# THE INFLUENCE OF STATISTICAL AGGREGATION MEASURES AND INTERVALS FOR PROCESSING AUTOMATED RUT DEPTH MEASUREMENTS ON PAVEMENT MANAGEMENT SYSTEMS

**CHRISTINA PAPADOURIS**

# THE INFLUENCE OF STATISTICAL AGGREGATION MEASURES AND INTERVALS FOR PROCESSING AUTOMATED RUT DEPTH MEASUREMENTS ON PAVEMENT MANAGEMENT SYSTEMS

**CHRISTINA PAPADOURIS**

**A dissertation submitted in partial fulfilment of the requirements for the degree of**

**MASTER OF ENGINEERING (TRANSPORTATION ENGINEERING)**

**In the**

**FACULTY OF ENGINEERING**

**UNIVERSITY OF PRETORIA**

**December 2021**

# DISSERTATION SUMMARY

# THE INFLUENCE OF STATISTICAL AGGREGATION MEASURES AND INTERVALS FOR PROCESSING AUTOMATED RUT DEPTH MEASUREMENTS ON PAVEMENT MANAGEMENT SYSTEMS

## CG PAPADOURIS

**Supervisor:** Professor WJvdM Steyn

**Co-Supervisor:** Doctor Raelize du Plooy

**Department:** Civil Engineering

**University:** University of Pretoria

**Degree:** Master of Engineering (Transportation engineering)

Rutting, an important indicator of structural integrity and a concern for road user safety, is measured using either manual or automated techniques. For simplification purposes, automated data consisting of high-density measurements obtained at short intervals is condensed by statistical measures, mostly averages, over larger intervals to characterise pavement sections. As longer pavement sections do not represent homogeneous performance conditions, with some sections deteriorating faster than others, the aggregation process causes valuable information to be lost, resulting in a possibly inaccurate representation of the pavement condition.

Using this aggregated data as an input in Pavement Management Systems (PMS) may result in inaccurate condition prediction, maintenance requirements, and budgetary forecasts. The level of aggregation, including the selected analysis pavement section lengths, influences the extent to which this information is inaccurately forecast.

This study investigates the potential effects, as influenced by varying aggregated section lengths, of using statistical aggregation measures, namely, averages and percentiles, to analyse high-density automated rutting data, on the distribution of rut depth over a pavement section, and the respective maintenance, funding, and pavement performance requirements.

A statistical and technical needs analysis was undertaken to study the influence of 20 m, 50 m, 100 m, 500 m, 1 000 m, and 10 000 m aggregated section lengths, considering the mean, and the $50^{th}$, $75^{th}$, $90^{th}$,

95th, and 99th percentiles as aggregation measures, on the distribution of rut depth over a pavement section and the respective maintenance, funding, and pavement performance requirements.

When using the mean as the statistical aggregation measure, the study indicated that the dispersion of rut depth reduces with increasing averaged section length, resulting in inaccurate condition and maintenance requirement forecasts. Introducing percentiles as the aggregation measure revealed that percentiles offer more accuracy over averages. For annual financial planning, the 50th percentile is most suitable. For technical needs planning, the 75th percentile is better suited as it presented with the lowest degree of error in estimating the total maintenance and rehabilitation need over the analysis period. Higher percentiles (90th to 99th) should be considered where high priority roads and performance requirements are a concern.

# ABSTRACT

**Title:** The Influence of Statistical Aggregation Measures and Intervals for Processing Automated Rut Depth Measurements on Pavement Management Systems

**Author:** C.G. Papadouris

**Supervisor:** Professor WJvdM Steyn

**Co-Supervisor:** Doctor Raelize du Plooy

**Department:** Civil Engineering

**University:** University of Pretoria

**Degree:** Master of Engineering (Transportation Engineering)

Automated rutting data is condensed by means of statistical measures, mostly averages, over larger intervals to characterise pavement sections, thereby reducing the amount of data required to be analysed. Longer pavement sections, however, do not necessarily represent homogeneous performance conditions, and valuable information is lost as a result of the aggregation process.

Using this aggregated data as an input in pavement management systems (PMS) may result in inaccurate condition prediction, maintenance requirements, and budgetary forecasts. The level of aggregation, including the selected analysis pavement section lengths, influences the extent to which this information is inaccurately forecast.

This study investigates the potential effects, as influenced by varying aggregated section lengths, of using statistical aggregation measures, namely, averages and percentiles, to analyse high-density automated rutting data, on the distribution of rut depth over a pavement section, and the respective maintenance, funding, and pavement performance requirements.

When using the mean as the statistical aggregation measure, the study indicated that the dispersion of rut depth reduces with increasing averaged section length, resulting in inaccurate condition and maintenance requirement forecasts. Introducing percentiles as the aggregation measure revealed that percentiles offer more accuracy over averages. For annual financial planning, the $50^{th}$ percentile is most suitable. For technical needs planning, the $75^{th}$ percentile is better suited, considering higher percentiles ($90^{th}$ to $99^{th}$) where high priority roads and performance requirements are a concern.

# DECLARATION

I, the undersigned, hereby declare that:

- I understand what plagiarism is, and I am aware of the University's policy in this regard;
- The work contained in this thesis is my own original work;
- I did not refer to the work of current or previous students, lecture notes, handbooks, or any other study material without proper referencing;
- Where other people's work has been used, this has been appropriately acknowledged and referenced;
- I have not allowed anyone to copy any part of my thesis;
- I have not previously, in its entirety or in part, submitted this thesis at any university for a degree.

**DISCLAIMER:**

**The work presented in this report is that of the student alone. Students were encouraged to take ownership of their projects and to develop and execute their experiments with limited guidance and assistance. The content of the research does not necessarily represent the views of the supervisor or any staff member of the University of Pretoria, Department of Civil Engineering. The supervisor did not read or edit the final report and is not responsible for any technical inaccuracies, statements, or errors. The conclusions and recommendations given in the report are also not necessarily that of the supervisor, sponsors, or companies involved in the research.**

**Signature of student:** 

**Name of student:** Christina Papadouris

**Student number:** 11008190

**Date:** 14/12/2021

# ACKNOWLEDGEMENTS

I wish to express my appreciation to the following organisations and persons who made this project dissertation possible:

a) Specialised Road Technologies (SRT) and Aurecon Africa (rebranded as Zutari) for the provision of data used in the analysis;

b) Aurecon Africa (rebranded as Zutari) for the provision of the dTIMS software and accompanying analysis models for the duration of the study;

c) Professor WJvdM Steyn, my supervisor, and Doctor Raelize du Plooy, my co-supervisor, for their guidance and support, and

d) My family for their encouragement and support during the study.

# TABLE OF CONTENTS

PAGE

# LIST OF APPENDICES

# LIST OF TABLES

PAGE

## LIST OF FIGURES

PAGE

# 1 INTRODUCTION

## 1.1 BACKGROUND

Rutting is a defect that develops in the pavement structure due to traffic loading (SANRAL, 2014; Wang, 2005). It is an important indicator of structural integrity and also impacts road user safety. Rut depth levels are, therefore, regularly monitored to obtain knowledge of the road's condition in order to maintain the pavements at an adequate level of service (COTO, 2016a; Mallela and Wang 2006).

Rut depths are measured using either manual or automated techniques (Mallela and Wang, 2006). Manual methods are simple to execute but are based on a limited number of actual measurements, as measurements are taken at large intervals due to traffic and time limitations. It is, therefore, difficult to obtain the entire profile of the road segment, and there is the potential of overlooking sections of road containing deeper than typical rutting. It is also labour intensive, dangerous for pavement condition raters when traffic control is limited, and there is a higher chance of measurement errors occurring (Wang, 2005; Hoffman and Sargand, 2011).

The importance of timely, safe, and efficient data collection resulted in the development of automated survey vehicles capable of collecting the data needed to assess and monitor the extent and severity of pavement rutting. Numerous rut measurements are obtained at short intervals along the road segment, allowing for a more comprehensive indication of the actual condition of the pavement, in a much shorter time period, without interfering with traffic flow, and the safety risk of the rating team is greatly reduced (Wang, 2005; Hoffman and Sargand, 2011).

For simplification purposes, high-density automated data is condensed by means of statistical measures, mostly averages, to characterise pavement sections. Through this aggregation process, valuable information is lost, resulting in a possibly inaccurate representation of the pavement condition (Kadar et al., 2015).

In South Africa, visual assessments used to assess the surfacing, structural, and functional condition of pavements are carried out in accordance with the COTO (2016b) TMH 9 visual assessment procedures. The scope of the assessment does not include the identification of uniform sections of condition and standard segment lengths of 2 km (± 1 km) are recommended for evaluating flexible pavements. While standard segment lengths are 2 km in length, segments provided often vary in length and can be as long as 10 km.

As per the COTO (2013) TMH 22, the average of the automated rut data should be recorded and stored at 10 m intervals and reported on at 100 m intervals.

As per the COLTO (1997) TRH 12 guidelines on the design of flexible pavement rehabilitation projects, rehabilitation requirements should be identified for uniform pavement sections. Uniform sections are determined based on similar functional properties, such as riding quality and rut depth, and similar types of materials, material conditions, and pavement structure. At project level, detailed measurements are typically considered in determining these uniform sections (COTO, 2013 and SANRAL, 2014).

However, at network level, detailed measurements are typically aggregated to some extent prior to determining uniform sections. In most PMSs, high-density automated data such as rut measurements recorded at 10 m intervals is aggregated by means of averages or percentiles to obtain an aggregated value per visually assessed segment discussed above without considering the variability of rut depth along these sections. Following this process, these visually assessed segments are further aggregated based on similar condition, pavement structure, and environmental characteristics to obtain more practical maintenance and rehabilitation project lengths, prior to determining maintenance/rehabilitation requirements. In doing so these longer sections are considered to be homogenous. However, as some shorter sections (10 m to 100 m) present with higher rutting than others, these aggregated sections do not represent homogeneous conditions.

Using this aggregated data as an input in pavement management systems (PMS) may result in inaccurate condition prediction, maintenance requirements, and budgetary forecasts. The extent to which this information is inaccurately forecast is influenced by the level of aggregation, including the selected analysis pavement section lengths (Kadar et al., 2015).

This study investigates the potential effects, as influenced by varying aggregated section lengths, of using statistical aggregation measures, namely, averages and percentiles, to analyse high-density automated rutting data, on the distribution of calculated rut depth over a pavement section and the respective maintenance and funding requirements.

## 1.2 OBJECTIVES OF THE STUDY

The objectives of the study are:

1. To study the influence of varying aggregated section lengths, considering the mean as the statistical aggregation measure, on the distribution of calculated rut depth over a pavement section, and the respective maintenance and funding requirements;
2. To study the influence of varying aggregated section lengths, considering varying percentiles as the statistical aggregation measure, on the distribution of calculated rut depth over a pavement section, and the respective maintenance and funding requirements;

3. Based on the abovementioned studies, determine which aggregation measure provides a more accurate representation of the pavement condition when compared to the discrete rut depth measurements, and
4. Apply the statistical aggregation measures within a selected specification to analyse the use of such methods in providing an accurate representation of whether or not pavement performance requirements are being met when compared to discrete rut depth measurements.

## 1.3 SCOPE OF THE STUDY

The scope of the data acquired for the analysis is summarised as follows:

- 13 Samples consisting of major and minor arterial/distributor paved roads located in the Northern Cape Province of South Africa were selected for the analysis. The number of samples was limited by the availability of data acquired for the analysis as well as the sample assessment length (only samples containing an assessment length considered to be sufficient to allow for the comparison of varying section lengths were selected for the analysis);
- The variability of rut depth measurements (distribution type and dispersion of rut depth values) is subject to the availability of data acquired for the analysis;
- Rut depth measurements were taken at 10 m intervals and are considered to be discrete measurements, and
- Accurate maintenance history of road segments indicating the nature of the treatment carried out, the date of application, and the length of the maintenance segment was not necessarily recorded/available, thus impacting the accuracy of the type of distribution of rut depth identified for longer pavement sections where pavement and environmental characteristics are not the only influencing factors.

The scope of the data analysis is summarised as follows:

- Only exponential, lognormal, and normal distributions are considered in identifying the type of distribution of rut depth;
- The influence of the following aggregated section lengths is considered: 20 m, 50 m, 100 m, 500 m, 1 000 m, and 10 000 m;
- The influence of the following percentiles is considered per aggregated section length: $50^{th}$, $75^{th}$, $90^{th}$, $95^{th}$, and $99^{th}$;

- The influence of data processing on the distribution of rut depth amongst condition categories is influenced by the bins defined in evaluating the severity of rut depth. The following bins are used to categorise rut depth: sound (rut < 5 mm), isolated (5 mm ≤ rut < 10 mm), moderate (10 mm ≤ rut ≤ 15 mm), warning (15 mm < rut ≤ 20 m), and severe (rut > 20 mm);
- The immediate annual maintenance and funding requirements are determined through a technical needs analysis for a 20-year period;
- The technical needs analysis does not incorporate any life-cycle optimisation in the determination of needs;
- The determined maintenance requirements are dependent on the pavement condition data, algorithms for pavement performance, and algorithms for maintenance;
- The determined funding requirements are additionally influenced by the specified treatment unit costs;
- Locally calibrated versions of the HDM-4 pavement performance models are used to predict the future performance of road segments and the subsequent maintenance and funding requirements;
- Major treatments considered in the maintenance needs analysis include reseals, light rehabilitation, and heavy rehabilitation;
- Minor treatments considered in the maintenance needs analysis include fog sprays. Fog spray maintenance requirements are not discussed in this report;
- Rutting is not the sole maintenance driver and the condition of roughness, cracking, patching, potholes, pumping, and ravelling is also considered in determining the maintenance requirements, and
- When studying the application of the statistical aggregation measures within a specification, the statistical aggregation measures were only tested against the performance requirements indicated in the South African NRA (1999) specification.

## 1.4 METHODOLOGY

A statistical and technical needs analysis was undertaken to study the influence of varying aggregated section lengths, considering the mean and percentiles as statistical aggregation measures, on the distribution of calculated rut depth over a pavement section, and the respective maintenance and funding requirements.

Two sets of road performance data from the Limpopo and Northern Cape Province were obtained for the analysis. The acquired road performance data consists of high-speed profile measurements, i.e., roughness and rut depth measurements, taken at 10 m intervals, non-destructive falling weight deflectometer measurements, visual assessments, traffic counts, and other inventory data affecting pavement deterioration and, therefore, the distribution of rut depth, and the respective maintenance and funding requirements.

From the datasets obtained, roads having an assessment length that was considered sufficient to allow for the comparison of different section lengths were selected for the analysis. As such, 13 roads located in the Northern Cape Province, ranging in length from approximately 52 km to 146 km, were selected for the analysis.

The average of the discrete 10 m rut depth measurements was taken per 20 m, 50 m, 100 m, 500 m, 1 000 m, and 10 000 m section lengths. Exponential, lognormal, and normal probability plots were plotted and compared per section length to study the influence of a change in averaged section length on the type of distribution of calculated rut depth values. Cumulative distributions of rut depth and distribution parameters (maximum, mean, variance, coefficient of variation, $20^{th}$ percentile, and $95^{th}$ percentile) were compared for all section lengths to study the influence of a change in averaged section length on the dispersion of rut depth values.

A technical (engineering) needs analysis was carried out in dTIMS (Deighton Total Infrastructure Management System) over a 20-year analysis period to study the influence of varying aggregated section lengths, considering the mean as the statistical aggregation measure, on the immediate annual maintenance requirements and the resulting funding need.

In an attempt to determine whether or not a percentile rather than the average might provide a better estimation of distribution/dispersion of rut depth values and the respective maintenance and funding requirements when compared to the discrete 10 m rut depth measurements, the $50^{th}$, $75^{th}$, $90^{th}$, $95^{th}$, and $99^{th}$ percentile of the discrete 10 m rut depth measurements were calculated per 20 m, 50 m, 100 m, 500 m, 1 000 m, and 10 000 m section lengths. Cumulative distributions of rut depth and distribution parameters (mean, minimum, maximum, and coefficient of variation) were compared for all percentiles and aggregated section lengths to study the influence of varying percentiles and aggregated section lengths on the dispersion of calculated rut depth values.

A technical needs analysis was rerun in dTIMS over a 20-year analysis period to study the influence of aggregated section lengths, considering varying percentiles as the statistical aggregation measure, on the immediate annual maintenance requirements and the resulting funding need.

The application of these statistical aggregation measures within the South African NRA (1999) specification was then additionally studied to analyse the use of such methods in providing an accurate representation of whether or not pavement performance requirements are being met when compared to discrete rut depth measurements.

The cumulative distribution was plotted for discrete 10 m, 100 m average, and 100 m $50^{th}$, $75^{th}$, $90^{th}$, $95^{th}$, and $99^{th}$ percentile rut depth measurements for 5 samples of varying rut depth severity. The resulting cumulative distribution graphs were then analysed according to the acceptance criteria specified in the NRA (1999) to determine if the statistical aggregation methods provide an accurate representation of whether the performance requirements are being met or not when compared to the results of the discrete 10 m rut depth measurements.

## 1.5 ORGANISATION OF THE REPORT

The report consists of the following chapters and appendices:

- Chapter 1 contains the introduction as well as the objectives, scope, methodology, and the outline of the remainder of the report;
- Chapter 2 contains the literature review of pavement management system components, methods for measuring pavement transverse profiles and rut depths using manual and automated equipment, measurement issues associated with point laser profilometers, methods of transitioning between manual and automated measurements, data aggregation issues, current specifications available for measuring rut, performance models for condition prediction, and definitions of condition-based maintenance treatments for flexible pavements;
- Chapter 3 discusses the data obtained for the analysis as well as the research methodology;
- Chapter 4 presents the discussion of results obtained from the study;
- Chapter 5 contains conclusions and recommendations;
- Chapter 6 contains the reference list, and
- Appendices

# 2 LITERATURE REVIEW

## 2.1 THE IMPORTANCE OF MAINTENANCE AND REHABILITATION

After construction, pavements deteriorate over time under the combined actions of traffic and the environment. Deterioration impedes the pavement's ability to perform functions, such as providing a smooth riding surface essential for riding comfort, ensuring road user safety under all conditions, and having sufficient structural capacity to support the applied axle loads (Steyn, 2012). As a result, vehicle operating costs and the cost of transporting goods are increased, and user safety, comfort, and travel speed are lowered. Deterioration also lowers the pavement's resilience to adverse circumstances such as natural hazards and manmade disasters, making it vulnerable to catastrophic failure, which could have widespread and economic consequences (Frangopol, 2007; Paterson, 1987).

Mismanagement and neglect accelerate the deterioration of the pavement structure. Maintenance is, therefore, required. Through pavement maintenance, protective and repair measures are carried out to limit the detrimental effects of traffic and the environment, thereby slowing the rate of deterioration and increasing the availability and reliability (i.e., improving the serviceability) as well as prolonging the useful life of the pavement (Atkinson, 1990). Satisfactory lifetime performance aids in sustaining economic growth and the social development of modern society (Frangopol, 2007).

When defects become too large/severe to be corrected through maintenance, rehabilitation of the pavement is required to improve the pavement condition (Steyn, 2012).

## 2.2 PAVEMENT MANAGEMENT SYSTEMS (PMS)

### 2.2.1 Importance

When maintaining or rehabilitating infrastructure, the following factors need to be taken into consideration (Gräbe, 2013):

- There are limited funds available to carry out maintenance and rehabilitation. Therefore, maintenance and rehabilitation needs should be prioritised and budgeted for;
- Maintenance should be carried out with minimal interference with the users of the facility, and
- To ensure that a productive maintenance and rehabilitation input is achieved, the correct maintenance and rehabilitation option should be selected and executed in a timely manner.

To ensure that all the factors mentioned are effectively put in place, maintenance and rehabilitation need to be managed. Pavement management systems are, therefore, utilised.

### 2.2.2 PMS components

The main components of a pavement management system are (Steyn, 2012):

- **Inventory**: Collection of information on road sections being managed. Relevant aspects include location, pavement structure, traffic, history, and drainage;
- **Condition monitoring:** Regular collection of data describing the condition of the pavement;
- **Condition prediction**: Prediction models describing pavement deterioration rates;
- **Decision criteria**: Criteria indicating when decisions regarding maintenance and rehabilitation actions need to be taken, and
- **Implementation procedures**: Procedures indicating the type of maintenance or rehabilitation to be performed.

Pavement management is conducted on a network and project level. On a network level, funding is optimised, and broad areas of maintenance, rehabilitation, and construction are prioritised for the entire road network. On a project level, detailed planning of maintenance and rehabilitation are made. The focus is on technical concerns, specific materials, procedures, and detailed design decisions (Steyn, 2012).

## 2.3 CONDITION MONITORING

Condition monitoring is used to determine the overall condition of the pavement, which is necessary for the evaluation and determination of maintenance needs (Gräbe, 2013).

### 2.3.1 Pavement deterioration

Pavement performance is primarily a function of the traffic and weather conditions to which the pavement is exposed. Traffic loads cause stresses and strains within the pavement layers, and under repeated loads, these responses lead to the deformation of the pavement layers. The degree of deformation depends on the characteristics of the load, the pavement layer thickness, and the pavement layer stiffness. Conditions such as weathering and solar radiation lead to the ageing of asphaltic materials causing the materials to become brittle and more susceptible to cracking. Once initiated, the severity of cracking continues to worsen, and eventually, potholes are formed. Furthermore, cracks allow surface water to permeate the pavement layers, which further accelerates the disintegration of the pavement. This cumulative deformation leads to wheel path rutting, which in effect increases pavement roughness (Odoki and Kerali, 2006).

### 2.3.2 Pavement condition parameters

Surfacing, structural, and functional condition assessments are used to describe the condition of flexible pavements. Surfacing condition assessments reflect the susceptibility of underlying pavement layers to surface exposure and water ingress. Surfacing condition parameters include surfacing texture, surfacing failures, surfacing patching, surfacing cracks, binder condition, aggregate loss, bleeding, and surfacing deformation. Structural condition assessments reflect the ability of the pavement to resist traffic and environmentally induced stress. Structural condition parameters include cracks, pumping, rutting, settlement, patching, and potholing. Functional condition assessments reflect the ability of the pavement to carry traffic comfortably and safely. Functional condition parameters include riding quality, skid resistance, surface drainage, edge defects, rutting, and potholing (COTO, 2016b; Gräbe, 2013; SANRAL, 2014; Steyn, 2012).

## 2.4 RUTTING DEFINITION

Rutting is a defect that develops in the pavement due to traffic loading. Axle loads cause consolidation or shear failure of one or more pavement layers, which results in the displacement of bituminous material that makes up part of the pavement structure, causing longitudinal depressions in the wheel path (SANRAL, 2014; Wang, 2005).

The formation of rutting associated with the asphalt layer due to compaction is illustrated in Figure 2-1. The formation of rutting associated with the asphalt layer due to mix design problems causing the lateral displacement of material is illustrated in Figure 2-2. The formation of rutting associated with a weak subgrade is illustrated in Figure 2-3 (Simpson, 2001).

The severity of rutting is influenced by pavement material properties, layer thickness, pavement age, climatic conditions, drainage conditions, traffic volume, and construction quality (SANRAL, 2020).

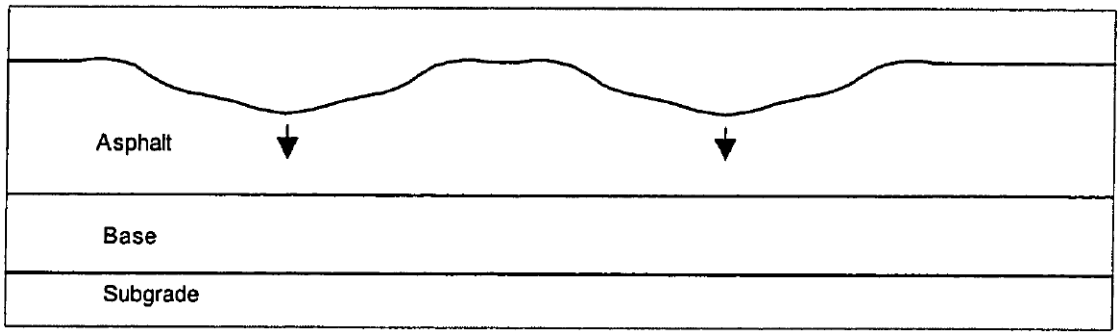


**Figure 2-1: Rutting due to densification of asphalt (Simpson, 2001)**

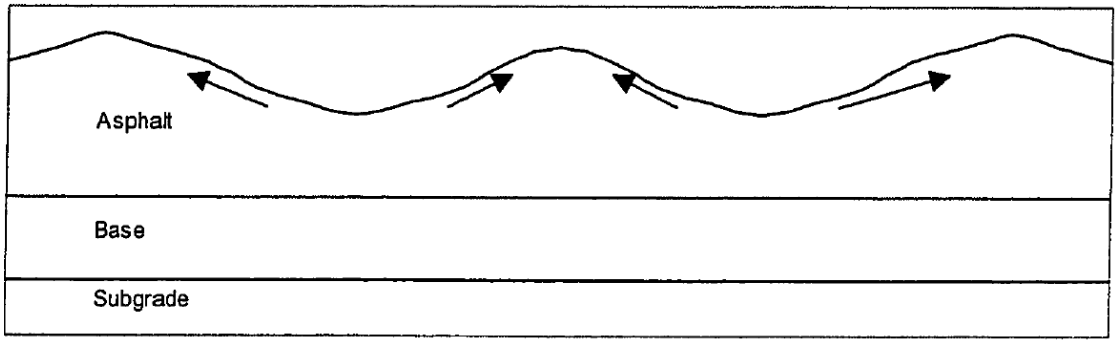


**Figure 2-2: Rutting due to lateral displacement of asphalt (Simpson, 2001)**

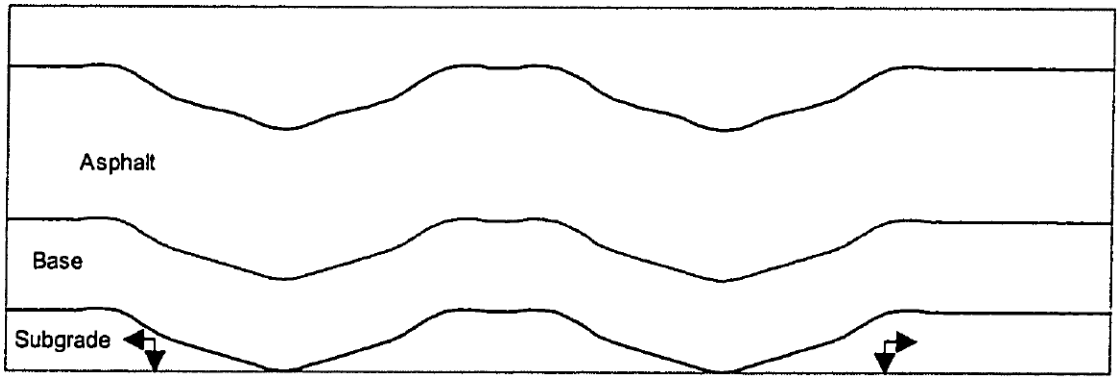


**Figure 2-3: Rutting within the subgrade (Simpson, 2001)**

Rutting is an indicator of the structural integrity of the pavement, i.e., the presence of rutting indicates that there might be a failure in one or more layers in the pavement (Adlinge and Gupta, 2013). Rutting also impacts road user safety. Deep rutting can cause vehicles to become unstable when trying to move out of the rut, and during wet weather, water tends to collect in the ruts and subjects the pavement to ponding and freezing, increasing pavement deterioration and the potential for hydroplaning and associated wet-weather accidents. Rutting also contributes to pavement roughness, which has a detrimental effect on the overall ride quality of the road and, hence, user satisfaction (COTO, 2016a; Wang, 2005).

For these reasons, rut depths are regularly monitored to obtain knowledge of the condition of the road and to detect unacceptable increases in the amount or severity of rutting in order to estimate the timing, type, and cost of maintenance needs and maintain the pavements at an adequate level of service (COTO, 2016a; Mallela and Wang, 2006). When evaluating the functional condition, rutting relates to the riding quality and safety experienced by the road user. In terms of structural performance, rutting is an important measure since it develops as a result of accumulated wheel load repetitions throughout the service life of the pavement (COTO, 2016a).

## 2.5 SURFACE TRANSVERSE PROFILE

The transverse profile, measured along a continuous lateral line on the pavement surface, as shown in Figure 2-4, is used to characterise rutting. Different rutting parameters can be determined from the transverse surface profile to characterise rutting. These parameters are discussed in Section 2.6 (COTO, 2016a; Sayers and Karamihas, 1998).

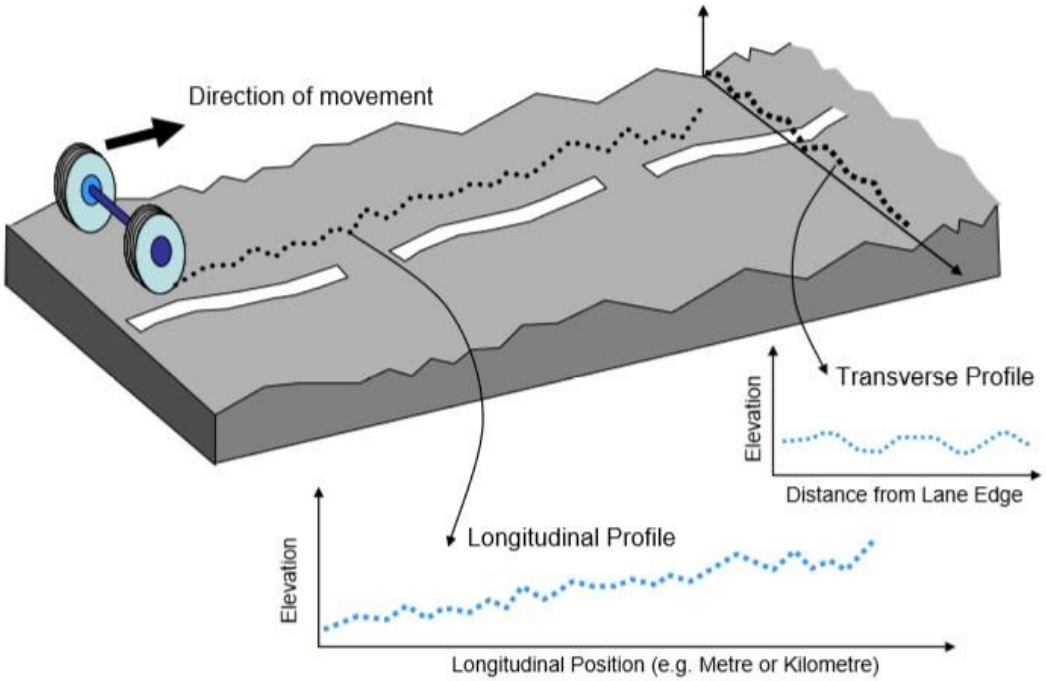


**Figure 2-4: Pavement surface profiles (COTO, 2016a)**

## 2.6 CHARACTERISATION OF RUTTING

Several rutting indices exist to characterise rutting and are grouped into rut depth, rut width, area, and ponding indices, as well as radius of curvature. The radius of curvature is not recommended for use due to the difficulties in defining and calculating the index and is, therefore, not discussed here (COTO, 2016a; Serigos et al., 2012).

**Rut depth index**

This is the most frequently used index for characterising rutting. Rut depth is the estimate of unevenness in the transverse direction of the road and is defined differently depending on the method or equipment used to measure it. The rut depth is most commonly defined as the maximum distance between the straightedge or wire line and the transverse profile, measured perpendicular to the straightedge or wire line, indicated as “RD” in Figure 2-5(a) (COTO, 2016a; Serigos et al., 2012).

**Rut width index**

Defined as the distance between the points at which the straightedge or wire is supported by the transverse profile, indicated as “RW” in Figure 2-5(b) (COTO, 2016a; Serigos et al., 2012).

**Area indices**

Area indices are divided into negative area index, positive area index, and fill area index. The negative area index is defined as the area formed below a straight (wire) line that connects the first and last coordinate of the lane and the transverse profile, as shown in Figure 2-5(c). The positive area index is defined as the area formed above a straight (wire) line that connects the first and last coordinate of the lane and the transverse profile, as shown in Figure 2-5(c). The negative and positive area indices are used to gain information on the severity and cause of the rutting. The fill (rut) area index is defined as the total area formed between the transverse profile and a straight (wire) line connecting the peaks of the profile, as shown in Figure 2-5(d). The fill (rut) area index is used to estimate the amount of material required to repair the pavement (COTO, 2016a; Serigos et al., 2012).

**Ponding indices**

Ponding indices include pond depth, pond width, and pond area. Pond depth is defined as the maximum vertical distance (obtained for each wheel path) between the transverse profile and a horizontal line positioned at the maximum point at which water would pond, indicated as “PD” in Figure 2-5(e) (Serigos et al., 2012). Pond width is defined as the horizontal distance between the points at which the horizontal line positioned at the maximum point at which water would pond meets the transverse profile, indicted as “PW” in Figure 2-5(f). Pond area is defined as the total area formed between the transverse profile and the horizontal line positioned at the maximum point at which water would pond, as shown in Figure 2-5(g) (COTO, 2016a).

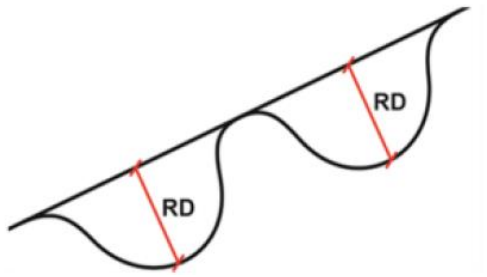


(a) Rut depth

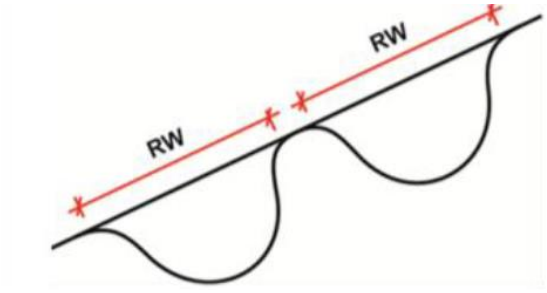


(b) Rut width

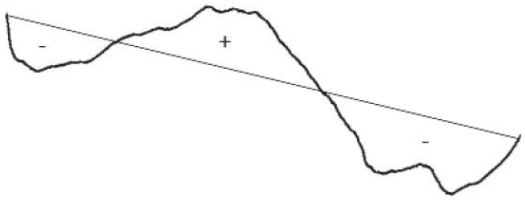


(b) Negative and positive area index

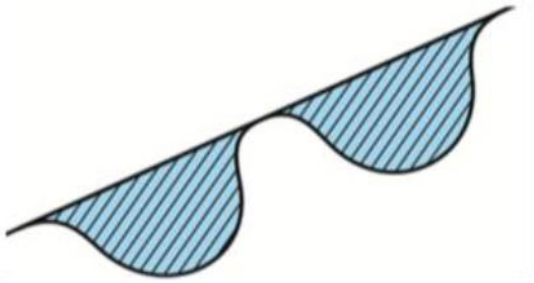

(d) Fill (rut) area


(e) Pond depth

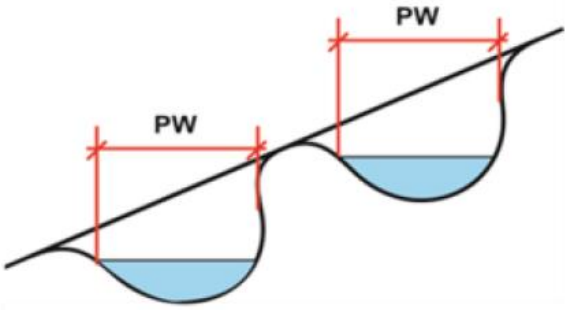


(f) Pond width

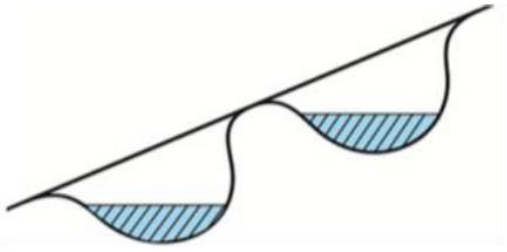

(g) Pond area

**Figure 2-5: Rutting indices available to characterise rutting (adapted from COTO, 2016a and Serigos et al., 2012)**

## 2.7 RUT DEPTH MEASUREMENT TECHNIQUES

Rut depths are measured using either manual or automated techniques (Mallela and Wang, 2006).

### 2.7.1 Manual measurement techniques

The most common manual methods for measuring maximum rut depth are the straightedge and the wire string (Serigos et al., 2012).

**Straightedge method**

The straightedge is placed across the wheel path perpendicular to the direction of traffic, contacting the road at the two highest points on either side of the wheel path. Several measurements are taken along the length of the straightedge to find the maximum vertical distance between the road surface and the bottom of the straightedge, which is defined as the rut depth. The straightedge method is illustrated in Figure 2-6 (Hoffman and Sargand, 2011).

The maximum rut depth obtained is affected by the length of the straightedge. ASTM International (2015) E1703/E1703M-10 requires that the straightedge length be in the range of 1.73 m to 4.88 m. In this range, the straightedge spans over at least half of the traffic lane, thereby ensuring that the straightedge is long enough to span over the two highest points on either side of the rut (Hajek et al., 1998; Serigos et al., 2012).

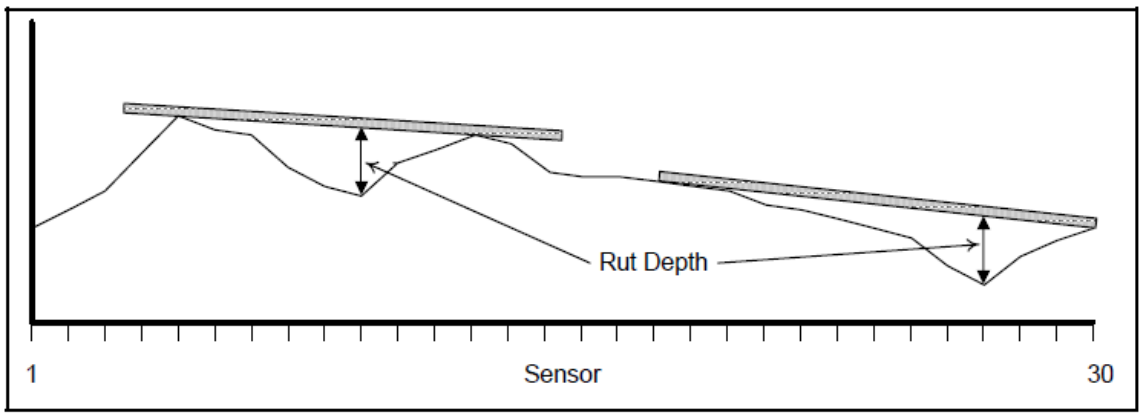


**Figure 2-6: Straightedge method (Mallela and Wang, 2006)**

The straightedge method is a widely accepted, standard rut measurement method. Therefore, rut depth measurements obtained using this method are used as a reference to the ground truth when evaluating the accuracy of any automated instrument (Huang et al., 2009).

**Wire string method**

The wire is stretched tense transversely across the pavement lane, enveloping the high points. The rut depth is defined as the maximum vertical distance measured between the tensed wire

and the pavement surface. The wire string method is illustrated in Figure 2-7 (Serigos et al., 2012).

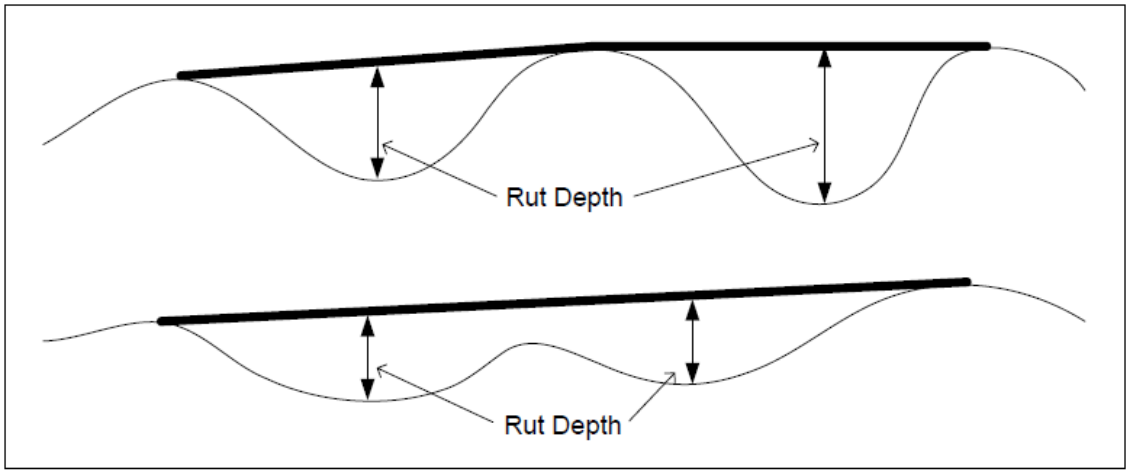


**Figure 2-7: Wire string method (Mallela and Wang, 2006)**

The straightedge and wire string method will provide the same rut depth as long as the straightedge length is long enough to cover the same high points at the ends of the wheel path (Serigos et al., 2012).

### 2.7.2 Disadvantages of manual methods

Manual methods are simple to execute but are based on a limited number of actual measurements (measurements are taken at large intervals) due to traffic and time limitations. It is, therefore, difficult to obtain the entire profile of the road segment, and there is the potential of overlooking sections of road containing deeper than typical rutting. It is also labour intensive, dangerous for pavement condition raters when traffic control is limited, and there is a higher chance of measurement errors occurring (Wang, 2005; Hoffman and Sargand, 2011).

### 2.7.3 Reference profile beams

In addition to the straightedge and wire string method, manually operated devices capable of accurately measuring the full transverse profile of a pavement surface in addition to the maximum rut depth have been developed for rut validation purposes. Such devices include the Transverse Profile Beam and the Manual Rut Reference Profiler (COTO, 2016a).

**Transverse Profile Beam (TPB)**

The TPB consists of a 3.6 m long beam supported by a wheel that is moved across the pavement by a motorised carriage, as shown in Figure 2-8. Vertical and horizontal transducers monitor the position and elevation of the wheel as it moves across the pavement. Rut depth is then calculated under a 2 m simulated straightedge. The results obtained using a TPB are virtually identical to those measured manually (Bennett, 2002; COTO, 2016a).

**Figure 2-8: Transverse Profile Beam (Bennett, 2002)**

**Manual Rut Reference Profiler (MRRP)**

The MRRP consists of a horizontal aluminium bar with a measurement width of 2 m and a motorised vertical tower equipped with a notebook stand for automated data collection. The vertical tower is guided across the pavement surface in such a manner that minimises the effect of texture (COTO, 2016a). The MRRP is shown in Figure 2-9.

**Figure 2-9: Manual Rut Reference Profiler (Scienceware, 2008)**

### 2.7.4 Automatic measurement techniques

The importance of timely, safe, and efficient data collection resulted in the development of automated survey vehicles capable of collecting the data needed to assess and monitor the extent and severity of pavement rutting (Wang, 2005).

The advantage of automated measurement techniques is that numerous rut measurements are obtained at short intervals along the road segment, allowing for a more comprehensive indication of the actual condition of the pavement, in a much shorter time period, without interfering with traffic flow and the safety risk of the rating team is greatly reduced (Hoffman and Sargand 2011).

There are four technologies available for estimating rut depth using automated techniques, namely, ultrasonics, point lasers, scanning lasers, and optical systems. Automatic measuring systems making use of ultrasonic or point laser technology are considered as point-based discrete systems, and systems making use of scanning laser or optical technology are considered as continuous profile systems (Mallela and Wang, 2006; Serigios et al., 2012).

**Ultrasonics**

Ultrasonic sensors (number varies) are mounted on a beam, which is usually mounted on the front of the survey vehicle. The sensors measure the distance to the pavement surface as the vehicle travels along the road to obtain the transverse profile of the pavement. Rut depths are then estimated from the transverse profile (Mallela and Wang, 2006; Serigios et al., 2012).

**Point lasers**

Systems making use of point laser technology consist of a beam mounted with several lasers (number varies), which measure the elevation at a point to obtain the transverse profile of the pavement as the vehicle travels over the road segment at highway speeds. Rut depths are then estimated from the transverse profile (Mallela and Wang, 2006; Serigios et al., 2012).

Point laser technology is much faster than ultrasonic technology and can therefore record the transverse profile at much smaller intervals (as low as 10 mm) along the road (Mallela and Wang, 2006; Serigios et al., 2012). Point lasers are described in more detail in Section 2.8.

**Scanning lasers**

Scanning lasers sample the full pavement width to produce a profile that is almost continuous, i.e., capable of measuring more than 1000 points across the pavement surface. Rut depths are then estimated from the transverse profile (Austroads, 2016; Mallela and Wang, 2006; Serigios et al., 2012).

**Optical systems**

Systems making use of optical systems project lasers to the pavement and, with the use of a special camera, measure the deformation of the laser line. Digitised images of the transverse profile are then analysed to estimate rut depths (Mallela and Wang, 2006; Serigios et al., 2012).

## 2.8 POINT LASERS

Point lasers (also known as laser profilometers) are the most popular automatic measurement systems used in South Africa. For this reason, they are the main focus of this project and are discussed in more detail in this section (COTO, 2016a).

### 2.8.1 Profilometer description

Profilometers are based on the concept of measuring the distance from a reference point on the survey vehicle to the pavement surface to establish the transverse profile (COTO, 2016a).

Laser profilometers consist of an accelerometer, a laser height sensor, and a distance measuring instrument, as shown in Figure 2-10 (Gillespie et al., 1987; Sayers and Karamihas, 1998). The reference elevation on the survey vehicle is defined by the accelerometer (Gillespie et al., 1987; Sayers and Karamihas, 1998). The accelerometer measures a vertical acceleration, which is converted to an inertial reference that defines the instant height of the accelerometer in the vehicle (Feingold, 2013; Sayers and Karamihas, 1998). The distance between the accelerometer and the pavement surface is measured with a non-contact laser sensor (Feingold, 2013; Sayers and Karamihas, 1998). A light source positioned on the measuring vehicle emits light to a point on the pavement surface, which is then reflected to a light receiver positioned on the measuring vehicle. The change in position of the lighted point on the pavement surface is detected by the optics associated with the light receiver (Hajek et al., 1998). The longitudinal travelled distance is measured by a distance transducer to provide registration of the profile along the road (ASTM International, 2004; Gillespie et al., 1987). The distance transducer produces a series of pulses, the intervals of which represent the distance travelled (ASTM International, 2004).

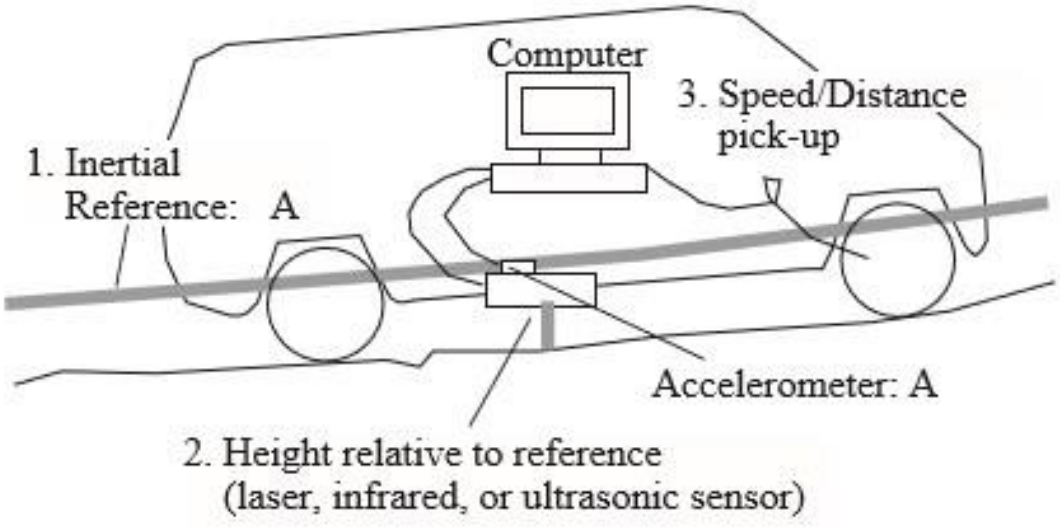


**Figure 2-10: Components of a profilometer (Sayers and Karamihas, 1998)**

Rut depth measurement requires simultaneous measurement of height from an array of height sensors distributed across the direction of travel (Gillespie et al., 1987). A point laser profilometer, therefore, utilises 3- or more point lasers (Li, 2012). The spacing configuration of point sensors is designed so as to assist the profilometer in locating the high and low points of the pavement surface (COTO, 2016a). Typical rut bar configurations for 3-, 5- and 9-point rut bar systems are shown in Figure 2-11.

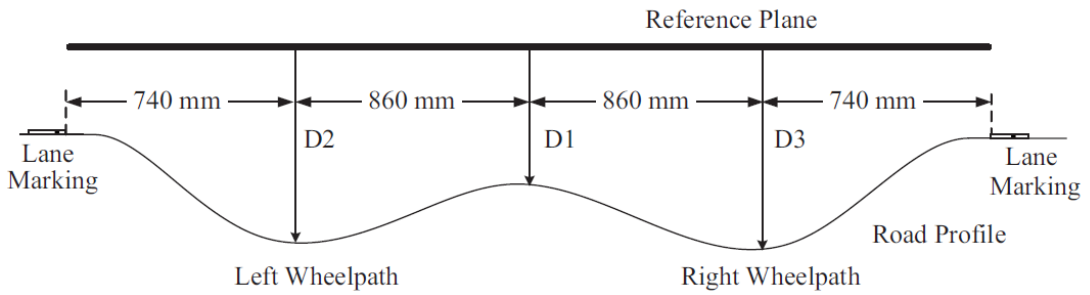


3-point rut bar configuration

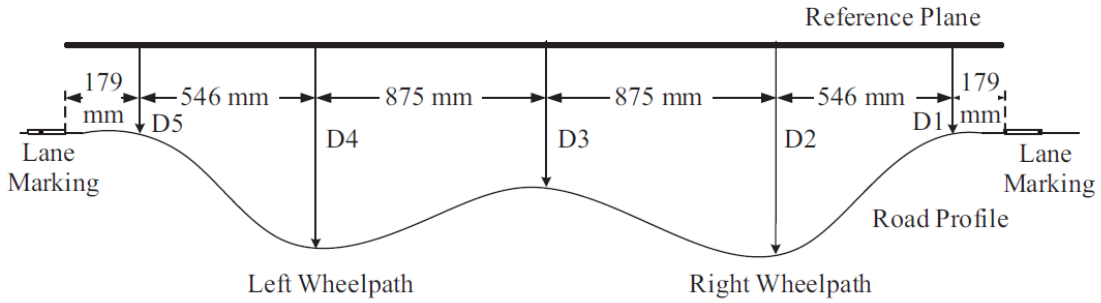


5-point rut bar configuration

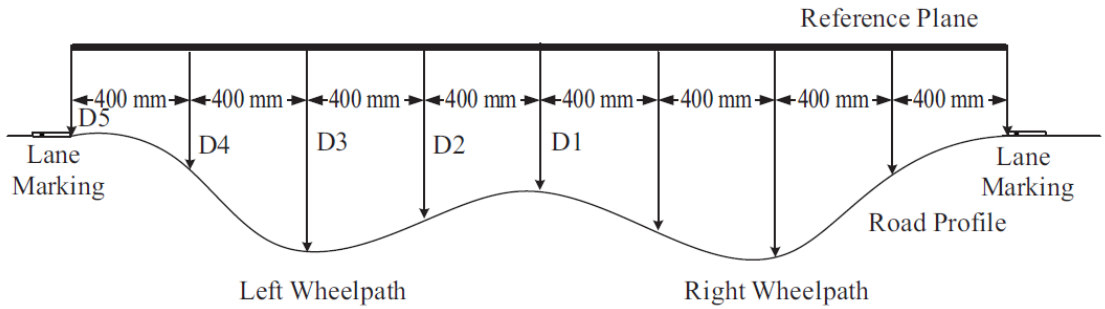


9-point rut bar configuration

**Figure 2-11: Rut bar configurations (Yichang et al., 2015)**

The measured transverse profile is analysed using algorithms to determine the rut depth (COTO, 2016a). The algorithms used are discussed in Section 2.9.

## 2.9 RUT DEPTH ALGORITHMS

Three algorithms exist to determine the rut depth from the measured transverse profile (Mallela and Wang, 2006).

### 2.9.1 Straightedge model

The straightedge model simulates the manual method of placing a straightedge across the pavement, as described in Section 2.7.1 (Mallela and Wang, 2006).

### 2.9.2 Wire string model

The wire string model simulates the manual method of stretching a wire across the pavement, as described in Section 2.7.1 (Mallela and Wang, 2006).

### 2.9.3 Pseudo-ruts

Pseudo-ruts are defined as the difference between a high and a low point, as shown in Figure 2-12 (Mallela and Wang, 2006). This method of determining rut depth was proposed for use in profiler systems producing a limited number of data points (3- or 5-point sensors) and is not considered a reliable method as it can produce poor results (COTO, 2016a; Hoffman and Sargand, 2011).

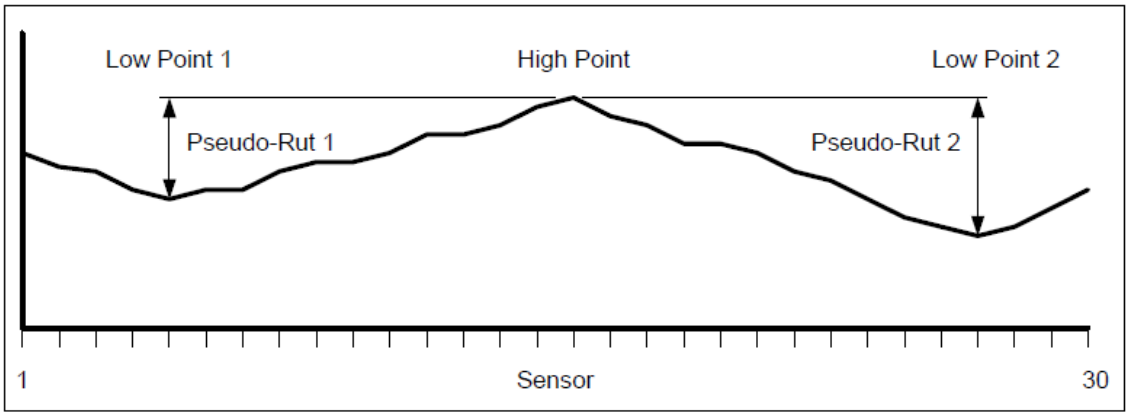


**Figure 2-12: Pseudo-ruts (Mallela and Wang, 2006)**

## 2.10 MEASUREMENT ISSUES

The accuracy of rut depth obtained from point-based discrete automatic measuring systems is primarily governed by the number and spacing configuration of sensors (sampling interval), the lateral placement of the survey vehicle, the measurement width, the lane width, the rut shape, severity of surface rutting, the pavement surface texture and analysis algorithm (Li, 2012; Mallela and Wang, 2006; Sayers and Karamihas, 1998).

### 2.10.1 Effect of the sampling interval

Based on the algorithms used to calculate rut depth, for the measured rut depth to correlate with the actual rut depth, the sensors would need to locate the high and low points in each wheel path being measured. However, since sensors are spaced at discrete intervals across the road, the lasers can easily miss these points, thereby underestimating the true rut depth. Figure 2-13 illustrates that the rut depth measured at discrete intervals (vertical axis) does not correlate with the rut depth obtained from a continuous transverse profile (horizontal axis) (Mallela and Wang, 2006).

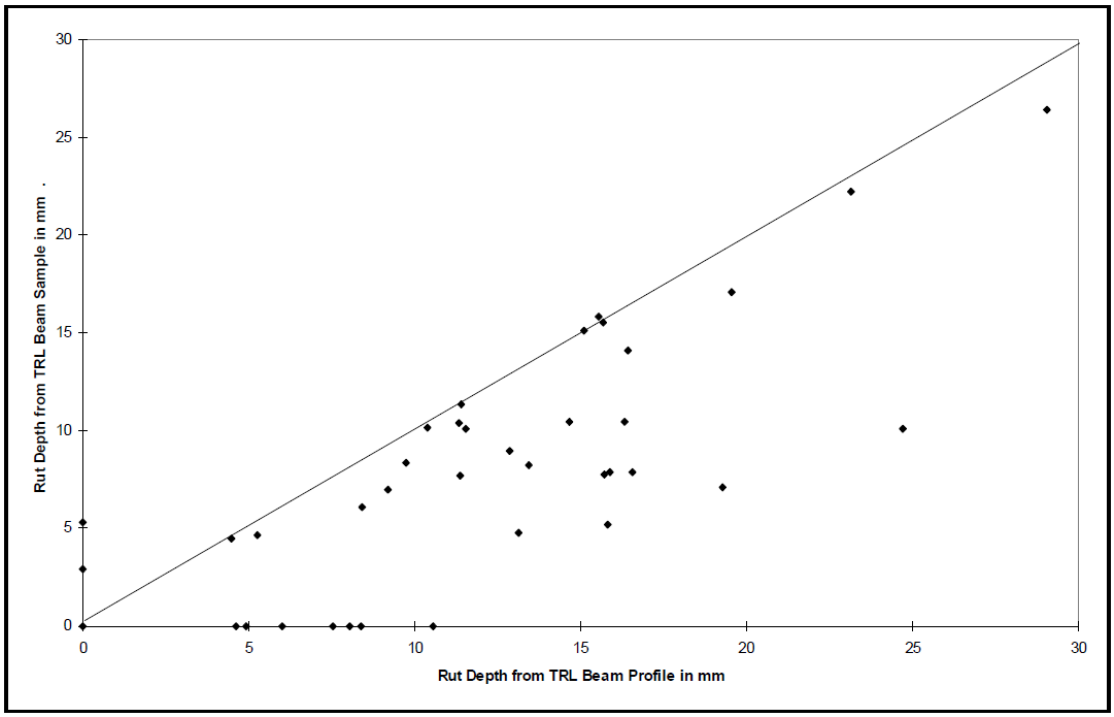


**Figure 2-13: Relationship between discrete and continuous rut depth data (Mallela and Wang, 2006)**

Figure 2-14 illustrates the effect of the number and spacing configuration of the sensors on the profilometer's ability to locate the high and low points in the profile. Different sensor density and spacing corresponds to different high and low points being recorded (Mallela and Wang, 2006).

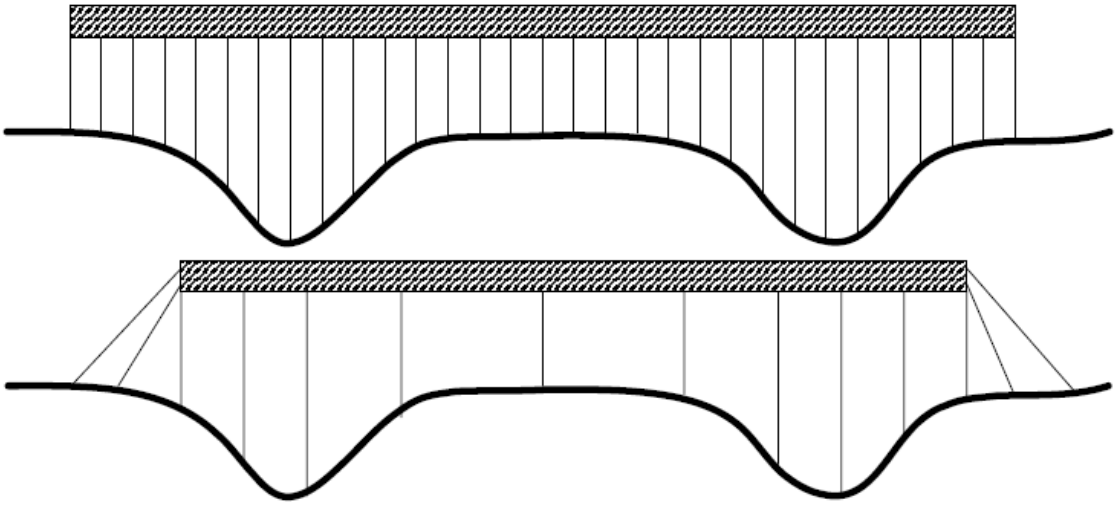

**Figure 2-14: Effect of the number and spacing configuration of sensors (Mallela and Wang, 2006)**

Increasing the number of sensors reduces the spacing between the sensors, thereby increasing the probability of locating high and low points and improving measurement accuracy (Mallela and Wang, 2006).

Mallela and Wang (2006) compared rut depths measured with different types of instrument configurations. When studying the effect of the number of sensors, an underestimation error of 2 mm to 4 mm was obtained for 13 to 30 sensors, and an error of 1 mm was obtained for 60 sensors. EquationsEquation 2-1 and Equation 2-2 represent the relationships identified between the standard error of measurements and the number of sensors. These relationships indicate that the accuracy of the measured rut depth significantly improves with an increasing number of sensors, the degree of improvement being much less significant with more than 25 sensors.

$$KerbERROR = 14.39 \times (SENSORS) - 0.5770 \times R^2 = 0.94 \quad \text{Equation 2-1}$$

$$CentreERROR = 11.40 \times (SENSORS) - 0.3831 \times R^2 = 0.90 \quad \text{Equation 2-2}$$

Where: ERROR is the standard error in mm

SENSORS is the number of sensors

Sjögren and Lundberg (2005) undertook an investigation to find the optimum configuration of a profilometer for measuring rut depth. Keeping the measurement width constant, Sjögren and Lundberg (2005) studied the effect of the number of sensors on the accuracy of the rut depth, considering the rut depth measured using continuous transverse sampling as the reference. The results obtained are shown in Figure 2-15 and Figure 2-16 and are summarised in Table 2-1. Based on the obtained results, it was deduced that the accuracy of the measured rut depth

increases with an increasing number of sensors, and 17 to 25 sensors are the optimum if the cost per extra sensor is considered.

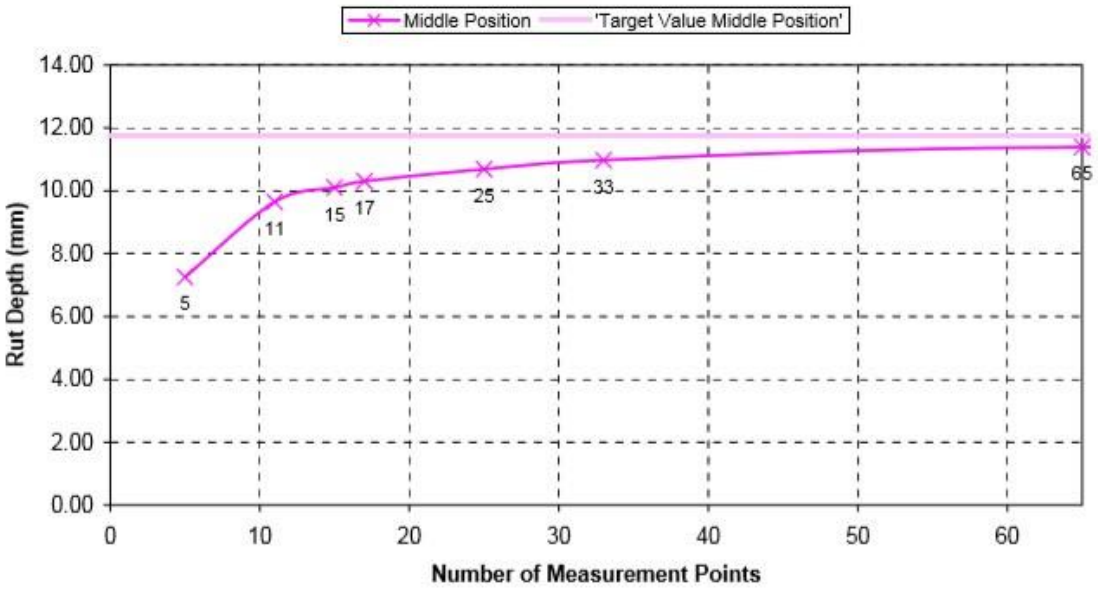


**Figure 2-15: Effect of the number of sensors on measurement accuracy (Sjögren and Lundberg, 2005)**

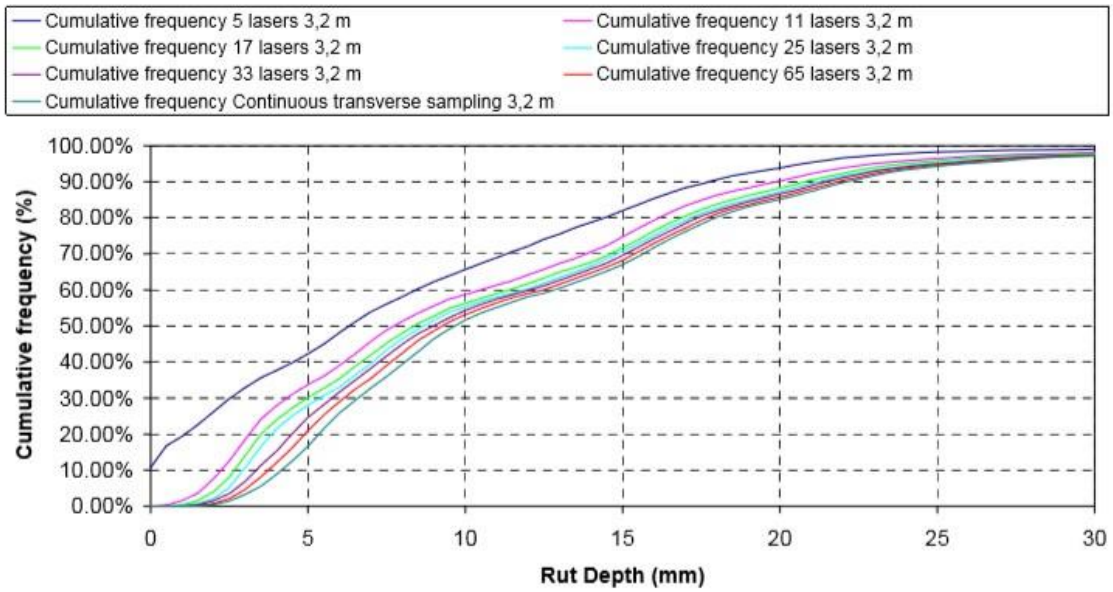


**Figure 2-16: Effect of the number of sensors on measured rut depth (Sjögren and Lundberg, 2005)**

**Table 2-1: Effect of the number of sensors on the measured rut depth (adapted from Sjögren and Lundberg, 2005)**

| Change in number of sensors | Change in rut depth (mm) |
|---|---|
| 17 to 25 | 0.4 |
| 17 to 33 | 0.6 |
| 17 to 65 | 1.1 |

### 2.10.2 Effect of lateral placement

The probability of locating high and low points also depends on the position of the survey vehicle on the road. If the vehicle is not positioned to allow the profilometer to sample the true high and low points, there will be an error (Mallela and Wang, 2006).

To accurately monitor the change in the rut condition of the pavement over time, the operator is required to position the vehicle in exactly the same wheel path between successive surveys, as shown in Figure 2-17(a). However, random variations in vehicle placement along the pavement section will likely occur, as shown in Figure 2-17(b), resulting in variability in the measurements obtained from the successive surveys. The source of variation in the measured rut depth is then attributed to the fact that different points are being profiled each time. It cannot be attributed to the change in pavement condition, thereby making it difficult to accurately trend the rutting data (Mallela and Wang, 2006).

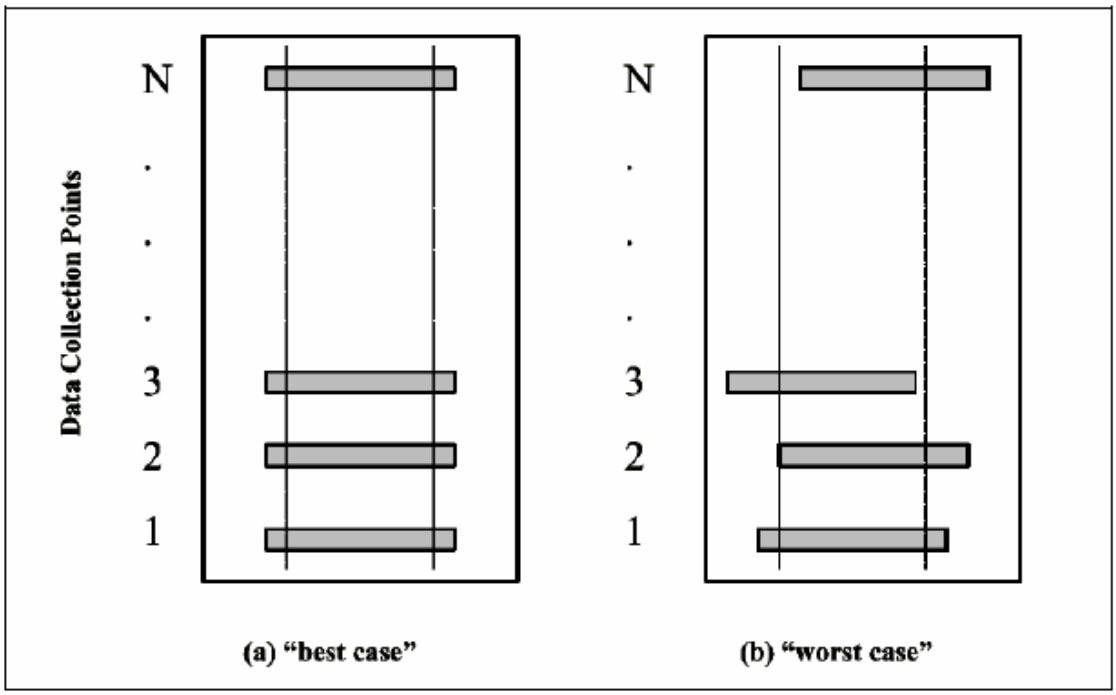


**Figure 2-17: Lateral placement of the survey vehicle (Mallela and Wang, 2006)**

Increasing the number of sensors and reducing the spacing between lasers reduces the impact of lateral variations (Mallela and Wang, 2006).

### 2.10.3 Effect of varying measurement and lane widths

Amongst the factors considered in the investigation undertaken by Sjögren and Lundberg (2005) was the effect of the measurement width of the rut bar on the rut depth. The influence of the measurement width on the rut depth obtained using continuous transverse sampling is shown in Figure 2-18. Increasing the measurement width increases the calculated rut depth. The width, however, should be adapted to the situation and type of road.

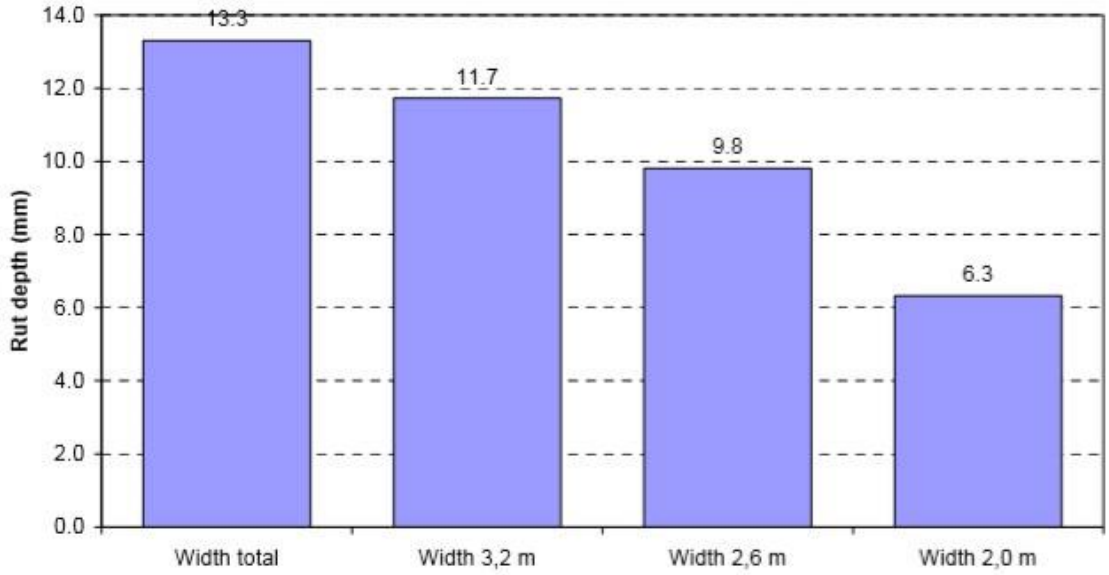


**Figure 2-18: Influence of measurement width (Sjögren and Lundberg, 2005)**

The influence of the lateral position, as influenced by the measurement width, on the rut depth obtained using continuous transverse sampling is shown in Figure 2-19. The influence of the lateral position reduces with increasing measurement width.

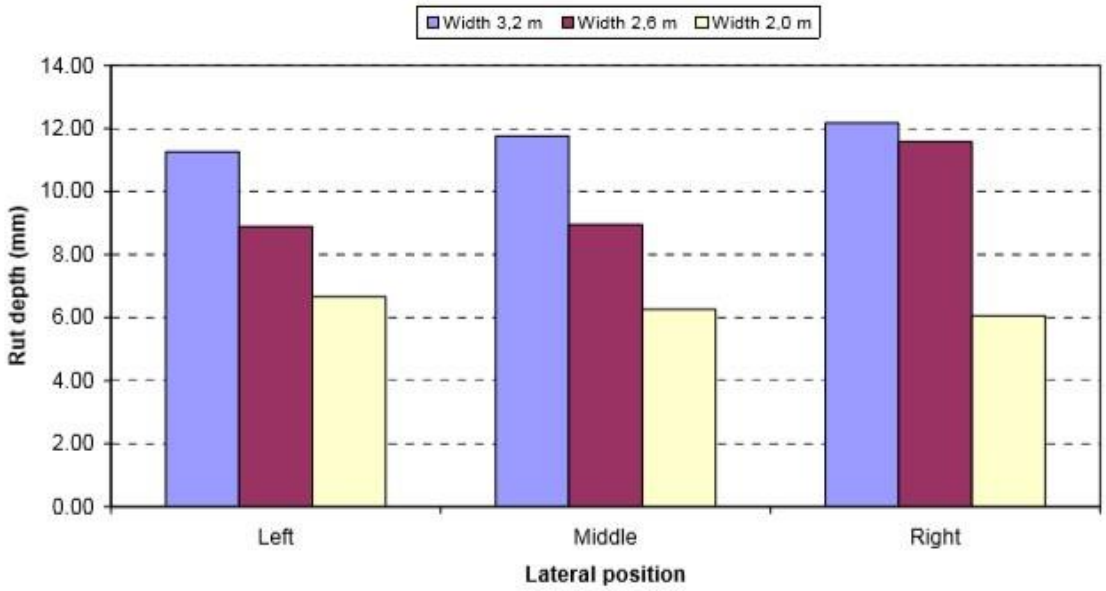


**Figure 2-19: Influence of measurement width on the effect of the lateral position (Sjögren and Lundberg, 2005)**

### 2.10.4 Effect of varying rut shapes

Yichang et al. (2015) assessed the rut depth measurement error of various point-based rut bar systems using 3D line laser technology. The effect of the rut shape on the measurement error was studied. Two main rut shapes were considered in the study, namely, V-shape and U-shape.

Results from the study indicated that for rut bar systems with fewer sensors, the rut shape has a greater effect on the rut depth measurement error. A U-shape rut has less impact on the rut depth measurement error introduced by a point-based rut bar system because the valley is flat and wide, and the possibility of a sensor located on it is high. A V-shape has a greater impact on the measurement error when a point-based rut bar system is used because the valley is narrow, making it harder for the sensor to be precisely located on the top of the valley. As the number of laser sensors increases, the ability of the rut bar system to capture rut shapes more accurately also increases.

Results also indicated that rut bar systems with fewer sensors perform inconsistently among various rut shapes, making it difficult for an optimal configuration to be found. Rut bar systems can capture rut shapes more accurately as the number of laser sensors increase.

### 2.10.5 Effect of surface rutting severity

Yichang et al. (2015) also studied the effect of rutting severity on the measurement error. For rut bar systems with fewer sensors, the measurement error increases with increasing rut depth. This trend does not apply to rut bar systems with more sensors.

### 2.10.6 Effect of pavement surface texture

The typical road profile encompasses a spectrum of sinusoidal wavelengths. If the true pavement profile is a sinusoid with a certain wavelength and the sampling interval selected for the analysis is too large, the samples will define a sinusoid with a much longer wavelength as the measured profile, as shown in Figure 2-20. This effect is called aliasing and is avoided by using a profiler containing an anti-aliasing filter or by using a smaller sampling interval (half the wavelength or smaller) (Sayers and Karamihas, 1998).

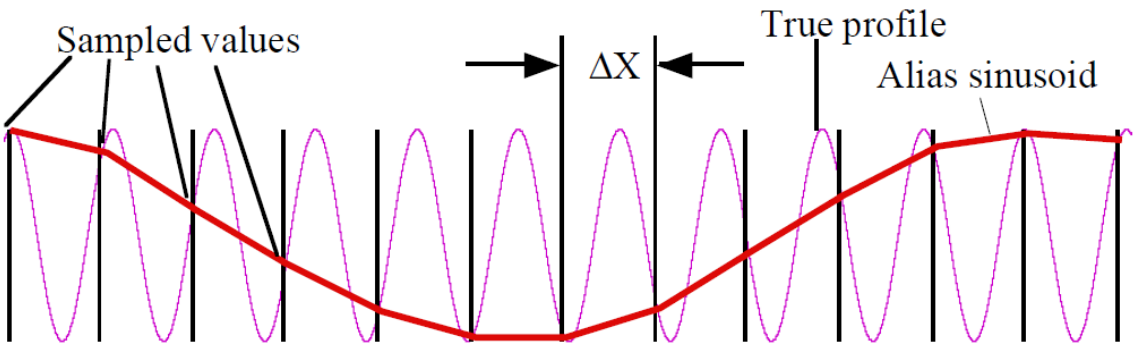


**Figure 2-20: The effect of aliasing (Sayers and Karamihas, 1998)**

## 2.11 TRANSITIONING BETWEEN MANUAL AND AUTOMATED MEASUREMENTS

As the accuracy of rut depth measurements obtained from point laser profilometers is governed by the measurement issues discussed in Section 2.10, discrepancies between manual and point laser automated systems are evident. Most condition indices presently being used as a measure of the pavement condition were developed based on manual condition ratings/measurements. With the replacement of manual measurements with automated measurements, methods of transitioning between manual and automated measurements are required to effectively apply condition indices as well as to account for measurement errors.

Mallela and Wang (2006) developed rut depth transfer functions to convert rut depths from automated systems back to a reference standard. The measurements of four profilometers (1 ultrasonic system and 3-point laser systems) were simulated on a reference transverse profile in Harmonisation of Rut Depth Software. The rut depth under a 2 m straightedge was predicted, considering the configuration of each profilometer and then compared to the rut depth for the reference profile through regression analyses. 348 Transverse profiles measured using a TPB were considered in the analysis. The linear regression transfer functions determined for the different point laser profilometers are presented in Table 2-2.

**Table 2-2: Transfer functions (adapted from Mallela and Wang, 2006)**

| Kerb side | Centre lane side | Profilometer |
|---|---|---|
| RD = 2.44 + 0.98 MEAS | RD = 3.05 + 0.80 MEAS | WDM 16-sensor[1] |
| RD = 2.09 + 0.96 MEAS | RD = 3.56 + 0.64 MEAS | PMS 15-sensor[2] |
| RD = 2.39 + 0.96 MEAS | RD = 3.20 + 0.77 MEAS | ARRB 13-sensor[3] |

Where: RD is 'true' 2 m straightedge rut depth of the reference profile in mm

MEAS is the rut depth measured by the profilometer in mm using the Strategic Highway Research Program (SHRP) 2 m straightedge simulation

Bandini (2010) carried out research to develop a procedure to effectively apply automated rut depth measurements in the New Mexico Department of Transportation's Pavement Serviceability Index (PSI) calculation, which was developed based on distress ratings (including rutting) and automated roughness data. The recommended approach was to convert automated rut depth data into equivalent severity and extent ratings for rutting. Regression analyses were carried out to minimise the difference between the PSI values computed based on rutting ratings from manual surveys and those computed using equivalent rutting ratings estimated from automated rut depth measurements.

## 2.12 BIG DATA

For simplification purposes, high-density automated data is condensed by means of statistical measures, mostly averages, over larger intervals to characterise pavement sections. This is also done to obtain more practical lengths for planning maintenance and rehabilitation projects. As longer pavement sections do not necessarily represent homogeneous performance conditions, with some sections deteriorating faster than others, the aggregation process results in valuable information being lost, resulting in a possibly inaccurate representation of the pavement condition (Jannat et al., 2016; Kadar et al., 2015).

### 2.12.1 Previous studies

Previous studies indicate that aggregating survey data leads to inaccurate condition and maintenance/rehabilitation predictions.

Jannat et al. (2016) investigated the influence of the interval used to aggregate the observed profile data on pavement performance monitoring and maintenance decisions. The rut depth, International Roughness Index (IRI), and overall pavement condition index (PCI) for 50 m, 500 m, 1 000 m, and 10 000 m pavement segment lengths were compared, and a Monte-Carlo

[1] 16-sensor WDM point laser system
[2] 15-sensor PMS point laser system
[3] 13-sensor Australian Road Research Board – Transport Research (ARRB TR) point laser system

simulation was carried out, considering rut depth as a random variable, to estimate the probability of maintenance works being triggered (PCI < 80%) for 50 m and 500 m section lengths. Based on analyses of the distributions, the distribution of rut depth was found to follow either a lognormal or normal distribution. For simplicity, a normal distribution was used to model the pavement conditions.

The comparison of the distribution of rut depth for varying section lengths yielded the following results:

- Shorter section lengths (50 m) present with higher rut depth than longer section lengths;
- Compared to long section lengths, short section lengths indicate a relatively evenly distribution of rut depth;
- The average, 50$^{th}$ percentile, and standard deviation vary significantly among varying section lengths, and
- The 75$^{th}$ percentile appeared to be a more stable statistical parameter.

The Monte-Carlo simulation indicated a higher probability of required maintenance for 50 m section lengths than for 500 m section lengths.

Kannemeyer (2003) presented the effects of aggregation on statistics for different aggregation intervals. The effects are shown in Table 2-3. With an increase in aggregation interval, there is a reduction in the degree of scatter in the data, i.e., the standard deviation decreases, and the minimum and maximum values converge.

**Table 2-3: Effect of aggregation on statistics (adapted from Kannemeyer, 2003)**

| Aggregation Interval (m) | Mean (mm) | Standard deviation | Length of section with mean rut >15 mm for a minimum length of 10 m |
|---|---|---|---|
| 10 | 11.0 | 4.0 | 120 |
| 20 | 11.0 | 3.0 | 100 |
| 50 | 10.9 | 2.8 | 20 |
| 100 | 10.9 | 2.4 | 0 |

Kannemeyer (2003) recommended that the resolution of the measuring device and the minimum pavement length that justifies a certain maintenance activity be considered in selecting the aggregation interval. In considering the measuring device resolution, a minimum interval of 10 m is considered sufficient to ensure that the individual rut depth values remain uncorrelated.

In obtaining practical lengths for planning maintenance and rehabilitation projects, common project management systems typically aggregate short (25 m to 100 m) survey sections to longer (1 km to 5 km) "homogeneous" sections based on similar condition characteristics prior to determining maintenance requirements. As the aggregation of data to longer "homogeneous" sections leads to a considerable loss of information and smoothing of peak condition values, Donev and Hoffmann (2018) recommended using the short survey sections (25 m to 50 m) for condition prediction and then combining sections into longer maintenance work-zones based on economic criteria. In this approach, work zones (timing, length, and location) yielding optimal maintenance rehabilitation costs, temporary traffic control costs, and work-zone related user and environmental costs are selected. Considering different aggregation lengths (200 m, 600 m, and 1 000 m), the results of this approach were compared to that of the "homogeneous" sections approach. The recommended approach performed better in all instances, providing more accurate predictions in terms of service life and life-cycle costing (Donev et al., 2020).

Kadar et al. (2015) recommended treating each data set as a stochastic information packet (SIP), thereby utilising the full data set and avoiding data inaccuracies. With SIPs, the input and output are distributions of the data, thereby considering the full dataset and not just a statistical characterisation of it. Modelling with SIPs allows for budget and condition forecasts to include the level of associated risks alongside the future condition and budget requirements.

### 2.12.2 Current practices in South Africa

In South Africa, visual assessments used to assess the surfacing, structural, and functional condition of pavements are carried out in accordance with the COTO (2016b) TMH 9 visual assessment procedures. The scope of the assessment does not include the identification of uniform sections of condition and standard segment lengths of 2 km (± 1 km) are recommended for evaluating flexible pavements. While standard segment lengths are 2 km in length, segments provided often vary in length and can be as long as 10 km.

As per the COTO (2013) TMH 22, the average of the automated rut data should be recorded and stored at 10 m intervals and reported on at 100 m intervals.

As per the COLTO (1997) TRH 12 guidelines on the design of flexible pavement rehabilitation projects, rehabilitation requirements should be identified for uniform pavement sections. Uniform sections are determined based on similar functional properties, such as riding quality and rut depth, and similar types of materials, material conditions, and pavement structure. At project level, detailed measurements are typically considered in determining these uniform sections (COTO, 2013 and SANRAL, 2014).

However, at network level, detailed measurements are typically aggregated to some extent prior to determining uniform sections. In most PMSs, high-density automated data such as rut measurements recorded at 10 m intervals is aggregated by means of averages or percentiles to obtain an aggregated value per visually assessed segment discussed above without considering the variability of rut depth along these sections. Following this process, these visually assessed segments are further aggregated based on similar condition, pavement structure, and environmental characteristics to obtain more practical maintenance and rehabilitation project lengths, prior to determining maintenance/rehabilitation requirements. In doing so these longer sections are considered to be homogenous. However, as some shorter sections (10 m to 100 m) present with higher rutting than others, these aggregated sections do not represent homogeneous conditions.

## 2.13 SPECIFICATIONS FOR MEASURING RUT DEPTH

Some other specifications currently available for measuring and processing rut depth are presented in Table 2-4. Data processing in all the specifications discussed consists of averaging rut depth values, measured at smaller intervals along the pavement surface, over a larger interval.

**Table 2-4: Specifications for measuring rut depth**

| Specification | NRA (1999) | AASHTO (2013) AASHTO R48-10 | Austroads (2016) AG:AM/T009 |
|---|---|---|---|
| **Measurement technique** | Manual/Automated | Automated | Automated |
| **Equipment** | No specific equipment is specified. Based on manual methods of measuring rut depth using a 2 m straightedge. | • Multi-sensor device (minimum of 5 sensors).<br>• Line-laser device. | • Multi-laser device (minimum of 11 lasers).<br>• Line-laser device. |
| **Rut depth algorithm** | The 2 m straightedge is the standard reference for rut measurements in South Africa. | Basic 5-point rut depth calculation or stringline method. | 2 m straightedge or stringline method. |
| **Data processing** | • Manual: 10 m testing interval specified.<br>• Automated (not specified): Average rut depth over the specified 10 m testing interval currently being done in practice to comply with specifications.<br>• The cumulative distribution of averaged rut depths over 1 km segment lengths is recorded. | • Transverse profiles are measured at a maximum interval of 10 m.<br>• The average rut depth in each wheel path within a longitudinal summary interval (generally 100 m) is recorded.<br>• The maximum rut depth in each wheel path within a longitudinal summary interval (generally 100 m) is recorded. | • The average rut depth in each wheel path over a given length of road (typically 20 m or 100 m) is recorded.<br>• The percentage of ruts falling into a specified series of rut bins for the given length of road is recorded. |

Intervals for measurement provided in the NRA (1999) are based on manual methods for measuring rut depth. However, since automated measuring techniques are used in practice, the average rut depth is obtained over 10 m intervals to comply with these specifications.

## 2.14 CONDITION PREDICTION

Condition data are used in performance models to predict pavement performance and maintenance and rehabilitation needs. Performance models can be categorised into deterministic, probabilistic, and soft computing methods such as neural networks and artificial intelligence (Morcous, 2005). Deterministic models can be described as either empirical, based on statistical analyses of observed deterioration trends, or mechanistic, based on theoretical and experimental analyses of pavement behaviour (Steyn, 2012).

### 2.14.1 HDM-4 models

The Highway Development and Management Model (HDM-4) combines both the theoretical and experimental bases of mechanistic models with the behaviour observed in empirical models to predict the annual pavement condition and evaluate maintenance and rehabilitation strategies (Odoki and Kerali, 2006).

Deterioration models have been developed for bituminous, concrete, and unsealed road surface classes, with each road surface class defining a family of distress modes (Odoki and Kerali, 2006).

The deterioration of bituminous pavements is modelled in terms of eight modes of distress, namely, cracking, ravelling, potholing, edge breaks, rutting, roughness, surface texture, and skid resistance. The interaction between the abovementioned distress modes is reflected in the performance models. Factors affecting pavement deterioration, namely, the climate and environment, traffic, pavement history, road geometry, pavement structural characteristics, and material properties, are also incorporated into the models (Odoki and Kerali, 2006).

As each distress mode develops and progresses at different rates in different environments, user-definable deterioration factors have been incorporated into the models to allow for the adjustment of deterioration rates to match those of local conditions, thus allowing the models to be applied universally (Odoki and Kerali, 2006).

## 2.15 MAINTENANCE AND REHABILITATION

Maintenance and rehabilitation affect the current pavement condition as well as the future rate of deterioration. When small pavement defects are present, maintenance can be applied to correct these defects and slow the rate of deterioration. If maintenance is not applied effectively and deterioration progresses, maintenance can no longer be applied to correct more severe

defects, and rehabilitation is required. With increasing pavement deterioration, the cost of maintenance and rehabilitation activities also increases. Therefore, undertaking maintenance and rehabilitation activities as soon as treatment is required increases their effectiveness, reduces treatment costs, and extends the overall pavement life (Steyn, 2012).

Table 2-5 discusses the condition-based maintenance treatments for flexible pavements.

**Table 2-5: Description of condition-based maintenance treatments for flexible pavements (adapted from Committee of State Road Authorities, 1992 and SANRAL, 2014)**

| Treatment Type | Description |
|---|---|
| Reseal | Application of a new surfacing layer |
| Light rehabilitation | Addition of a new surfacing layer with more extensive preparation work than required for a reseal and/or reworking of the base layer |
| Heavy rehabilitation | Addition of a new surfacing and base layer and/or reworking of deeper layers |

## 2.16 SUMMARY

From previous studies, it can be seen that aggregating survey data leads to inaccurate condition and maintenance/rehabilitation predictions.

In most network level PMS applications in South Africa, high-density automated data such as rut measurements recorded at 10 m intervals is aggregated to longer sections by means of averages or percentiles without considering the variability of the rut depth along those sections. This aggregated data is used as an input in PMSs, thereby resulting in possibly inaccurate condition predictions, maintenance requirements, and budgetary forecasts. The extent to which this information is inaccurately forecast is influenced by the aggregation measure used as well as the section length selected for aggregation.

# 3 RESEARCH METHODOLOGY

## 3.1 INTRODUCTION

A statistical and technical needs analysis was undertaken to study the influence of varying aggregated section lengths[4], considering the mean and percentiles as statistical aggregation measures, on the distribution of calculated rut depth over a pavement section, and the respective maintenance and funding requirements. The distribution of the calculated rut depth and the resulting maintenance and funding requirements estimated based on these statistical aggregation measures were compared to that of the discrete rut depth measurements to determine which aggregation measure provides a more accurate representation of the pavement condition and treatment needs.

The application of these statistical aggregation measures within a selected specification was then additionally studied to analyse the use of such methods in providing an accurate representation of whether or not pavement performance requirements are being met when compared to discrete rut depth measurements. A summary of the methodology is provided in Figure 3-1.

[4] Aggregated sections are not based on uniform conditions of rut. Rut depth measurements taken at short intervals are aggregated over longer intervals without considering the variability of rut depth along these sections. In this way, the consequences of not considering the variability in the aggregation process is studied.

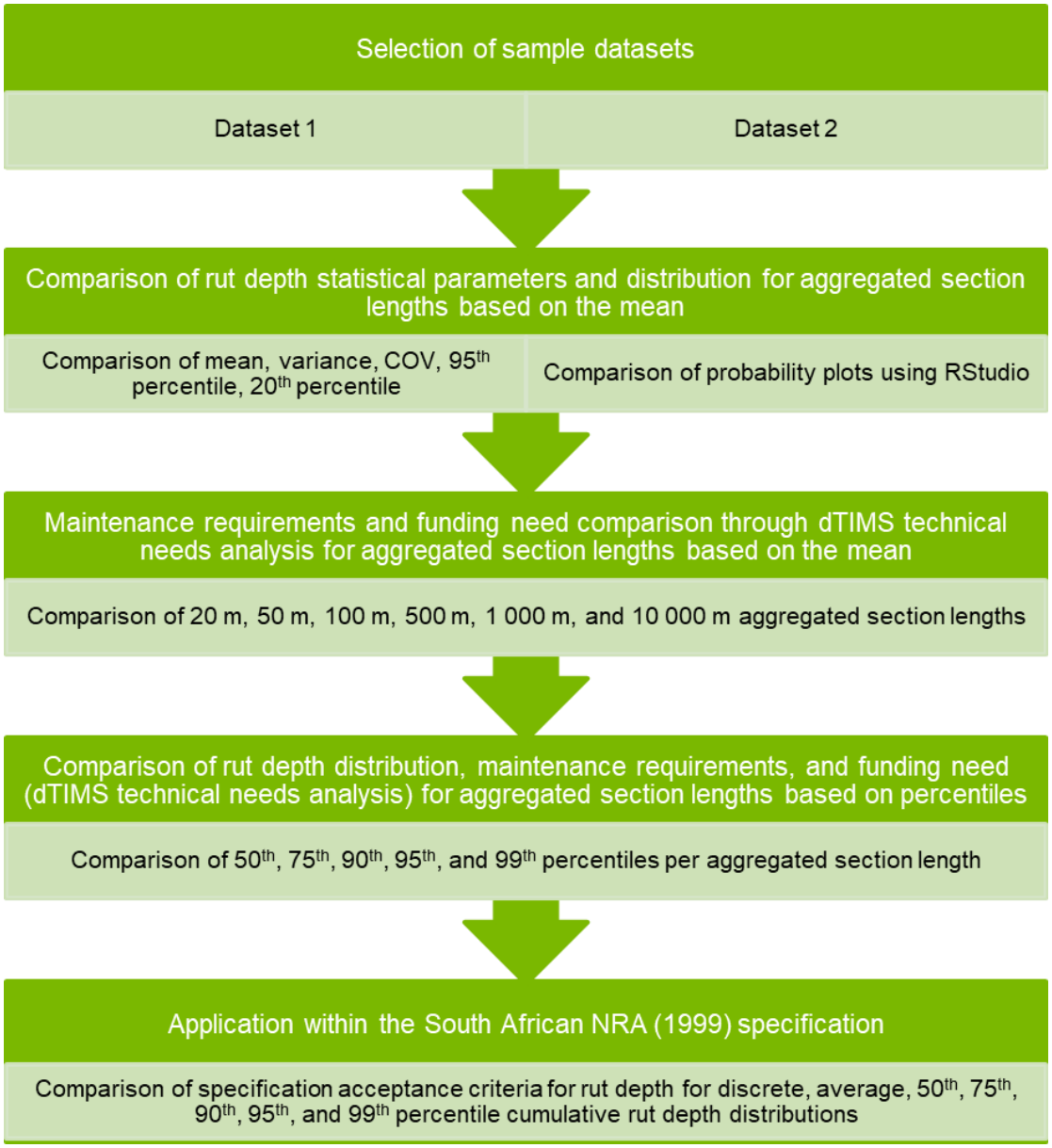


**Figure 3-1: Research methodology**

## 3.2 SAMPLE DATASETS

Two sets of road performance data were obtained for the analysis. Profile measurements were carried out by Specialised Road Technologies (SRT) with the Dynatest 5051 Mark III Road Surface Profiler (RSP), equipped with 17 lasers.

### 3.2.1 Dataset 1

Dataset 1 consists of 522.37 km of paved road segments located in the Limpopo Province of South Africa. 5 Profilometer samples of rut depth measurements taken at 10 m intervals were obtained from high-speed profile measurements carried out in 2016.

#### 3.2.1.1 Inventory

1) Road Class and Traffic

Table 3-1 provides the road class and Average Annual Daily Traffic (AADT) per sample road segment.

**Table 3-1: Road class and traffic per sample road segment**

| Profilometer Sample | Road Name(s) | Length (km) | RISFSA Class[5] | AADT | Heavy Vehicles |
|---|---|---|---|---|---|
| 1 | N1 | 200.01 | 1 | >9 000 to 20 000 | >1 700 to 3 000 (>14%) |
| 2 | N1 | 66.67 | 1 | >6 000 to 14 000 | >900 to 2 500 (>15%) |
| 3 | N1 | 43.41 | 1 | >3 000 to 4 500 | >800 to 1 000 (>24%) |
| 4 | R521 | 153.39 | 3 | >1 700 to 3 000 | >300 to 600 (>19%) |
| 5 | R521 | 58.89 | 3 | >1 700 to 3 000 | >300 to 600 (>19%) |

2) Climate and environment

**Moisture**

The average annual precipitation in the regions of Limpopo surrounding the sample road segments ranges from 300 mm to 600 mm (World Bank Group, 2017). According to Odoki and Kerali (2006), areas experiencing low rainfall with an annual precipitation ranging from 300 mm to 800 mm, are classified as *Semi-Arid*.

**Temperature**

The regions of Limpopo surrounding the sample road segments experience average monthly temperatures ranging from approximately 12˚C to 28˚C throughout the year (World Bank Group, 2017). According to Odoki and Kerali (2006), areas experiencing high day and cool night temperatures ranging from -5˚C to 45˚C are classified as *Sub-Tropical to Hot*.

### 3.2.2 Dataset 2

Dataset 2 consists of 1 076.1 km of paved roads located in the Northern Cape Province of South Africa. High-speed profile measurements, visual assessments, and traffic counts were carried out in 2015, and non-destructive Falling Weight Deflectometer (FWD) measurements were carried out in 2013. High-speed profile measurements include roughness and rut depth measurements measured at 10 m intervals. Visual assessments were carried out in accordance

[5] Road Infrastructure Strategic Framework for South Africa (RISFSA) Classification: 1 = Primary distributor; 3 = District distributor

with the Committee of State Road Authorities (1992) TMH 9 visual assessment procedures and included surfacing, structural, and functional assessments.

Of the roads that were assessed, roads having an assessment length that was considered sufficient to allow for the comparison of different section lengths were selected for the analysis. As a result, 13 roads were selected for the analysis. A map depicting the selected road sections is presented in Figure 3-2.

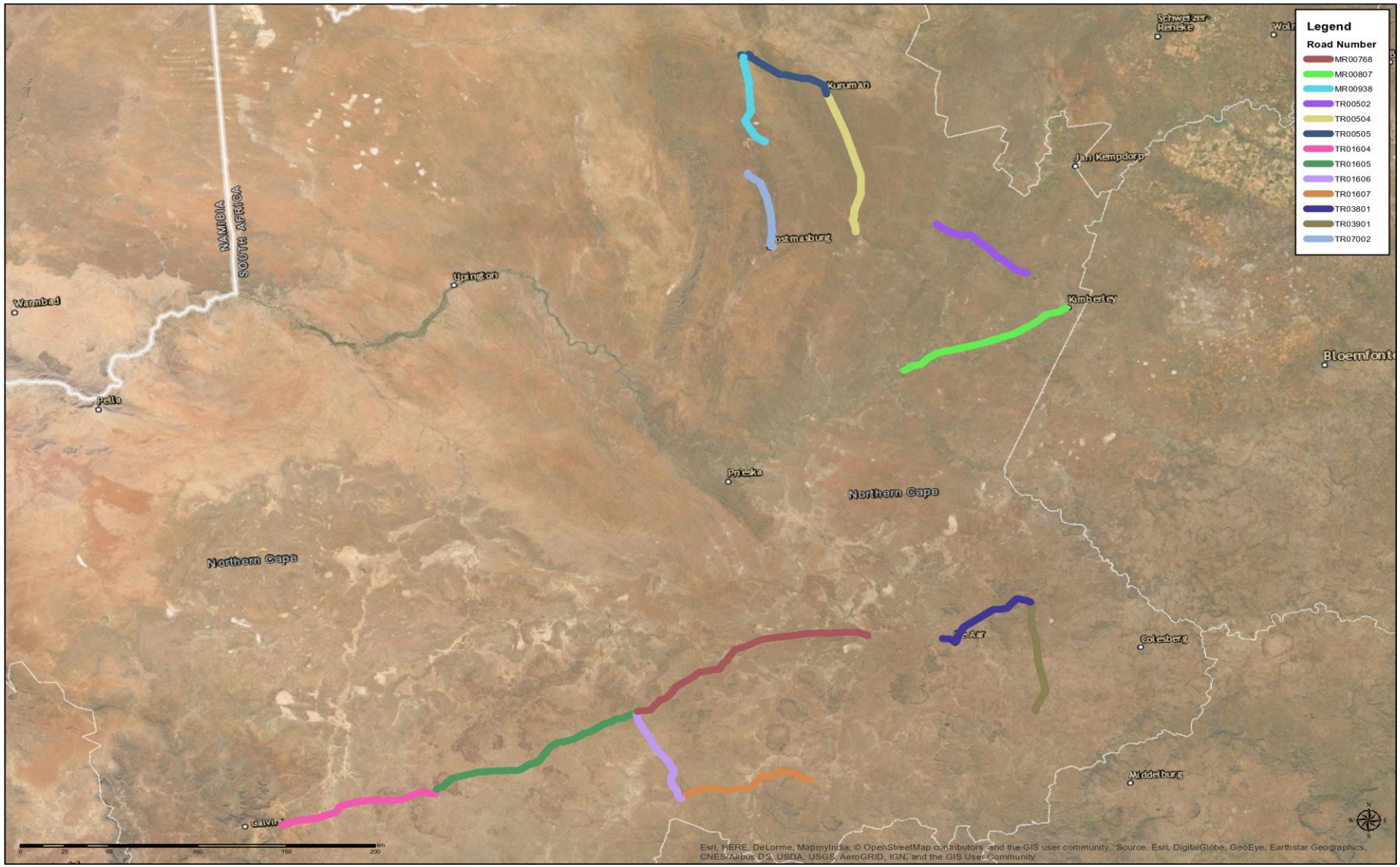


**Figure 3-2: Map of selected road sections for dataset 2**

#### 3.2.2.1 Inventory

Table 3-2 provides a summary of the inventory obtained for Dataset 2.

**Table 3-2: Dataset 2 inventory**

| Road Name | Length (km) | RCAM Class[6] | Surface Type[7] | Surface Age | Base Type[8] | Base Age | Average SNP[9] | Average AADT | % Heavy Vehicles | Terrain | Moisture | Temperature |
|---|---|---|---|---|---|---|---|---|---|---|---|---|
| MR00768 | 146.18 | R2 | ST | 16 to 38 | GB | 33 to 38 | 3.78 | 149 | 21.06 | Rolling | Arid | Sub-Tropical to Hot |
| MR00807 | 101.48 | R2 | ST | 1 to 32 | GB | 42 to 50 | 3.54 | 2 328 | 9.28 | Rolling | Arid | Sub-Tropical to Hot |
| MR00938 | 60.22 | R3 | ST | 11 to 41 | GB | 11 to 41 | 4.32 | 2 957 | 15.00 | Rolling | Arid | Sub-Tropical to Hot |
| TR00502 | 61.28 | R2 | ST | 1 to 20 | GB | 80 | 4.20 | 3 803 | 18.81 | Rolling | Arid | Sub-Tropical to Hot |
| TR00504 | 92.5 | R2 | ST | 28 to 80 | GB | 40 to 80 | 4.85 | 1 660 | 21.03 | Rolling | Arid | Sub-Tropical to Hot |
| TR00505 | 60.29 | R2 | ST | 21 to 80 | GB | 1 to 80 | 6.21 | 2 476 | 29.02 | Rolling | Arid | Sub-Tropical to Hot |
| TR01604 | 94.37 | R2 | ST | 24 to 80 | GB | 39 to 80 | 3.50 | 271 | 21.67 | Rolling | Arid | Sub-Tropical to Hot |
| TR01605 | 127.89 | R2 | ST | 22 to 53 | GB | 44 to 53 | 3.59 | 179 | 26.24 | Rolling | Arid | Sub-Tropical to Hot |
| TR01606 | 62.89 | R2 | ST | 31 to 51 | GB | 50 to 51 | 3.40 | 109 | 16.05 | Rolling | Arid | Sub-Tropical to Hot |
| TR01607 | 81.04 | R2 | ST | 13 to 80 | GB | 49 to 80 | 3.26 | 141 | 15.12 | Rolling | Arid | Sub-Tropical to Hot |
| TR03801 | 62.5 | R3 | ST | 19 to 80 | GB | 51 to 80 | 3.16 | 599 | 12.47 | Rolling | Arid | Sub-Tropical to Hot |
| TR03901 | 72.25 | R2 | ST | 11 to 41 | GB | 41 to 47 | 3.21 | 185 | 35.34 | Rolling | Arid | Sub-Tropical to Hot |
| TR07002 | 52.85 | R2 | ST | 23 to 34 | GB | 44 | 5.74 | 2 894 | 17.82 | Rolling | Arid | Sub-Tropical to Hot |

[6] South African Road Classification and Access Management (RCAM) Classification: R2 = Rural major arterial/distributor carrying inter-regional traffic; R3 = Rural minor arterial/distributor carrying inter-district traffic
[7] Surface Type: ST = Surface Treatment
[8] Base Type: GB = Granular Base
[9] SNP = Adjusted Structural Number

## 3.3 DATASET DISTRIBUTIONS

### 3.3.1 Selecting a method of identifying distributions

Three methods were considered for identifying the type of distribution describing the rut depth values, namely, goodness of fit tests, quantile-quantile plots, and probability plots. In selecting a method, the nature of the data being studied as well as the factors affecting the statistical method were considered. The following is of note for each method:

1) Goodness of fit tests

For large samples, small deviations from the distribution have a large impact on the p-value (Lin et al., 2013).

2) Quantile-Quantile and probability plots

As the maintenance history of road segments is not always available or accurately recorded, accurate information on the nature of the treatment carried out, the date of application, and the length of the maintenance segment is not always available. Thus, a long road segment possessing the same pavement structure, environment, terrain, and traffic characteristics, can possess shorter segments with different maintenance histories and, thereby, different condition and rut depth distributions.

Dummy data was generated in RStudio to study the sensitivity of the quantile-quantile and probability plots to a change in sample size and distribution type.

Pavements exhibit three distributions of rut depth throughout their lifetime. With a limited amount of rutting, pavements initially present with a negative exponential distribution. As they age and begin to rut, there is a transition to a lognormal distribution and then to a normal distribution later in life (Kannemeyer, 2003). Exponential, lognormal, and normal distributions were therefore considered in the sensitivity analysis. 15 Samples were generated and analysed as follows:

a) 4 Samples containing 10, 50, 100, and 1 000 observations, respectively, were generated from a standard exponential distribution with a rate, $\lambda$, of 1. Exponential probability and quantile-quantile plots were plotted;

b) 4 Samples containing 10, 50, 100, and 1 000 observations, respectively, were generated from a standard lognormal distribution with a mean, $\mu$, of 0 and a standard deviation, $\sigma$, of 1. Lognormal probability and quantile-quantile plots were plotted;

c) 4 Samples containing 10, 50, 100, and 1 000 observations, respectively, were generated from a standard normal distribution with a mean, μ, of 0 and a standard deviation, σ, of 1. Normal probability and quantile-quantile plots were plotted;

d) 1 Sample of 1 000 observations was generated from a standard exponential and lognormal distribution, and 500 observations were generated from each distribution type. Exponential and lognormal probability plots were plotted;

e) 1 Sample of 1 000 observations was generated from a standard exponential and normal distribution, and 500 observations were generated from each distribution type. Normal probability and quantile-quantile plots were plotted. Exponential plots could not be plotted as all observations must be positive to be fitted with an exponential distribution, and

f) 1 Sample of 1 000 observations was generated from a standard lognormal and normal distribution, and 500 observations were generated from each distribution type. Normal probability and quantile-quantile plots were plotted. Lognormal plots could not be plotted as all observations must be positive to be fitted with a lognormal distribution.

The results of this sensitivity analysis are provided in Appendix A. The results indicate that the probability plot is less sensitive to both the sample size and distribution type than the quantile-quantile plot. Where a combination of distributions exists, a distribution type is more discernible on a probability plot than on a quantile-quantile plot.

The limited maintenance history available on the road segments hinders the ability to accurately identify a distribution type. As the focus of this study is not the accuracy of identifying the initial distribution type of the rut depth but rather the impact of the aggregated section lengths on the distribution, the probability plot was chosen as the method for identifying the distribution type.

### 3.3.2 Dataset 1

Probability plots were plotted for left and right rut depth measurements for all 5 samples. In all samples, left rut depth measurements presented with a poor correlation ($R^2 < 0.9$) to all distributions considered. In sample 3, both left and right rut depth measurements presented with a poor correlation to all distributions considered. To identify the possible causes of the poor correlation obtained, additional variables, such as historic maintenance activities, affecting pavement deterioration and, therefore, the distribution of rut depth, were considered, in addition to pavement type and traffic volume. To consider the impact of maintenance activities on the distribution, sample 1 with the longest segment length was split into smaller segment lengths. As the history of maintenance activities and maintenance segment lengths is not known, sample lengths of 50 km and 1 km were considered. For 50 km segments, left rut depth measurements

still presented with a poor correlation to all distributions. Improved correlation is observed in a segment length of 1 km. A summary of the results is presented in Table 3-3. Probability plots for all samples and segment lengths considered are provided in Appendix B.

**Table 3-3: Dataset 1 distribution summary**

| Sample | Left rut depth | | | Right rut depth | | |
|---|---|---|---|---|---|---|
| | Total Sample Length | 50 km Segment Length | 1 km Segment Length | Total Sample Length | 50 km Segment Length | 1 km Segment Length |
| 1 | Poor correlation | Poor correlation | Exponential, $R^2 > 0.9$ | Normal, $R^2 > 0.9$ | Normal, $R^2 > 0.9$ | Normal, $R^2 > 0.9$ |
| 2 | Poor correlation | - | - | Normal, $R^2 > 0.9$ | - | - |
| 3 | Poor correlation | - | - | Poor correlation | - | - |
| 4 | Poor correlation | - | - | Exponential, $R^2 > 0.9$ | - | - |
| 5 | Poor correlation | - | - | Exponential, $R^2 > 0.9$ | - | - |

### 3.3.3 Dataset 2

Probability plots were plotted for left and right rut depth measurements for each of the 13 roads selected for the analysis. Probability plots are provided in Appendix C. A summary of the results is presented in Table 3-4. For left rut depth measurements, 1 sample presents with an exponential distribution, ten samples present with a lognormal distribution, and the remaining two samples present with a normal distribution. For right rut depth measurements, all samples present with a lognormal distribution. Therefore, the left rut depth measurements were selected for the analysis as these measurements present with higher variability across the samples.

**Table 3-4: Dataset 2 distribution summary**

| Sample | Left rut depth | | | | | | Right rut depth | | | | | |
|---|---|---|---|---|---|---|---|---|---|---|---|---|
| | Distribution | Sound[10] (%) | Isolated[10] (%) | Moderate[10] (%) | Warning[10] (%) | Severe[10] (%) | Distribution | Sound[10] (%) | Isolated[10] (%) | Moderate[10] (%) | Warning[10] (%) | Severe[10] (%) |
| 1 | Lognormal | 57.85 | 39.70 | 2.39 | 0.07 | 0.00 | Lognormal | 81.05 | 18.13 | 0.79 | 0.03 | 0.00 |
| 2 | Lognormal | 53.08 | 39.52 | 6.51 | 0.80 | 0.09 | Lognormal | 86.72 | 12.47 | 0.73 | 0.09 | 0.00 |
| 3 | Lognormal | 43.84 | 46.05 | 9.08 | 0.98 | 0.05 | Lognormal | 65.16 | 31.38 | 3.40 | 0.05 | 0.00 |
| 4 | Exponential | 52.74 | 35.82 | 9.55 | 1.73 | 0.16 | Lognormal | 64.08 | 27.32 | 6.95 | 1.47 | 0.18 |
| 5 | Normal | 48.29 | 45.81 | 5.63 | 0.23 | 0.04 | Lognormal | 64.50 | 31.45 | 3.45 | 0.55 | 0.05 |
| 6 | Lognormal | 73.45 | 26.05 | 0.48 | 0.02 | 0.00 | Lognormal | 70.48 | 26.12 | 2.79 | 0.56 | 0.05 |
| 7 | Lognormal | 61.96 | 34.80 | 2.97 | 0.28 | 0.00 | Lognormal | 88.31 | 11.19 | 0.50 | 0.00 | 0.00 |
| 8 | Lognormal | 75.58 | 23.08 | 1.13 | 0.16 | 0.04 | Lognormal | 93.19 | 6.18 | 0.46 | 0.11 | 0.05 |
| 9 | Lognormal | 69.12 | 28.45 | 2.15 | 0.25 | 0.03 | Lognormal | 90.90 | 8.55 | 0.52 | 0.02 | 0.00 |
| 10 | Lognormal | 60.59 | 33.61 | 4.34 | 1.01 | 0.44 | Lognormal | 70.58 | 27.48 | 1.78 | 0.11 | 0.05 |
| 11 | Lognormal | 50.85 | 39.99 | 6.75 | 1.73 | 0.69 | Lognormal | 66.41 | 25.18 | 6.46 | 1.63 | 0.32 |
| 12 | Lognormal | 55.38 | 39.11 | 4.94 | 0.53 | 0.04 | Lognormal | 77.13 | 19.50 | 3.07 | 0.22 | 0.07 |
| 13 | Normal | 31.47 | 52.94 | 14.23 | 1.32 | 0.04 | Lognormal | 81.99 | 16.95 | 0.98 | 0.06 | 0.02 |
| Average | - | 56.48 | 37.30 | 5.40 | 0.70 | 0.13 | - | 76.96 | 20.15 | 2.45 | 0.38 | 0.06 |

As dataset 2 contains longer sample lengths presenting with a higher correlation to the distributions considered than dataset 1, dataset 2 was used in the analysis.

[10] Rut depth condition categories adapted from COTO (2016), as discussed in Table 3-5 of Section 3.4.2.

## 3.4 INFLUENCE OF SECTION LENGTH ON RUT DEPTH DISTRIBUTION USING AVERAGES

### 3.4.1 Aggregated section lengths

For each of the 13 samples (road segments) considered, the average of the discrete 10 m rut depth measurements were taken per 20 m, 50 m, 100 m, 500 m, 1 000 m, and 10 000 m section lengths. The average is calculated by taking the average of 2 points for 20 m sections, 5 points for 50 m sections, and so forth.

### 3.4.2 Statistical parameters and distributions

For each aggregated section length considered, exponential, lognormal, and normal probability plots were plotted per sample and compared to study the influence of the change in averaged section length on the type of distribution of calculated rut depth values.

Cumulative distributions of rut depth were also plotted per aggregated section length, and the maximum, mean, variance, Coefficient of Variation (COV), $20^{th}$ percentile, and $95^{th}$ percentile distribution parameters were compared to study the influence of the change in averaged section length on the dispersion of calculated rut depth values.

The change in the distribution of calculated rut depth amongst the condition categories listed in Table 3-5 was also compared per aggregated section length considered.

**Table 3-5: Rut depth condition categories adapted from COTO (2016b)**

| Condition category | Rut depth, RD (mm) |
|---|---|
| Sound | $RD < 5$ |
| Isolated | $5 \leq RD < 10$ |
| Moderate | $10 \leq RD \leq 15$ |
| Warning | $15 < RD \leq 20$ |
| Severe | $RD > 20$ |

## 3.5 INFLUENCE OF SECTION LENGTH ON MAINTENANCE REQUIREMENTS AND FUNDING NEED USING AVERAGES

A technical (engineering) needs analysis was carried out in dTIMS over a 20-year analysis period to study the influence of varying aggregated section lengths, considering the mean as the statistical aggregation measure, on the immediate annual maintenance requirements and the resulting funding need. The analysis entailed the prediction of the future performance of the road segments under investigation using the current condition and pavement performance

prediction models. The immediate needs were determined based on the current and past condition status of the road segment per year.

### 3.5.1 dTIMS

dTIMS is an asset management software application with the capabilities of (Deighton, 2019):

- Creating and maintaining an inventory integrating all types of assets in one place;
- Performing a technical needs analysis, through which one can determine the immediate maintenance, preservation, and rehabilitation actions on each asset, and
- Performing a life-cycle cost analysis, through which one can analyse and report on the current and future asset condition, as well as determine the best maintenance, preservation, and rehabilitation actions on each asset for various alternative budget scenarios.

### 3.5.2 Technical needs analysis components

The input and output components of the technical needs analysis performed for the pavement assets investigated in this study are summarised in Figure 3-3.

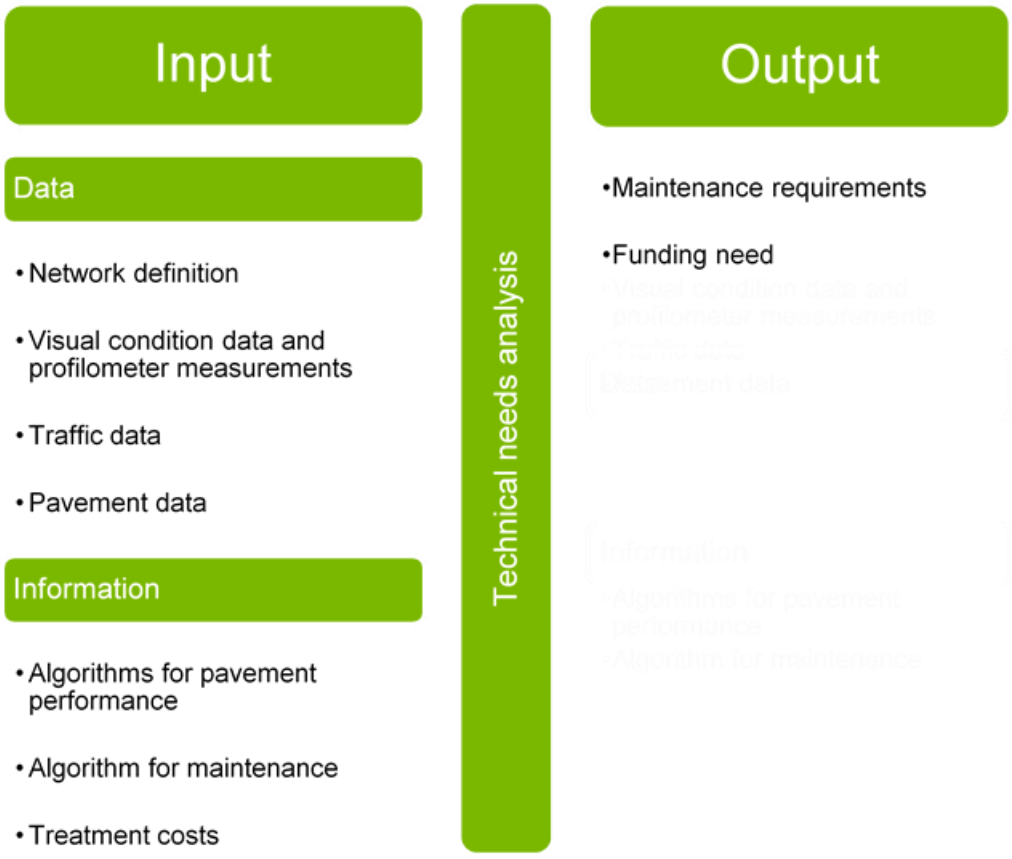


**Figure 3-3: Components of technical needs analysis**

**Data**

Committee of State Road Authorities (1992) TMH 9 visual assessments, high-speed profile measurements, FWD measurements, traffic counts, pavement ages, and environmental conditions such as moisture, temperature, and terrain, detailed in Section 3.2.2, served as the starting point for the prediction of future performance of the road segments included in the analysis.

To study the influence of aggregated section lengths on the maintenance and funding requirements, considering solely the change in rut depth as a variable, an average constant (determined from the data acquired per sample road segment) was used for all other maintenance drivers. The only variables included rut depth and the maintenance drivers influenced by a change in rut depth, namely, roughness and the overall condition index.

**Algorithms for pavement performance**

Locally calibrated versions of the Odoki and Kerali (2006) HDM-4 pavement performance models have been modelled in dTIMS and used in the analysis. Pavement performance is modelled in terms of cracking, rutting, ravelling, potholes, and roughness.

The Odoki and Kerali (2006) HDM-4 pavement performance models include a calibration factor aimed at adjusting the model predictions to local conditions. The calibration factors used in the analysis were derived from the latest (2013) calibration study completed in South Africa at the time of the analysis. This study remains unpublished and, at the request of the commissioning provincial department of transport, cannot be wholly published in this report. The owner of the data obtained from this study is, therefore, unspecified in this report.

Aurecon Africa (rebranded as Zutari) was commissioned to conduct a Bennett and Peterson (2000) HDM-4 level 2 calibration to study the rate of local pavement deterioration.

A total of 37 pavement sections, which best represent the composition of the paved road network in the respective province, were selected. These sections cover a variety of traffic, pavement and surface types, climate regions, and pavement conditions. The selected pavement sections were monitored annually by means of visual surveys and physical measurements since 1996. The collected deterioration data was then used to compare predicted and observed pavement behaviour in order to determine the calibration factors providing the best adjustment of the predicted behaviour towards the observed behaviour. The calibration factors derived from the study are provided in Table 3-6.

**Table 3-6: Calibration factors for HDM-4 performance prediction models**

| Distress parameter | Calibration factor |
|---|---|
| All crack initiation | 1.2 |
| Wide crack initiation | 1.0 |

| Distress parameter | Calibration factor |
|---|---|
| All crack progression | 0.12 |
| Wide crack progression | 0.12 |
| Ravelling initiation | 1.0 |
| Ravelling progression | 0.12 |
| Pothole initiation | 1.0 |
| Pothole progression | 1.0 |
| Rutting initiation | 1.0 |
| Rutting progression | 3.1 |
| Roughness progression (structural component) | 1.0 |
| Roughness progression (environmental coefficient) | 2.8 |

As the TMH 9 and the HDM-4 do not express distresses in the same units of measurement, the TMH 9 distress ratings require a conversion to the HDM-4 distress ratings before the HDM-4 pavement performance models can be utilised to predict future performance. Aurecon Africa (rebranded as Zutari) was additionally commissioned to determine the conversion factors by studying the relationship between the TMH 9 and HDM-4 distress ratings for the above-mentioned 37 pavement sections. This study also remains unpublished and, at the request of the commissioning provincial department of transport, cannot be wholly published in this report. The owner of the data obtained from this study is, therefore, unspecified in this report. The conversions used in the analysis are provided in Table 3-7, Table 3-8, and Table 3-9.

The conversion of the TMH 9 degree and extent for surface cracks to a percentage cracked area, as defined in the HDM-4, is presented in Table 3-7.

**Table 3-7: TMH 9 to HDM-4 conversion of surface cracks**

| TMH 9 Degree | % Area with surface cracks | | | | |
|---|---|---|---|---|---|
| | TMH 9 Extent | | | | |
| | 1 | 2 | 3 | 4 | 5 |
| 1 to 5 | 1 | 1 | 7.1 | 8.2 | 13.6 |

The conversion of the TMH 9 degree and extent for crocodile cracks to a percentage cracked area, as defined in the HDM-4, is presented in Table 3-8.

**Table 3-8: TMH 9 to HDM-4 conversion of crocodile cracks**

| TMH 9 Degree | % Area with crocodile cracks | | | | |
|---|---|---|---|---|---|
| | TMH 9 Extent | | | | |
| | **1** | **2** | **3** | **4** | **5** |
| 1 | 0.01 | 1 | 2 | 5.1 | 9 |
| 2 | 0.14 | 2 | 4 | 8 | 10 |
| 3 | 1 | 3.5 | 6.8 | 11 | 16 |
| 4 | 1 | 3.5 | 6.8 | 11 | 16 |
| 5 | 1 | 3.5 | 6.8 | 11 | 16 |

The conversion of the TMH 9 degree and extent for potholes to the number of 0.1 $m^2$ sized potholes, as defined in the HDM-4, is presented in Table 3-9.

**Table 3-9: TMH 9 to HDM-4 conversion of potholes**

| TMH 9 Degree | Number of 0.1 $m^2$ potholes | | | | |
|---|---|---|---|---|---|
| | TMH 9 Extent | | | | |
| | **1** | **2** | **3** | **4** | **5** |
| 1 | 0 | 1 | 2 | 3 | 5 |
| 2 | 0 | 2 | 3 | 5 | 7 |
| 3 | 0 | 2 | 4 | 6 | 10 |
| 4 | 1 | 4 | 7 | 11 | 17 |
| 5 | 1 | 8 | 13 | 21 | 31 |

**Algorithms for maintenance**

Table 3-10 provides the treatments used in the analysis along with the criteria that need to be met in order for the respective treatment to be triggered on a pavement segment, as well as the effects of the treatment on the pavement strength, distresses, and condition. Treatment triggers and resets as previously used by Aurecon Africa (rebranded as Zutari) were derived based on the guidelines provided by the Committee of State Road Authorities (1994) TRH 22, COTO (2013) TMH 22, and Odoki and Kerali (2006) HDM-4, and adjusted considering engineering judgement and experience gained in pavement management and dTIMS strategic analyses.

**Table 3-10: Treatments, triggers, and resets**

| Treatment | Trigger | Resets |
|---|---|---|
| Reseal | ((AADT > 4000 AND All cracks ≥ 2%) OR (AADT ≤ 4000 AND All cracks ≥ 5%)) AND (Rut ≤ 20 mm AND Condition index ≥ 35% AND Wide cracks ≤ 10% AND IRI ≤ 4.5 AND NOT (Condition index ≤ 45% And IRI ≥ 4.0)) | SNP = Old SNP + 0.21<br>Cracking = 0%<br>Ravelling = 0%<br>Potholes = 0<br>Patching = 0%<br>Rut = 95% of old value<br>IRI = 97.5% of old value<br>Condition recalculated |
| Light rehabilitation | ((Wide cracks ≥ 10% AND IRI ≤ 4.5) OR (Wide cracks ≤ 10% AND IRI ≥ 4.5) OR (Condition index ≤ 45% AND IRI ≥ 4.0)) AND NOT (IRI ≥ 4.5 And Wide cracks ≥ 10%) AND NOT (IRI ≥ 4.5 And Condition index ≤ 45%) AND NOT (Wide cracks ≥ 10% AND Condition index ≤ 45%) AND IRI ≤ 6.6 AND Rut ≤ 20 mm AND Condition index ≥ 35% | SNP = Old SNP + 0.61<br>Cracking = 0%<br>Ravelling = 0%<br>Potholes = 0<br>Patching = 0%<br>Rut is recalculated<br>IRI = 2<br>Condition is recalculated |
| Heavy rehabilitation | IRI ≥ 6.6 OR Rut ≥ 20 mm OR (IRI ≥ 4.5 AND Wide cracks ≥ 10%) OR (Condition index ≤ 45% AND IRI ≥ 4.5) OR (Condition index ≤ 45% AND Wide cracks ≥ 10%) OR Condition index ≤ 35% | SNP = Old SNP + 0.96<br>Cracking = 0%<br>Ravelling = 0%<br>Potholes = 0<br>Patching = 0%<br>Rut is recalculated<br>IRI = 1.4<br>Condition is recalculated |

**Treatment unit costs**

The treatment unit costs used in the analysis are provided in Table 3-11. Unit costs are provided in 2016 Rand value. Inflation is not taken into account in the analysis.

**Table 3-11: Treatment unit costs**

| Treatment | Unit costs (R/m$^2$) |
|---|---|
| Reseal | 149 |
| Light rehabilitation | 664 |
| Heavy rehabilitation | 1 073 |

## 3.6 INFLUENCE OF SECTION LENGTH ON RUT DEPTH DISTRIBUTION, MAINTENANCE REQUIREMENTS, AND FUNDING NEED USING PERCENTILES

### 3.6.1 Aggregated section lengths

For each of the 13 samples (road segments) considered, the 50$^{th}$, 75$^{th}$, 90$^{th}$, 95$^{th}$, and 99$^{th}$ percentile of the discrete 10 m rut depth measurements were calculated per 20 m, 50 m, 100 m, 500 m, 1 000 m, and 10 000 m section lengths. Percentiles are calculated by taking the 50$^{th}$, 75$^{th}$, 90$^{th}$, 95$^{th}$, and 99$^{th}$ percentile of 2 points for 20 m sections, 5 points for 50 m sections, and so forth.

### 3.6.2 Statistical parameters and distributions

Cumulative distributions of rut depth were plotted per percentile, and the COV, as well as the mean, minimum, and maximum rut depth values were compared to study the influence varying aggregated section lengths, considering varying percentiles as the statistical aggregation measure, on the dispersion of calculated rut depth values.

The change in the distribution of calculated rut depth amongst warning to severe condition categories, described in Table 3-5, was also compared per percentile and aggregated section length.

### 3.6.3 Maintenance requirements and funding need

The technical (engineering) needs analysis specified in Section 3.5 was rerun in dTIMS over a 20-year analysis period to study the influence of varying aggregated section lengths, considering varying percentiles as the statistical aggregation measure, on the immediate annual maintenance requirements and the resulting funding need.

## 3.7 APPLICATION WITHIN THE SOUTH AFRICAN NRA (1999) SPECIFICATION

The NRA (1999) specifies performance requirements for functional and structural aspects of a road pavement. As per the NRA (1999), rut depth measurements taken at 10 m intervals should be processed to produce cumulative distribution graphs over 1 km segments. Using the cumulative distribution graph for each segment, the rut depth measurements must meet the acceptance criteria specified in Table 3-12.

**Table 3-12: Acceptance criteria for rut depth (NRA, 1999)**

| Limiting rut depth (mm) | Maximum length (%) of segment with rut depth worse than limiting value |
|---|---|
| 15 | 10 |
| 20 | 5 |
| 25 | 0 |

In practice, the automated rut depth measurements taken at 25 mm intervals are averaged over 10 m intervals to comply with the specification. In order to study the influence of average and percentile statistical aggregation measures on the acceptance criteria presented in Table 3-12, the cumulative distributions of 5 samples of varying rut depth severity (based on discrete 10 m interval measurements) were analysed. 5 Segments of 1 km in length were selected from sample 11 according to the criteria listed in Table 3-13.

**Table 3-13: Selection criteria for samples**

| Sample | Selection criteria |
|---|---|
| 1 | Sound to moderate rut depth and all acceptance criteria are met |
| 2 | Sound to warning rut depth and all acceptance criteria are met |
| 3 | Sound to severe rut depth and all acceptance criteria are met |
| 4 | Sound to severe rut depth and not all acceptance criteria are met |
| 5 | Sound to severe rut depth and none of the acceptance criteria are met |

The distribution of rut depth amongst the condition categories described in Section 3.4.2 is presented in Table 3-14 for each sample.

**Table 3-14: Distribution amongst rut depth condition categories per sample**

| Sample | Condition category (%) | | | | |
|---|---|---|---|---|---|
| | Sound | Isolated | Moderate | Warning | Severe |
| 1 | 61 | 27 | 12 | 0 | 0 |
| 2 | 19 | 51 | 21 | 9 | 0 |
| 3 | 44 | 43 | 7 | 4 | 2 |
| 4 | 44 | 42 | 9 | 2 | 3 |
| 5 | 26 | 22 | 23 | 20 | 9 |

As 10 m interval rut depth measurements are taken as discrete measurements for the purposes of this study, the 10 m measurements have been processed over 100 m intervals (typical

reporting interval as per the COTO (2013) TMH 22, AASHTO (2013) AASHTO R48-10 and Austroads (2016) AG:AM/T009 specifications) for each 1 km segment.

The cumulative distribution was plotted for discrete 10 m, 100 m average, and 100 m 50$^{th}$, 75$^{th}$, 90$^{th}$, 95$^{th}$, and 99$^{th}$ percentile rut depth measurements (see Appendix I). The resulting cumulative distribution graphs were then analysed according to the specified acceptance criteria to determine if the statistical aggregation measures provide an accurate representation of whether these performance requirements are met or not when compared to the results of the discrete 10 m rut depth measurements.

# 4 DISCUSSION OF RESULTS

The results of the statistical and technical needs analysis undertaken to study the influence of varying aggregated section lengths, considering the mean and percentiles as the statistical aggregation measures, on the distribution of calculated rut depth and the respective maintenance, funding, and pavement performance requirements, are discussed in this chapter.

## 4.1 AGGREGATED SECTION LENGTHS USING AVERAGES

### 4.1.1 Descriptive statistics

A comparison of descriptive statistics and the cumulative distribution for the different averaged section lengths reveals that the dispersion of rut depth around the mean reduces with increasing averaged section length. Table 4-1 presents the descriptive statistics for sample 11. As seen in Table 4-1, the variance decreases with increasing section length, and the maximum value, 95$^{th}$ percentile, and 20$^{th}$ percentile converge towards the mean with increasing section length. All samples convey similar results. The descriptive statistics for all samples are provided in Appendix D.

**Table 4-1: Sample 11 descriptive statistics**

| Distribution Parameter | 10 m Sections | 20 m Sections | 50 m Sections | 100 m Sections | 500 m Sections | 1 000 m Sections | 10 000 m Sections |
|---|---|---|---|---|---|---|---|
| Maximum (mm) | 29.85 | 27.75 | 20.60 | 20.52 | 13.66 | 10.89 | 6.45 |
| % Change in maximum | | -7% | -31% | -31% | -54% | -64% | -78% |
| Mean (mm) | 5.63 | 5.63 | 5.63 | 5.63 | 5.63 | 5.63 | 5.62 |
| % Change in mean | | 0% | 0% | 0% | 0% | 0% | 0% |
| Variance (mm$^2$) | 11.94 | 10.70 | 8.82 | 7.13 | 3.14 | 1.98 | 0.31 |
| % Change in variance | | -10% | -26% | -40% | -74% | -83% | -97% |
| COV | 0.61 | 0.58 | 0.53 | 0.47 | 0.32 | 0.25 | 0.10 |
| % Change in COV | | -5% | -13% | -23% | -48% | -59% | -84% |
| 95$^{th}$ Percentile (mm) | 12.03 | 11.57 | 11.01 | 10.61 | 8.39 | 8.64 | 6.37 |
| % Change in 95$^{th}$ percentile | | -4% | -8% | -12% | -30% | -28% | -47% |
| 20$^{th}$ Percentile (mm) | 2.97 | 3.15 | 3.34 | 3.60 | 4.32 | 4.64 | 5.38 |
| % Change in 20$^{th}$ percentile | | 6% | 12% | 21% | 45% | 56% | 81% |

### 4.1.2 Distribution of rut depth

Table 4-2 presents the change in distribution type with changing averaged section lengths for all samples analysed. 46% of samples transition from an exponential or lognormal distribution to a normal distribution with increasing averaged section length, 23% of samples transition

from a normal or lognormal distribution to an exponential distribution, and the remaining 31% remain a lognormal distribution. Probability plots are provided in Appendix E.

**Table 4-2: Change in distribution type**

| Sample | Distribution of rut depth | | | | | | |
|---|---|---|---|---|---|---|---|
| | 10 m Sections | 20 m Sections | 50 m Sections | 100 m Sections | 500 m Sections | 1 000 m Sections | 10 000 m Sections |
| 1 | Lognormal | Lognormal | Lognormal | Lognormal | Normal | Normal | Normal |
| 2 | Lognormal | Lognormal | Lognormal | Lognormal | Lognormal | Lognormal | Lognormal |
| 3 | Lognormal | Lognormal | Lognormal | Lognormal | Lognormal | Lognormal | Normal |
| 4 | Exponential | Exponential | Lognormal | Normal | Normal | Normal | Normal |
| 5 | Normal | Lognormal | Lognormal | Lognormal | Lognormal | Lognormal | Exponential |
| 6 | Lognormal | Lognormal | Lognormal | Lognormal | Lognormal | Lognormal | Lognormal |
| 7 | Lognormal | Lognormal | Lognormal | Lognormal | Lognormal | Lognormal | Exponential |
| 8 | Lognormal | Lognormal | Lognormal | Lognormal | Lognormal | Lognormal | Normal |
| 9 | Lognormal | Lognormal | Lognormal | Lognormal | Normal | Normal | Normal |
| 10 | Lognormal | Lognormal | Lognormal | Lognormal | Lognormal | Lognormal | Lognormal |
| 11 | Lognormal | Lognormal | Lognormal | Lognormal | Lognormal | Lognormal | Lognormal |
| 12 | Lognormal | Lognormal | Lognormal | Lognormal | Lognormal | Lognormal | Normal |
| 13 | Normal | Normal | Lognormal | Lognormal | Lognormal | Lognormal | Exponential |

Figure 4-1 presents the cumulative distributions for the different averaged section lengths for sample 11. The distribution is initially a wider, flatter S-curve, indicating a higher dispersion and range of possible rut depth values. With increasing averaged section length, the slope of the S-curve becomes steeper, indicating lower dispersion. All samples convey similar results. Cumulative distributions for all samples are provided in Appendix F.2.

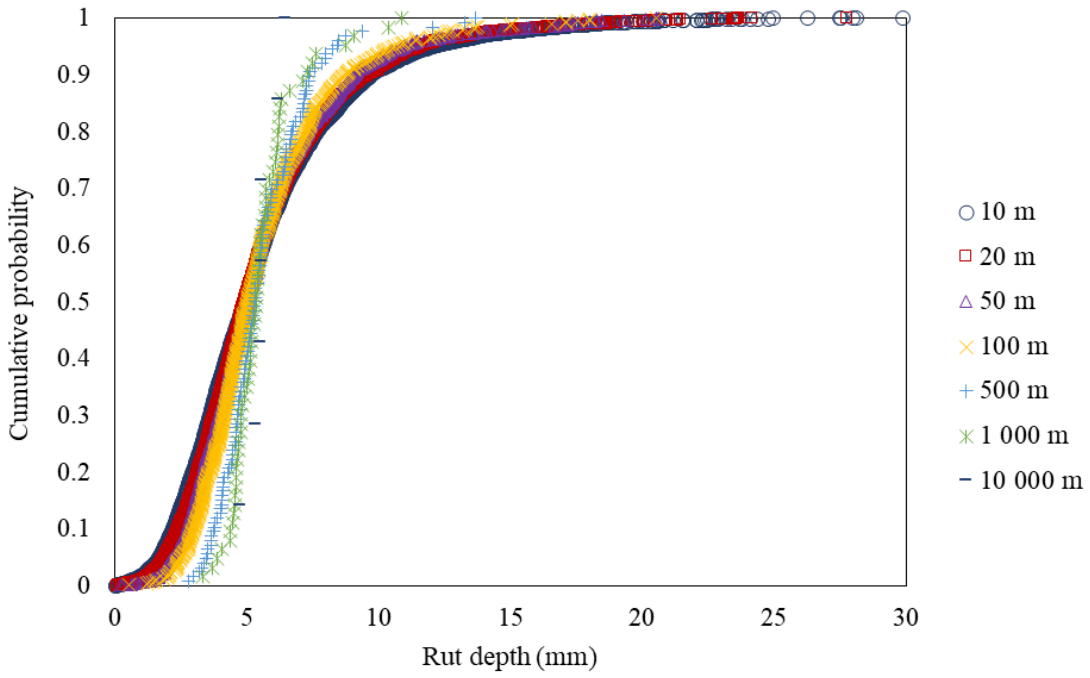


**Figure 4-1: Sample 11 cumulative distribution**

For each sample, over 80% of 10 m interval rut depth values are classified as sound and isolated. As such, with increasing averaged section length, the minority of rut depth values classified as moderate, warning, and severe are averaged out amongst the majority lower rut depth values. The percentage moderate, warning, and severe rut depth values reduce with increasing averaged section length. An example of the change in distribution amongst the rut depth condition categories with increasing averaged section length is provided in Figure 4-2 for sample 11. All samples convey similar results. The results for all samples are provided in Appendix F.3.

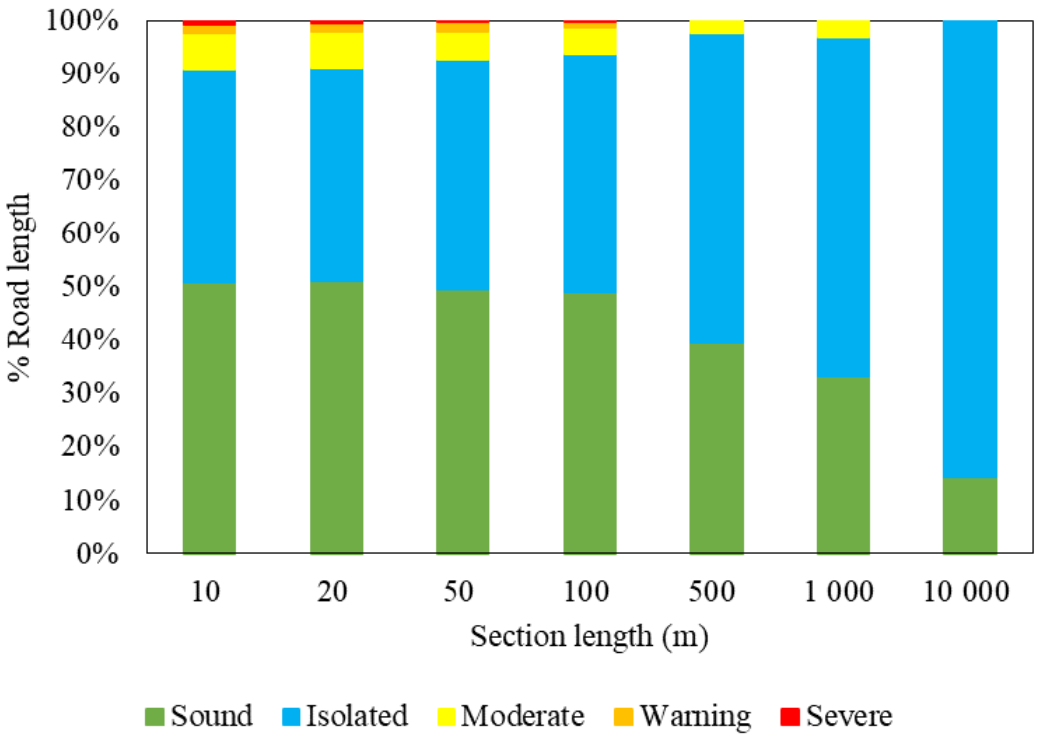


**Figure 4-2: Distribution of rut depth values amongst condition categories for sample 11**

The degree to which these rut depth values are averaged out depends on the averaged section length, the distribution of rut depth values amongst the different rut depth severity categories, as well as the distribution of rut depth values over the length of the road segment.

### 4.1.3 Maintenance requirements

Figure 4-3 presents the distribution of maintenance treatments triggered on the 10 m sections over the entire analysis period for the 13 samples studied. Treatment lengths are provided per sample and represent the total treatment length triggered over the entire analysis period. Reseal and light rehabilitation treatments are triggered on 99% to 100% of road lengths, with heavy rehabilitation being triggered on the remaining 0% to 1% of road lengths.

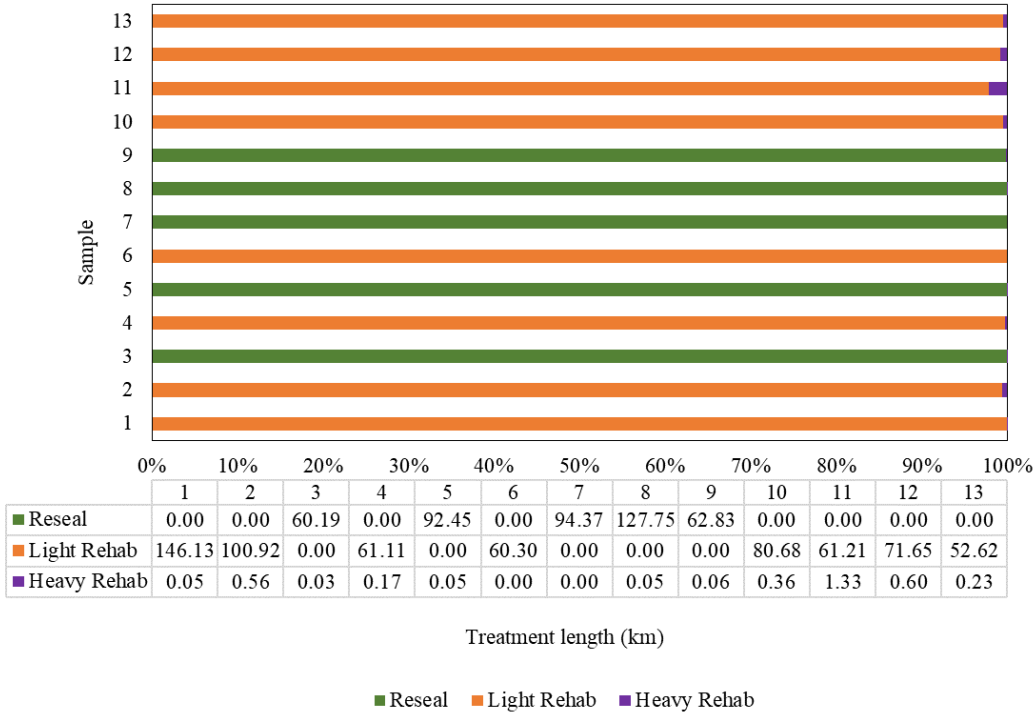


| | 1 | 2 | 3 | 4 | 5 | 6 | 7 | 8 | 9 | 10 | 11 | 12 | 13 |
|---|---|---|---|---|---|---|---|---|---|---|---|---|---|
| Reseal | 0.00 | 0.00 | 60.19 | 0.00 | 92.45 | 0.00 | 94.37 | 127.75 | 62.83 | 0.00 | 0.00 | 0.00 | 0.00 |
| Light Rehab | 146.13 | 100.92 | 0.00 | 61.11 | 0.00 | 60.30 | 0.00 | 0.00 | 0.00 | 80.68 | 61.21 | 71.65 | 52.62 |
| Heavy Rehab | 0.05 | 0.56 | 0.03 | 0.17 | 0.05 | 0.00 | 0.00 | 0.05 | 0.06 | 0.36 | 1.33 | 0.60 | 0.23 |

**Figure 4-3: Distribution of maintenance treatments triggered on 10 m sections**

Table 4-3 presents the change in heavy rehabilitation treatment length with changing averaged section length. With increasing averaged section length, the minority of severe (>20 mm) rut depth values are averaged out amongst the majority lower rut depth values, thereby decreasing heavy rehabilitation treatment lengths. The rate of decrease in treatment length is influenced by the averaged section length, the distribution of rut depth values amongst different rut depth severity categories, the distribution of rut depth values over the segment length, and the condition of other maintenance drivers, including roughness, cracking, patching, potholes, and ravelling, which are influenced by temperature and moisture conditions, pavement and surface type, pavement strength, pavement, and surface age, surface thickness, deflection, relative compaction, construction defects, and traffic loading.

**Table 4-3: Change in heavy rehabilitation treatment length**

| Sample | Heavy rehabilitation treatment length (km) | | | | | | |
|---|---|---|---|---|---|---|---|
| | 10 m Sections | 20 m Sections | 50 m Sections | 100 m Sections | 500 m Sections | 1 000 m Sections | 10 000 m Sections |
| 1 | 0.05 | 0.00 | 0.00 | 0.00 | 0.00 | 0.00 | 0.00 |
| 2 | 0.56 | 0.46 | 0.20 | 0.20 | 0.00 | 0.00 | 0.00 |
| 3 | 0.03 | 0.02 | 0.00 | 0.00 | 0.00 | 0.00 | 0.00 |
| 4 | 0.17 | 0.12 | 0.10 | 0.00 | 0.00 | 0.00 | 0.00 |
| 5 | 0.05 | 0.04 | 0.05 | 0.00 | 0.00 | 0.00 | 0.00 |
| 6 | - | - | - | - | - | - | - |
| 7 | - | - | - | - | - | - | - |
| 8 | 0.05 | 0.04 | 0.00 | 0.00 | 0.00 | 0.00 | 0.00 |
| 9 | 0.06 | 0.04 | 0.05 | 0.00 | 0.00 | 0.00 | 0.00 |
| 10 | 0.36 | 0.30 | 0.25 | 0.20 | 0.00 | 0.00 | 0.00 |
| 11 | 1.33 | 1.20 | 1.15 | 0.70 | 0.00 | 0.00 | 0.00 |
| 12 | 0.60 | 0.50 | 0.40 | 0.20 | 0.00 | 0.00 | 0.00 |
| 13 | 0.23 | 0.08 | 0.00 | 0.00 | 0.00 | 0.00 | 0.00 |

Figure 4-4 presents the change in light rehabilitation treatment length and treatment year with changing averaged section length for sample 1. For sample 1, light rehabilitation is triggered in years 2022, 2023, and 2024, where the road sections respectively contain warning (approximately 16 mm to 19 mm) rut depth, isolated to moderate (approximately 6 mm to 15 mm) rut depth, and isolated (5 mm to 7 mm) rut depth.

For a section of a road segment to be triggered for light rehabilitation, the section needs to contain rut depth less than 20 mm. Within this criterion for rut depth, the year in which light rehabilitation is selected as the maintenance decision is dependent on the state of cracking, roughness, potholes, patching, and the overall visual condition index, influenced by temperature and moisture conditions, pavement strength, pavement age, and traffic loading, i.e., in 2022, pavement sections triggering a light rehabilitation present with more severe rutting, and consequently higher roughness and a poorer overall visual condition index, while other distresses are in a less severe state; in 2024, pavement sections triggering a light rehabilitation present with less severe rutting, whereas other distresses have deteriorated slightly over time and are now in a more severe state, and consequently so is the section's roughness and the overall visual condition index, just as in 2022.

As all above-mentioned parameters, except for rut depth and those dependent on rut depth, remain constant across road segments throughout the analysis, the impact of the averaged section length on the selection of light rehabilitation as a maintenance decision is therefore dependent on the resulting change in rut depth, and consequently the change in roughness as well as the overall condition index.

Influenced by the distribution of rut depth values over the segment length, the minority of warning rut depth values are averaged out amongst the majority lower rut depth values with increasing averaged section length, resulting in road sections with similar isolated to moderate rut depth; consequently, the length of segments requiring light rehabilitation treatments in years 2022 and 2024 reduces. Increasing the averaged section length to 10 000 m results in all light rehabilitation treatments being triggered in 2023.

Sample 1 contains sections requiring heavy and light rehabilitation in multiple years, resulting in a change in both treatment year and length with increasing averaged section length. All samples containing multiple treatment types, with the majority treatment (light rehabilitation / reseal) triggering in multiple years, convey similar results. The results for all such samples are provided in Appendix G.2.

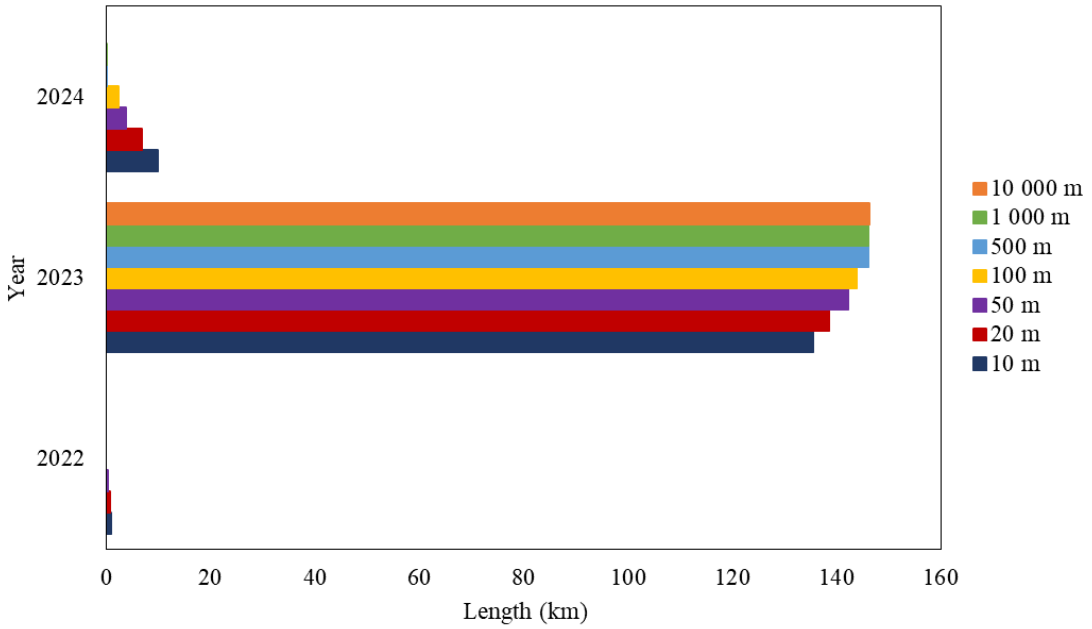


**Figure 4-4: Change in light rehabilitation treatment year and length for sample 1**

On average, 42% (as indicated in Table 4-4) of averaged sections triggering a light rehabilitation one year later than what deemed necessary, when considering the 'true' pavement conditions as indicated by the discrete 10 m sections, can no longer be effectively treated with a light rehabilitation and rather require a heavy rehabilitation.

**Table 4-4: Percentage of sections on which a light rehabilitation is ineffectively applied**

| Averaged Section Length (m) | Sections on which light rehabilitation is no longer effective | |
|---|---|---|
| | Average Section Length (km) | Average Percentage Length (%) |
| 20 | 0.02 | 41% |
| 50 | 0.04 | 42% |
| 100 | 0.06 | 42% |
| 500 | 0.10 | 43% |
| 1 000 | 0.11 | 43% |
| 10 000 | 0.11 | 43% |
| Average | 0.07 | 42% |

Samples containing multiple treatment types, with the majority treatment (light rehabilitation / reseal) triggering in a single year, undergo a change in treatment length but no change in treatment year. Figure 4-5 presents the change in reseal treatment year and length with changing averaged section length for sample 3. Sample 3 contains sections requiring heavy rehabilitation and reseals in 2016.

As previously discussed, with increasing averaged section length, the minority of severe (>20 mm) rut depth values are averaged out amongst the majority lower rut depth values, thereby decreasing heavy rehabilitation treatment lengths, and increasing reseal treatment lengths. The rate of decrease in treatment length is influenced by the averaged section length, the distribution of rut depth values amongst different rut depth severity categories, the distribution of rut depth values over the segment length, and the condition of other maintenance drivers, including roughness, cracking, patching, potholes, and ravelling, which are influenced by temperature and moisture conditions, pavement and surface type, pavement strength, pavement, and surface age, surface thickness, deflection, relative compaction, construction defects, and traffic loading.

The selection of a reseal as a maintenance decision is dependent on the state of rut depth, cracking, roughness, patching, potholes, pumping, and the overall visual condition index, influenced by temperature and moisture conditions, pavement strength, pavement age, and traffic loading.

The results for all samples containing multiple treatment types, with the majority treatment triggering in a single year, are provided in Appendix G.3.

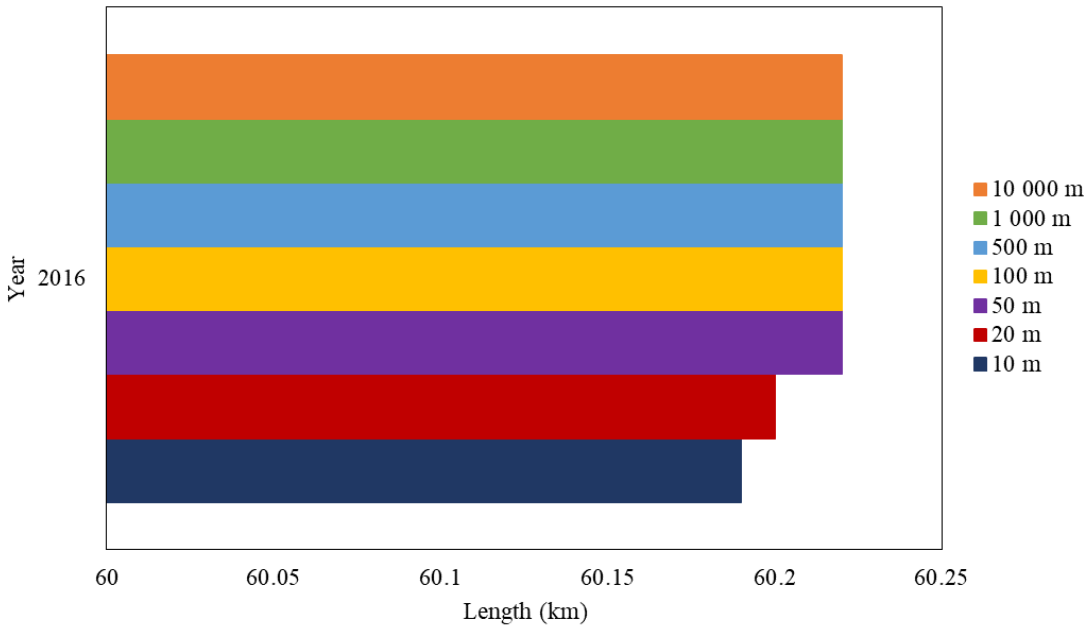


**Figure 4-5: Change in reseal treatment year and length for sample 3**

Samples containing a single treatment (light rehabilitation / reseal), triggering in a single year, undergo no change in treatment year or length. Figure 4-6 presents the change in light rehabilitation treatment year and length with changing averaged section length for sample 6. Sample 6 contains sections requiring light rehabilitation in 2016. The below results pertain to treatment lengths being greater than the averaged section length, were the averaged section length to be greater than the treatment length (as determined with the 10 m section length), there would be a change in treatment length regardless of the number of treatments triggered per year. The results for all samples containing a single treatment triggering in a single year are provided in Appendix G.4.

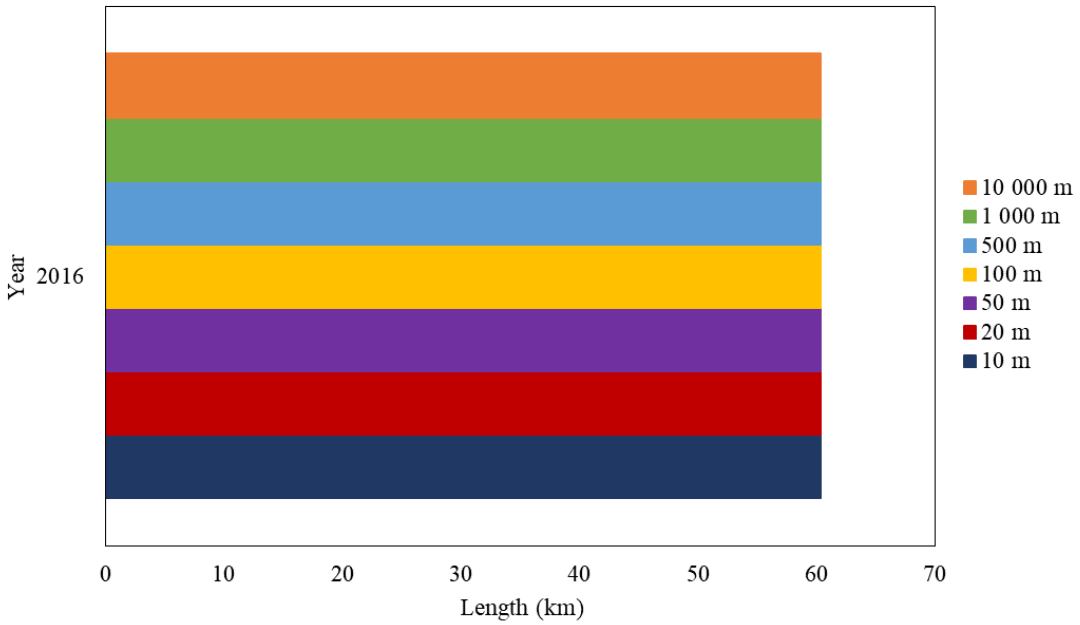


**Figure 4-6: Change in light rehabilitation treatment year and length for sample 6**

Table 4-5 to Table 4-8 respectively present the error in the overall maintenance decision, heavy rehabilitation maintenance decision, light rehabilitation maintenance decision, and reseal maintenance decision for all samples with changing averaged section length, as well as some of the parameters influencing the degree of error. The percentage error shown is the total error incurred as a result of a change in treatment type, year, and length.

The rut depth COV and the percentage of the sample segment length containing sound and isolated rutting are used to indicate the influence of rut depth on the error in maintenance decisions. IRI and the Visual Condition Index (VCI) have been used to indicate the influence of other maintenance drivers. Other influencing parameters include the number of treatments triggered per road sample segment (for 10 m section lengths) as well as the number of different years in which these treatments have been triggered. A parameter that has not been shown here is the distribution of rut depth values over the segment length. This parameter should be taken into consideration when studying the results shown.

From the results obtained, the following is evident:

- The percentage error in the overall maintenance decision increases with increasing averaged section length, resulting in inaccurate treatment types, treatment lengths, and treatment years;
- No direct relationship is evident between the degree of the error in maintenance decisions and the dispersion of rut depth values;

- Samples with a single treatment and treatment year contain no error;
- For samples with multiple treatments and a single treatment year, no error can be seen in the overall maintenance decision as there is no error in the overall treatment length. However, an error is present when looking at individual treatments. From Table 4-8, it can be seen that for multiple treatments in a single year, samples with a lower VCI and percentage sound and isolated rutting, and a higher IRI, result in a higher degree of error;
- For samples with multiple treatments and a higher number of treatment years (3 to 9), the degree of error is influenced by the rut depth COV, the percentage length containing sound and isolated rutting, IRI, and VCI. Higher COV and IRI, and lower VCI and percentage sound and isolated rutting result in a higher degree of error. Not all of these parameters need to be true for one sample to result in a higher degree of error than another; there is no direct relationship, and
- Samples containing multiple treatments and a high number of treatment years (10) result in a high degree of error.

**Table 4-5: Error in overall maintenance decision**

| Sample | Parameters | | | | | | Error in overall maintenance decision (%) | | | | | | |
|---|---|---|---|---|---|---|---|---|---|---|---|---|---|
| | Rut depth COV | Sound and Isolated Rutting (% Length) | IRI | VCI | Number of treatments triggered | Number of treatment years | 10 m Sections | 20 m Sections | 50 m Sections | 100 m Sections | 500 m Sections | 1 000 m Sections | 10 000 m Sections |
| 1 | 0.46 | 98 | 2.85 | 83 | 2 | 5 | - | 4.34 | 9.15 | 11.62 | 14.52 | 14.52 | 14.76 |
| 2 | 0.56 | 93 | 2.86 | 68 | 2 | 7 | - | 6.09 | 15.21 | 21.27 | 35.26 | 38.21 | 48.07 |
| 3 | 0.51 | 90 | 3.55 | 50 | 2 | 1 | - | 0.00 | 0.00 | 0.00 | 0.00 | 0.00 | 0.00 |
| 4 | 0.66 | 89 | 3.35 | 69 | 2 | 3 | - | 1.34 | 2.38 | 4.01 | 13.15 | 13.15 | 16.42 |
| 5 | 0.49 | 94 | 2.51 | 57 | 2 | 2 | - | 0.00 | 0.11 | 0.09 | 0.09 | 0.09 | 0.09 |
| 6 | 0.38 | 100 | 4.24 | 79 | 1 | 1 | - | 0.00 | 0.00 | 0.00 | 0.00 | 0.00 | 0.00 |
| 7 | 0.54 | 97 | 2.69 | 67 | 1 | 1 | - | 0.00 | 0.00 | 0.00 | 0.00 | 0.00 | 0.00 |
| 8 | 0.56 | 99 | 2.27 | 68 | 2 | 1 | - | 0.00 | 0.00 | 0.00 | 0.00 | 0.00 | 0.00 |
| 9 | 0.62 | 98 | 2.36 | 72 | 2 | 3 | - | 0.06 | 0.13 | 0.13 | 0.13 | 0.13 | 0.13 |
| 10 | 0.68 | 94 | 4.32 | 59 | 2 | 1 | - | 0.00 | 0.00 | 0.00 | 0.00 | 0.00 | 0.00 |
| 11 | 0.61 | 91 | 2.78 | 85 | 2 | 9 | - | 2.43 | 5.31 | 6.59 | 9.82 | 14.61 | 14.61 |
| 12 | 0.56 | 94 | 2.56 | 85 | 2 | 10 | - | 2.16 | 4.29 | 7.45 | 20.18 | 22.95 | 66.55 |
| 13 | 0.46 | 84 | 2.97 | 74 | 2 | 5 | - | 4.31 | 10.14 | 15.44 | 26.41 | 35.88 | 47.23 |

**Table 4-6: Error in heavy rehabilitation maintenance decision**

| Sample | Parameters | | | | | | Error in heavy rehabilitation maintenance decision (%) | | | | | | |
|---|---|---|---|---|---|---|---|---|---|---|---|---|---|
| | Rut depth COV | Sound and Isolated Rutting (% Length) | IRI | VCI | Number of treatments triggered | Number of treatment years | 10 m Sections | 20 m Sections | 50 m Sections | 100 m Sections | 500 m Sections | 1 000 m Sections | 10 000 m Sections |
| 1 | 0.46 | 98 | 2.85 | 83 | 2 | 5 | - | 100.00 | 100.00 | 100.00 | 100.00 | 100.00 | 100.00 |
| 2 | 0.56 | 93 | 2.86 | 68 | 2 | 7 | - | 35.71 | 92.86 | 64.29 | 100.00 | 100.00 | 100.00 |
| 3 | 0.51 | 90 | 3.55 | 50 | 2 | 1 | - | 33.33 | 100.00 | 100.00 | 100.00 | 100.00 | 100.00 |
| 4 | 0.66 | 89 | 3.35 | 69 | 2 | 3 | - | 41.18 | 76.47 | 100.00 | 100.00 | 100.00 | 100.00 |
| 5 | 0.49 | 94 | 2.51 | 57 | 2 | 2 | - | 20.00 | 200.00 | 100.00 | 100.00 | 100.00 | 100.00 |
| 6 | 0.38 | 100 | 4.24 | 79 | 1 | 1 | - | - | - | - | - | - | - |
| 7 | 0.54 | 97 | 2.69 | 67 | 1 | 1 | - | - | - | - | - | - | - |
| 8 | 0.56 | 99 | 2.27 | 68 | 2 | 1 | - | 20.00 | 100.00 | 100.00 | 100.00 | 100.00 | 100.00 |
| 9 | 0.62 | 98 | 2.36 | 72 | 2 | 3 | - | 100.00 | 116.67 | 100.00 | 100.00 | 100.00 | 100.00 |
| 10 | 0.68 | 94 | 4.32 | 59 | 2 | 1 | - | 16.67 | 30.56 | 44.44 | 100.00 | 100.00 | 100.00 |
| 11 | 0.61 | 91 | 2.78 | 85 | 2 | 9 | - | 20.30 | 49.62 | 75.94 | 100.00 | 100.00 | 100.00 |
| 12 | 0.56 | 94 | 2.56 | 85 | 2 | 10 | - | 56.67 | 60.00 | 73.33 | 100.00 | 100.00 | 100.00 |
| 13 | 0.46 | 84 | 2.97 | 74 | 2 | 5 | - | 73.91 | 100.00 | 100.00 | 100.00 | 100.00 | 100.00 |

**Table 4-7: Error in light rehabilitation maintenance decision**

| Sample | Parameters | | | | | | Error in light rehabilitation maintenance decision (%) | | | | | | |
|---|---|---|---|---|---|---|---|---|---|---|---|---|---|
| | Rut depth COV | Sound and Isolated Rutting (% Length) | IRI | VCI | Number of treatments triggered | Number of treatment years | 10 m Sections | 20 m Sections | 50 m Sections | 100 m Sections | 500 m Sections | 1 000 m Sections | 10 000 m Sections |
| 1 | 0.46 | 98 | 2.85 | 83 | 2 | 5 | - | 4.30 | 9.12 | 11.59 | 14.49 | 14.49 | 14.73 |
| 2 | 0.56 | 93 | 2.86 | 68 | 2 | 7 | - | 6.06 | 15.08 | 21.13 | 35.30 | 38.27 | 48.18 |
| 3 | 0.51 | 90 | 3.55 | 50 | 2 | 1 | - | - | - | - | - | - | - |
| 4 | 0.66 | 89 | 3.35 | 69 | 2 | 3 | - | 1.26 | 2.27 | 3.75 | 12.91 | 12.91 | 16.18 |
| 5 | 0.49 | 94 | 2.51 | 57 | 2 | 2 | - | - | - | - | - | - | - |
| 6 | 0.38 | 100 | 4.24 | 79 | 1 | 1 | - | 0.00 | 0.00 | 0.00 | 0.00 | 0.00 | 0.00 |
| 7 | 0.54 | 97 | 2.69 | 67 | 1 | 1 | - | - | - | - | - | - | - |
| 8 | 0.56 | 99 | 2.27 | 68 | 2 | 1 | - | - | - | - | - | - | - |
| 9 | 0.62 | 98 | 2.36 | 72 | 2 | 3 | - | - | - | - | - | - | - |
| 10 | 0.68 | 94 | 4.32 | 59 | 2 | 1 | - | 0.07 | 0.14 | 0.20 | 0.45 | 0.45 | 0.45 |
| 11 | 0.61 | 91 | 2.78 | 85 | 2 | 9 | - | 2.04 | 4.35 | 5.08 | 7.86 | 12.76 | 12.76 |
| 12 | 0.56 | 94 | 2.56 | 85 | 2 | 10 | - | 2.04 | 3.96 | 7.17 | 20.01 | 22.81 | 66.77 |
| 13 | 0.46 | 84 | 2.97 | 74 | 2 | 5 | - | 4.35 | 10.24 | 15.56 | 26.59 | 36.09 | 47.49 |

**Table 4-8: Error in reseal maintenance decision**

| Sample | Parameters | | | | | | Error in reseal maintenance decision (%) | | | | | | |
|---|---|---|---|---|---|---|---|---|---|---|---|---|---|
| | Rut depth COV | Sound and Isolated Rutting (% Length) | IRI | VCI | Number of treatments triggered | Number of treatment years | 10 m Sections | 20 m Sections | 50 m Sections | 100 m Sections | 500 m Sections | 1 000 m Sections | 10 000 m Sections |
| 1 | 0.46 | 98 | 2.85 | 83 | 2 | 5 | - | - | - | - | - | - | - |
| 2 | 0.56 | 93 | 2.86 | 68 | 2 | 7 | - | - | - | - | - | - | - |
| 3 | 0.51 | 90 | 3.55 | 50 | 2 | 1 | - | 0.02 | 0.05 | 0.05 | 0.05 | 0.05 | 0.05 |
| 4 | 0.66 | 89 | 3.35 | 69 | 2 | 3 | - | - | - | - | - | - | - |
| 5 | 0.49 | 94 | 2.51 | 57 | 2 | 2 | - | 0.01 | 0.00 | 0.05 | 0.05 | 0.05 | 0.05 |
| 6 | 0.38 | 100 | 4.24 | 79 | 1 | 1 | - | - | - | - | - | - | - |
| 7 | 0.54 | 97 | 2.69 | 67 | 1 | 1 | - | 0.00 | 0.00 | 0.00 | 0.00 | 0.00 | 0.00 |
| 8 | 0.56 | 99 | 2.27 | 68 | 2 | 1 | - | 0.01 | 0.04 | 0.04 | 0.04 | 0.04 | 0.04 |
| 9 | 0.62 | 98 | 2.36 | 72 | 2 | 3 | - | 0.03 | 0.02 | 0.10 | 0.10 | 0.10 | 0.10 |
| 10 | 0.68 | 94 | 4.32 | 59 | 2 | 1 | - | - | - | - | - | - | - |
| 11 | 0.61 | 91 | 2.78 | 85 | 2 | 9 | - | - | - | - | - | - | - |
| 12 | 0.56 | 94 | 2.56 | 85 | 2 | 10 | - | - | - | - | - | - | - |
| 13 | 0.46 | 84 | 2.97 | 74 | 2 | 5 | - | - | - | - | - | - | - |

### 4.1.4 Funding implications

Incorrectly identified maintenance requirements resulting from using averages to analyse automated rutting data results in inaccurate maintenance and rehabilitation budgetary forecasts.

On average, across all samples, the total portion of the predicted budget being incorrectly allocated due to an inaccurately estimated financial need per year and/or treatment type is shown in Figure 4-7 per averaged section length. The degree to which the budget is inaccurately estimated per year and/or treatment type increases with increasing averaged section length.

For an averaged section length of 20 m, on average 1.7% (R7 million) of the forecasted budget is incorrectly allocated, with 0.9% being an underestimation and 0.8% being an overestimation.

For an averaged section length of 10 000 m, on average 16.2% (R62 million) of the forecasted budget is incorrectly allocated, with 8.3% being an underestimation and 8.0% being an overestimation.

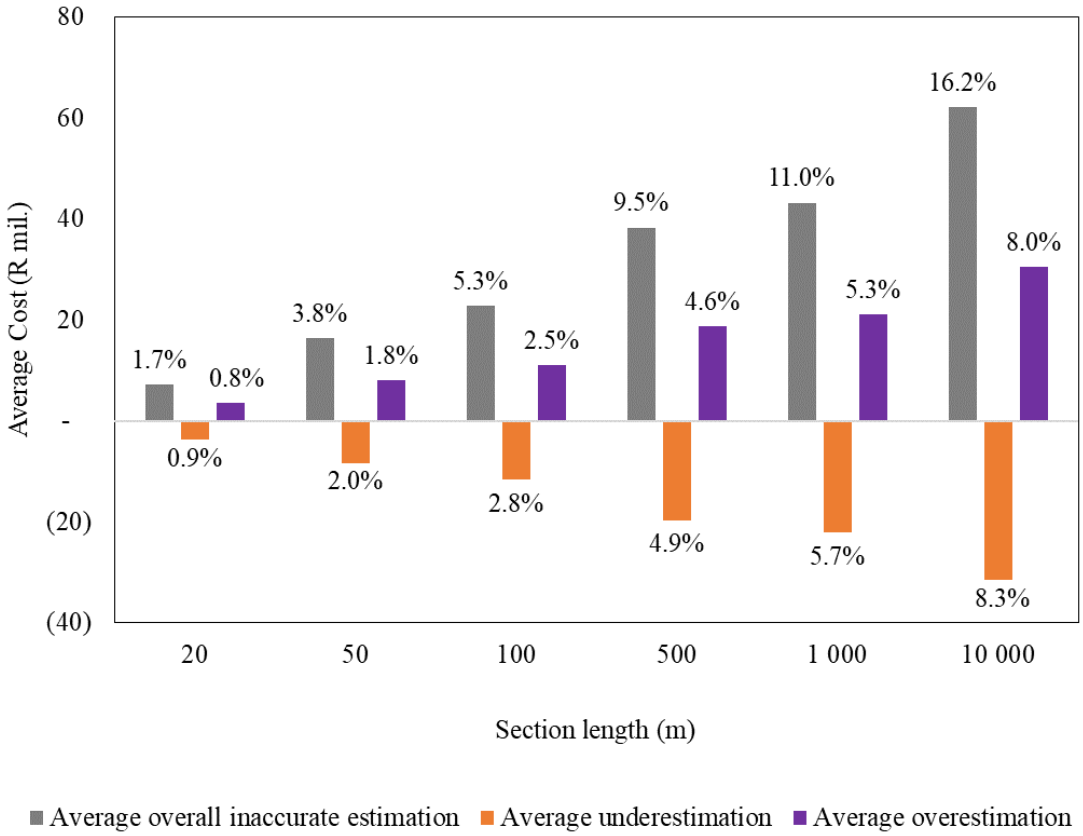


**Figure 4-7: Influence of averaged section lengths on budgetary forecasts**

## 4.2 AGGREGATED SECTION LENGTHS USING PERCENTILES

### 4.2.1 Descriptive statistics

Table 4-9 presents the average mean, minimum, and maximum rut depth across all samples per aggregated section length and percentile investigated. The average mean, minimum, and maximum rut depth increases with increasing section length and percentile, with the average minimum and maximum rut depth converging towards the mean with increasing section length.

**Table 4-9: Overall descriptive statistics per percentile**

| Distribution Parameter | | 20 m Sections | 50 m Sections | 100 m Sections | 500 m Sections | 1 000 m Sections | 10 000 m Sections |
|---|---|---|---|---|---|---|---|
| 50th Percentile (mm) | Mean | 5.079 | 4.997 | 4.948 | 4.809 | 4.769 | 4.635 |
| | Min | 0.247 | 0.372 | 0.633 | 1.655 | 1.987 | 3.240 |
| | Max | 22.492 | 18.834 | 16.908 | 10.733 | 8.849 | 5.989 |
| 75th Percentile (mm) | Mean | 5.416 | 5.782 | 6.041 | 6.367 | 6.418 | 6.482 |
| | Min | 0.280 | 0.662 | 1.006 | 2.400 | 2.851 | 4.740 |
| | Max | 24.323 | 20.808 | 19.473 | 13.900 | 11.993 | 8.380 |
| 90th Percentile (mm) | Mean | 5.618 | 6.411 | 6.918 | 7.876 | 8.097 | 8.456 |
| | Min | 0.297 | 0.769 | 1.259 | 2.987 | 3.698 | 6.190 |
| | Max | 25.580 | 23.301 | 21.369 | 17.225 | 15.445 | 11.027 |
| 95th Percentile (mm) | Mean | 5.685 | 6.621 | 7.349 | 8.736 | 9.126 | 9.776 |
| | Min | 0.302 | 0.791 | 1.327 | 3.430 | 4.196 | 7.155 |
| | Max | 26.040 | 24.779 | 23.348 | 19.407 | 17.569 | 12.922 |
| 99th Percentile (mm) | Mean | 5.739 | 6.789 | 7.694 | 9.989 | 10.833 | 12.790 |
| | Min | 0.306 | 0.806 | 1.365 | 4.105 | 4.922 | 8.995 |
| | Max | 26.442 | 26.160 | 25.796 | 23.194 | 21.681 | 17.605 |

### 4.2.2 Distribution of rut depth

Figure 4-8 to Figure 4-12 respectively present the cumulative distribution for the 50$^{th}$, 75$^{th}$, 90$^{th}$, 95$^{th}$, and 99$^{th}$ percentile for 20 m aggregated section lengths in comparison to the discrete 10 m section lengths for sample 1. An increase in the percentile results in an increased shift of the distribution towards the maximum 10 m section rut depth values. The dispersion of rut depth values (as indicated by the COV) remains approximately the same with increasing percentiles. All samples convey similar results. Results for all samples are provided in Appendix H.

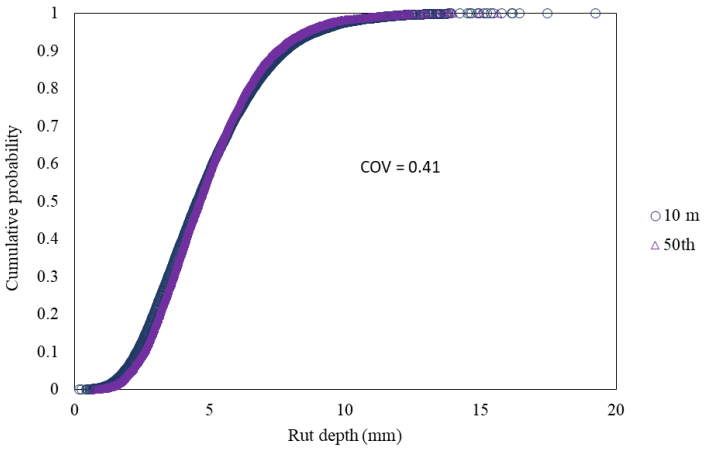


**Figure 4-8: Sample 1 cumulative distribution for 50th percentile 20 m section lengths**

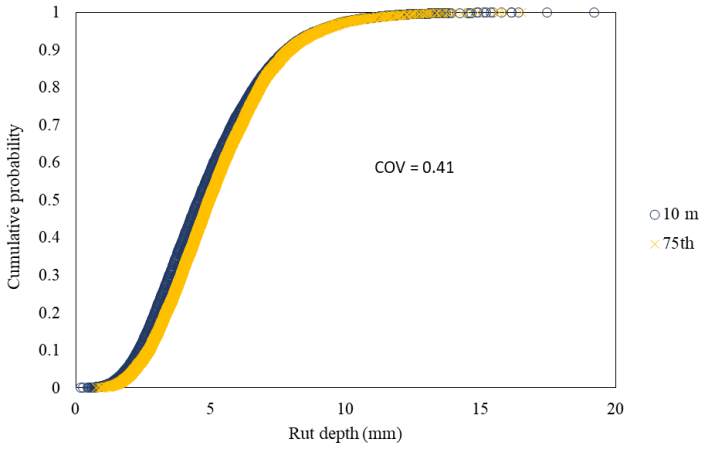


**Figure 4-9: Sample 1 cumulative distribution for 75th percentile 20 m section lengths**

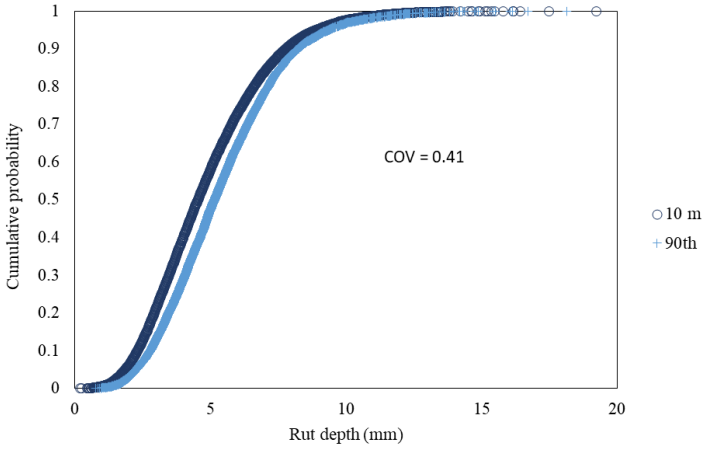


**Figure 4-10: Sample 1 cumulative distribution for 90th percentile 20 m section lengths**

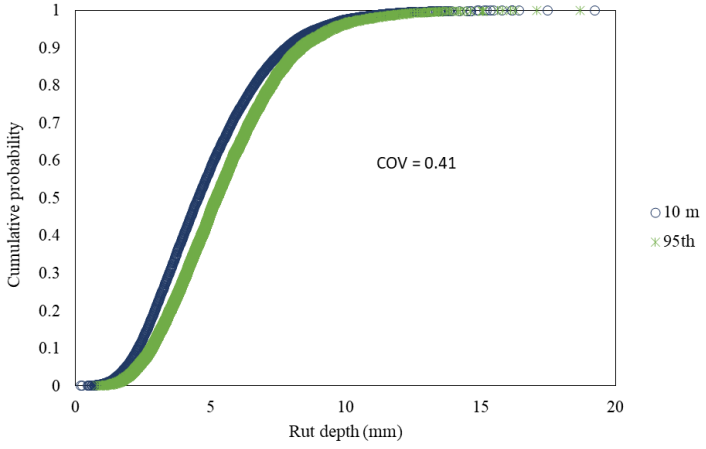


**Figure 4-11: Sample 1 cumulative distribution for 95th percentile 20 m section lengths**

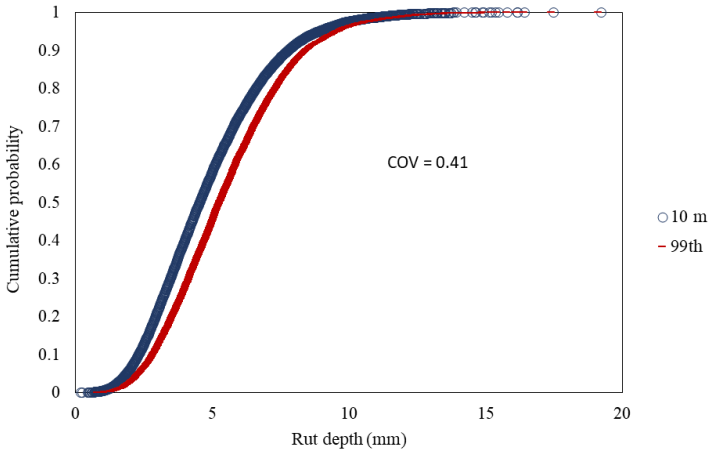


**Figure 4-12: Sample 1 cumulative distribution for 99th percentile 20 m section lengths**

Table 4-10 presents the average absolute percentage error in warning to severe rut depth condition categories across all samples per percentile. All percentiles present with an error in the estimation of percentage warning to severe rut depth. The minimum absolute error in warning to severe rut depth occurs in the 75$^{th}$ percentile for all aggregated section lengths investigated, with the minimum error occurring in 20 m section lengths and increasing with increasing section length.

In the comparison of the distribution of rut depth among varying aggregated section lengths, Jannat et al. (2015) similarly found that the 75$^{th}$ percentile appeared to be a more stable statistical parameter.

**Table 4-10: Overall average percentage error in warning to severe rut depth per percentile**

| Section Length (m) | Absolute error in warning to severe rut depth (%) | | | | | |
|---|---|---|---|---|---|---|
| | Average | 50th Percentile | 75th Percentile | 90th Percentile | 95th Percentile | 99th Percentile |
| 20 | 0.151 | 0.151 | 0.082 | 0.247 | 0.313 | 0.369 |
| 50 | 0.300 | 0.268 | 0.227 | 0.663 | 0.970 | 1.270 |
| 100 | 0.526 | 0.451 | 0.256 | 1.106 | 1.674 | 2.461 |
| 500 | 0.778 | 0.825 | 0.488 | 1.196 | 3.803 | 8.564 |
| 1 000 | 0.825 | 0.825 | 0.703 | 1.196 | 3.947 | 12.046 |
| 10 000 | 0.825 | 0.825 | 0.825 | 0.825 | 4.139 | 24.270 |
| Average | 0.568 | 0.558 | 0.430 | 0.872 | 2.474 | 8.163 |

Table 4-11 presents the percentage of samples presenting with an underestimation in the percentage warning to severe rut depth per percentile. Table 4-12 presents the percentage of samples presenting with an overestimation in the percentage warning to severe rut depth per percentile. The occurrence of an underestimation reduces with an increasing percentile, and the occurrence of an overestimation increases with an increasing percentile.

On average, overall, the 75$^{th}$ percentile presents with an underestimation in the percentage warning to severe rut depth in 64% of samples and an overestimation in the remaining 36% of samples. The 75$^{th}$ percentile, therefore, has a higher probability of underestimating the percentage warning to severe rut depth.

Should the importance of the road be considered, a percentile with a higher probability of overestimating the percentage warning to severe rut depth might be preferred for data processing. The 90$^{th}$, 95$^{th}$, and 99$^{th}$ percentiles all present with high probabilities of overestimation, i.e., 68%, 81%, and 94%, respectively. However, the average overall absolute average error increases with an increasing percentile, with the 90$^{th}$ percentile presenting with the smallest error, as shown in Table 4-10 above.

**Table 4-11: Percentage occurrence of underestimation in warning to severe rut depth per percentile**

| Section Length (m) | % Occurrence of underestimation in warning to severe rut depth | | | | | |
|---|---|---|---|---|---|---|
| | Average | 50th Percentile | 75th Percentile | 90th Percentile | 95th Percentile | 99th Percentile |
| 20 | 100 | 100 | 23 | 0 | 0 | 0 |
| 50 | 100 | 100 | 15 | 8 | 0 | 0 |
| 100 | 100 | 100 | 46 | 8 | 8 | 0 |
| 500 | 100 | 100 | 100 | 23 | 15 | 8 |
| 1 000 | 100 | 100 | 100 | 54 | 23 | 8 |
| 10 000 | 100 | 100 | 100 | 100 | 69 | 23 |
| Average | 100 | 100 | 64 | 32 | 19 | 6 |

**Table 4-12: Percentage occurrence of overestimation in warning to severe rut depth per percentile**

| Section Length (m) | % Occurrence of overestimation in warning to severe rut depth | | | | | |
|---|---|---|---|---|---|---|
| | Average | 50th Percentile | 75th Percentile | 90th Percentile | 95th Percentile | 99th Percentile |
| 20 | 0 | 0 | 77 | 100 | 100 | 100 |
| 50 | 0 | 0 | 85 | 92 | 100 | 100 |
| 100 | 0 | 0 | 54 | 92 | 92 | 100 |
| 500 | 0 | 0 | 0 | 77 | 85 | 92 |
| 1 000 | 0 | 0 | 0 | 46 | 77 | 92 |
| 10 000 | 0 | 0 | 0 | 0 | 31 | 77 |
| Average | 0 | 0 | 36 | 68 | 81 | 94 |

Samples 6 and 7, not presenting with any severe rut depth in the discrete 10 m sections, do not present with an error in the estimation of severe rut depth for percentile aggregated section lengths. As discussed previously, an increase in percentile results in an increased shift of the distribution towards the maximum 10 m section rut depth values; this maximum is not exceeded. Additionally, with the dispersion of rut depth around the mean reducing with increasing aggregated section lengths, the maximum rut depth converges towards the mean, i.e., percentiles values converge towards the mean with increasing aggregated section lengths.

### 4.2.3 Maintenance requirements

Table 4-13 illustrates the average absolute percentage error in heavy rehabilitation (minority treatment) length across all samples per percentile and aggregated section length investigated. The error discussed only considers the change in treatment length; no change in treatment year is taken into account.

The average minimum absolute error occurs in the 75$^{th}$ percentile for all section lengths investigated, with the minimum error occurring in 20 m section lengths and increasing with increasing section length. On average, the 75$^{th}$ percentile also presented with the highest occurrence of a 0% error in treatment length.

The average minimum absolute error in the 75$^{th}$ percentile is approximately 40% or less in section lengths up to 100 m, with the error increasing to 70% and above for section lengths of 500 m and above. An error less than that occurring in the averaged 20 m section length occurs in the 75$^{th}$ percentile of 50 m section lengths.

On average, overall, the 75$^{th}$ percentile presented with an underestimation of the heavy rehabilitation treatment length in 55% of samples and an overestimation in 24% of samples. The 75$^{th}$ percentile, therefore, has a higher probability of underestimating the heavy rehabilitation treatment length. The minimum error for the abovementioned 79% of samples occurred in the 75$^{th}$ percentile. No error occurred in the remaining 21% of samples.

Should the importance of the road be considered, a percentile with a higher probability of overestimating the heavy rehabilitation treatment length might be preferred for data processing. The 90$^{th}$, 95$^{th}$, and 99$^{th}$ percentiles all present with high probabilities of overestimation, i.e., 51%, 59%, and 79%, respectively. However, the average overall absolute average error increases with an increasing percentile, with the 90$^{th}$ percentile presenting with the smallest error. The minimum error occurred in the 90$^{th}$ percentile in 29% of the 51% of samples presenting with an overestimation in the 90$^{th}$ percentile. Of the samples presenting with an overestimation in the 95$^{th}$ and 99$^{th}$ percentiles, only 17% and 28% presented with the minimum error in these percentiles.

The 90$^{th}$ percentile presents with a smaller error in 100 m section lengths than in 50 m section lengths.

**Table 4-13: Average error in heavy rehabilitation maintenance decision per percentile for samples overall**

| Section length | Percentile | % Minimum underestimated[1] (%) | Average underestimated error[2] (%) | % Minimum overestimated[3] (%) | Average overestimated error[4] (%) | No error[5] (%) | % Overall underestimated[6] (%) | % Overall overestimated[7] (%) | Absolute overall error[8] (%) |
|---|---|---|---|---|---|---|---|---|---|
| 20 m | Average | 62 | -24 | 0 | - | 15 | 85 | 0 | 29 |
| | 50th | 62 | -24 | 0 | - | 15 | 85 | 0 | 29 |
| | 75th | 38 | -26 | 46 | 18 | 15 | 38 | 46 | 18 |
| | 90th | 0 | - | 31 | 34 | 23 | 0 | 77 | 34 |
| | 95th | 0 | - | 23 | 32 | 23 | 0 | 77 | 39 |
| | 99th | 0 | - | 15 | 27 | 15 | 0 | 85 | 47 |
| 50 m | Average | 54 | -58 | 0 | - | 23 | 77 | 0 | 46 |
| | 50th | 38 | -58 | 8 | 18 | 31 | 62 | 8 | 33 |
| | 75th | 15 | -51 | 46 | 28 | 38 | 15 | 46 | 21 |
| | 90th | 0 | - | 38 | 174 | 15 | 0 | 85 | 113 |
| | 95th | 0 | - | 15 | 300 | 15 | 0 | 85 | 145 |
| | 99th | 0 | - | 15 | 300 | 15 | 0 | 85 | 162 |
| 100 m | Average | 62 | -89 | 0 | - | 15 | 85 | 0 | 72 |
| | 50th | 77 | -79 | 0 | - | 15 | 85 | 0 | 66 |
| | 75th | 31 | -78 | 46 | 42 | 23 | 31 | 46 | 43 |
| | 90th | 8 | -100 | 46 | 102 | 15 | 8 | 77 | 94 |
| | 95th | 0 | - | 15 | 500 | 15 | 0 | 85 | 249 |
| | 99th | 0 | - | 8 | 900 | 15 | 0 | 85 | 338 |
| 500 m | Average | 77 | -100 | 0 | - | 15 | 85 | 0 | 85 |
| | 50th | 77 | -100 | 0 | - | 15 | 85 | 0 | 85 |
| | 75th | 77 | -92 | 8 | 39 | 15 | 77 | 8 | 74 |
| | 90th | 46 | -100 | 31 | 199 | 15 | 46 | 38 | 121 |
| | 95th | 23 | -100 | 31 | 541 | 15 | 23 | 62 | 306 |
| | 99th | 0 | - | 38 | 1 933 | 15 | 0 | 85 | 1 285 |
| 1 000 m | Average | 77 | -100 | 0 | - | 15 | 85 | 0 | 85 |
| | 50th | 77 | -100 | 0 | - | 15 | 85 | 0 | 85 |
| | 75th | 85 | -93 | 0 | - | 15 | 85 | 0 | 79 |
| | 90th | 54 | -100 | 31 | 131 | 15 | 54 | 31 | 94 |
| | 95th | 46 | -100 | 8 | 488 | 15 | 46 | 38 | 210 |
| | 99th | 0 | - | 46 | 2 501 | 15 | 0 | 85 | 1 644 |
| 10 000 m | Average | 85 | -100 | 0 | - | 15 | 85 | 0 | 85 |
| | 50th | 85 | -100 | 0 | - | 15 | 85 | 0 | 85 |
| | 75th | 85 | -100 | 0 | - | 15 | 85 | 0 | 85 |
| | 90th | 85 | -100 | 0 | - | 15 | 85 | 0 | 85 |
| | 95th | 77 | -100 | 8 | 652 | 15 | 77 | 8 | 127 |
| | 99th | 31 | -100 | 46 | 9 134 | 15 | 31 | 54 | 4 470 |
| Overall | Average | 69 | | 0 | | | 83 | 0 | 67 |
| | 50th | 69 | | 1 | | | 81 | 1 | 64 |
| | 75th | 55 | | 24 | | | 55 | 24 | 53 |
| | 90th | 32 | | 29 | | | 32 | 51 | 90 |
| | 95th | 24 | | 17 | | | 24 | 59 | 179 |
| | 99th | 5 | | 28 | | | 5 | 79 | 1 324 |

[1]Percentage of samples presenting with a minimum underestimated error in the respective percentile
[2]The average minimum underestimated error
[3]Percentage of samples presenting with a minimum overestimated error in the respective percentile
[4]The average minimum overestimated error
[5]The percentage of samples presenting with no error in the respective percentile
[6]Percentage of samples presenting with an underestimated error in the respective percentile
[7]Percentage of samples presenting with an overestimated error in the respective percentile
[8]Absolute average overall error

Table 4-14 illustrates the average absolute percentage error in light rehabilitation / reseal (majority treatment) length across all samples per percentile and aggregated section length investigated. The error discussed only considers the change in treatment length; no change in treatment year is taken into account.

The error in light rehabilitation / reseal length is marginal in comparison to the treatment length. However, the average minimum absolute error occurs in the 75$^{th}$ percentile for all section lengths investigated. The 20 m section length presents will the smallest error, followed by the 100 m section length, 50 m section length, 500 m section length, and finally, the 10 000 m section length. On average, the 75$^{th}$ percentile also presented with the highest occurrence of a 0% error in treatment length.

An error approximately equal to that occurring in the averaged 20 m section length occurs in the 75th percentile of up to 100 m section lengths.

Where heavy rehabilitation is overestimated in the 75th percentile, light rehabilitation / reseal is underestimated, and vice versa.

**Table 4-14: Average error in light rehabilitation / reseal maintenance decision per percentile for samples overall**

| Section length | Percentile | % Minimum underestimated[1] (%) | Average underestimated error[2] (%) | % Minimum overestimated[3] (%) | Average overestimated error[4] (%) | No error[5] (%) | % Overall underestimated[6] (%) | % Overall overestimated[7] (%) | Absolute overall error[8] (%) |
|---|---|---|---|---|---|---|---|---|---|
| 20 m | Average | 0 | - | 62 | 0.084 | 15 | 0 | 85 | 0.082 |
| | 50th | 0 | - | 62 | 0.084 | 15 | 0 | 85 | 0.082 |
| | 75th | 46 | -0.065 | 38 | 0.029 | 15 | 46 | 38 | 0.041 |
| | 90th | 31 | -0.069 | 0 | - | 23 | 77 | 0 | 0.113 |
| | 95th | 23 | -0.035 | 0 | - | 23 | 77 | 0 | 0.145 |
| | 99th | 15 | -0.022 | 0 | - | 15 | 85 | 0 | 0.173 |
| 50 m | Average | 0 | - | 54 | 0.118 | 23 | 0 | 77 | 0.135 |
| | 50th | 8 | -0.049 | 38 | 0.084 | 31 | 8 | 62 | 0.124 |
| | 75th | 46 | -0.189 | 15 | 0.030 | 38 | 46 | 15 | 0.092 |
| | 90th | 38 | -0.150 | 0 | - | 15 | 85 | 0 | 0.333 |
| | 95th | 15 | -0.139 | 0 | - | 15 | 85 | 0 | 0.434 |
| | 99th | 15 | -0.139 | 0 | - | 15 | 85 | 0 | 0.577 |
| 100 m | Average | 0 | - | 62 | 0.183 | 15 | 0 | 85 | 0.248 |
| | 50th | 0 | - | 77 | 0.245 | 15 | 0 | 85 | 0.216 |
| | 75th | 46 | -0.159 | 31 | 0.046 | 23 | 46 | 31 | 0.087 |
| | 90th | 46 | -0.324 | 8 | 0.050 | 15 | 77 | 8 | 0.493 |
| | 95th | 15 | -0.252 | 0 | - | 15 | 85 | 0 | 0.820 |
| | 99th | 8 | -0.449 | 0 | - | 15 | 85 | 0 | 1 |
| 500 m | Average | 0 | - | 77 | 0.283 | 15 | 0 | 85 | 0.385 |
| | 50th | 0 | - | 77 | 0.283 | 15 | 0 | 85 | 0.385 |
| | 75th | 8 | -0.174 | 77 | 0.292 | 15 | 8 | 77 | 0.238 |
| | 90th | 31 | -2 | 46 | 0.118 | 15 | 38 | 46 | 0.715 |
| | 95th | 31 | -0.798 | 23 | 0.041 | 15 | 62 | 23 | 1 |
| | 99th | 38 | -0.917 | 0 | - | 15 | 85 | 0 | 4 |
| 1 000 m | Average | 0 | - | 77 | 0.283 | 15 | 0 | 85 | 0.385 |
| | 50th | 0 | - | 77 | 0.283 | 15 | 0 | 85 | 0.385 |
| | 75th | 0 | - | 85 | 0.306 | 15 | 0 | 85 | 0.259 |
| | 90th | 31 | -2 | 54 | 0.141 | 15 | 31 | 54 | 0.549 |
| | 95th | 8 | -1 | 46 | 0.118 | 15 | 38 | 46 | 1 |
| | 99th | 46 | -3 | 0 | - | 15 | 85 | 0 | 6 |
| 10 000 m | Average | 0 | - | 85 | 0.454 | 15 | 0 | 85 | 0.385 |
| | 50th | 0 | - | 85 | 0.454 | 15 | 0 | 85 | 0.385 |
| | 75th | 0 | - | 85 | 0.454 | 15 | 0 | 85 | 0.385 |
| | 90th | 0 | - | 85 | 0.454 | 15 | 0 | 85 | 0.385 |
| | 95th | 8 | -14 | 77 | 0.283 | 15 | 8 | 77 | 1 |
| | 99th | 46 | -20 | 31 | 0.056 | 15 | 54 | 31 | 14 |
| Overall | Average | 0 | | 69 | | | 0 | 83 | 0.270 |
| | 50th | 1 | | 69 | | | 1 | 81 | 0.263 |
| | 75th | 24 | | 55 | | | 24 | 55 | 0.184 |
| | 90th | 29 | | 32 | | | 51 | 32 | 0.431 |
| | 95th | 17 | | 24 | | | 59 | 24 | 0.901 |
| | 99th | 28 | | 5 | | | 79 | 5 | 4 |

[1]Percentage of samples presenting with a minimum underestimated error in the respective percentile
[2]The average minimum underestimated error
[3]Percentage of samples presenting with a minimum overestimated error in the respective percentile
[4]The average minimum overestimated error
[5]The percentage of samples presenting with no error in the respective percentile
[6]Percentage of samples presenting with an underestimated error in the respective percentile
[7]Percentage of samples presenting with an overestimated error in the respective percentile
[8]Absolute average overall error

Samples 6 and 7, containing only a light rehabilitation or reseal, do not present with any error in treatment length. The severity of rut depth and the condition of other maintenance drivers did not warrant a heavy rehabilitation in the discrete 10 m sections. These samples do not present with any severe (>20 mm) rut depth in the discrete 10 m sections, which is the only instance in which rut depth solely influences the requirement for a heavy rehabilitation. For

sections containing sound to warning rut depth (<20 mm), the requirement for a heavy rehabilitation is additionally dependent on the condition of other maintenance drivers. Introducing higher percentiles, which increases the shift of the distribution towards the maximum 10 m section rut depth value (<20 mm), does not sufficiently increase maintenance drivers, influenced by rut depth, such as roughness and the overall condition index to trigger a heavy rehabilitation requirement as the condition of other maintenance drivers still play a role.

However, it should be noted that should the condition of other maintenance drivers be severe enough that maintenance drivers influenced by rut depth are just below the criteria required to trigger a heavy rehabilitation, introducing higher percentile rut depth might sufficiently increase the condition of these maintenance drivers to trigger a heavy rehabilitation.

### 4.2.4 Funding implications

On average, across all aggregated section lengths and samples, the total portion of the predicted budget being incorrectly allocated due to an inaccurately estimated financial need per treatment type over the analysis period is shown in Figure 4-13 and Figure 4-14 per percentile. The inaccuracies discussed here only consider errors in the predicted treatment type and not errors in treatment years. Therefore, inaccuracies in the annual financial need are not considered; only inaccuracies in the total financial need over the analysis period are considered.

Figure 4-13 shows the inaccurately estimated financial need for heavy rehabilitation. When compared to the mean, the 50$^{th}$ and 75$^{th}$ percentile present with a lower overall inaccuracy in the predicted financial need for heavy rehabilitation, with the 75$^{th}$ percentile presenting with the lowest inaccuracy. On average, overall, 53% (R1 million) of the forecasted budget is incorrectly allocated, which is 14% lower than the inaccuracy yielded from using the average as the statistical aggregation measure. On average, 71% (R1.1 million) of the budget is underestimated, and 29% (R0.7 million) is overestimated with the 75$^{th}$ percentile.

After the 75$^{th}$ percentile, the degree to which the budget is inaccurately estimated for heavy rehabilitation increases with increasing percentile.

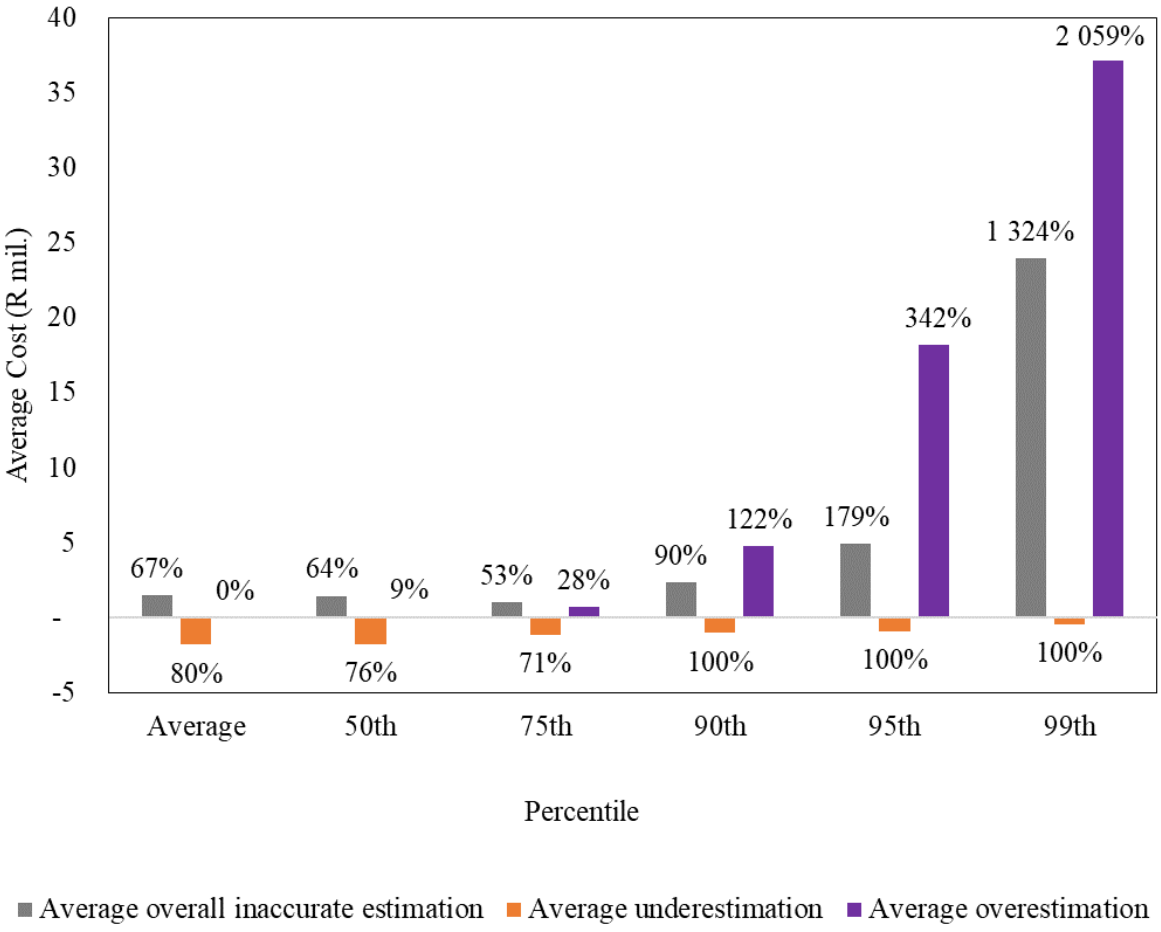


**Figure 4-13: Influence of percentiles on heavy rehabilitation budgetary forecasts (not considering inaccuracies in the annual financial need)**

Figure 4-14 shows the inaccurately estimated financial need for light rehabilitation / reseals. The 75$^{th}$ percentile presents with the lowest overall inaccuracy in the predicted financial need for light rehabilitation / reseals. On average, overall, 0.2% (R0.6 million) of the forecasted budget is incorrectly allocated, which is 0.1% lower than the inaccuracy yielded from using the average as the statistical aggregation measure. On average, 0.1% (R0.5 million) of the budget is underestimated, and 0.2% (R0.6 million) is overestimated with the 75$^{th}$ percentile.

After the 75$^{th}$ percentile, the degree to which the budget is inaccurately estimated for light rehabilitation / reseals increases with increasing percentile.

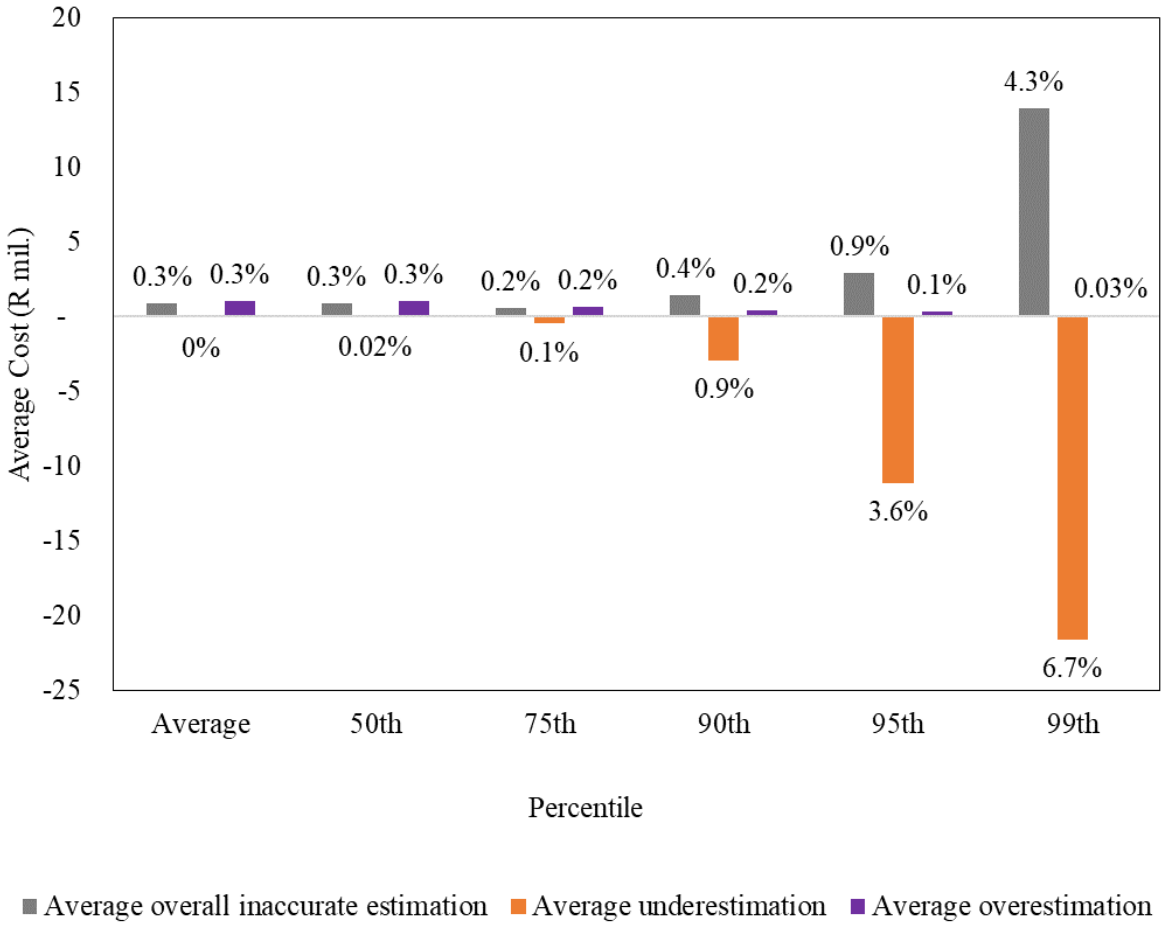


**Figure 4-14: Influence of percentiles on light rehabilitation / reseal budgetary forecasts (not considering inaccuracies in the annual financial need)**

On average, across all aggregated section lengths and samples, the total portion of the predicted budget being incorrectly allocated due to an inaccurately estimated financial need per year and/or treatment type is shown in Figure 4-15 and Figure 4-16 per percentile. Inaccuracies in the annual financial need are considered here.

Figure 4-15 shows the inaccurately estimated financial need for heavy rehabilitation. When compared to the mean, the 50$^{th}$ and 75$^{th}$ percentile present with a lower overall inaccuracy in the predicted financial need for heavy rehabilitation, with the 75$^{th}$ percentile presenting with the lowest inaccuracy. On average, overall, 68% (R1.5 million) of the forecasted budget is incorrectly allocated, which is 6% lower than the inaccuracy yielded from using the average as the statistical aggregation measure. On average, 53% (R1.1 million) of the budget is underestimated, and 14% (R0.4 million) is overestimated with the 75$^{th}$ percentile.

After the 75$^{th}$ percentile, the degree to which the budget is inaccurately estimated for heavy rehabilitation increases with increasing percentile.

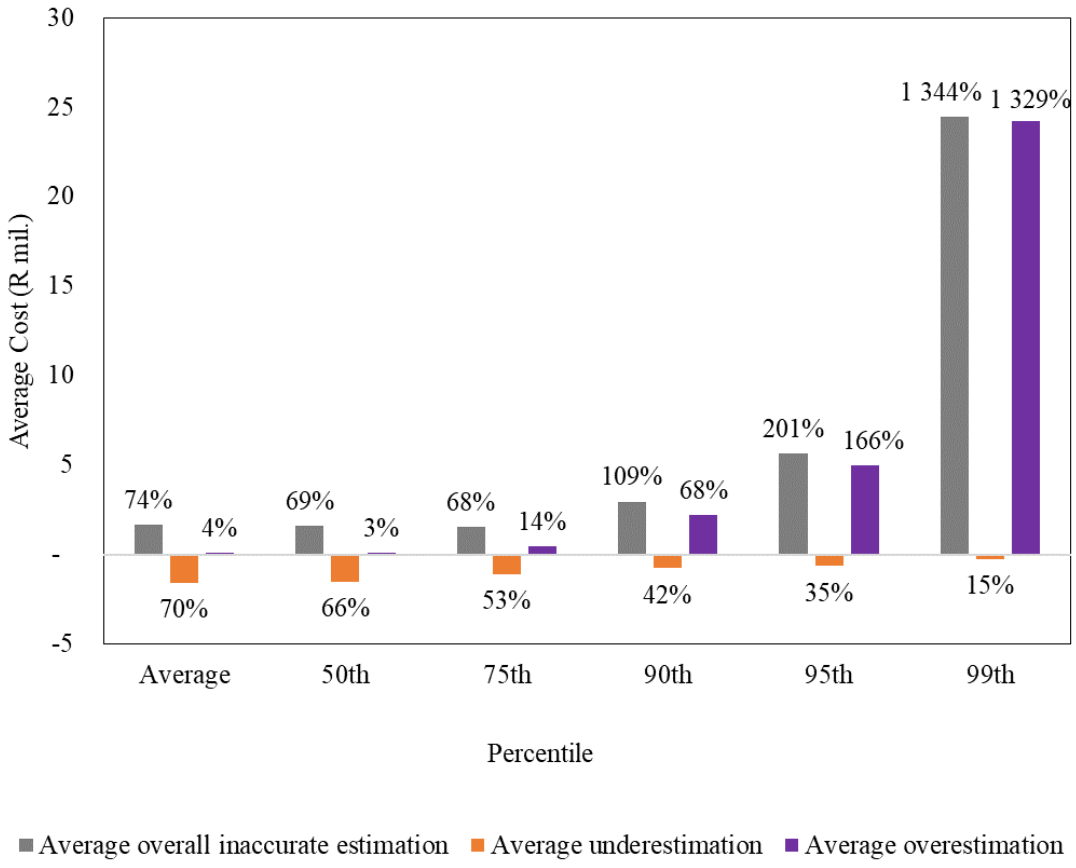


**Figure 4-15: Influence of percentiles on heavy rehabilitation budgetary forecasts (considering inaccuracies in the annual financial need)**

Figure 4-16 shows the inaccurately estimated financial need for light rehabilitation / reseals. When compared to the mean, only the 50$^{th}$ percentile presents with a lower overall inaccuracy in the predicted financial need for light rehabilitation / reseals. Under the 50$^{th}$ percentile, 6% (R23 million) of the forecasted budget is incorrectly allocated on average overall, which is 2% lower than the inaccuracy yielded from using the average as the statistical aggregation measure. On average, 3% (R11 million) of the budget is underestimated, and 3% (R11 million) is overestimated with the 50$^{th}$ percentile. Under the 75$^{th}$ percentile, 11% (R42 million) of the forecasted budget is incorrectly allocated on average overall, which is 3% higher than the inaccuracy yielded from using the average as the statistical aggregation measure. On average, 5% (R21 million) of the budget is underestimated, and 5% (R21 million) is overestimated with the 75$^{th}$ percentile.

The degree to which the budget is inaccurately estimated for light rehabilitation / reseals increases with increasing percentile.

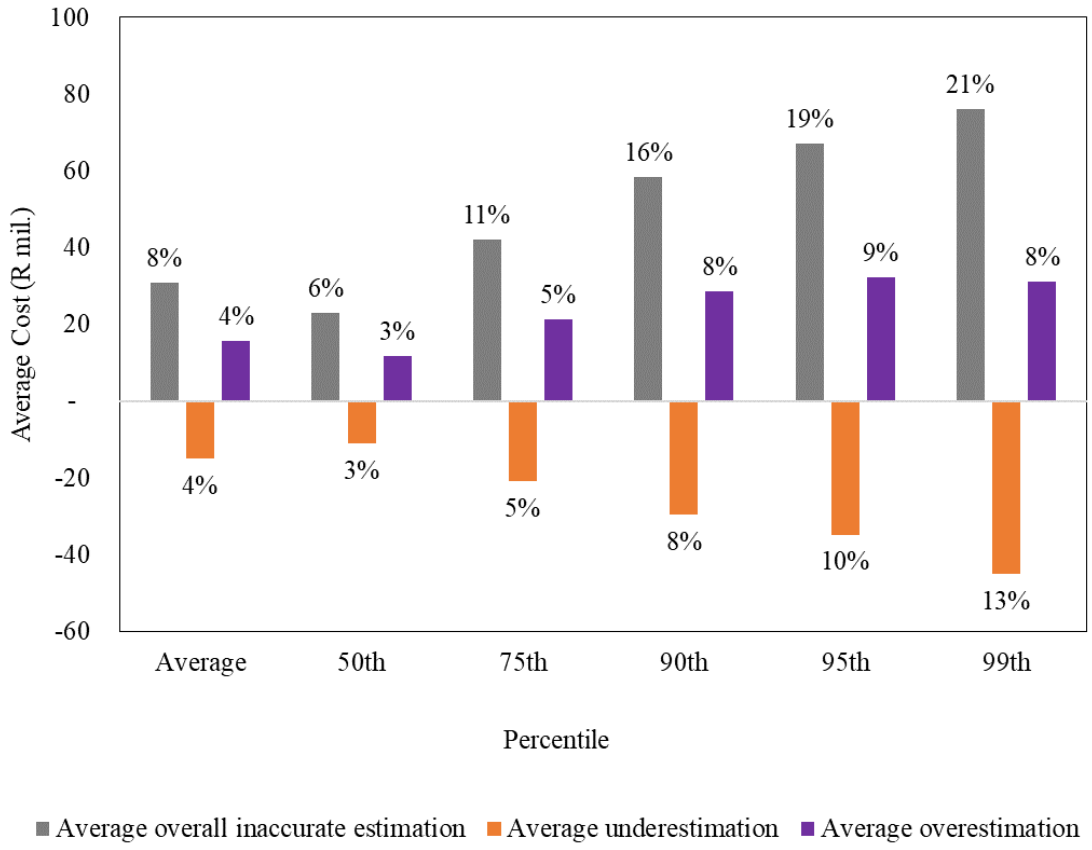


**Figure 4-16: Influence of percentiles on light rehabilitation / reseal budgetary forecasts (considering inaccuracies in the annual financial need)**

## 4.3 APPLICATION WITHIN THE SOUTH AFRICAN NRA (1999) SPECIFICATION

The influence of average and percentile statistical aggregation measures on the acceptance criteria specified in the NRA (1999) is presented in Table 4-15.

**Table 4-15: Influence of statistical aggregation measures on NRA (1999) acceptance criteria**

| Sample | Statistical Aggregation Measure | Acceptance Criteria for Rut Depth | | | | | |
|---|---|---|---|---|---|---|---|
| | | Maximum 10% of segment worse than 15 mm | | Maximum 5% of segment worse than 20 mm | | Maximum 0% of segment worse than 25 mm | |
| | | % exceeding 15 mm | Within limits? | % exceeding 20 mm | Within limits? | % exceeding 25 mm | Within limits? |
| 1 | 10 m Discrete | 0 | Yes | 0 | Yes | 0 | Yes |
| | 100 m Average | 0 | Yes | 0 | Yes | 0 | Yes |
| | 100 m 50$^{th}$ Percentile | 0 | Yes | 0 | Yes | 0 | Yes |
| | 100 m 75$^{th}$ Percentile | 0 | Yes | 0 | Yes | 0 | Yes |

| Sample | Statistical Aggregation Measure | Acceptance Criteria for Rut Depth | | | | | |
|---|---|---|---|---|---|---|---|
| | | Maximum 10% of segment worse than 15 mm | | Maximum 5% of segment worse than 20 mm | | Maximum 0% of segment worse than 25 mm | |
| | | % exceeding 15 mm | Within limits? | % exceeding 20 mm | Within limits? | % exceeding 25 mm | Within limits? |
| | 100 m 90th Percentile | 0 | Yes | 0 | Yes | 0 | Yes |
| | 100 m 95th Percentile | 0 | Yes | 0 | Yes | 0 | Yes |
| | 100 m 99th Percentile | 0 | Yes | 0 | Yes | 0 | Yes |
| 2 | 10 m Discrete | 8 | Yes | 0 | Yes | 0 | Yes |
| | 100 m Average | 0 | Yes | 0 | Yes | 0 | Yes |
| | 100 m 50th Percentile | 0 | Yes | 0 | Yes | 0 | Yes |
| | 100 m 75th Percentile | 3 | Yes | 0 | Yes | 0 | Yes |
| | 100 m 90th Percentile | 20 | No | 0 | Yes | 0 | Yes |
| | 100 m 95th Percentile | 22 | No | 0 | Yes | 0 | Yes |
| | 100 m 99th Percentile | 48 | No | 0 | Yes | 0 | Yes |
| 3 | 10 m Discrete | 5 | Yes | 2 | Yes | 0 | Yes |
| | 100 m Average | 0 | Yes | 0 | Yes | 0 | Yes |
| | 100 m 50th Percentile | 0 | Yes | 0 | Yes | 0 | Yes |
| | 100 m 75th Percentile | 5 | Yes | 0 | Yes | 0 | Yes |
| | 100 m 90th Percentile | 12 | No | 0 | Yes | 0 | Yes |
| | 100 m 95th Percentile | 15 | No | 10 | No | 0 | Yes |
| | 100 m 99th Percentile | 15 | No | 12 | No | 0 | Yes |
| 4 | 10 m Discrete | 5 | Yes | 3 | Yes | 2 | No |
| | 100 m Average | 2 | Yes | 0 | Yes | 0 | Yes |
| | 100 m 50th Percentile | 1 | Yes | 0 | Yes | 0 | Yes |
| | 100 m 75th Percentile | 6 | Yes | 3 | Yes | 1 | No |
| | 100 m 90th Percentile | 7 | Yes | 4 | Yes | 2 | No |
| | 100 m 95th Percentile | 8 | Yes | 5 | Yes | 2 | No |
| | 100 m 99th Percentile | 8 | Yes | 5 | Yes | 2 | No |
| 5 | 10 m Discrete | 28 | No | 8 | No | 1 | No |
| | 100 m Average | 22 | No | 0 | Yes | 0 | Yes |
| | 100 m 50th Percentile | 30 | No | 0 | Yes | 0 | Yes |
| | 100 m 75th Percentile | 42 | No | 0 | Yes | 0 | Yes |
| | 100 m 90th Percentile | 47 | No | 23 | No | 0 | Yes |
| | 100 m 95th Percentile | 49 | No | 27 | No | 0 | Yes |

| Sample | Statistical Aggregation Measure | Acceptance Criteria for Rut Depth | | | | | |
|---|---|---|---|---|---|---|---|
| | | Maximum 10% of segment worse than 15 mm | | Maximum 5% of segment worse than 20 mm | | Maximum 0% of segment worse than 25 mm | |
| | | % exceeding 15 mm | Within limits? | % exceeding 20 mm | Within limits? | % exceeding 25 mm | Within limits? |
| | 100 m 99$^{th}$ Percentile | 51 | No | 40 | No | 7 | No |

While the percentage of the road segment presenting with rut depth worse than the specified limiting value cannot always be accurately predicted with average and statistical aggregation measures, when compared to the results of the 'discrete' 10 m rut depth measurements, the 75$^{th}$ percentile presents with the highest occurrence (4 out of 5 samples) of providing an accurate representation of whether these performance requirements are being met or not.

The 75$^{th}$ percentile does not always accurately represent the "maximum 0% of segment worse than 25 mm" acceptance criteria, underestimating this percentage in one sample. The 99$^{th}$ percentile accurately represents the "maximum 0% of segment worse than 25 mm" acceptance criteria in all samples. However, the "maximum 5% of segment worse than 20 mm" and "maximum 10% of segment worse than 15 mm" acceptance criteria are inaccurately represented with overestimation in 2 out of the 5 samples. The importance of the road being maintained should once again be taken into consideration when selecting a percentile for data processing.

Table 4-16 summarises the number of samples for which the average and statistical aggregation measures provide an accurate representation of whether these performance requirements are being met or not.

**Table 4-16: Summary of samples correctly representing NRA (1999) acceptance criteria per statistical aggregation measure**

| Statistical Aggregation Measure | Number of samples correctly representing NRA (1999) acceptance criteria |
|---|---|
| Average | 3 |
| 50$^{th}$ Percentile | 3 |
| 75$^{th}$ Percentile | 4 |
| 90$^{th}$ Percentile | 2 |
| 95$^{th}$ Percentile | 2 |
| 99$^{th}$ Percentile | 3 |

The aggregation interval, distribution of rut depth values amongst different rut depth severity categories, and the distribution of rut depth values over the segment length influence the results of this study. It is recommended that the study be repeated with a larger sample size and an aggregation interval of 10 m, as used in practice, to determine the accuracy of these results.

# 5 CONCLUSIONS AND RECOMMENDATIONS

## 5.1 CONCLUSIONS

This study investigated the potential effects, as influenced by varying aggregated section lengths, of using statistical aggregation measures, namely, averages and percentiles, to analyse high-density automated rutting data, on the distribution of calculated rut depth over a pavement section and the respective maintenance, funding, and pavement performance requirements.

### 5.1.1 Aggregated section lengths using averages

The following findings were obtained from studying the influence of varying aggregated section lengths, considering mean as the statistical aggregation measure, on the distribution of calculated rut depth and the respective maintenance and funding requirements.

**1. Descriptive statistics**

The dispersion of rut depth around the mean reduces with increasing averaged section length, with the minimum and maximum rut depth values converging towards the mean.

**2. Distribution of rut depth**

46% of samples transition from an exponential or lognormal distribution to a normal distribution with increasing averaged section length, 23% of samples transition from a normal or lognormal distribution to an exponential distribution, and the remaining 31% remain a lognormal distribution.

With the dispersion and range of possible rut depth values reducing with increasing averaged section length, the percentage of minority rut depth values classified as moderate to severe also reduces.

**3. Maintenance requirements**

- The percentage error in the overall maintenance decision increases with increasing averaged section length, resulting in inaccurate treatment types, treatment lengths, and treatment years;
- No direct relationship is evident between the degree of the error in maintenance decisions and the dispersion of rut depth values. The degree of error is influenced by the averaged section length, the distribution of rut depth values amongst different rut depth severity categories, the distribution of rut depth values over the segment length, and the condition of other maintenance drivers such as roughness, cracking, patching, potholes, and ravelling;
- With increasing averaged section length, the minority of severe (>20 mm) rut depth values are averaged out amongst the majority lower rut depth values, thereby decreasing heavy

rehabilitation treatment lengths and increasing light rehabilitation / reseal treatment lengths, and

- On average, 42% of averaged sections triggering a light rehabilitation one year later than what was deemed necessary, when considering the 'true' pavement conditions as indicated by the discrete 10 m sections, can no longer be effectively treated with a light rehabilitation and rather require a heavy rehabilitation.

**4. Funding implications**

- Incorrectly identified maintenance requirements resulting from using averages to analyse automated rutting data results in inaccurate maintenance and rehabilitation budgetary forecasts;
- The total portion of the predicted budget being incorrectly allocated due to an inaccurately estimated financial need per year and/or treatment type increases with increasing averaged section length;
- For an averaged section length of 20 m, on average 1.7% (R7 million) of the forecasted budget is incorrectly allocated, with 0.9% being an underestimation and 0.8% being an overestimation, and
- For an averaged section length of 10 000 m, on average 16.2% (R62 million) of the forecasted budget is incorrectly allocated, with 8.3% being an underestimation and 8.0% being an overestimation.

### 5.1.2 Aggregated section lengths using percentiles

The following findings were obtained from studying the influence of varying aggregated section lengths, considering percentiles as the statistical aggregation measure, on the distribution of calculated rut depth and the respective maintenance and funding requirements.

**1. Descriptive statistics**

The mean, minimum, and maximum rut depth increases with increasing aggregated section length and percentile, with the minimum and maximum rut depth converging towards the mean with increasing section length.

**2. Distribution of rut depth**

- An increase in the percentile results in an increased shift of the distribution towards the maximum discrete 10 m section rut depth values. The dispersion of rut depth remains approximately the same with increasing percentiles;

- All percentiles present with an error in the estimation of percentage warning to severe rut depth;
- The minimum absolute error in warning to severe rut depth occurs in the 75$^{th}$ percentile for all aggregated section lengths investigated, with the error increasing with increasing section length;
- The 75$^{th}$ percentile presented with an underestimation in the percentage warning to severe rut depth in 64% of samples and an overestimation in the remaining 36% of samples;
- The 90$^{th}$, 95$^{th}$, and 99$^{th}$ percentiles present with higher probabilities of overestimation, i.e., 68%, 81%, and 94%, respectively. The 90$^{th}$ percentile, however, presents with a lower error in the estimation of percentage warning to severe rut depth than the 95$^{th}$ and 99$^{th}$ percentile, and
- Samples not presenting with any severe rut depth in the discrete 10 m sections do not present with an error in the estimation of severe rut depth.

**3. Maintenance requirements**

- The minimum absolute error in treatment length occurs in the 75$^{th}$ percentile for all section lengths investigated;
- For heavy rehabilitation (minority treatment), the average minimum absolute error in the 75$^{th}$ percentile is approximately 40% or less in section lengths up to 100 m, with the error increasing to 70% and above for section lengths of 500 m and above. An error less than that occurring in the averaged 20 m section length occurs in the 75$^{th}$ percentile of 50 m section lengths;
- For light rehabilitation / reseal (majority treatment), an error approximately equal to that occurring in the averaged 20 m section length occurs in the 75$^{th}$ percentile of up to 100 m section lengths;
- On average, the 75$^{th}$ percentile also presented with the highest probability of a 0% error in treatment length;
- The 75$^{th}$ percentile presented with an underestimation of heavy rehabilitation treatment length and an overestimation of light rehabilitation / reseal length in 55% of samples;
- The 75$^{th}$ percentile presented with an overestimation of heavy rehabilitation treatment length and an underestimation of light rehabilitation / reseal length in 24% of samples;

- The 90th, 95th, and 99th percentiles all present with high probabilities of overestimation in heavy rehabilitation, i.e., 51%, 59%, and 79%, respectively. The 90th percentile, however, presents with a lower error in treatment length than the 95th and 99th percentile, and
- The 90th percentile presents with a smaller error (in heavy rehabilitation length) in 100 m section lengths than in 50 m section lengths.

## 4. Funding implications

When considering the total financial need over the analysis period, where only the inaccurately estimated financial need per treatment type is considered (excluding errors in treatment years), the 75th percentile presents with the lowest overall inaccuracy. The following implications on the total financial need are evident from the study:

- On average overall for heavy rehabilitation, 53% (R1 million) of the forecasted budget is incorrectly allocated with the 75th percentile, which is 14% lower than the inaccuracy yielded from using the average as the statistical aggregation measure. On average, 71% (R1.1 million) of the budget is underestimated, and 29% (R0.7 million) is overestimated with the 75th percentile, and
- On average overall for light rehabilitation / reseals, 0.2% (R0.6 million) of the forecasted budget is incorrectly allocated with the 75th percentile, which is 0.1% lower than the inaccuracy yielded from using the average as the statistical aggregation measure. On average, 0.1% (R0.5 million) of the budget is underestimated, and 0.2% (R0.6 million) is overestimated with the 75th percentile.

When considering the annual financial need, where the inaccurately estimated financial need per treatment type and/or year is considered, the 75th percentile presents with the lowest overall inaccuracy in the predicted financial need for heavy rehabilitation, while the 50th percentile presents with the lowest overall inaccuracy in the predicted financial need for light rehabilitation / reseals. The following implications on the annual financial need are evident from the study:

- On average overall for heavy rehabilitation, 68% (R1.5 million) of the forecasted budget is incorrectly allocated with the 75th percentile, which is 6% lower than the inaccuracy yielded from using the average as the statistical aggregation measure. On average, 53% (R1.1 million) of the budget is underestimated, and 14% (R0.4 million) is overestimated with the 75th percentile, and
- On average overall for light rehabilitation / reseals, 6% (R23 million) of the forecasted budget is incorrectly allocated with the 50th percentile, which is 2% lower than the inaccuracy yielded from using the average as the statistical aggregation measure. On

average, 3% (R11 million) of the budget is underestimated, and 3% (R11 million) is overestimated with the 50th percentile

### 5.1.3 Application within the South African NRA (1999) specification

The following findings were obtained from studying the influence of average and percentile statistical aggregation measures on the acceptance criteria specified in the NRA (1999).

- When compared to discrete rut depth measurements, the use of statistical aggregation measures does not always provide an accurate representation of whether or not pavement performance requirements are being met. The 75th percentile, however, presented with the highest occurrence of providing an accurate representation, proving to be inaccurate only when providing an indication of whether the percentage of the most severe rut depth (>25 mm) is exceeding the recommended limits, and
- The 99th percentile is the only percentile to accurately provide an indication of whether or not the percentage of rut depth greater than 25 mm is exceeding the recommended limits. However, the 99th percentile has a higher probability of overestimating the percentage warning to severe rut depth, and in 2 out of the 5 samples inaccurately indicated that the sample was exceeding the recommended limits for rut depth greater than 15 mm and 20 mm.

## 5.2 RECOMMENDATIONS

Based on the findings obtained in the study, the following is recommended:

- The importance of the road being maintained should be taken into consideration when selecting a statistical aggregation measure for data processing;
- While no statistical aggregation measure can accurately characterise the distribution of rutting along a pavement section, percentiles offer more accuracy over averages and are recommended for data processing;
- While the aggregation process reduces the percentage warning to severe rutting (>15 mm), the 75th percentile presented with the lowest degree of error and proved to be the most accurate in estimating the total maintenance and rehabilitation need over a 20-year analysis period. The 75th percentile, however, has a higher probability of underestimating the percentage warning to severe rutting and, therefore, the need for heavy rehabilitation;
- Higher percentiles, namely, the 90th, 95th, and 99th, which have a higher probability of overestimating the percentage warning to severe rutting and the need for heavy rehabilitation, are better suited for data processing when the importance of the road is a

priority. The 90th percentile presents with the lowest error. The 99th percentile, however, is the only percentile to accurately provide an indication of whether or not the percentage of rut depth greater than 25 mm is exceeding the recommended limits (0% of the road segment should contain rutting greater than 25 mm, as indicated in the South African NRA (1999) specification). This study should be repeated for other specifications containing different performance requirements;

- The abovementioned results relate to the total maintenance and financial need over the analysis period and do not consider inaccuracies in annual financial estimates. With regards to the annual financial need, the 75th percentile proved to be the most accurate in predicting the annual financial need in heavy rehabilitation, while the 50th percentile proved to be the most accurate in predicting the annual financial need for light rehabilitation / reseals. For annual financial planning, the 50th percentile is most suitable. For technical needs planning, the 75th percentile is better suited, considering higher percentiles where high priority roads and performance requirements are a concern;
- The minimum pavement length that can be economically maintained should be considered in selecting the aggregation interval. However, with the degree of error increasing with increasing aggregated section length, it is recommended that the aggregation interval not exceed 100 m. Therefore, to allow for shorter intervals to be used in condition and needs prediction, these shorter intervals should rather only be combined into more practical maintenance project lengths, based on economic criteria, after condition prediction;
- A larger sample size containing a higher variability of rut depth measurements (distribution type and dispersion of rut depth values) should be analysed in future studies, and
- As-built plans of road segments investigated should be obtained to accurately identify the distribution of rut depth in future studies.

# 6 REFERENCES

AASHTO 2013. *Standard Practice for Determining Rut Depth in Pavements*, (AASHTO R48-10). AASHTO, United States.

Adlinge, S.S. and Gupta A.K. 2013. Pavement Deterioration and its Causes. *International Journal of Innovative Research & Development*, Vol 2, No 4, April, pp 437-450.

ASTM International 2004. *Standard Test Method for Measuring the Longitudinal Profile of Traveled Surfaces with an Accelerometer Established Inertial Profiling Reference*, (ASTM E950-98). ASTM International, United States.

ASTM International 2015. *Standard Test Method for Measuring Rut-Depth of Pavement Surfaces Using a Straightedge*, (ASTM E1703/E1703M-10). ASTM International, United States.

Atkinson, J.K. 1990. *Highway Maintenance Handbook*. 1st ed. Thomas Telford Ltd, London.

Austroads 2016. *Austroads Test Method AG:AM/T009 Pavement Rutting Measurement with a Laser Profilometer*. Austroads, Sydney, NSW.

Bandini, P. Pham, H.V. 2010. *Transition from Manual to Automatic Rutting Measurements: Effects on Pavement Serviceability Index Values*. New Mexico Department of Transportation. Research Report N. NM 08SAF-02. New Mexico.

Bennett, C.R. 2002. *Establishing Reference Profiles for Rut Depth Measurements*. Data Collection Limited, New Zealand.

Bennett, C.R., Peterson, W.D.O., 2000. *HDM-4 Highway Development and Management, Volume 5, A Guide to Calibration and Adaption*. International Study of Highway Development and Management Tools (ISOHDM). World Road Association (PIARC), Paris and The World Bank, Washington, DC.

COLTO 1997. Draft TRH 12 *Flexible Pavement Rehabilitation Investigation and Design*. Department of Transport, Pretoria, South Africa.

Committee of State Road Authorities 1992. *TMH 9 Pavement Management Systems: Standard Visual Assessment Manual for Flexible Pavements*. Department of Transport, Pretoria, South Africa.

Committee of State Road Authorities 1994. *Draft TRH 22 Pavement Management Systems. Department of Transport*, Pretoria, South Africa.

COTO 2013. *Draft TMH 22 Road Asset Management Manual*. The South African National Roads Agency, Pretoria, South Africa.

COTO 2016a. *TMH 13 Automated Road Condition Assessments Part D: Rutting*. Committee of Transportation Officials (COTO), South Africa.

COTO 2016b. *TMH 9 Manual for Visual Assessment of Road Pavements*. The South African National Roads Agency, Pretoria, South Africa.

Council for Scientific and Industrial Research 1985. *TRH 6 Nomenclature and Methods for Describing the Condition of Asphalt Pavements*. National Institute for Transport and Road Research, Pretoria, South Africa.

Deighton, 2019. Viewed 20 April 2019, https://www.deighton.com/

Donev, V. and Hoffmann, M. 2018. Optimisation of pavement maintenance and rehabilitation activities, timing and work zones for short survey sections and multiple distress types. *International Journal of Pavement Engineering*, Vol 21, No 5, July, pp 583-607.

Donev, V. Hoffmann, M. and Blab, R. 2020. Aggregation of condition survey data in pavement management: shortcomings of a homogeneous sections approach and how to avoid them. *Structures and Infrastructure Engineering*, Vol 17, No 1, February, pp 1-13.

Feingold, J. 2013. High Speed Inertial Profiler: Smoother rides for Florida's traveling public. *Florida Asphalt*, Vol 12, No 2, pp 17.

Frangopol, D.M. and Liu, M. 2007. Maintenance and management of civil infrastructure based on condition, safety, optimization, and life-cycle cost. *Structure and Infrastructure Engineering*, Vol 3, No 1, March, pp 29-41.

Gillespie, T.D. Sayers, M.W. and Hagan, M.R. 1987. *Methodology for Road Roughness Profiling and Rut Depth Measurement*. The University of Michigan Transportation Research Institute. Technical Report FHWA/RD-87-042. Michigan, United States.

Gräbe P.J. 2013. Infrastructure maintenance management. Lecture notes distributed in the unit, SSI 790 Infrastructure Management, University of Pretoria. 2015.

Hajek, J.J. Musgrove, G. and Kazmierowski, T.J. 1998. Measurement, management and utilization of rutting data. *4th International Conference on Managing Pavements*. Ontario Ministry of Transportation. Canada.

Hoffman, B.R. and Sargand, S.M. 2011. *Verification of Rut Depth Collected with the INO Laser Rut Measurement System (LRMS)*. Ohio Research Institute for Transportation and the Environment. Student Study FHWA/OH-2011/18. Ohio.

Huang, Y.R. Hempel, P. and Copenhaver, T. 2009. *A Rut Measurement System Based on Continuous Transverse Profiles from a 3-D System*. Texas Department of Transportation. Research and Development Project Report DHT 49. Texas.

Jannat, G.E. Henning, T.F.P. Zhang, C. Tighe, S.L. and Ningyuan, L. 2016. Road Section Length Variability on Pavement Management Decision Making for Ontario Highway Systems. *Transportation Research Record: Journal of the Transportation Research Board*, Vol 2589, No 1, pp 87-96.

Kadar, P. Martin, T. and Sen, R. 2015. Addressing Uncertainties of Performance Modelling with Stochastic Information Packages – Incorporating Uncertainty in Performance and Budget Forecasts. *9th International Conference on Managing Pavement Assets*. Alexandria, Virginia, USA.

Kannemeyer, L. 2003. *Modelling Rutting in Flexible Pavements in HDM-4*. Draft Report.

Li, F. 2012. *A Methodology for Characterizing Pavement Rutting Condition Using Emerging 3D Line Laser Imaging Technology*. PhD thesis. Georgia Institute of Technology.

Lin, M. Lucas, H.C. and Shmueli, G. 2013. Too Big to Fail: Large Samples and the P-Value Problem. *Information Systems Research*, Vol 24, No 4, October, pp 906-917.

Mallela, R. and Wang, H. 2006. *Harmonising Automated Rut Depth Measurements – Stage 2*. Data Collection Ltd. Land Transport New Zealand Research Report 277. New Zealand.

Morcous, G. Lounis, Z. 2005. Maintenance Optimization of Infrastructure Networks Using Genetic Algorithms. *Journal of Automation in Construction*, Vol 14, No 1, January, pp 129-142.

NRA 1999. *Concession Contract for the Design, Construction, Financing, Operating and Maintenance of a Portion of National Route 3 from Cedara in KwaZulu-Natal to Heidelberg South Interchange in Gauteng as a Toll Highway with Developments and Associated Facilities*. The South African National Roads Agency (SANRAL), South Africa.

Odoki, J.B., Kerali, H.G.R., 2006. *HDM-4 Highway Development and Management, Volume 4, Analytical Framework and Model Descriptions*, 2nd ed. International Study of Highway Development and Management Tools (ISOHDM). World Road Association (PIARC), Paris and The World Bank, Washington, DC.

Paterson, W.D.O. 1987. *Road Deterioration and Maintenance Effects*. 1st ed. The Johns Hopkins University Press, Baltimore.

Richter, C. 2001. *Adequacy of rut bar data collection. US Department of Transportation Federal Highway* Administration. Publication No. FHWA-RD-01-027. McLean, Virginia.

SANRAL 2014. *South African Pavement Engineering Manual*. South African National Roads Agency (SANRAL). South Africa.

SANRAL 2020. *Routine Road Maintenance Manual, Chapter 8 Road Pavement Repairs – Flexible Pavements*, viewed 28 September 2020, https://www.nra.co.za/wpfd_file/chapter-8/

Sayers, M.W. and Karamihas, S.M. 1998. *The Little Book of Profiling*.1st ed. The Regent of the University of Michigan, Michigan.

Scienceware. 2008. *Manual Rut Reference Profiler*. Scientific and Commercial Software Development, Centurion, South Africa.

Serigos, P.A. Prozzi, J.A. Nam, B.H. and Murphy, M.R. 2012. *Field Evaluation of Automated Rutting Measuring Equipment*. Center for Transportation Research. Technical Report FHWA/TX-12/0-6663-1. Austin, Texas.

Simpson, A.L. 2001. *Measurement of Rutting in Asphalt Pavements*. PhD thesis. The University of Texas at Austin.

Sjögren, L. and Lundberg, T. 2005. Designing an up to date rut depth monitoring profilometer, requirements and limitations. *2nd European Pavement and Asset Management Conference, 21st–23rd March 2004, Berlin, Germany*. The Swedish National Road and Transport Research Institute, Sweden, pp 1-13.

Steyn, W.J.vdM. 2012. Study guide and core notes – 2012. Lecture notes distributed in the unit, SGM 221 Pavement materials and design, University of Pretoria. June 2012.

Wang, H. 2005. *Development of Laser System to Measure Pavement Rutting*. MSc thesis. University of South Florida.

World Bank Group, 2017. Viewed 1 February 2017, https://climateknowledgeportal.worldbank.org/

Yichang, T.J. Zhaohua, W. and Feng, L. 2015. Assessment of Rut Depth Measurement Accuracy of Point-Based Rut Bar Systems Using Emerging 3D Line Laser Imaging Technology. *Journal of Marine Science and Technology*, Vol 23, No 3, pp 322-330.

# APPENDIX A

# DUMMY DATA GENERATED FOR SELECTING A METHOD OF IDENTIFYING DISTRIBUTIONS

# APPENDIX A DUMMY DATA GENERATED FOR SELECTING A METHOD OF IDENTIFYING DISTRIBUTIONS

## A.1 INTRODUCTION

The results of the sensitivity analysis discussed in Section **Error! Reference source not found.** are presented in the sections that follow. For the discussion of the results, refer to Section **Error! Reference source not found.**.

## A.2 SAMPLES GENERATED FROM EXPONENTIAL DISTRIBUTION

Figure A-1 to Figure A-4 present the probability and quantile-quantile plots of samples generated from a standard exponential distribution with sample sizes, 10, 50, 100, and 1 000, respectively.

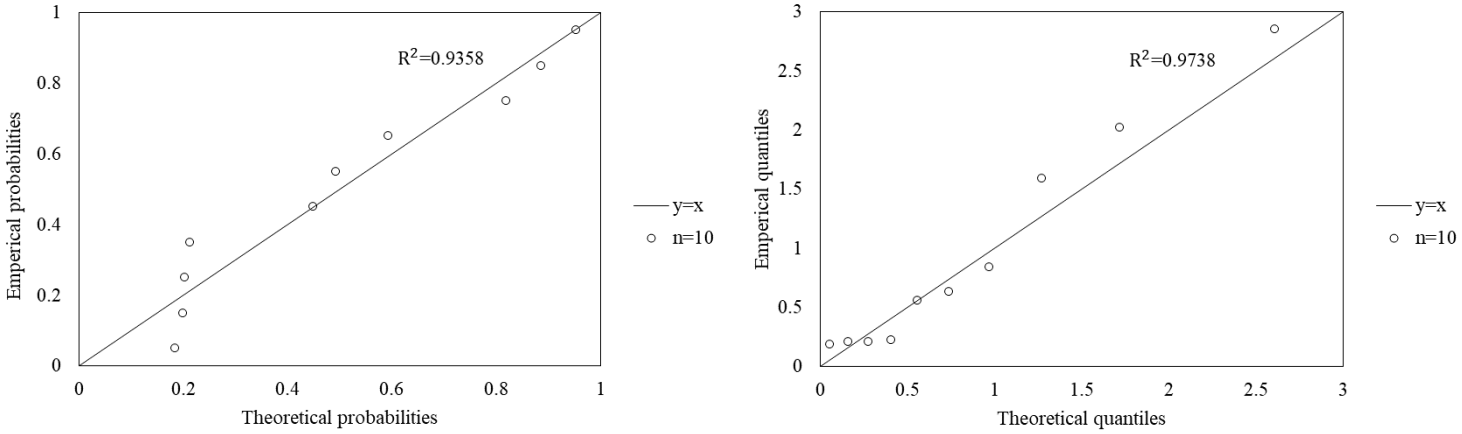


**Figure A-1: Sample generated from a standard exponential distribution with sample size, n=10: (a) probability plot; (b) quantile-quantile plot**

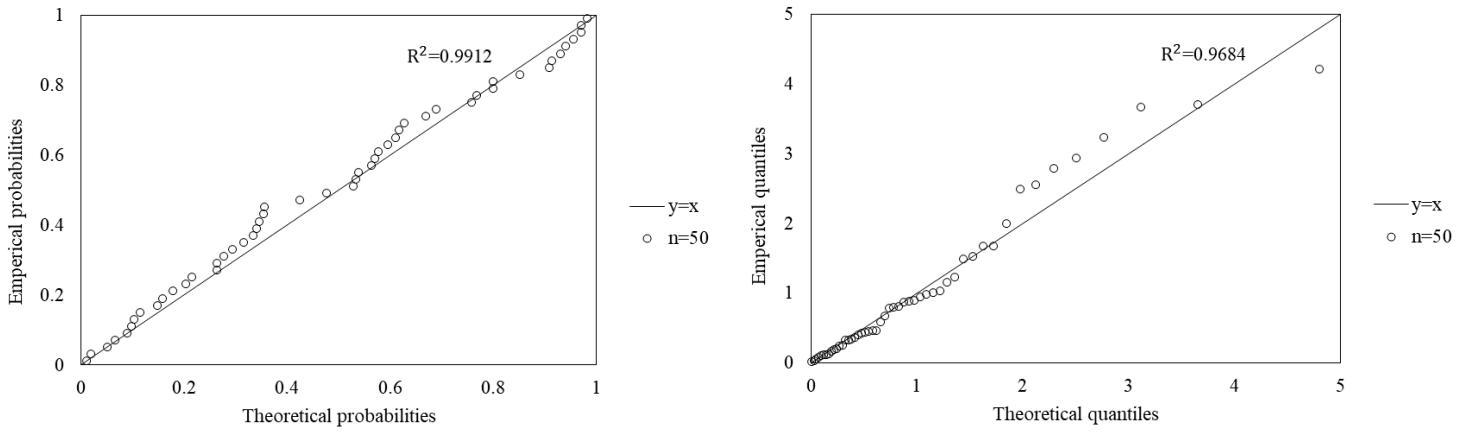


(a) (b)

**Figure A-2: Sample generated from a standard exponential distribution with sample size, n=50: (a) probability plot; (b) quantile-quantile plot**

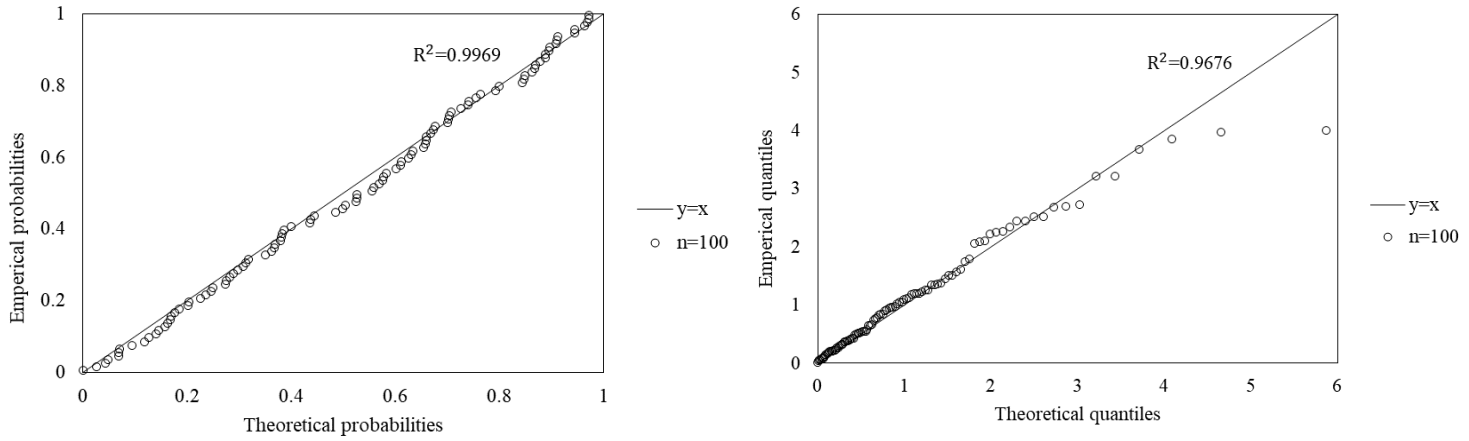


(a) (b)

**Figure A-3: Sample generated from a standard exponential distribution with sample size, n=100: (a) probability plot; (b) quantile-quantile plot**

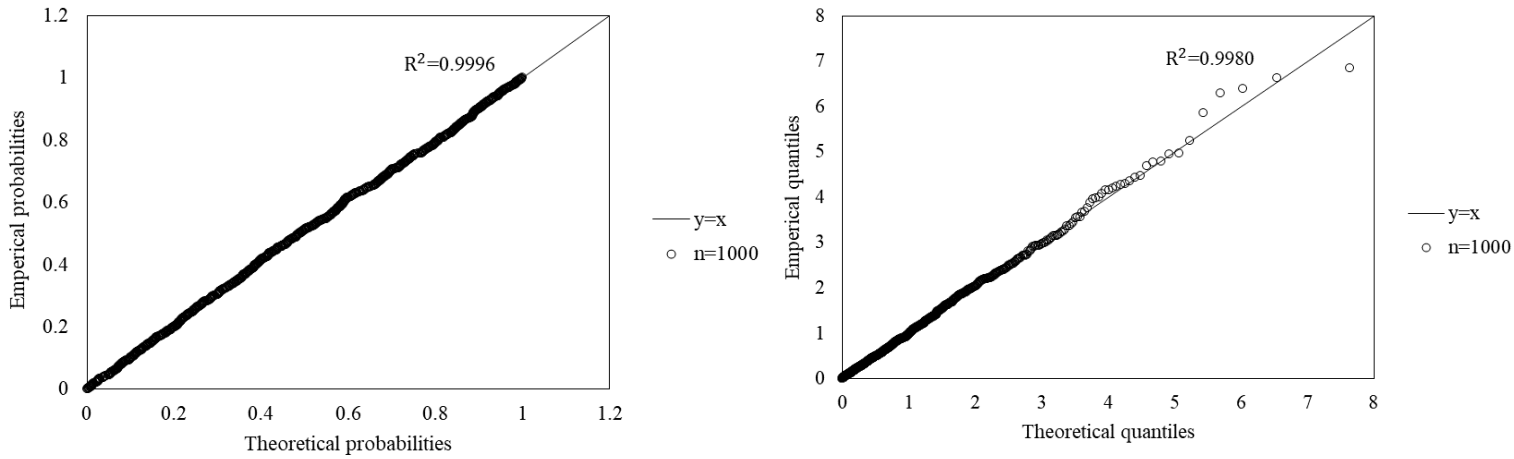


(a) (b)

**Figure A-4: Sample generated from a standard exponential distribution with sample size, n=1 000: (a) probability plot; (b) quantile-quantile plot**

Figure A-5 presents the probability and quantile-quantile plot for all samples generated from a standard exponential distribution.

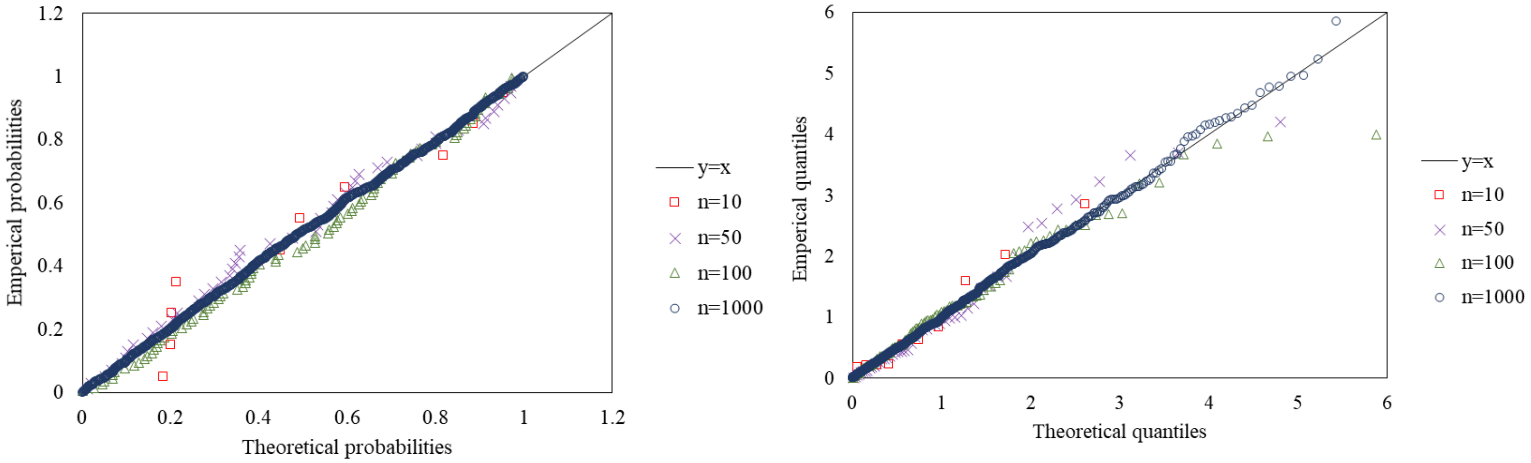


(a) (b)

**Figure A-5: Samples generated from a standard exponential distribution: (a) probability plot; (b) quantile-quantile plot**

## A.3 SAMPLES GENERATED FROM LOGNORMAL DISTRIBUTION

Figure A-6 to Figure A-9 present the probability and quantile-quantile plots of samples generated from a standard lognormal distribution with sample sizes, 10, 50, 100, and 1 000, respectively.

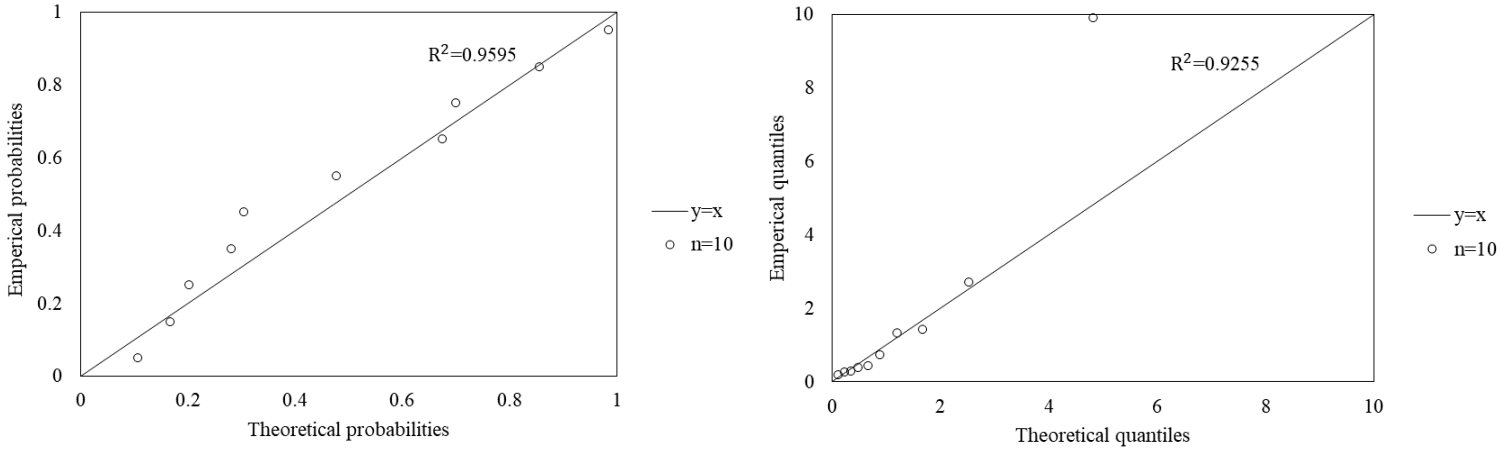


(a) (b)

**Figure A-6: Sample generated from a standard lognormal distribution with sample size, n=10: (a) probability plot; (b) quantile-quantile plot**

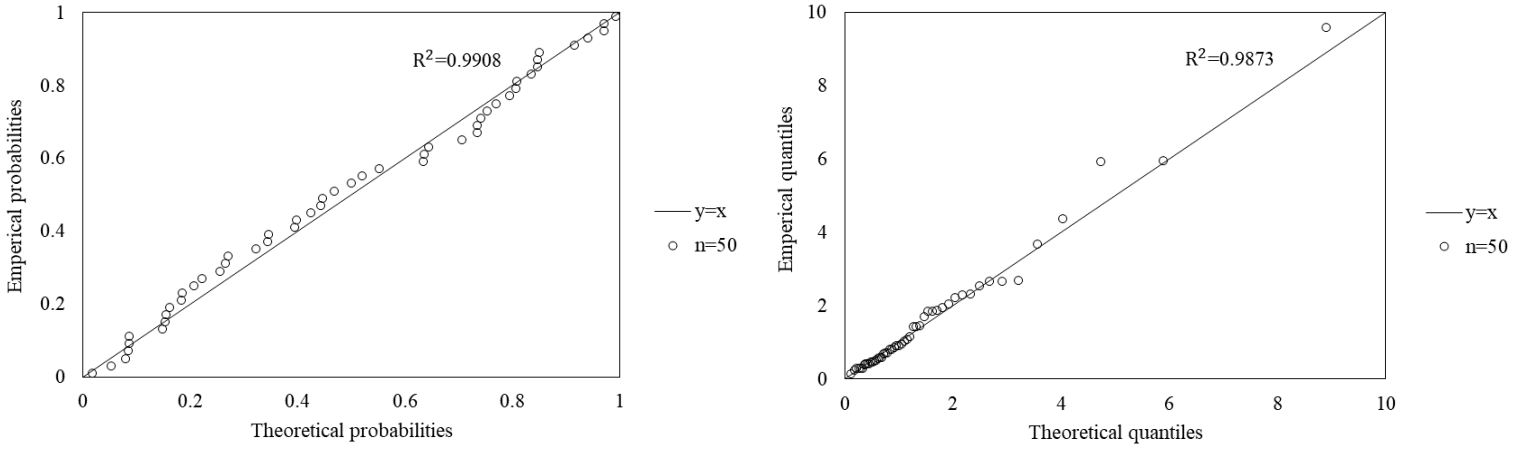


(a) (b)

**Figure A-7: Sample generated from a standard lognormal distribution with sample size, n=50: (a) probability plot; (b) quantile-quantile plot**

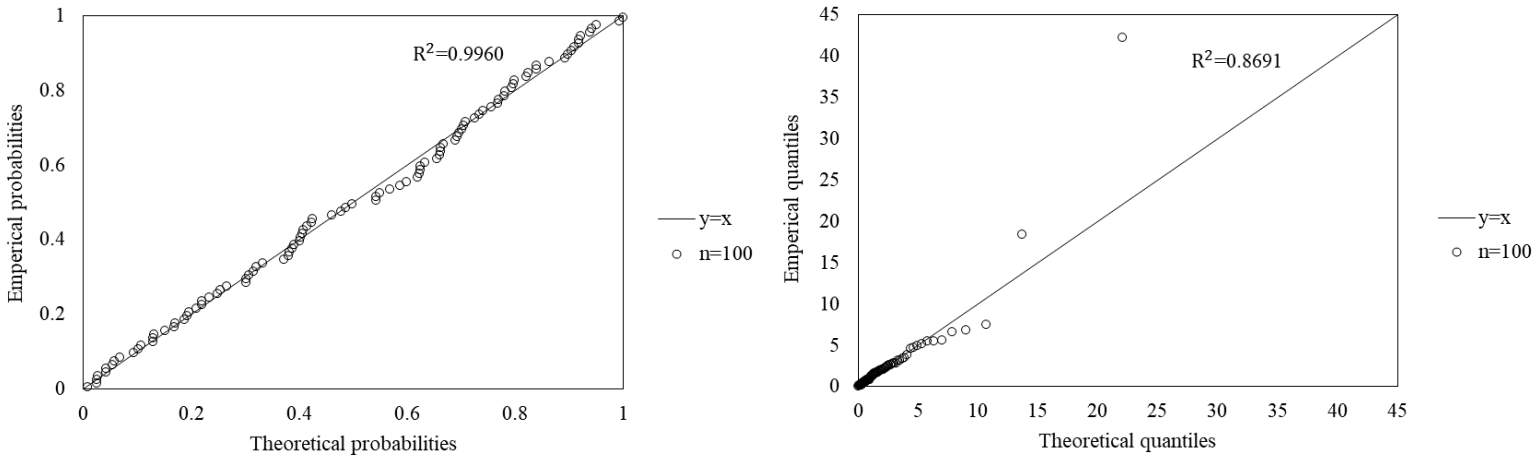


(a) (b)

**Figure A-8: Sample generated from a standard lognormal distribution with sample size, n=100: (a) probability plot; (b) quantile-quantile plot**

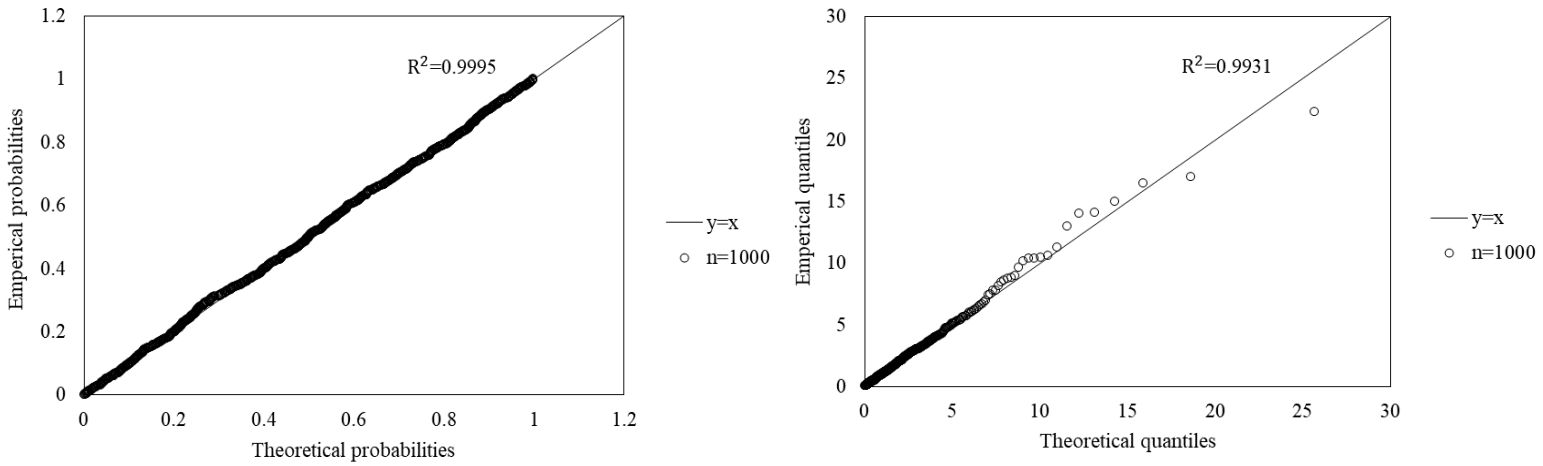


(a) (b)

**Figure A-9: Sample generated from a standard lognormal distribution with sample size, n=1 000: (a) probability plot; (b) quantile-quantile plot**

Figure A-10 presents the probability and quantile-quantile plot for all samples generated from a standard lognormal distribution.

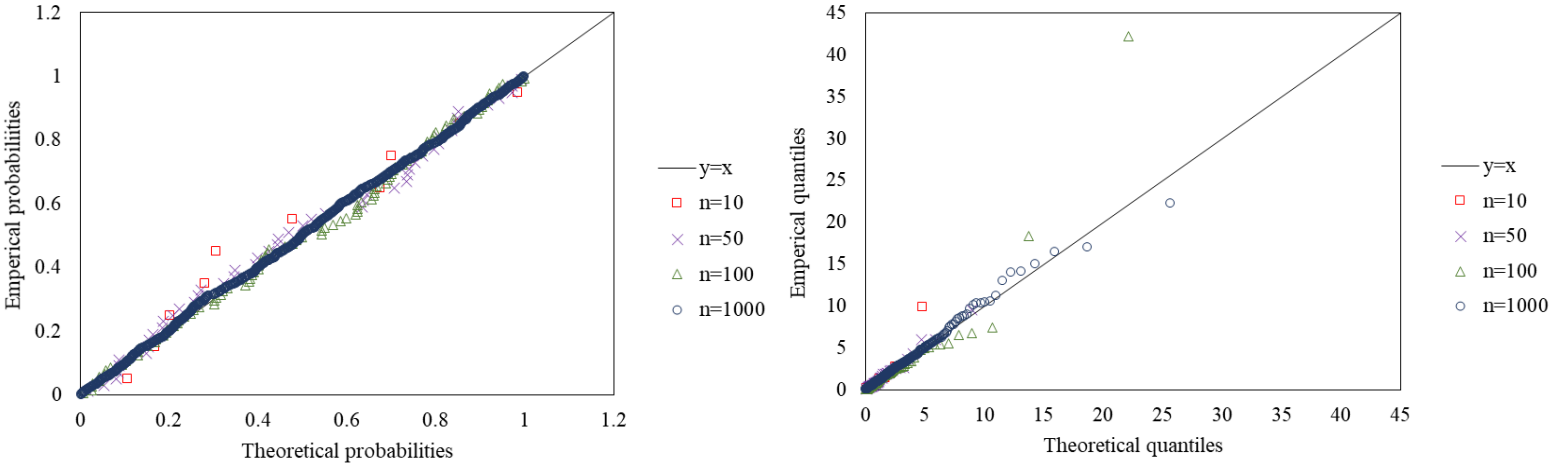


(a) (b)

**Figure A-10: Samples generated from a standard lognormal distribution: (a) probability plot; (b) quantile-quantile plot**

## A.4 SAMPLES GENERATED FROM NORMAL DISTRIBUTION

Figure A-11 to Figure A-14 present the probability and quantile-quantile plots of samples generated from a standard normal distribution with sample sizes, 10, 50, 100, and 1 000, respectively.

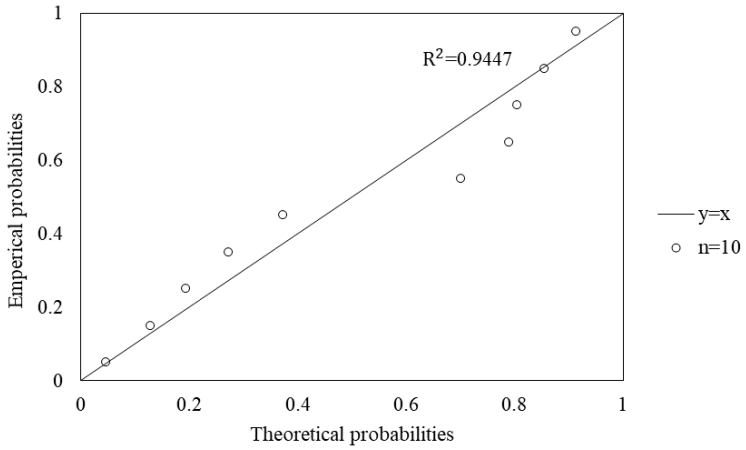


(a)

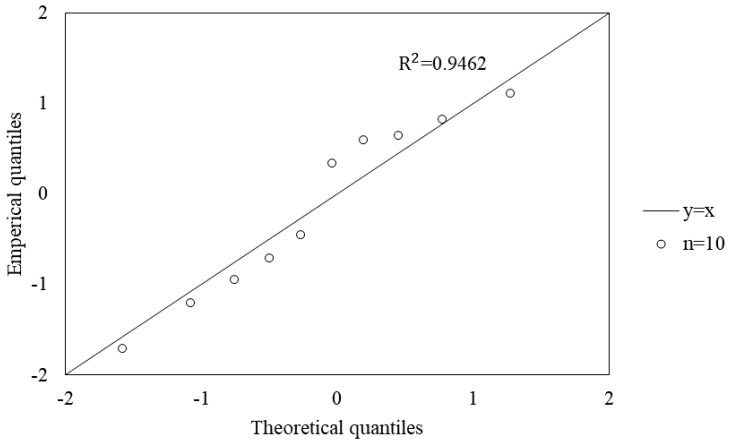


(b)

**Figure A-11: Sample generated from a standard normal distribution with sample size, n=10: (a) probability plot; (b) quantile-quantile plot**

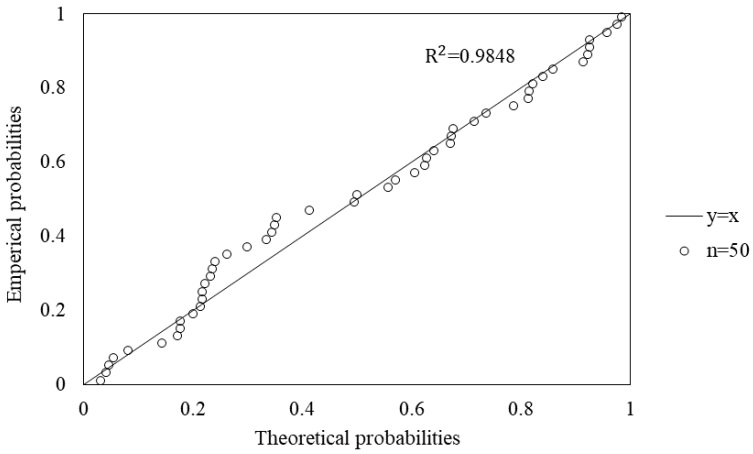


(a)

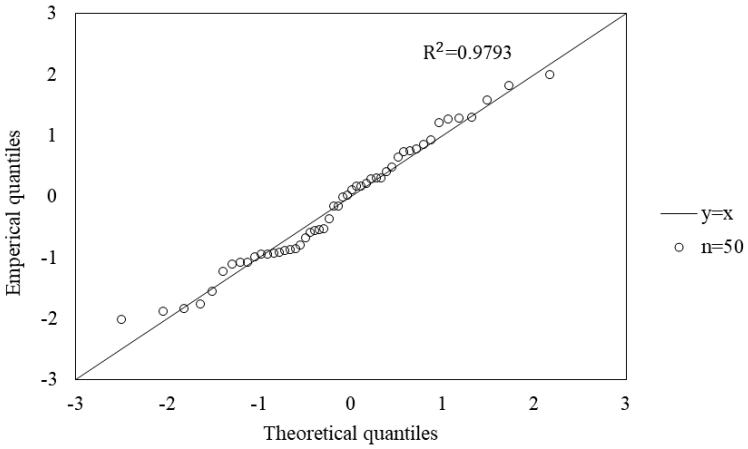


(b)

**Figure A-12: Sample generated from a standard normal distribution with sample size, n=50: (a) probability plot; (b) quantile-quantile plot**

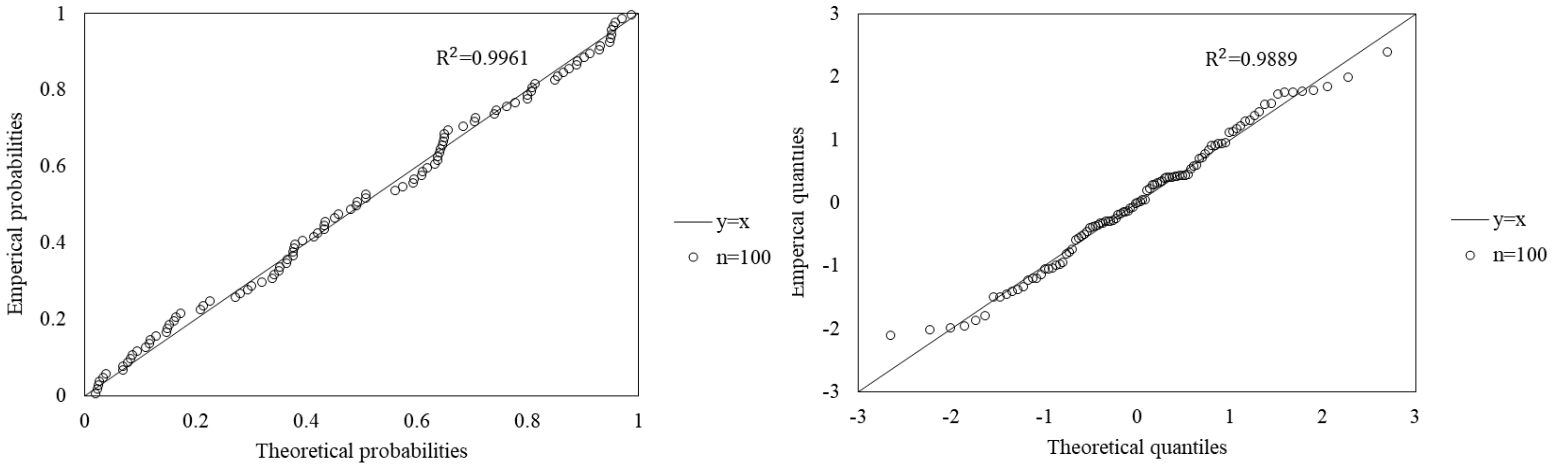


(a) (b)

**Figure A-13: Sample generated from a standard normal distribution with sample size, n=100: (a) probability plot; (b) quantile-quantile plot**

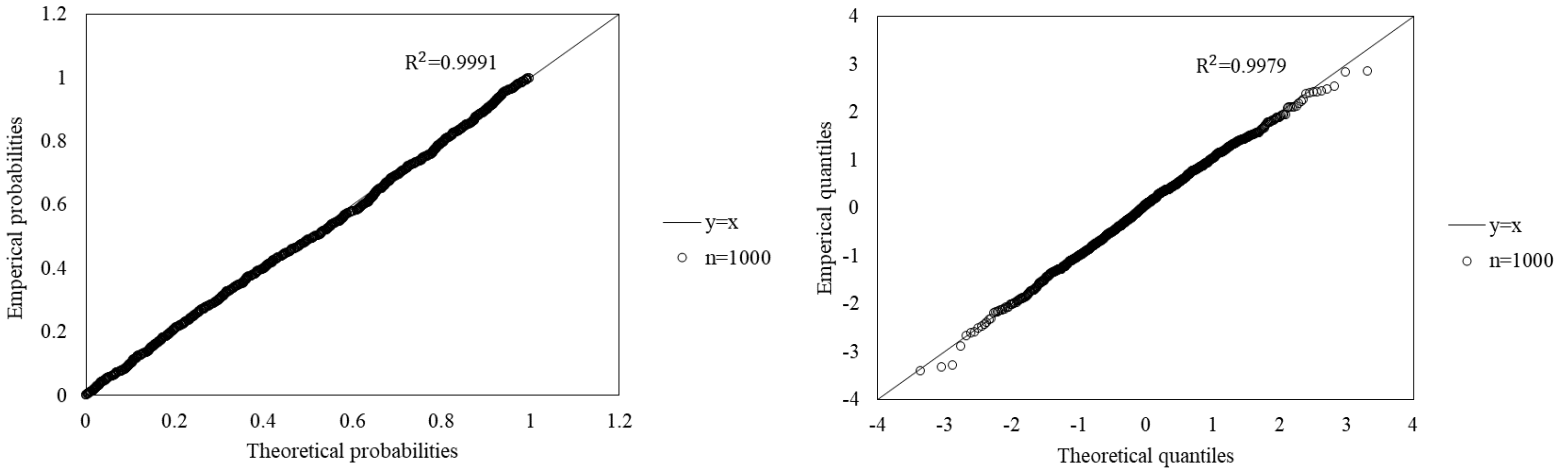


(a) (b)

**Figure A-14: Sample generated from a standard normal distribution with sample size, n=1 000: (a) probability plot; (b) quantile-quantile plot**

Figure A-15 presents the probability and quantile-quantile plot for all samples generated from a standard normal distribution.

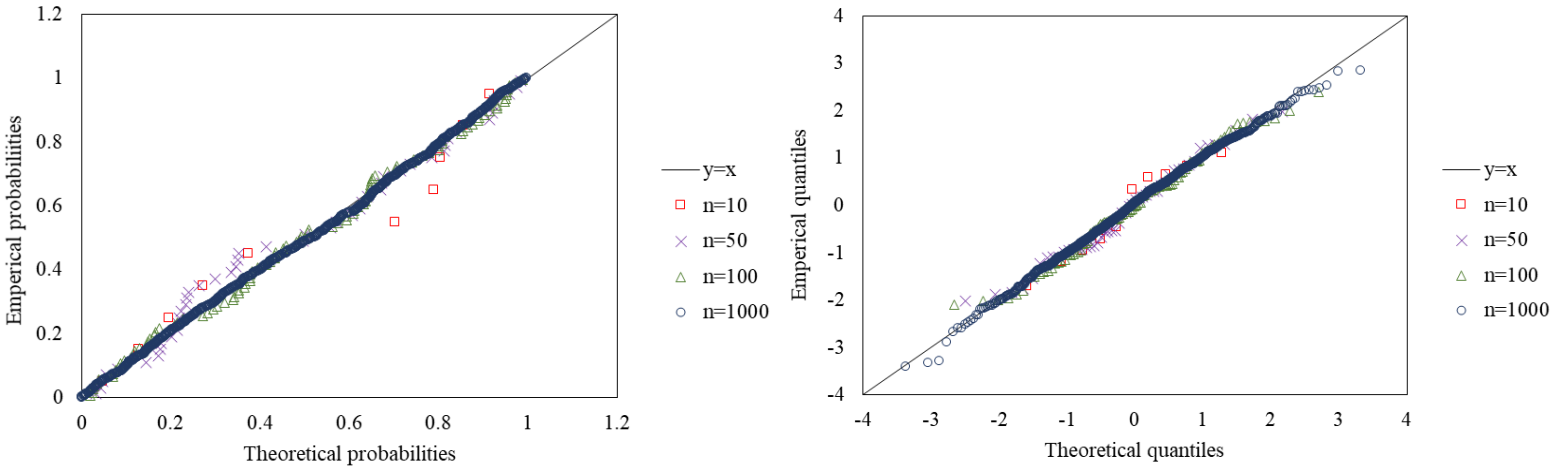


(a) (b)

**Figure A-15: Samples generated from a standard normal distribution: (a) probability plot; (b) quantile-quantile plot**

## A.5 SAMPLES GENERATED FROM EXPONENTIAL AND LOGNORMAL DISTRIBUTION

Figure A-16 and Figure A-17 respectively present exponential and lognormal probability and quantile-quantile plots for samples generated from standard exponential and lognormal distributions.

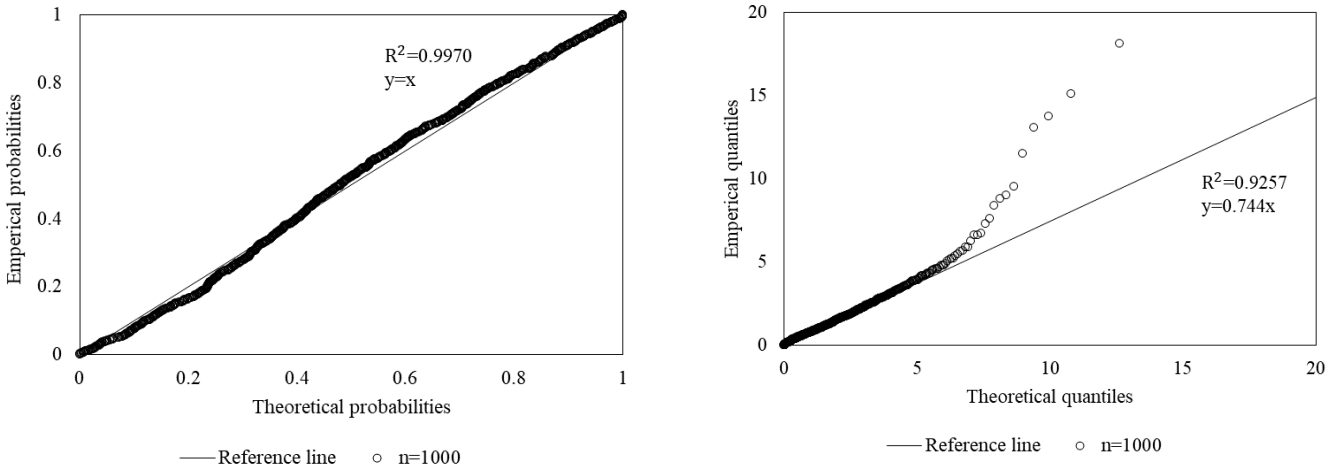


(a) (b)

**Figure A-16: Sample generated from standard exponential (n=500) and lognormal (n=500) distribution: (a) exponential probability plot; (b) exponential quantile-quantile plot**

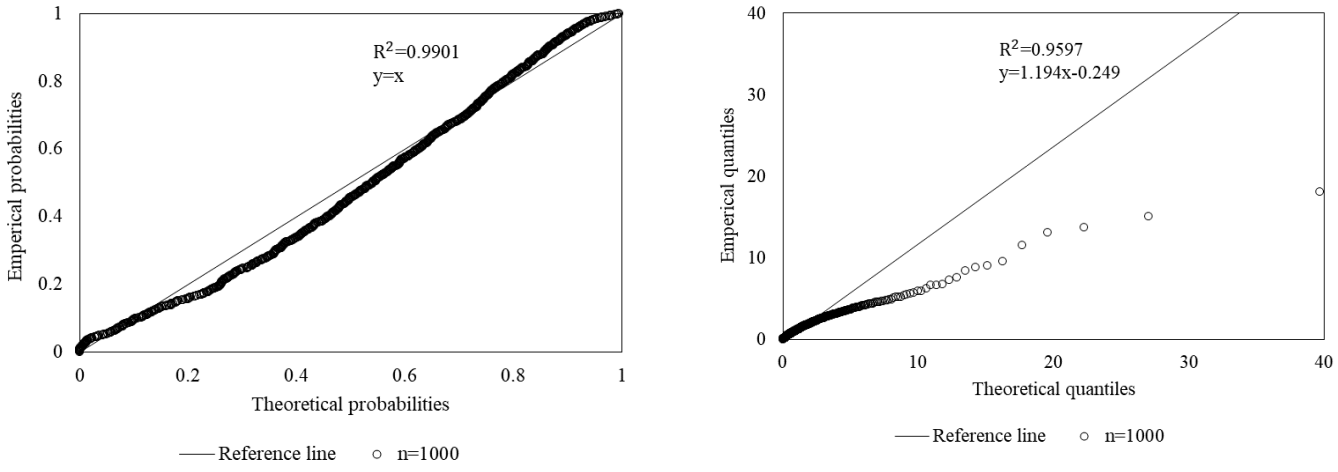


(a) (b)

**Figure A-17: Sample generated from standard exponential (n=500) and lognormal (n=500) distribution: (a) lognormal probability plot; (b) lognormal quantile-quantile plot**

## A.6 SAMPLES GENERATED FROM EXPONENTIAL AND NORMAL DISTRIBUTION

Figure A-18 presents normal probability and quantile-quantile plots for samples generated from standard exponential and normal distributions.

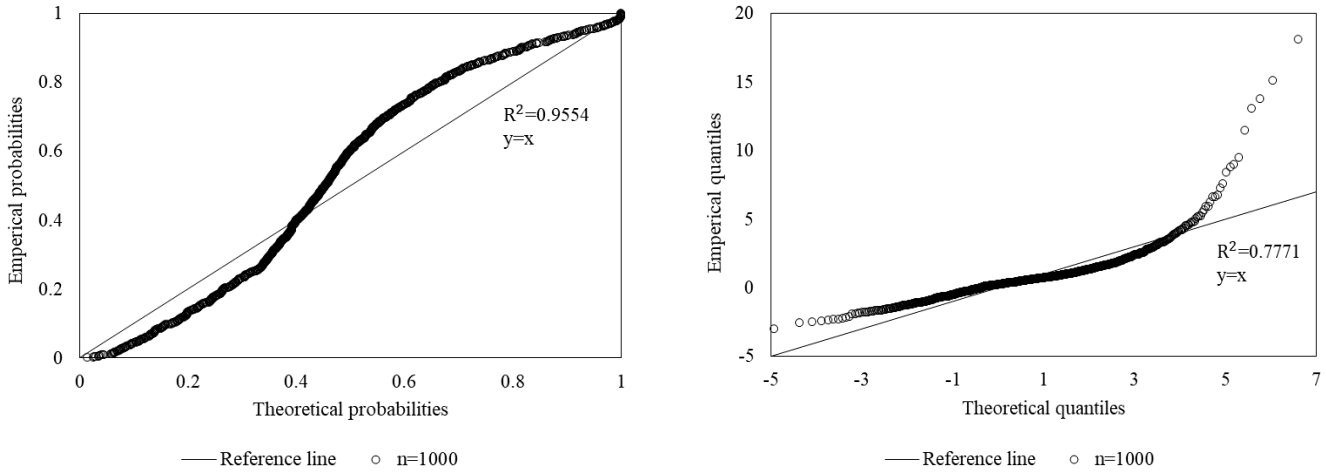


(a) (b)

**Figure A-18: Sample generated from standard exponential (n=500) and normal (n=500) distribution: (a) normal probability plot; (b) normal quantile-quantile plot**

## A.7 SAMPLES GENERATED FROM LOGNORMAL AND NORMAL DISTRIBUTION

Figure A-19 presents normal probability and quantile-quantile plots for samples generated from standard lognormal and normal distributions.

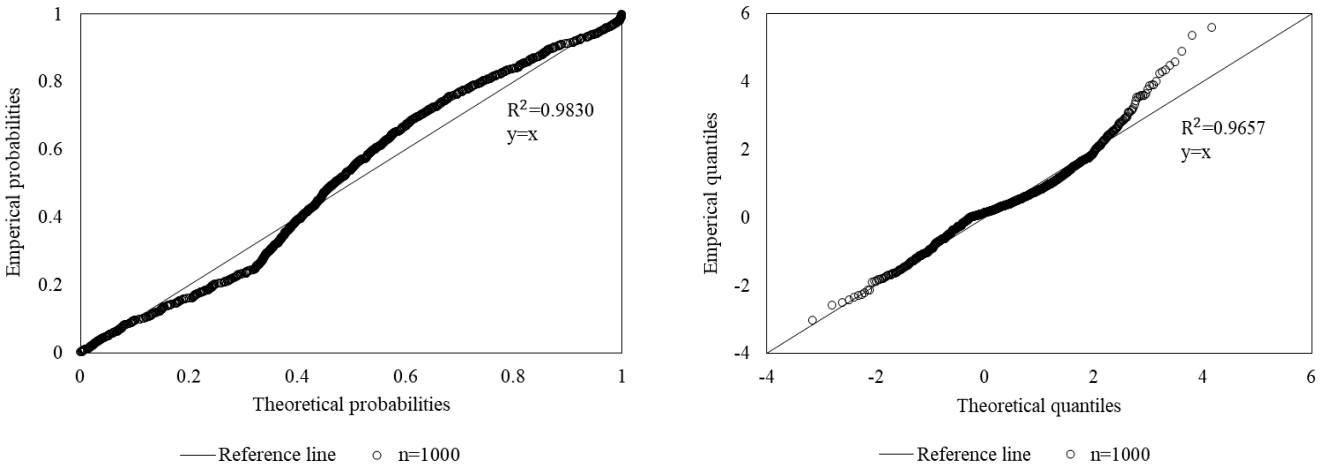


(a) (b)

**Figure A-19: Sample generated from standard lognormal (n=500) and normal (n=500) distribution: (a) normal probability plot; (b) normal quantile-quantile plot**

# APPENDIX B

# LEFT AND RIGHT RUT DEPTH PROBABILITY PLOTS FOR DATASET 1 SAMPLES

# APPENDIX B LEFT AND RIGHT RUT DEPTH PROBABILITY PLOTS FOR DATASET 1 SAMPLES

## B.1 INTRODUCTION

The exponential, lognormal, and normal probability plots plotted in R-Studio for left and right rut depth 10 m measurements for each of the 5 samples obtained are presented in the sections that follow.

## B.2 LEFT RUT DEPTH PROBABILITY PLOTS

Figure B-1 to Figure B-15 present the full sample length exponential, lognormal, and normal probability plots for the left rut depth of samples obtained for the analysis.

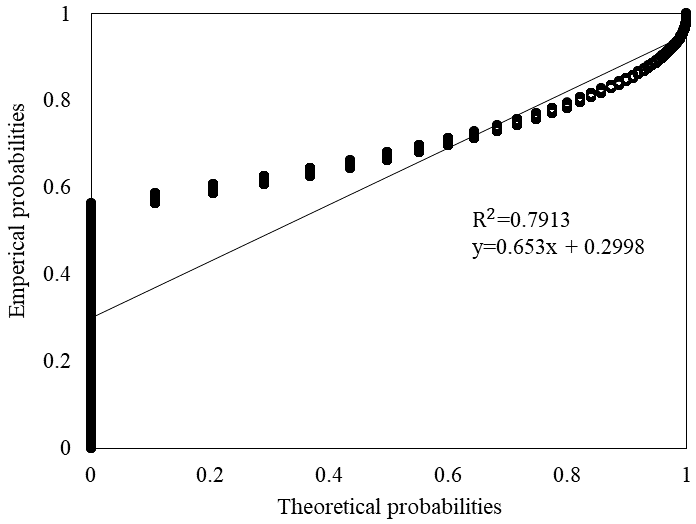


**Figure B-1: Sample 1 left rut exponential probability plot**

N/A

**Figure B-2: Sample 1 left rut lognormal probability plot**

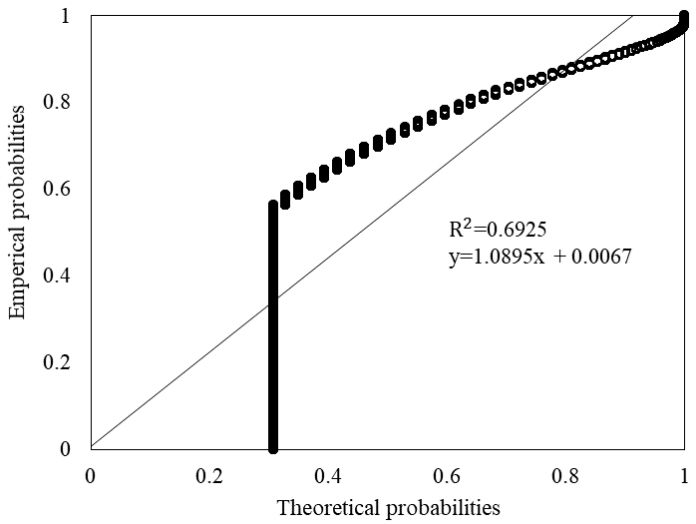


**Figure B-3: Sample 1 left rut normal probability plot**

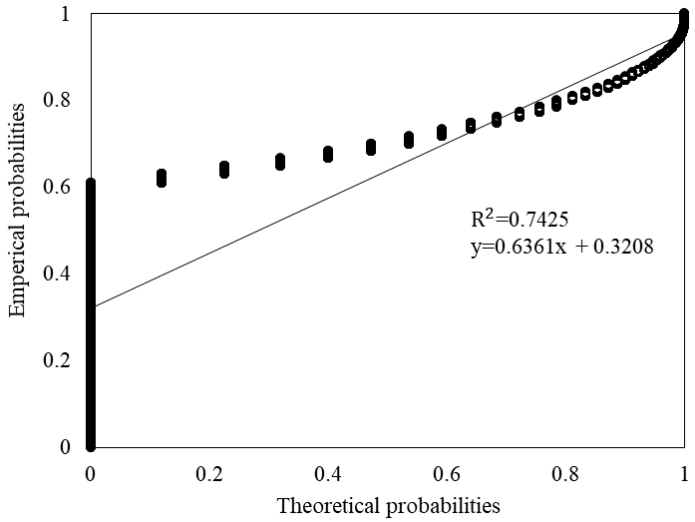


**Figure B-4: Sample 2 left rut exponential probability plot**

N/A

**Figure B-5: Sample 2 left rut lognormal probability plot**

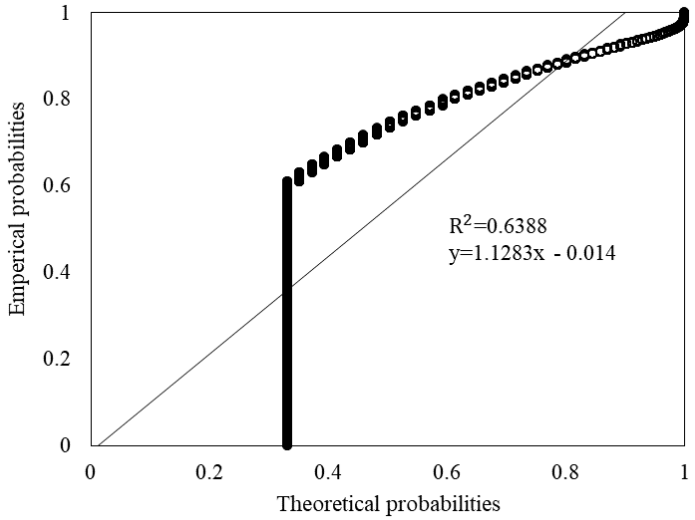


**Figure B-6: Sample 2 left rut normal probability plot**

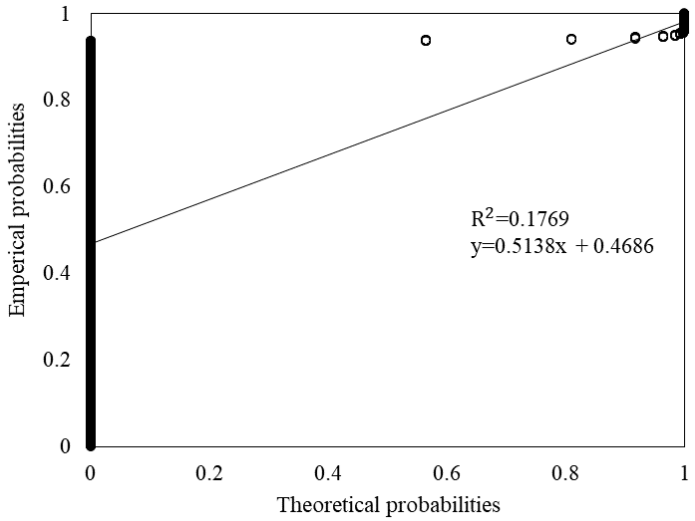


**Figure B-7: Sample 3 left rut exponential probability plot**

N/A

**Figure B-8: Sample 3 left rut lognormal probability plot**

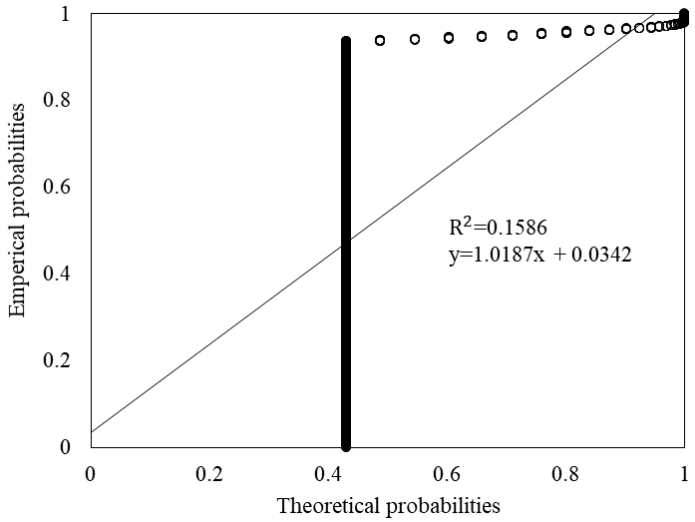


**Figure B-9: Sample 3 left rut normal probability plot**

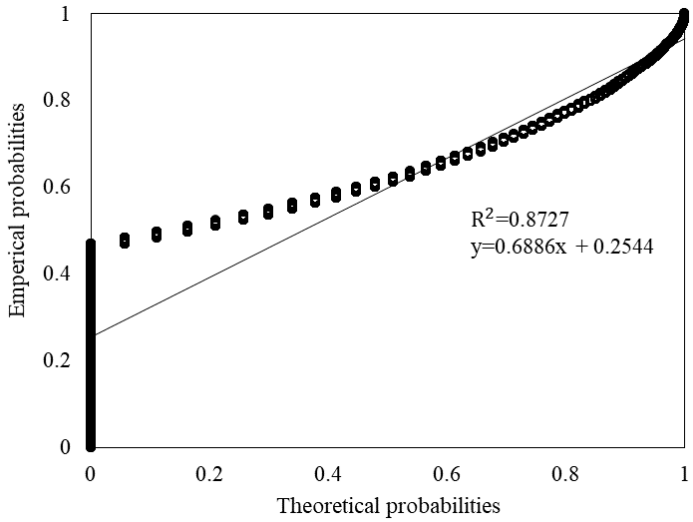


**Figure B-10: Sample 4 left rut exponential probability plot**

N/A

**Figure B-11: Sample 4 left rut lognormal probability plot**

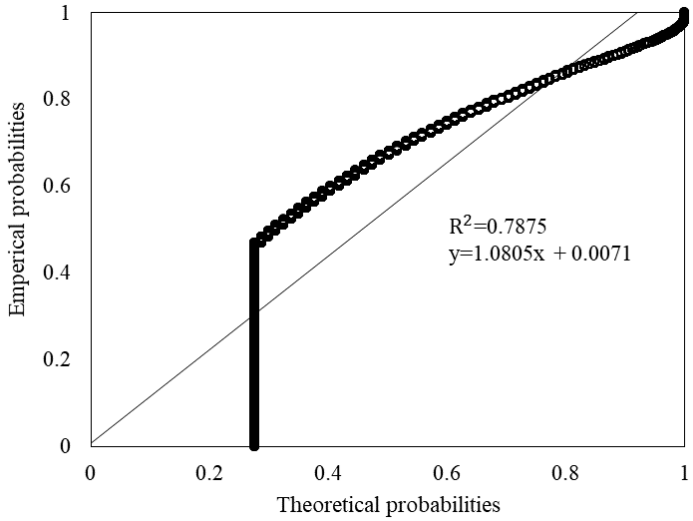


**Figure B-12: Sample 4 left rut normal probability plot**

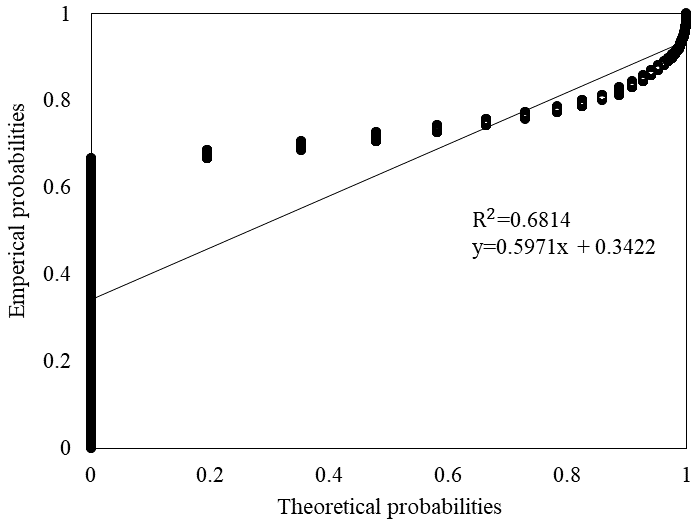


**Figure B-13: Sample 5 left rut exponential probability plot**

N/A

**Figure B-14: Sample 5 left rut lognormal probability plot**

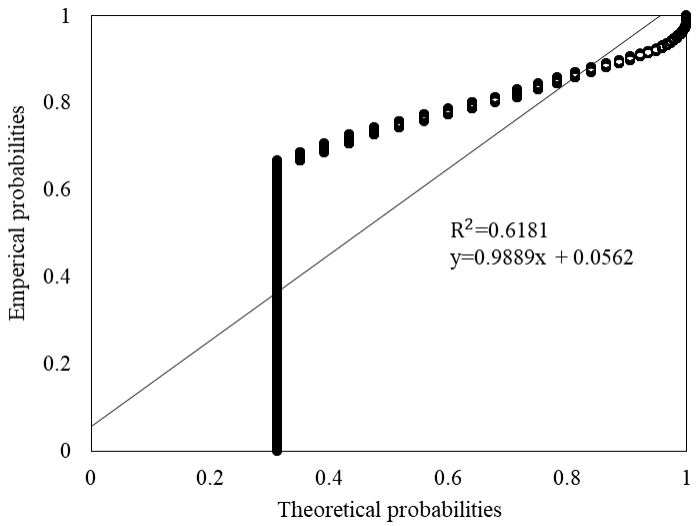


**Figure B-15: Sample 5 left rut normal probability plot**

Figure B-16 to Figure B-27 present the 50 km sample length exponential, lognormal, and normal probability plots for sample 1 left rut depth measurements.

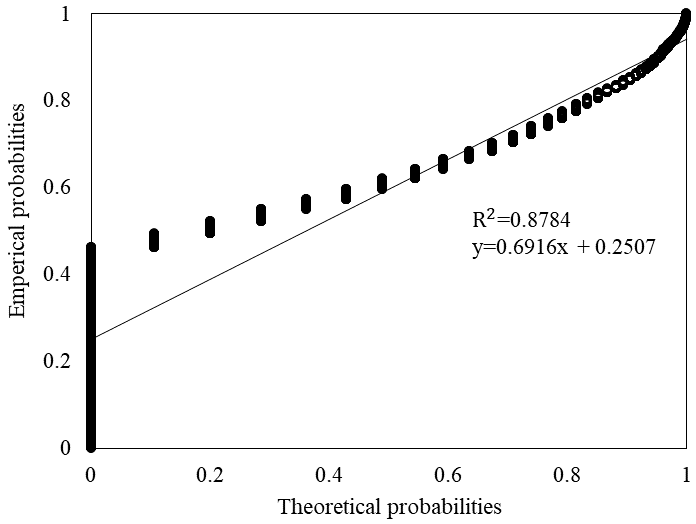


**Figure B-16: Sample 1.1 left rut exponential probability plot**

N/A

**Figure B-17: Sample 1.1 left rut lognormal probability plot**

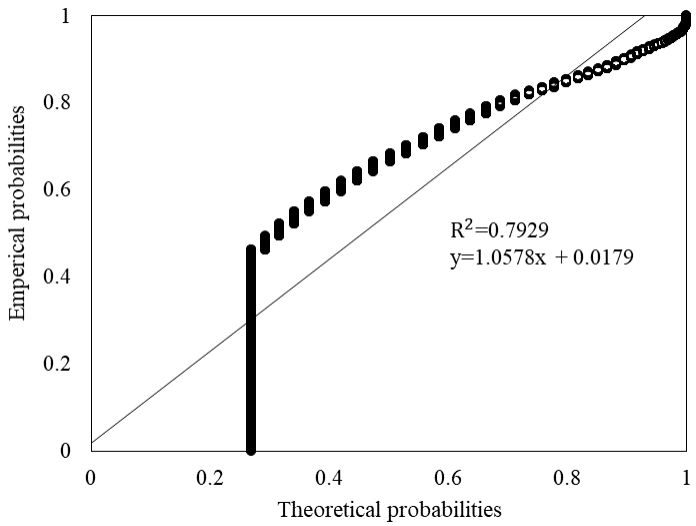


**Figure B-18: Sample 1.1 left rut normal probability plot**

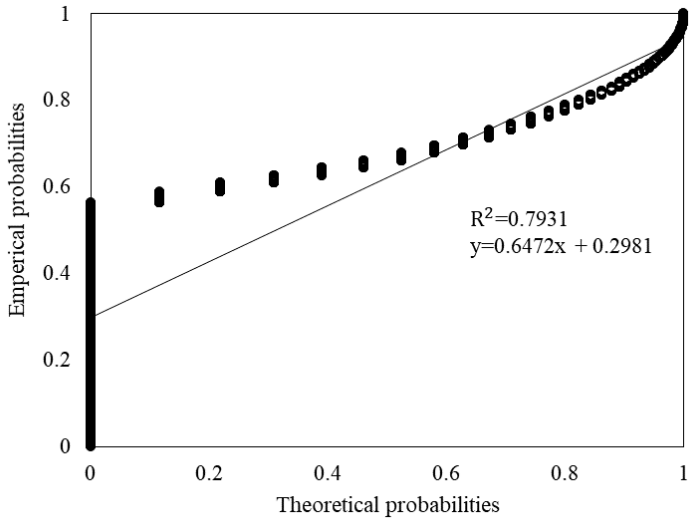


**Figure B-19: Sample 1.2 left rut exponential probability plot**

N/A

**Figure B-20: Sample 1.2 left rut lognormal probability plot**

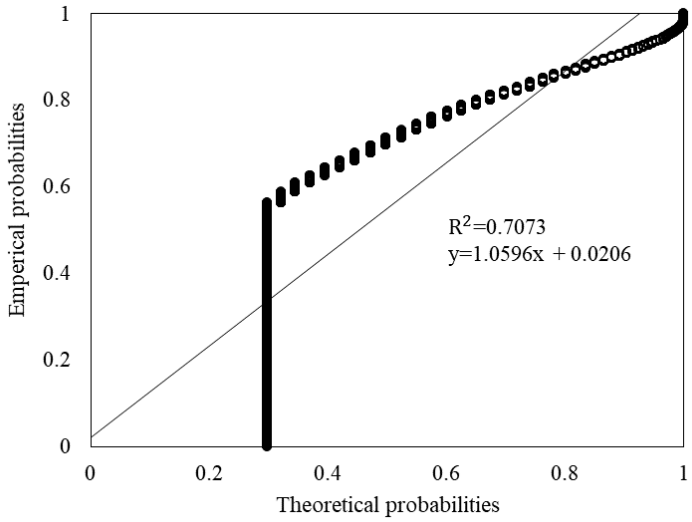


**Figure B-21: Sample 1.2 left rut normal probability plot**

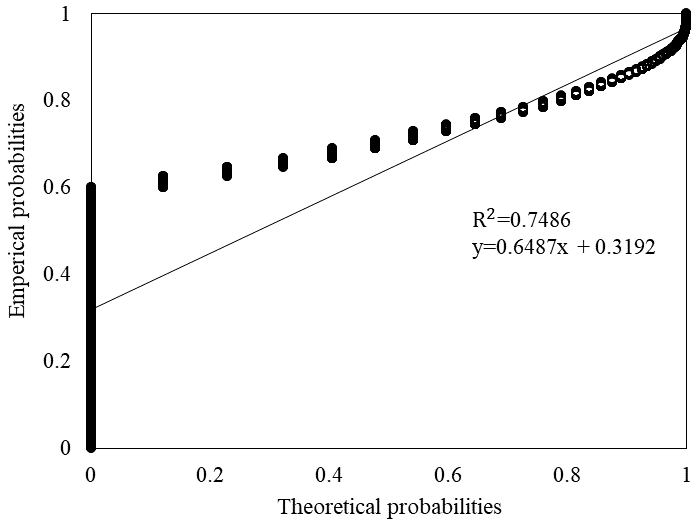


**Figure B-22: Sample 1.3 left rut exponential probability plot**

N/A

**Figure B-23: Sample 1.3 left rut lognormal probability plot**

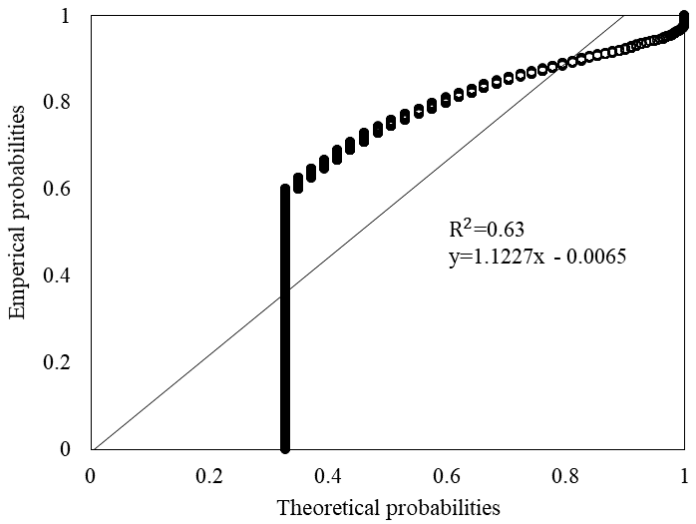


**Figure B-24: Sample 1.3 left rut normal probability plot**

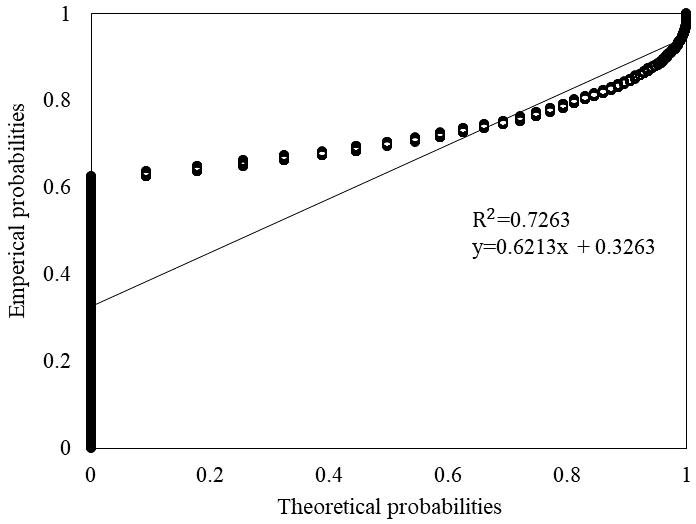


**Figure B-25: Sample 1.4 left rut exponential probability plot**

N/A

**Figure B-26: Sample 1.4 left rut lognormal probability plot**

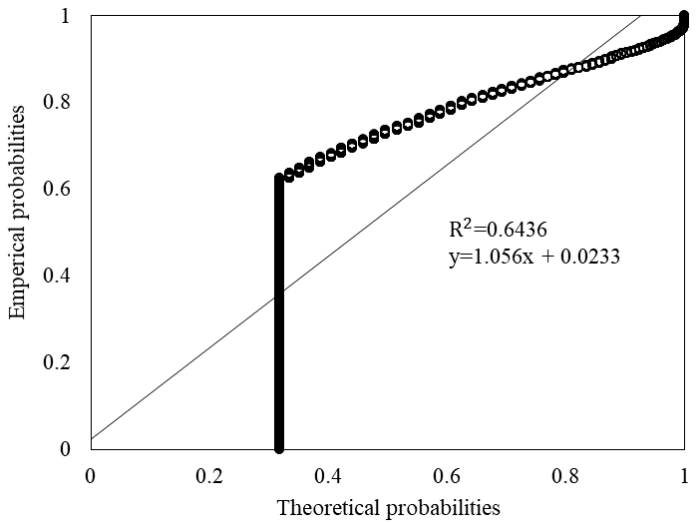


**Figure B-27: Sample 1.4 left rut normal probability plot**

Figure B-28 to Figure B-30 present the 1 km sample length exponential, lognormal, and normal probability plots for sample 1 left rut depth measurements.

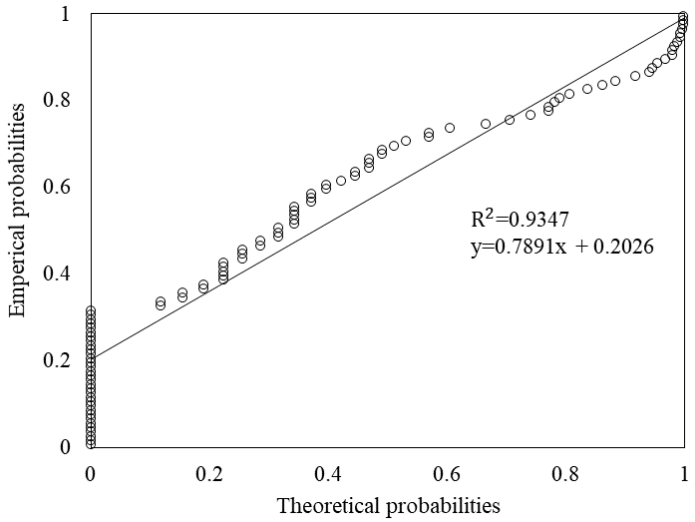


**Figure B-28: Sample 1.1 left rut exponential probability plot**

N/A

**Figure B-29: Sample 1.1 left rut lognormal probability plot**

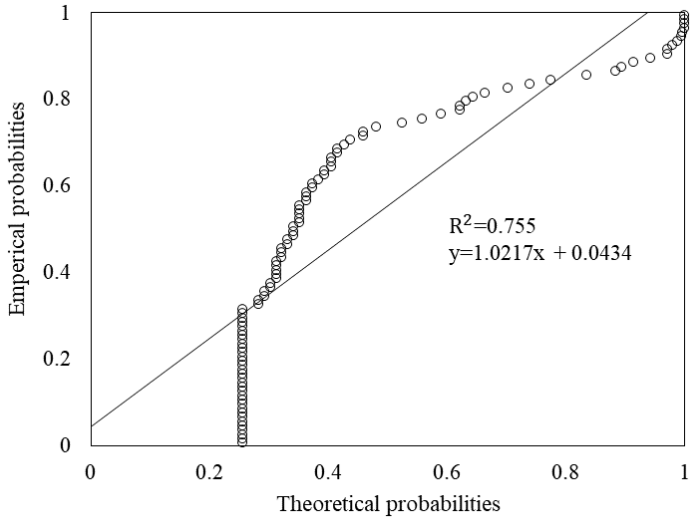


**Figure B-30: Sample 1.1 left rut normal probability plot**

## B.3 RIGHT RUT DEPTH PROBABILITY PLOTS

Figure B-31 to Figure B-45 present the full sample length exponential, lognormal, and normal probability plots for the right rut depth of samples obtained for the analysis.

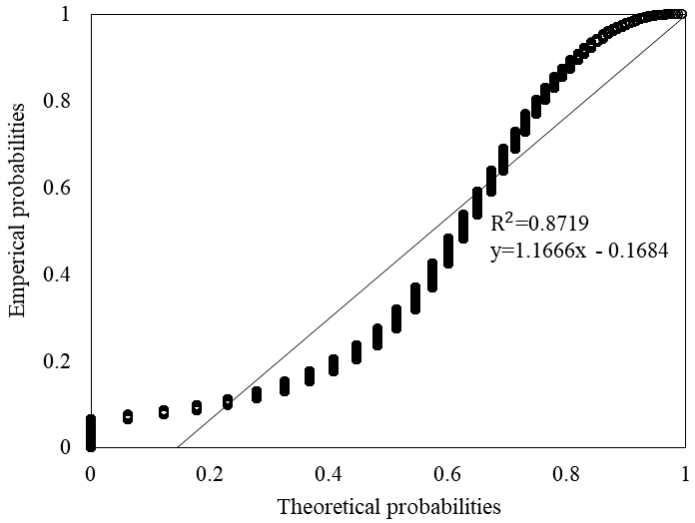


**Figure B-31: Sample 1 right rut exponential probability plot**

N/A

**Figure B-32: Sample 1 right rut lognormal probability plot**

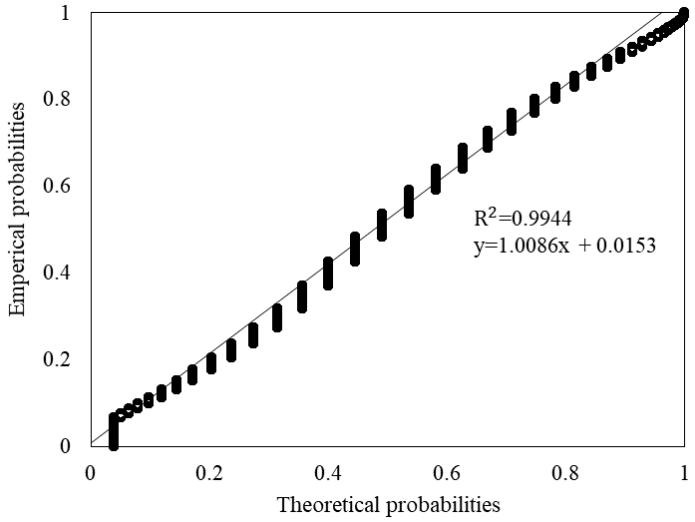


**Figure B-33: Sample 1 right rut normal probability plot**

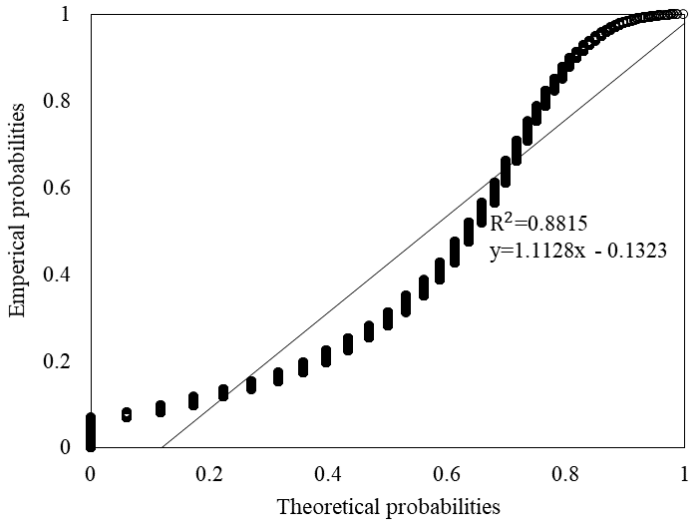


**Figure B-34: Sample 2 right rut exponential probability plot**

N/A

**Figure B-35: Sample 2 right rut lognormal probability plot**

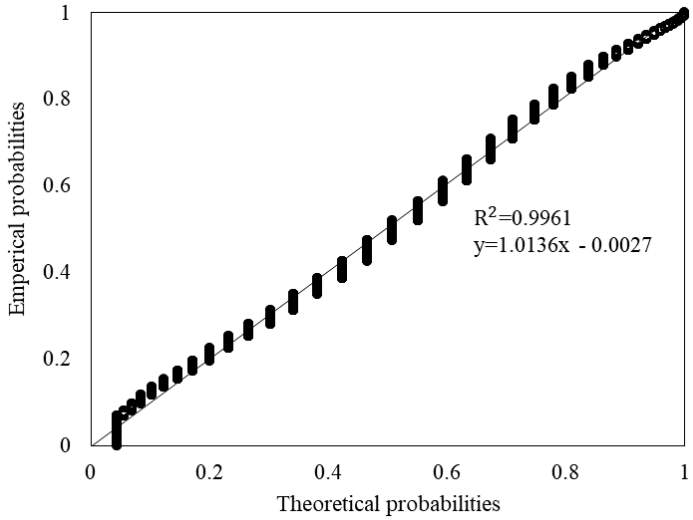


**Figure B-36: Sample 2 right rut normal probability plot**

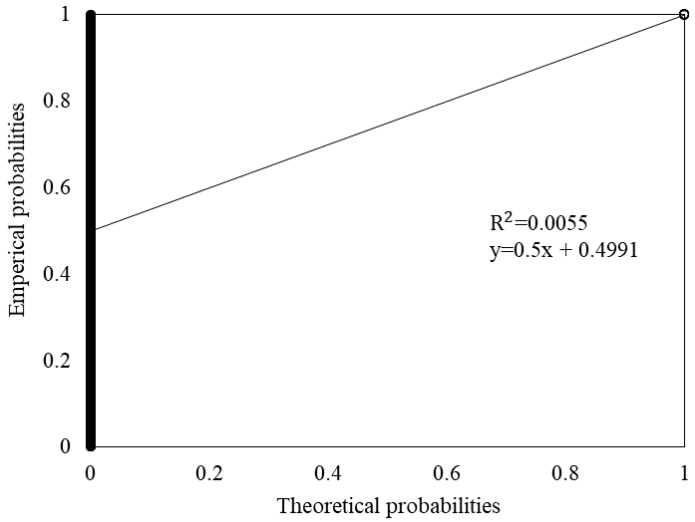


**Figure B-37: Sample 3 right rut exponential probability plot**

N/A

**Figure B-38: Sample 3 right rut lognormal probability plot**

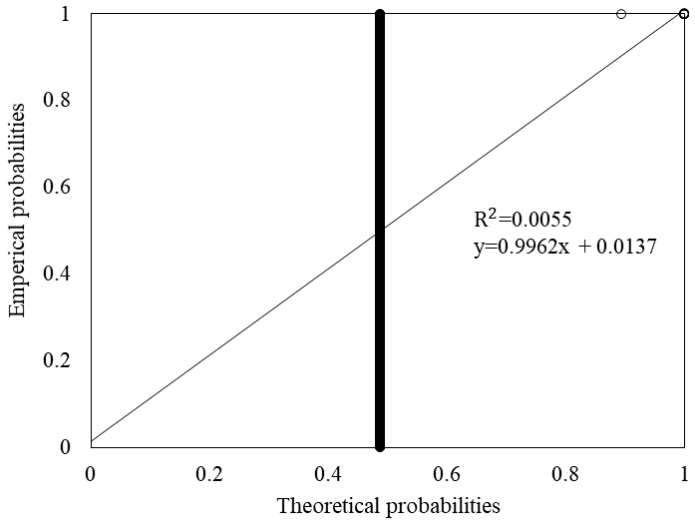


**Figure B-39: Sample 3 right rut normal probability plot**

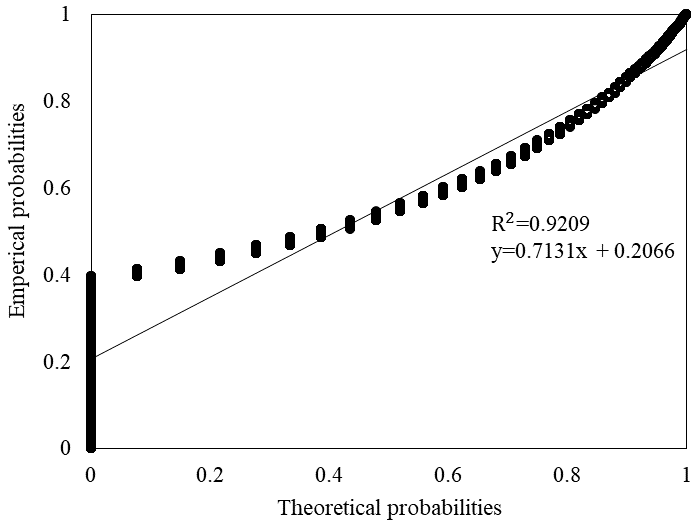


**Figure B-40: Sample 4 right rut exponential probability plot**

N/A

**Figure B-41: Sample 4 right rut lognormal probability plot**

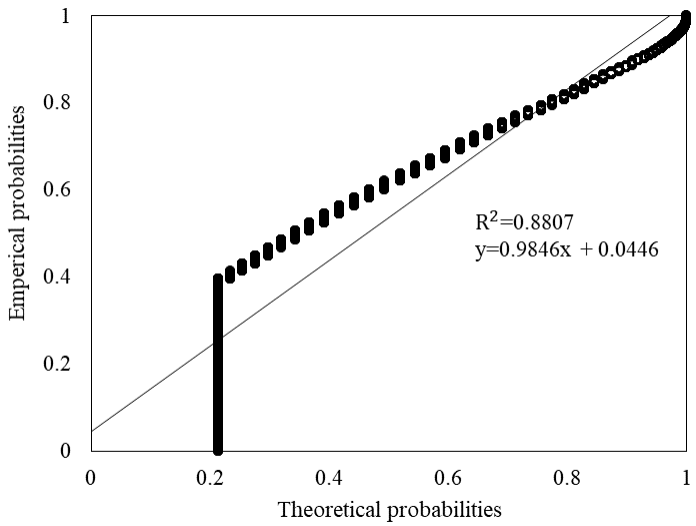


**Figure B-42: Sample 4 right rut normal probability plot**

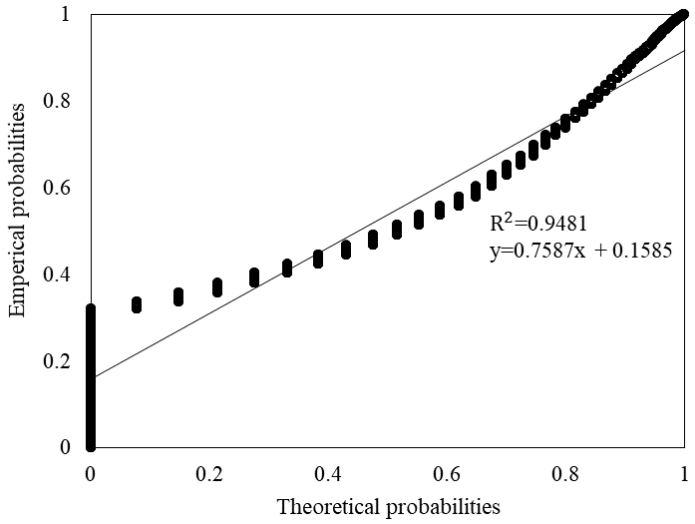


**Figure B-43: Sample 5 right rut exponential probability plot**

N/A

**Figure B-44: Sample 5 right rut lognormal probability plot**

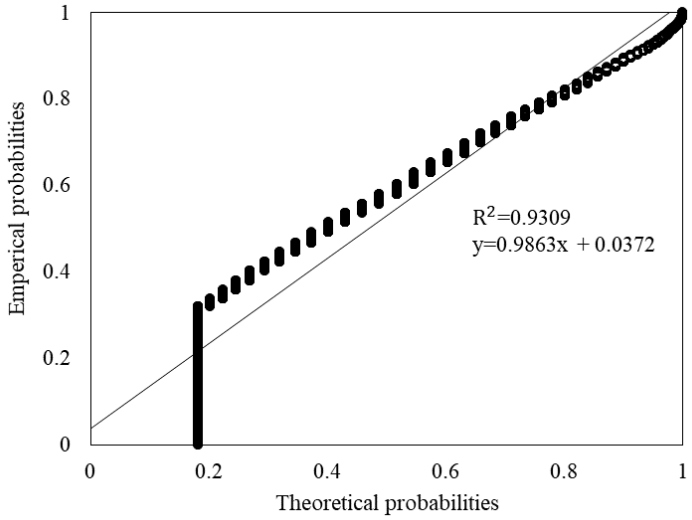


**Figure B-45: Sample 5 right rut normal probability plot**

Figure B-46 to Figure B-57 present the 50 km sample length exponential, lognormal, and normal probability plots for sample 1 right rut depth measurements.

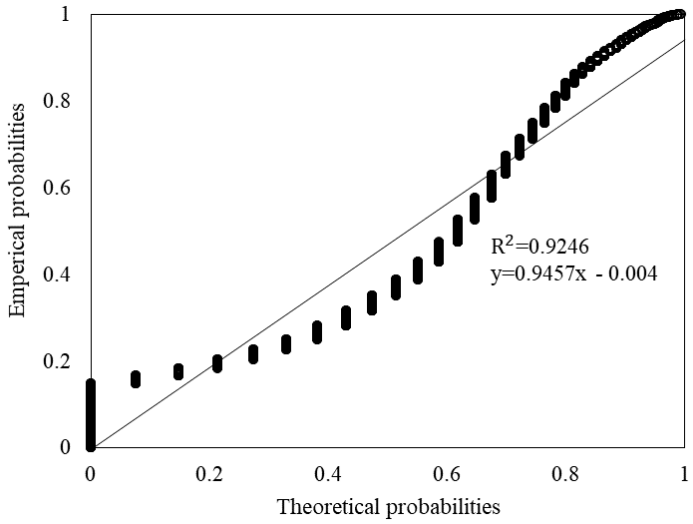


**Figure B-46: Sample 1.1 right rut exponential probability plot**

N/A

**Figure B-47: Sample 1.1 right rut lognormal probability plot**

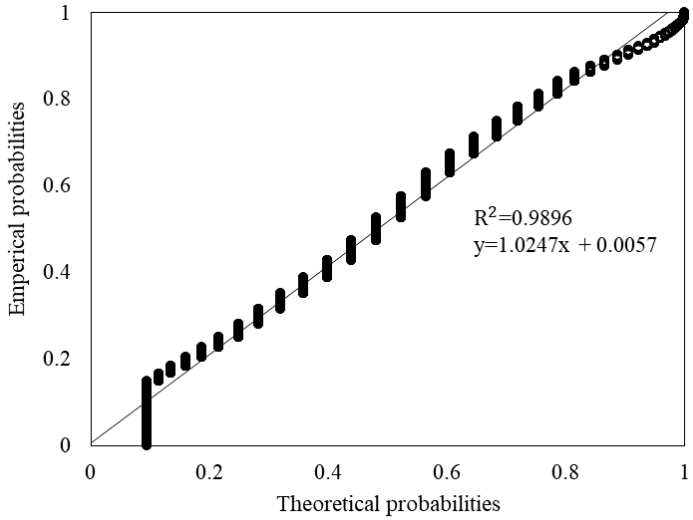


**Figure B-48: Sample 1.1 right rut normal probability plot**

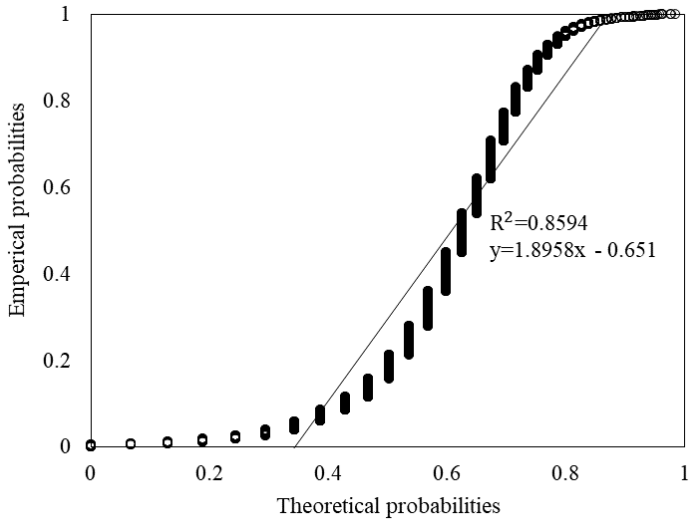


**Figure B-49: Sample 1.2 right rut exponential probability plot**

N/A

**Figure B-50: Sample 1.2 right rut lognormal probability plot**

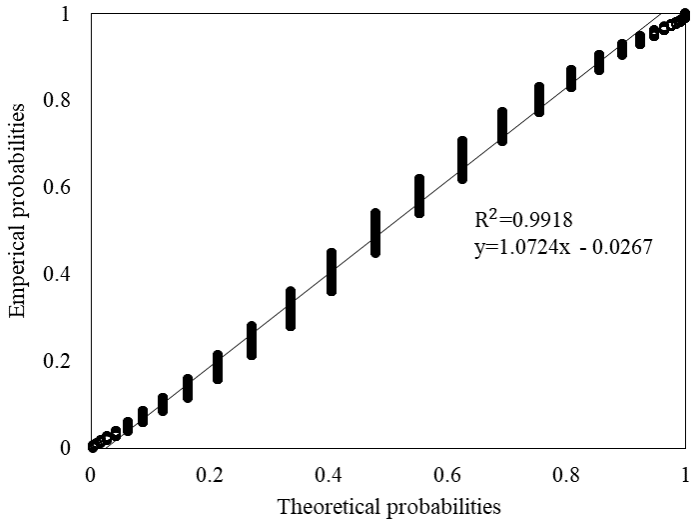


**Figure B-51: Sample 1.2 right rut normal probability plot**

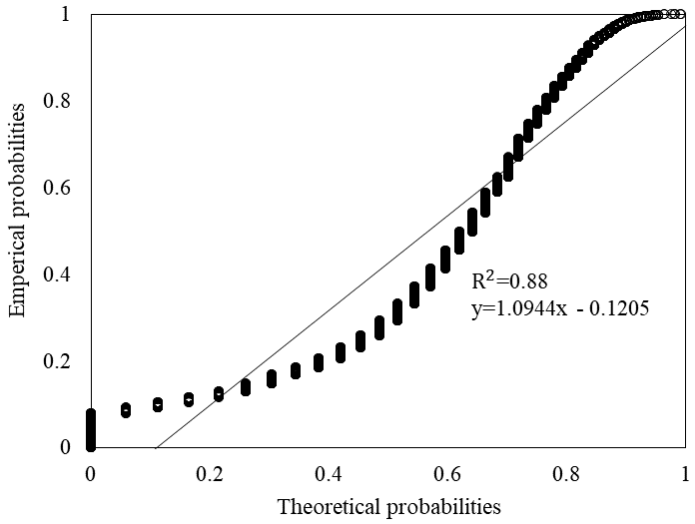


**Figure B-52: Sample 1.3 right rut exponential probability plot**

N/A

**Figure B-53: Sample 1.3 right rut lognormal probability plot**

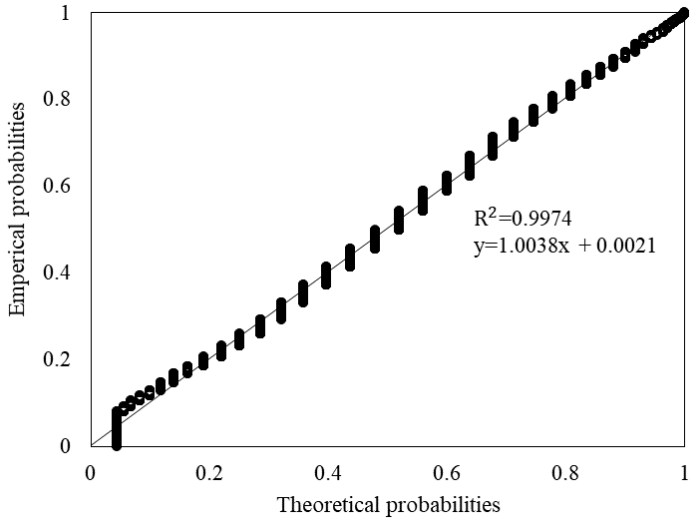


**Figure B-54: Sample 1.3 right rut normal probability plot**

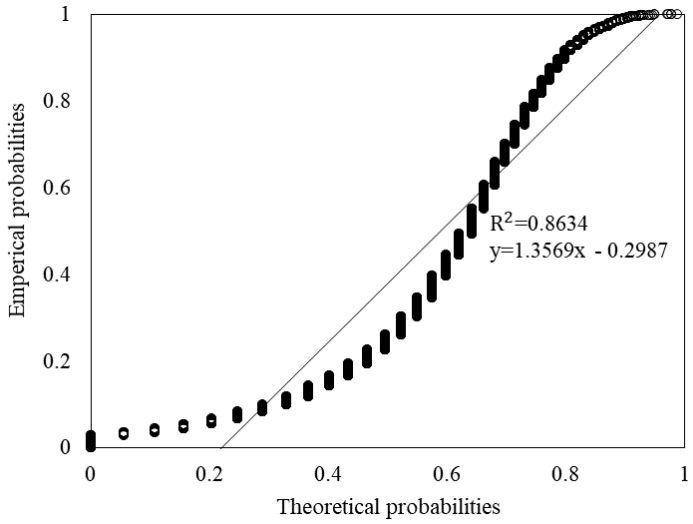


**Figure B-55: Sample 1.4 right rut exponential probability plot**

N/A

**Figure B-56: Sample 1.4 right rut lognormal probability plot**

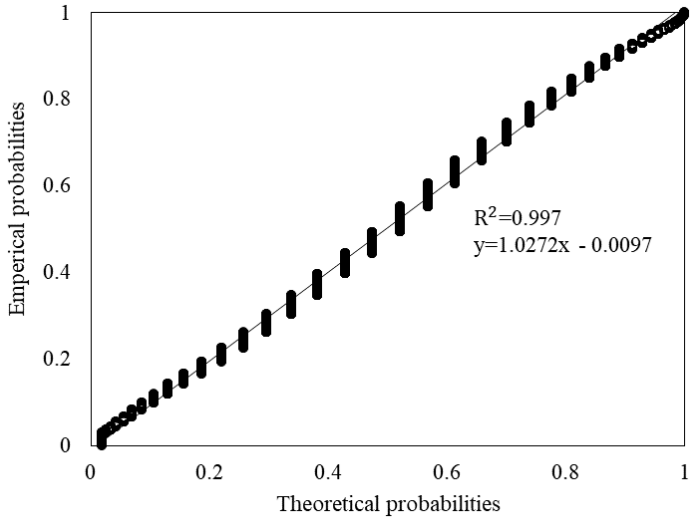


**Figure B-57: Sample 1.4 right rut normal probability plot**

Figure B-58 to Figure B-60 present the 1 km sample length exponential, lognormal, and normal probability plots for sample 1 right rut depth measurements.

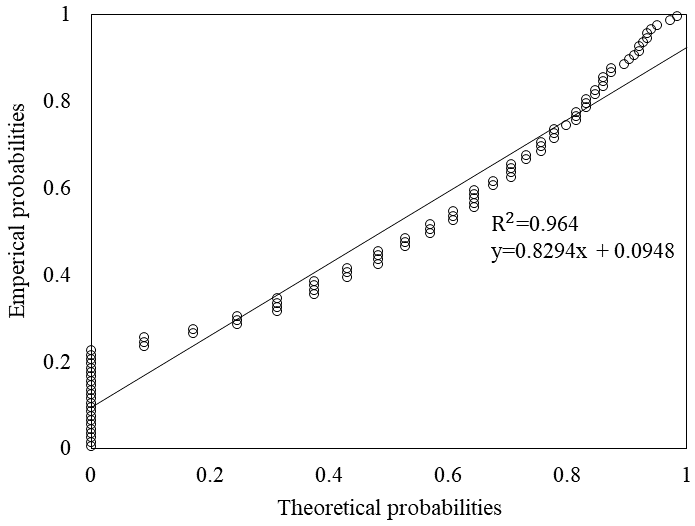


**Figure B-58: Sample 1.1 right rut exponential probability plot**

N/A

**Figure B-59: Sample 1.1 right rut lognormal probability plot**

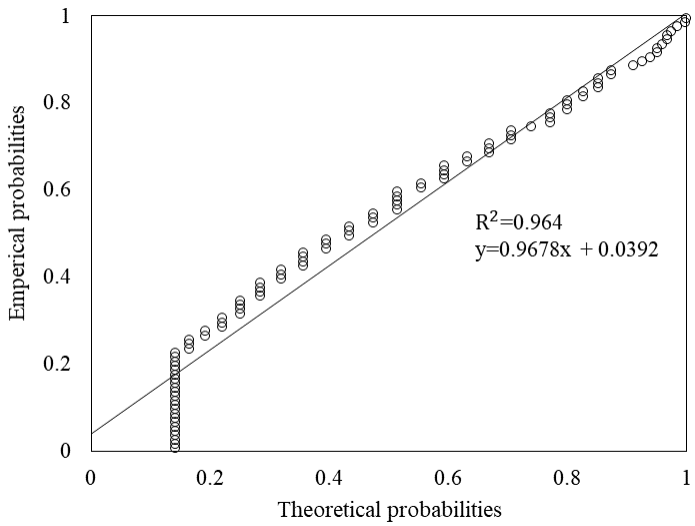


**Figure B-60: Sample 1.1 right rut normal probability plot**

# APPENDIX C

# LEFT AND RIGHT RUT DEPTH PROBABILITY PLOTS FOR DATASET 2 SAMPLES

# APPENDIX C LEFT AND RIGHT RUT DEPTH PROBABILITY PLOTS FOR DATASET 2 SAMPLES

## C.1 INTRODUCTION

The exponential, lognormal, and normal probability plots plotted in R-Studio for left and right rut depth 10 m measurements for each of the 13 roads selected for the analysis are presented in the sections that follow.

## C.2 LEFT RUT DEPTH PROBABILITY PLOTS

Figure C-1 to Figure C-39 present exponential, lognormal, and normal probability plots for the left rut depth of roads selected for the analysis.

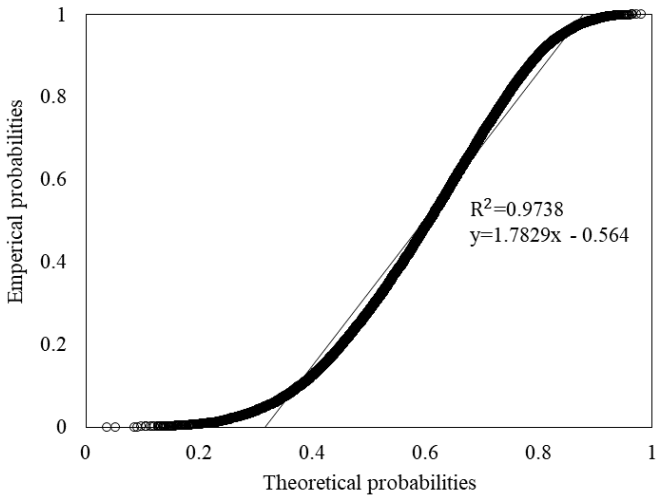


**Figure C-1: Sample 1 left rut exponential probability plot**

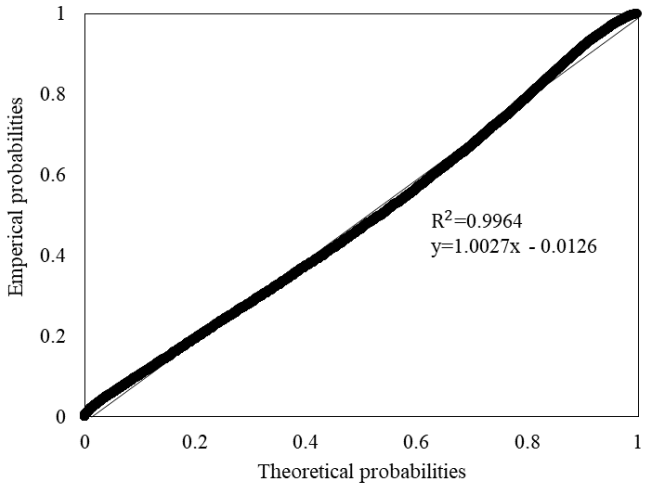


**Figure C-2: Sample 1 left rut lognormal probability plot**

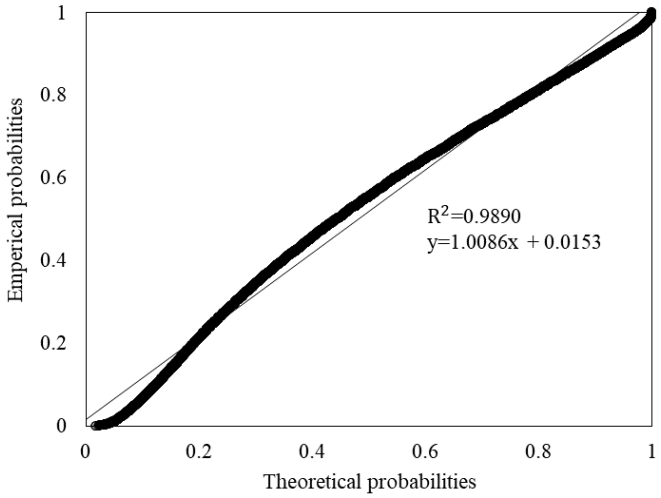


**Figure C-3: Sample 1 left rut normal probability plot**

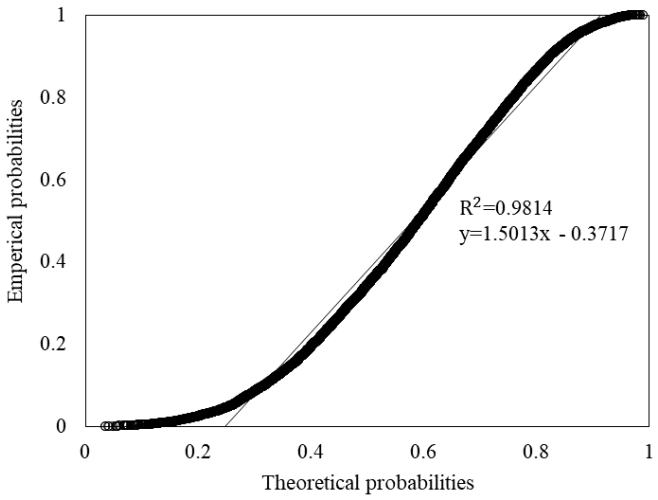


**Figure C-4: Sample 2 left rut exponential probability plot**

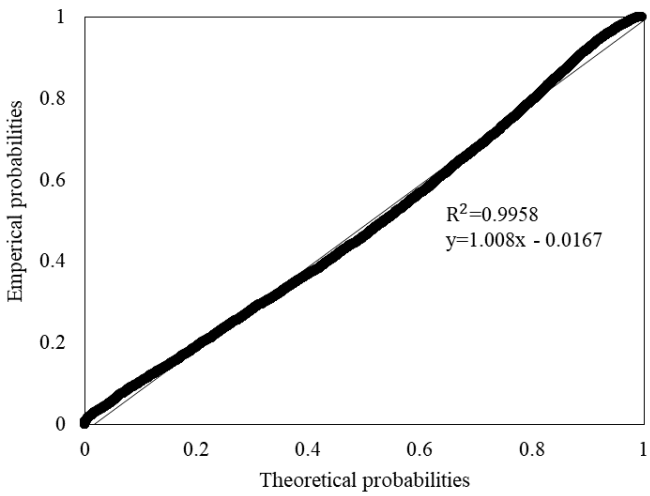


**Figure C-5: Sample 2 left rut lognormal probability plot**

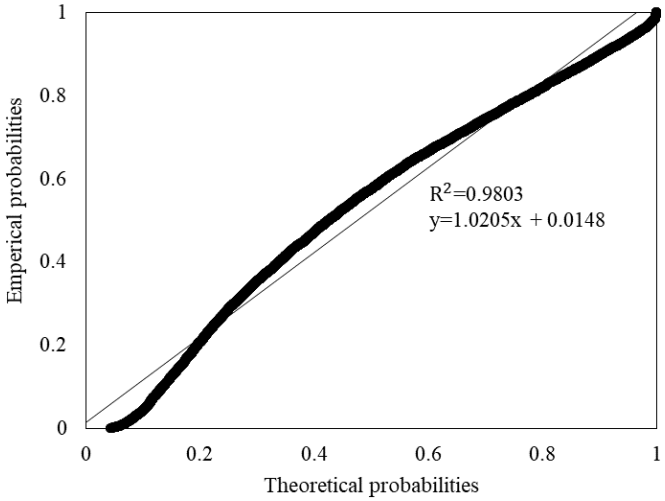


**Figure C-6: Sample 2 left rut normal probability plot**

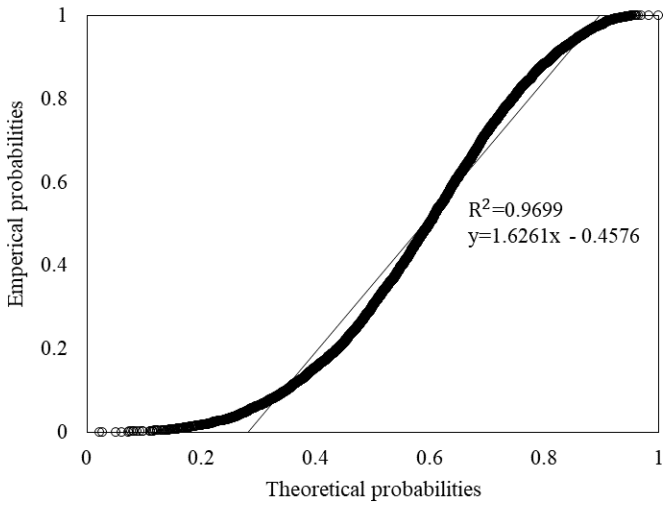


**Figure C-7: Sample 3 left rut exponential probability plot**

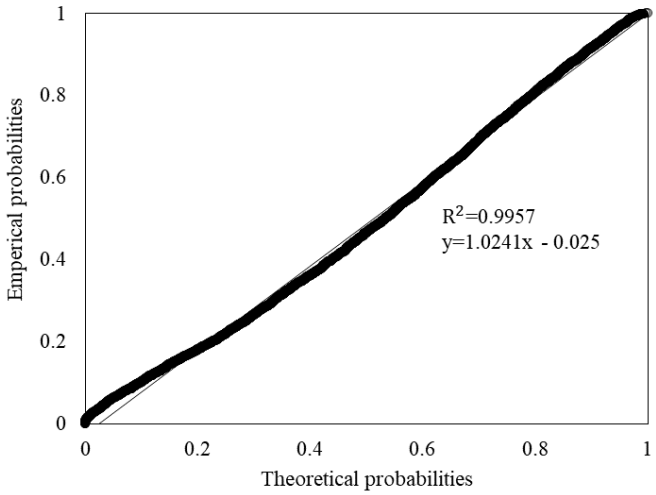


**Figure C-8: Sample 3 left rut lognormal probability plot**

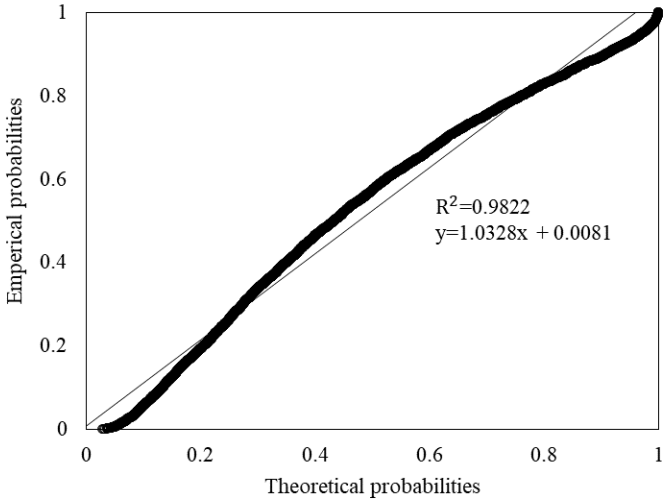


**Figure C-9: Sample 3 left rut normal probability plot**

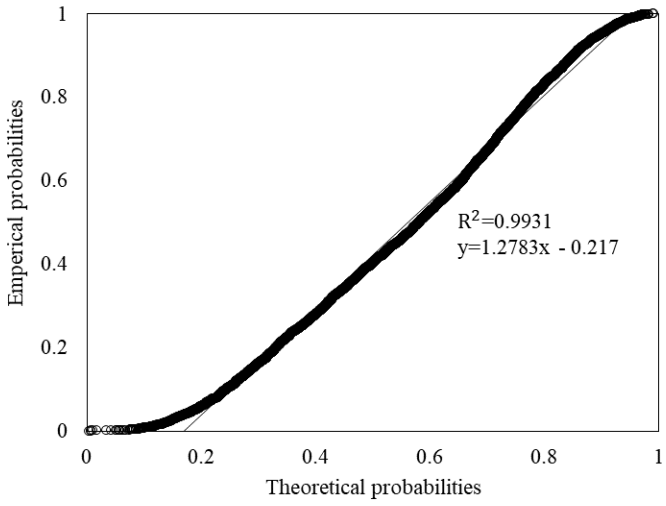


**Figure C-10: Sample 4 left rut exponential probability plot**

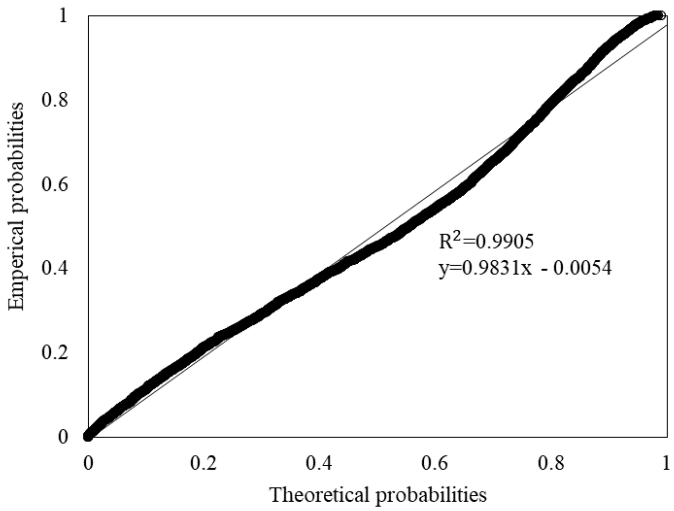


**Figure C-11: Sample 4 left rut lognormal probability plot**

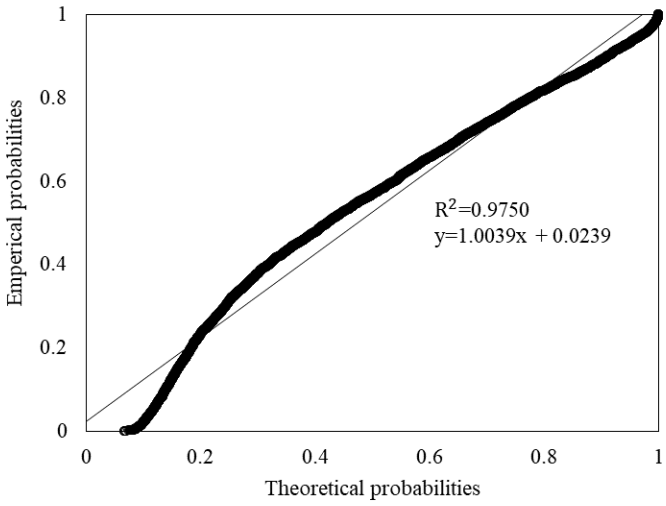


**Figure C-12: Sample 4 left rut normal probability plot**

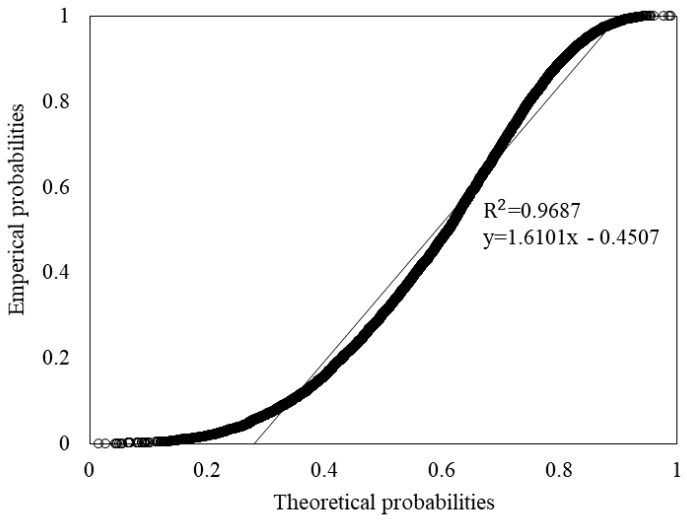


**Figure C-13: Sample 5 left rut exponential probability plot**

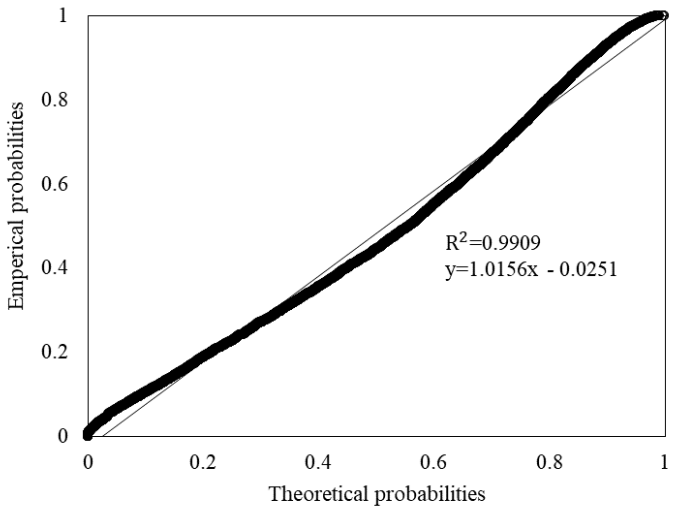


**Figure C-14: Sample 5 left rut lognormal probability plot**

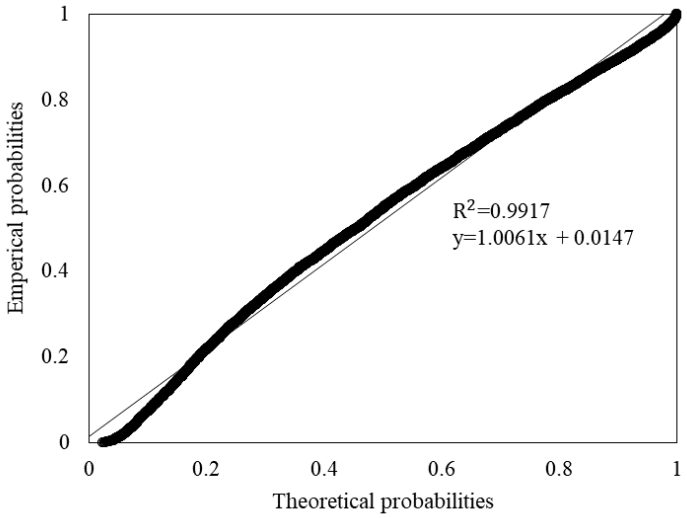


**Figure C-15: Sample 5 left rut normal probability plot**

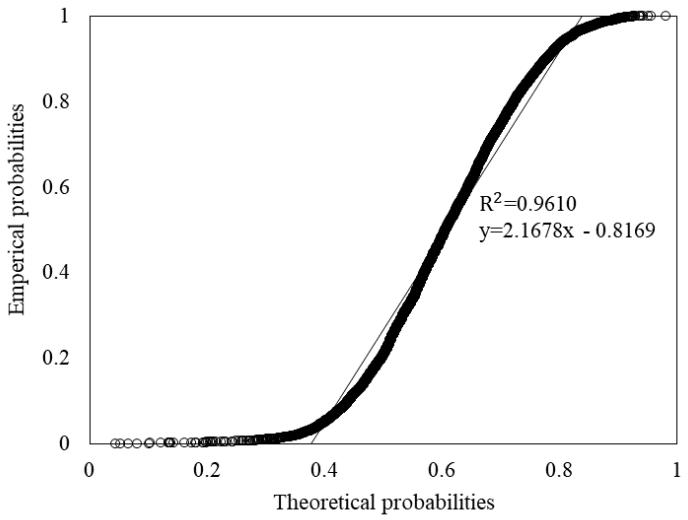


**Figure C-16: Sample 6 left rut exponential probability plot**

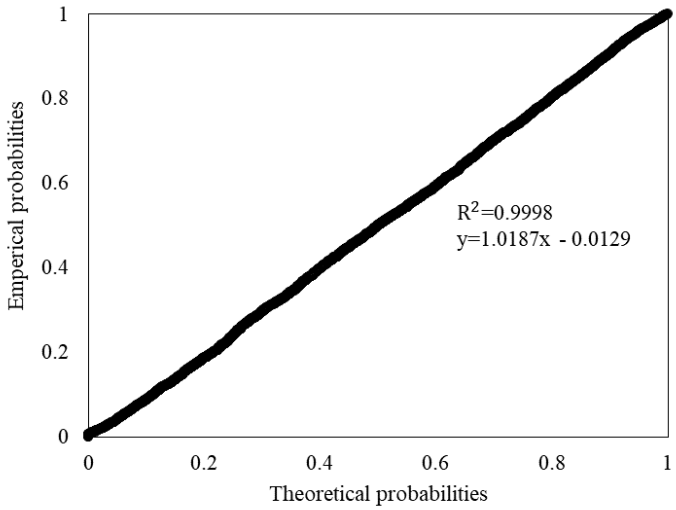


**Figure C-17: Sample 6 left rut lognormal probability plot**

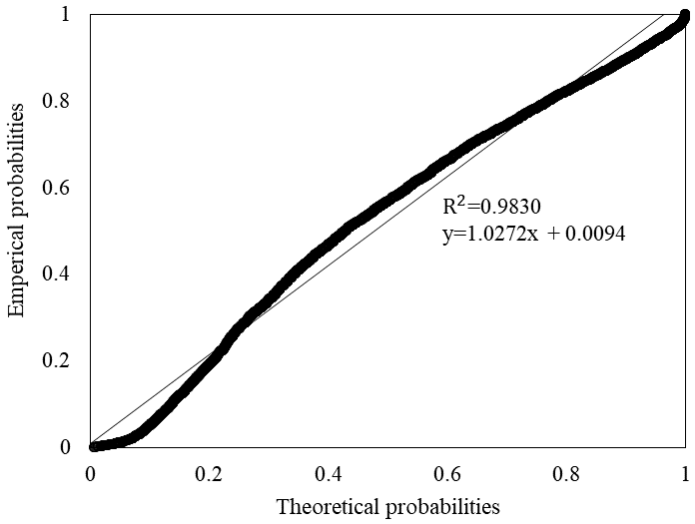


**Figure C-18: Sample 6 left rut normal probability plot**

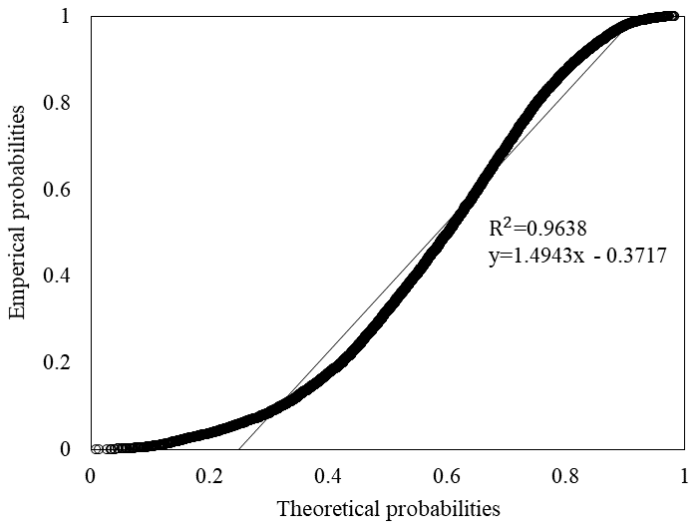


**Figure C-19: Sample 7 left rut exponential probability plot**

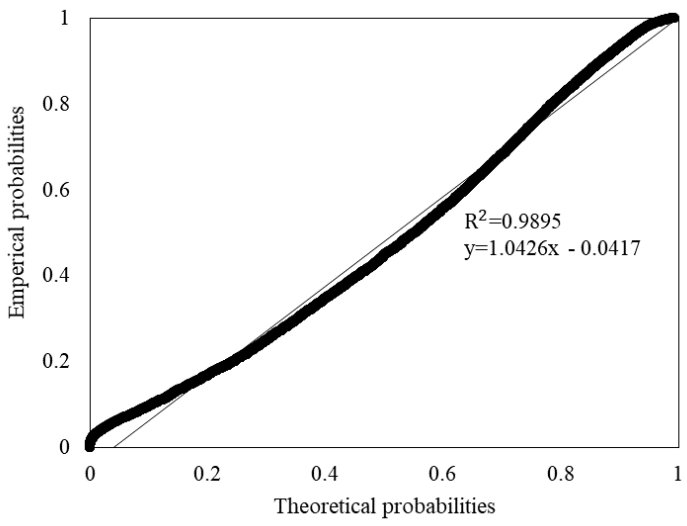


**Figure C-20: Sample 7 left rut lognormal probability plot**

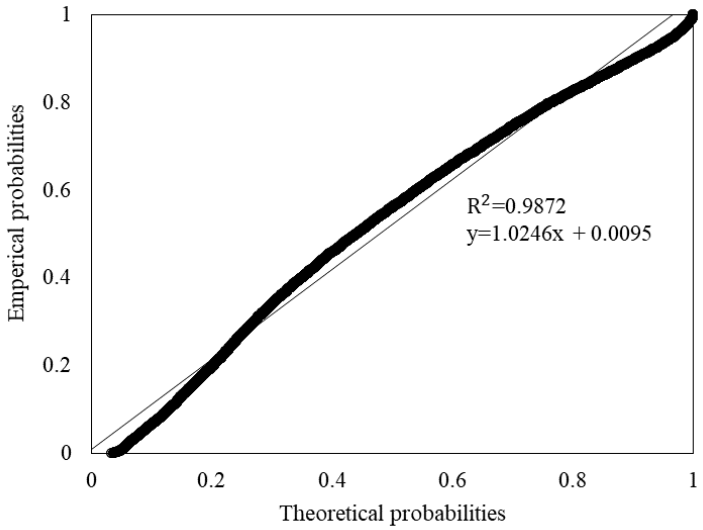


**Figure C-21: Sample 7 left rut normal probability plot**

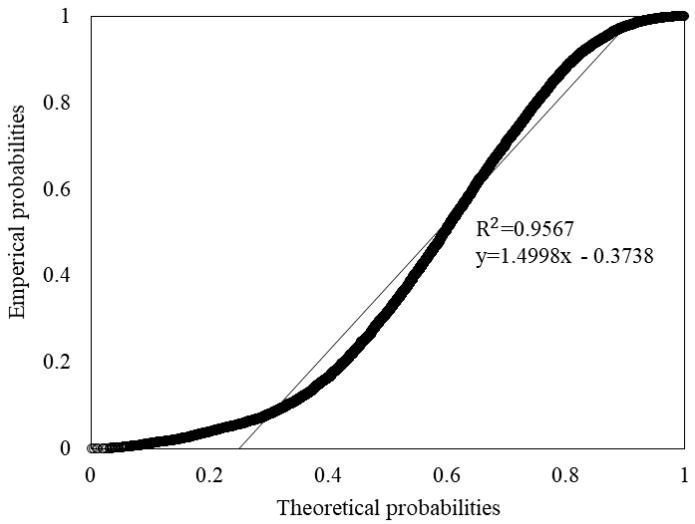


**Figure C-22: Sample 8 left rut exponential probability plot**

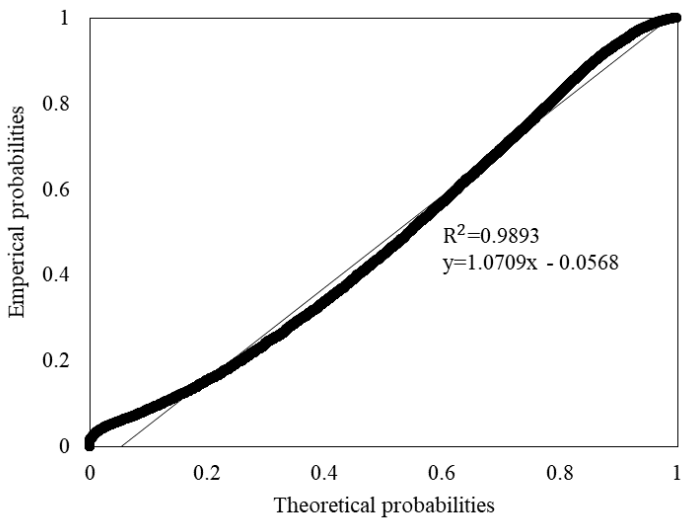


**Figure C-23: Sample 8 left rut lognormal probability plot**

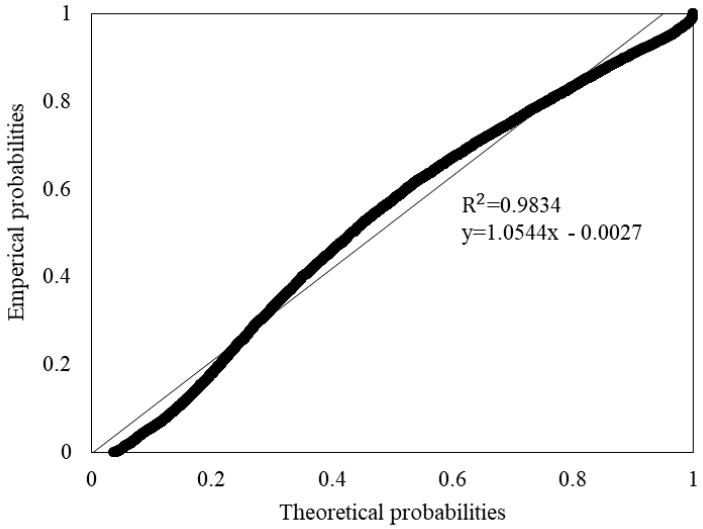


**Figure C-24: Sample 8 left rut normal probability plot**

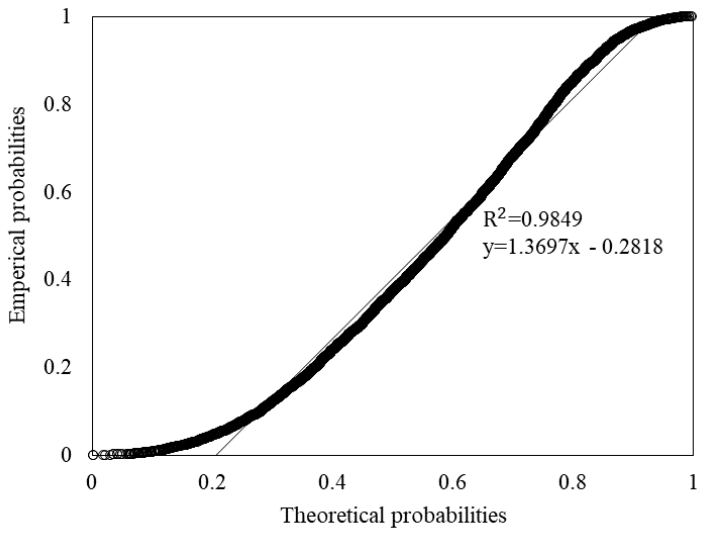


**Figure C-25: Sample 9 left rut exponential probability plot**

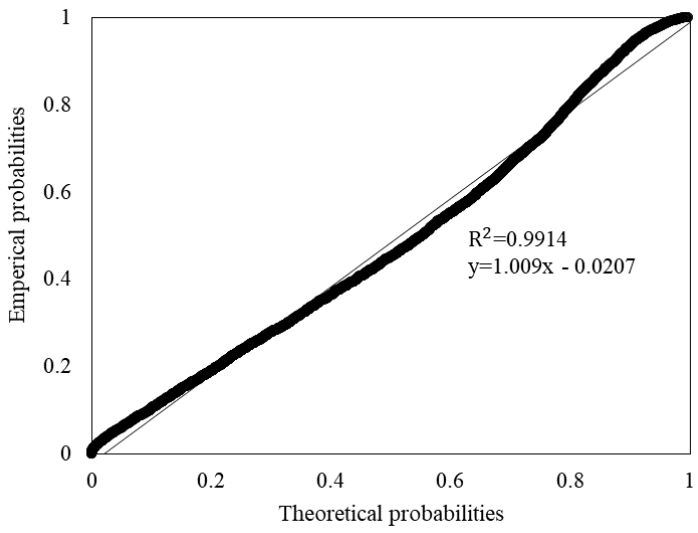


**Figure C-26: Sample 9 left rut lognormal probability plot**

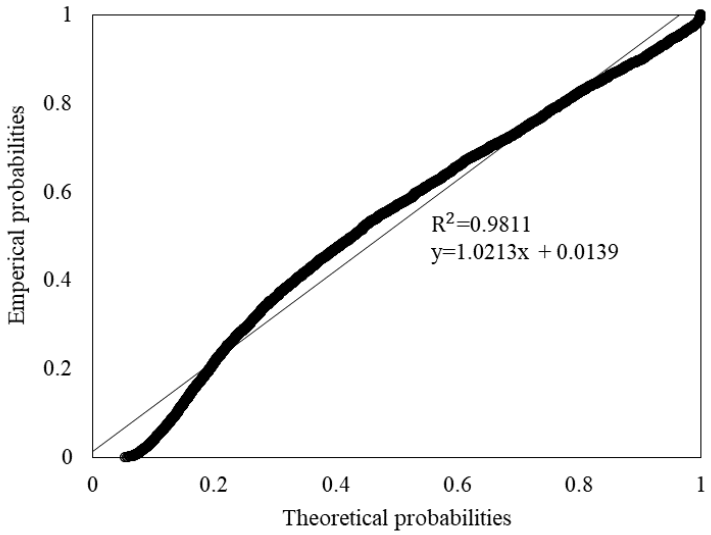


**Figure C-27: Sample 9 left rut normal probability plot**

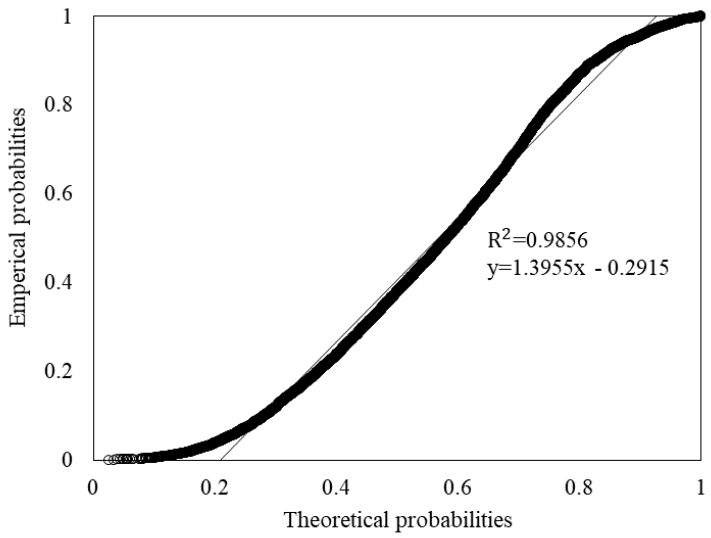


**Figure C-28: Sample 10 left rut exponential probability plot**

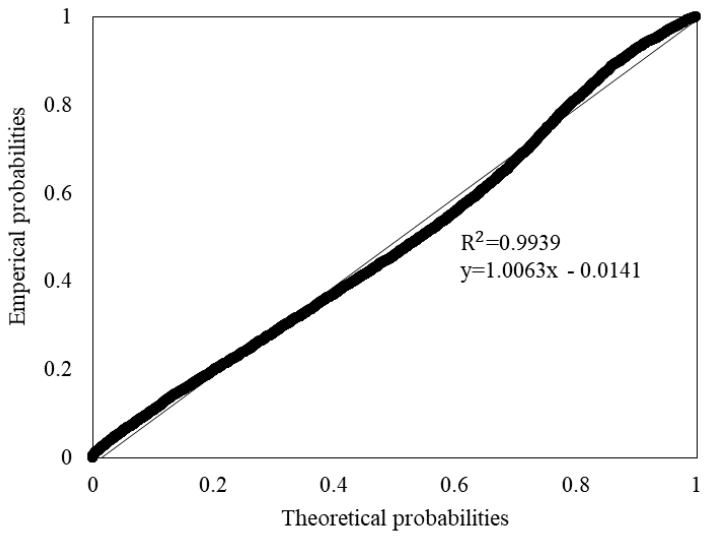


**Figure C-29: Sample 10 left rut lognormal probability plot**

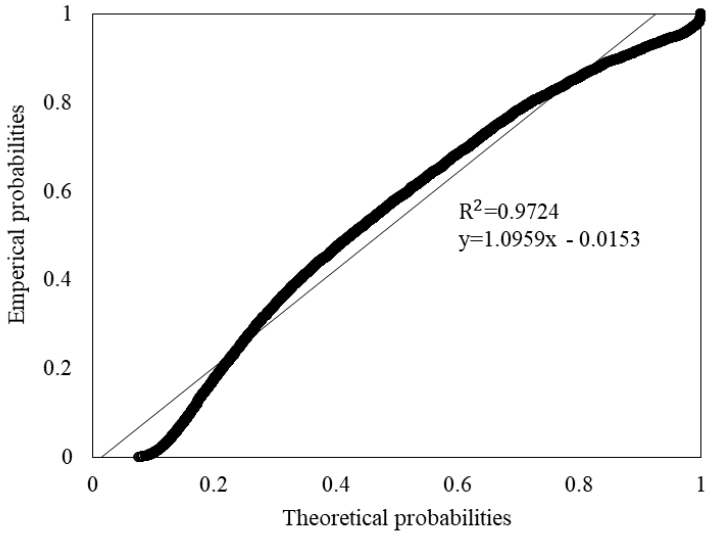


**Figure C-30: Sample 10 left rut normal probability plot**

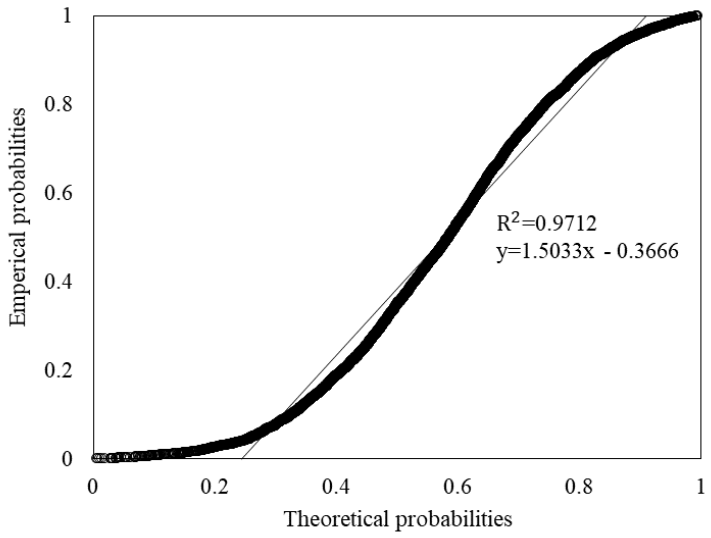


**Figure C-31: Sample 11 left rut exponential probability plot**

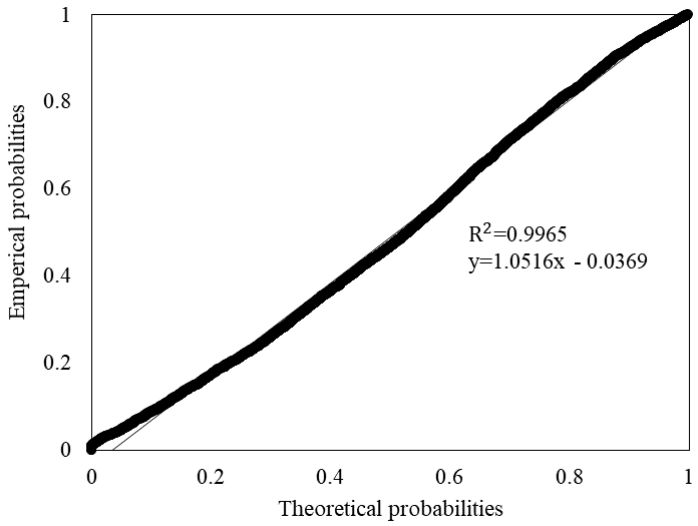


**Figure C-32: Sample 11 left rut lognormal probability plot**

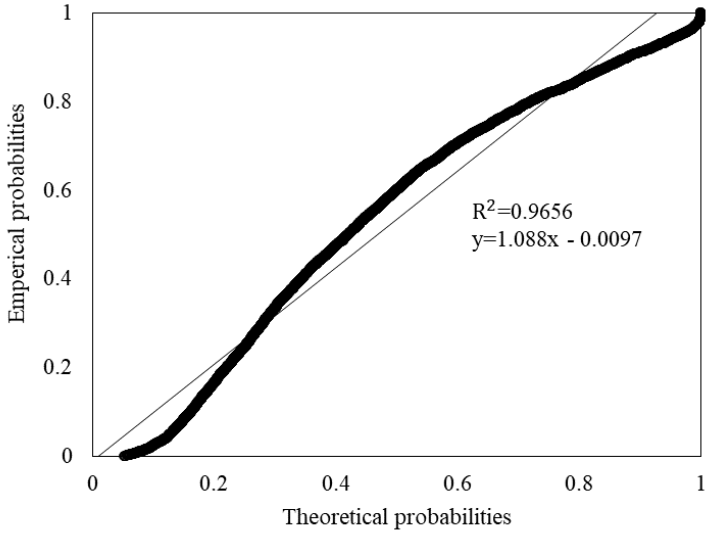


**Figure C-33: Sample 11 left rut normal probability plot**

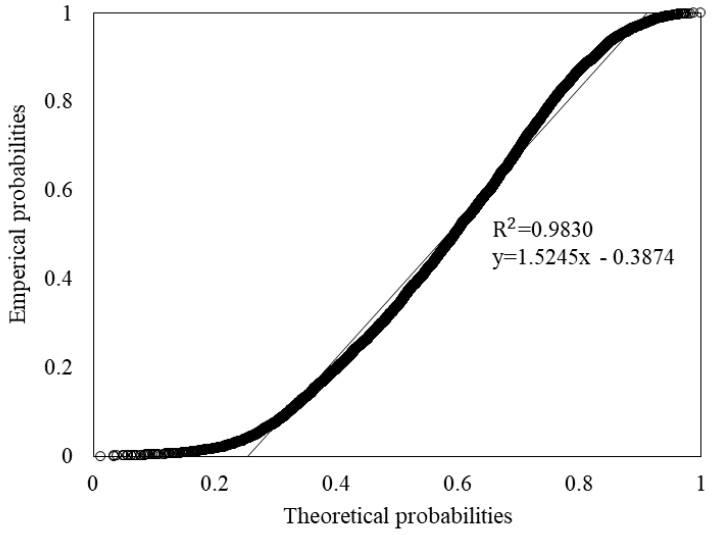


**Figure C-34: Sample 12 left rut exponential probability plot**

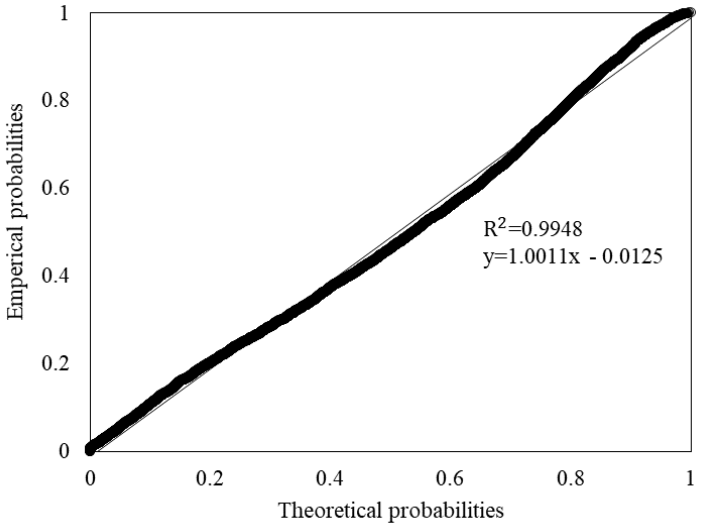


**Figure C-35: Sample 12 left rut lognormal probability plot**

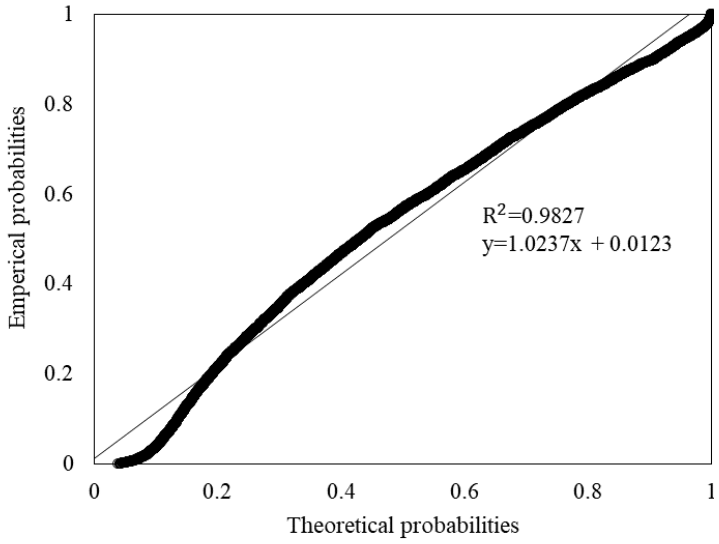


**Figure C-36: Sample 12 left rut normal probability plot**

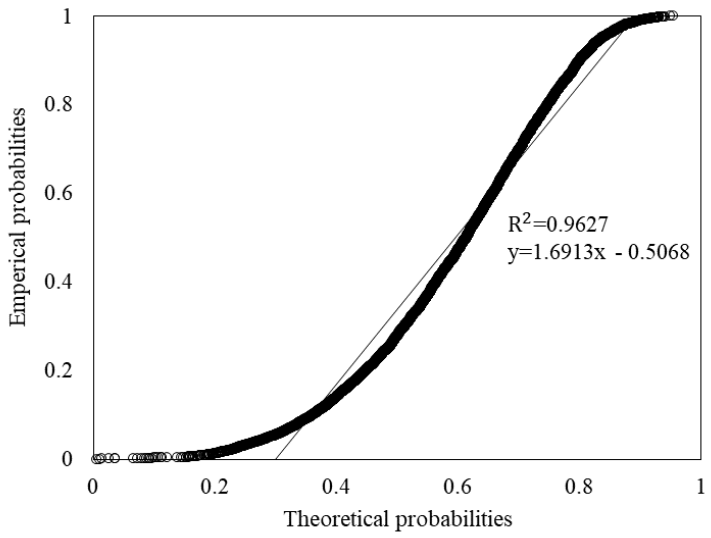


**Figure C-37: Sample 13 left rut exponential probability plot**

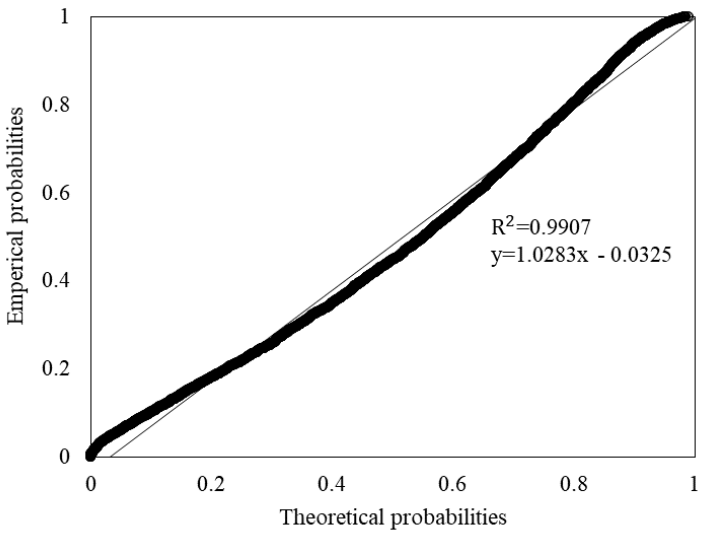


**Figure C-38: Sample 13 left rut lognormal probability plot**

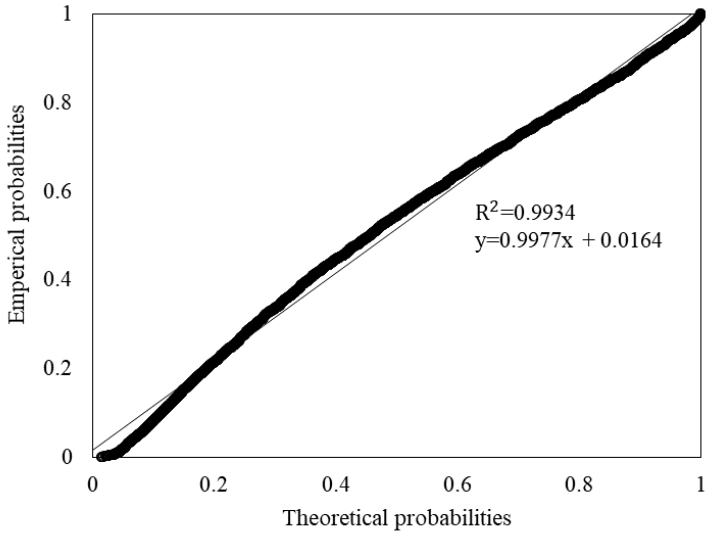


**Figure C-39: Sample 13 left rut normal probability plot**

## C.3 RIGHT RUT DEPTH PROBABILITY PLOTS

Figure C-40 to Figure C-78 present exponential, lognormal, and normal probability plots for the right rut depth of roads selected for the analysis.

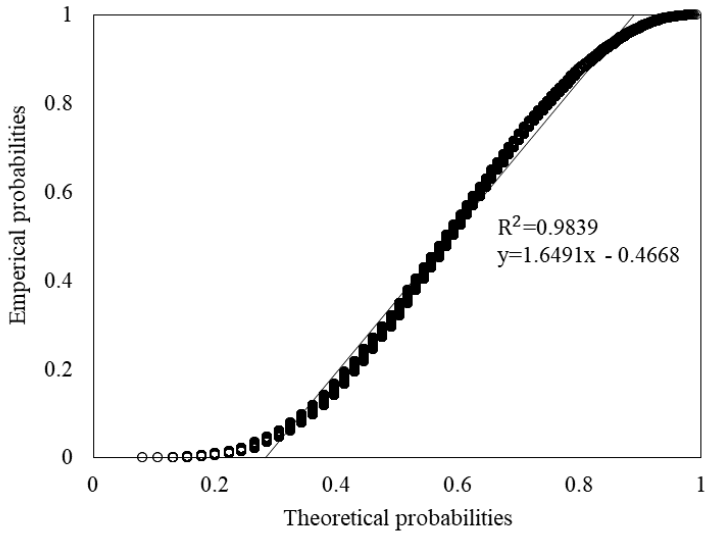


**Figure C-40: Sample 1 right rut exponential probability plot**

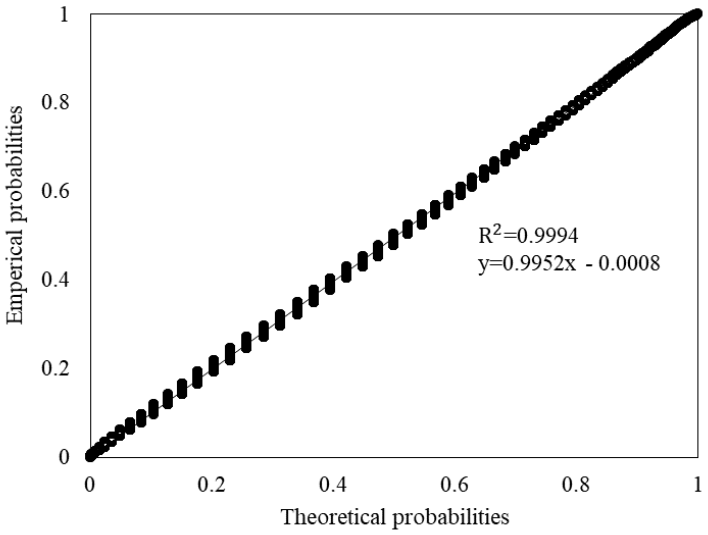


**Figure C-41: Sample 1 right rut lognormal probability plot**

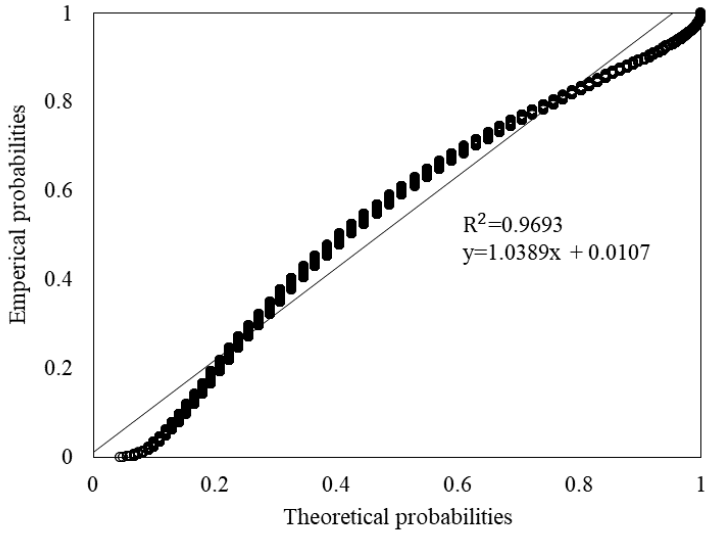


**Figure C-42: Sample 1 right rut normal probability plot**

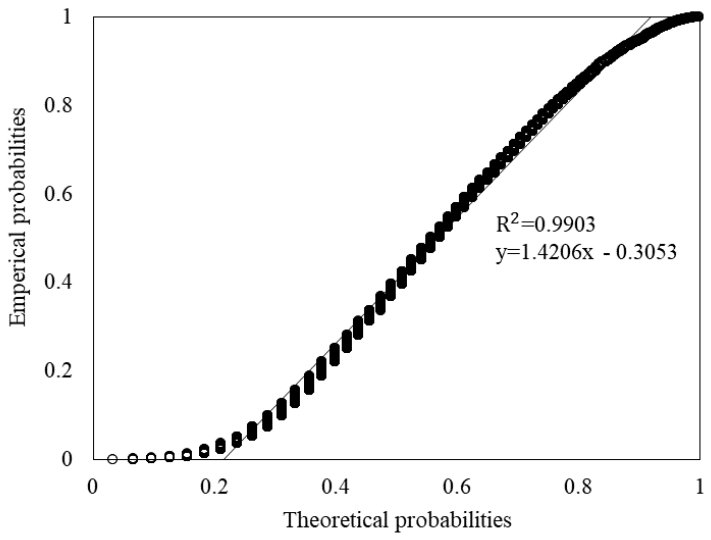


**Figure C-43: Sample 2 right rut exponential probability plot**

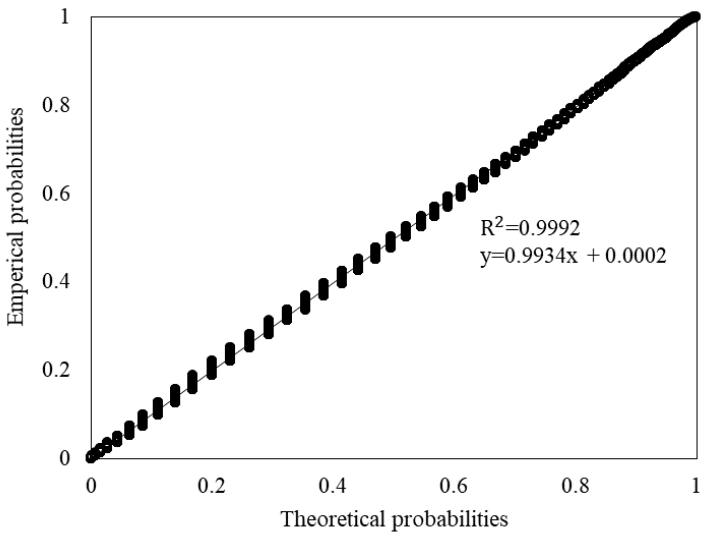


**Figure C-44: Sample 2 right rut lognormal probability plot**

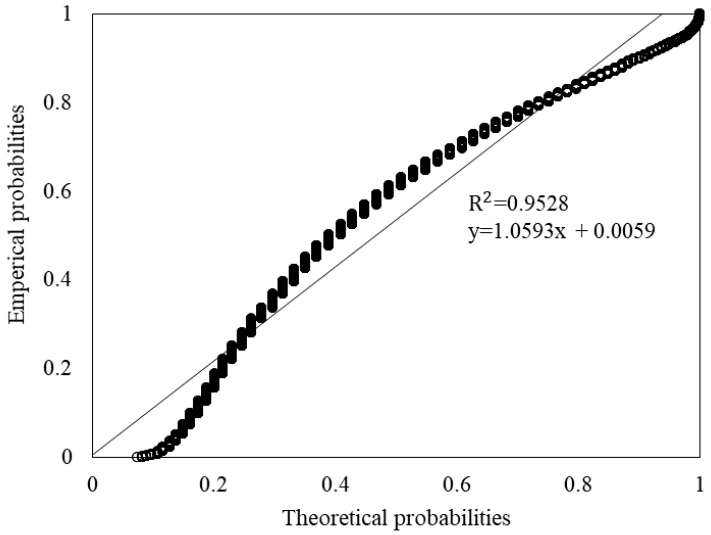


**Figure C-45: Sample 2 right rut normal probability plot**

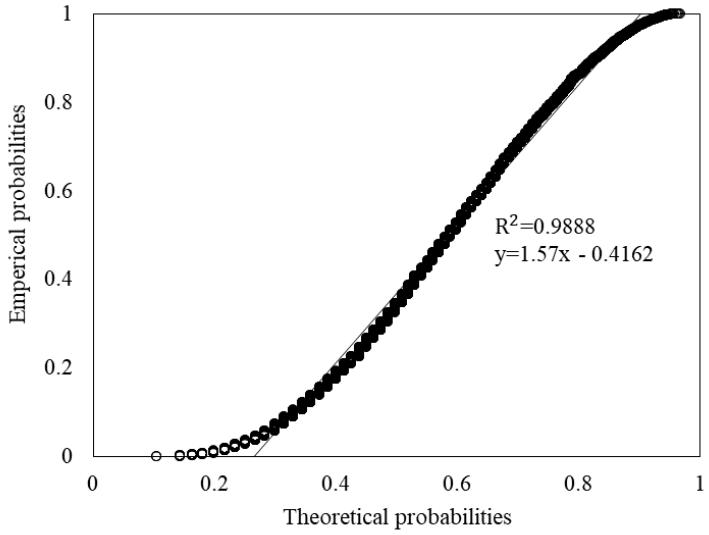


**Figure C-46: Sample 3 right rut exponential probability plot**

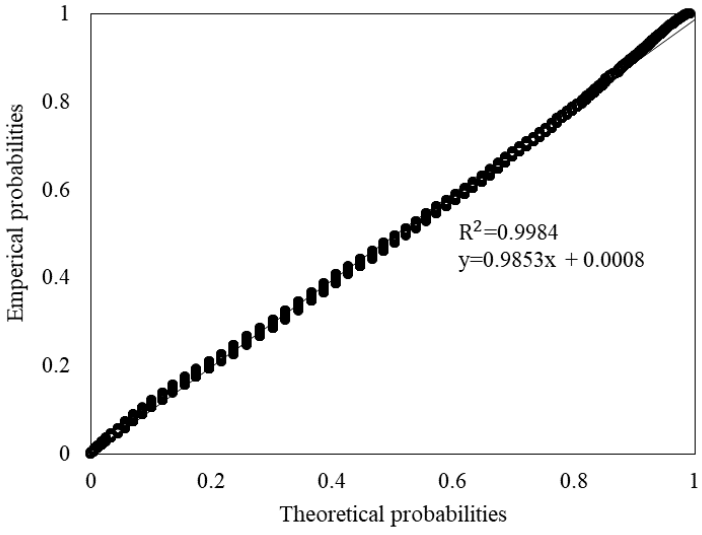


**Figure C-47: Sample 3 right rut lognormal probability plot**

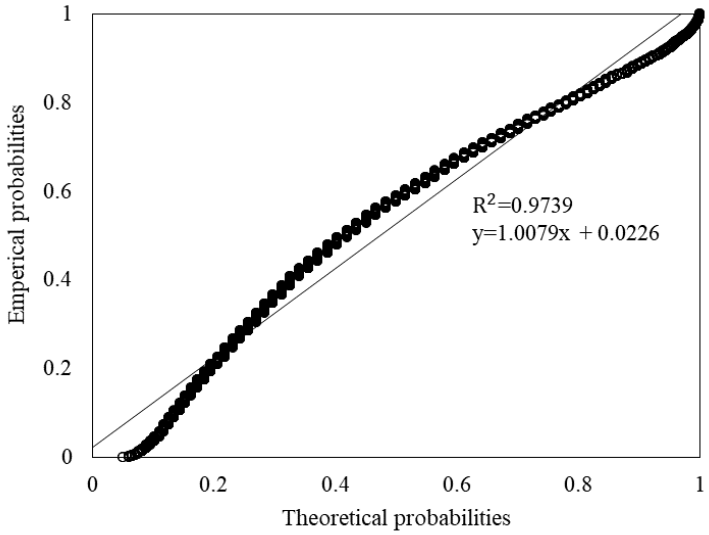


**Figure C-48: Sample 3 right rut normal probability plot**

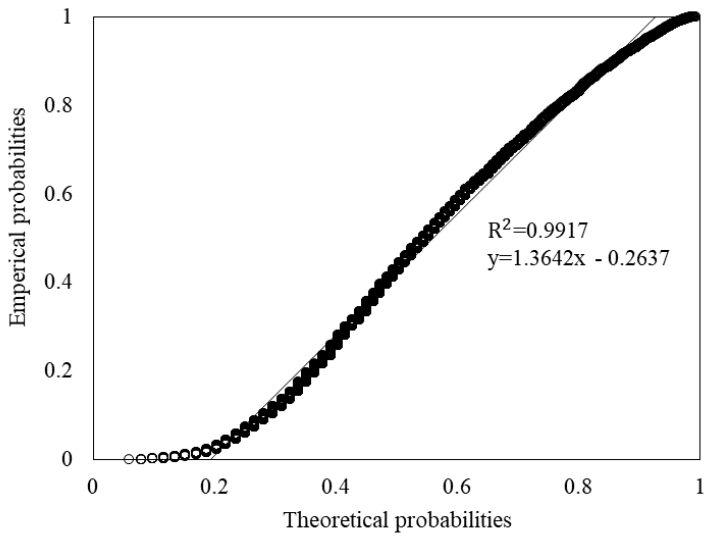


**Figure C-49: Sample 4 right rut exponential probability plot**

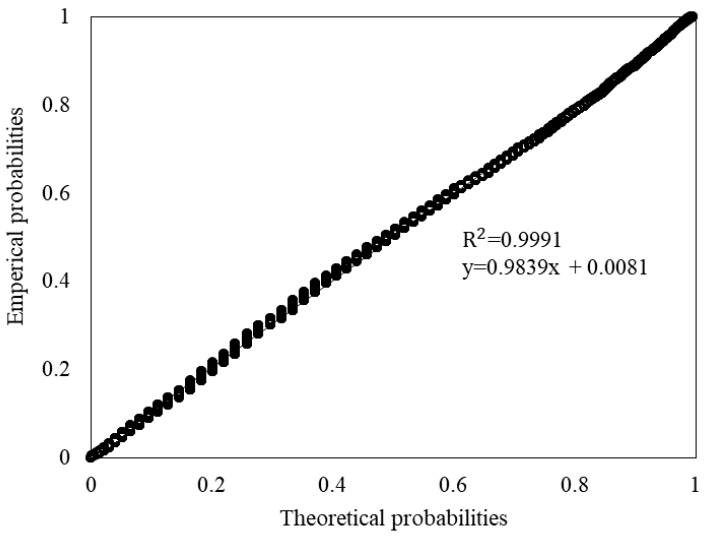


**Figure C-50: Sample 4 right rut lognormal probability plot**

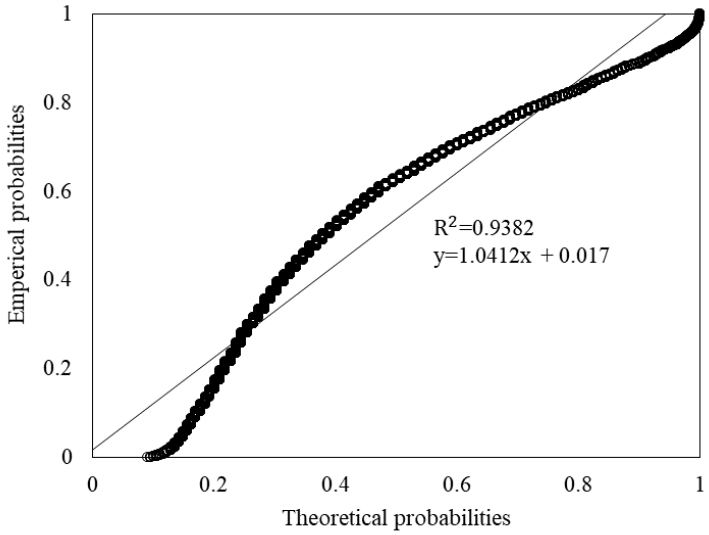


**Figure C-51: Sample 4 right rut normal probability plot**

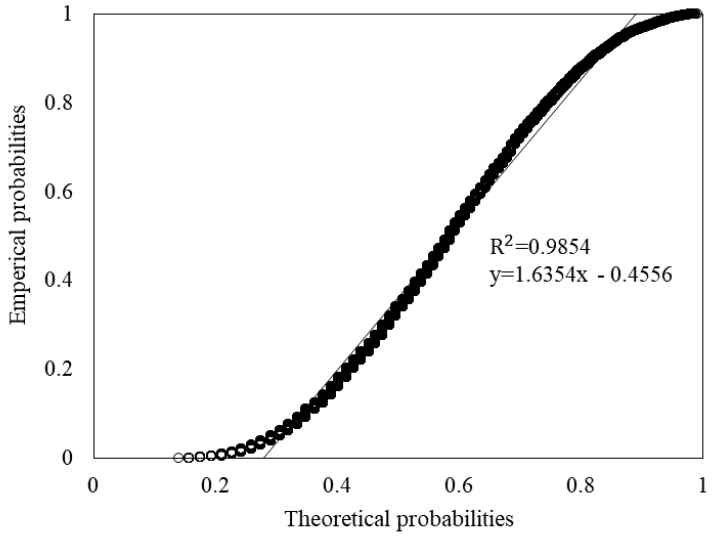


**Figure C-52: Sample 5 right rut exponential probability plot**

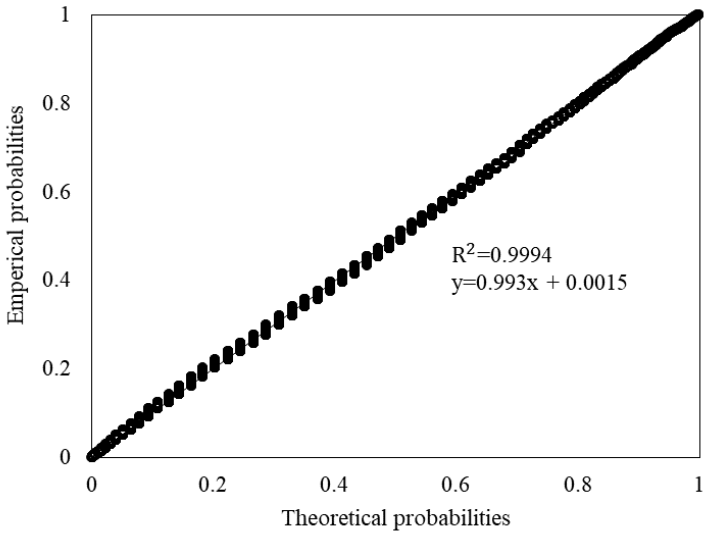


**Figure C-53: Sample 5 right rut lognormal probability plot**

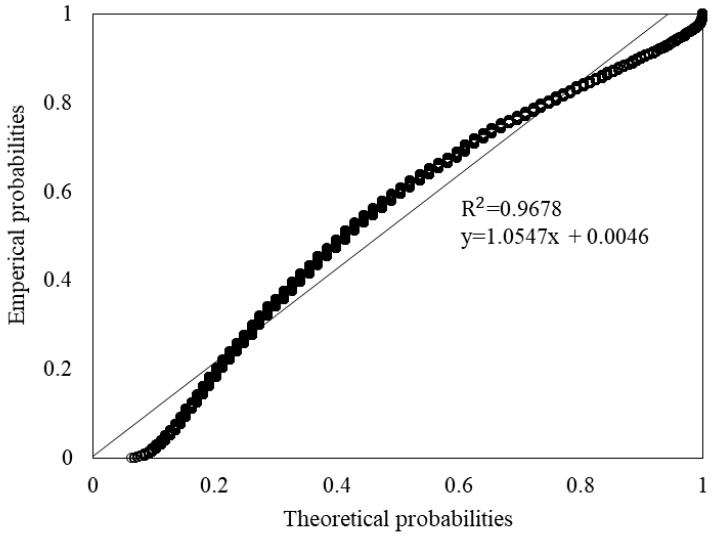


**Figure C-54: Sample 5 right rut normal probability plot**

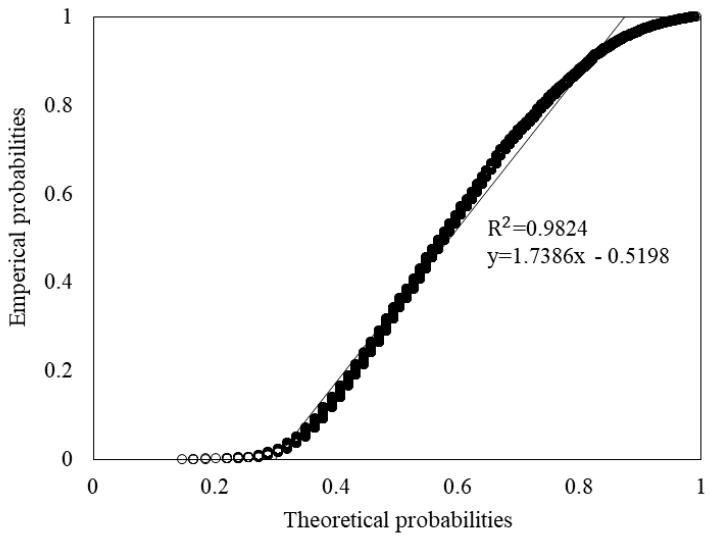


**Figure C-55: Sample 6 right rut exponential probability plot**

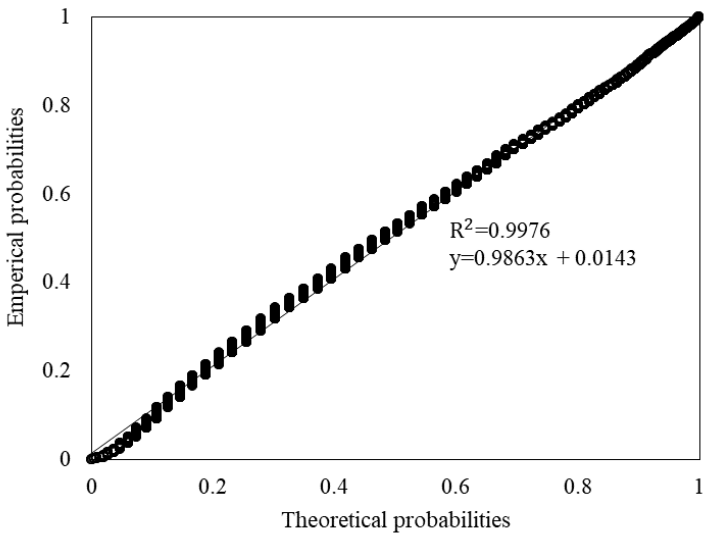


**Figure C-56: Sample 6 right rut lognormal probability plot**

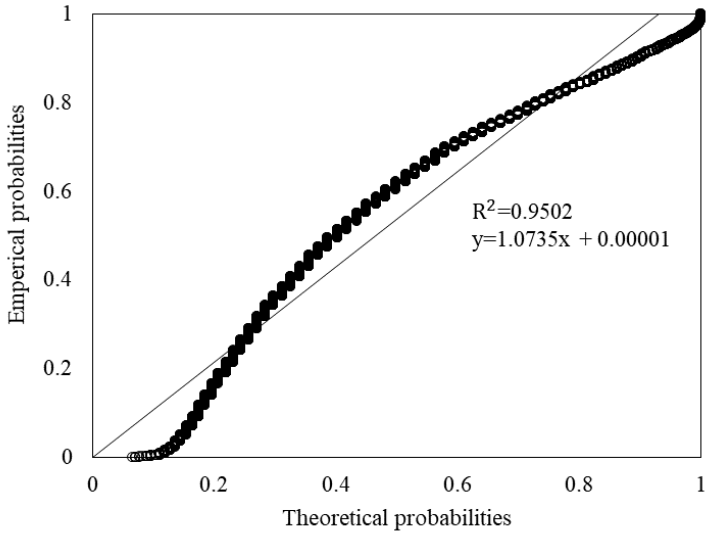


**Figure C-57: Sample 6 right rut normal probability plot**

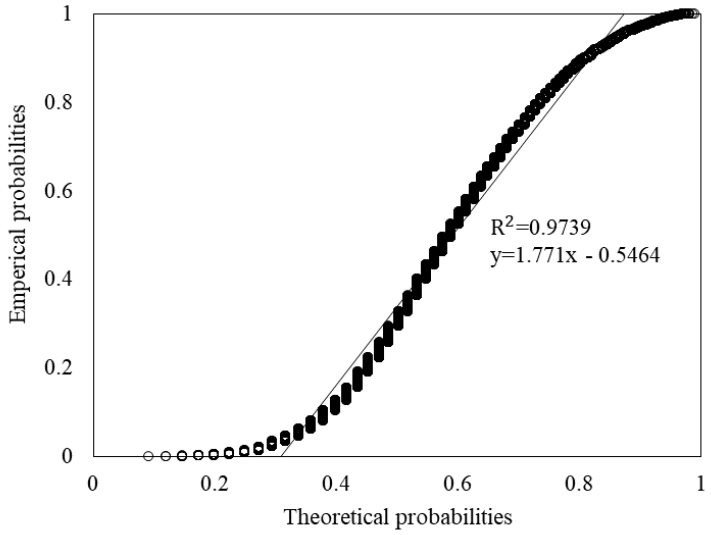


**Figure C-58: Sample 7 right rut exponential probability plot**

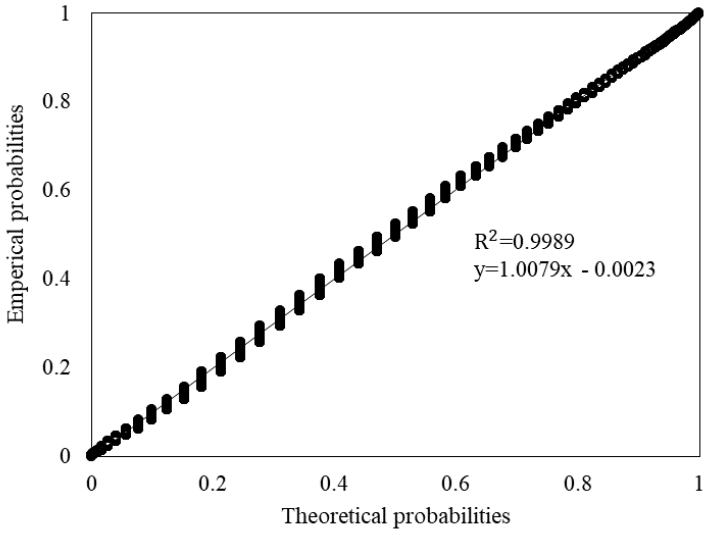


**Figure C-59: Sample 7 right rut lognormal probability plot**

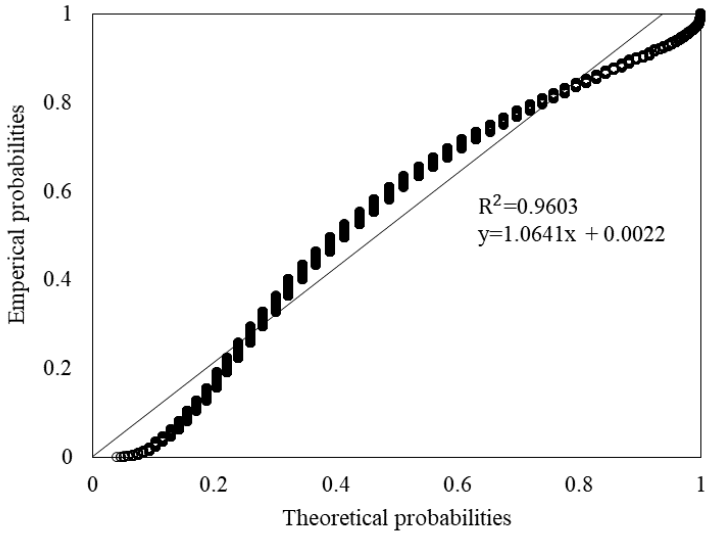


**Figure C-60: Sample 7 right rut normal probability plot**

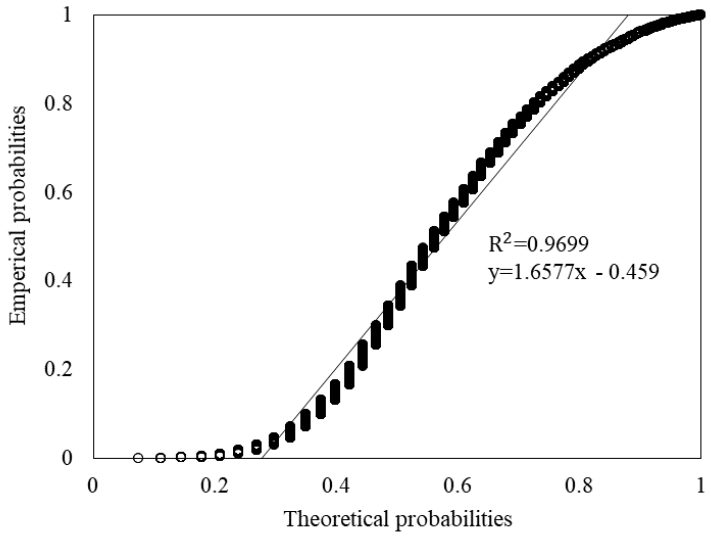


**Figure C-61: Sample 8 right rut exponential probability plot**

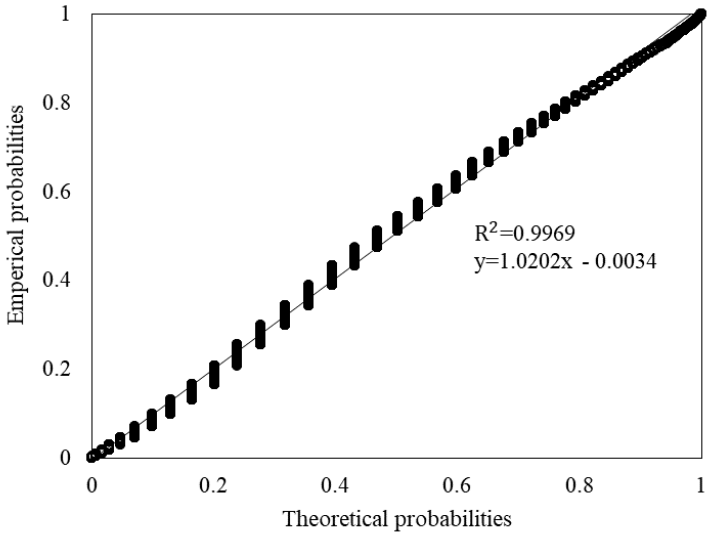


**Figure C-62: Sample 8 right rut lognormal probability plot**

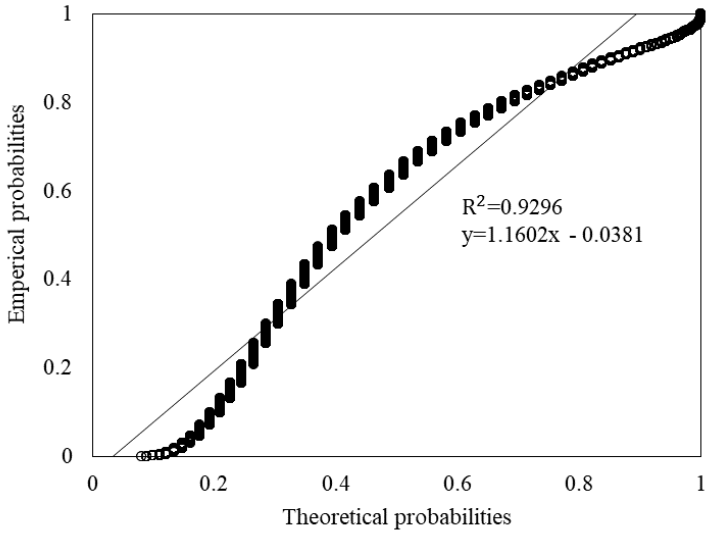


**Figure C-63: Sample 8 right rut normal probability plot**

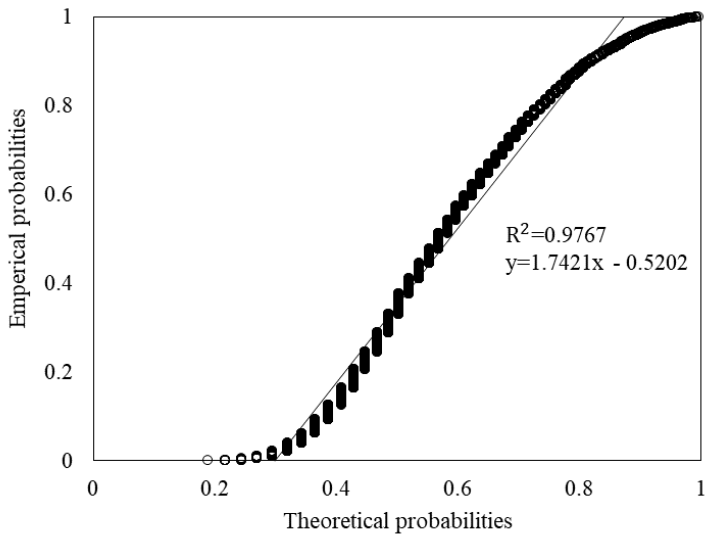


**Figure C-64: Sample 9 right rut exponential probability plot**

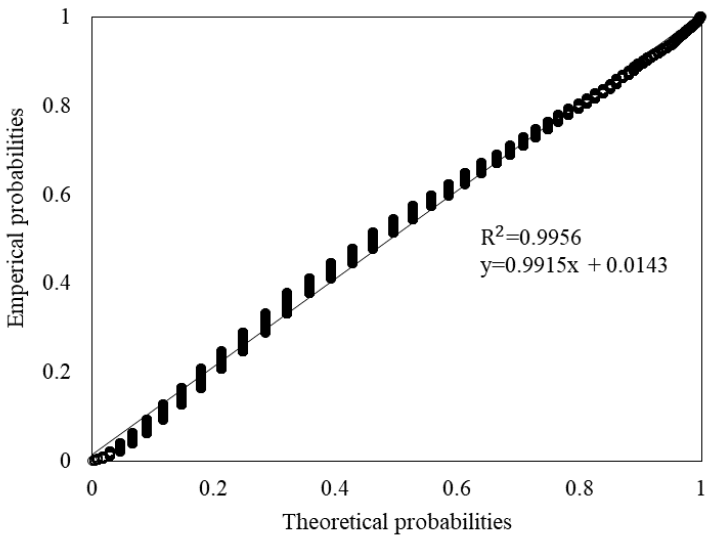


**Figure C-65: Sample 9 right rut lognormal probability plot**

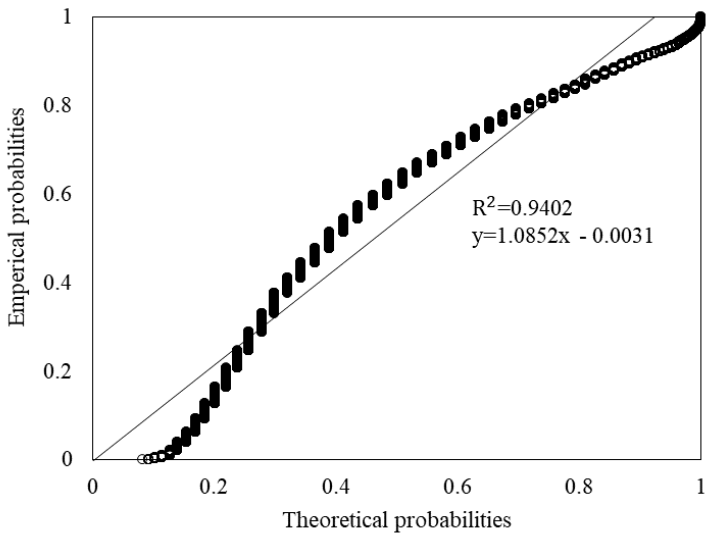


**Figure C-66: Sample 9 right rut normal probability plot**

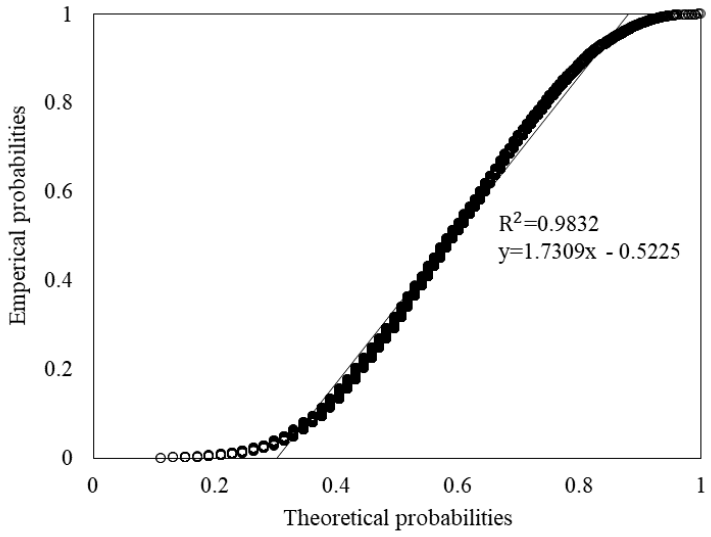


**Figure C-67: Sample 10 right rut exponential probability plot**

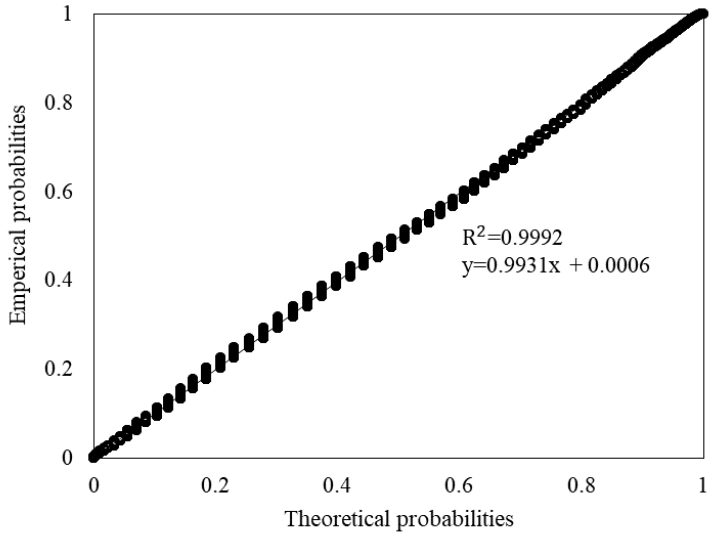


**Figure C-68: Sample 10 right rut lognormal probability plot**

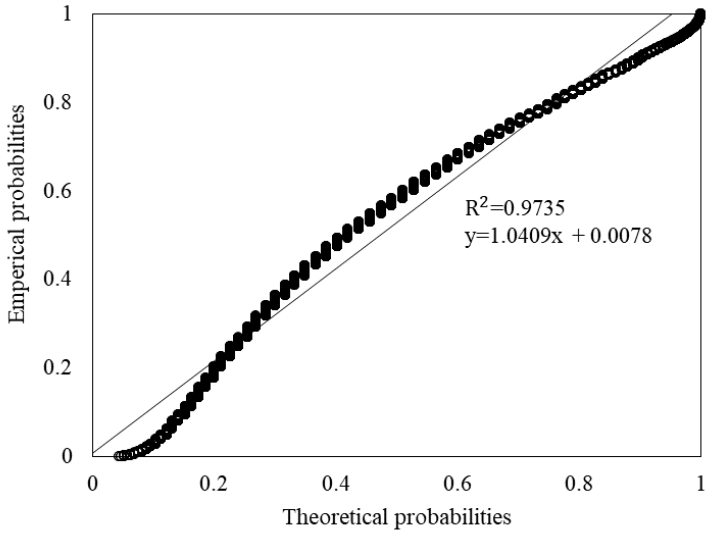


**Figure C-69: Sample 10 right rut normal probability plot**

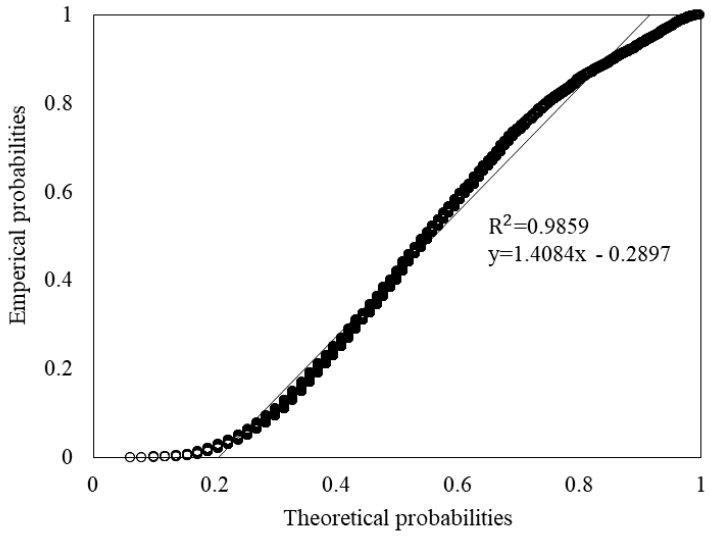


**Figure C-70: Sample 11 right rut exponential probability plot**

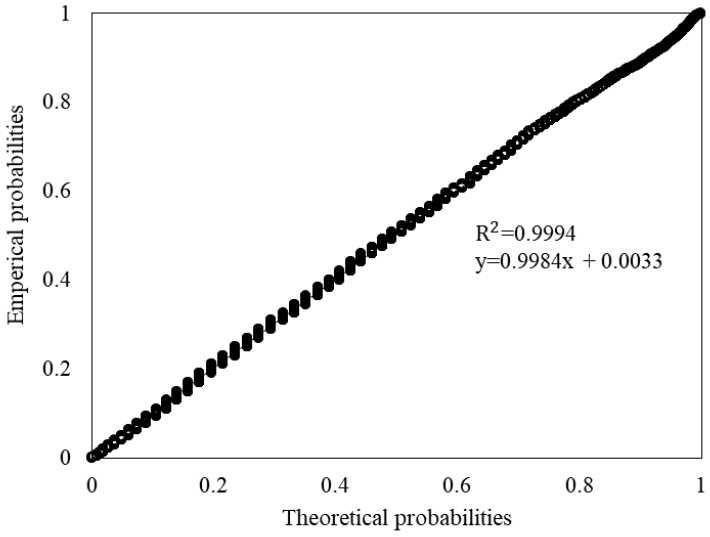


**Figure C-71: Sample 11 right rut lognormal probability plot**

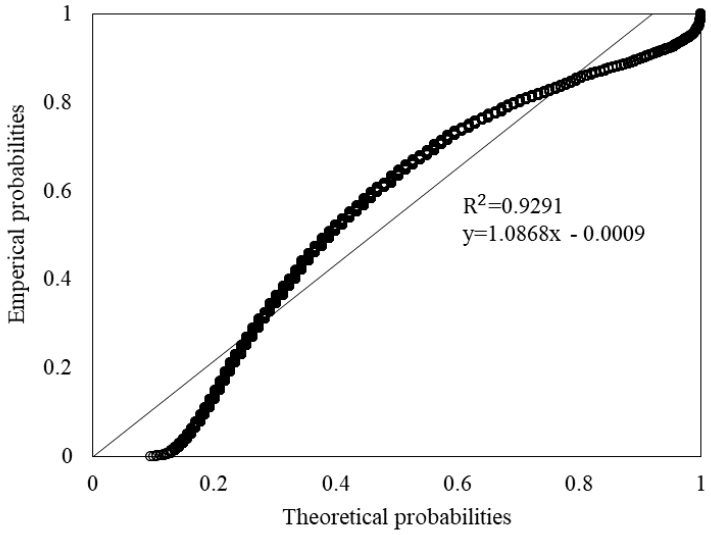


**Figure C-72: Sample 11 right rut normal probability plot**

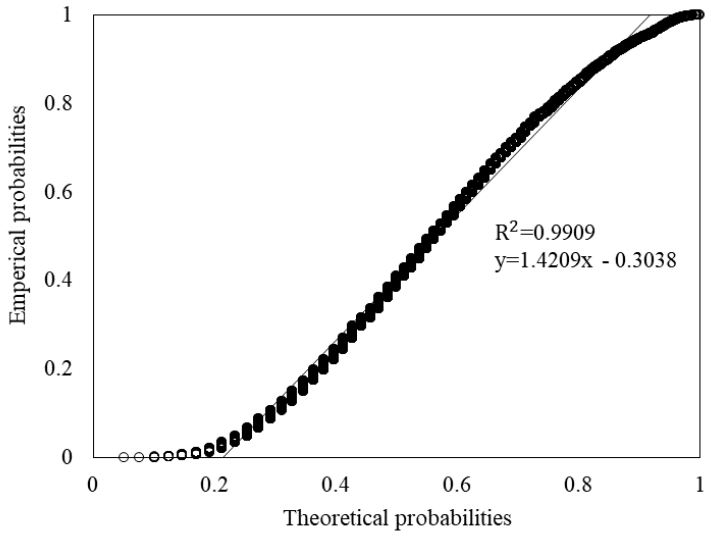


**Figure C-73: Sample 12 right rut exponential probability plot**

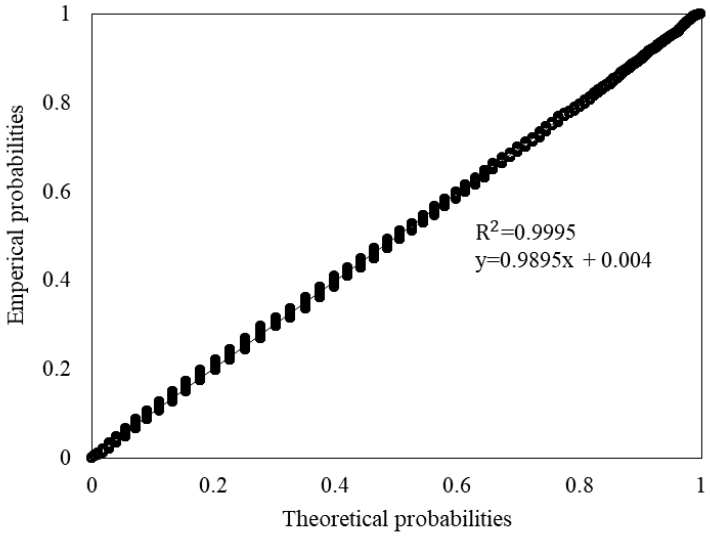


**Figure C-74: Sample 12 right rut lognormal probability plot**

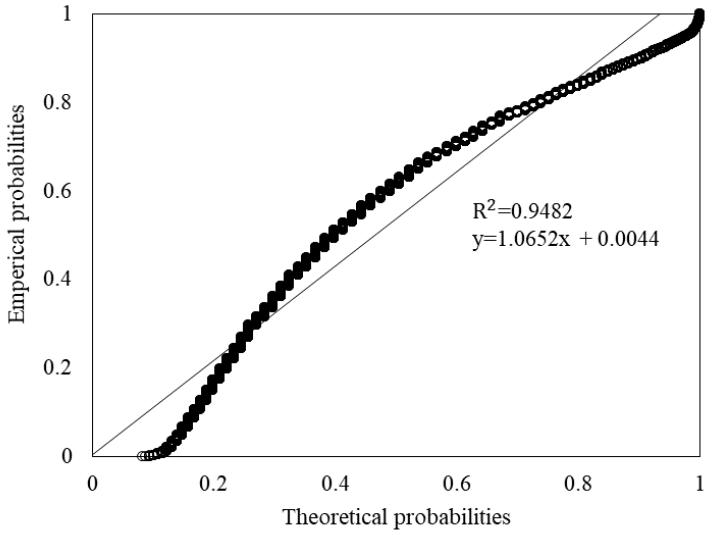


**Figure C-75: Sample 12 right rut normal probability plot**

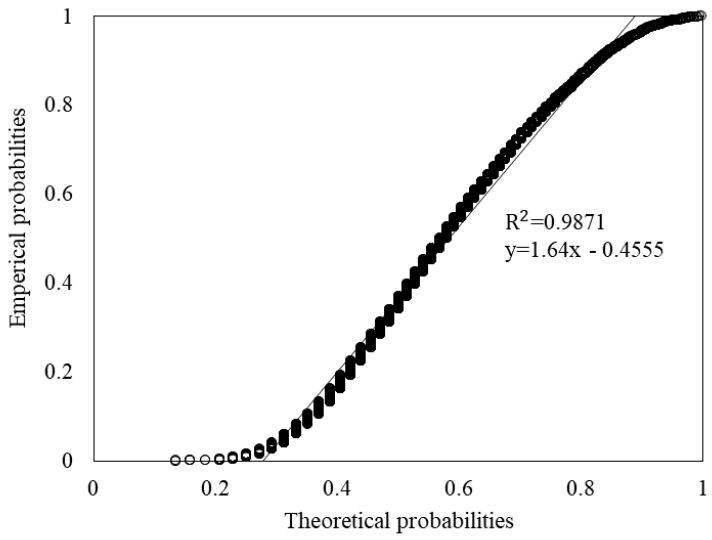


**Figure C-76: Sample 13 right rut exponential probability plot**

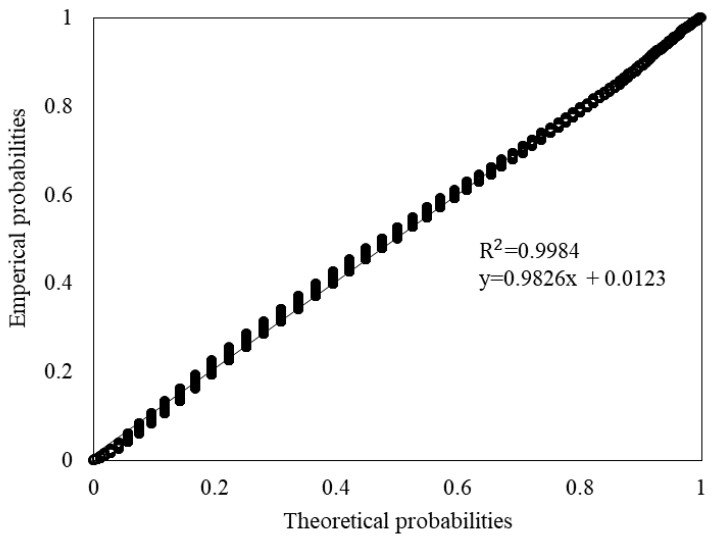


**Figure C-77: Sample 13 right rut lognormal probability plot**

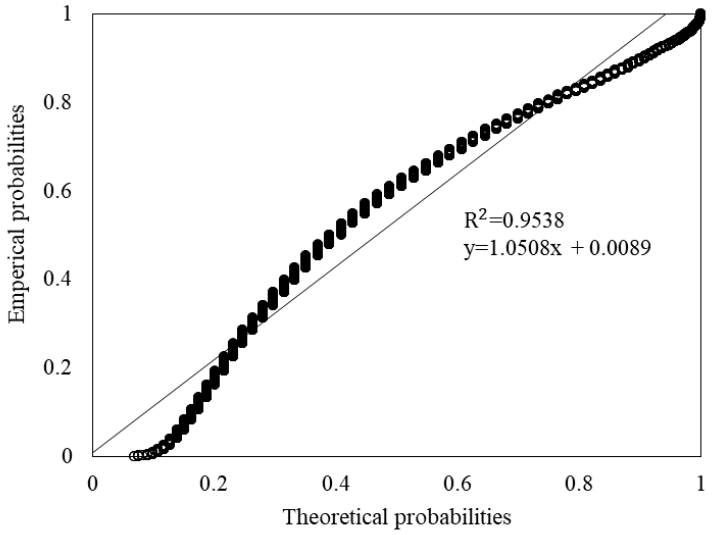


**Figure C-78: Sample 13 right rut normal probability plot**

# APPENDIX D

# DATASET 2 AVERAGED SECTION LENGTH DESCRIPTIVE STATISTICS

# APPENDIX D DATASET 2 AVERAGED SECTION LENGTH DESCRIPTIVE STATISTICS

## D.1 INTRODUCTION

The descriptive statistics per averaged section length discussed in Section 4.1.1 are presented for all samples analysed in the sections that follow.

## D.2 DESCRIPTIVE STATISTICS

Table D-1 to Table D-13 present the influence of averaged section length on the maximum value, mean, variance, COV, 95$^{th}$ percentile, and 20$^{th}$ percentile.

**Table D-1: Sample 1 descriptive statistics**

| Distribution Parameter | 10 m Sections | 20 m Sections | 50 m Sections | 100 m Sections | 500 m Sections | 1 000 m Sections | 10 000 m Sections |
|---|---|---|---|---|---|---|---|
| Maximum (mm) | 19.22 | 15.64 | 13.81 | 11.35 | 11.35 | 7.94 | 5.74 |
| % Change in maximum | | -19% | -28% | -41% | -41% | -59% | -70% |
| Mean (mm) | 4.86 | 4.86 | 4.86 | 4.86 | 4.85 | 4.84 | 4.81 |
| % Change in mean | | 0% | 0% | 0% | 0% | 0% | -1% |
| Variance (mm$^2$) | 4.89 | 4.02 | 3.04 | 2.48 | 1.34 | 1.04 | 0.53 |
| % Change in variance | | -18% | -38% | -49% | -73% | -79% | -89% |
| COV | 0.46 | 0.41 | 0.36 | 0.32 | 0.24 | 0.21 | 0.15 |
| % Change in COV | | -11% | -22% | -30% | -48% | -54% | -67% |
| 95$^{th}$ Percentile (mm) | 8.92 | 8.52 | 7.95 | 7.72 | 6.90 | 6.41 | 5.73 |
| % Change in 95$^{th}$ percentile | | -4% | -11% | -13% | -23% | -28% | -36% |
| 20$^{th}$ Percentile (mm) | 2.93 | 3.14 | 3.38 | 3.58 | 3.90 | 4.07 | 4.21 |
| % Change in 20$^{th}$ percentile | | 7% | 15% | 22% | 33% | 39% | 44% |

**Table D-2: Sample 2 descriptive statistics**

| Distribution Parameter | 10 m Sections | 20 m Sections | 50 m Sections | 100 m Sections | 500 m Sections | 1 000 m Sections | 10 000 m Sections |
|---|---|---|---|---|---|---|---|
| Maximum (mm) | 24.46 | 21.27 | 18.59 | 16.59 | 12.81 | 10.89 | 6.87 |
| % Change in maximum | | -13% | -24% | -32% | -48% | -55% | -72% |
| Mean (mm) | 5.33 | 5.33 | 5.33 | 5.33 | 5.33 | 5.32 | 5.20 |
| % Change in mean | | 0% | 0% | 0% | 0% | 0% | -2% |
| Variance ($mm^2$) | 8.98 | 7.90 | 6.51 | 5.33 | 3.16 | 2.41 | 1.12 |
| % Change in variance | | -12% | -28% | -41% | -65% | -73% | -88% |
| COV | 0.56 | 0.53 | 0.48 | 0.43 | 0.33 | 0.29 | 0.20 |
| % Change in COV | | -5% | -14% | -23% | -41% | -48% | -64% |
| $95^{th}$ Percentile (mm) | 10.91 | 10.57 | 10.25 | 9.70 | 8.67 | 7.89 | 6.84 |
| % Change in $95^{th}$ percentile | | -3% | -6% | -11% | -21% | -28% | -37% |
| $20^{th}$ Percentile (mm) | 2.76 | 2.96 | 3.24 | 3.34 | 3.85 | 4.00 | 4.15 |
| % Change in $20^{th}$ percentile | | 7% | 17% | 21% | 39% | 45% | 50% |

**Table D-3: Sample 3 descriptive statistics**

| Distribution Parameter | 10 m Sections | 20 m Sections | 50 m Sections | 100 m Sections | 500 m Sections | 1 000 m Sections | 10 000 m Sections |
|---|---|---|---|---|---|---|---|
| Maximum (mm) | 41.82 | 27.99 | 19.98 | 15.49 | 12.89 | 10.51 | 8.02 |
| % Change in maximum | | -33% | -52% | -63% | -69% | -75% | -81% |
| Mean (mm) | 5.93 | 5.93 | 5.93 | 5.93 | 5.93 | 5.94 | 5.99 |
| % Change in mean | | 0% | 0% | 0% | 0% | 0% | 1% |
| Variance ($mm^2$) | 9.31 | 8.15 | 6.96 | 6.02 | 4.14 | 3.51 | 2.22 |
| % Change in variance | | -12% | -25% | -35% | -56% | -62% | -76% |
| COV | 0.51 | 0.48 | 0.44 | 0.41 | 0.34 | 0.32 | 0.25 |
| % Change in COV | | -6% | -14% | -20% | -33% | -37% | -51% |
| $95^{th}$ Percentile (mm) | 11.8 | 11.43 | 10.86 | 10.57 | 9.54 | 9.46 | 7.86 |
| % Change in $95^{th}$ percentile | | -3% | -8% | -10% | -19% | -20% | -33% |
| $20^{th}$ Percentile (mm) | 3.43 | 3.63 | 3.79 | 3.94 | 4.31 | 4.63 | 4.52 |
| % Change in $20^{th}$ percentile | | 6% | 10% | 15% | 26% | 35% | 32% |

**Table D-4: Sample 4 descriptive statistics**

| Distribution Parameter | 10 m Sections | 20 m Sections | 50 m Sections | 100 m Sections | 500 m Sections | 1 000 m Sections | 10 000 m Sections |
|---|---|---|---|---|---|---|---|
| Maximum (mm) | 25.29 | 22.52 | 19.68 | 18.52 | 13.18 | 11.17 | 8.35 |
| % Change in maximum | | -11% | -22% | -27% | -48% | -56% | -67% |
| Mean (mm) | 5.44 | 5.44 | 5.44 | 5.44 | 5.44 | 5.43 | 5.52 |
| % Change in mean | | 0% | 0% | 0% | 0% | 0% | 1% |
| Variance ($mm^2$) | 13.06 | 11.98 | 10.45 | 9.22 | 6.71 | 5.84 | 4.02 |
| % Change in variance | | -8% | -20% | -29% | -49% | -55% | -69% |
| COV | 0.66 | 0.64 | 0.59 | 0.56 | 0.48 | 0.44 | 0.36 |
| % Change in COV | | -3% | -11% | -15% | -27% | -33% | -45% |
| $95^{th}$ Percentile (mm) | 12.36 | 12.07 | 11.5 | 11.33 | 10.09 | 8.88 | 8.03 |
| % Change in $95^{th}$ percentile | | -2% | -7% | -8% | -18% | -28% | -35% |
| $20^{th}$ Percentile (mm) | 2.19 | 2.34 | 2.48 | 2.59 | 2.95 | 3.19 | 3.57 |
| % Change in $20^{th}$ percentile | | 7% | 13% | 18% | 35% | 46% | 63% |

**Table D-5: Sample 5 descriptive statistics**

| Distribution Parameter | 10 m Sections | 20 m Sections | 50 m Sections | 100 m Sections | 500 m Sections | 1 000 m Sections | 10 000 m Sections |
|---|---|---|---|---|---|---|---|
| Maximum (mm) | 24.83 | 24.02 | 19.87 | 16.31 | 10.12 | 8.11 | 6.10 |
| % Change in maximum | | -3% | -20% | -34% | -59% | -67% | -75% |
| Mean (mm) | 5.42 | 5.42 | 5.42 | 5.42 | 5.42 | 5.42 | 5.38 |
| % Change in mean | | 0% | 0% | 0% | 0% | 0% | -1% |
| Variance ($mm^2$) | 7.14 | 6.15 | 4.95 | 3.94 | 1.71 | 1.17 | 0.24 |
| % Change in variance | | -14% | -31% | -45% | -76% | -84% | -97% |
| COV | 0.49 | 0.46 | 0.41 | 0.37 | 0.24 | 0.20 | 0.09 |
| % Change in COV | | -6% | -16% | -24% | -51% | -59% | -82% |
| $95^{th}$ Percentile (mm) | 10.26 | 9.97 | 9.58 | 9.18 | 7.61 | 7.38 | 6.09 |
| % Change in $95^{th}$ percentile | | -3% | -7% | -11% | -26% | -28% | -41% |
| $20^{th}$ Percentile (mm) | 3.05 | 3.31 | 3.61 | 3.74 | 4.33 | 4.58 | 4.89 |
| % Change in $20^{th}$ percentile | | 9% | 18% | 23% | 42% | 50% | 60% |

**Table D-6: Sample 6 descriptive statistics**

| Distribution Parameter | 10 m Sections | 20 m Sections | 50 m Sections | 100 m Sections | 500 m Sections | 1 000 m Sections | 10 000 m Sections |
|---|---|---|---|---|---|---|---|
| Maximum (mm) | 16.87 | 13.87 | 10.19 | 9.10 | 7.29 | 6.63 | 6.63 |
| % Change in maximum | | -18% | -40% | -46% | -57% | -61% | -61% |
| Mean (mm) | 4.21 | 4.21 | 4.21 | 4.21 | 4.22 | 4.24 | 4.55 |
| % Change in mean | | 0% | 0% | 0% | 0% | 1% | 8% |
| Variance ($mm^2$) | 2.60 | 2.20 | 1.75 | 1.46 | 0.88 | 0.73 | 1.15 |
| % Change in variance | | -15% | -33% | -44% | -66% | -72% | -56% |
| COV | 0.38 | 0.35 | 0.31 | 0.29 | 0.22 | 0.20 | 0.24 |
| % Change in COV | | -8% | -18% | -24% | -42% | -47% | -37% |
| $95^{th}$ Percentile (mm) | 7.17 | 6.82 | 6.54 | 6.34 | 5.82 | 5.99 | 6.17 |
| % Change in $95^{th}$ percentile | | -5% | -9% | -12% | -19% | -16% | -14% |
| $20^{th}$ Percentile (mm) | 2.90 | 2.99 | 3.11 | 3.20 | 3.38 | 3.48 | 3.78 |
| % Change in $20^{th}$ percentile | | 3% | 7% | 10% | 17% | 20% | 30% |

**Table D-7: Sample 7 descriptive statistics**

| Distribution Parameter | 10 m Sections | 20 m Sections | 50 m Sections | 100 m Sections | 500 m Sections | 1 000 m Sections | 10 000 m Sections |
|---|---|---|---|---|---|---|---|
| Maximum (mm) | 18.80 | 17.36 | 15.56 | 15.25 | 8.76 | 8.20 | 5.43 |
| % Change in maximum | | -8% | -17% | -19% | -53% | -56% | -71% |
| Mean (mm) | 4.61 | 4.61 | 4.61 | 4.61 | 4.61 | 4.61 | 4.61 |
| % Change in mean | | 0% | 0% | 0% | 0% | 0% | 0% |
| Variance ($mm^2$) | 6.23 | 5.33 | 4.31 | 3.49 | 1.76 | 1.18 | 0.44 |
| % Change in variance | | -14% | -31% | -44% | -72% | -81% | -93% |
| COV | 0.54 | 0.50 | 0.45 | 0.41 | 0.29 | 0.24 | 0.14 |
| % Change in COV | | -7% | -17% | -24% | -46% | -56% | -74% |
| $95^{th}$ Percentile (mm) | 9.30 | 8.91 | 8.38 | 8.04 | 7.15 | 6.54 | 5.42 |
| % Change in $95^{th}$ percentile | | -4% | -10% | -14% | -23% | -30% | -42% |
| $20^{th}$ Percentile (mm) | 2.54 | 2.76 | 2.94 | 3.19 | 3.53 | 3.64 | 3.99 |
| % Change in $20^{th}$ percentile | | 9% | 16% | 26% | 39% | 43% | 57% |

**Table D-8: Sample 8 descriptive statistics**

| Distribution Parameter | 10 m Sections | 20 m Sections | 50 m Sections | 100 m Sections | 500 m Sections | 1 000 m Sections | 10 000 m Sections |
|---|---|---|---|---|---|---|---|
| Maximum (mm) | 25.20 | 24.20 | 18.84 | 15.72 | 7.60 | 6.96 | 4.46 |
| % Change in maximum | | -4% | -25% | -38% | -70% | -72% | -82% |
| Mean (mm) | 3.84 | 3.84 | 3.84 | 3.84 | 3.84 | 3.84 | 3.84 |
| % Change in mean | | 0% | 0% | 0% | 0% | 0% | 0% |
| Variance ($mm^2$) | 4.61 | 4.00 | 3.24 | 2.61 | 1.32 | 0.95 | 0.25 |
| % Change in variance | | -13% | -30% | -43% | -71% | -79% | -95% |
| COV | 0.56 | 0.52 | 0.47 | 0.42 | 0.30 | 0.25 | 0.13 |
| % Change in COV | | -7% | -16% | -25% | -46% | -55% | -77% |
| 95$^{th}$ Percentile (mm) | 7.69 | 7.38 | 6.87 | 6.48 | 5.85 | 5.55 | 4.42 |
| % Change in 95$^{th}$ percentile | | -4% | -11% | -16% | -24% | -28% | -43% |
| 20$^{th}$ Percentile (mm) | 2.14 | 2.30 | 2.47 | 2.65 | 2.98 | 3.06 | 3.50 |
| % Change in 20$^{th}$ percentile | | 7% | 15% | 24% | 39% | 43% | 64% |

**Table D-9: Sample 9 descriptive statistics**

| Distribution Parameter | 10 m Sections | 20 m Sections | 50 m Sections | 100 m Sections | 500 m Sections | 1 000 m Sections | 10 000 m Sections |
|---|---|---|---|---|---|---|---|
| Maximum (mm) | 23.81 | 21.69 | 18.22 | 17.71 | 7.31 | 6.27 | 4.66 |
| % Change in maximum | | -9% | -23% | -26% | -69% | -74% | -80% |
| Mean (mm) | 4.06 | 4.07 | 4.07 | 4.07 | 4.07 | 4.07 | 4.03 |
| % Change in mean | | 0% | 0% | 0% | 0% | 0% | -1% |
| Variance ($mm^2$) | 6.34 | 5.48 | 4.43 | 3.57 | 1.35 | 0.83 | 0.27 |
| % Change in variance | | -14% | -30% | -44% | -79% | -87% | -96% |
| COV | 0.62 | 0.58 | 0.52 | 0.46 | 0.29 | 0.22 | 0.13 |
| % Change in COV | | -6% | -16% | -26% | -53% | -65% | -79% |
| 95$^{th}$ Percentile (mm) | 8.56 | 8.21 | 7.85 | 7.42 | 6.21 | 5.52 | 4.53 |
| % Change in 95$^{th}$ percentile | | -4% | -8% | -13% | -27% | -36% | -47% |
| 20$^{th}$ Percentile (mm) | 1.89 | 2.05 | 2.30 | 2.50 | 3.14 | 3.46 | 3.81 |
| % Change in 20$^{th}$ percentile | | 8% | 22% | 32% | 66% | 83% | 102% |

**Table D-10: Sample 10 descriptive statistics**

| Distribution Parameter | 10 m Sections | 20 m Sections | 50 m Sections | 100 m Sections | 500 m Sections | 1 000 m Sections | 10 000 m Sections |
|---|---|---|---|---|---|---|---|
| Maximum (mm) | 33.68 | 33.19 | 28.15 | 27.75 | 15.28 | 10.78 | 7.28 |
| % Change in maximum | | -1% | -16% | -18% | -55% | -68% | -78% |
| Mean (mm) | 4.80 | 4.80 | 4.80 | 4.80 | 4.79 | 4.77 | 4.65 |
| % Change in mean | | 0% | 0% | 0% | 0% | -1% | -3% |
| Variance ($mm^2$) | 10.56 | 9.59 | 8.21 | 6.63 | 3.30 | 2.35 | 1.26 |
| % Change in variance | | -9% | -22% | -37% | -69% | -78% | -88% |
| COV | 0.68 | 0.64 | 0.60 | 0.54 | 0.38 | 0.32 | 0.24 |
| % Change in COV | | -6% | -12% | -21% | -44% | -53% | -65% |
| $95^{th}$ Percentile (mm) | 10.64 | 10.28 | 9.76 | 9.34 | 8.36 | 7.67 | 6.42 |
| % Change in $95^{th}$ percentile | | -3% | -8% | -12% | -21% | -28% | -40% |
| $20^{th}$ Percentile (mm) | 2.22 | 2.44 | 2.69 | 3.02 | 3.51 | 3.74 | 4.05 |
| % Change in $20^{th}$ percentile | | 10% | 21% | 36% | 58% | 68% | 82% |

**Table D-11: Sample 11 descriptive statistics**

| Distribution Parameter | 10 m Sections | 20 m Sections | 50 m Sections | 100 m Sections | 500 m Sections | 1 000 m Sections | 10 000 m Sections |
|---|---|---|---|---|---|---|---|
| Maximum (mm) | 29.85 | 27.75 | 20.60 | 20.52 | 13.66 | 10.89 | 6.45 |
| % Change in maximum | | -7% | -31% | -31% | -54% | -64% | -78% |
| Mean (mm) | 5.63 | 5.63 | 5.63 | 5.63 | 5.63 | 5.63 | 5.62 |
| % Change in mean | | 0% | 0% | 0% | 0% | 0% | 0% |
| Variance ($mm^2$) | 11.94 | 10.70 | 8.82 | 7.13 | 3.14 | 1.98 | 0.31 |
| % Change in variance | | -10% | -26% | -40% | -74% | -83% | -97% |
| COV | 0.61 | 0.58 | 0.53 | 0.47 | 0.32 | 0.25 | 0.10 |
| % Change in COV | | -5% | -13% | -23% | -48% | -59% | -84% |
| $95^{th}$ Percentile (mm) | 12.03 | 11.57 | 11.01 | 10.61 | 8.39 | 8.64 | 6.37 |
| % Change in $95^{th}$ percentile | | -4% | -8% | -12% | -30% | -28% | -47% |
| $20^{th}$ Percentile (mm) | 2.97 | 3.15 | 3.34 | 3.60 | 4.32 | 4.64 | 5.38 |
| % Change in $20^{th}$ percentile | | 6% | 12% | 21% | 45% | 56% | 81% |

**Table D-12: Sample 12 descriptive statistics**

| Distribution Parameter | 10 m Sections | 20 m Sections | 50 m Sections | 100 m Sections | 500 m Sections | 1 000 m Sections | 10 000 m Sections |
|---|---|---|---|---|---|---|---|
| Maximum (mm) | 40.22 | 22.22 | 18.04 | 14.96 | 9.85 | 9.15 | 5.77 |
| % Change in maximum | | -45% | -55% | -63% | -76% | -77% | -86% |
| Mean (mm) | 5.08 | 5.08 | 5.08 | 5.08 | 5.08 | 5.09 | 4.92 |
| % Change in mean | | 0% | 0% | 0% | 0% | 0% | -3% |
| Variance ($mm^2$) | 8.00 | 7.03 | 5.81 | 4.72 | 2.42 | 1.82 | 0.68 |
| % Change in variance | | -12% | -27% | -41% | -70% | -77% | -92% |
| COV | 0.56 | 0.52 | 0.47 | 0.43 | 0.31 | 0.27 | 0.17 |
| % Change in COV | | -7% | -16% | -23% | -45% | -52% | -70% |
| $95^{th}$ Percentile (mm) | 10.23 | 9.97 | 9.49 | 9.16 | 8.02 | 7.52 | 5.73 |
| % Change in $95^{th}$ percentile | | -3% | -7% | -10% | -22% | -26% | -44% |
| $20^{th}$ Percentile (mm) | 2.61 | 2.82 | 3.00 | 3.27 | 3.82 | 3.95 | 4.31 |
| % Change in $20^{th}$ percentile | | 8% | 15% | 25% | 46% | 51% | 65% |

**Table D-13: Sample 13 descriptive statistics**

| Distribution Parameter | 10 m Sections | 20 m Sections | 50 m Sections | 100 m Sections | 500 m Sections | 1 000 m Sections | 10 000 m Sections |
|---|---|---|---|---|---|---|---|
| Maximum (mm) | 21.04 | 20.66 | 16.98 | 16.15 | 12.99 | 11.11 | 7.81 |
| % Change in maximum | | -2% | -19% | -23% | -38% | -47% | -63% |
| Mean (mm) | 6.80 | 6.80 | 6.80 | 6.80 | 6.80 | 6.79 | 6.60 |
| % Change in mean | | 0% | 0% | 0% | 0% | 0% | -3% |
| Variance ($mm^2$) | 9.73 | 8.59 | 7.37 | 6.54 | 4.23 | 3.48 | 1.39 |
| % Change in variance | | -12% | -24% | -33% | -57% | -64% | -86% |
| COV | 0.46 | 0.43 | 0.40 | 0.38 | 0.30 | 0.27 | 0.18 |
| % Change in COV | | -7% | -13% | -17% | -35% | -41% | -61% |
| $95^{th}$ Percentile (mm) | 12.30 | 12.10 | 11.62 | 11.28 | 10.59 | 9.98 | 7.78 |
| % Change in $95^{th}$ percentile | | -2% | -6% | -8% | -14% | -19% | -37% |
| $20^{th}$ Percentile (mm) | 4.05 | 4.26 | 4.47 | 4.70 | 5.33 | 5.34 | 5.50 |
| % Change in $20^{th}$ percentile | | 5% | 10% | 16% | 32% | 32% | 36% |

# APPENDIX E

# DATASET 2 LEFT RUT DEPTH PROBABILITY PLOTS FOR AVERAGED SECTION LENGTHS

# APPENDIX E DATASET 2 LEFT RUT DEPTH PROBABILITY PLOTS FOR AVERAGED SECTION LENGTHS

## E.1 INTRODUCTION

The averaged section length exponential, lognormal, and normal probability plots plotted in R-Studio for left rut depth measurements for each of the 13 roads selected for the analysis are presented in the sections that follow.

## E.2 LEFT RUT DEPTH PROBABILITY PLOTS

Figure E-1 to Figure E-18 present the averaged section length exponential, lognormal, and normal probability plots for sample 1 left rut depth measurements.

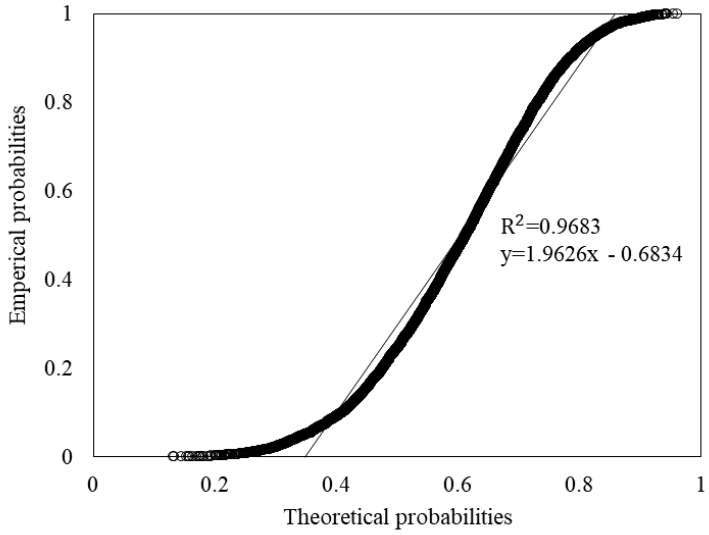


**Figure E-1: Sample 1 left rut exponential probability plot for 20 m averaged section length**

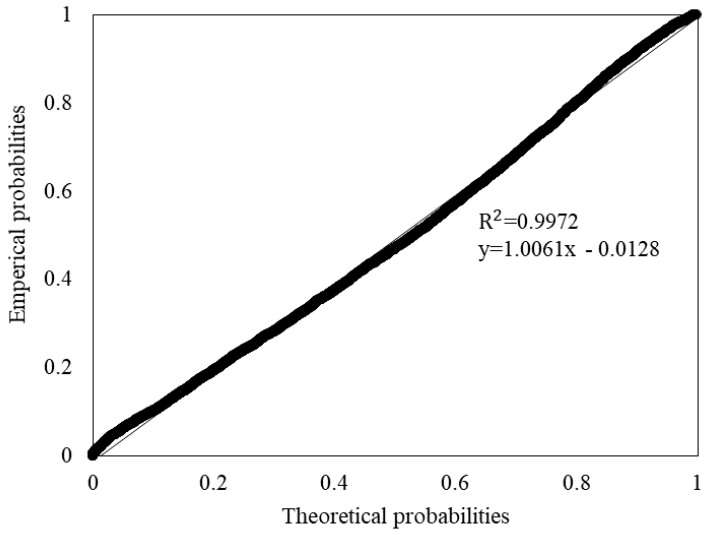


**Figure E-2: Sample 1 left rut lognormal probability plot for 20 m averaged section length**

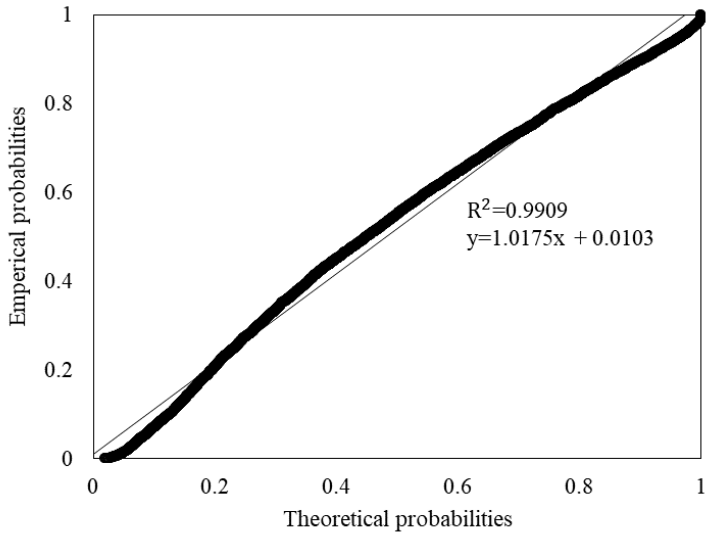


**Figure E-3: Sample 1 left rut normal probability plot for 20 m averaged section length**

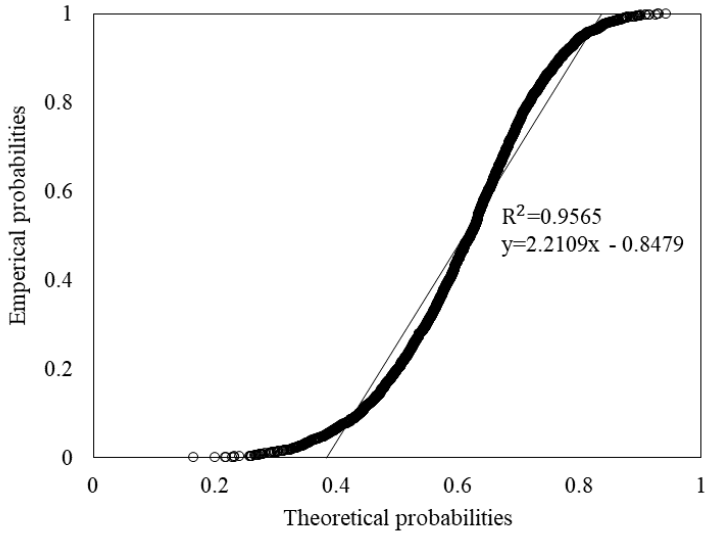


**Figure E-4: Sample 1 left rut exponential probability plot for 50 m averaged section length**

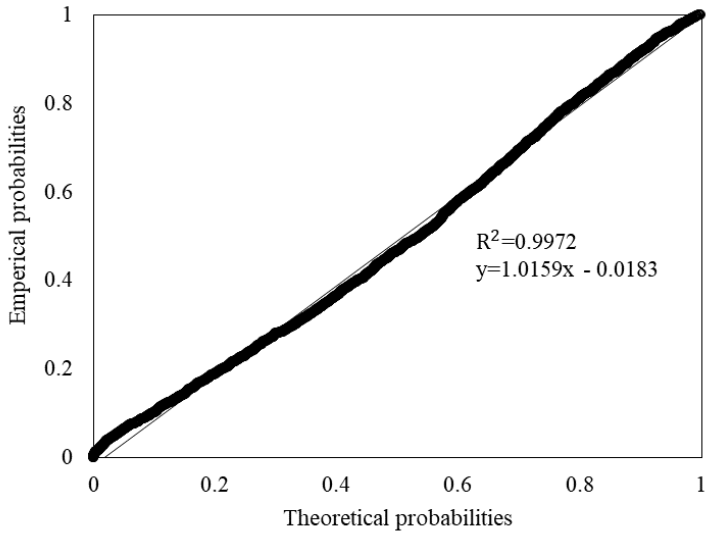


**Figure E-5: Sample 1 left rut lognormal probability plot for 50 m averaged section length**

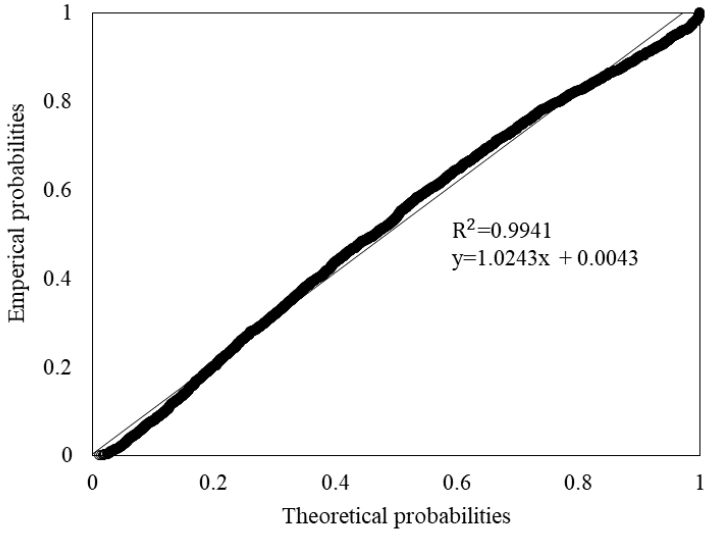


**Figure E-6: Sample 1 left rut normal probability plot for 50 m averaged section length**

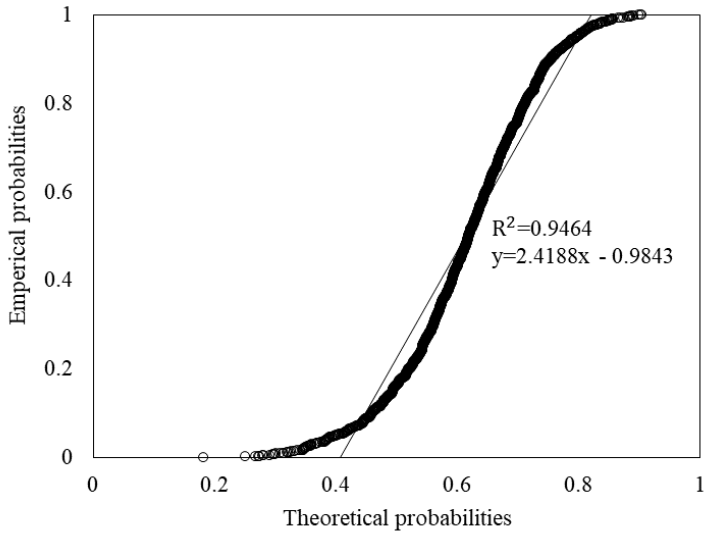


**Figure E-7: Sample 1 left rut exponential probability plot for 100 m averaged section length**

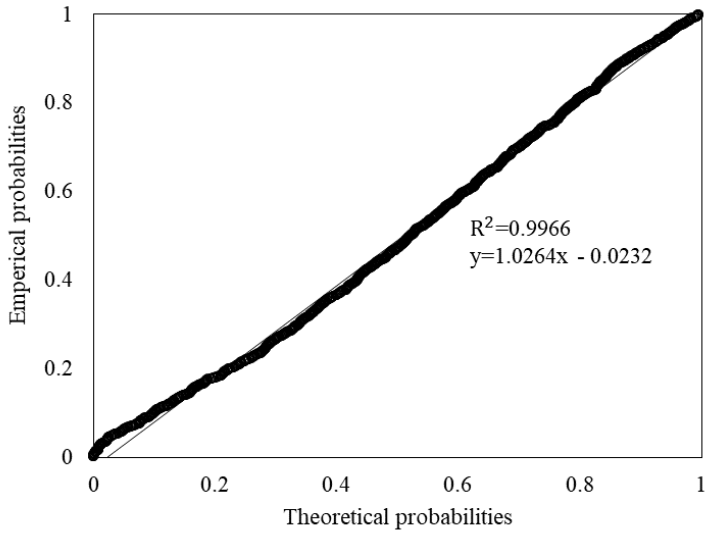


**Figure E-8: Sample 1 left rut lognormal probability plot for 100 m averaged section length**

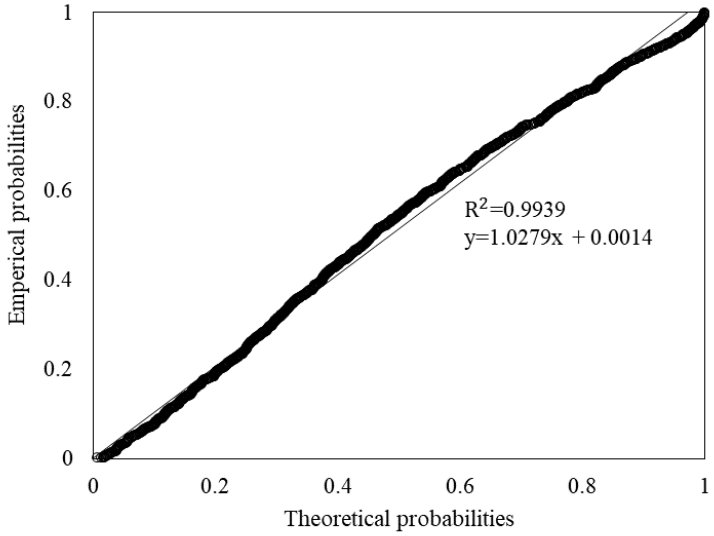


**Figure E-9: Sample 1 left rut normal probability plot for 100 m averaged section length**

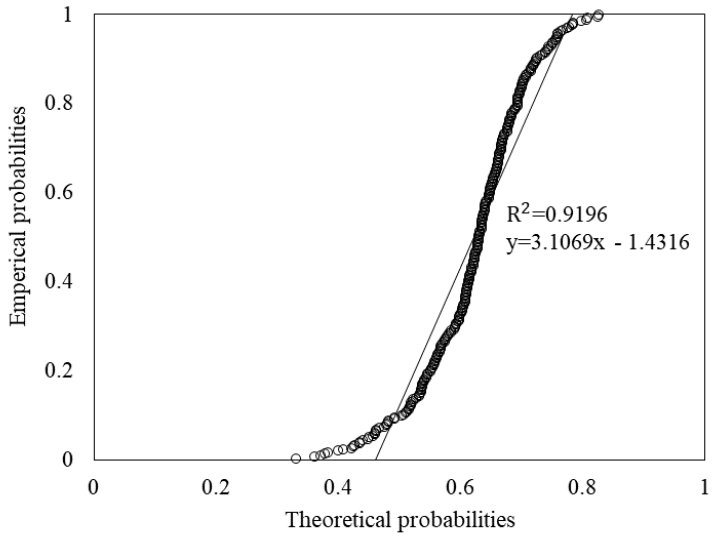


**Figure E-10: Sample 1 left rut exponential probability plot for 500 m averaged section length**

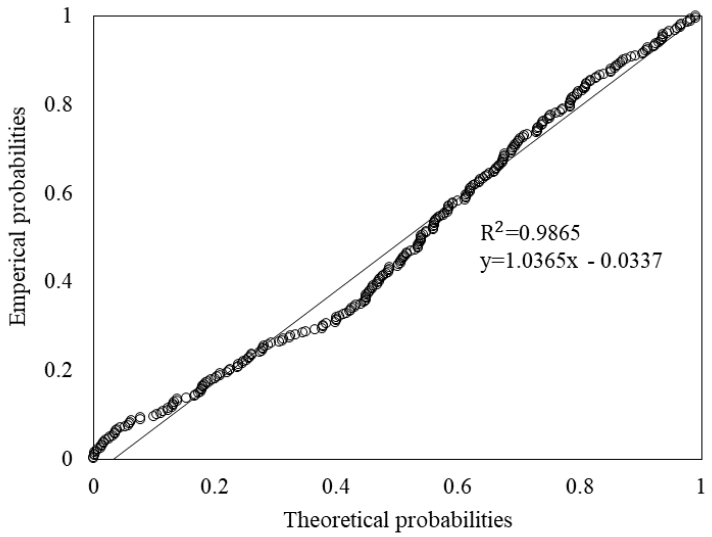


**Figure E-11: Sample 1 left rut lognormal probability plot for 500 m averaged section length**

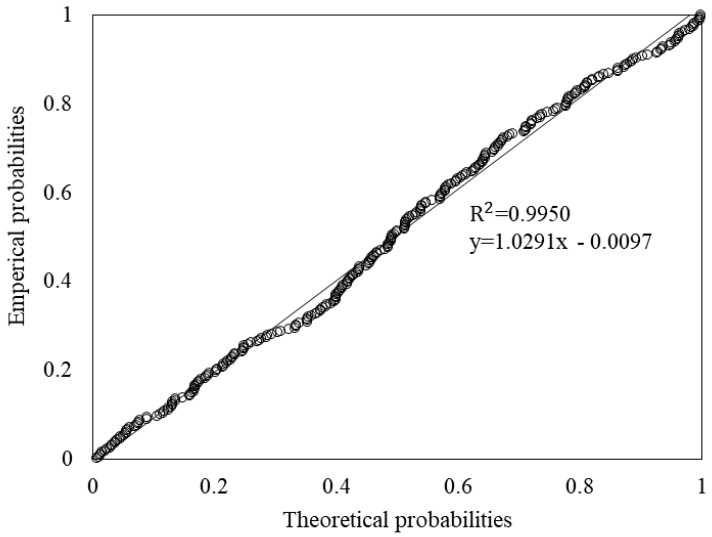


**Figure E-12: Sample 1 left rut normal probability plot for 500 m averaged section length**

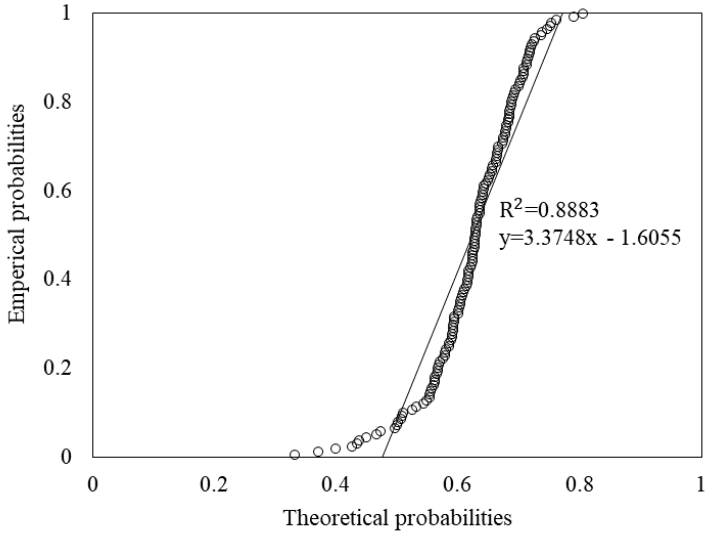


**Figure E-13: Sample 1 left rut exponential probability plot for 1 000 m averaged section length**

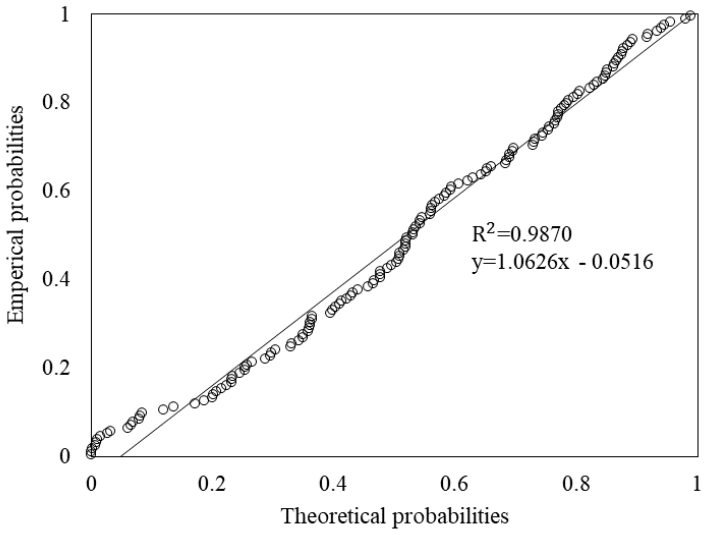


**Figure E-14: Sample 1 left rut lognormal probability plot for 1 000 m averaged section length**

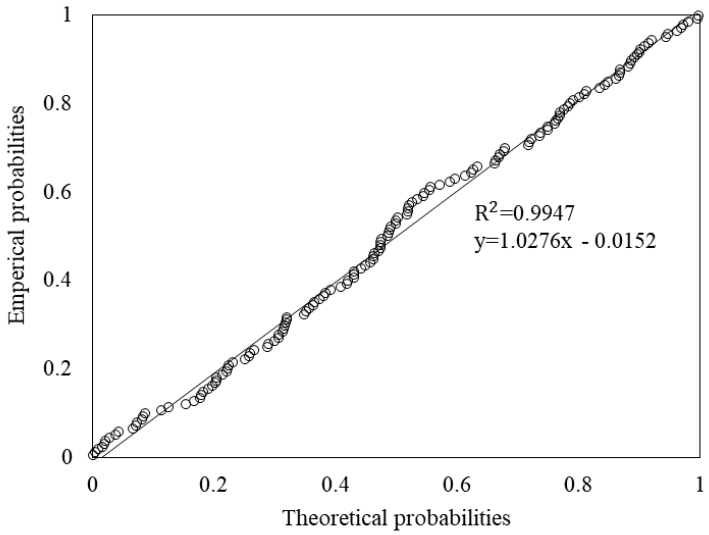


**Figure E-15: Sample 1 left rut normal probability plot for 1 000 m averaged section length**

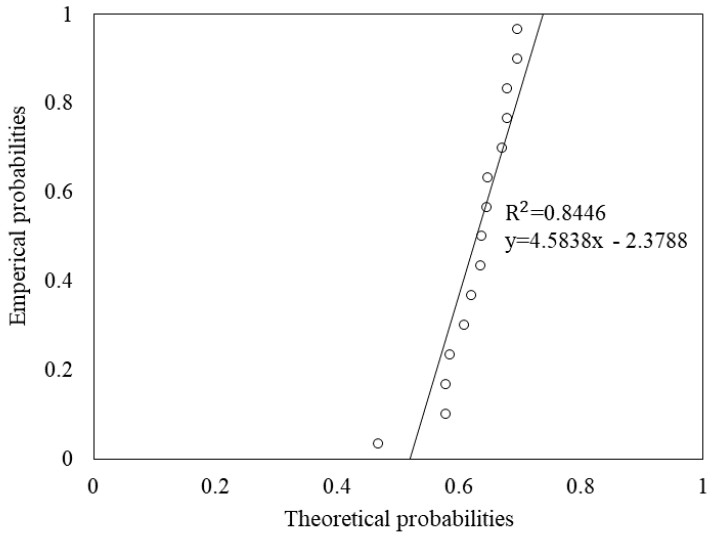


**Figure E-16: Sample 1 left rut exponential probability plot for 10 000 m averaged section length**

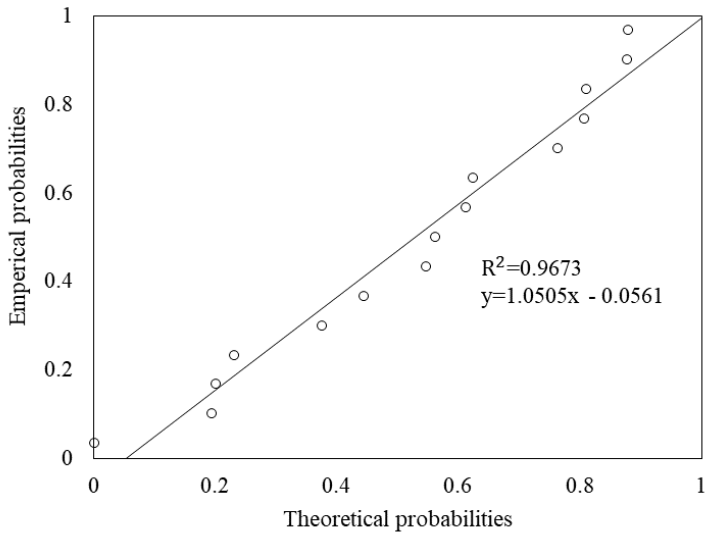


**Figure E-17: Sample 1 left rut lognormal probability plot for 10 000 m averaged section length**

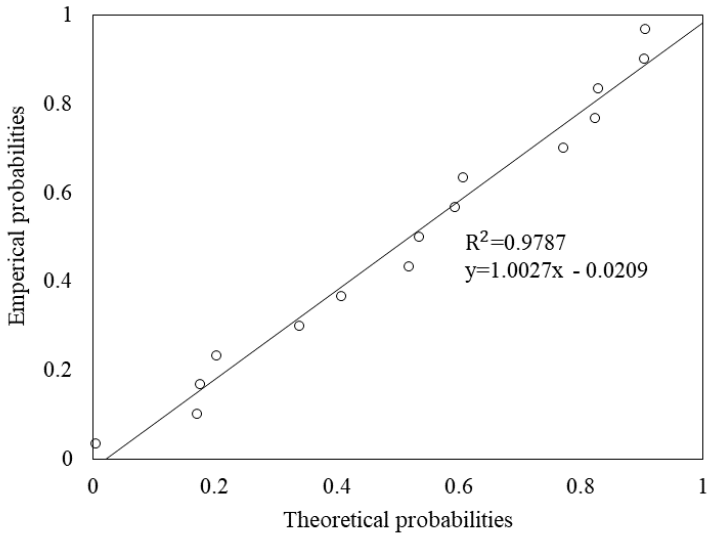


**Figure E-18: Sample 1 left rut normal probability plot for 10 000 m averaged section length**

Figure E-19 to Figure E-36 present the averaged section length exponential, lognormal, and normal probability plots for sample 2 left rut depth measurements.

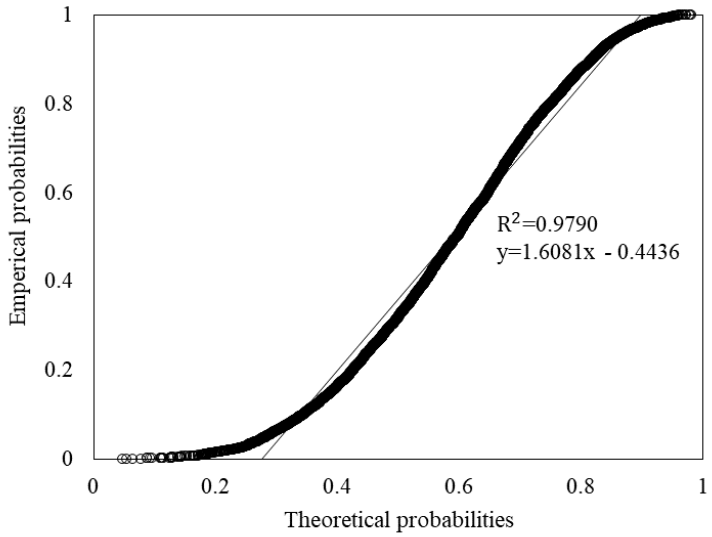


**Figure E-19: Sample 2 left rut exponential probability plot for 20 m averaged section length**

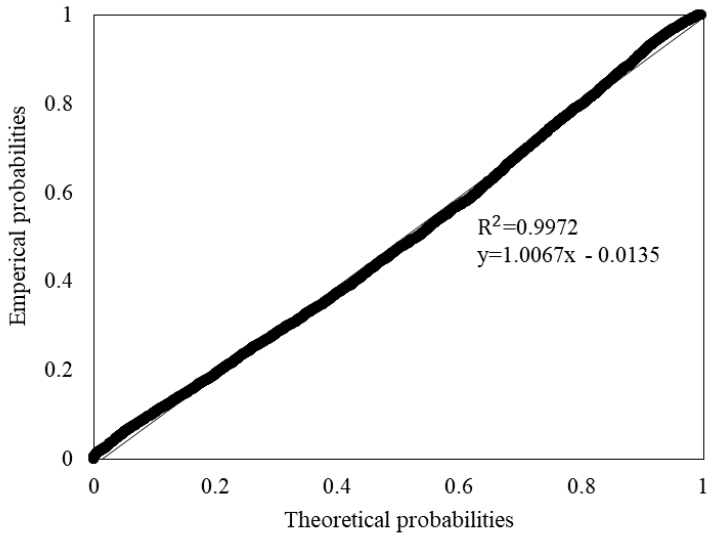


**Figure E-20: Sample 2 left rut lognormal probability plot for 20 m averaged section length**

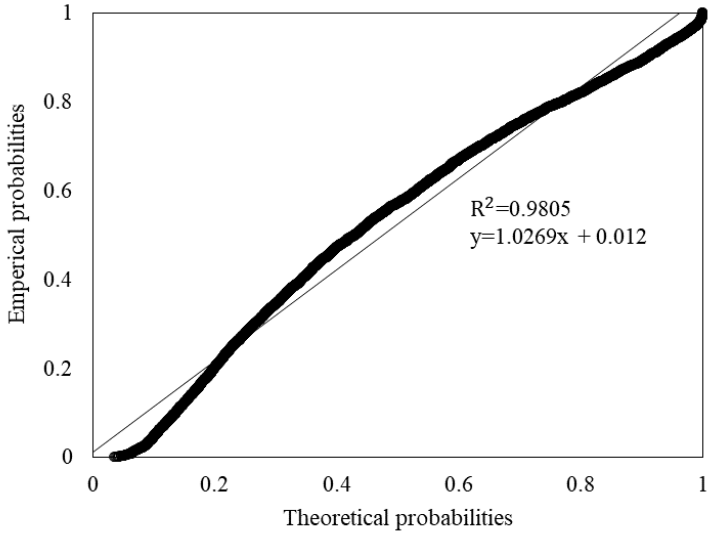


**Figure E-21: Sample 2 left rut normal probability plot for 20 m averaged section length**

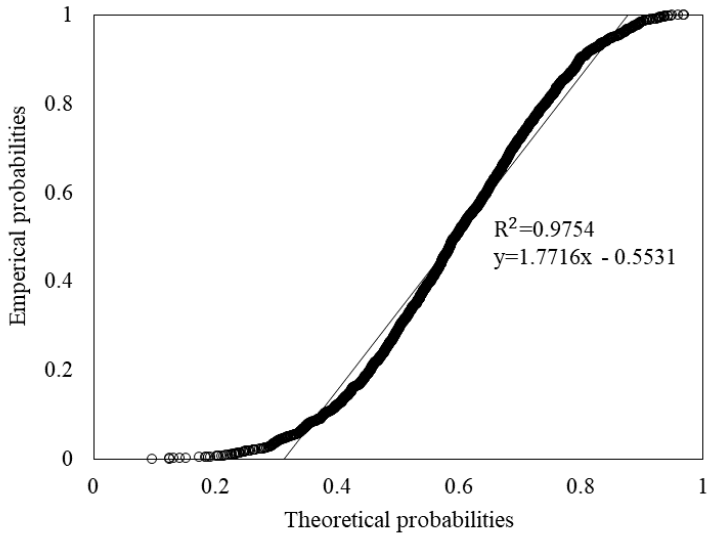


**Figure E-22: Sample 2 left rut exponential probability plot for 50 m averaged section length**

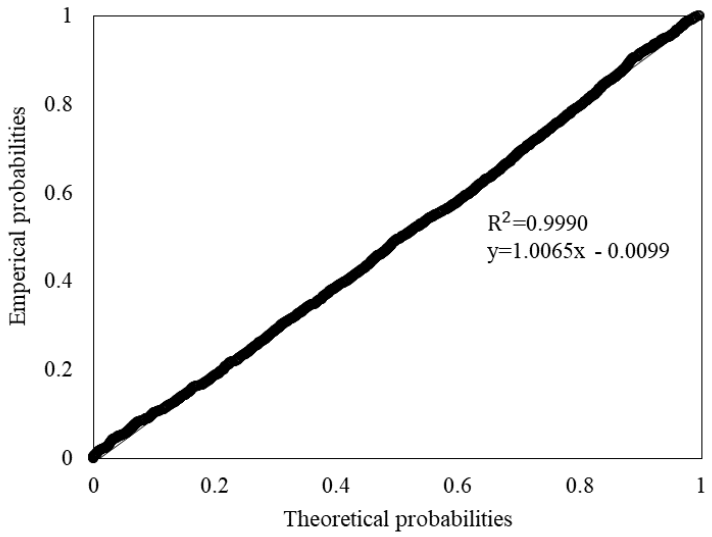


**Figure E-23: Sample 2 left rut lognormal probability plot for 50 m averaged section length**

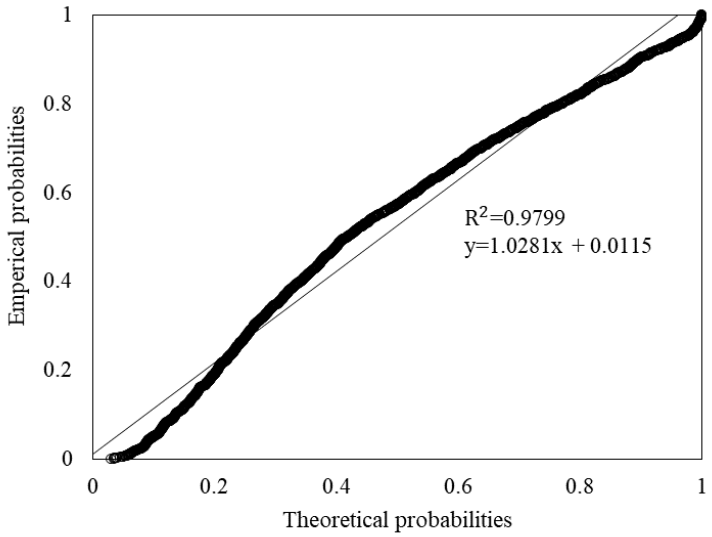


**Figure E-24: Sample 2 left rut normal probability plot for 50 m averaged section length**

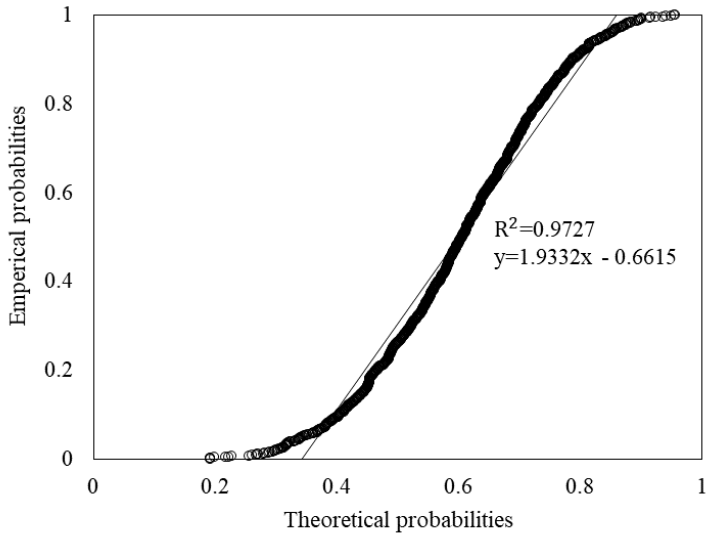


**Figure E-25: Sample 2 left rut exponential probability plot for 100 m averaged section length**

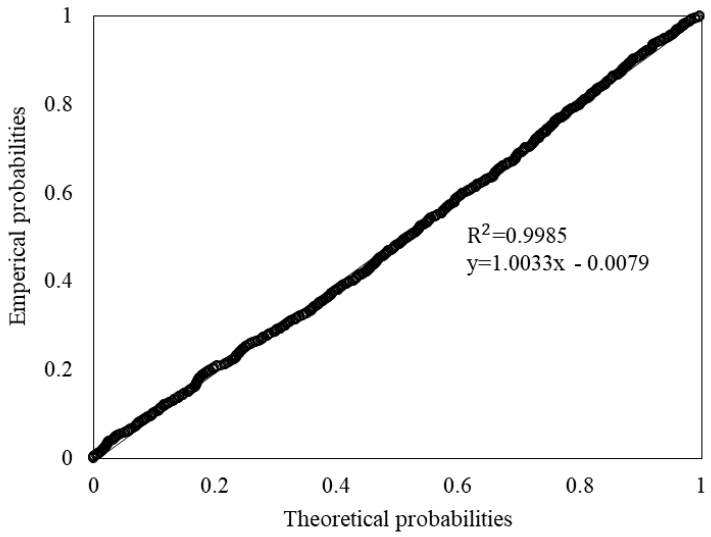


**Figure E-26: Sample 2 left rut lognormal probability plot for 100 m averaged section length**

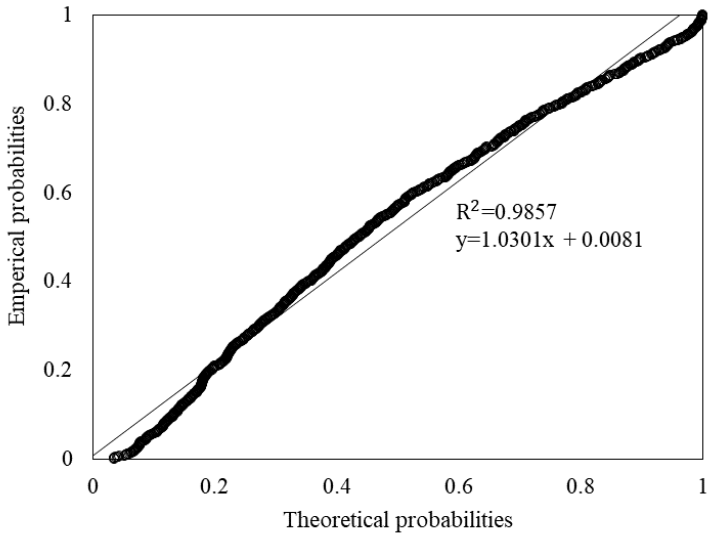


**Figure E-27: Sample 2 left rut normal probability plot for 100 m averaged section length**

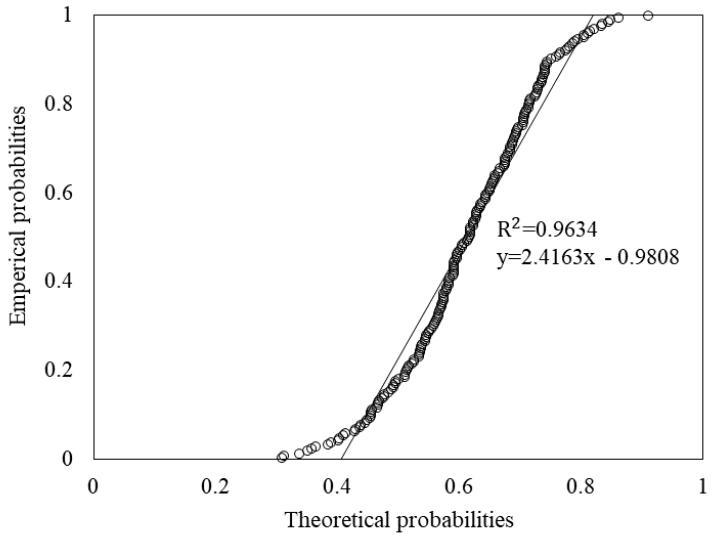


**Figure E-28: Sample 2 left rut exponential probability plot for 500 m averaged section length**

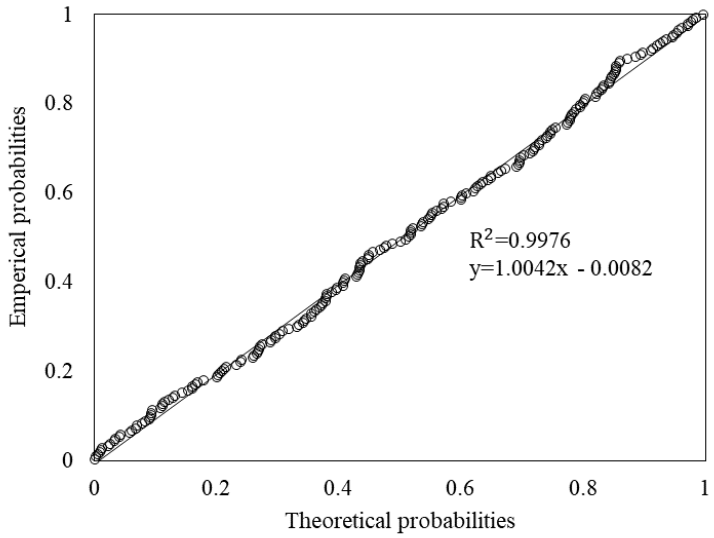


**Figure E-29: Sample 2 left rut lognormal probability plot for 500 m averaged section length**

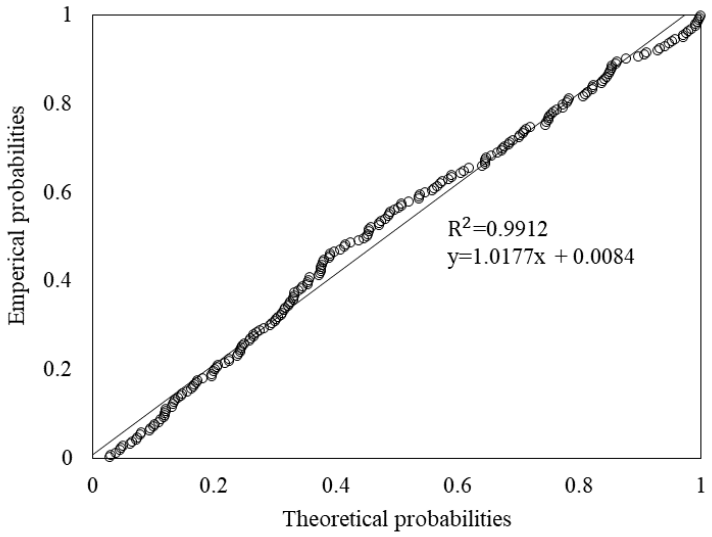


**Figure E-30: Sample 2 left rut normal probability plot for 500 m averaged section length**

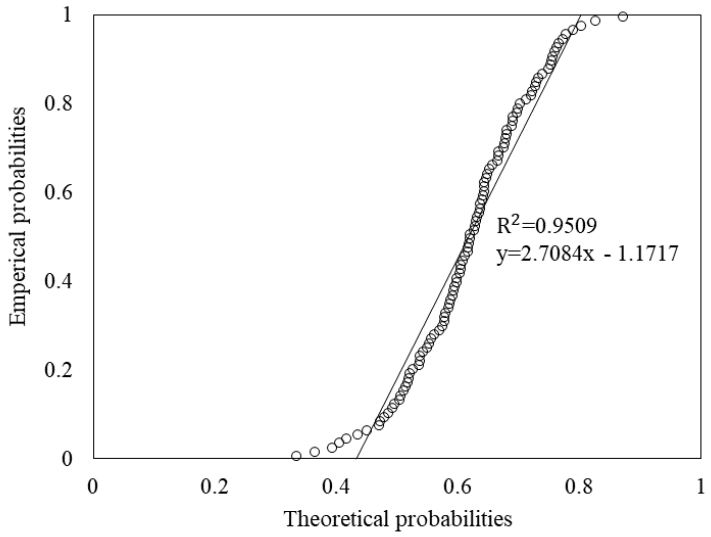


**Figure E-31: Sample 2 left rut exponential probability plot for 1 000 m averaged section length**

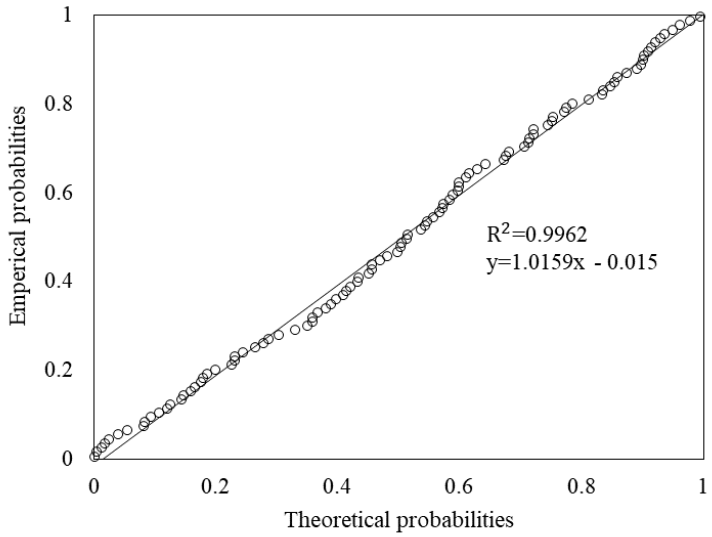


**Figure E-32: Sample 2 left rut lognormal probability plot for 1 000 m averaged section length**

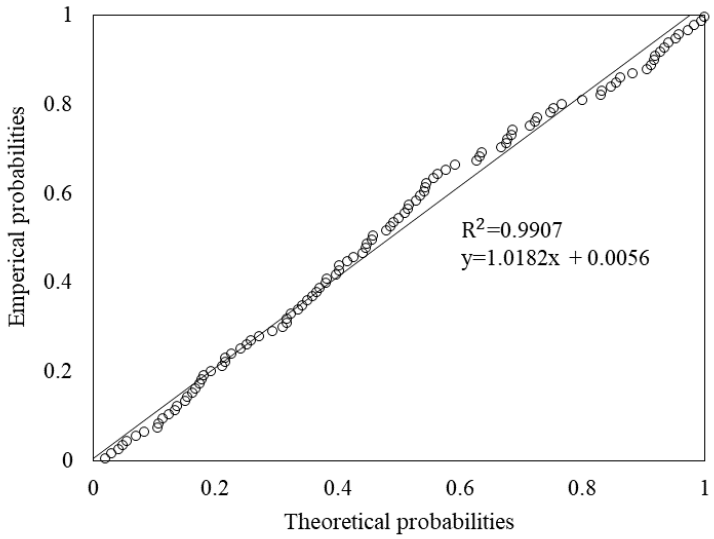


**Figure E-33: Sample 2 left rut normal probability plot for 1 000 m averaged section length**

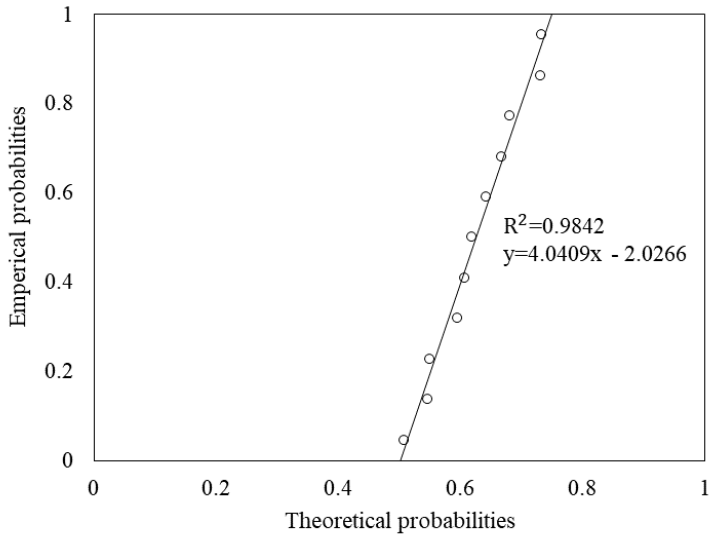


**Figure E-34: Sample 2 left rut exponential probability plot for 10 000 m averaged section length**

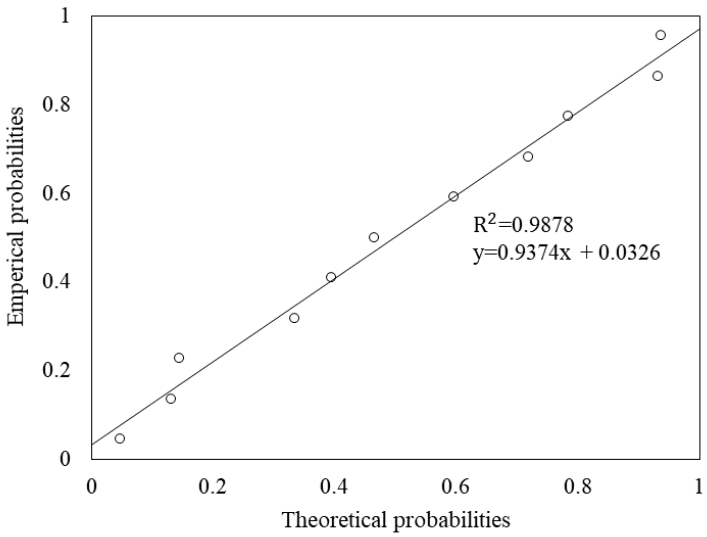


**Figure E-35: Sample 2 left rut lognormal probability plot for 10 000 m averaged section length**

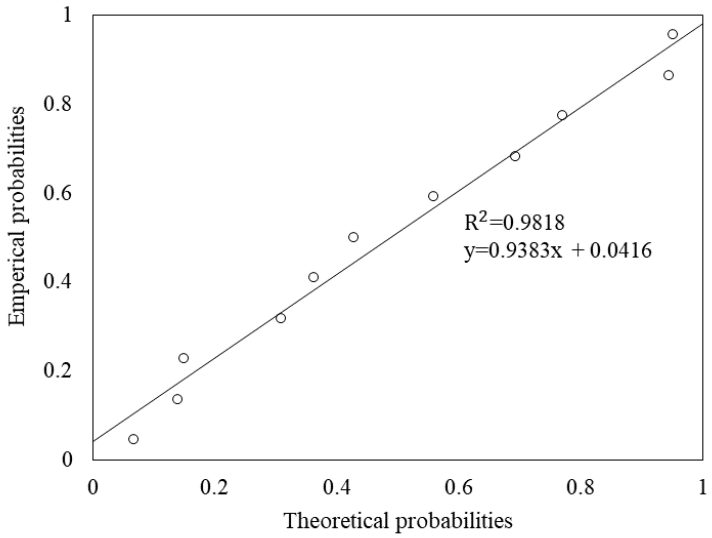


**Figure E-36: Sample 2 left rut normal probability plot for 10 000 m averaged section length**

Figure E-37 to Figure E-54 present the averaged section length exponential, lognormal, and normal probability plots for sample 3 left rut depth measurements.

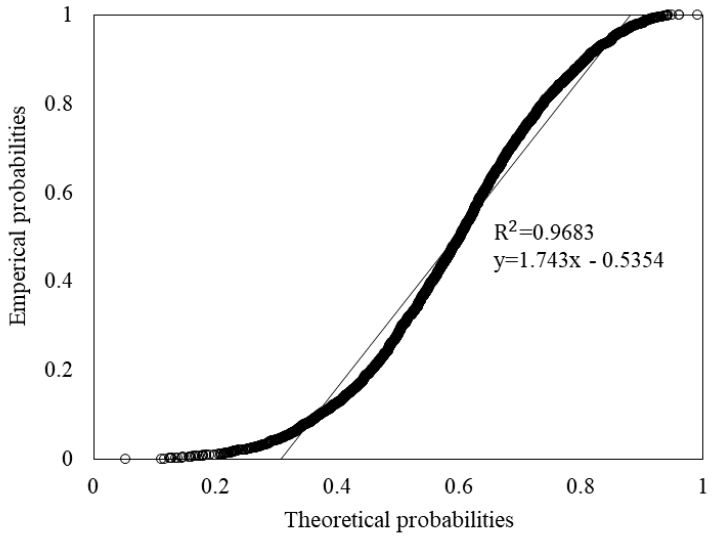


**Figure E-37: Sample 3 left rut exponential probability plot for 20 m averaged section length**

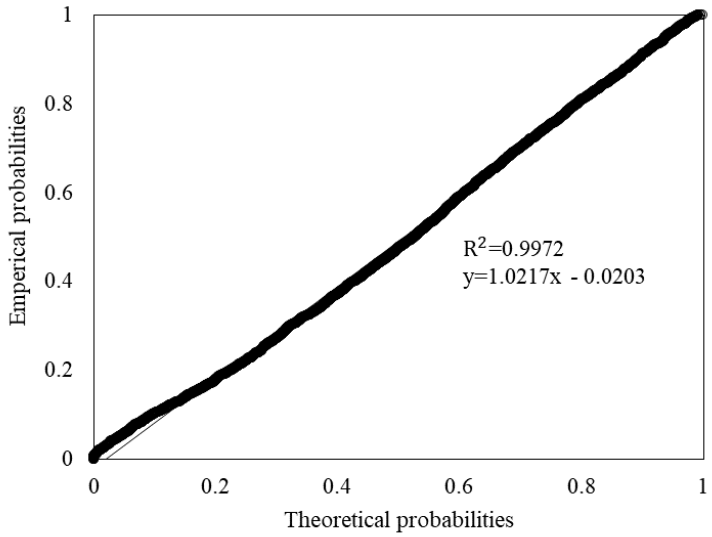


**Figure E-38: Sample 3 left rut lognormal probability plot for 20 m averaged section length**

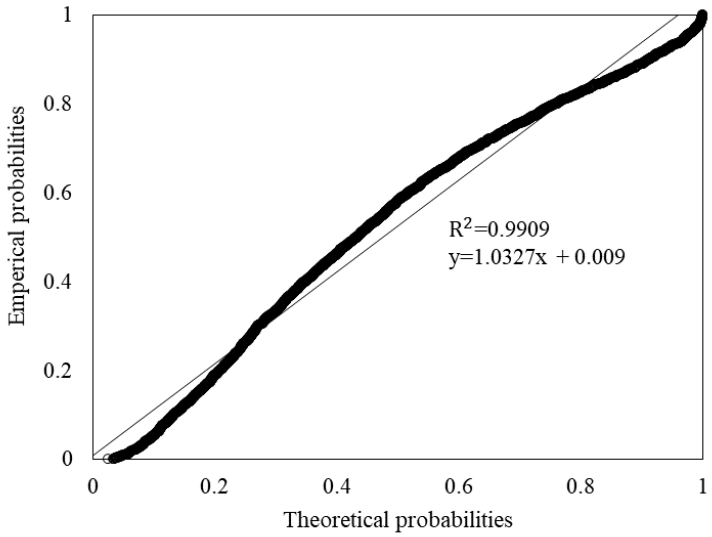


**Figure E-39: Sample 3 left rut normal probability plot for 20 m averaged section length**

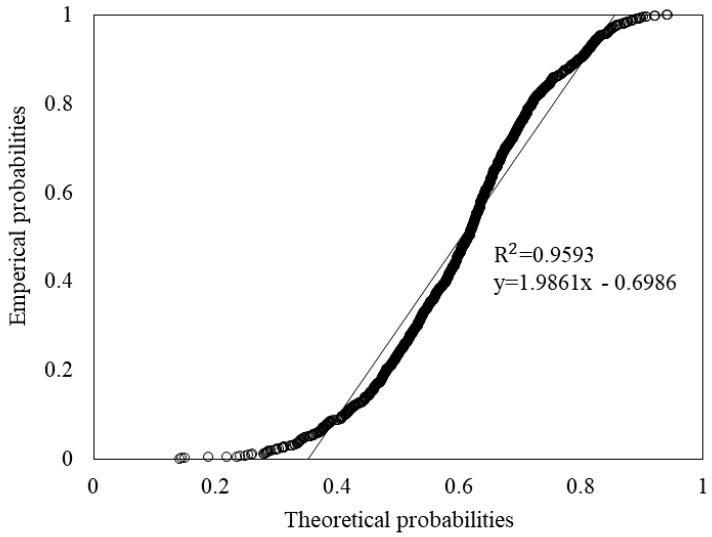


**Figure E-40: Sample 3 left rut exponential probability plot for 50 m averaged section length**

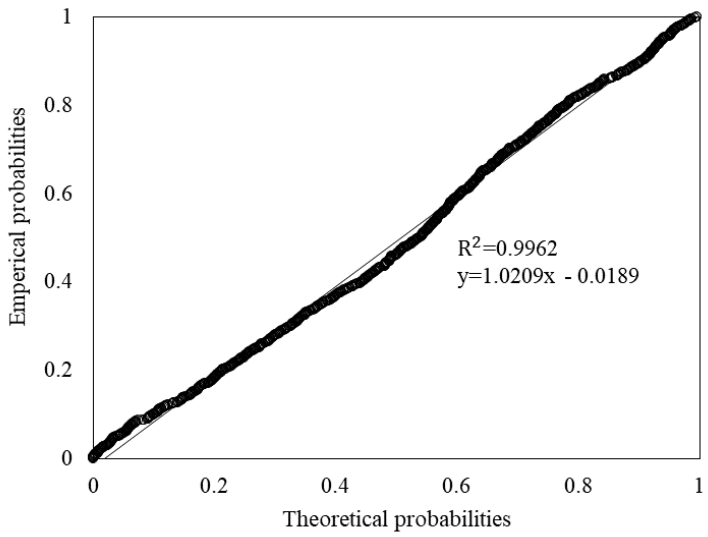


**Figure E-41: Sample 3 left rut lognormal probability plot for 50 m averaged section length**

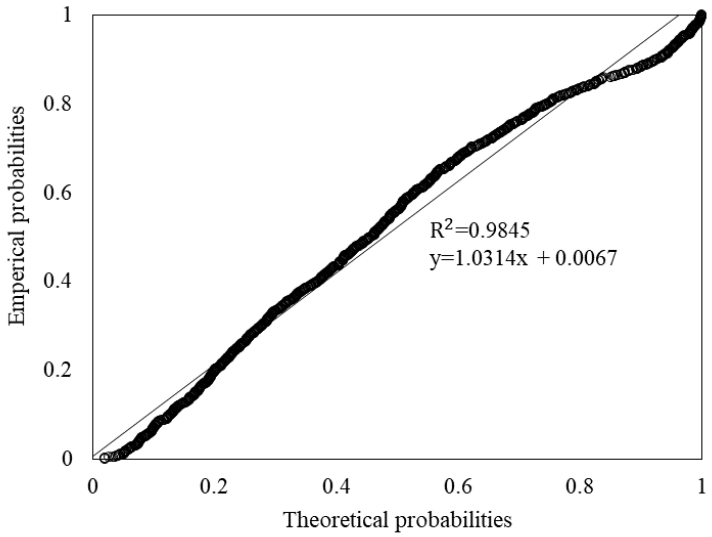


**Figure E-42: Sample 3 left rut normal probability plot for 50 m averaged section length**

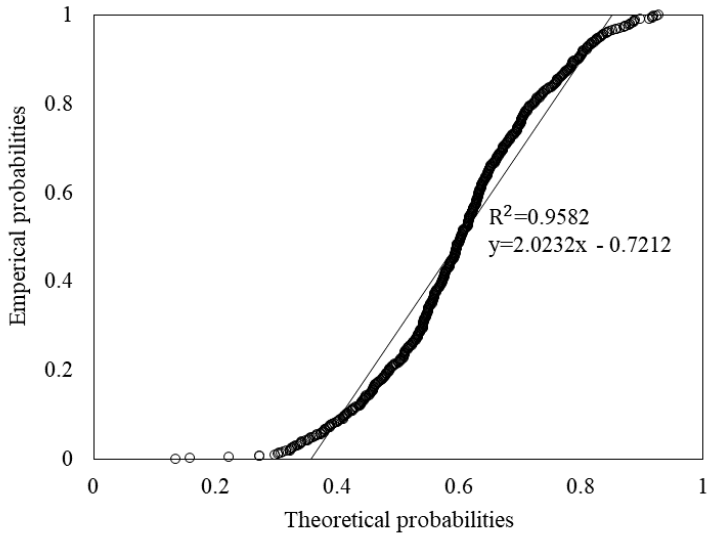


**Figure E-43: Sample 3 left rut exponential probability plot for 100 m averaged section length**

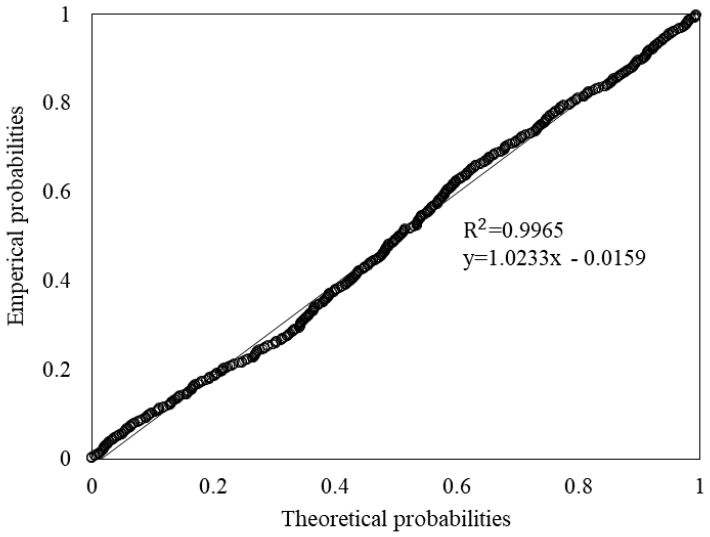


**Figure E-44: Sample 3 left rut lognormal probability plot for 100 m averaged section length**

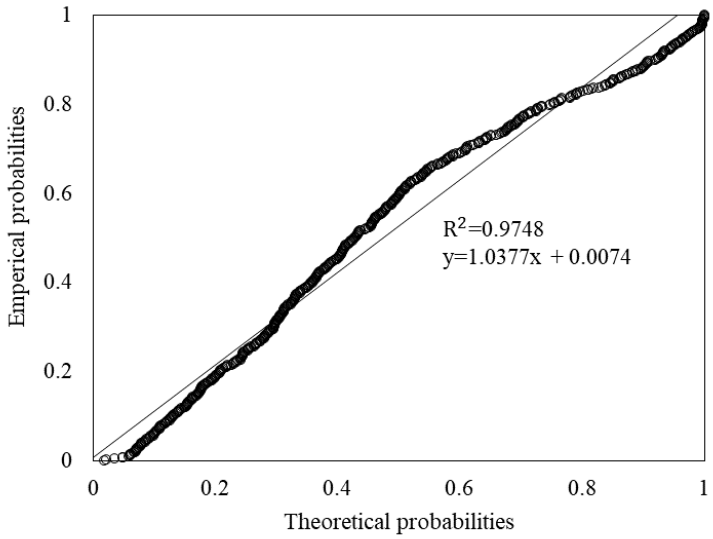


**Figure E-45: Sample 3 left rut normal probability plot for 100 m averaged section length**

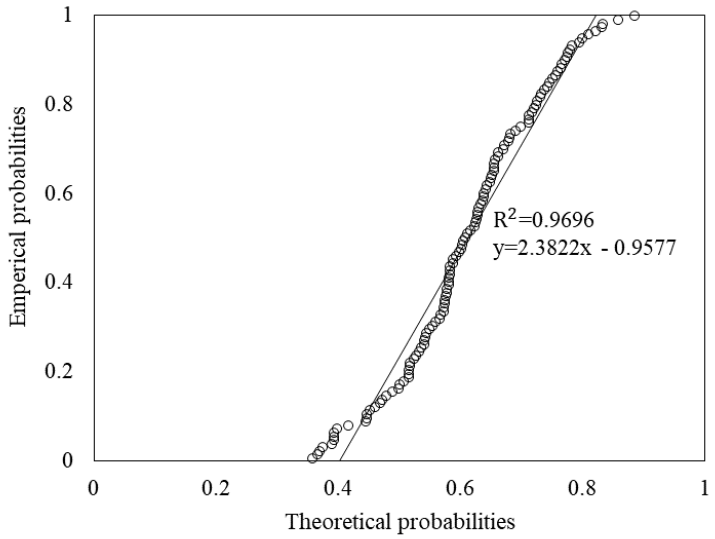


**Figure E-46: Sample 3 left rut exponential probability plot for 500 m averaged section length**

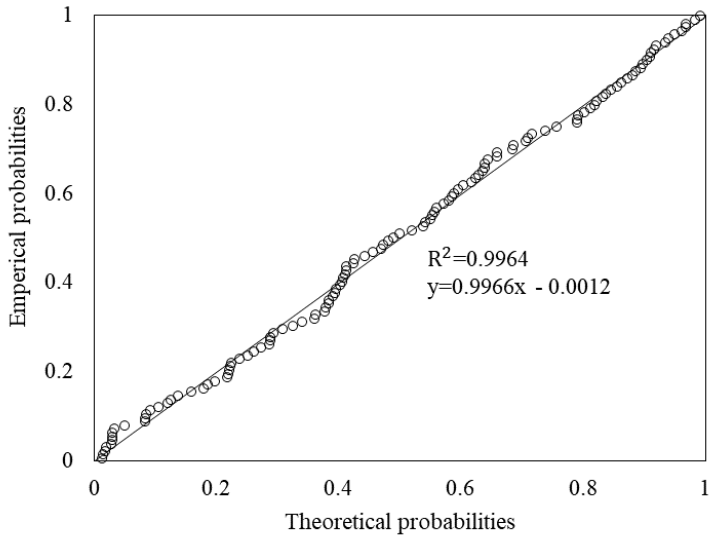


**Figure E-47: Sample 3 left rut lognormal probability plot for 500 m averaged section length**

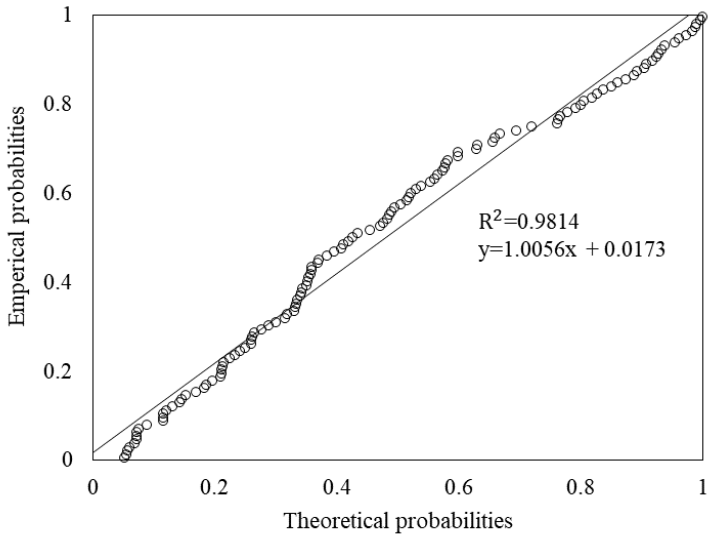


**Figure E-48: Sample 3 left rut normal probability plot for 500 m averaged section length**

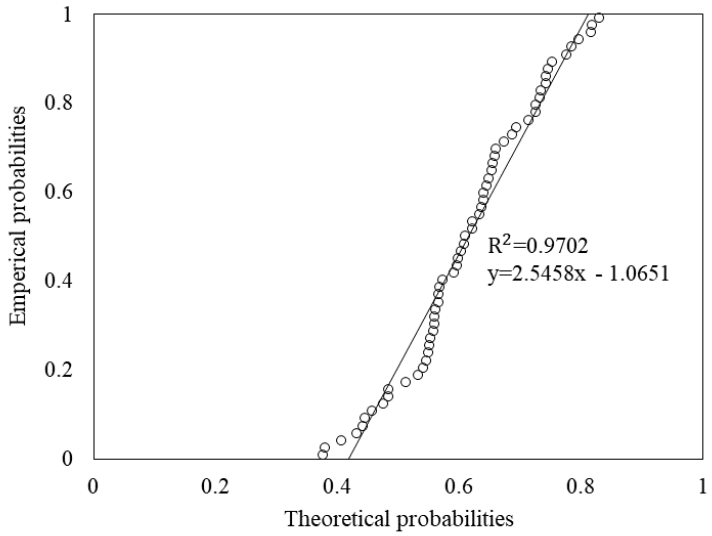


**Figure E-49: Sample 3 left rut exponential probability plot for 1 000 m averaged section length**

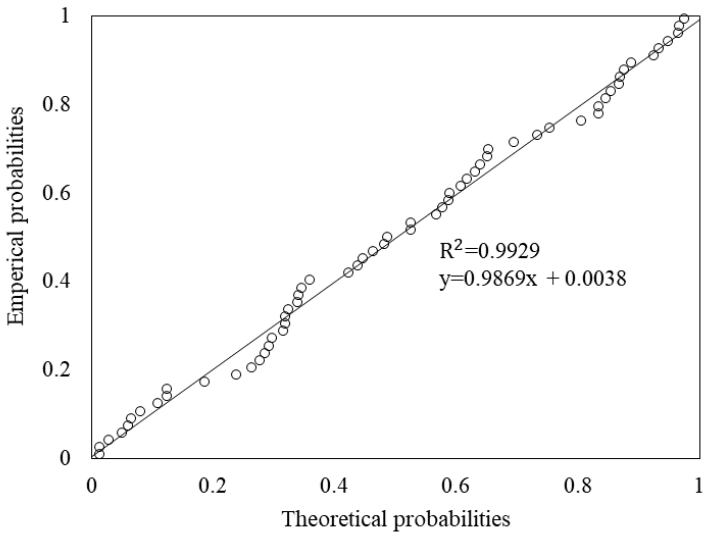


**Figure E-50: Sample 3 left rut lognormal probability plot for 1 000 m averaged section length**

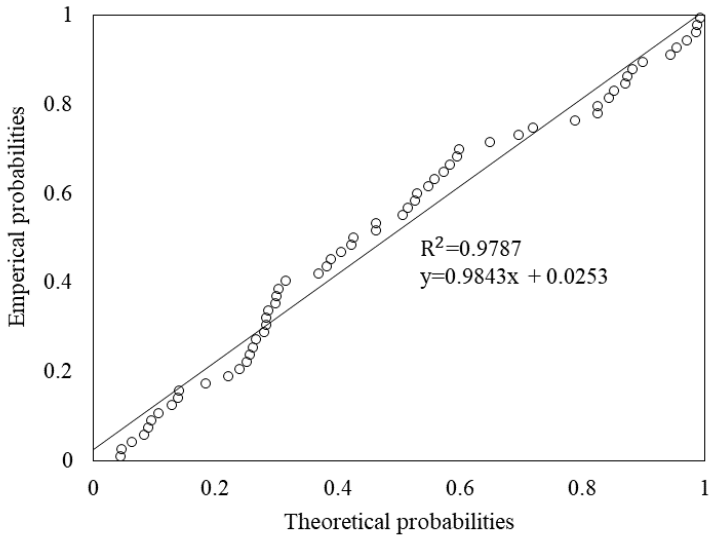


**Figure E-51: Sample 3 left rut normal probability plot for 1 000 m averaged section length**

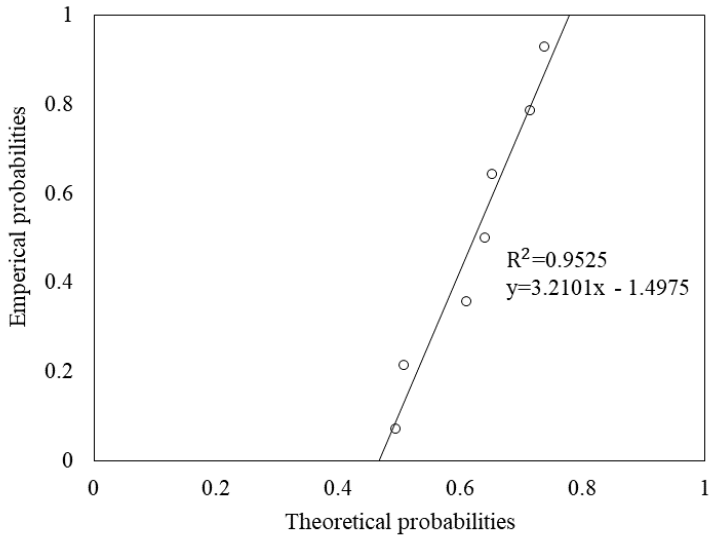


**Figure E-52: Sample 3 left rut exponential probability plot for 10 000 m averaged section length**

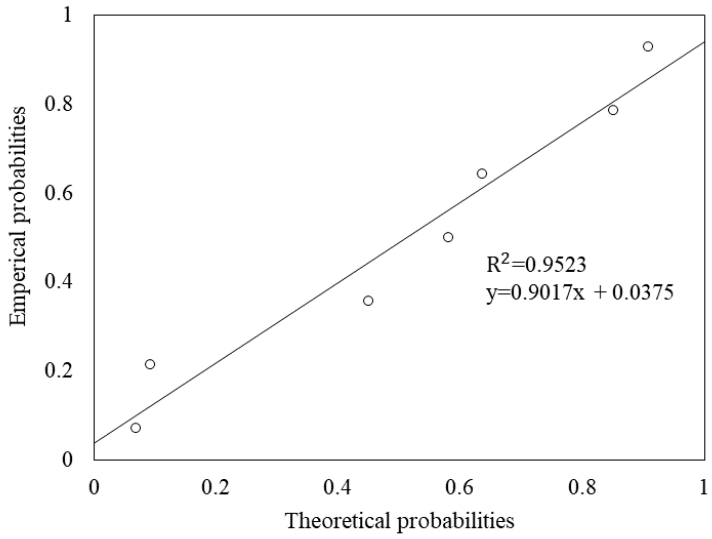


**Figure E-53: Sample 3 left rut lognormal probability plot for 10 000 m averaged section length**

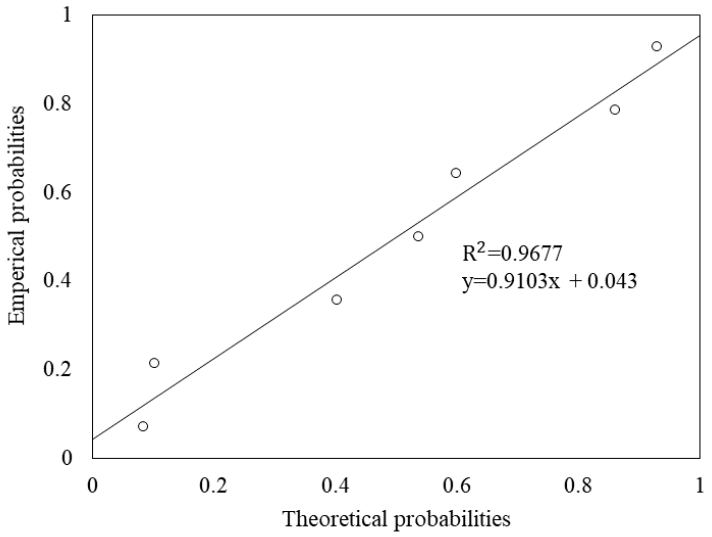


**Figure E-54: Sample 3 left rut normal probability plot for 10 000 m averaged section length**

Figure E-55 to Figure E-72 present the averaged section length exponential, lognormal, and normal probability plots for sample 4 left rut depth measurements.

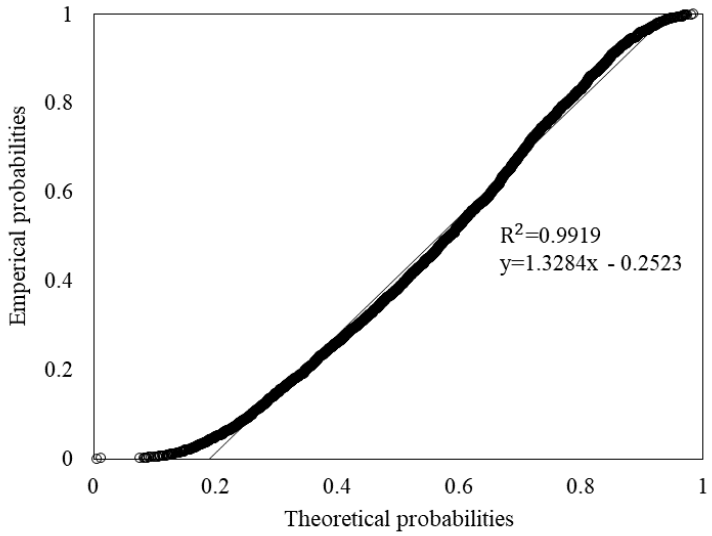


**Figure E-55: Sample 4 left rut exponential probability plot for 20 m averaged section length**

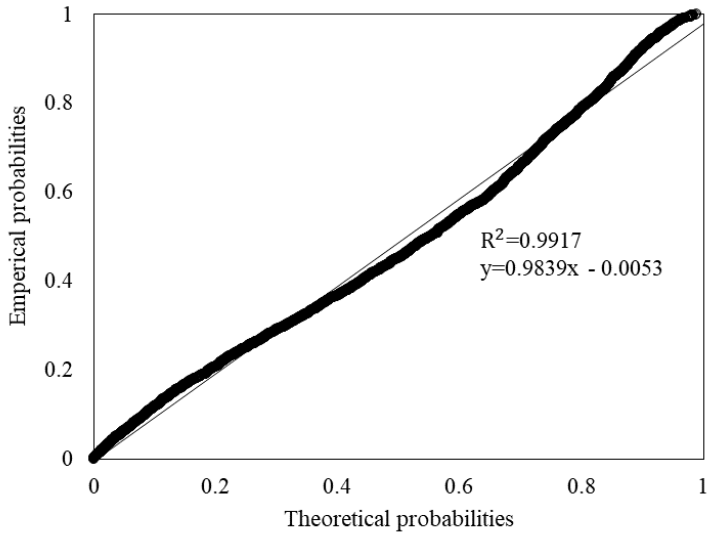


**Figure E-56: Sample 4 left rut lognormal probability plot for 20 m averaged section length**

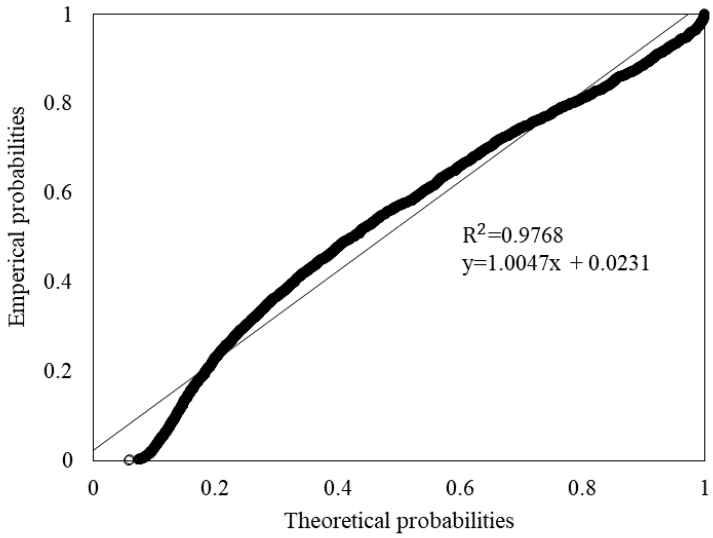


**Figure E-57: Sample 4 left rut normal probability plot for 20 m averaged section length**

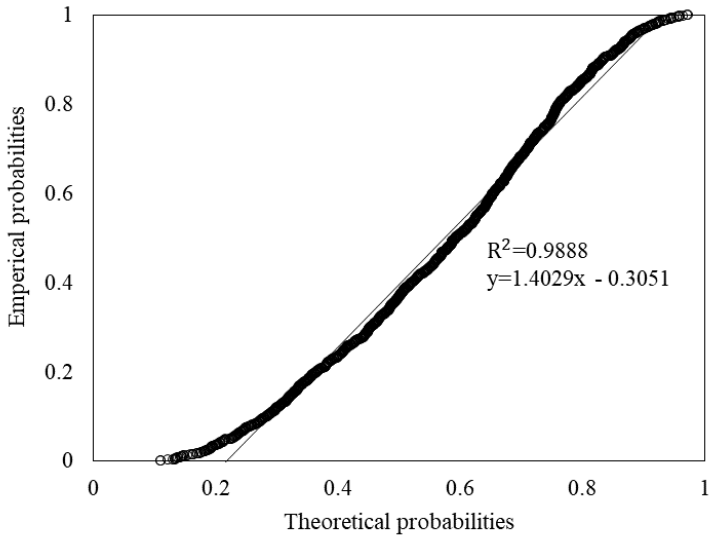


**Figure E-58: Sample 4 left rut exponential probability plot for 50 m averaged section length**

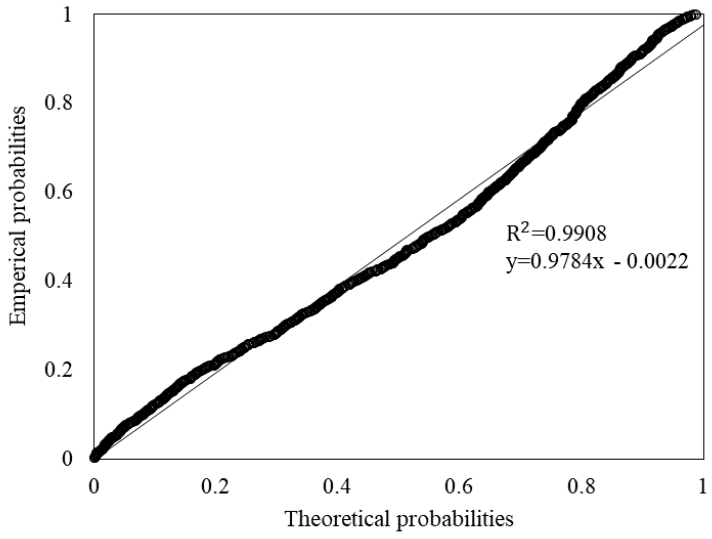


**Figure E-59: Sample 4 left rut lognormal probability plot for 50 m averaged section length**

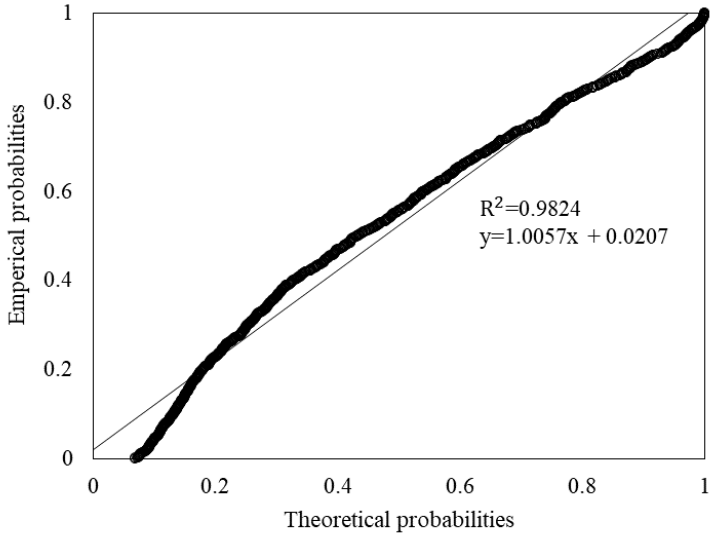


**Figure E-60: Sample 4 left rut normal probability plot for 50 m averaged section length**

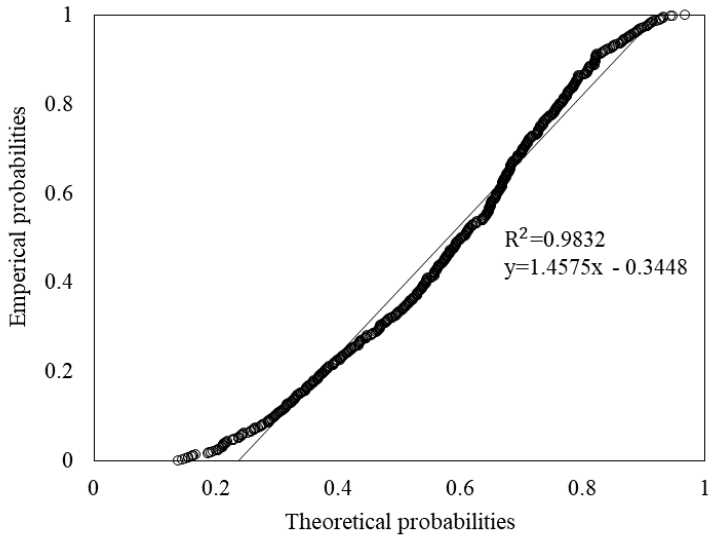


**Figure E-61: Sample 4 left rut exponential probability plot for 100 m averaged section length**

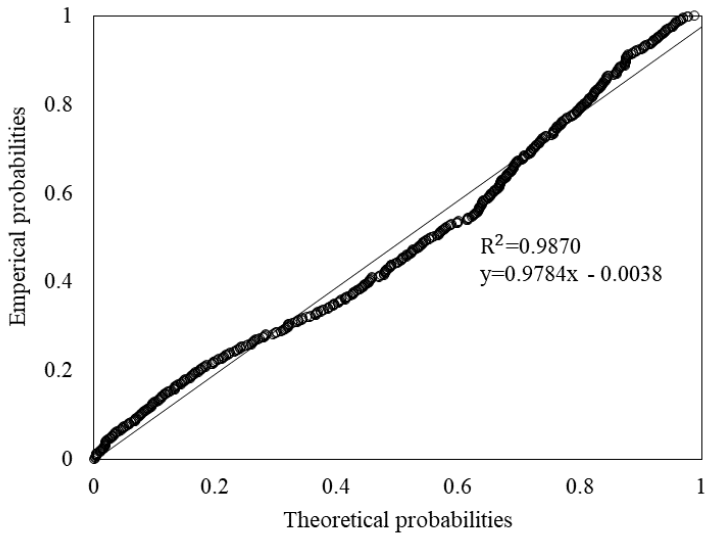


**Figure E-62: Sample 4 left rut lognormal probability plot for 100 m averaged section length**

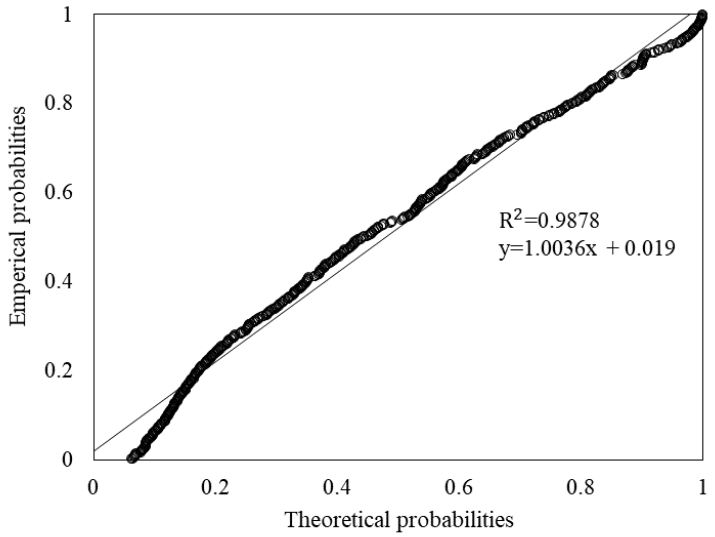


**Figure E-63: Sample 4 left rut normal probability plot for 100 m averaged section length**

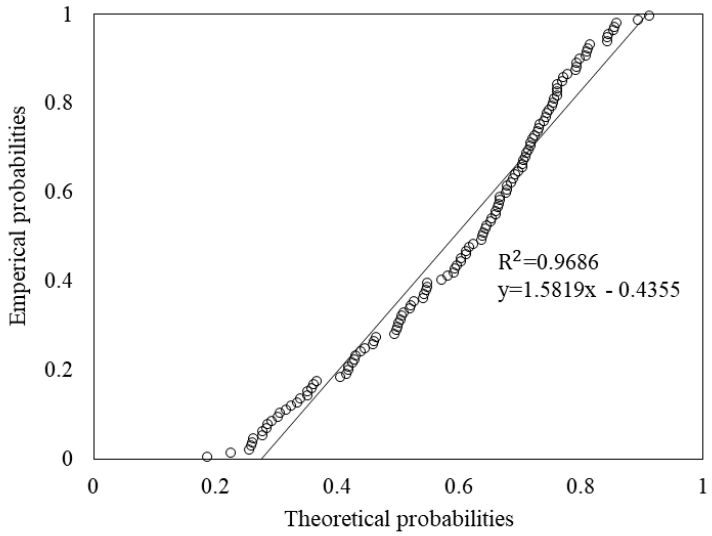


**Figure E-64: Sample 4 left rut exponential probability plot for 500 m averaged section length**

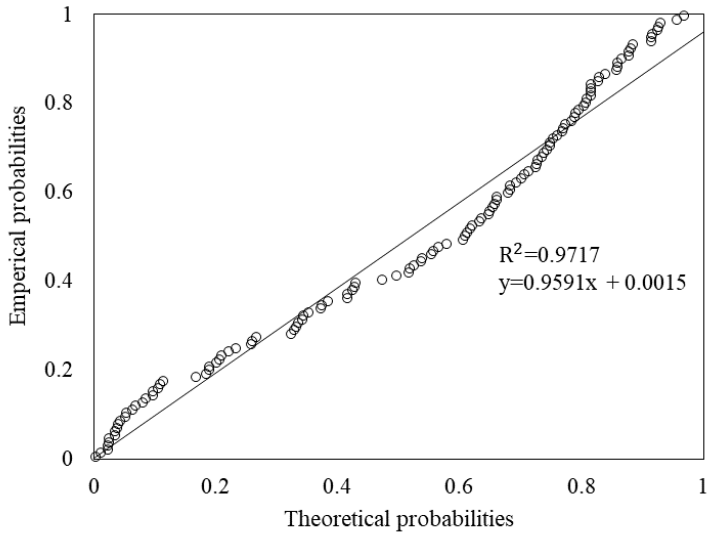


**Figure E-65: Sample 4 left rut lognormal probability plot for 500 m averaged section length**

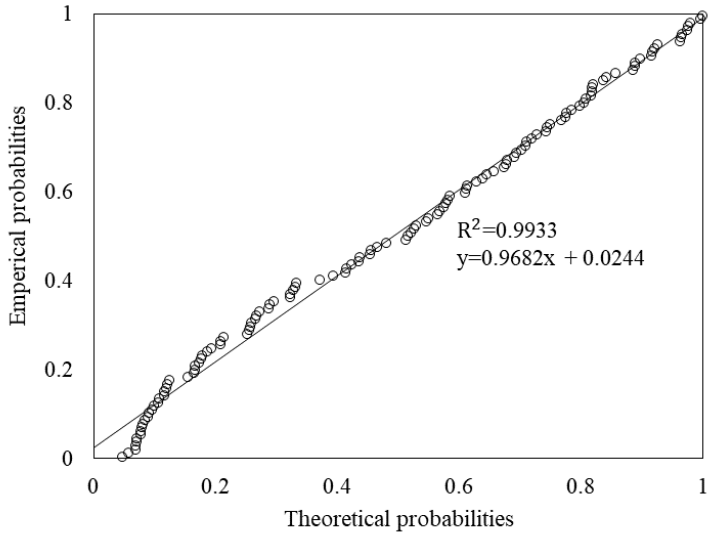


**Figure E-66: Sample 4 left rut normal probability plot for 500 m averaged section length**

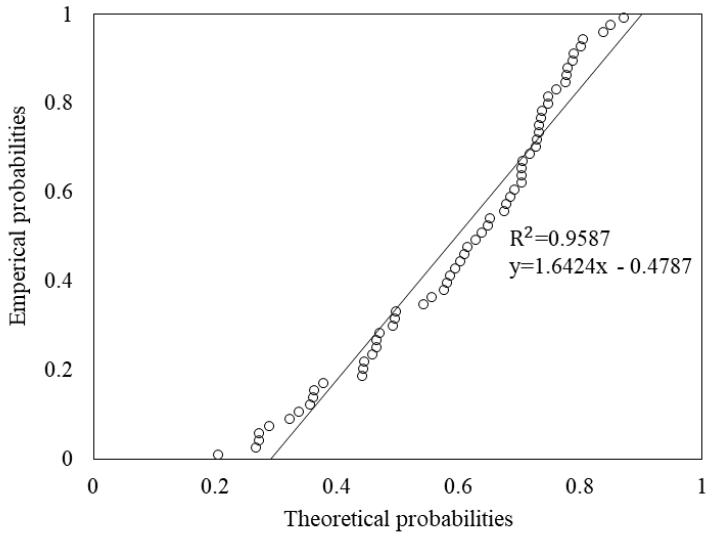


**Figure E-67: Sample 4 left rut exponential probability plot for 1 000 m averaged section length**

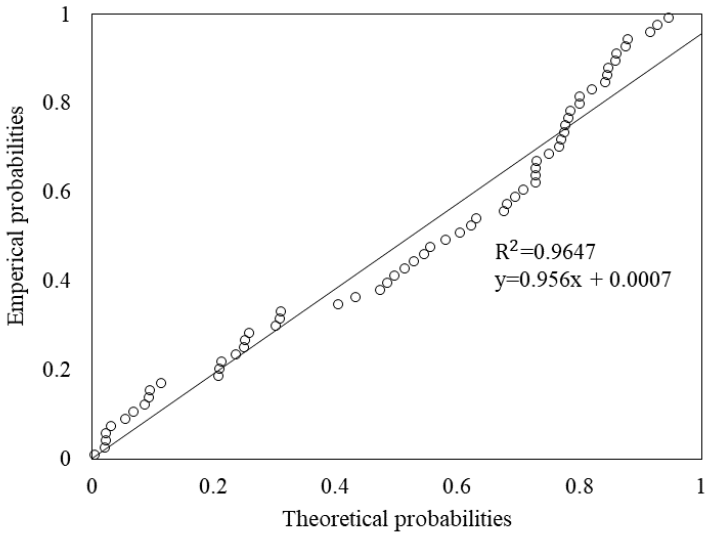


**Figure E-68: Sample 4 left rut lognormal probability plot for 1 000 m averaged section length**

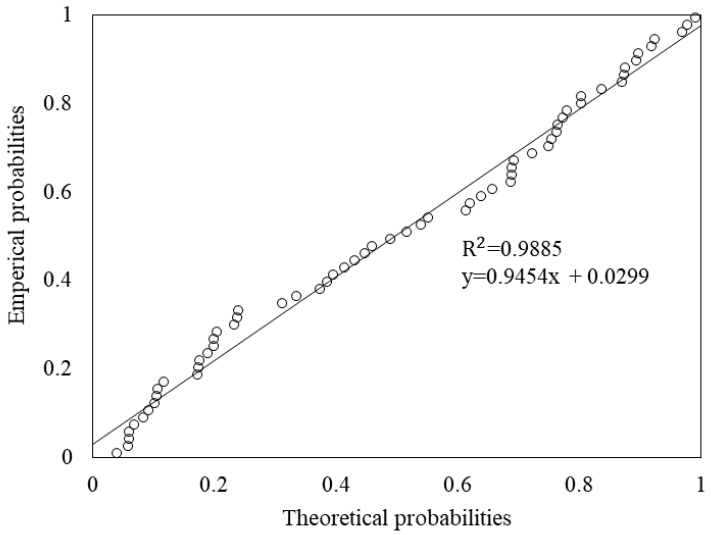


**Figure E-69: Sample 4 left rut normal probability plot for 1 000 m averaged section length**

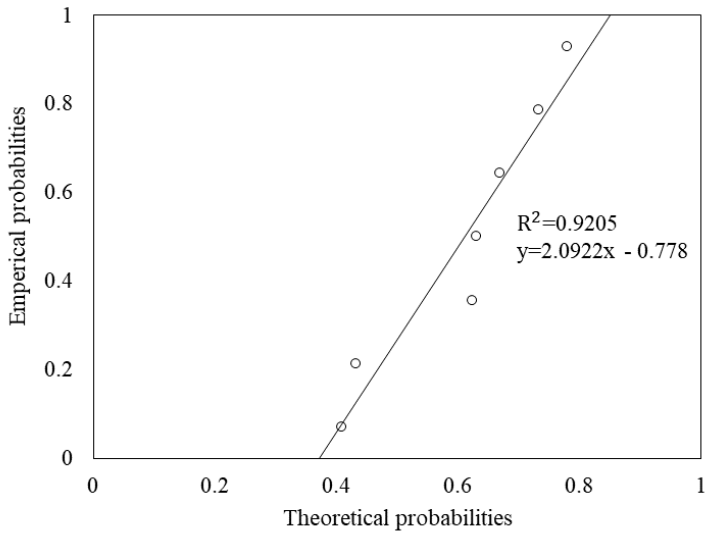


**Figure E-70: Sample 4 left rut exponential probability plot for 10 000 m averaged section length**

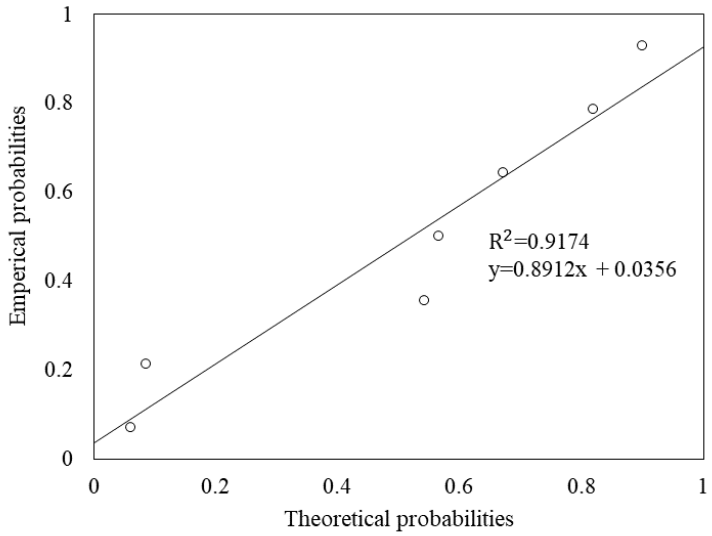


**Figure E-71: Sample 4 left rut lognormal probability plot for 10 000 m averaged section length**

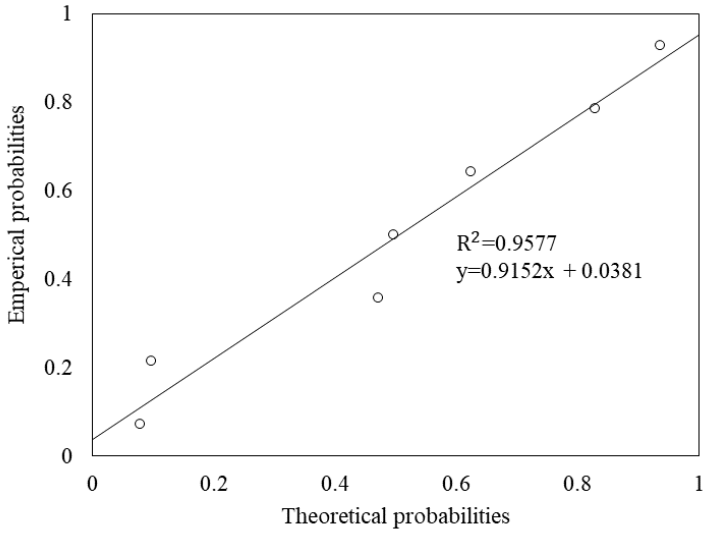


**Figure E-72: Sample 4 left rut normal probability plot for 10 000 m averaged section length**

Figure E-73 to Figure E-90 present the averaged section length exponential, lognormal, and normal probability plots for sample 5 left rut depth measurements.

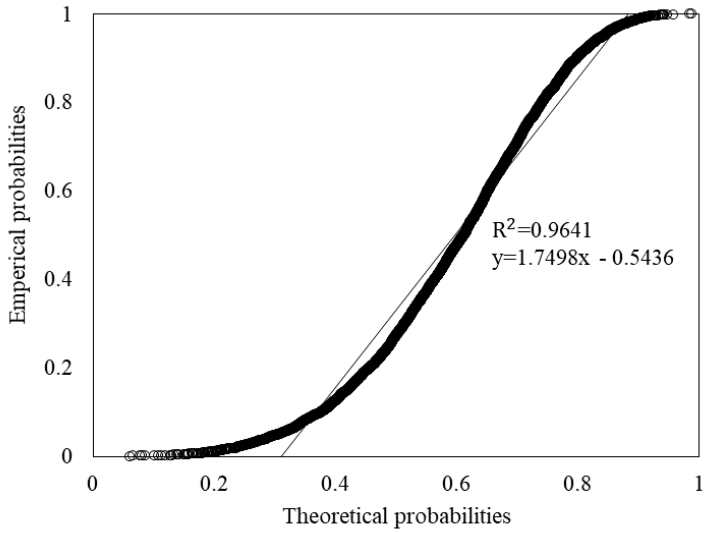


**Figure E-73: Sample 5 left rut exponential probability plot for 20 m averaged section length**

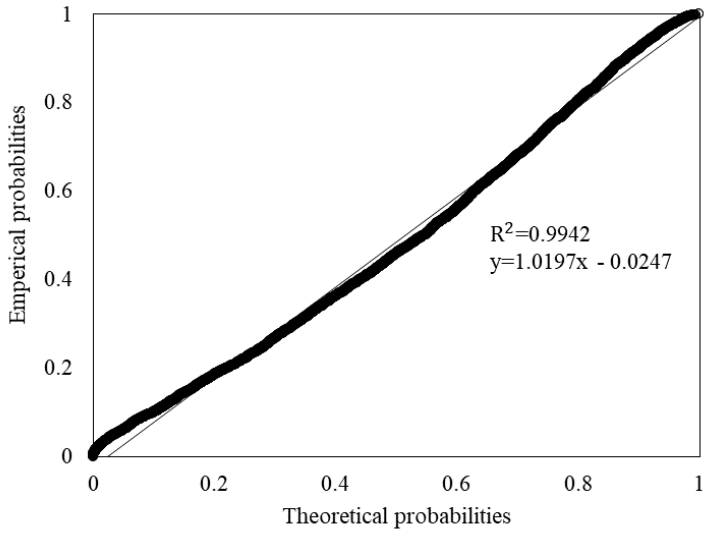


**Figure E-74: Sample 5 left rut lognormal probability plot for 20 m averaged section length**

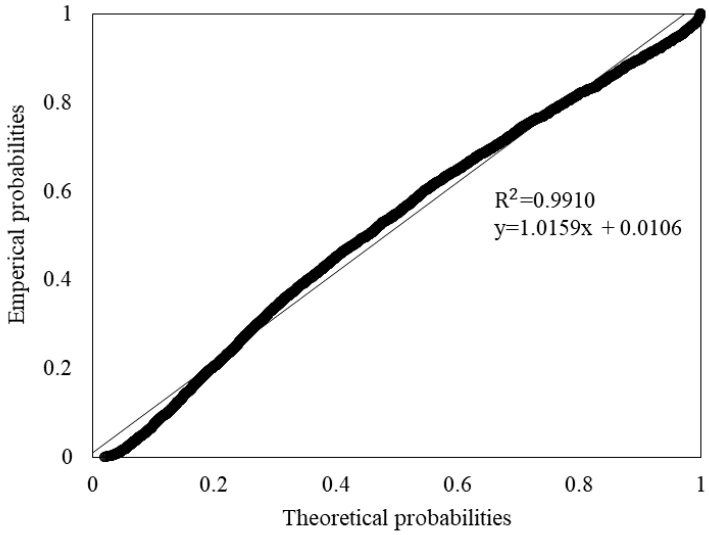


**Figure E-75: Sample 5 left rut normal probability plot for 20 m averaged section length**

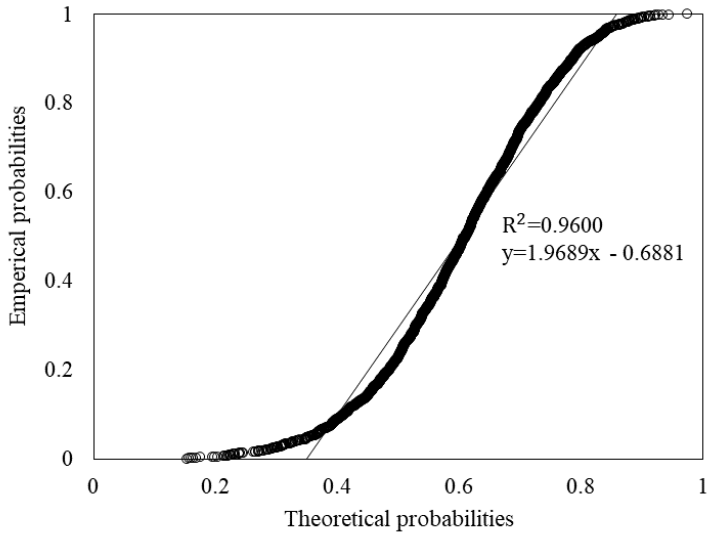


**Figure E-76: Sample 5 left rut exponential probability plot for 50 m averaged section length**

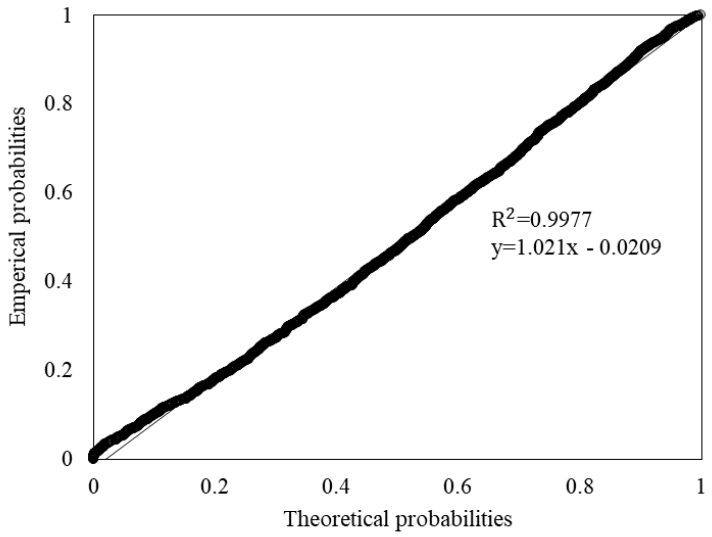


**Figure E-77: Sample 5 left rut lognormal probability plot for 50 m averaged section length**

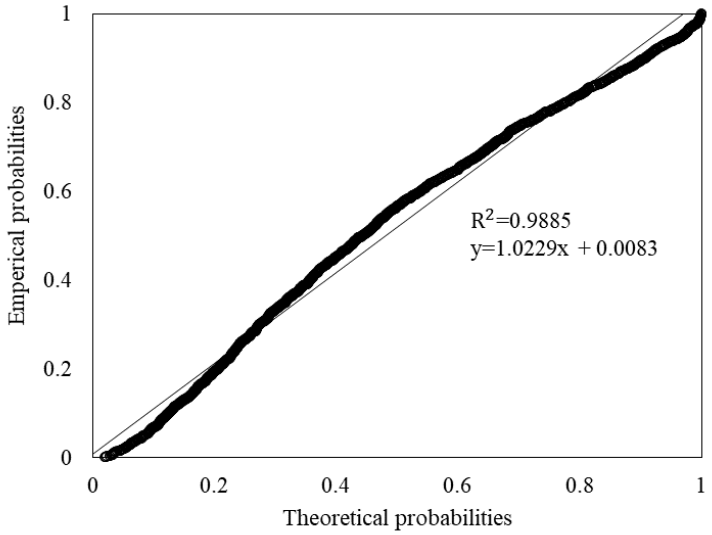


**Figure E-78: Sample 5 left rut normal probability plot for 50 m averaged section length**

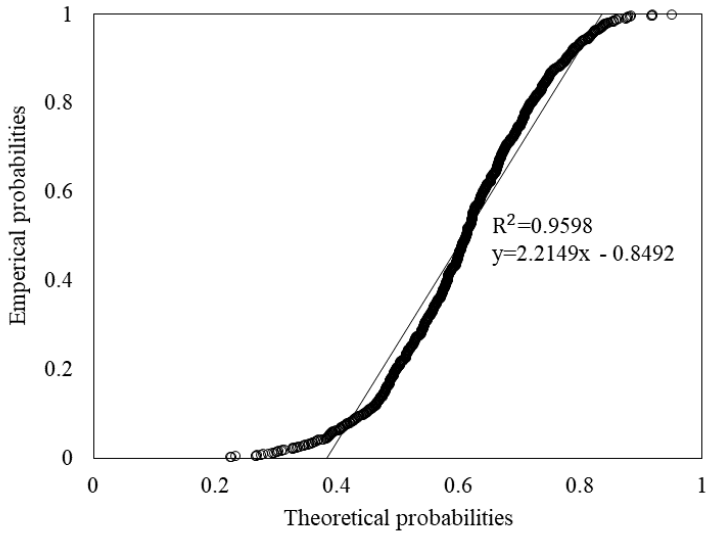


**Figure E-79: Sample 5 left rut exponential probability plot for 100 m averaged section length**

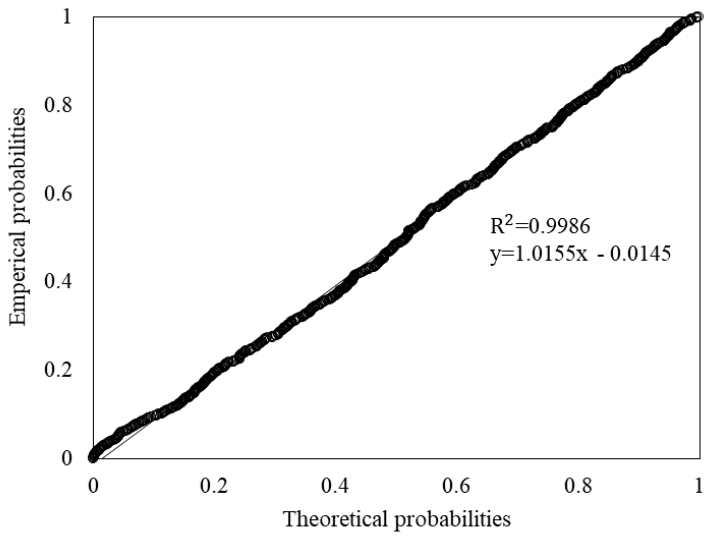


**Figure E-80: Sample 5 left rut lognormal probability plot for 100 m averaged section length**

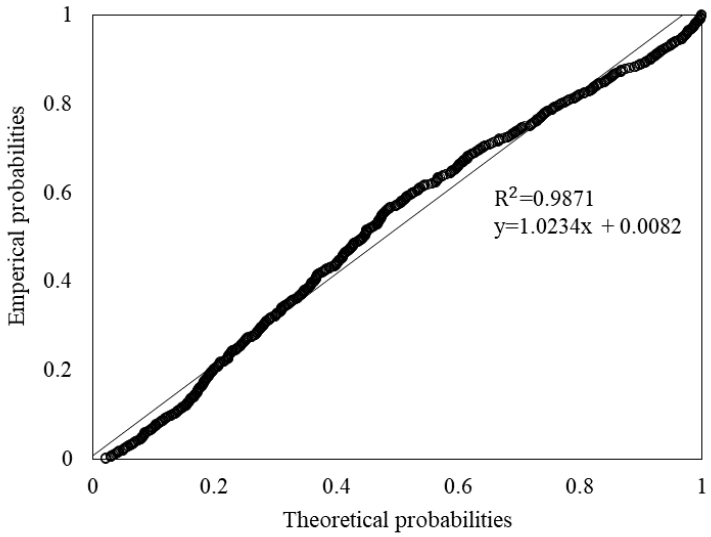


**Figure E-81: Sample 5 left rut normal probability plot for 100 m averaged section length**

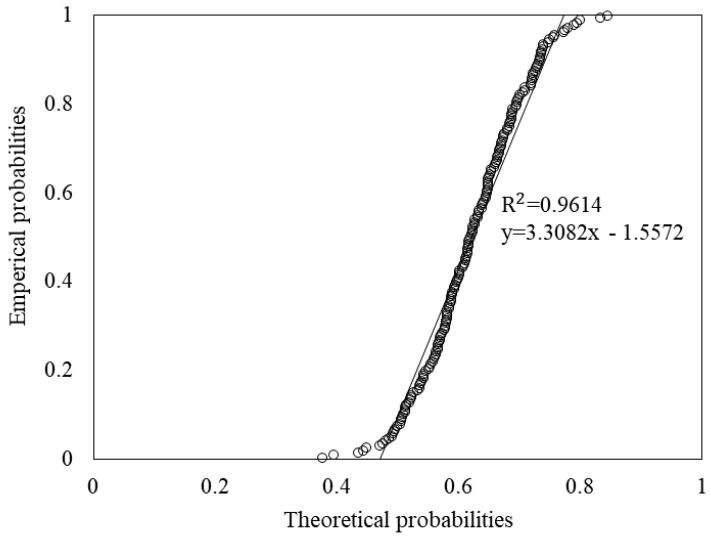


**Figure E-82: Sample 5 left rut exponential probability plot for 500 m averaged section length**

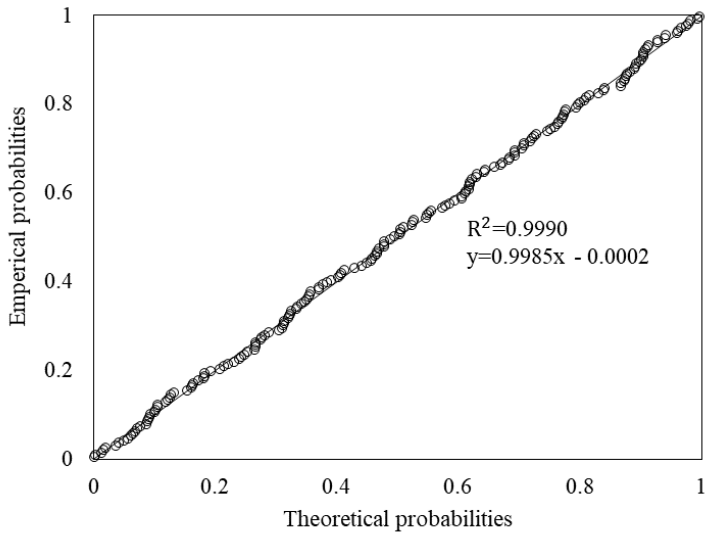


**Figure E-83: Sample 5 left rut lognormal probability plot for 500 m averaged section length**

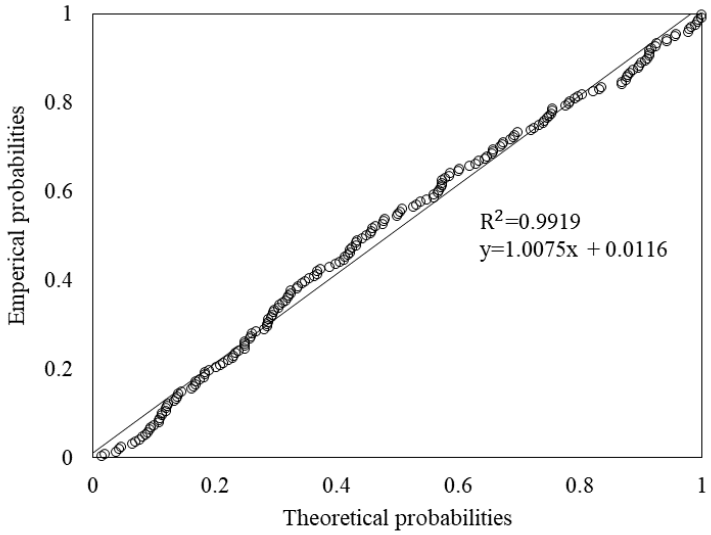


**Figure E-84: Sample 5 left rut normal probability plot for 500 m averaged section length**

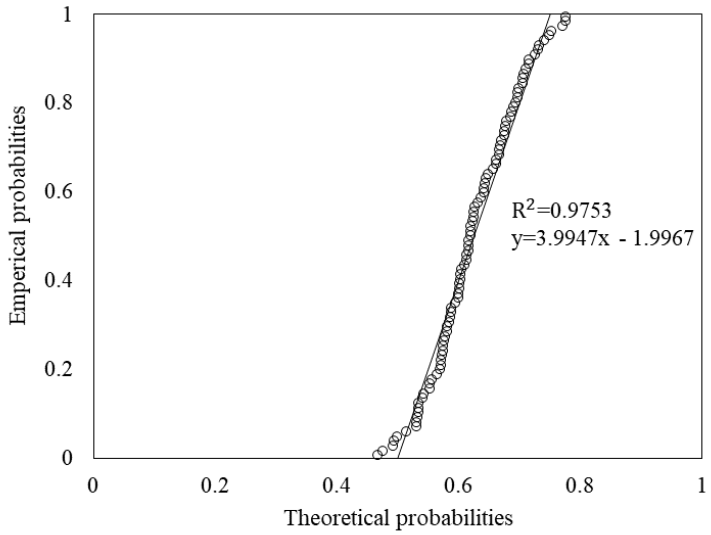


**Figure E-85: Sample 5 left rut exponential probability plot for 1 000 m averaged section length**

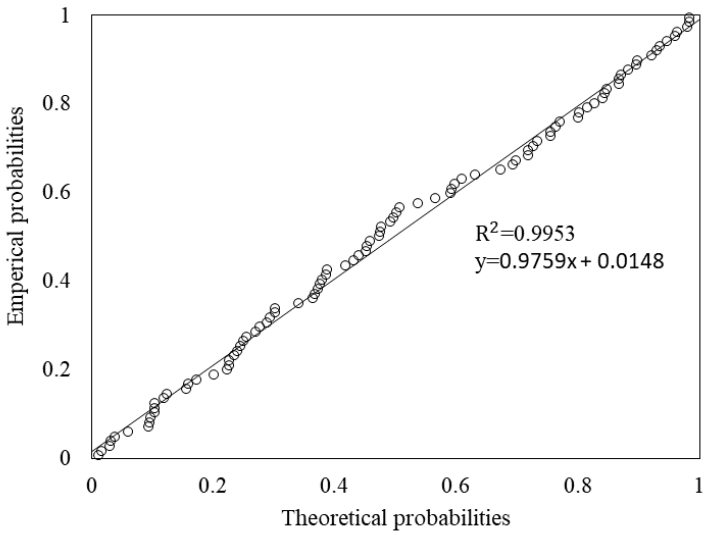


**Figure E-86: Sample 5 left rut lognormal probability plot for 1 000 m averaged section length**

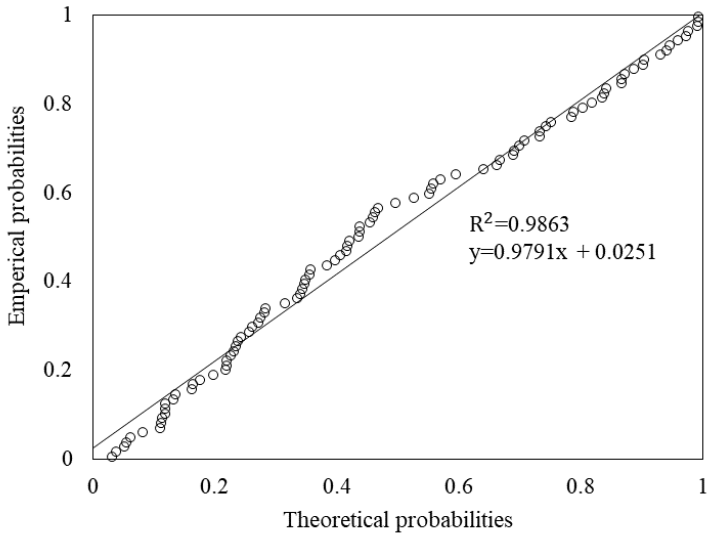


**Figure E-87: Sample 5 left rut normal probability plot for 1 000 m averaged section length**

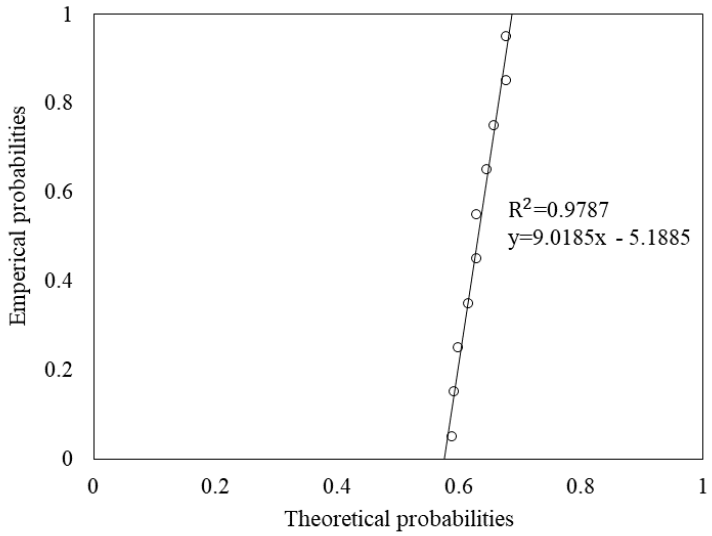


**Figure E-88: Sample 5 left rut exponential probability plot for 10 000 m averaged section length**

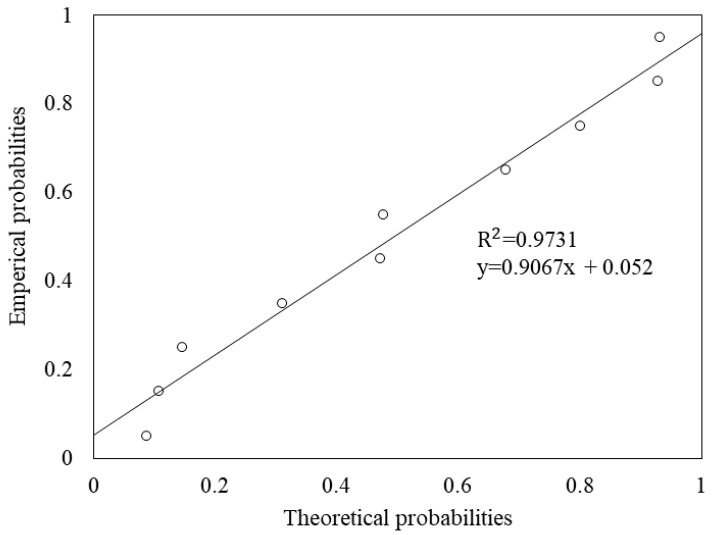


**Figure E-89: Sample 5 left rut lognormal probability plot for 10 000 m averaged section length**

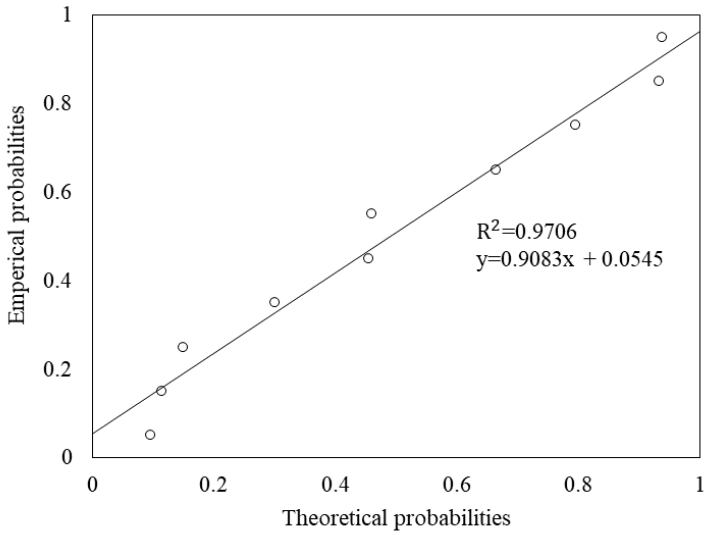


**Figure E-90: Sample 5 left rut normal probability plot for 10 000 m averaged section length**

Figure E-91 to Figure E-108 present the averaged section length exponential, lognormal, and normal probability plots for sample 6 left rut depth measurements.

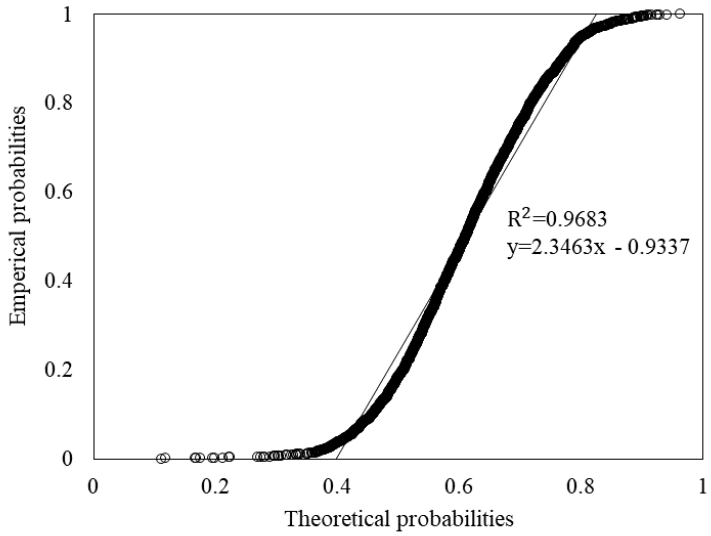


**Figure E-91: Sample 6 left rut exponential probability plot for 20 m averaged section length**

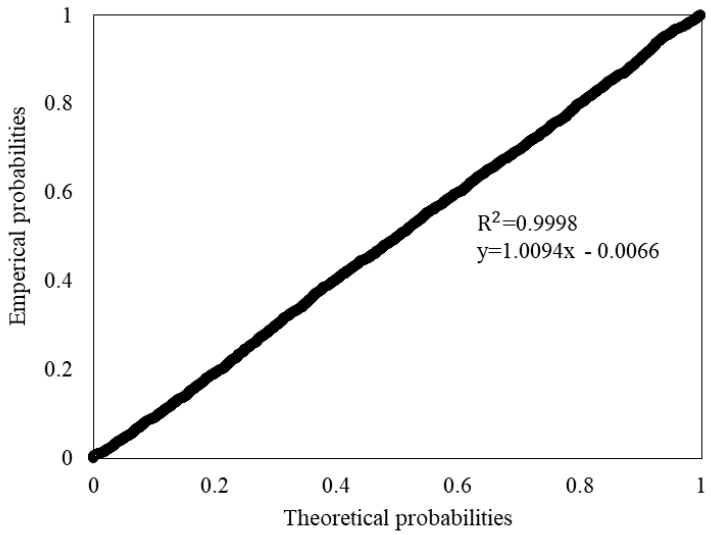


**Figure E-92: Sample 6 left rut lognormal probability plot for 20 m averaged section length**

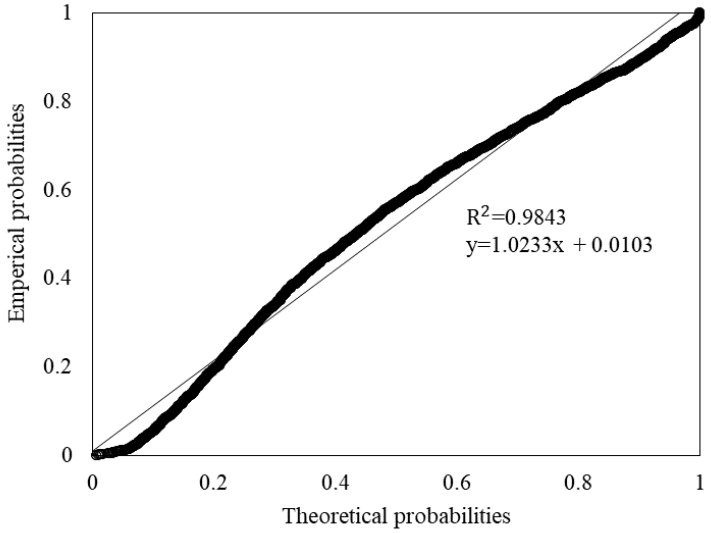


**Figure E-93: Sample 6 left rut normal probability plot for 20 m averaged section length**

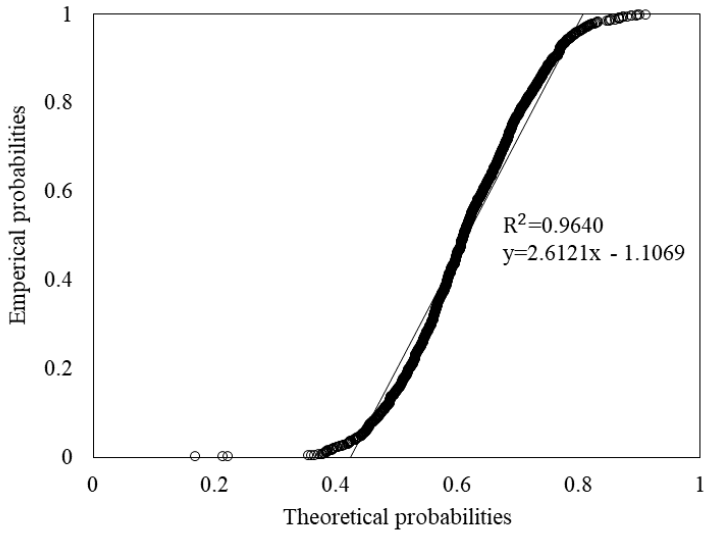


**Figure E-94: Sample 6 left rut exponential probability plot for 50 m averaged section length**

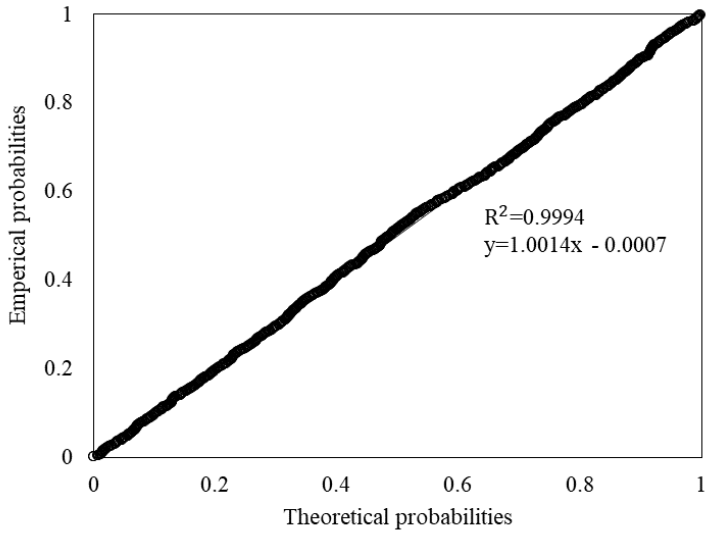


**Figure E-95: Sample 6 left rut lognormal probability plot for 50 m averaged section length**

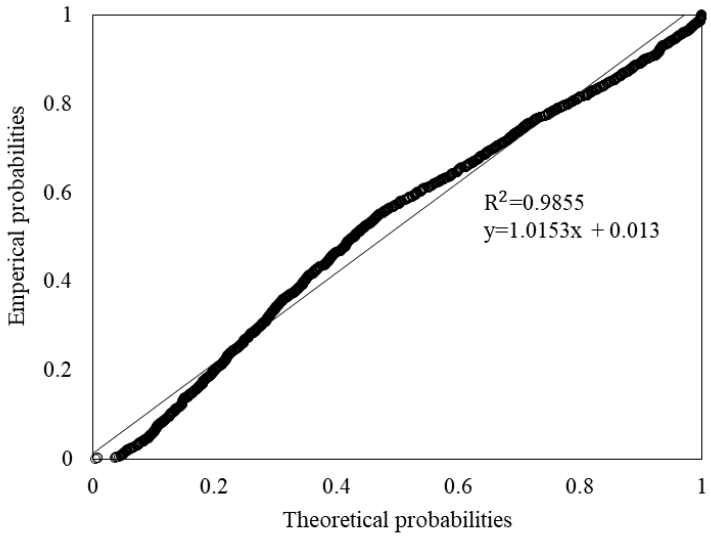


**Figure E-96: Sample 6 left rut normal probability plot for 50 m averaged section length**

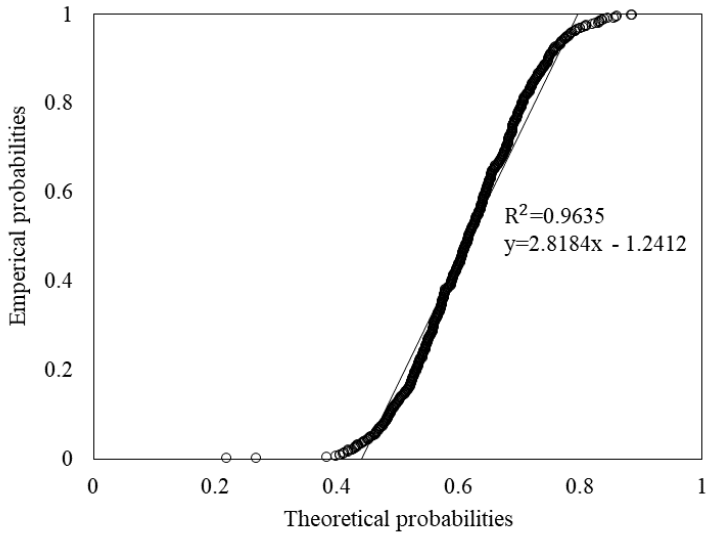


**Figure E-97: Sample 6 left rut exponential probability plot for 100 m averaged section length**

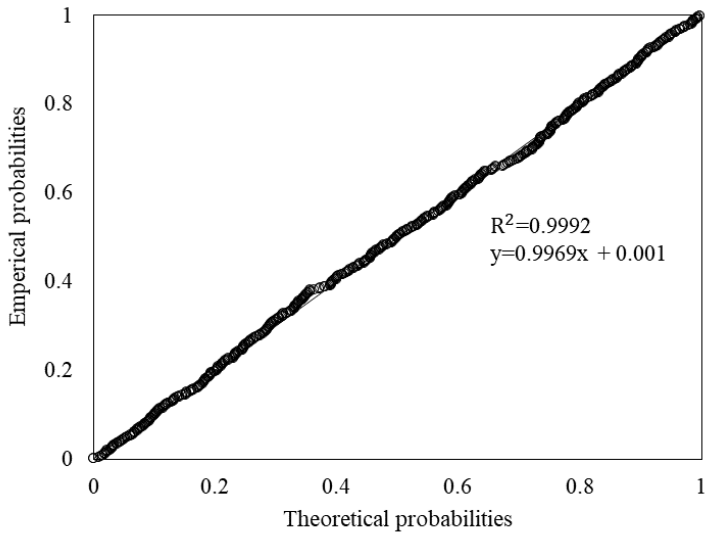


**Figure E-98: Sample 6 left rut lognormal probability plot for 100 m averaged section length**

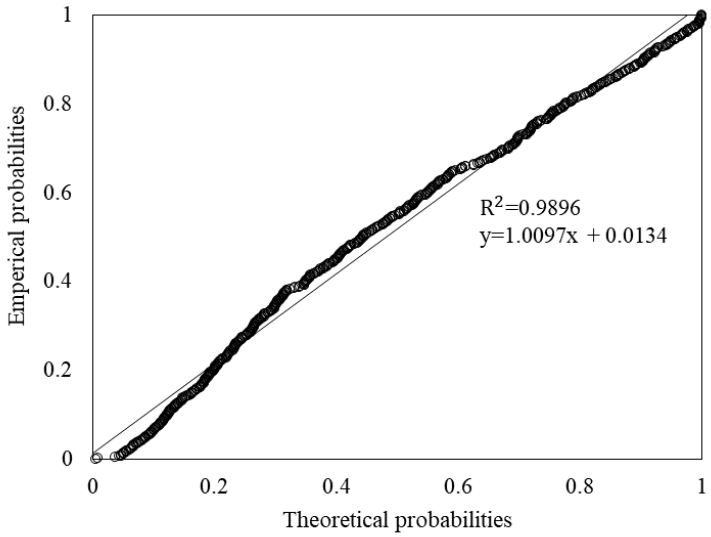


**Figure E-99: Sample 6 left rut normal probability plot for 100 m averaged section length**

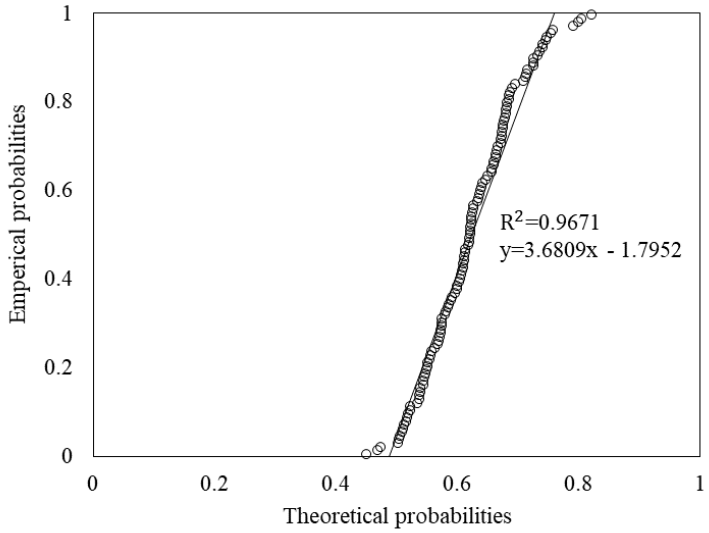


**Figure E-100: Sample 6 left rut exponential probability plot for 500 m averaged section length**

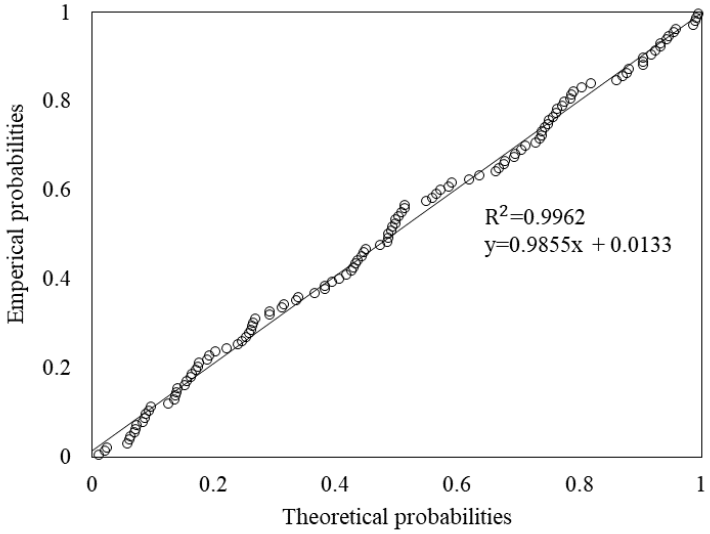


**Figure E-101: Sample 6 left rut lognormal probability plot for 500 m averaged section length**

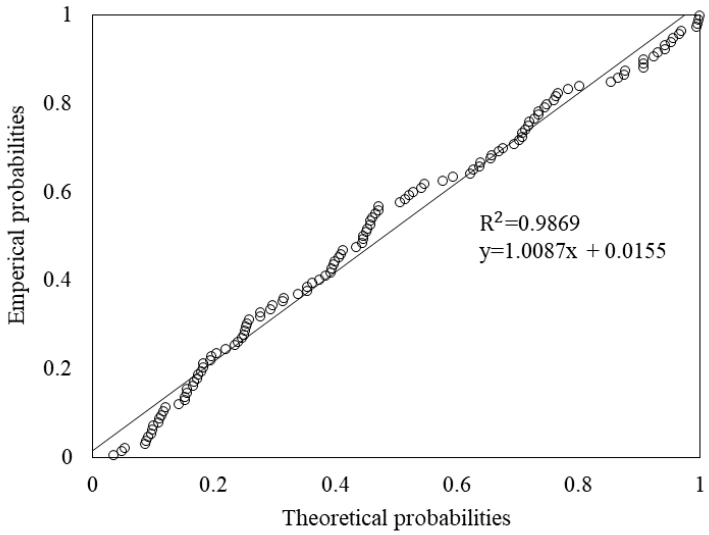


**Figure E-102: Sample 6 left rut normal probability plot for 500 m averaged section length**

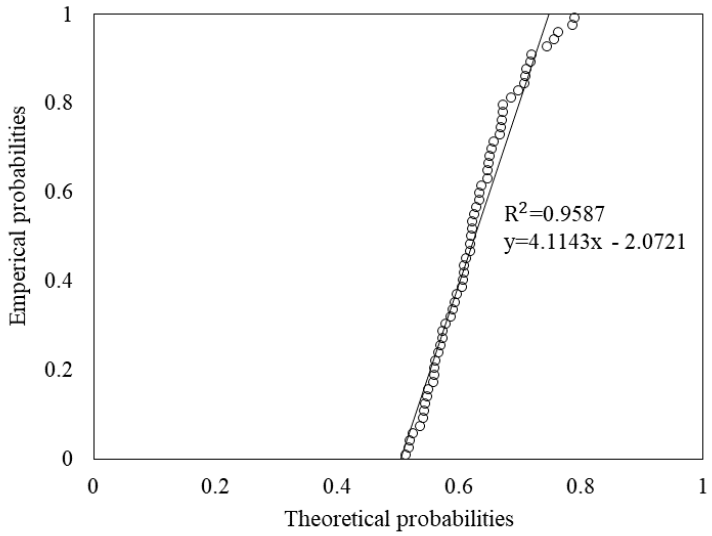


**Figure E-103: Sample 6 left rut exponential probability plot for 1 000 m averaged section length**

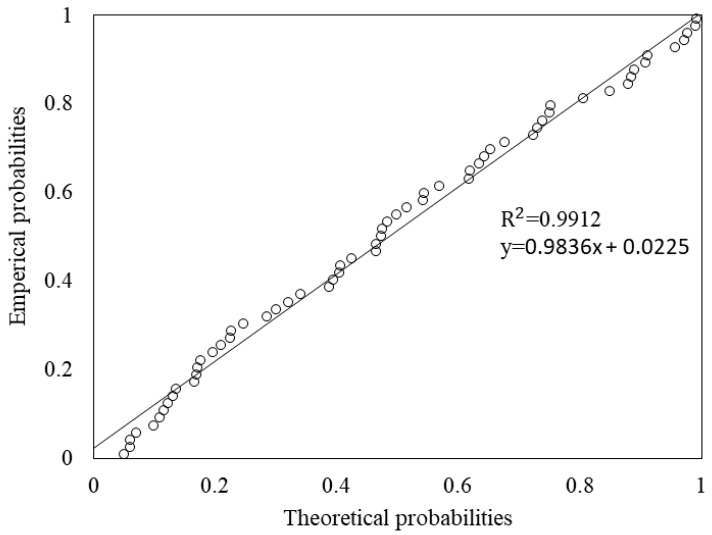


**Figure E-104: Sample 6 left rut lognormal probability plot for 1 000 m averaged section length**

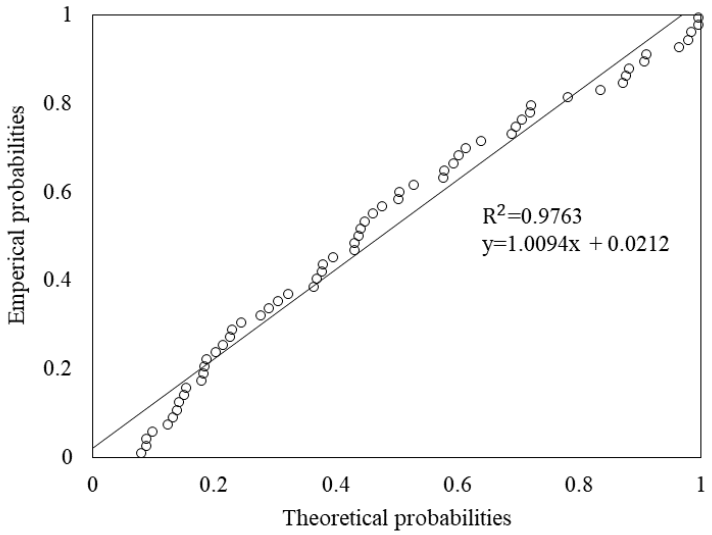


**Figure E-105: Sample 6 left rut normal probability plot for 1 000 m averaged section length**

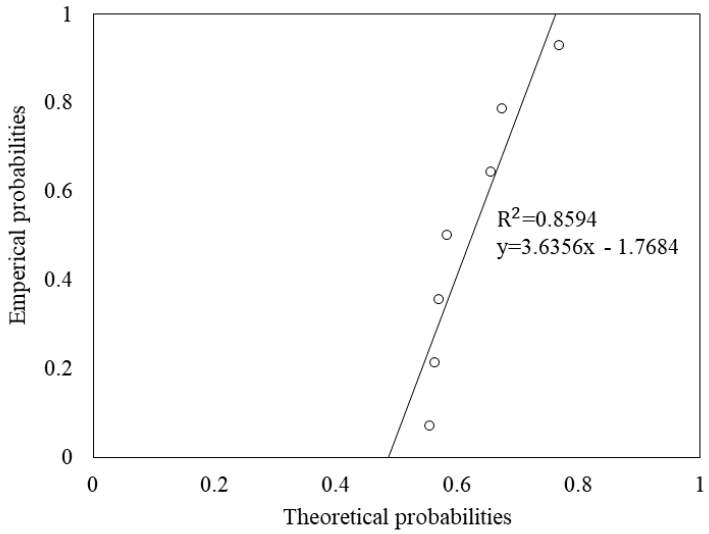


**Figure E-106: Sample 6 left rut exponential probability plot for 10 000 m averaged section length**

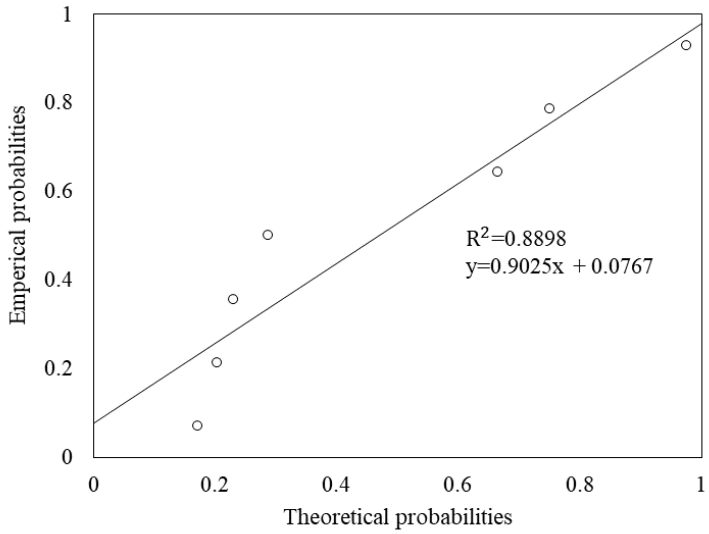


**Figure E-107: Sample 6 left rut lognormal probability plot for 10 000 m averaged section length**

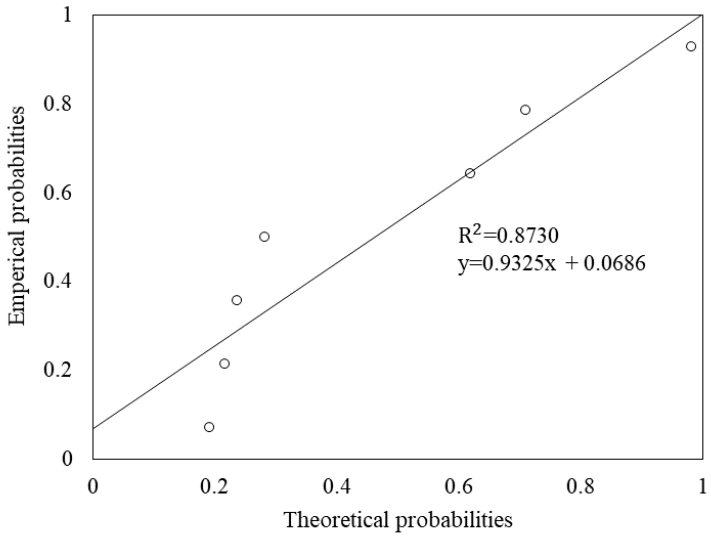


**Figure E-108: Sample 6 left rut normal probability plot for 10 000 m averaged section length**

Figure E-109 to Figure E-126 present the averaged section length exponential, lognormal, and normal probability plots for sample 7 left rut depth measurements.

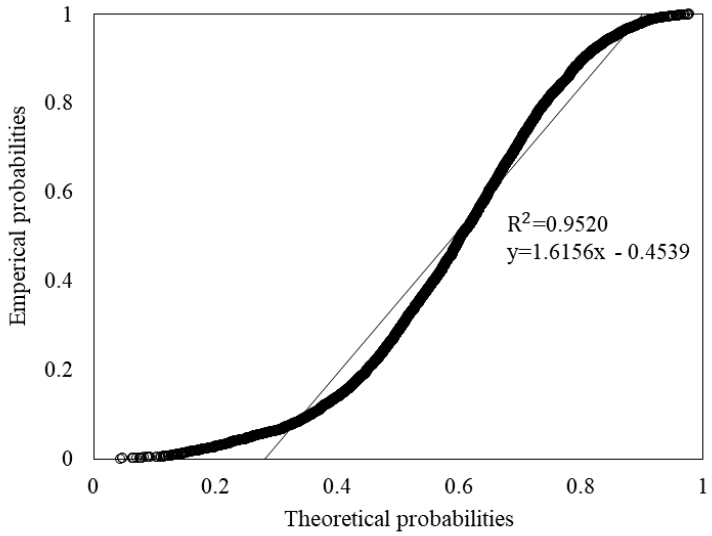


**Figure E-109: Sample 7 left rut exponential probability plot for 20 m averaged section length**

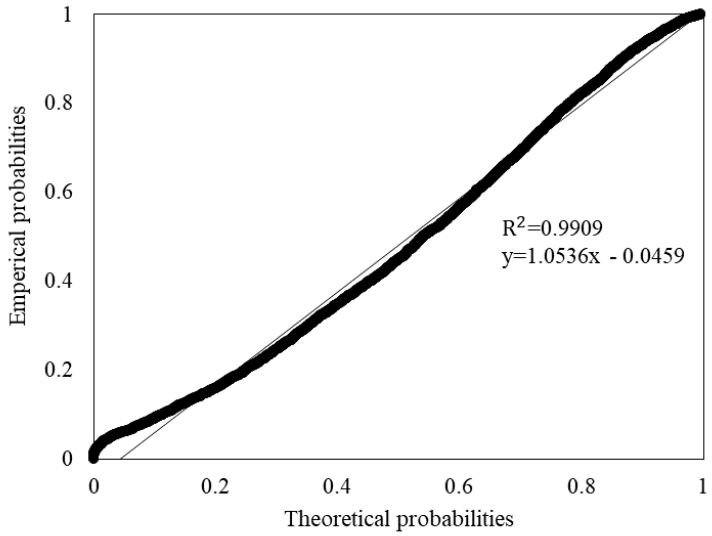


**Figure E-110: Sample 7 left rut lognormal probability plot for 20 m averaged section length**

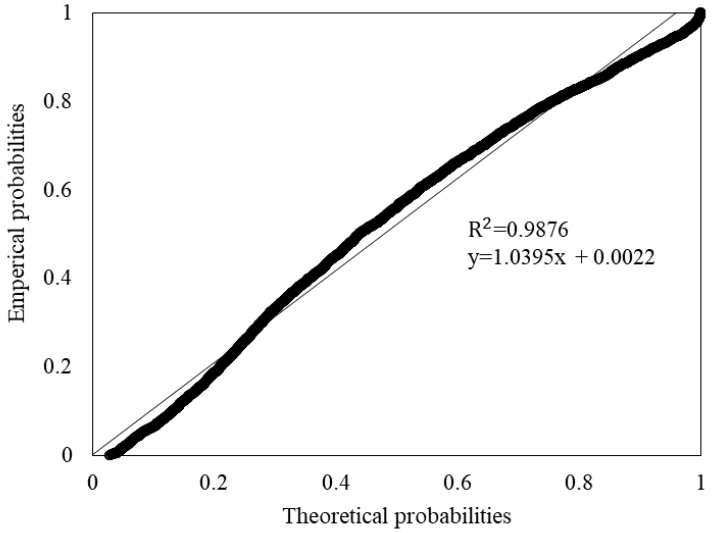


**Figure E-111: Sample 7 left rut normal probability plot for 20 m averaged section length**

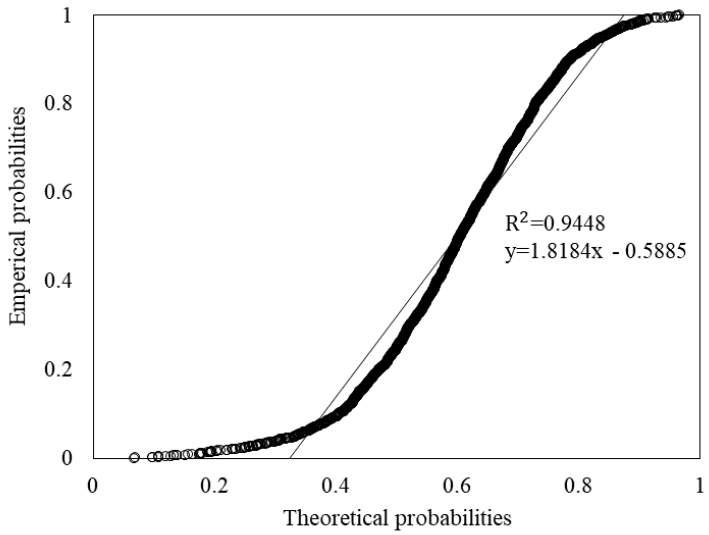


**Figure E-112: Sample 7 left rut exponential probability plot for 50 m averaged section length**

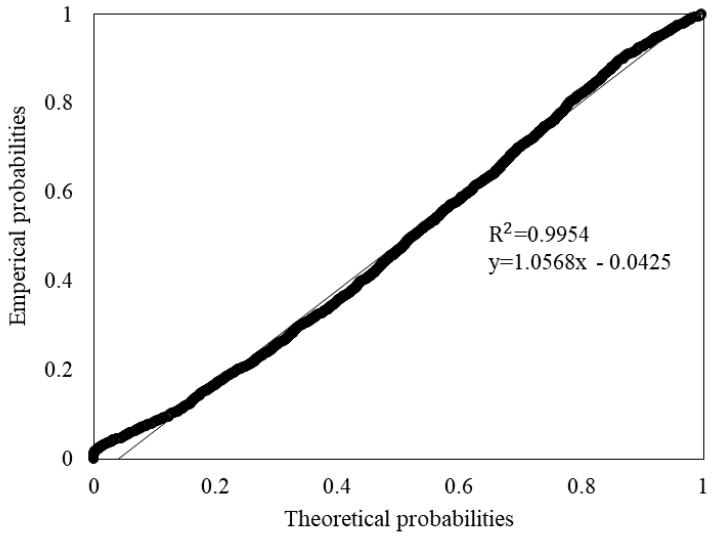


**Figure E-113: Sample 7 left rut lognormal probability plot for 50 m averaged section length**

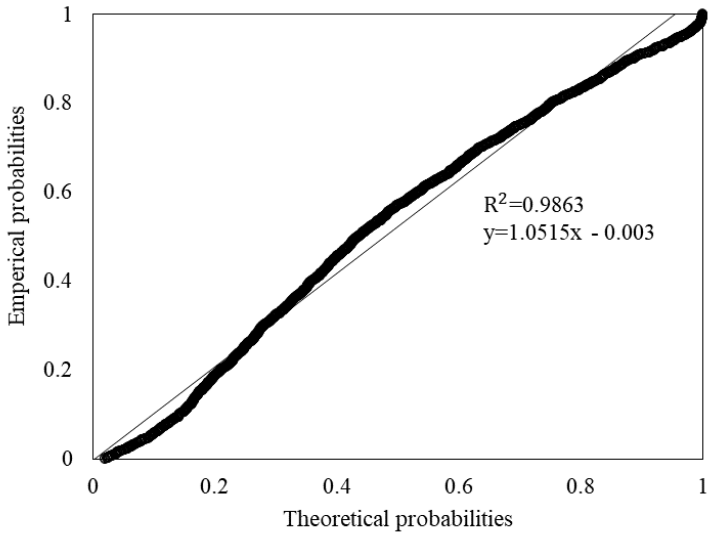


**Figure E-114: Sample 7 left rut normal probability plot for 50 m averaged section length**

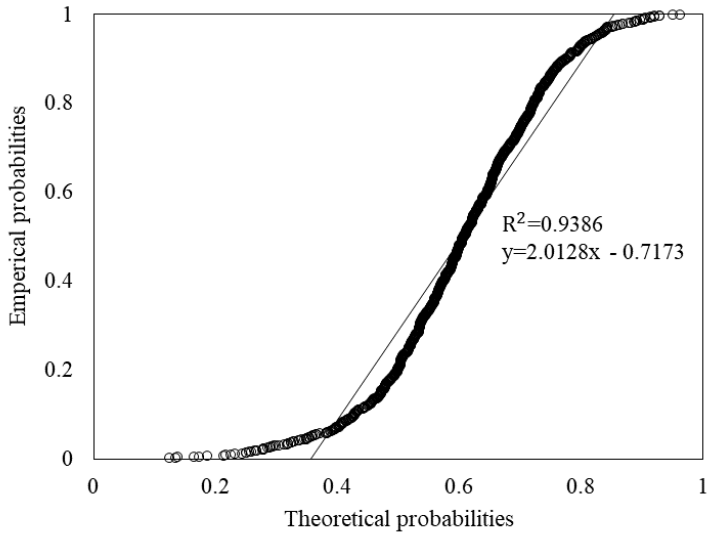


**Figure E-115: Sample 7 left rut exponential probability plot for 100 m averaged section length**

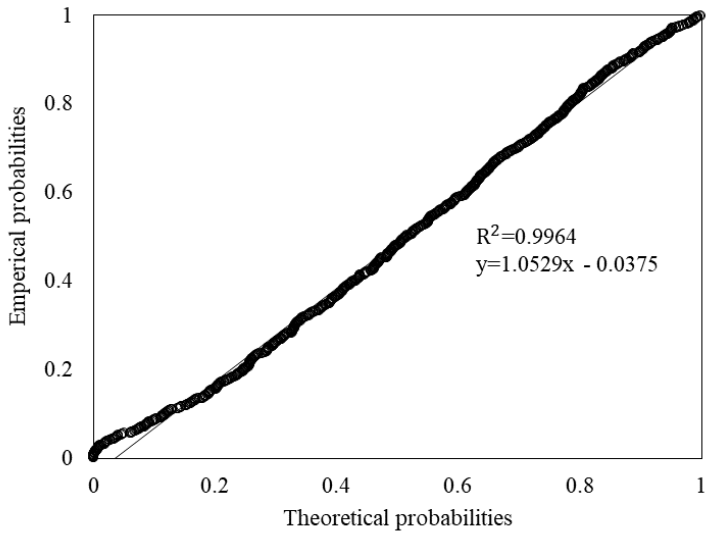


**Figure E-116: Sample 7 left rut lognormal probability plot for 100 m averaged section length**

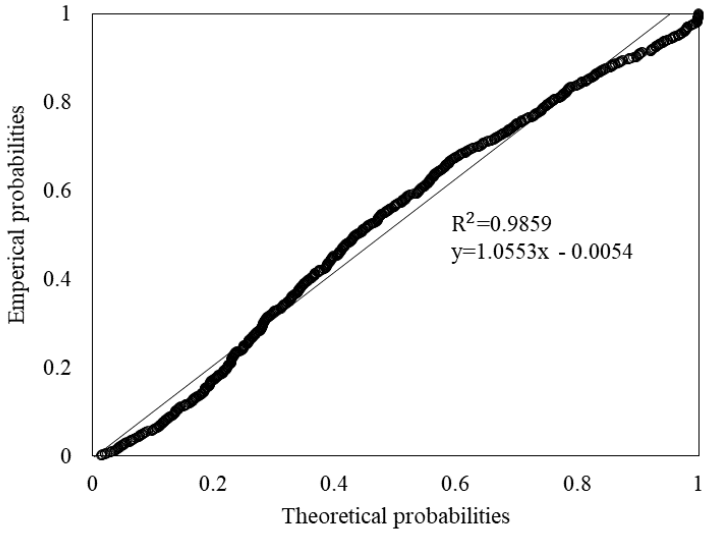


**Figure E-117: Sample 7 left rut normal probability plot for 100 m averaged section length**

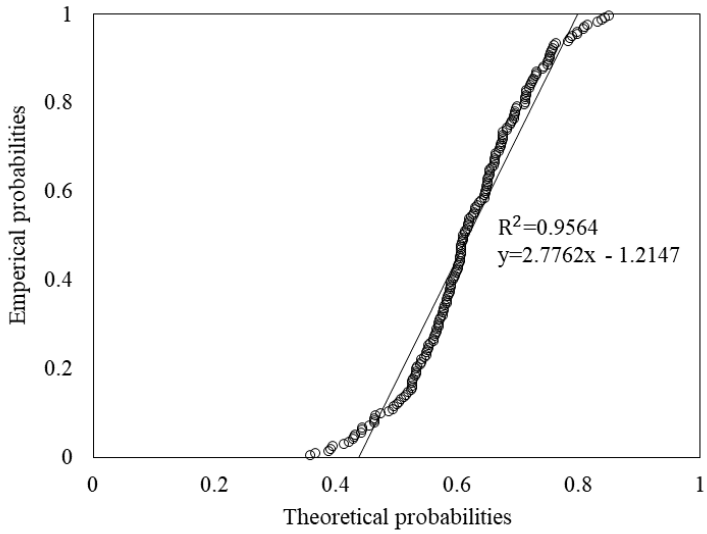


**Figure E-118: Sample 7 left rut exponential probability plot for 500 m averaged section length**

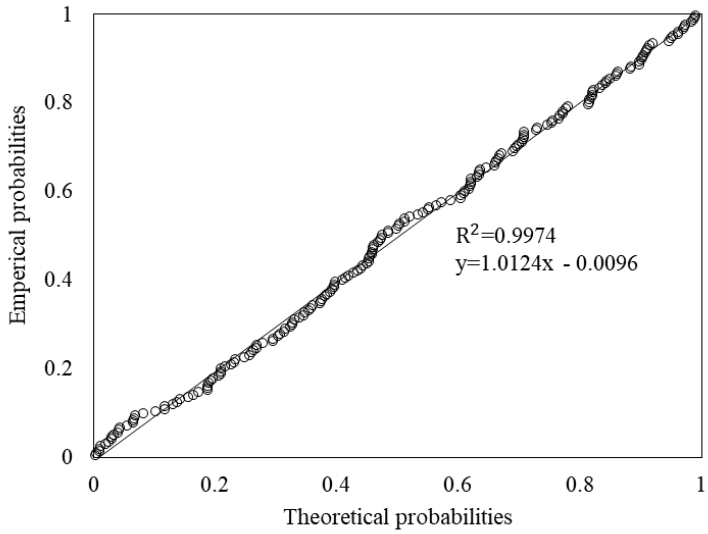


**Figure E-119: Sample 7 left rut lognormal probability plot for 500 m averaged section length**

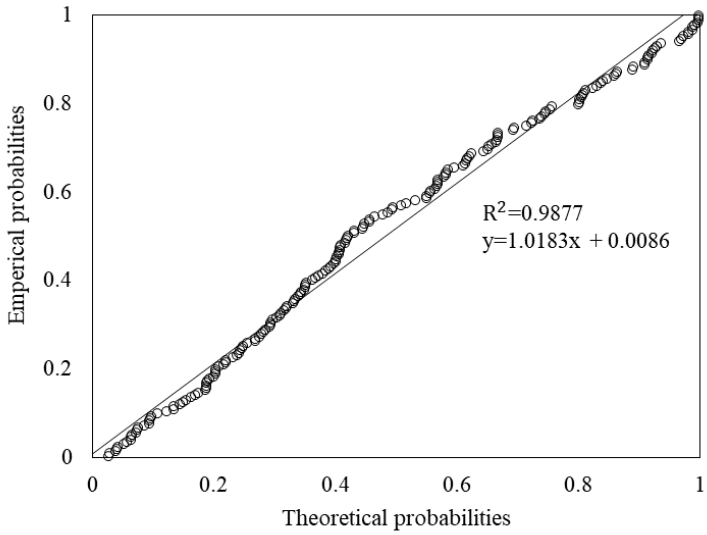


**Figure E-120: Sample 7 left rut normal probability plot for 500 m averaged section length**

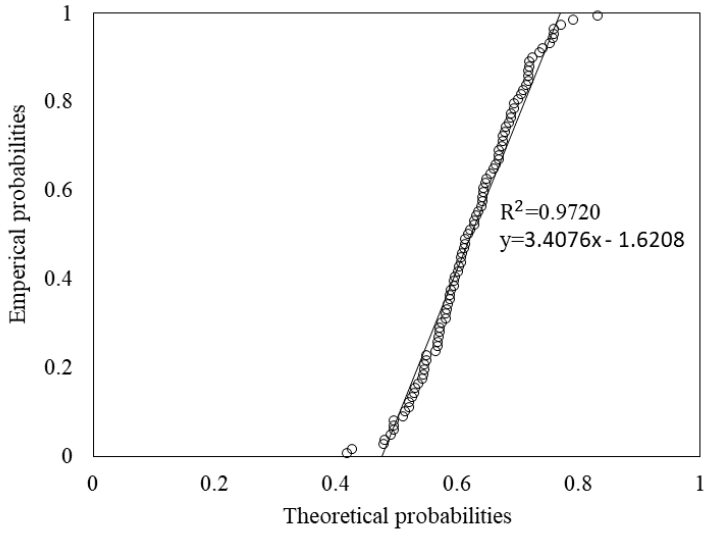


**Figure E-121: Sample 7 left rut exponential probability plot for 1 000 m averaged section length**

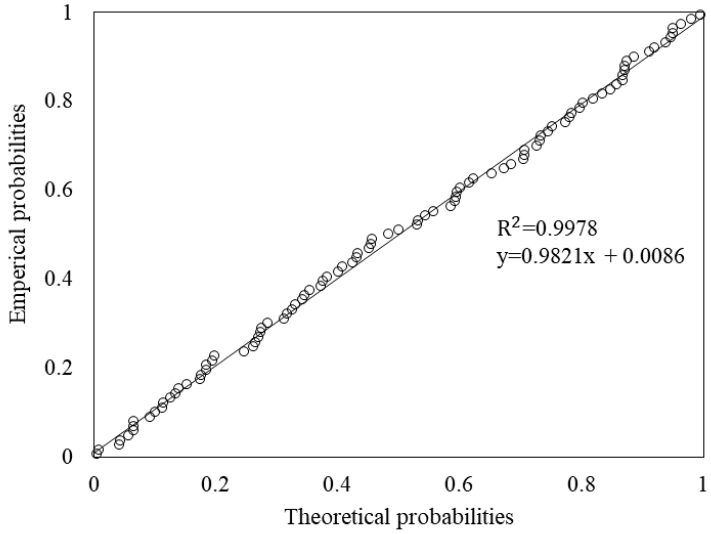


**Figure E-122: Sample 7 left rut lognormal probability plot for 1 000 m averaged section length**

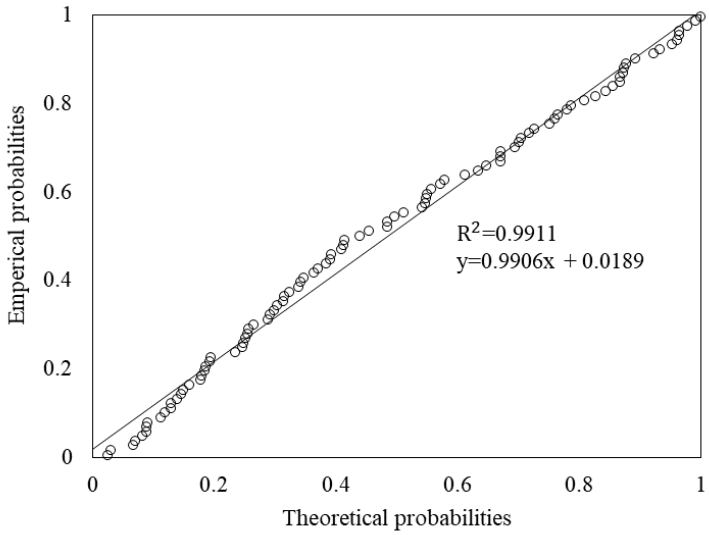


**Figure E-123: Sample 7 left rut normal probability plot for 1 000 m averaged section length**

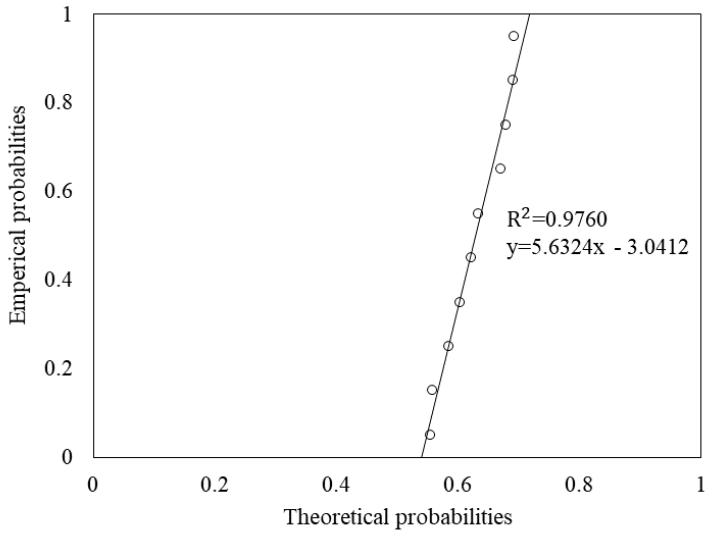


**Figure E-124: Sample 7 left rut exponential probability plot for 10 000 m averaged section length**

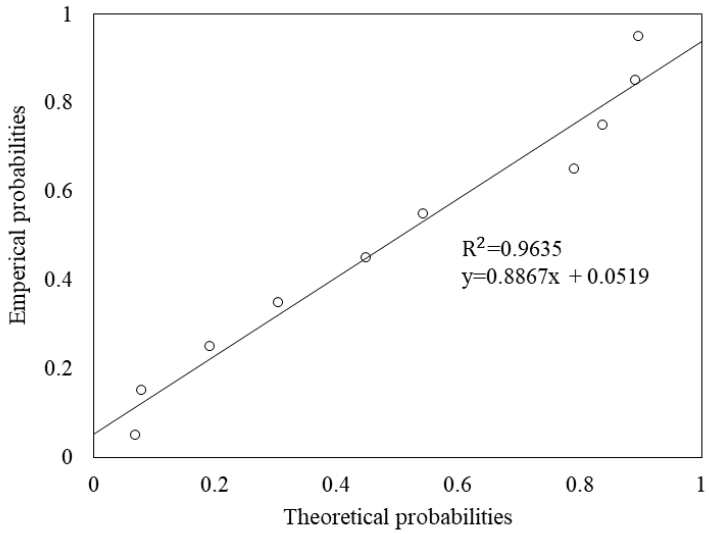


**Figure E-125: Sample 7 left rut lognormal probability plot for 10 000 m averaged section length**

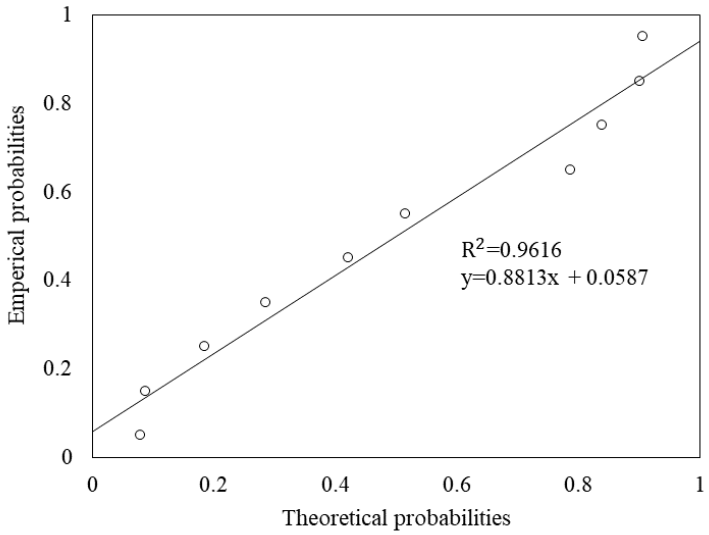


**Figure E-126: Sample 7 left rut normal probability plot for 10 000 m averaged section length**

Figure E-127 to Figure E-144 present the averaged section length exponential, lognormal, and normal probability plots for sample 8 left rut depth measurements.

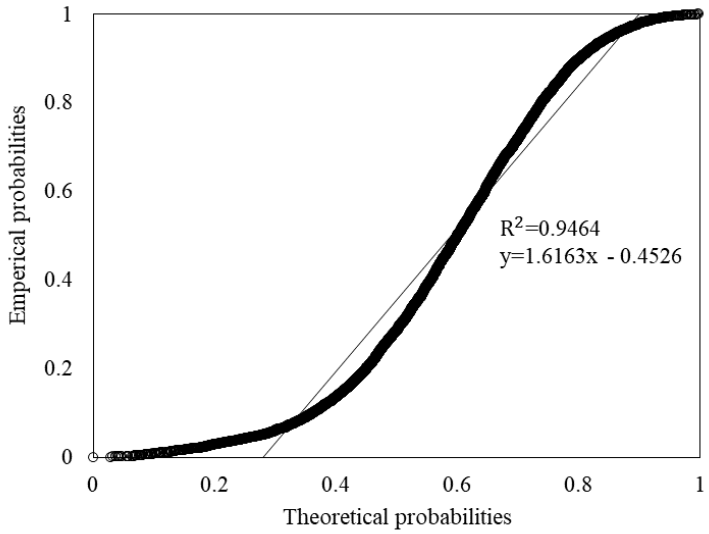


**Figure E-127: Sample 8 left rut exponential probability plot for 20 m averaged section length**

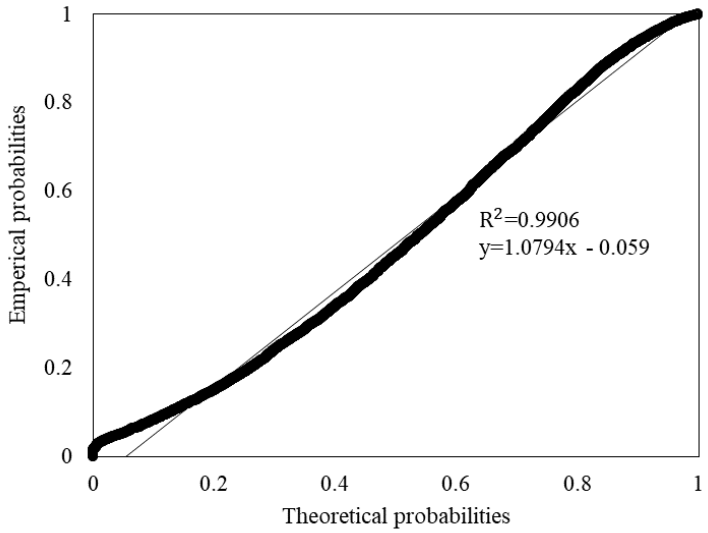


**Figure E-128: Sample 8 left rut lognormal probability plot for 20 m averaged section length**

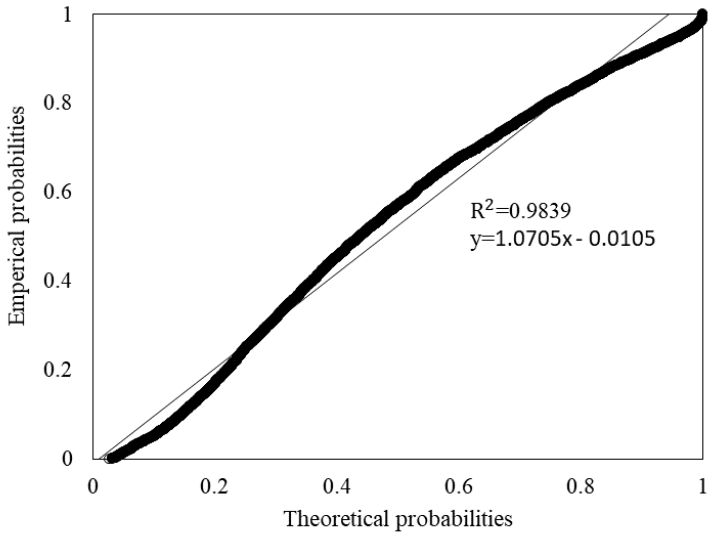


**Figure E-129: Sample 8 left rut normal probability plot for 20 m averaged section length**

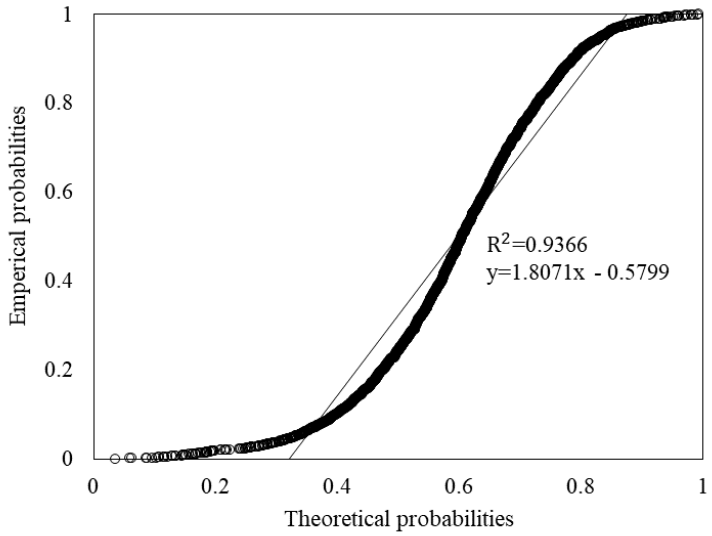


**Figure E-130: Sample 8 left rut exponential probability plot for 50 m averaged section length**

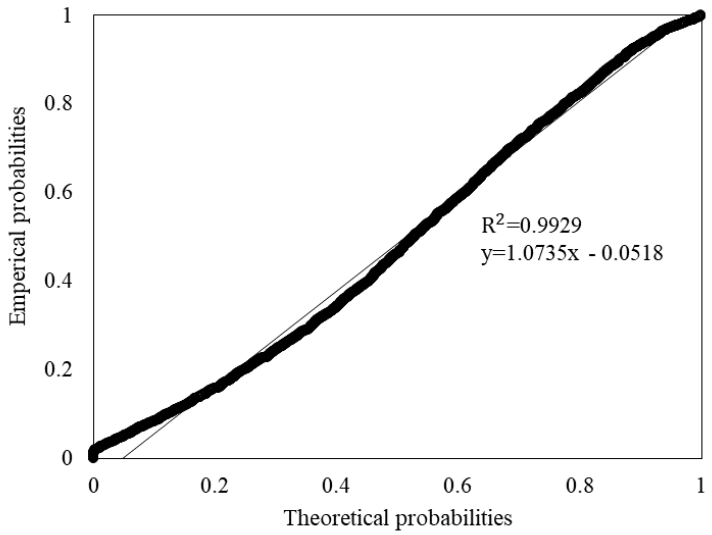


**Figure E-131: Sample 8 left rut lognormal probability plot for 50 m averaged section length**

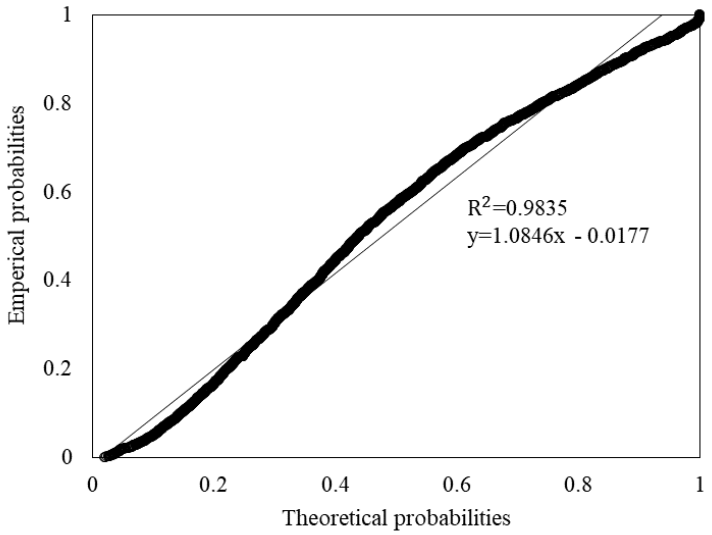


**Figure E-132: Sample 8 left rut normal probability plot for 50 m averaged section length**

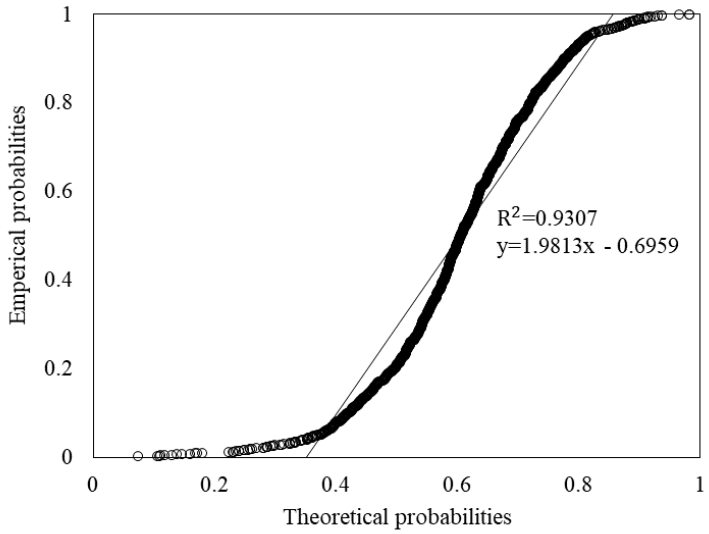


**Figure E-133: Sample 8 left rut exponential probability plot for 100 m averaged section length**

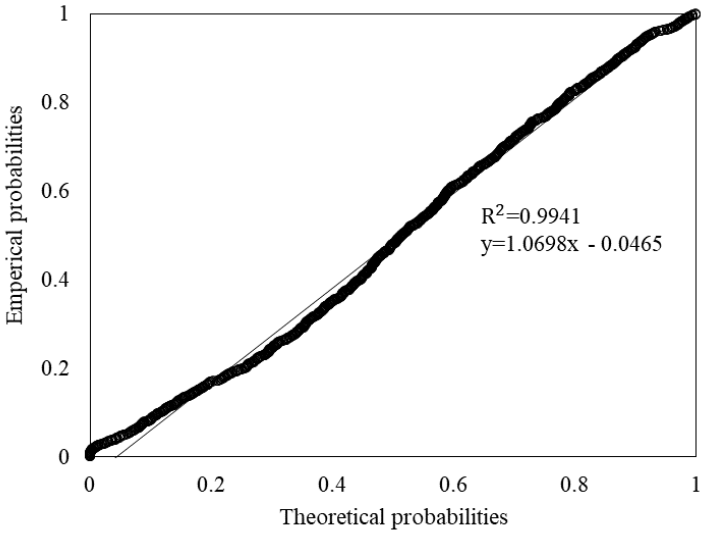


**Figure E-134: Sample 8 left rut lognormal probability plot for 100 m averaged section length**

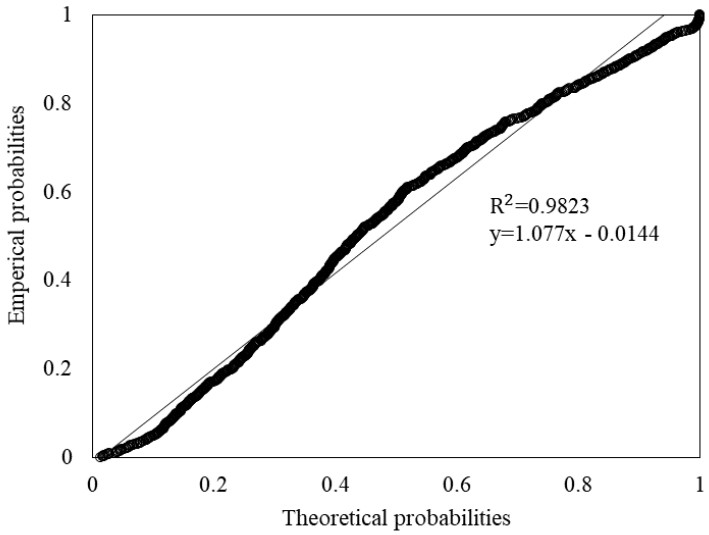


**Figure E-135: Sample 8 left rut normal probability plot for 100 m averaged section length**

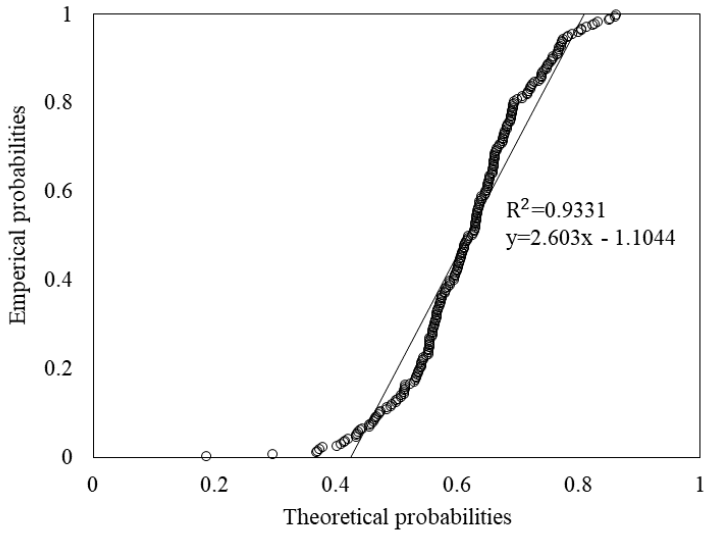


**Figure E-136: Sample 8 left rut exponential probability plot for 500 m averaged section length**

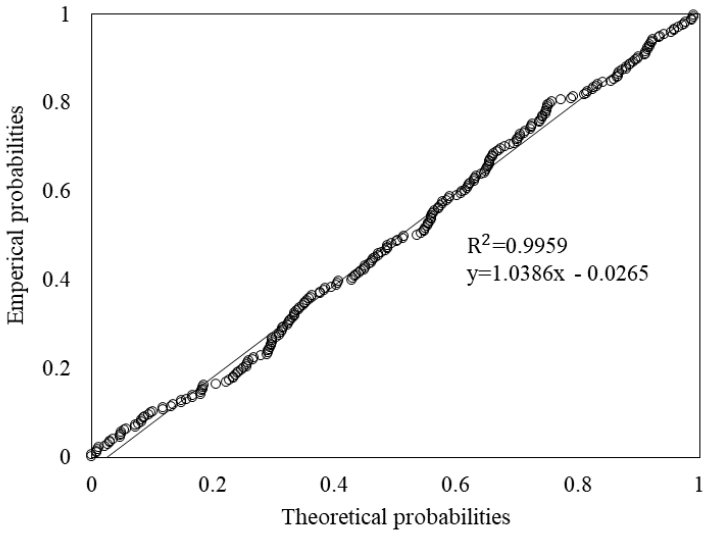


**Figure E-137: Sample 8 left rut lognormal probability plot for 500 m averaged section length**

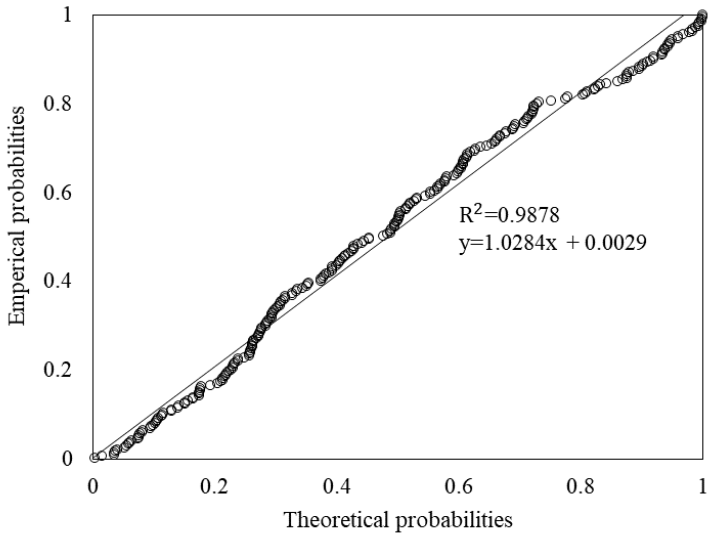


**Figure E-138: Sample 8 left rut normal probability plot for 500 m averaged section length**

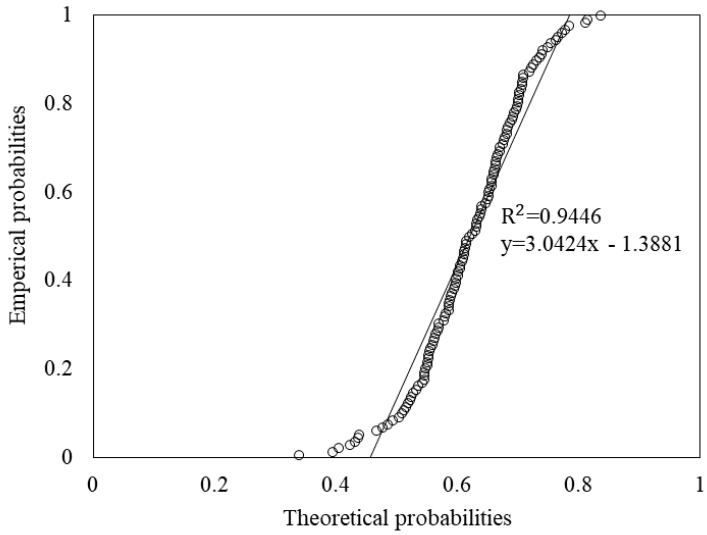


**Figure E-139: Sample 8 left rut exponential probability plot for 1 000 m averaged section length**

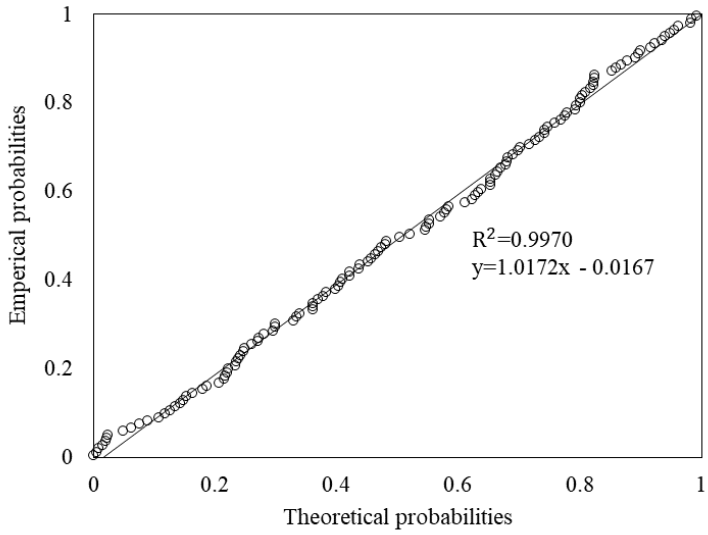


**Figure E-140: Sample 8 left rut lognormal probability plot for 1 000 m averaged section length**

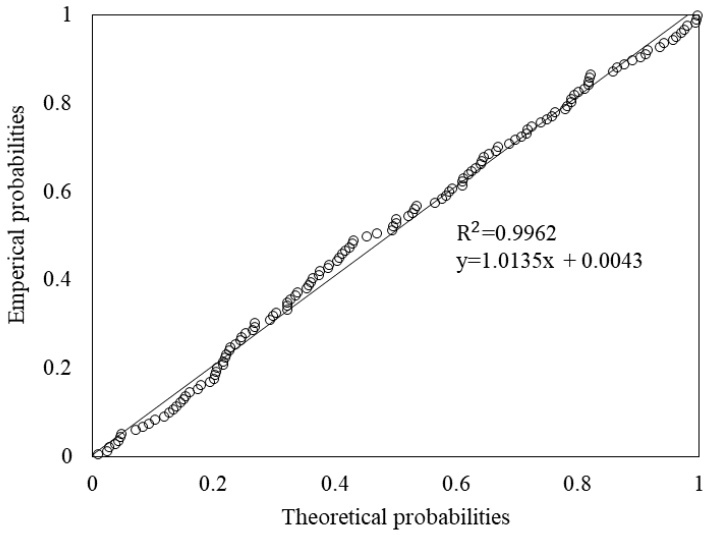


**Figure E-141: Sample 8 left rut normal probability plot for 1 000 m averaged section length**

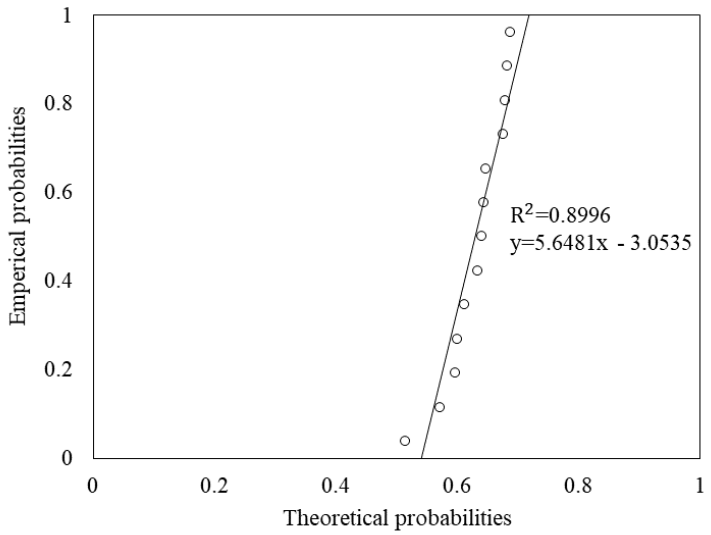


**Figure E-142: Sample 8 left rut exponential probability plot for 10 000 m averaged section length**

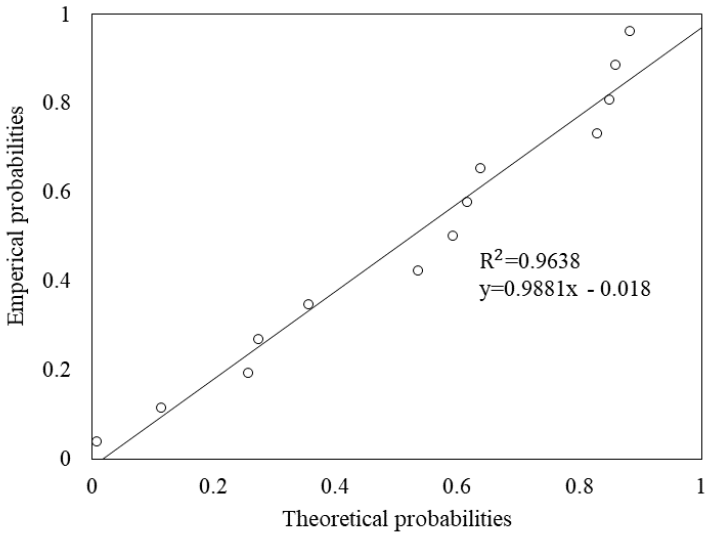


**Figure E-143: Sample 8 left rut lognormal probability plot for 10 000 m averaged section length**

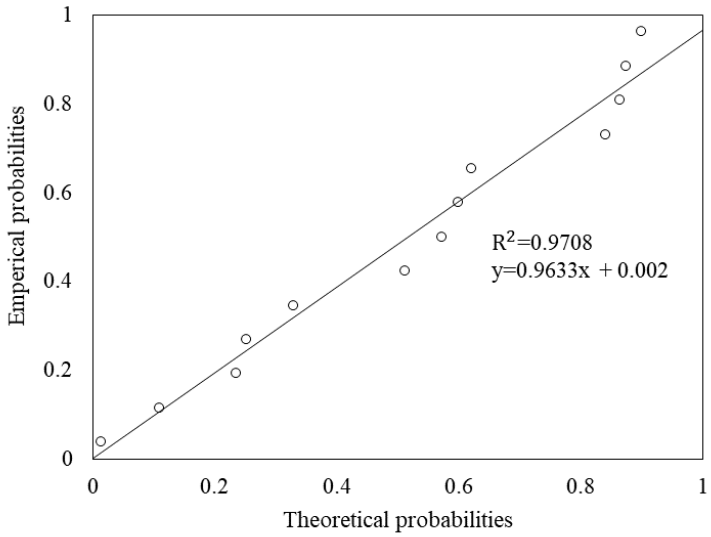


**Figure E-144: Sample 8 left rut normal probability plot for 10 000 m averaged section length**

Figure E-145 to Figure E-162 present the averaged section length exponential, lognormal, and normal probability plots for sample 9 left rut depth measurements.

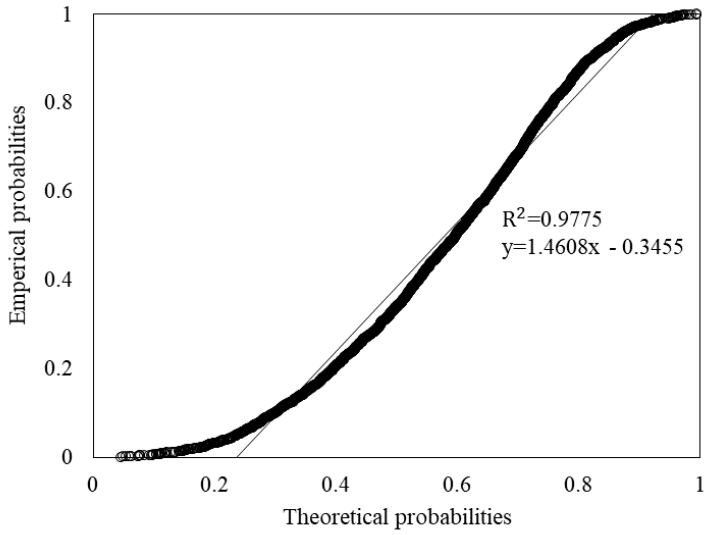


**Figure E-145: Sample 9 left rut exponential probability plot for 20 m averaged section length**

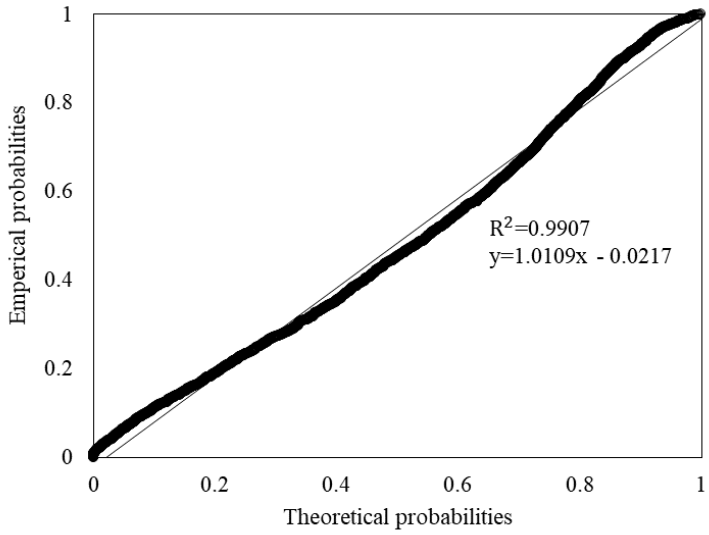


**Figure E-146: Sample 9 left rut lognormal probability plot for 20 m averaged section length**

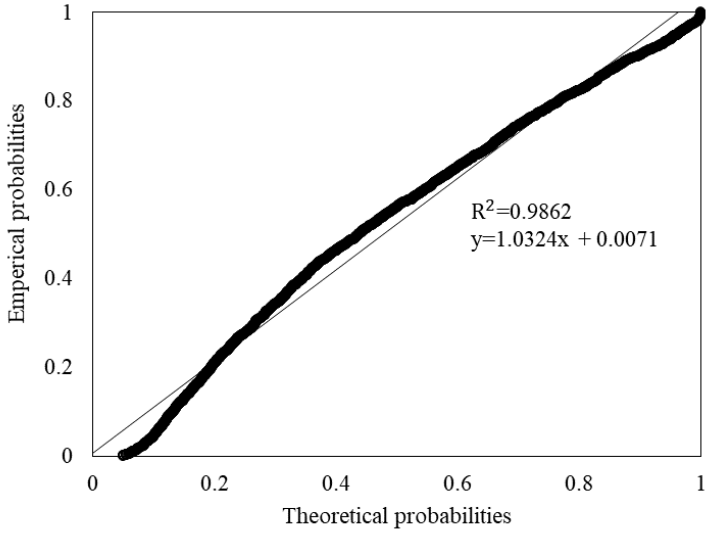


**Figure E-147: Sample 9 left rut normal probability plot for 20 m averaged section length**

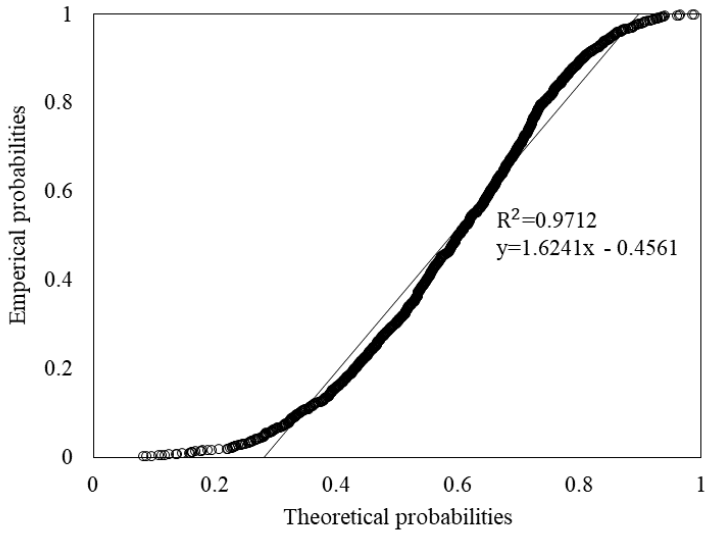


**Figure E-148: Sample 9 left rut exponential probability plot for 50 m averaged section length**

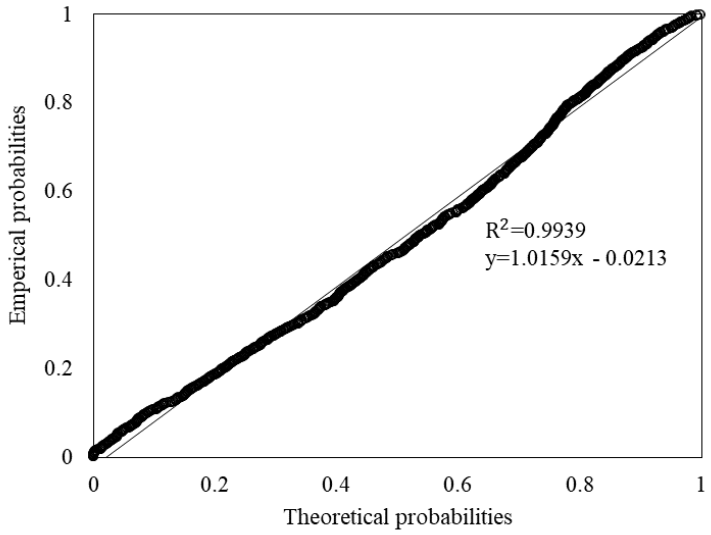


**Figure E-149: Sample 9 left rut lognormal probability plot for 50 m averaged section length**

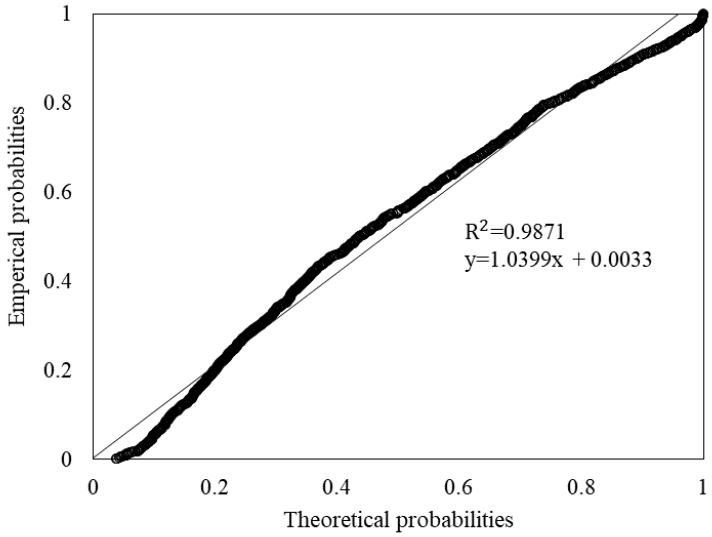


**Figure E-150: Sample 9 left rut normal probability plot for 50 m averaged section length**

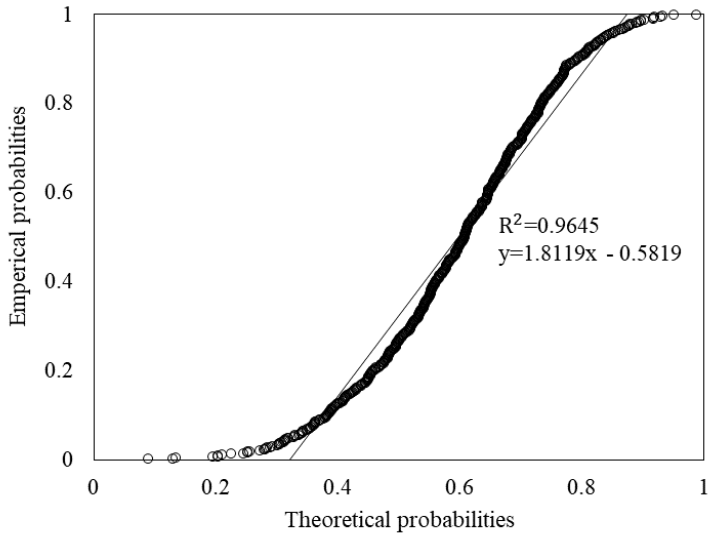


**Figure E-151: Sample 9 left rut exponential probability plot for 100 m averaged section length**

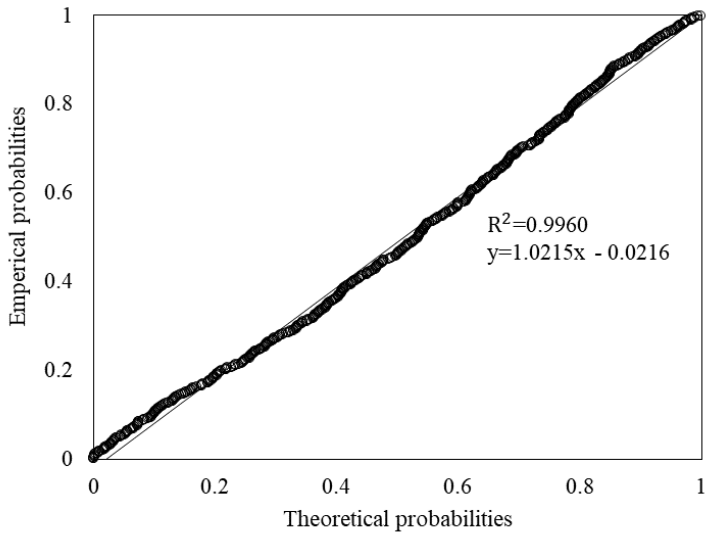


**Figure E-152: Sample 9 left rut lognormal probability plot for 100 m averaged section length**

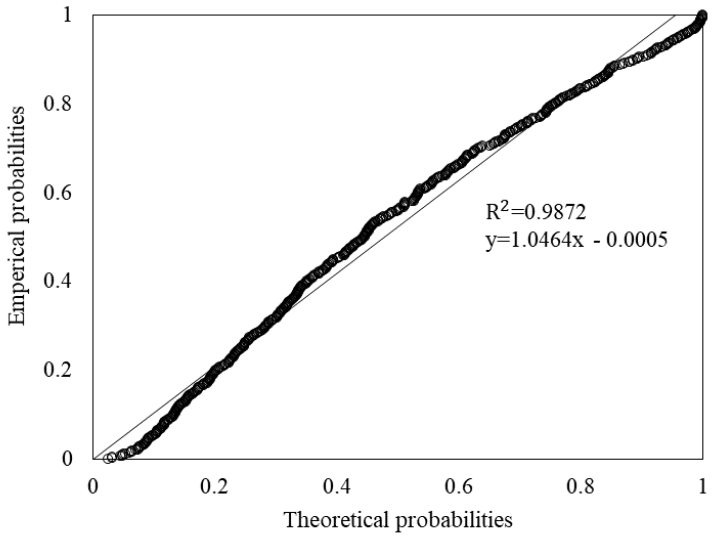


**Figure E-153: Sample 9 left rut normal probability plot for 100 m averaged section length**

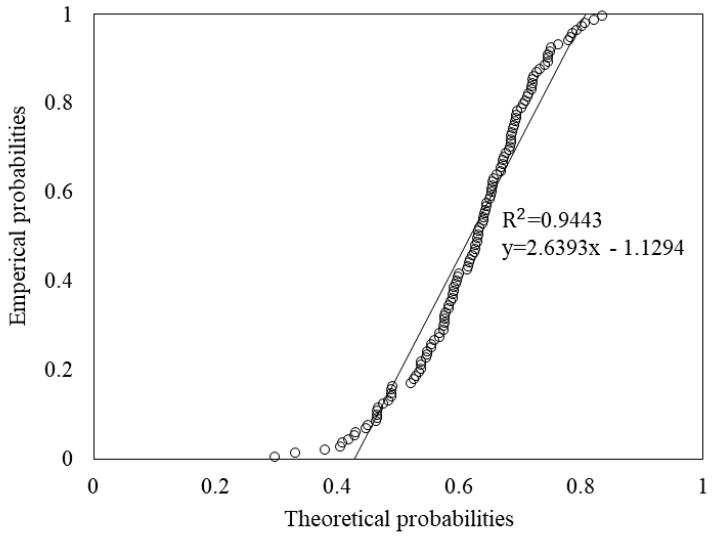


**Figure E-154: Sample 9 left rut exponential probability plot for 500 m averaged section length**

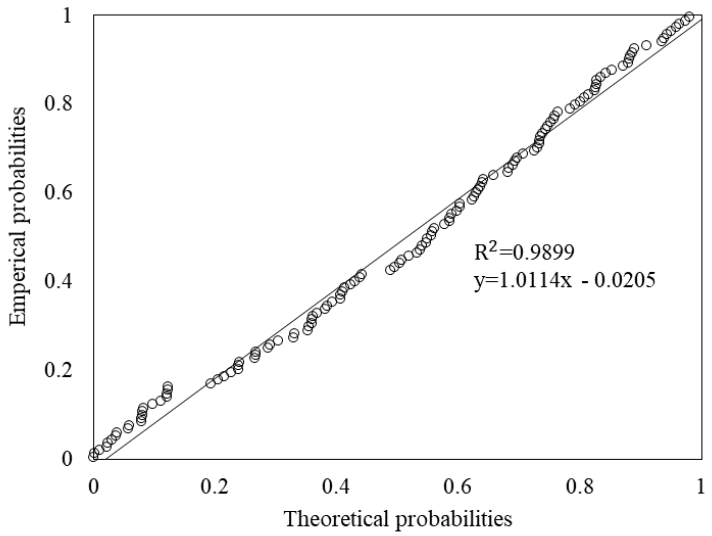


**Figure E-155: Sample 9 left rut lognormal probability plot for 500 m averaged section length**

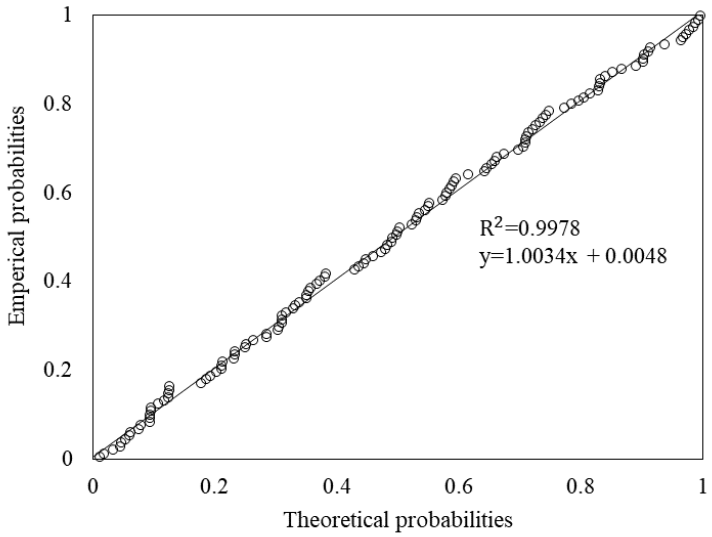


**Figure E-156: Sample 9 left rut normal probability plot for 500 m averaged section length**

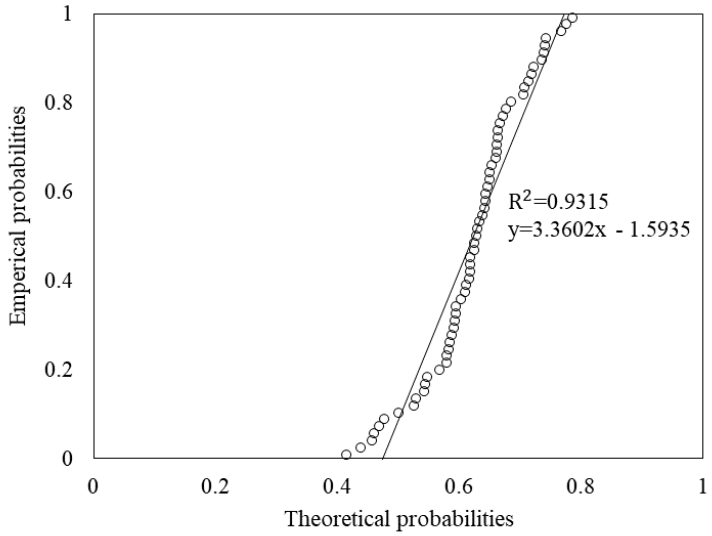


**Figure E-157: Sample 9 left rut exponential probability plot for 1 000 m averaged section length**

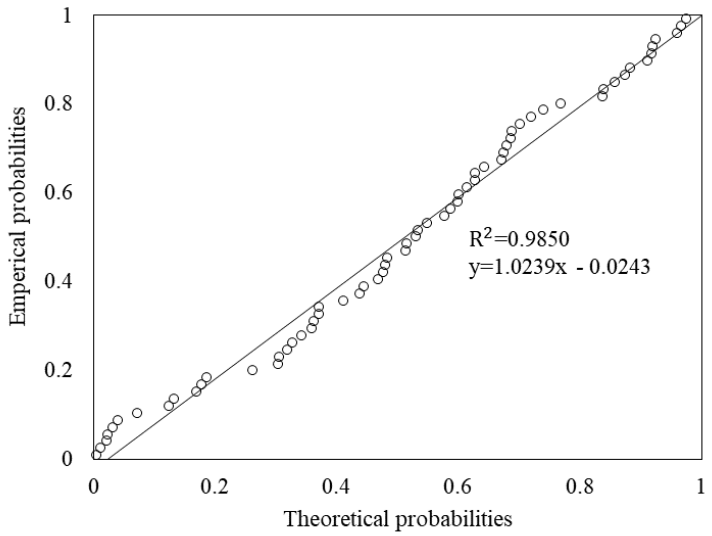


**Figure E-158: Sample 9 left rut lognormal probability plot for 1 000 m averaged section length**

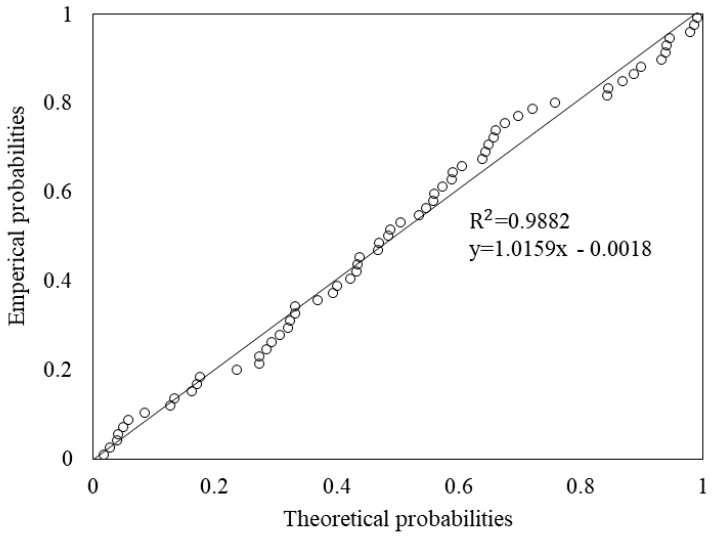


**Figure E-159: Sample 9 left rut normal probability plot for 1 000 m averaged section length**

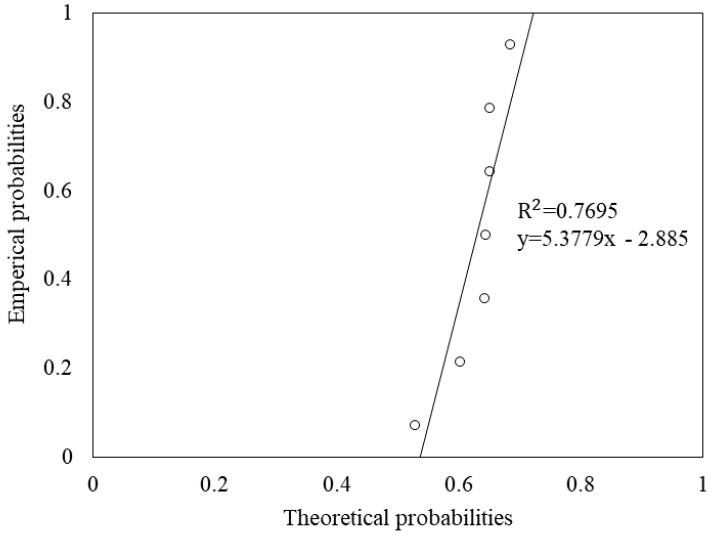


**Figure E-160: Sample 9 left rut exponential probability plot for 10 000 m averaged section length**

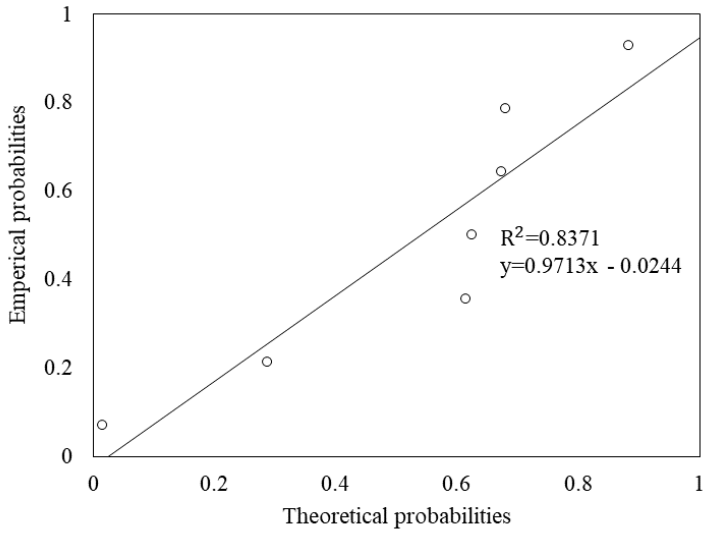


**Figure E-161: Sample 9 left rut lognormal probability plot for 10 000 m averaged section length**

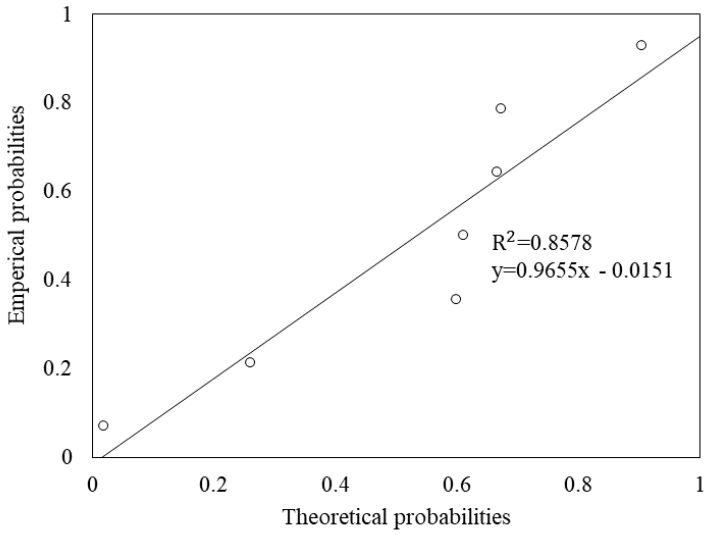


**Figure E-162: Sample 9 left rut normal probability plot for 10 000 m averaged section length**

Figure E-163 to Figure E-180 present the averaged section length exponential, lognormal, and normal probability plots for sample 10 left rut depth measurements.

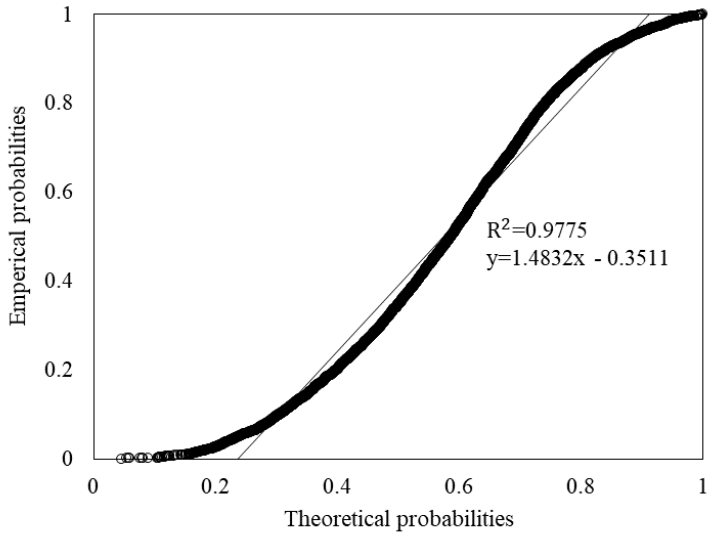


**Figure E-163: Sample 10 left rut exponential probability plot for 20 m averaged section length**

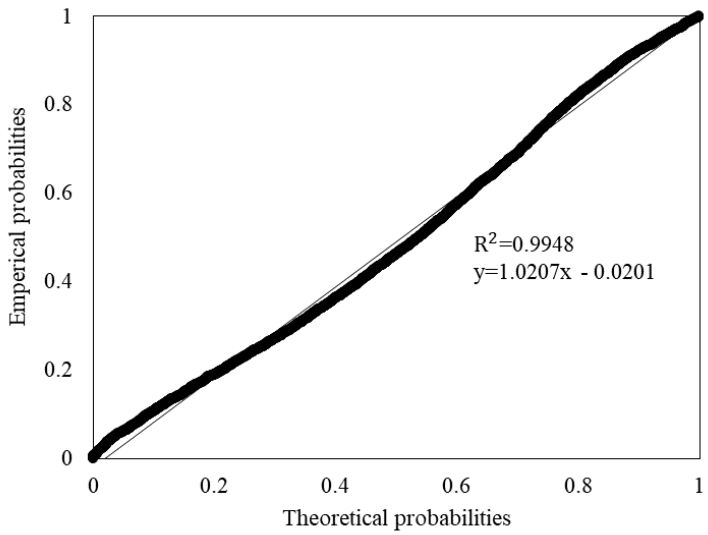


**Figure E-164: Sample 10 left rut lognormal probability plot for 20 m averaged section length**

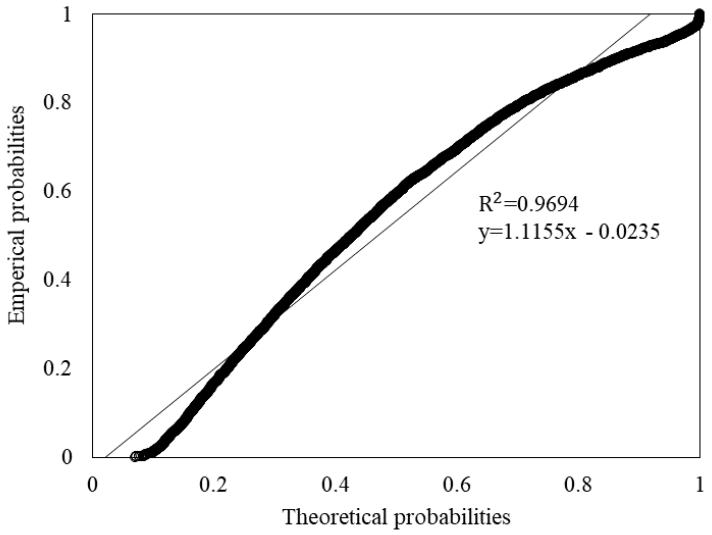


**Figure E-165: Sample 10 left rut normal probability plot for 20 m averaged section length**

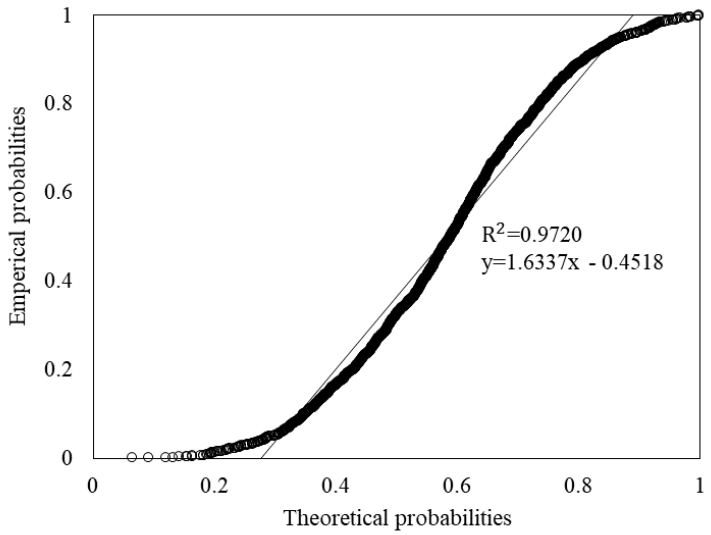


**Figure E-166: Sample 10 left rut exponential probability plot for 50 m averaged section length**

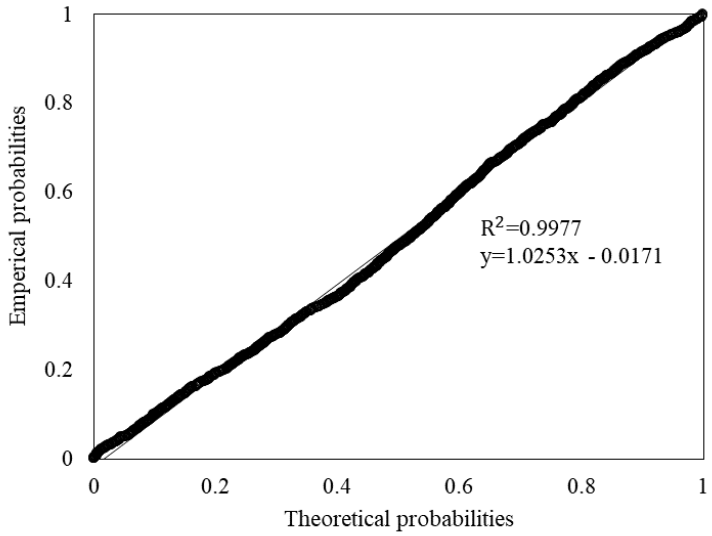


**Figure E-167: Sample 10 left rut lognormal probability plot for 50 m averaged section length**

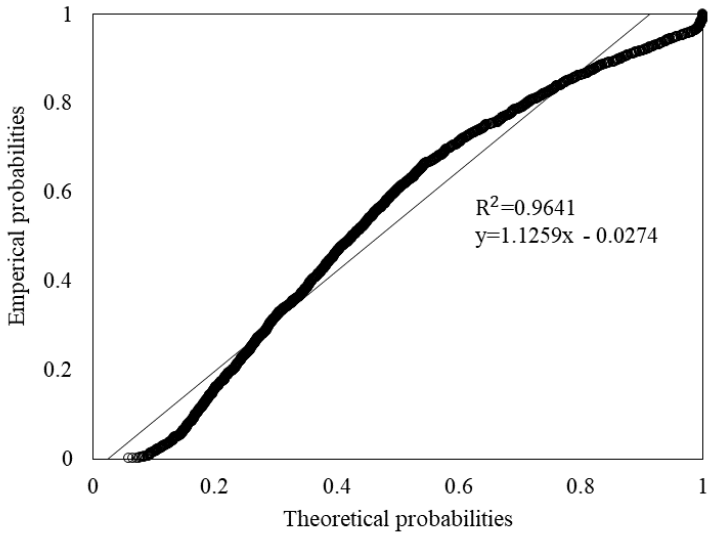


**Figure E-168: Sample 10 left rut normal probability plot for 50 m averaged section length**

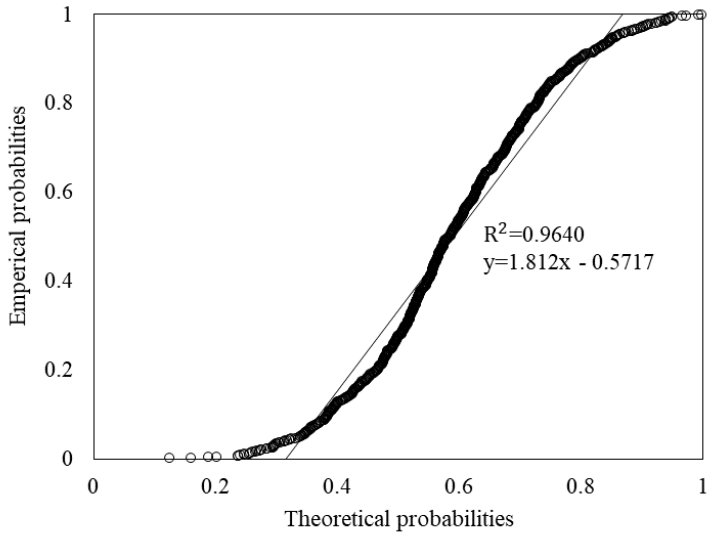


**Figure E-169: Sample 10 left rut exponential probability plot for 100 m averaged section length**

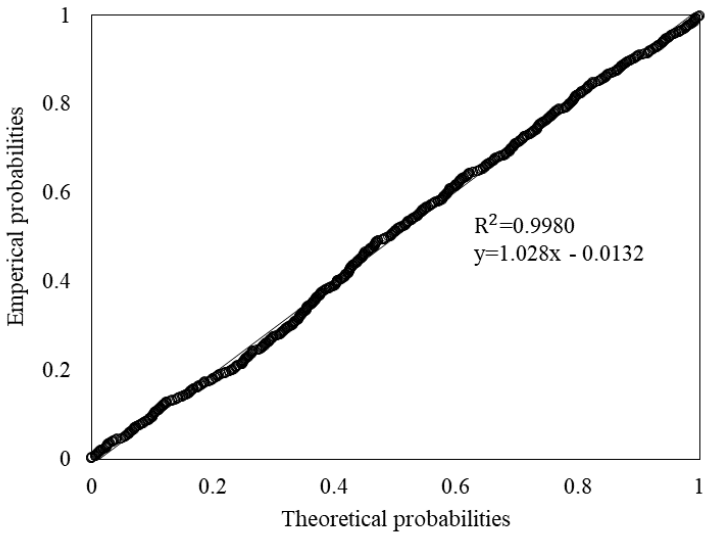


**Figure E-170: Sample 10 left rut lognormal probability plot for 100 m averaged section length**

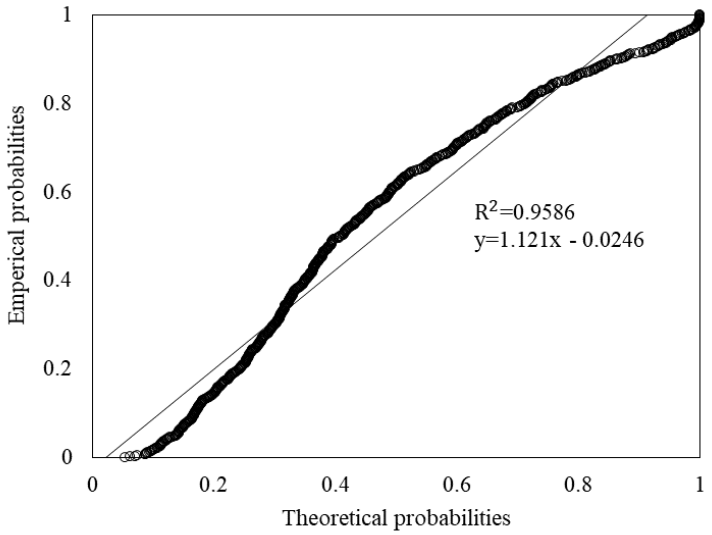


**Figure E-171: Sample 10 left rut normal probability plot for 100 m averaged section length**

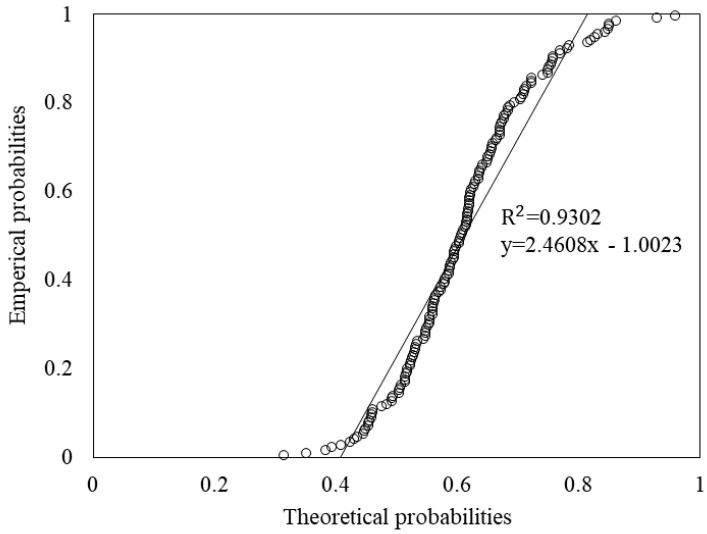


**Figure E-172: Sample 10 left rut exponential probability plot for 500 m averaged section length**

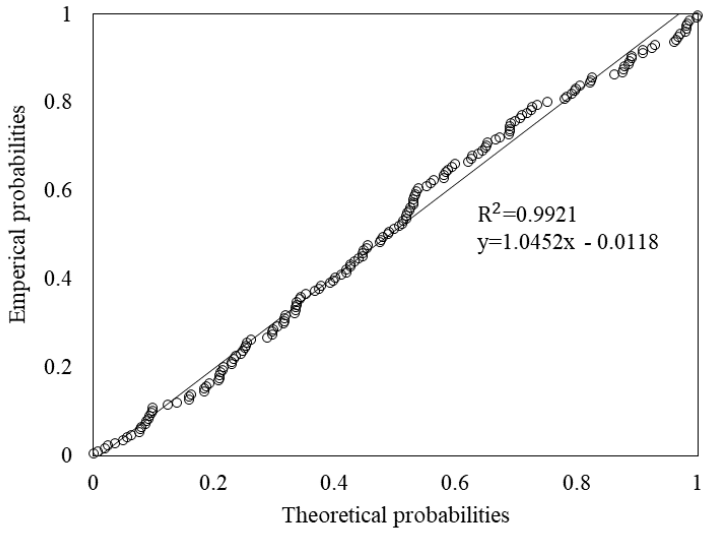


**Figure E-173: Sample 10 left rut lognormal probability plot for 500 m averaged section length**

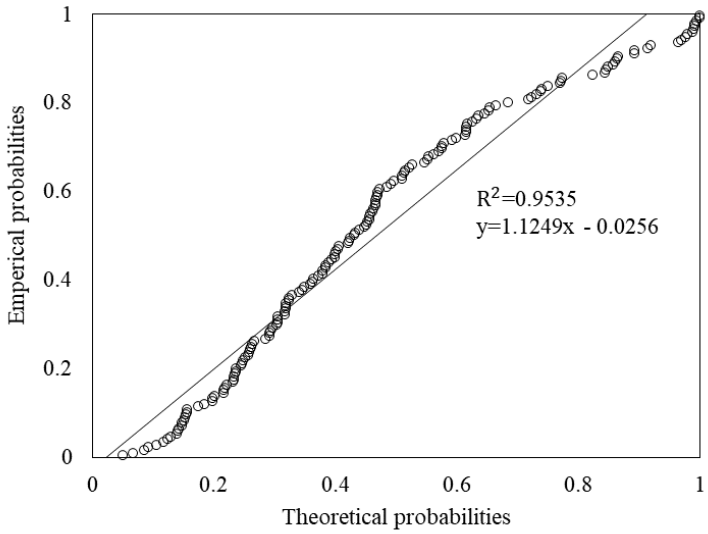


**Figure E-174: Sample 10 left rut normal probability plot for 500 m averaged section length**

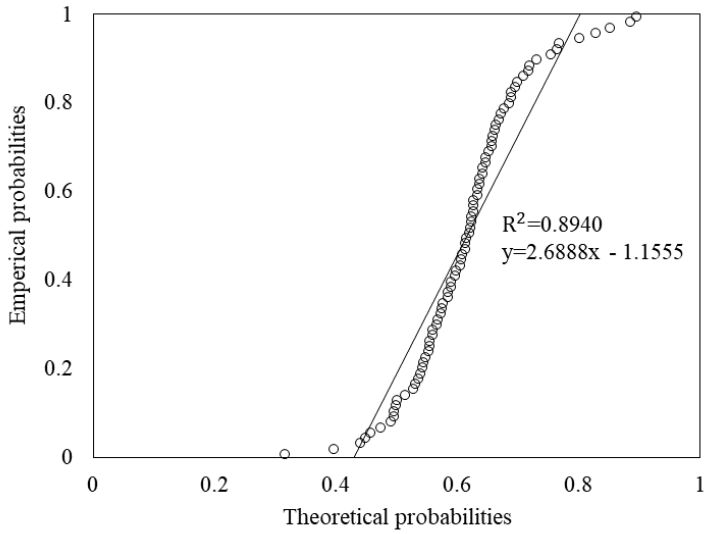


**Figure E-175: Sample 10 left rut exponential probability plot for 1 000 m averaged section length**

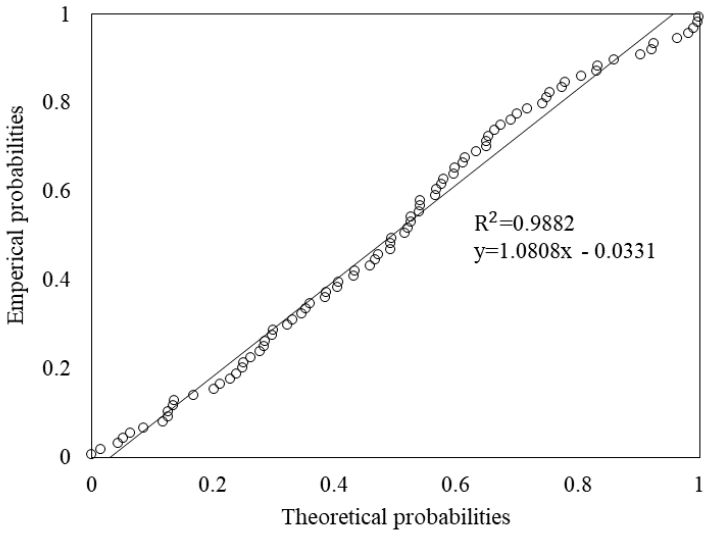


**Figure E-176: Sample 10 left rut lognormal probability plot for 1 000 m averaged section length**

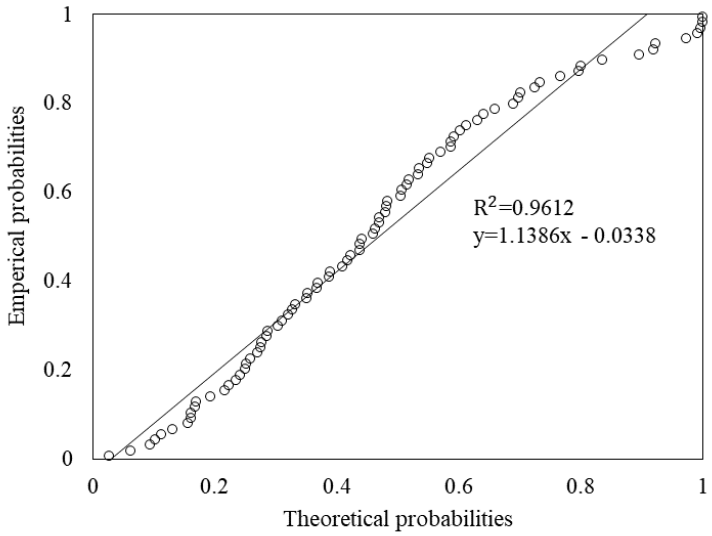


**Figure E-177: Sample 10 left rut normal probability plot for 1 000 m averaged section length**

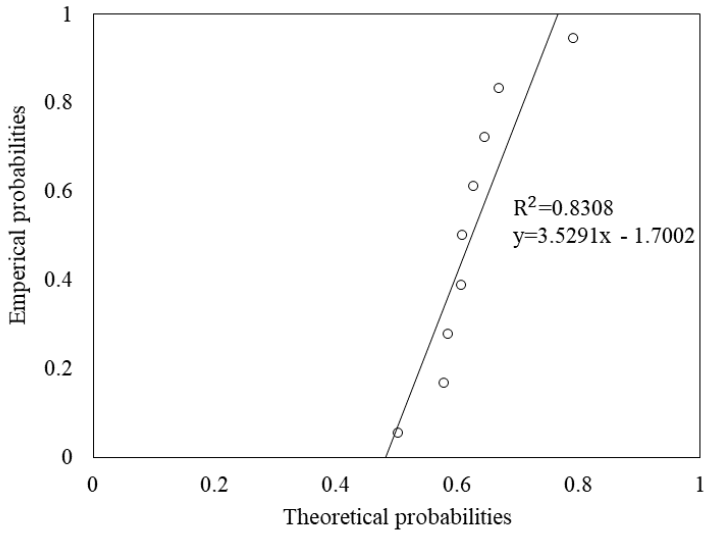


**Figure E-178: Sample 10 left rut exponential probability plot for 10 000 m averaged section length**

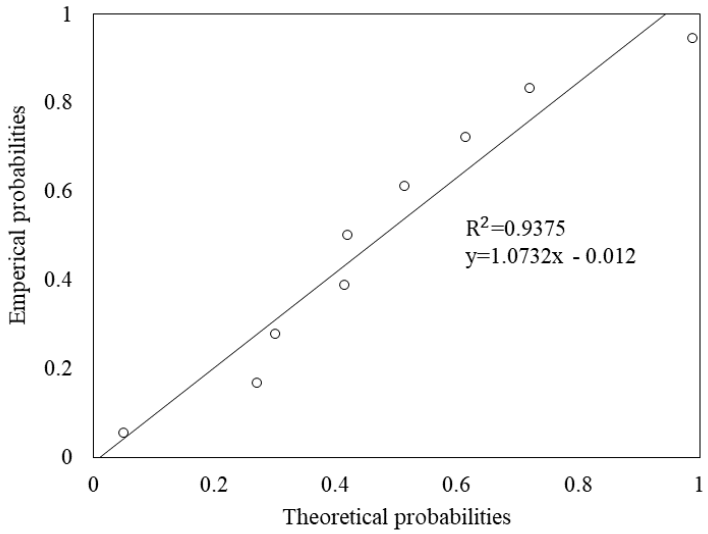


**Figure E-179: Sample 10 left rut lognormal probability plot for 10 000 m averaged section length**

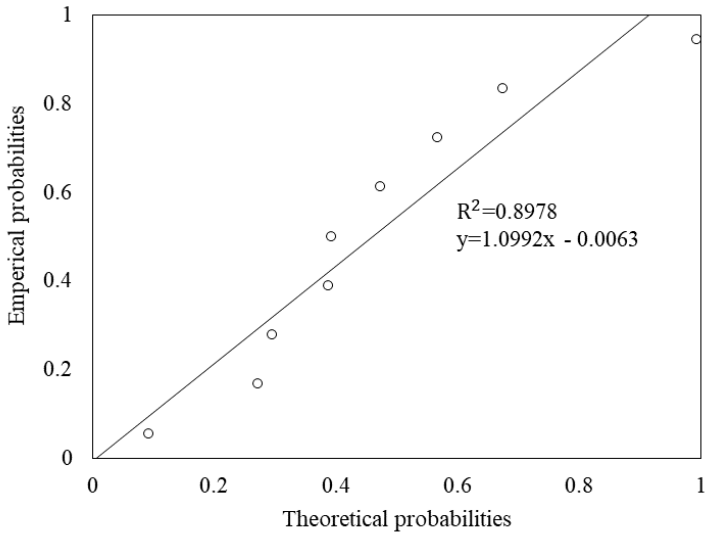


**Figure E-180: Sample 10 left rut normal probability plot for 10 000 m averaged section length**

Figure E-181 to Figure E-198 present the averaged section length exponential, lognormal, and normal probability plots for sample 11 left rut depth measurements.

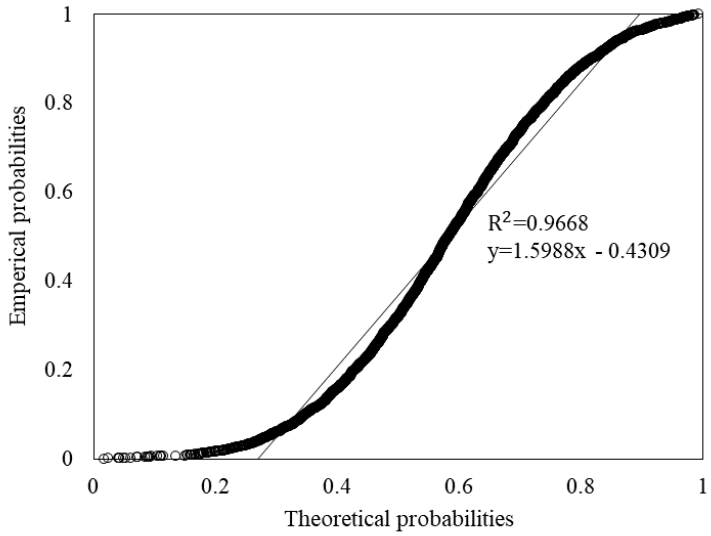


**Figure E-181: Sample 11 left rut exponential probability plot for 20 m averaged section length**

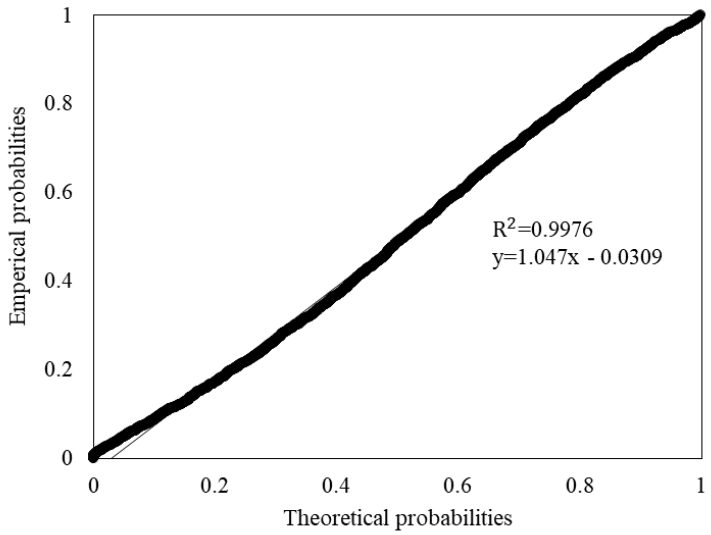


**Figure E-182: Sample 11 left rut lognormal probability plot for 20 m averaged section length**

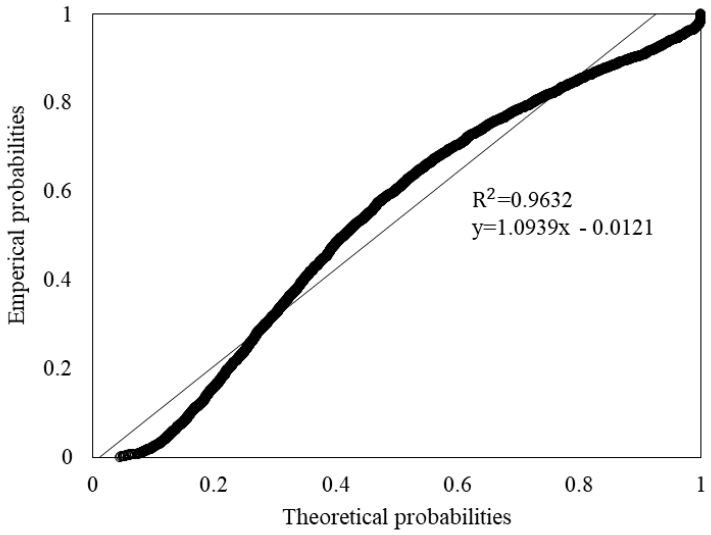


**Figure E-183: Sample 11 left rut normal probability plot for 20 m averaged section length**

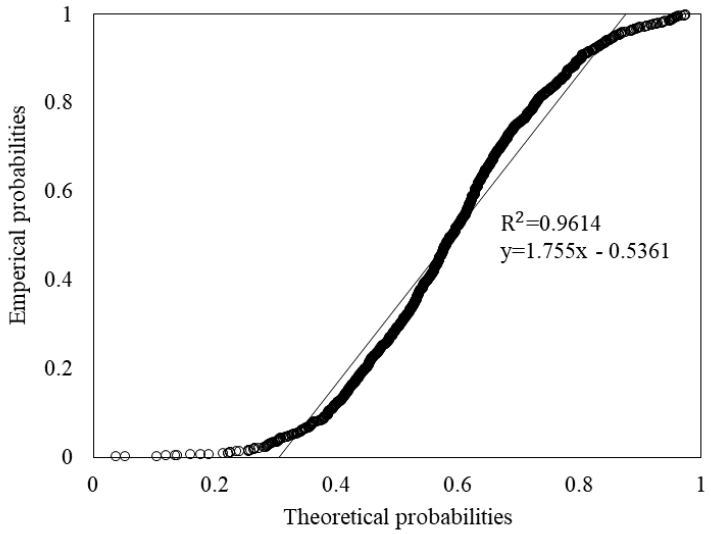


**Figure E-184: Sample 11 left rut exponential probability plot for 50 m averaged section length**

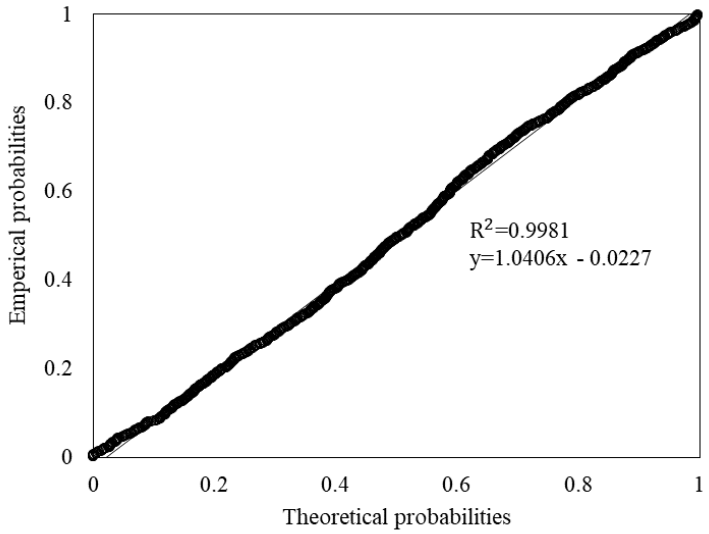


**Figure E-185: Sample 11 left rut lognormal probability plot for 50 m averaged section length**

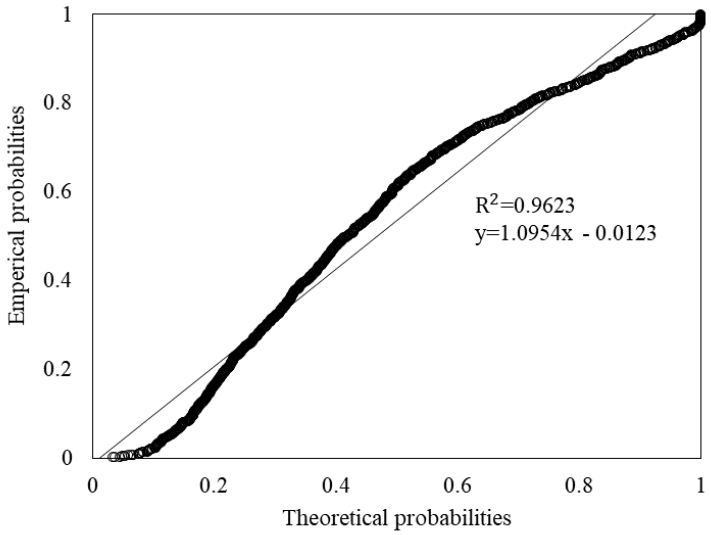


**Figure E-186: Sample 11 left rut normal probability plot for 50 m averaged section length**

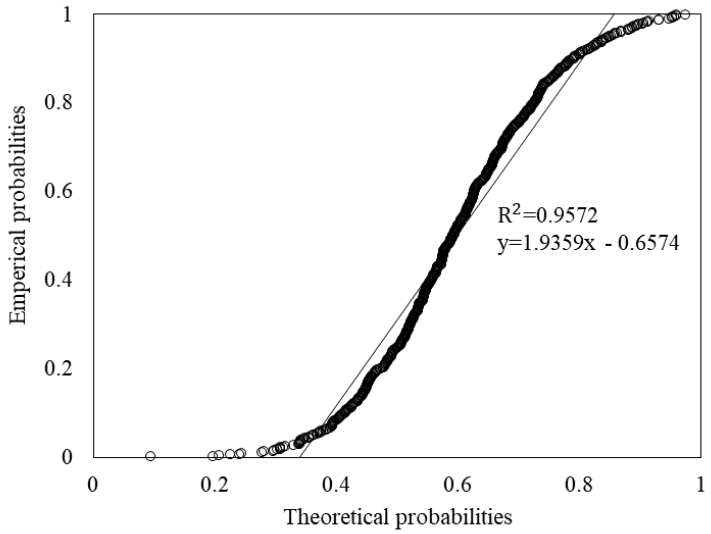


**Figure E-187: Sample 11 left rut exponential probability plot for 100 m averaged section length**

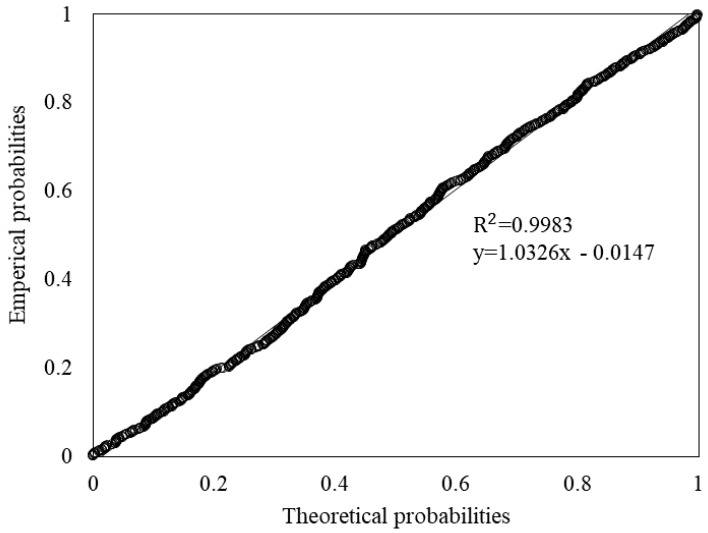


**Figure E-188: Sample 11 left rut lognormal probability plot for 100 m averaged section length**

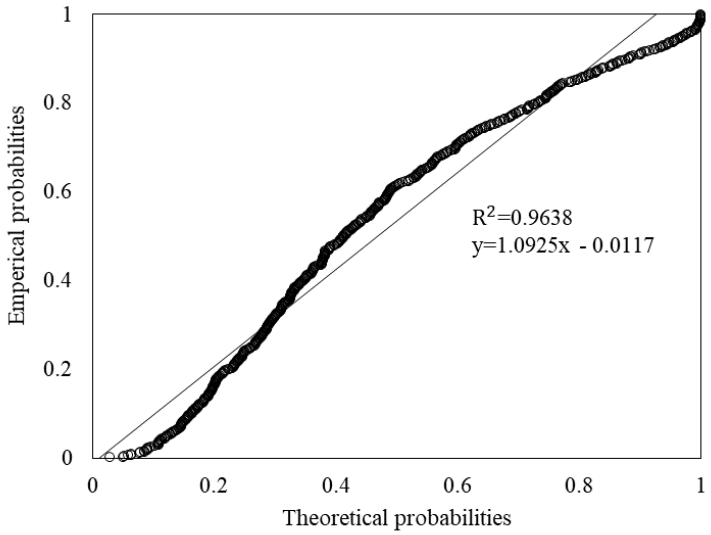


**Figure E-189: Sample 11 left rut normal probability plot for 100 m averaged section length**

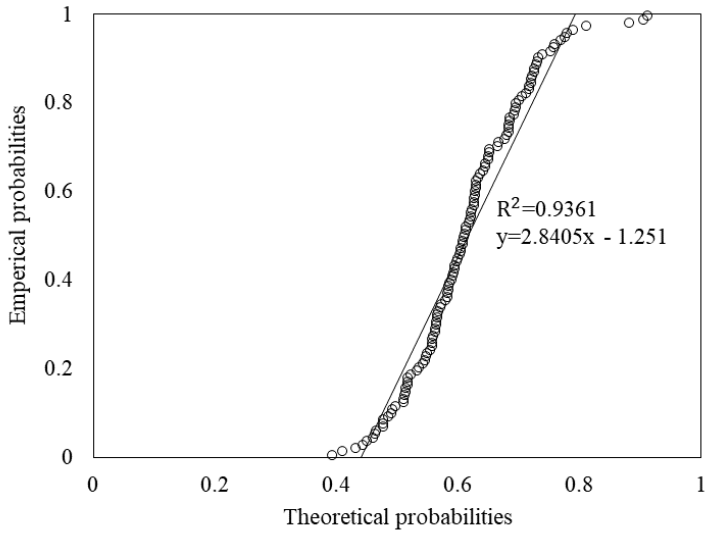


**Figure E-190: Sample 11 left rut exponential probability plot for 500 m averaged section length**

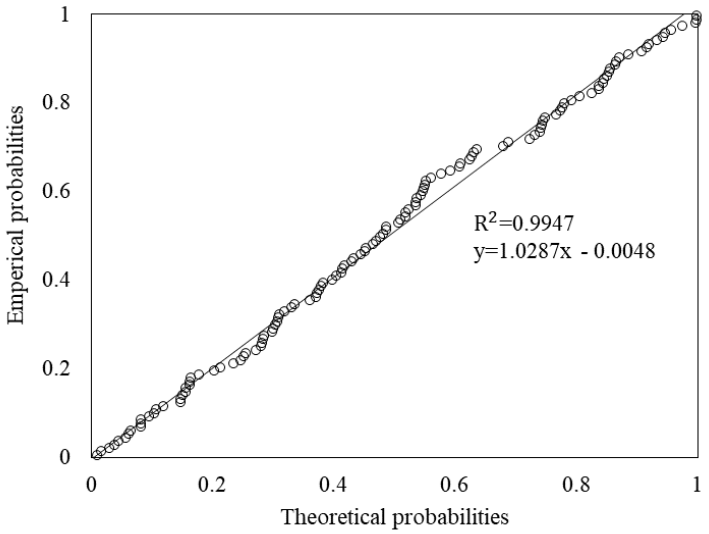


**Figure E-191: Sample 11 left rut lognormal probability plot for 500 m averaged section length**

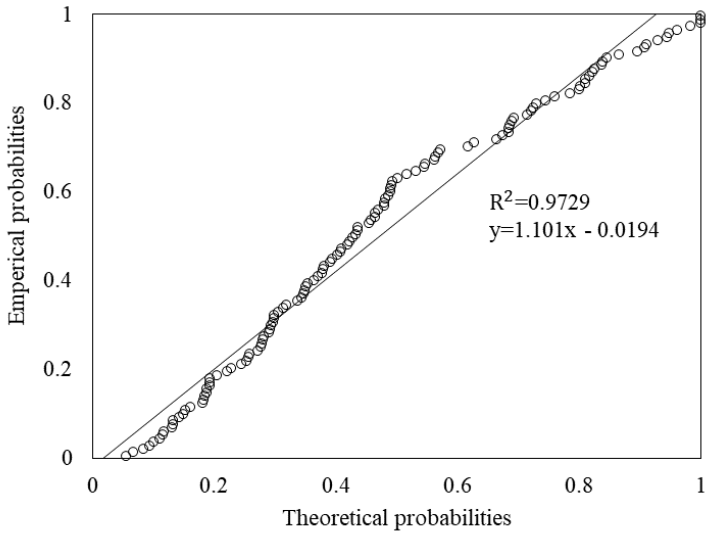


**Figure E-192: Sample 11 left rut normal probability plot for 500 m averaged section length**

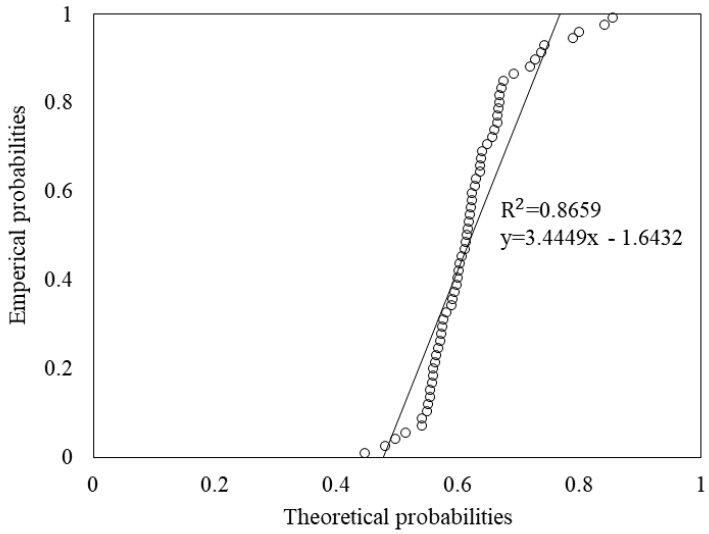


**Figure E-193: Sample 11 left rut exponential probability plot for 1 000 m averaged section length**

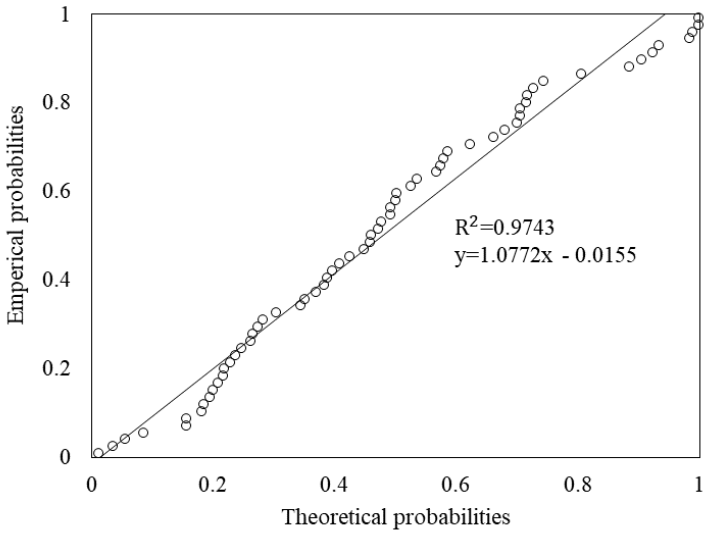


**Figure E-194: Sample 11 left rut lognormal probability plot for 1 000 m averaged section length**

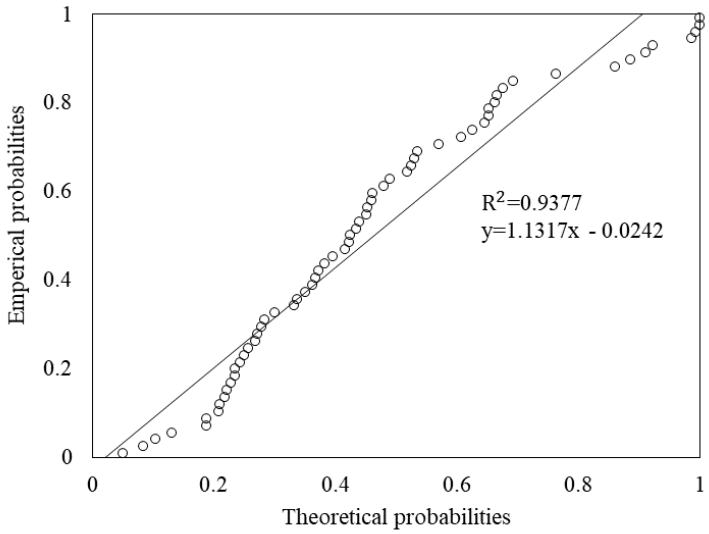


**Figure E-195: Sample 11 left rut normal probability plot for 1 000 m averaged section length**

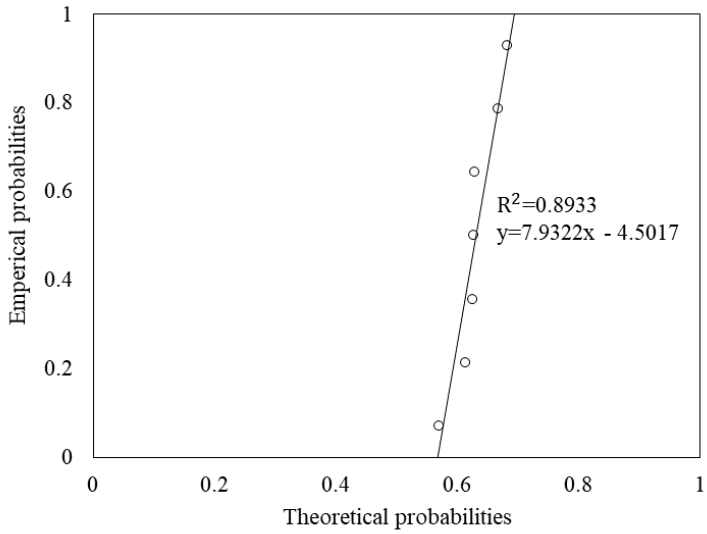


**Figure E-196: Sample 11 left rut exponential probability plot for 10 000 m averaged section length**

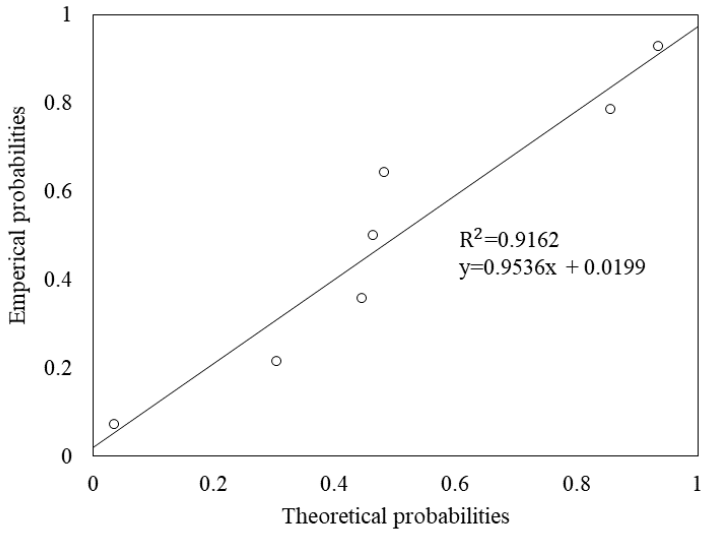


**Figure E-197: Sample 11 left rut lognormal probability plot for 10 000 m averaged section length**

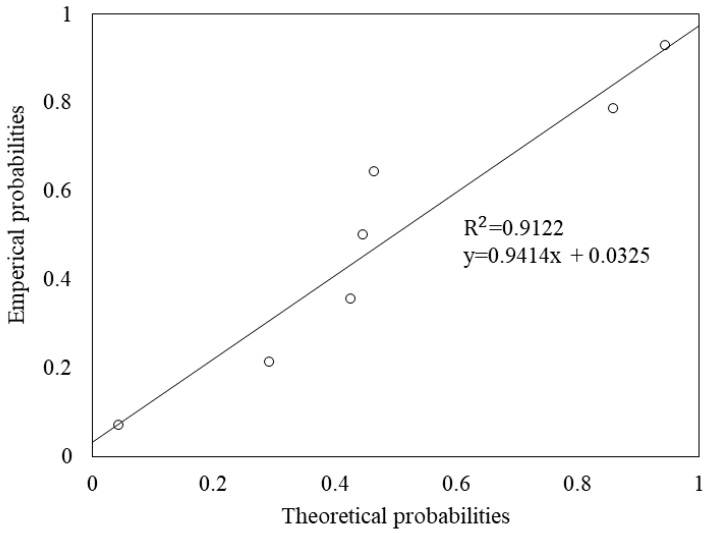


**Figure E-198: Sample 11 left rut normal probability plot for 10 000 m averaged section length**

Figure E-199 to Figure E-216 present the averaged section length exponential, lognormal, and normal probability plots for sample 12 left rut depth measurements.

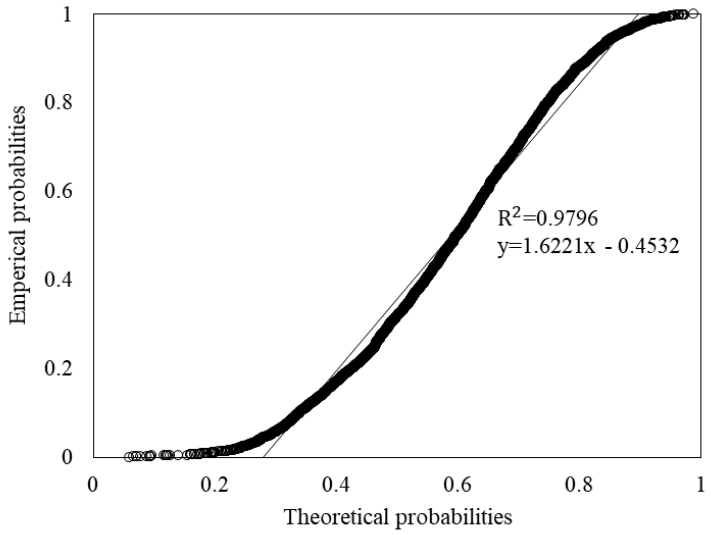


**Figure E-199: Sample 12 left rut exponential probability plot for 20 m averaged section length**

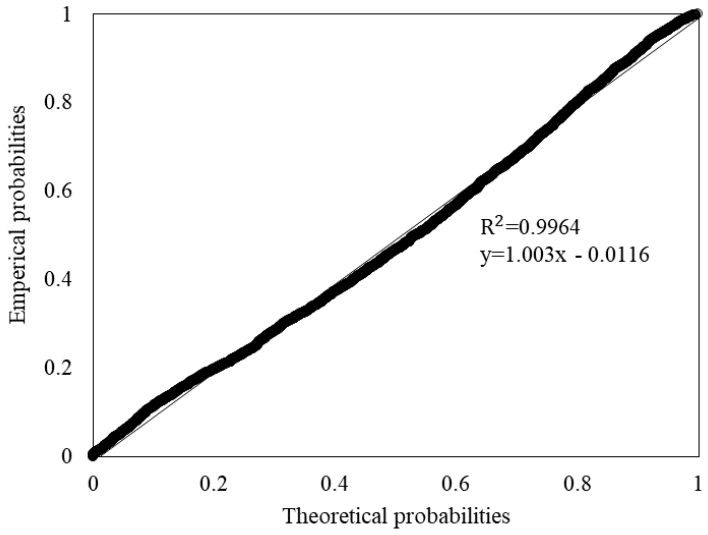


**Figure E-200: Sample 12 left rut lognormal probability plot for 20 m averaged section length**

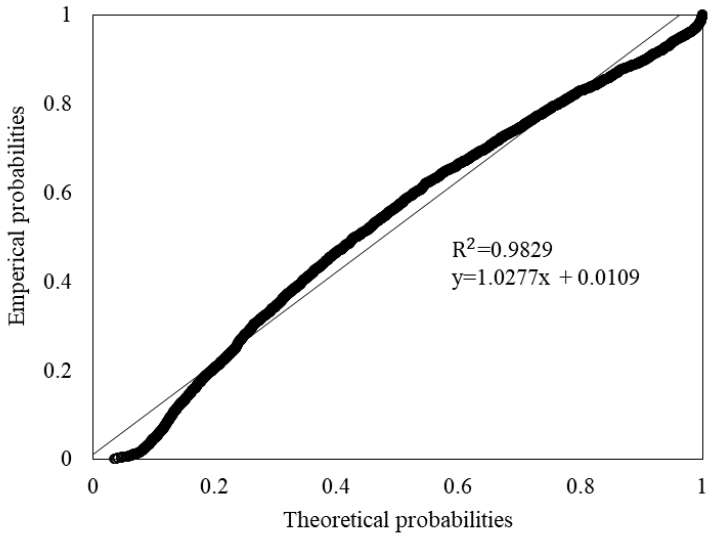


**Figure E-201: Sample 12 left rut normal probability plot for 20 m averaged section length**

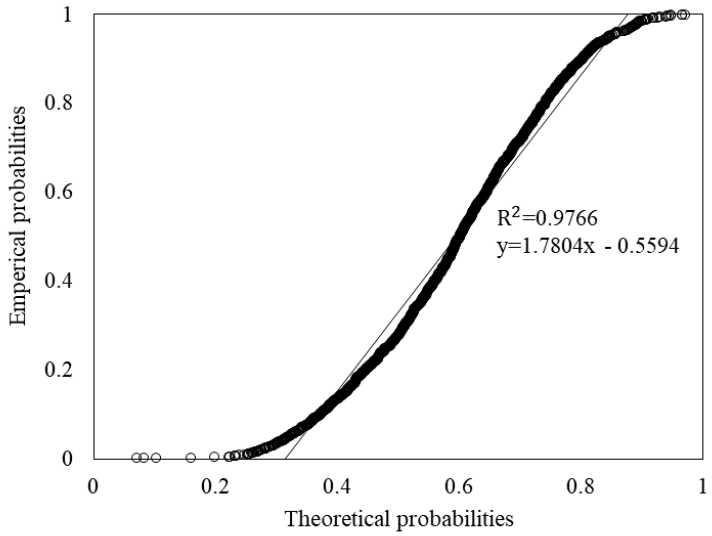


**Figure E-202: Sample 12 left rut exponential probability plot for 50 m averaged section length**

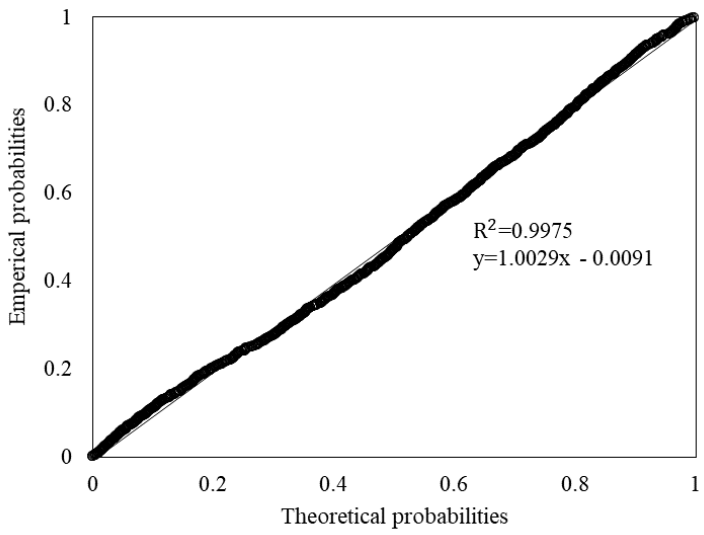


**Figure E-203: Sample 12 left rut lognormal probability plot for 50 m averaged section length**

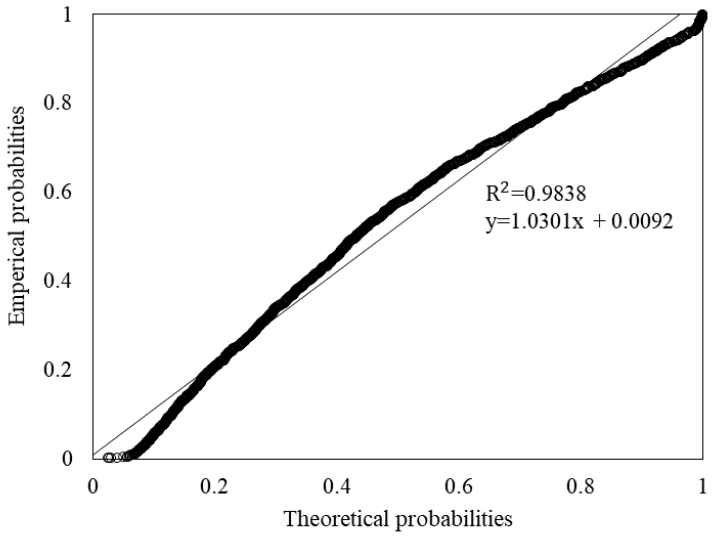


**Figure E-204: Sample 12 left rut normal probability plot for 50 m averaged section length**

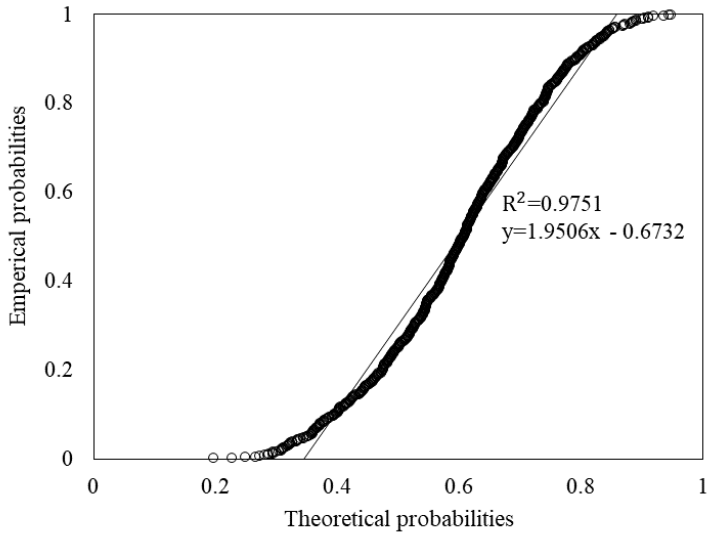


**Figure E-205: Sample 12 left rut exponential probability plot for 100 m averaged section length**

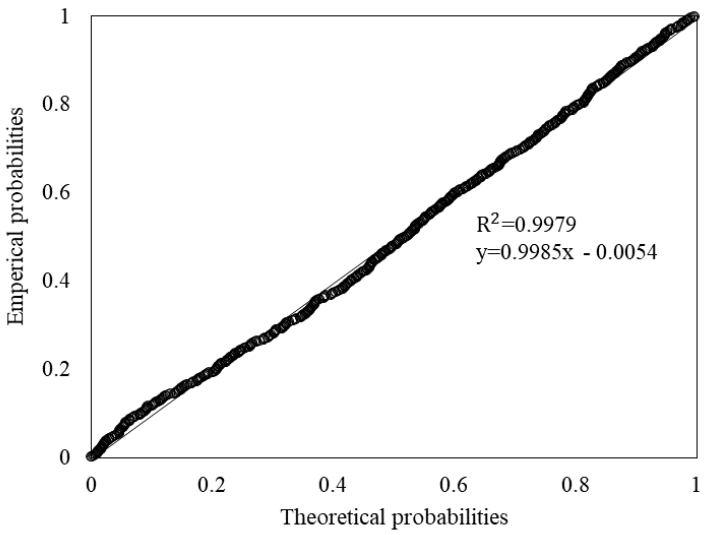


**Figure E-206: Sample 12 left rut lognormal probability plot for 100 m averaged section length**

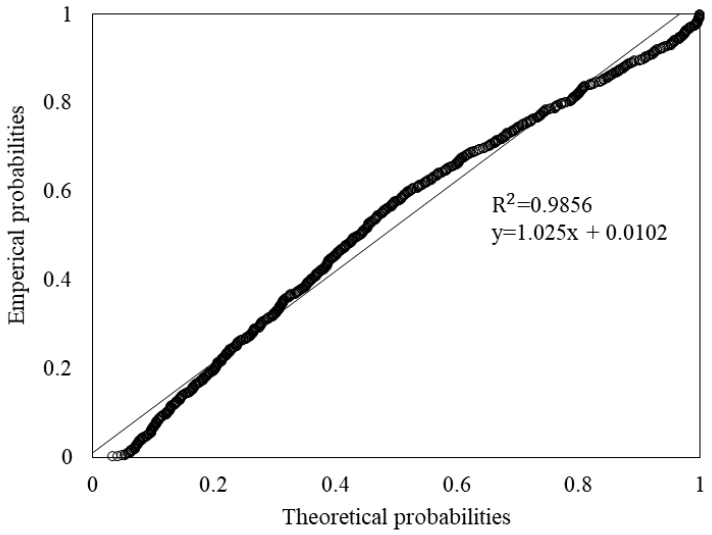


**Figure E-207: Sample 12 left rut normal probability plot for 100 m averaged section length**

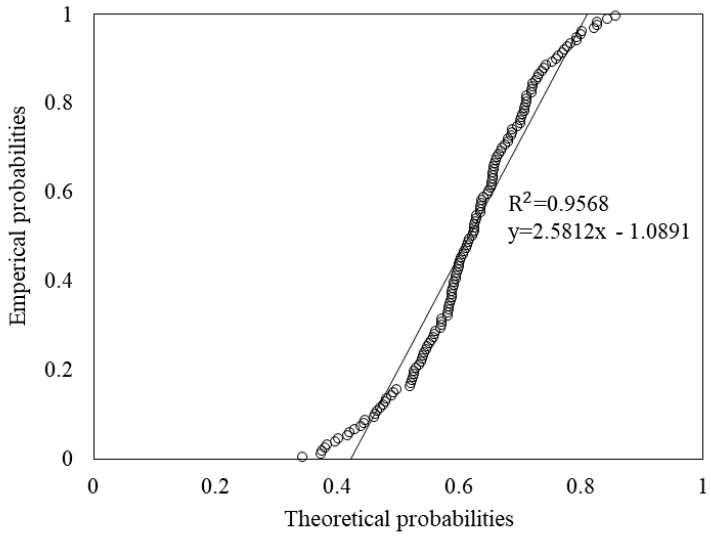


**Figure E-208: Sample 12 left rut exponential probability plot for 500 m averaged section length**

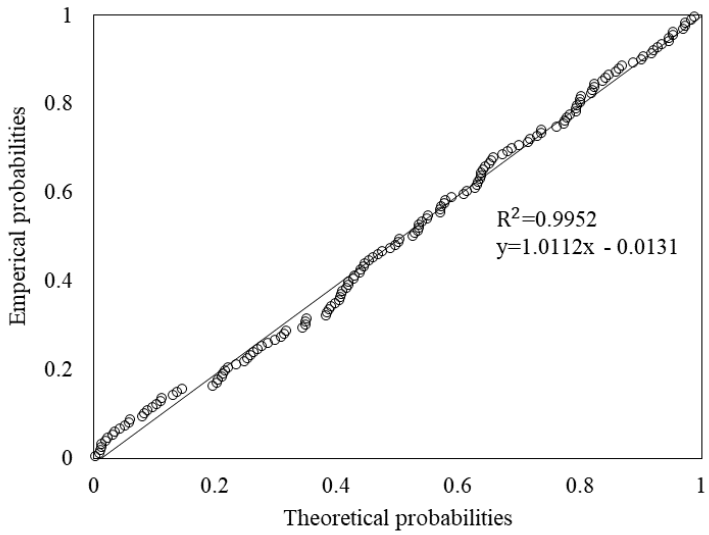


**Figure E-209: Sample 12 left rut lognormal probability plot for 500 m averaged section length**

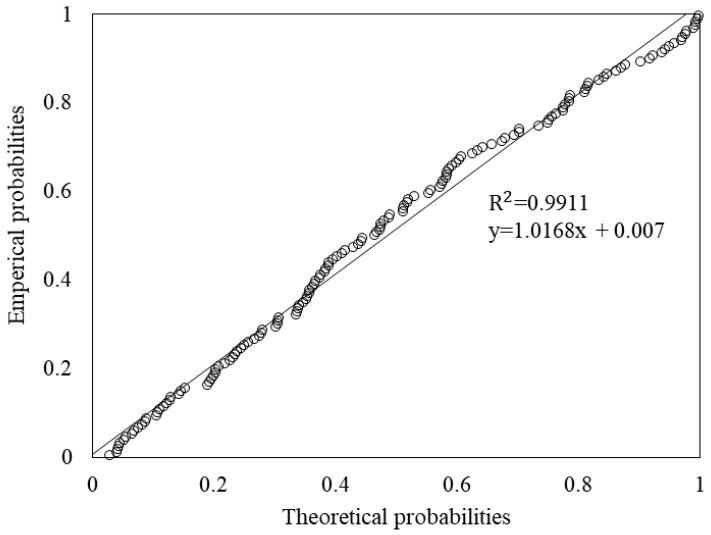


**Figure E-210: Sample 12 left rut normal probability plot for 500 m averaged section length**

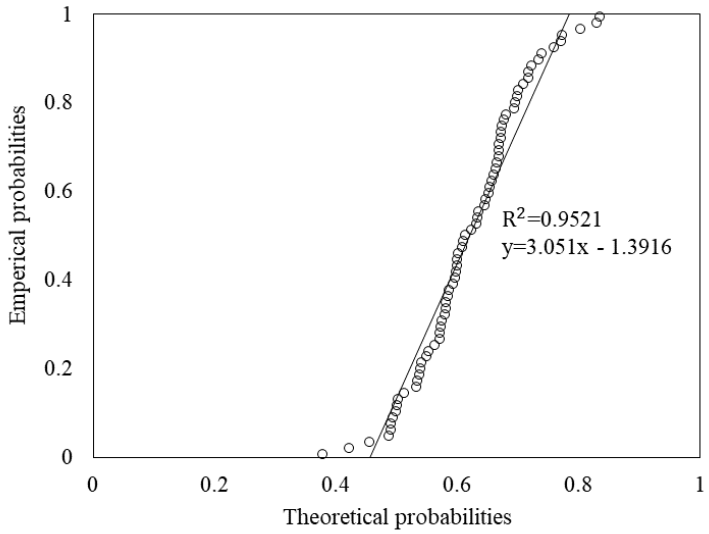


**Figure E-211: Sample 12 left rut exponential probability plot for 1 000 m averaged section length**

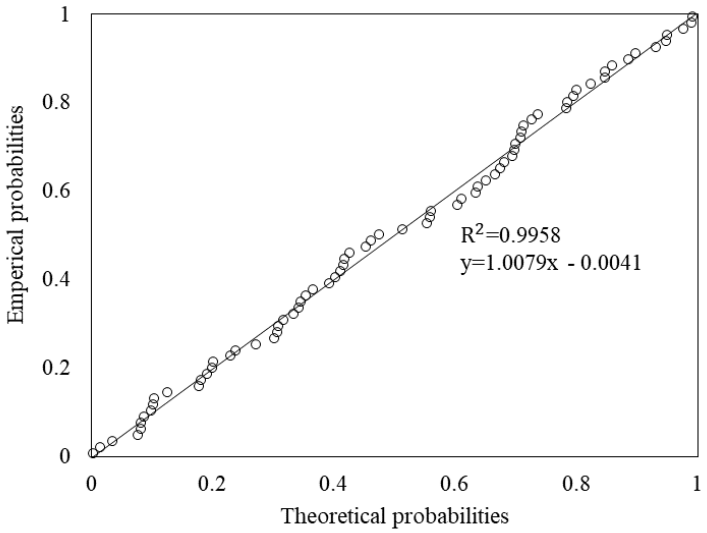


**Figure E-212: Sample 12 left rut lognormal probability plot for 1 000 m averaged section length**

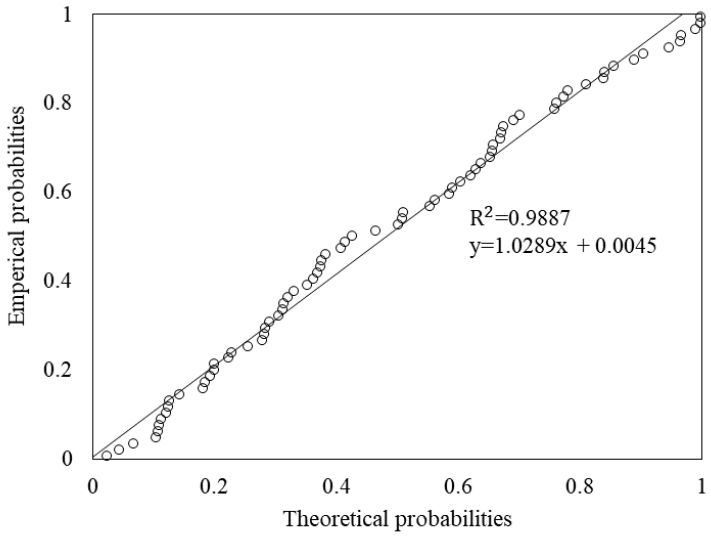


**Figure E-213: Sample 12 left rut normal probability plot for 1 000 m averaged section length**

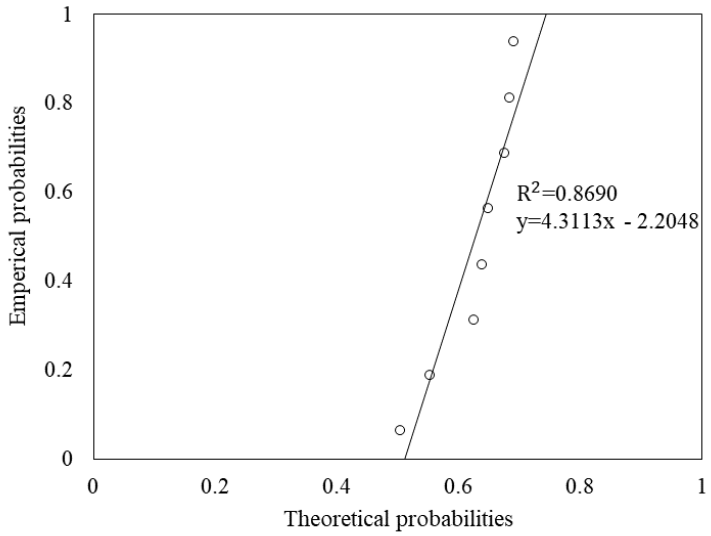


**Figure E-214: Sample 12 left rut exponential probability plot for 10 000 m averaged section length**

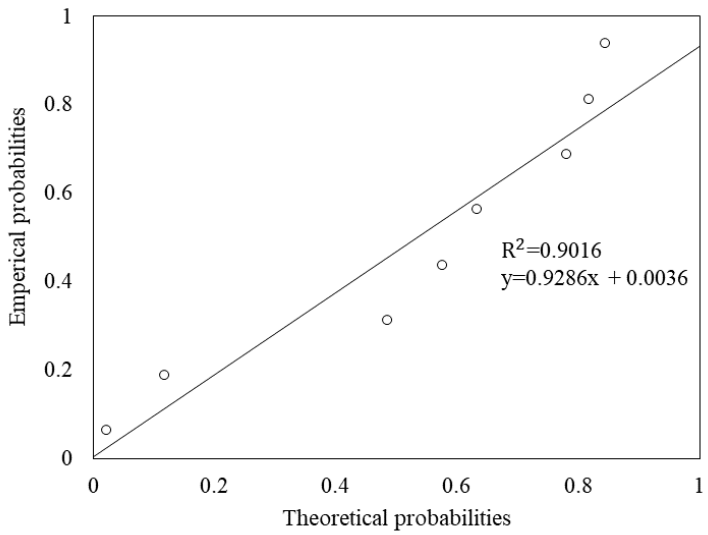


**Figure E-215: Sample 12 left rut lognormal probability plot for 10 000 m averaged section length**

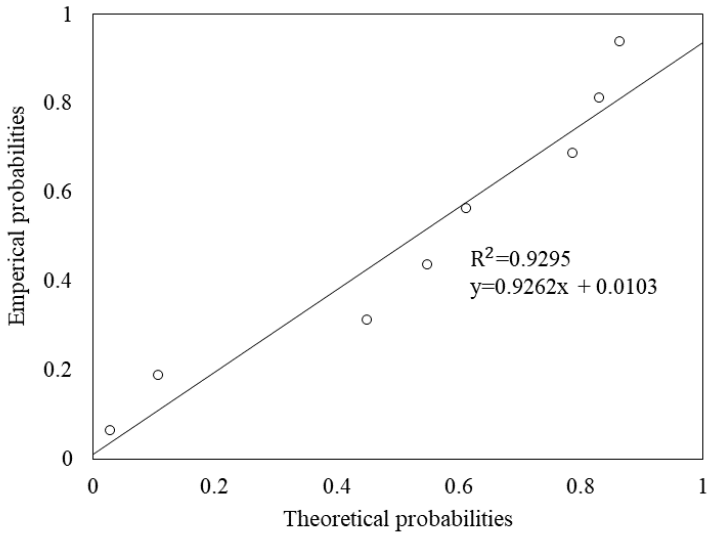


**Figure E-216: Sample 12 left rut normal probability plot for 10 000 m averaged section length**

Figure E-217 to Figure E-234 present the averaged section length exponential, lognormal, and normal probability plots for sample 13 left rut depth measurements.

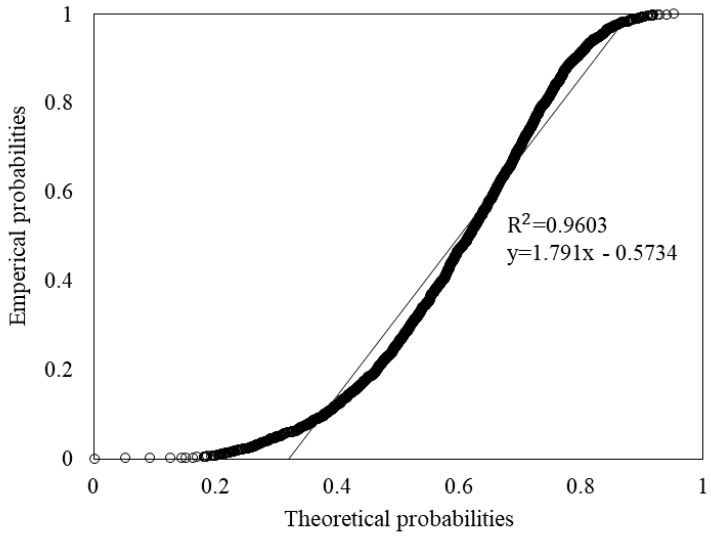


**Figure E-217: Sample 13 left rut exponential probability plot for 20 m averaged section length**

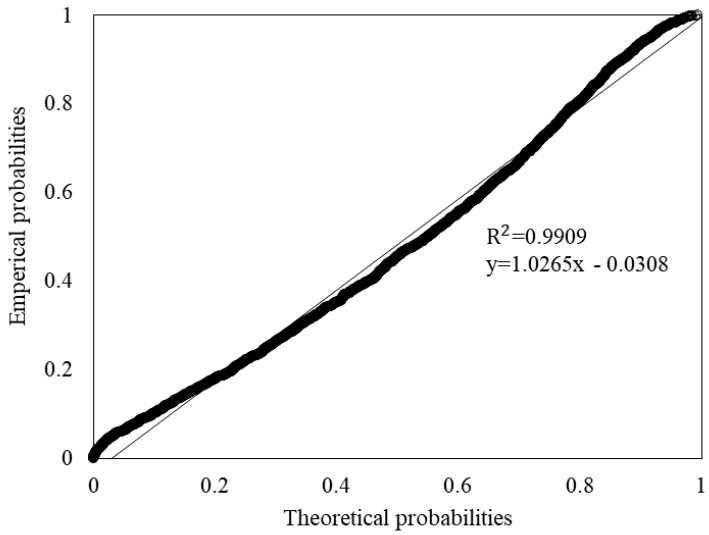


**Figure E-218: Sample 13 left rut lognormal probability plot for 20 m averaged section length**

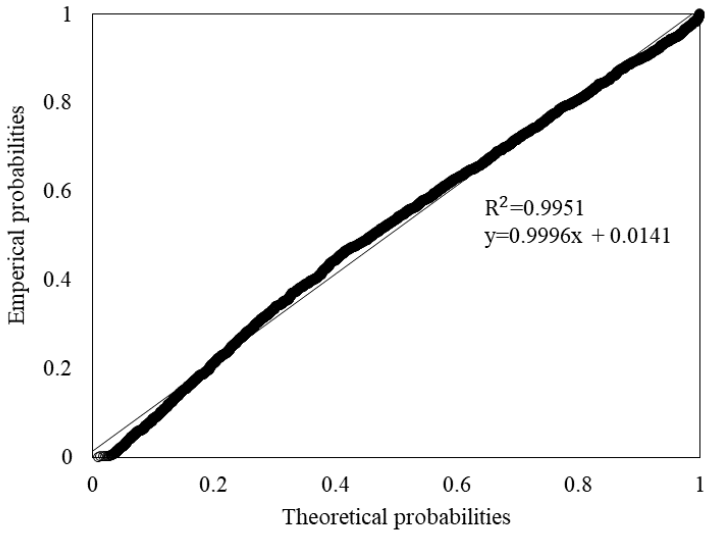


**Figure E-219: Sample 13 left rut normal probability plot for 20 m averaged section length**

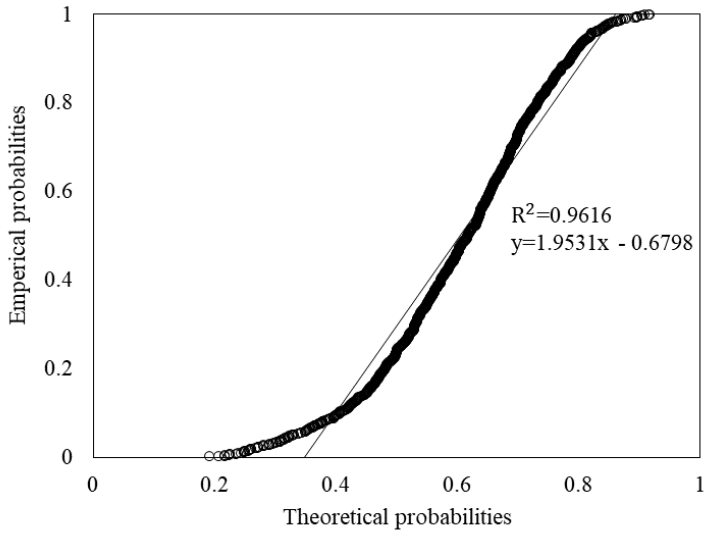


**Figure E-220: Sample 13 left rut exponential probability plot for 50 m averaged section length**

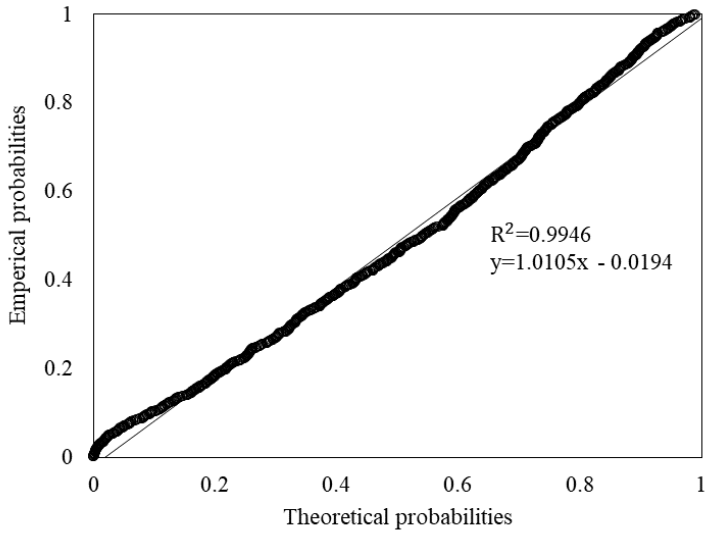


**Figure E-221: Sample 13 left rut lognormal probability plot for 50 m averaged section length**

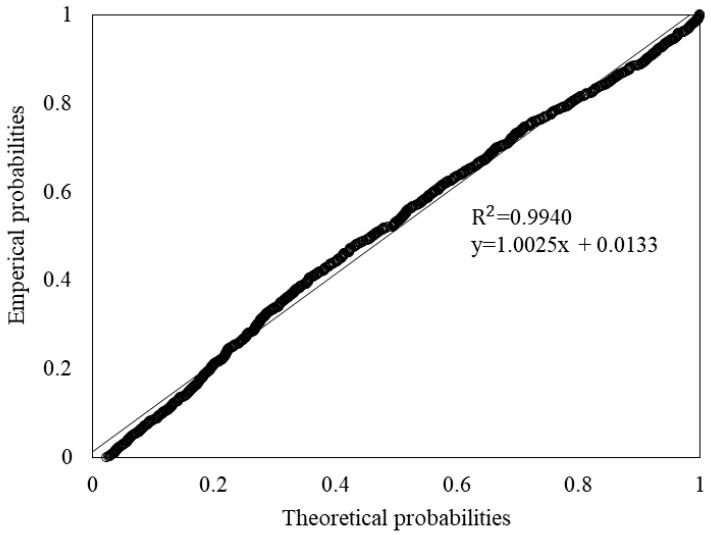


**Figure E-222: Sample 13 left rut normal probability plot for 50 m averaged section length**

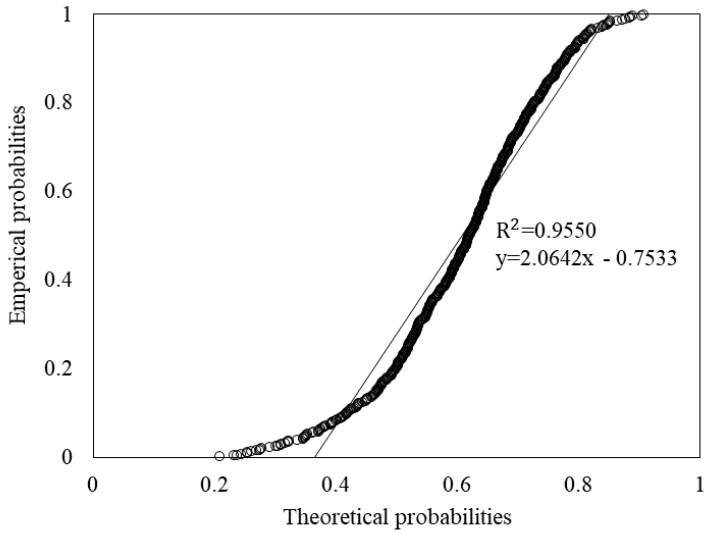


**Figure E-223: Sample 13 left rut exponential probability plot for 100 m averaged section length**

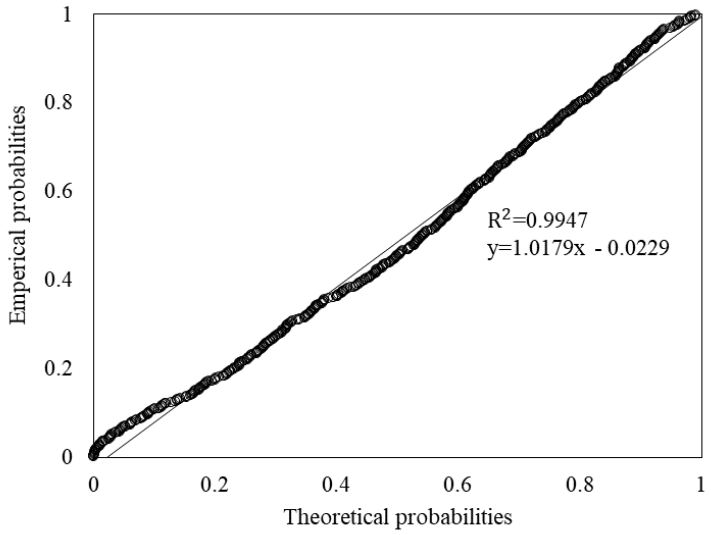


**Figure E-224: Sample 13 left rut lognormal probability plot for 100 m averaged section length**

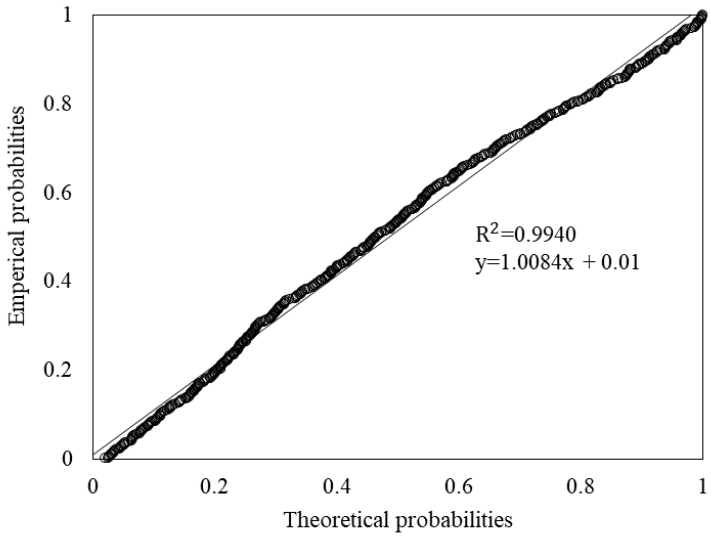


**Figure E-225: Sample 13 left rut normal probability plot for 100 m averaged section length**

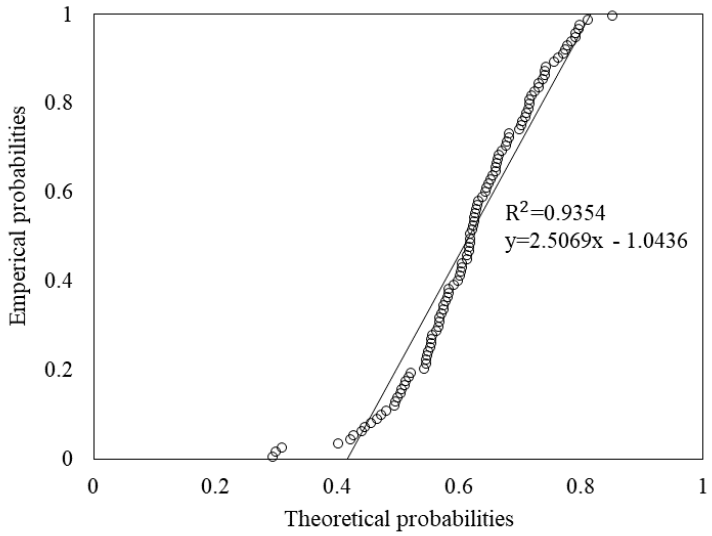


**Figure E-226: Sample 13 left rut exponential probability plot for 500 m averaged section length**

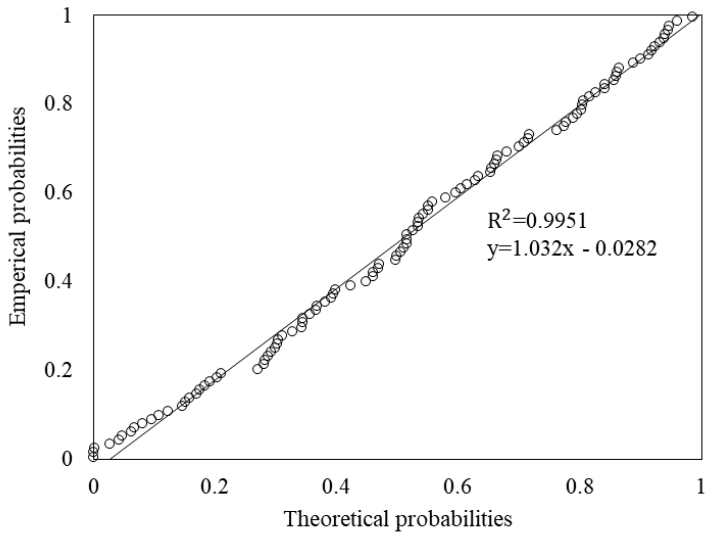


**Figure E-227: Sample 13 left rut lognormal probability plot for 500 m averaged section length**

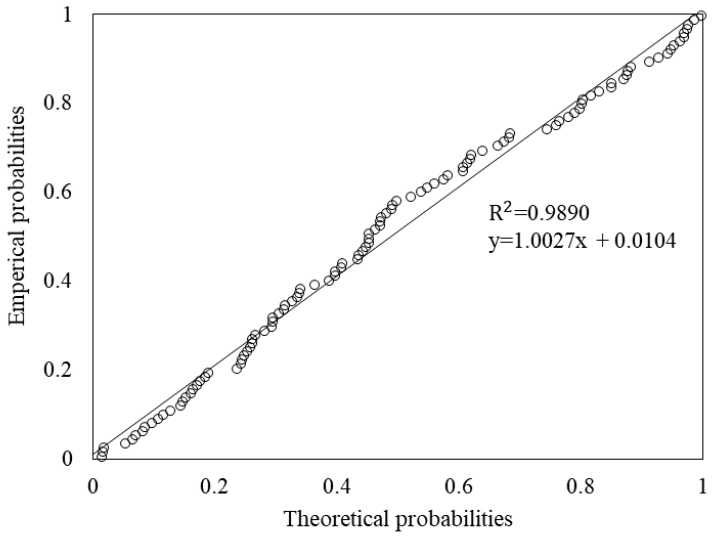


**Figure E-228: Sample 13 left rut normal probability plot for 500 m averaged section length**

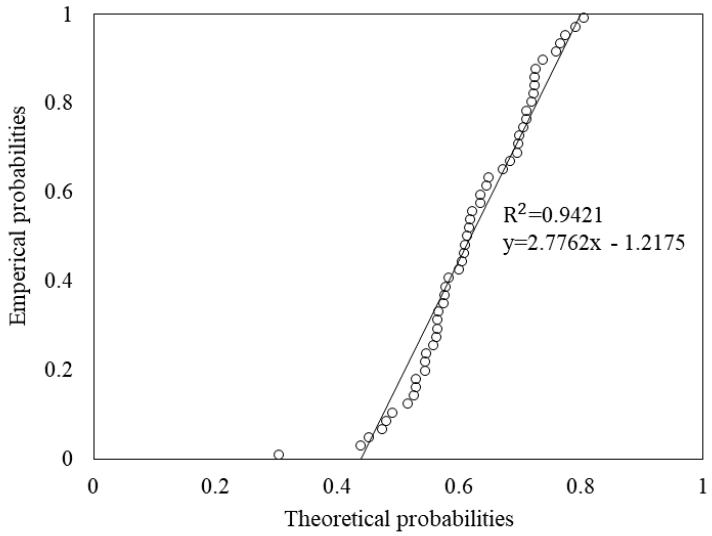


**Figure E-229: Sample 13 left rut exponential probability plot for 1 000 m averaged section length**

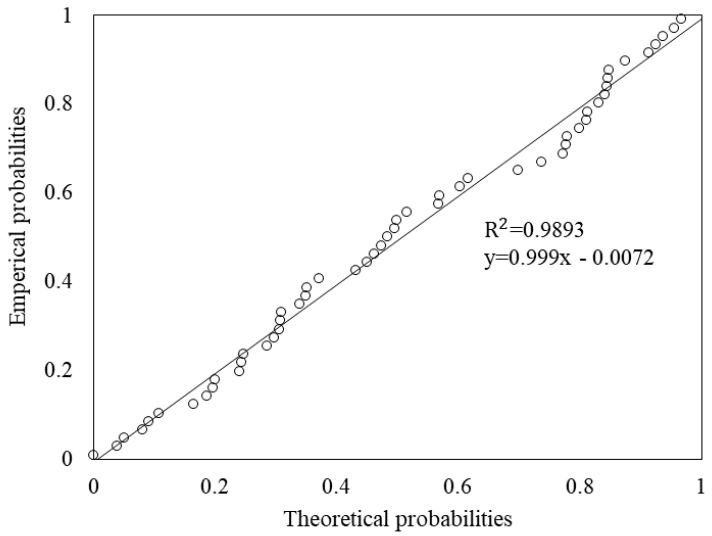


**Figure E-230: Sample 13 left rut lognormal probability plot for 1 000 m averaged section length**

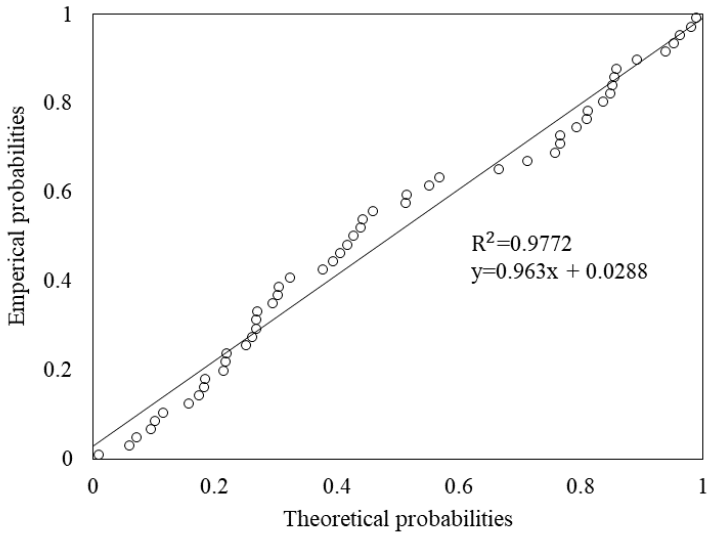


**Figure E-231: Sample 13 left rut normal probability plot for 1 000 m averaged section length**

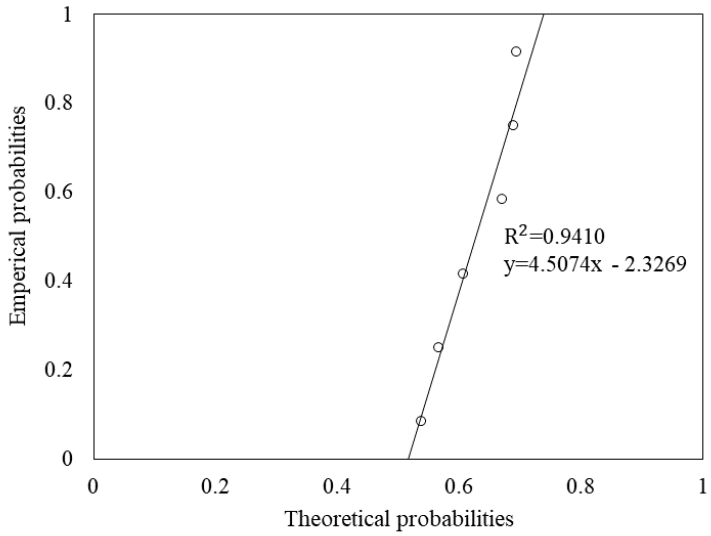


**Figure E-232: Sample 13 left rut exponential probability plot for 10 000 m averaged section length**

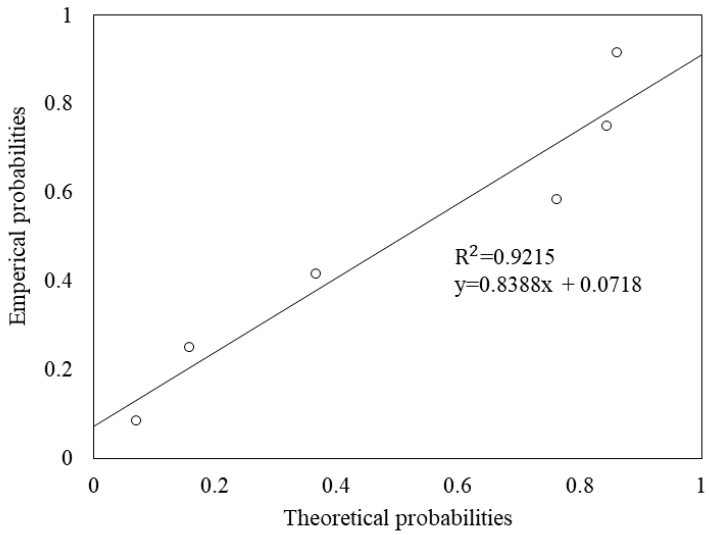


**Figure E-233: Sample 13 left rut lognormal probability plot for 10 000 m averaged section length**

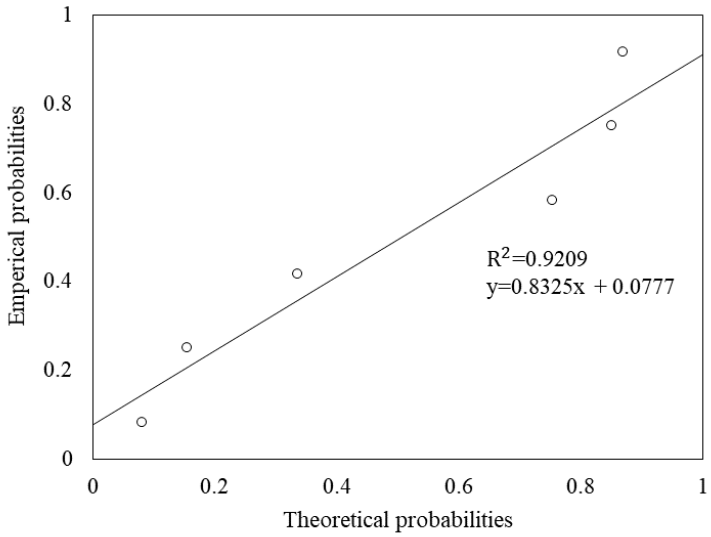


**Figure E-234: Sample 13 left rut normal probability plot for 10 000 m averaged section length**

# APPENDIX F

# DATASET 2 DISTRIBUTION OF RUT DEPTH FOR AVERAGED SECTION LENGTHS

# APPENDIX F DATASET 2 DISTRIBUTION OF RUT DEPTH FOR AVERAGED SECTION LENGTHS

## F.1 INTRODUCTION

The results from the comparison of the distribution of rut depth for different averaged section lengths discussed in Section 4.1.2 are presented in the sections that follow.

## F.2 CUMULATIVE DISTRIBUTION OF RUT DEPTH

Figure F-1 to Figure F-13 present the cumulative distributions of rut depth for the averaged section lengths investigated for samples 1 to 13, respectively.

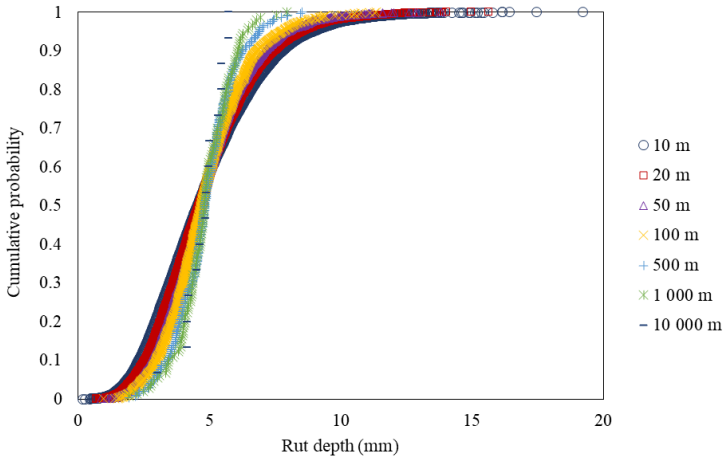


**Figure F-1: Sample 1 cumulative distribution**

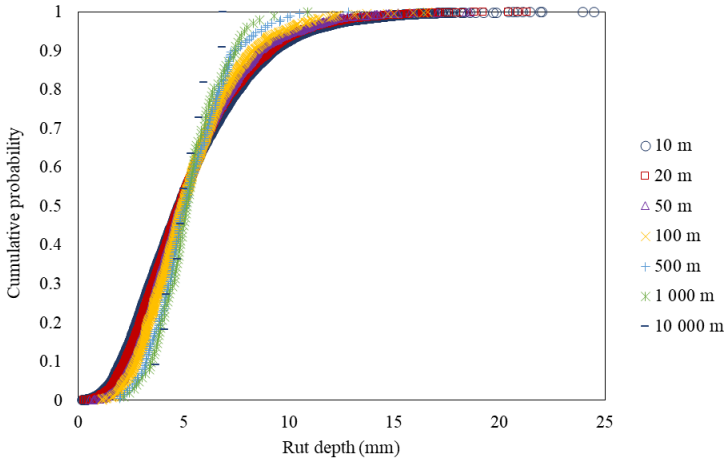


**Figure F-2: Sample 2 cumulative distribution**

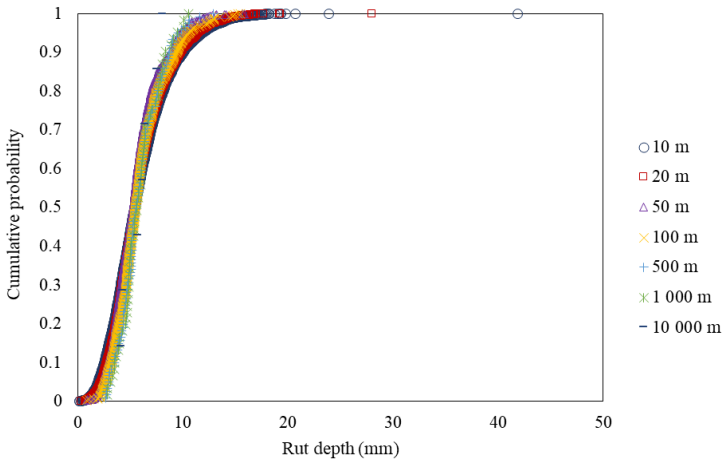


**Figure F-3: Sample 3 cumulative distribution**

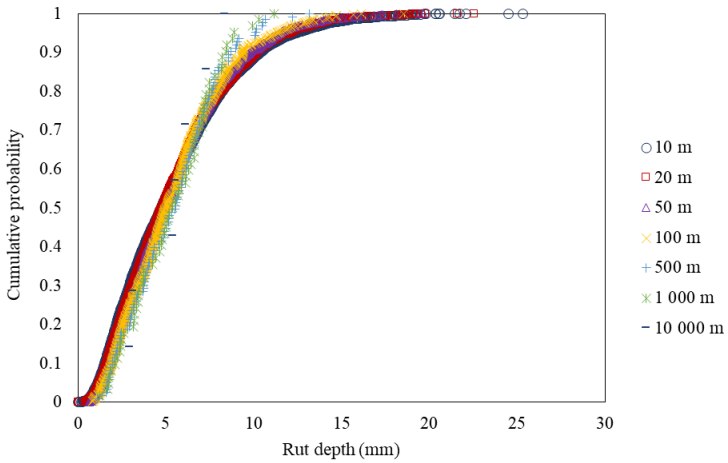


**Figure F-4: Sample 4 cumulative distribution**

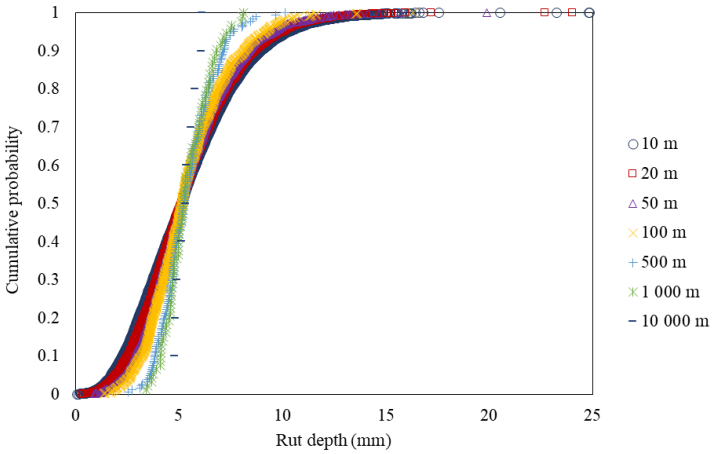


**Figure F-5: Sample 5 cumulative distribution**

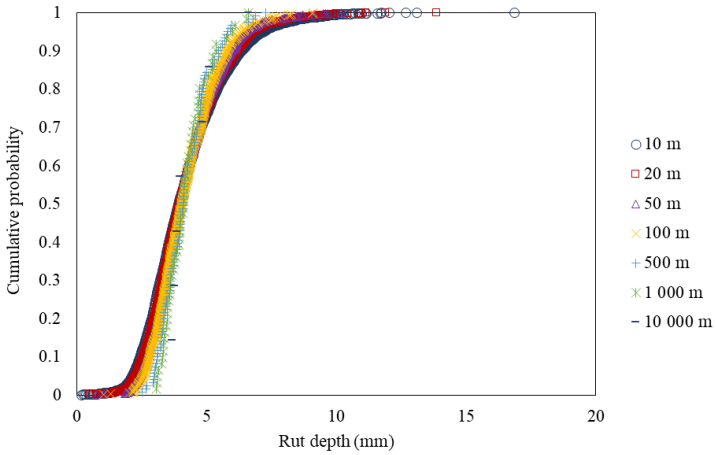


**Figure F-6: Sample 6 cumulative distribution**

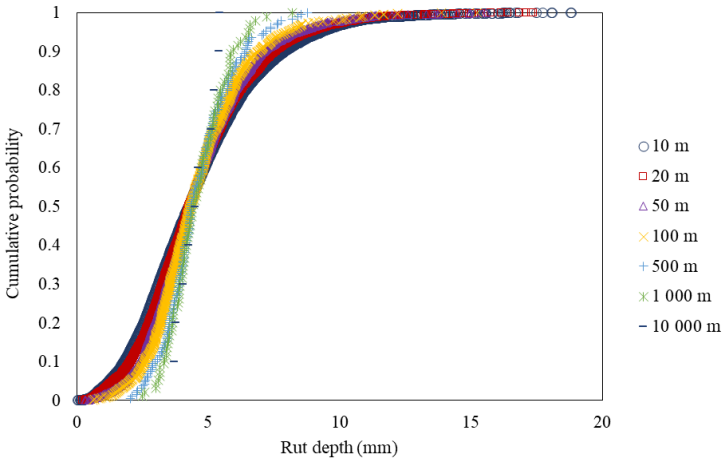


**Figure F-7: Sample 7 cumulative distribution**

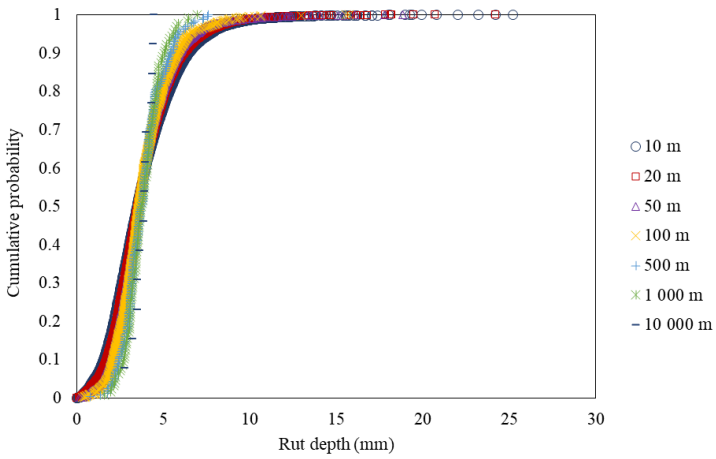


**Figure F-8: Sample 8 cumulative distribution**

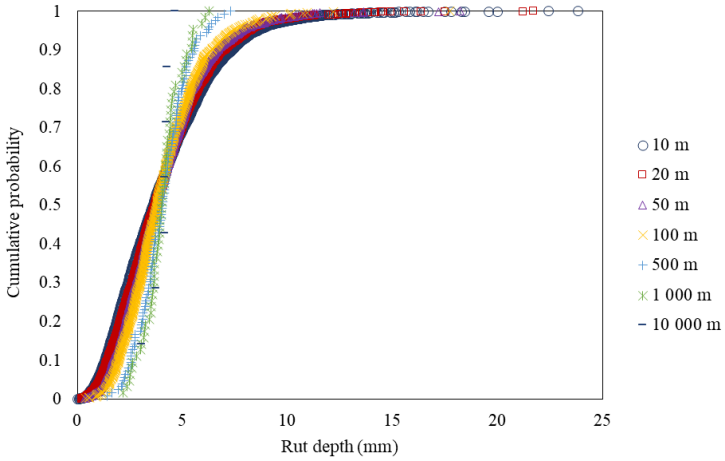


**Figure F-9: Sample 9 cumulative distribution**

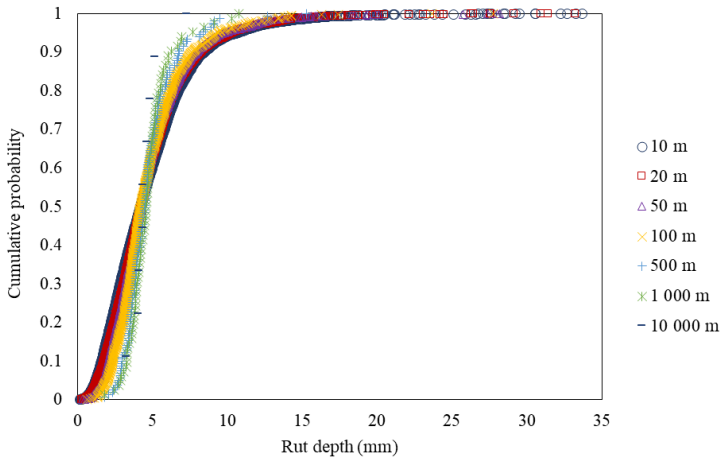


**Figure F-10: Sample 10 cumulative distribution**

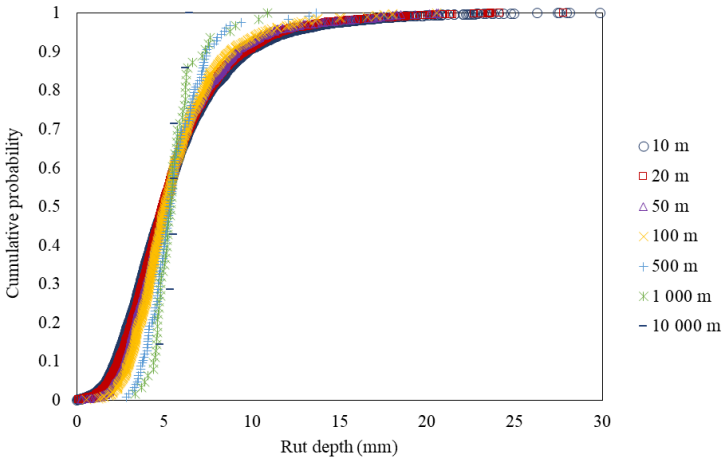


**Figure F-11: Sample 11 cumulative distribution**

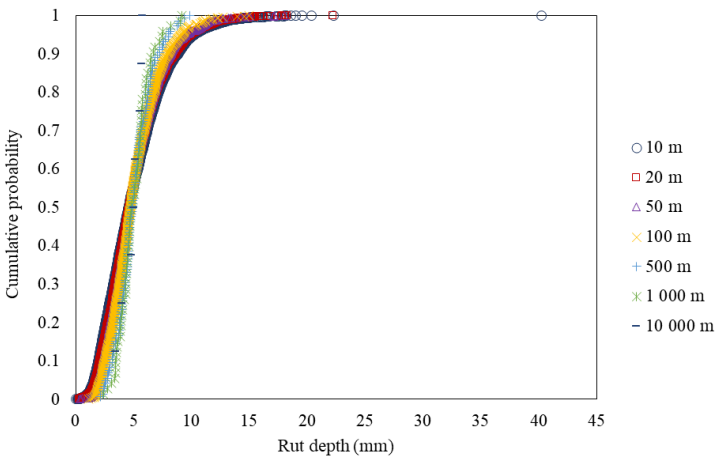


**Figure F-12: Sample 12 cumulative distribution**

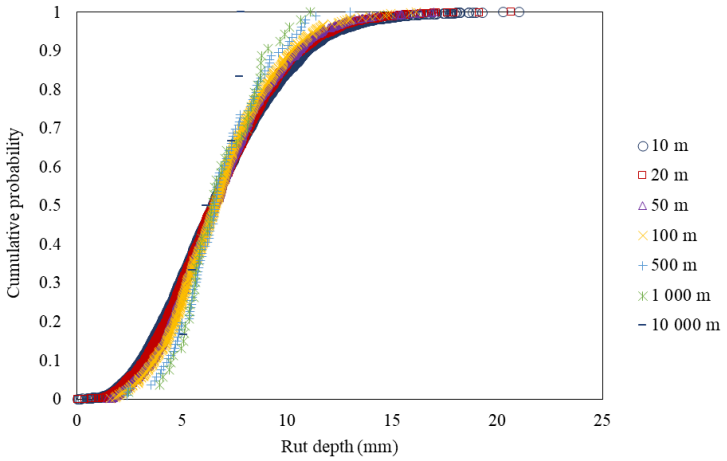


**Figure F-13: Sample 13 cumulative distribution**

## F.3 DISTRIBUTION OF RUT DEPTH VALUES AMONGST CONDITION CATEGORIES

Figure F-14 to Figure F-26 present the change in distribution amongst rut depth condition categories with increasing averaged section lengths for samples 1 to 13, respectively.

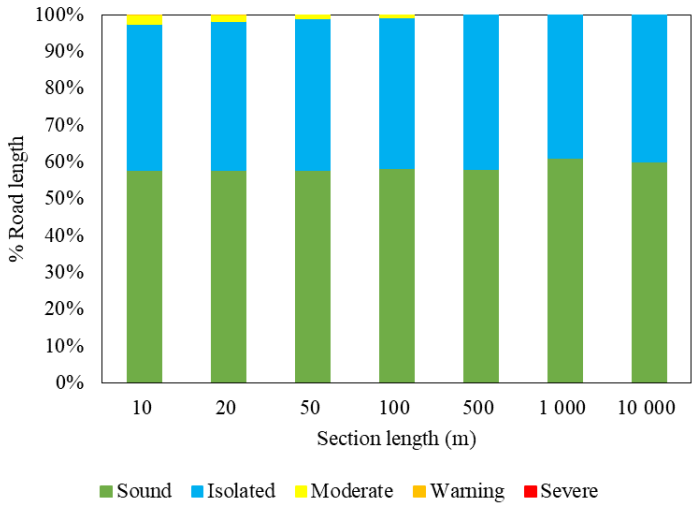


**Figure F-14: Distribution of rut depth amongst condition categories for sample 1**

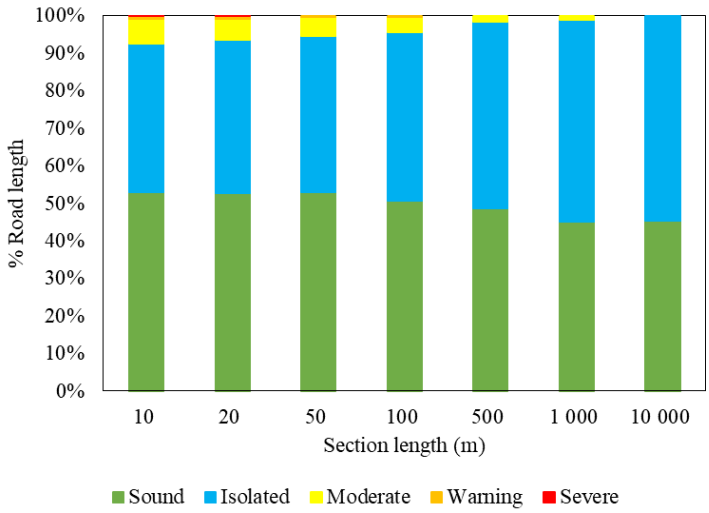


**Figure F-15: Distribution of rut depth amongst condition categories for sample 2**

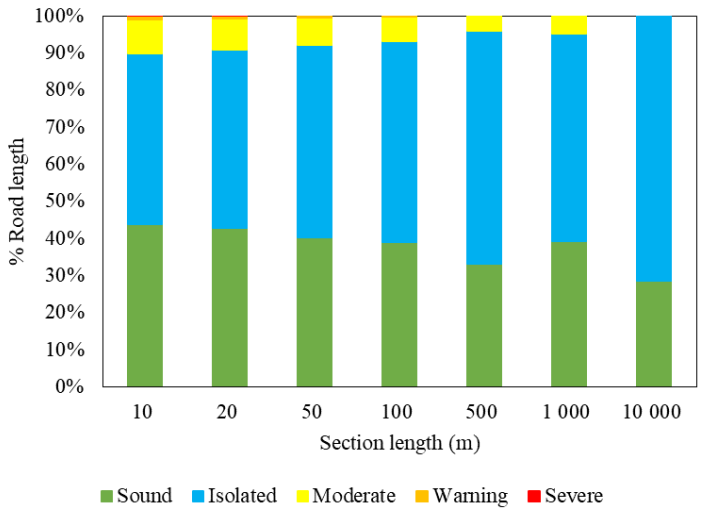


**Figure F-16: Distribution of rut depth amongst condition categories for sample 3**

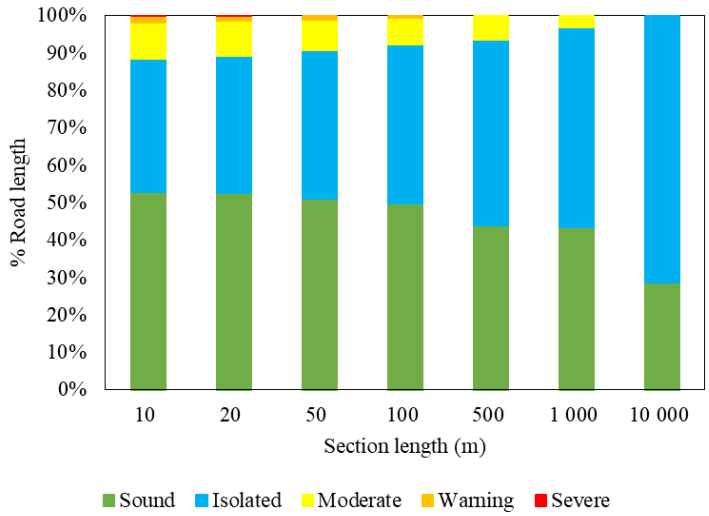


**Figure F-17: Distribution of rut depth amongst condition categories for sample 4**

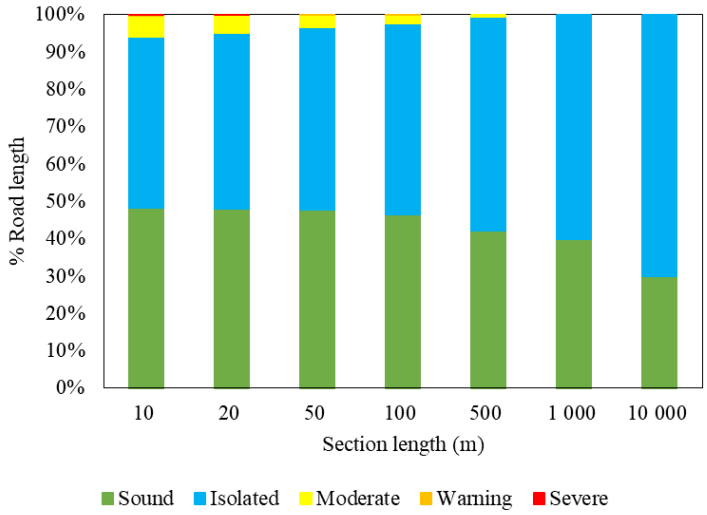


**Figure F-18: Distribution of rut depth amongst condition categories for sample 5**

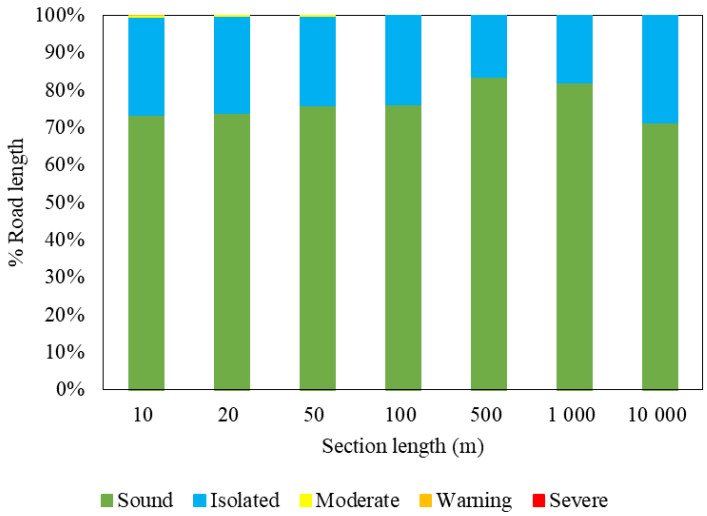


**Figure F-19: Distribution of rut depth amongst condition categories for sample 6**

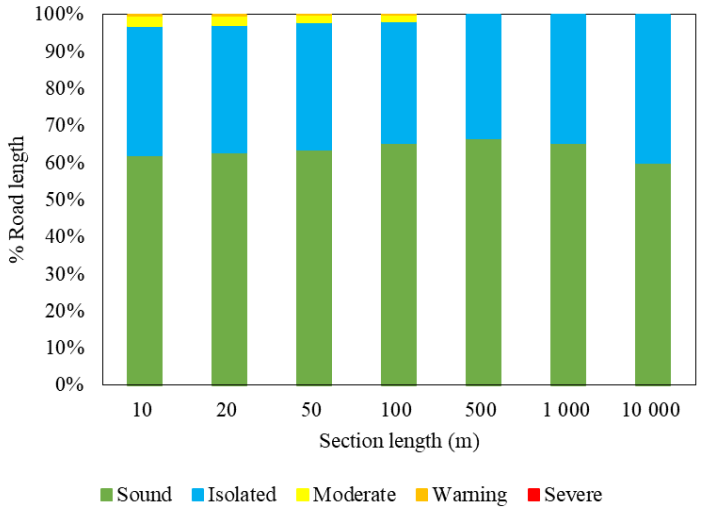


**Figure F-20: Distribution of rut depth amongst condition categories for sample 7**

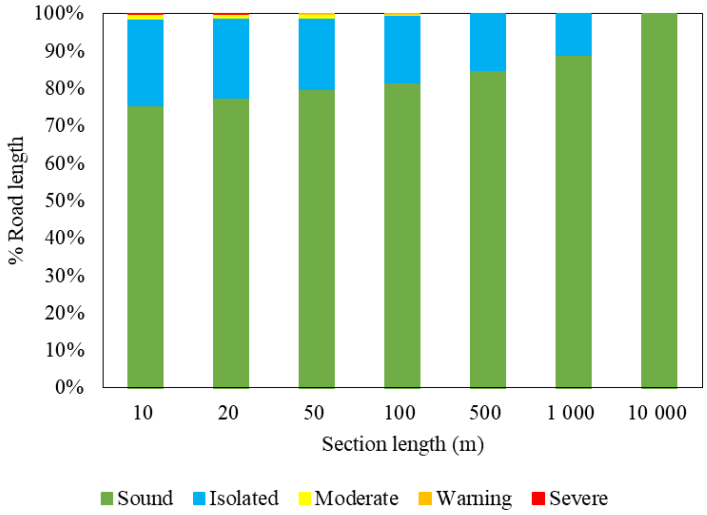


**Figure F-21: Distribution of rut depth amongst condition categories for sample 8**

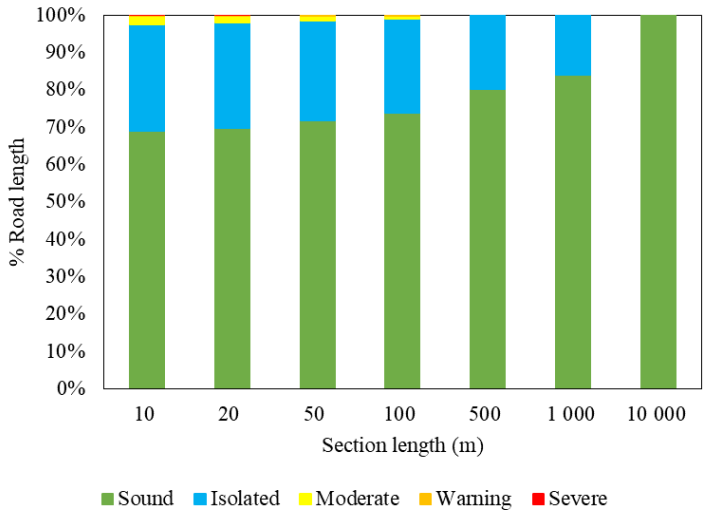


**Figure F-22: Distribution of rut depth amongst condition categories for sample 9**

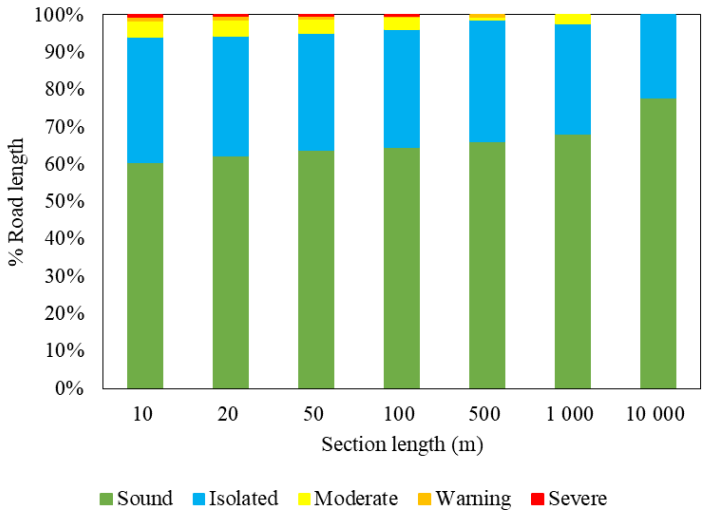


**Figure F-23: Distribution of rut depth amongst condition categories for sample 10**

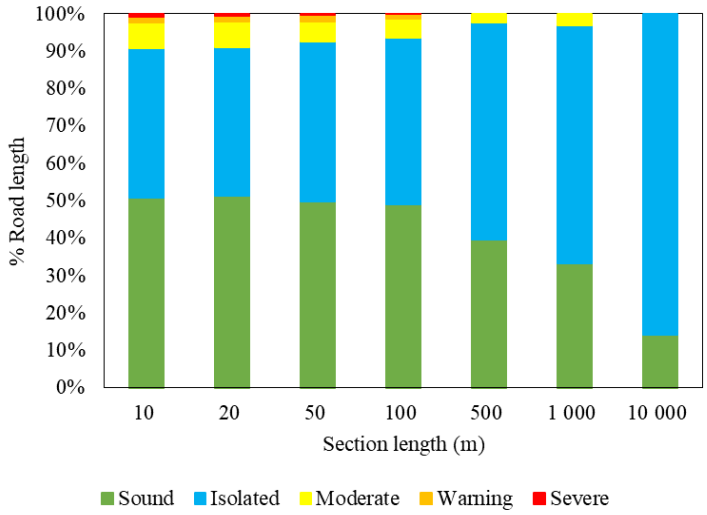


**Figure F-24: Distribution of rut depth amongst condition categories for sample 11**

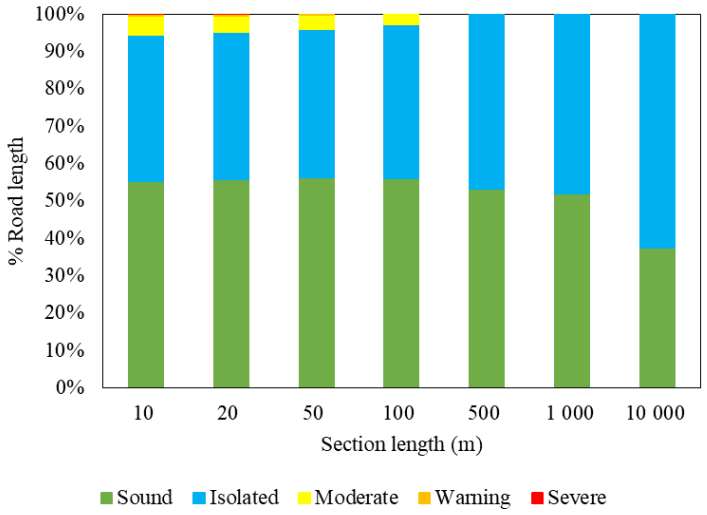


**Figure F-25: Distribution of rut depth amongst condition categories for sample 12**

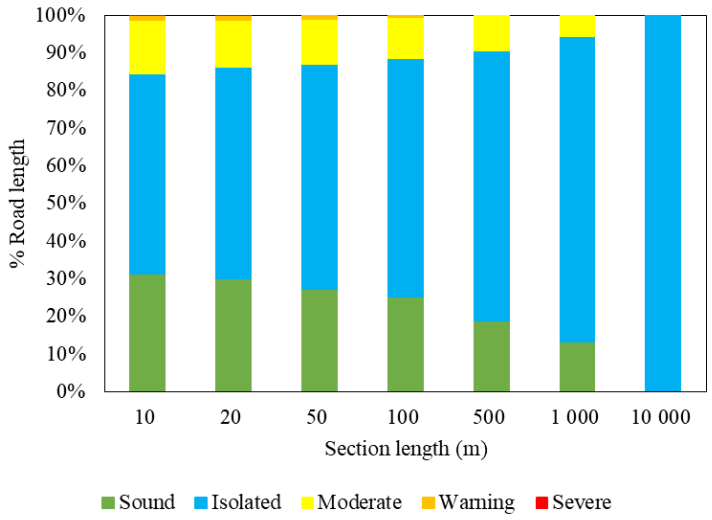


**Figure F-26: Distribution of rut depth amongst condition categories for sample 13**

# APPENDIX G

# DATASET 2 MAINTENANCE REQUIREMENTS

# APPENDIX G DATASET 2 MAINTENANCE REQUIREMENTS

## G.1 INTRODUCTION

The maintenance requirements results, obtained from the dTIMS technical needs analysis discussed in Section 4.1.3, are presented in the sections that follow.

## G.2 SAMPLES CONTAINING MULTIPLE TREATMENTS WITH THE MAJORITY TREATMENT TRIGGERED IN MULTIPLE YEARS

Figure G-1 to Figure G-13, where applicable, present the change in light rehabilitation / reseal year and length with increasing averaged section lengths for samples containing multiple treatments (light rehabilitation / reseal and heavy rehabilitation) with the majority treatment (light rehabilitation / reseal) triggered in multiple years.

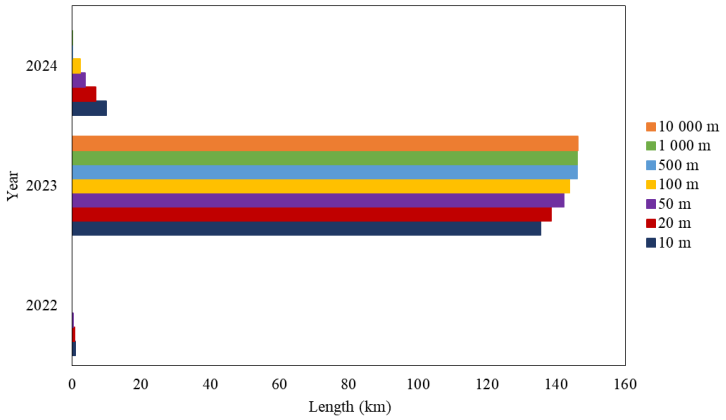


**Figure G-1: Change in light rehabilitation treatment year and length for sample 1**

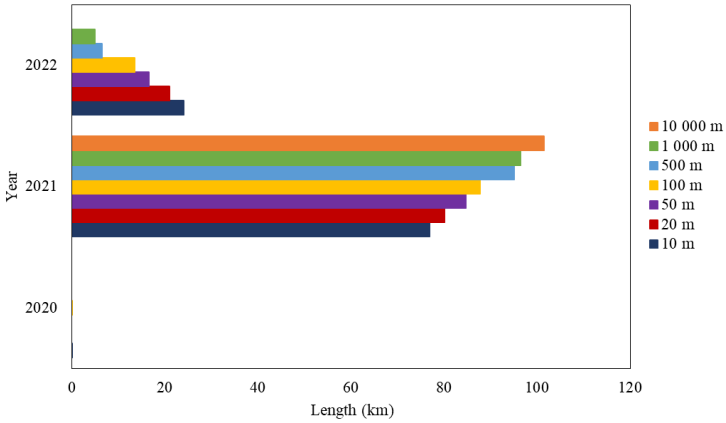


**Figure G-2: Change in light rehabilitation treatment year and length for sample 2**

N/A

**Figure G-3: Change in reseal treatment year and length for sample 3**

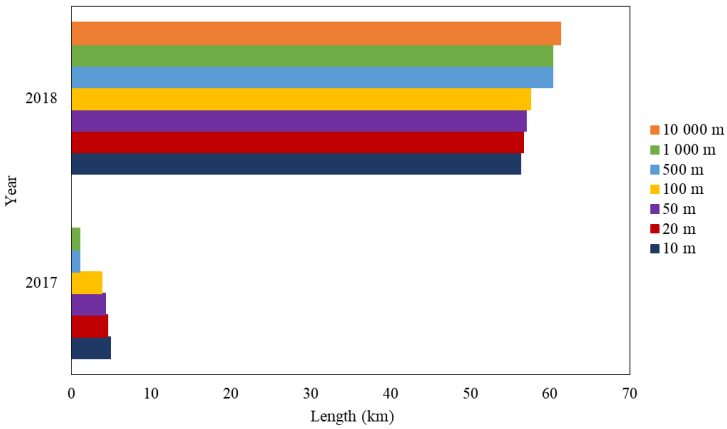


**Figure G-4: Change in light rehabilitation treatment year and length for sample 4**

N/A

**Figure G-5: Change in reseal treatment year and length for sample 5**

N/A

**Figure G-6: Change in light rehabilitation treatment year and length for sample 6**

N/A

**Figure G-7: Change in reseal treatment year and length for sample 7**

N/A

**Figure G-8: Change in reseal treatment year and length for sample 8**

N/A

**Figure G-9: Change in reseal treatment year and length for sample 9**

N/A

**Figure G-10: Change in light rehabilitation treatment year and length for sample 10**

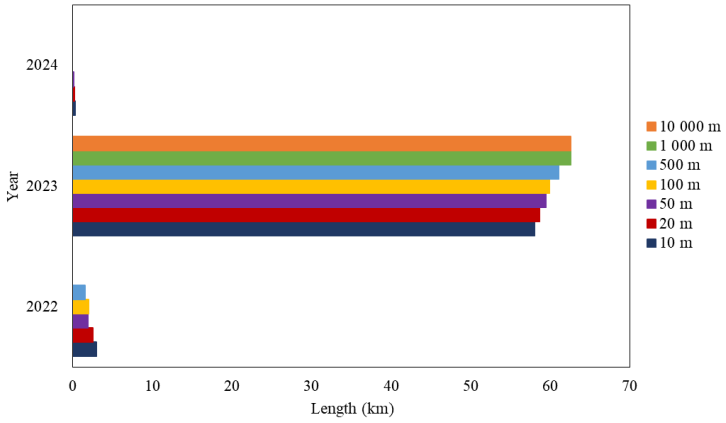


**Figure G-11: Change in light rehabilitation treatment year and length for sample 11**

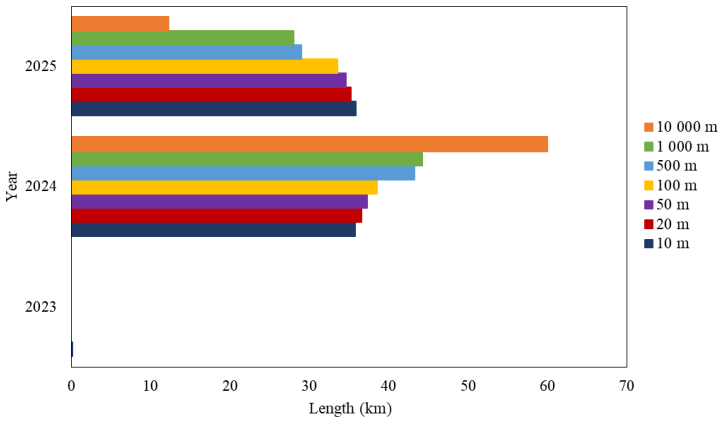


**Figure G-12: Change in light rehabilitation treatment year and length for sample 12**

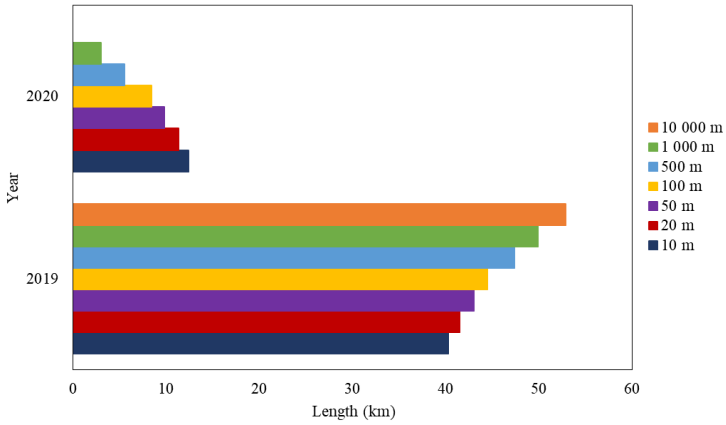


**Figure G-13: Change in light rehabilitation treatment year and length for sample 13**

## G.3 SAMPLES CONTAINING MULTIPLE TREATMENTS WITH THE MAJORITY TREATMENT TRIGGERED IN A SINGLE YEAR

Figure G-14 to Figure G-26, where applicable, present the change in light rehabilitation / reseal year and length with increasing averaged section lengths for samples containing multiple treatments (light rehabilitation / reseal and heavy rehabilitation) with the majority treatment (light rehabilitation / reseal) triggered in a single year.

N/A

**Figure G-14: Change in light rehabilitation treatment year and length for sample 1**

N/A

**Figure G-15: Change in light rehabilitation treatment year and length for sample 2**

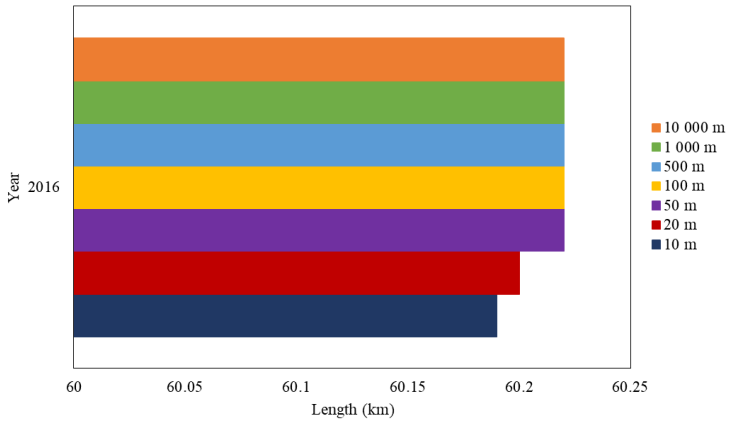


**Figure G-16: Change in reseal treatment year and length for sample 3**

N/A

**Figure G-17: Change in light rehabilitation treatment year and length for sample 4**

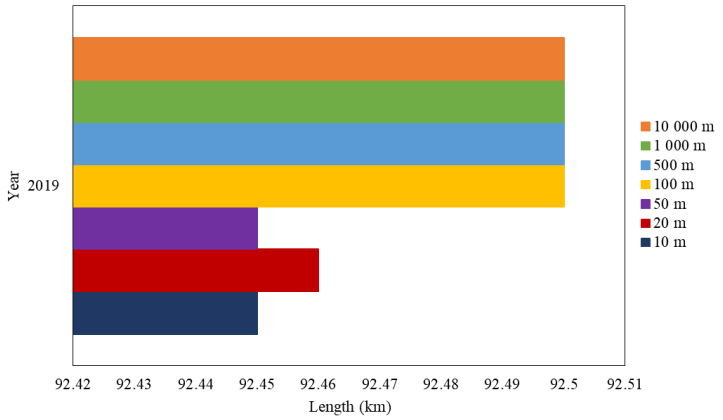


**Figure G-18: Change in reseal treatment year and length for sample 5**

N/A

**Figure G-19: Change in light rehabilitation treatment year and length for sample 6**

N/A

**Figure G-20: Change in reseal treatment year and length for sample 7**

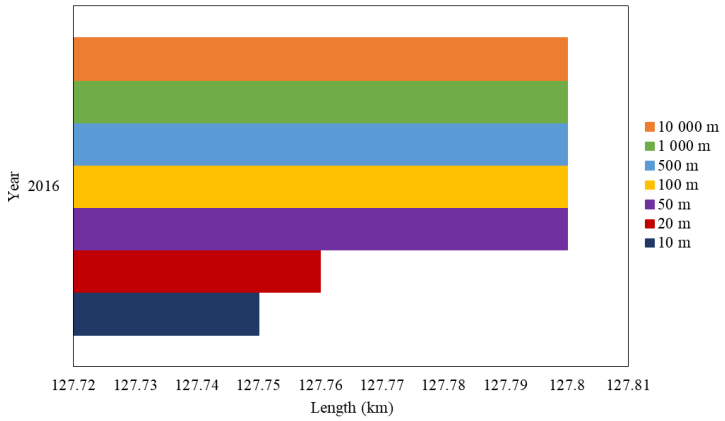


**Figure G-21: Change in reseal treatment year and length for sample 8**

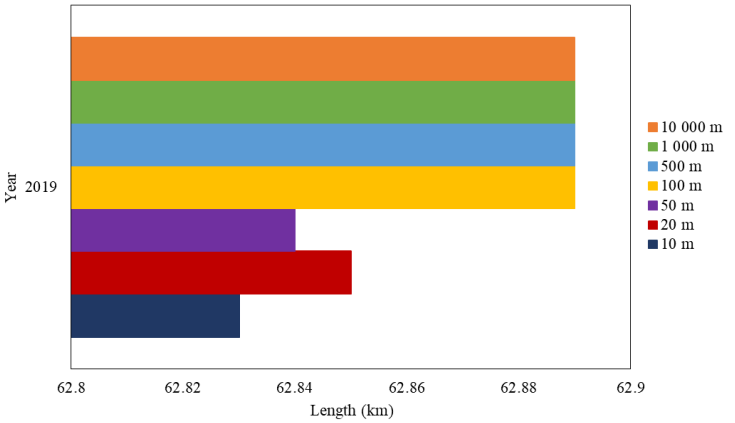


**Figure G-22: Change in reseal treatment year and length for sample 9**

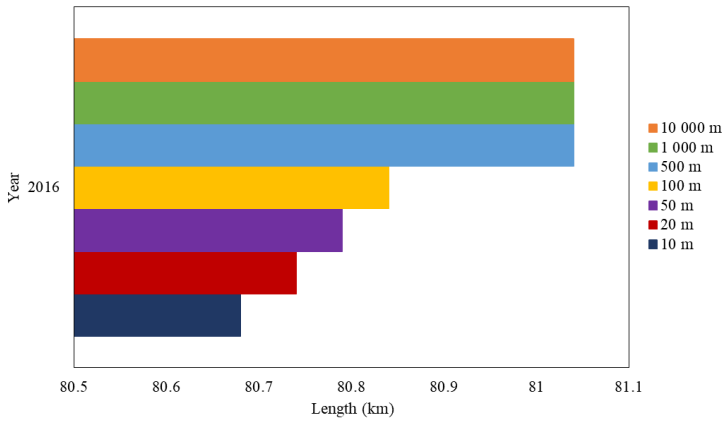


**Figure G-23: Change in light rehabilitation treatment year and length for sample 10**

N/A

**Figure G-24: Change in light rehabilitation treatment year and length for sample 11**

N/A

**Figure G-25: Change in light rehabilitation treatment year and length for sample 12**

N/A

**Figure G-26: Change in light rehabilitation treatment year and length for sample 13**

## G.4 SAMPLES CONTAINING A SINGLE TREATMENT TRIGGERED IN A SINGLE YEAR

Figure G-27 to Figure G-39, where applicable, present the change in light rehabilitation / reseal year and length with increasing averaged section lengths for samples containing a single treatment (light rehabilitation / reseal) triggered in a single year.

N/A

**Figure G-27: Change in light rehabilitation treatment year and length for sample 1**

N/A

**Figure G-28: Change in light rehabilitation treatment year and length for sample 2**

N/A

**Figure G-29: Change in reseal treatment year and length for sample 3**

N/A

**Figure G-30: Change in light rehabilitation treatment year and length for sample 4**

N/A

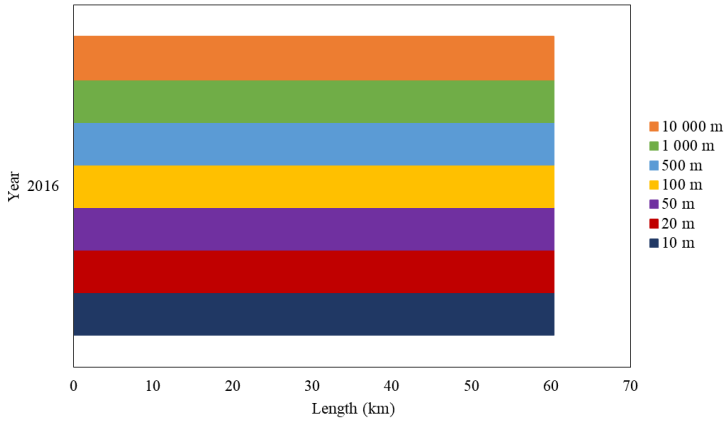


**Figure G-31: Change in reseal treatment year and length for sample 5**

**Figure G-32: Change in light rehabilitation treatment year and length for sample 6**

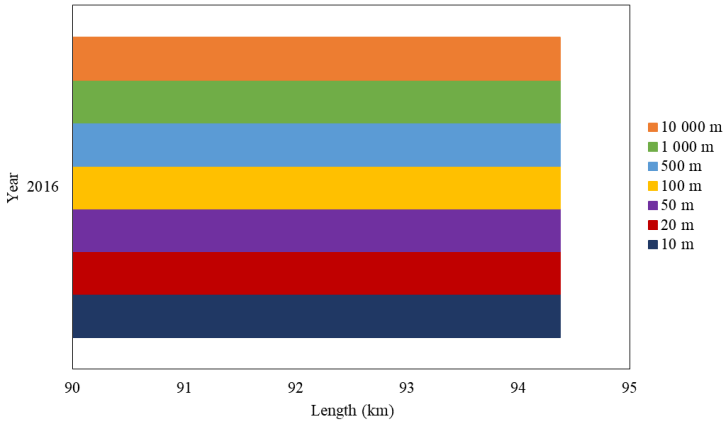


**Figure G-33: Change in reseal treatment year and length for sample 7**

N/A

**Figure G-34: Change in reseal treatment year and length for sample 8**

N/A

**Figure G-35: Change in reseal treatment year and length for sample 9**

N/A

**Figure G-36: Change in light rehabilitation treatment year and length for sample 10**

N/A

**Figure G-37: Change in light rehabilitation treatment year and length for sample 11**

N/A

**Figure G-38: Change in light rehabilitation treatment year and length for sample 12**

N/A

**Figure G-39: Change in light rehabilitation treatment year and length for sample 13**

# APPENDIX H

# DATASET 2 CUMULATIVE DISTRIBUTION OF RUT DEPTH BASED ON PERCENTILES

# APPENDIX H DATASET 2 CUMULATIVE DISTRIBUTION OF RUT DEPTH BASED ON PERCENTILES

## H.1 INTRODUCTION

The results from the comparison of the distribution of rut depth for the different percentiles discussed in Section 4.2.2 are presented in the sections that follow.

## H.2 CUMULATIVE DISTRIBUTION OF RUT DEPTH

Figure H-1 to Figure H-65 present the cumulative distributions of rut depth for the 50$^{th}$, 75$^{th}$, 90$^{th}$, 95$^{th}$, and 99$^{th}$ percentile for 20 m section lengths in comparison to 10 m section lengths for each of the 13 roads considered in the analysis.

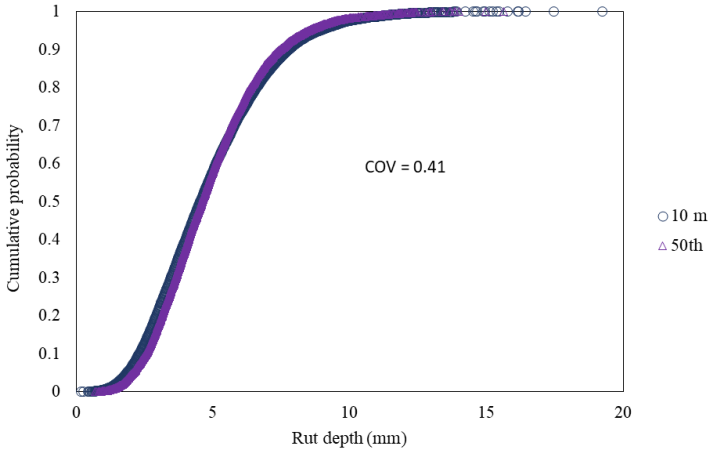


**Figure H-1: Sample 1 cumulative distribution for 50$^{th}$ percentile 20 m section lengths**

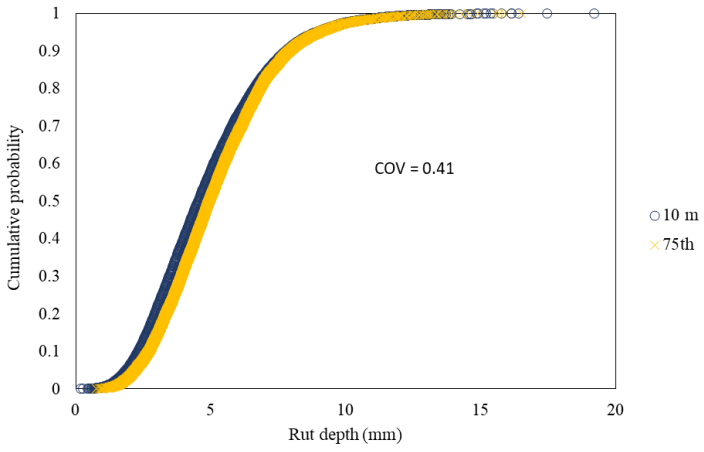


**Figure H-2: Sample 1 cumulative distribution for 75$^{th}$ percentile 20 m section lengths**

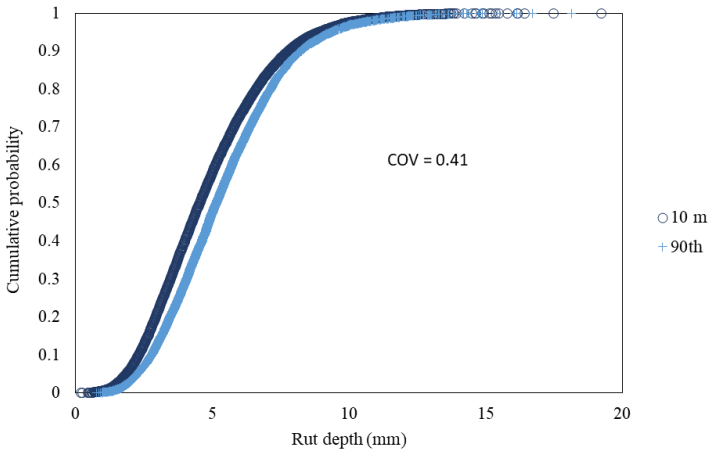


**Figure H-3: Sample 1 cumulative distribution for 90th percentile 20 m section lengths**

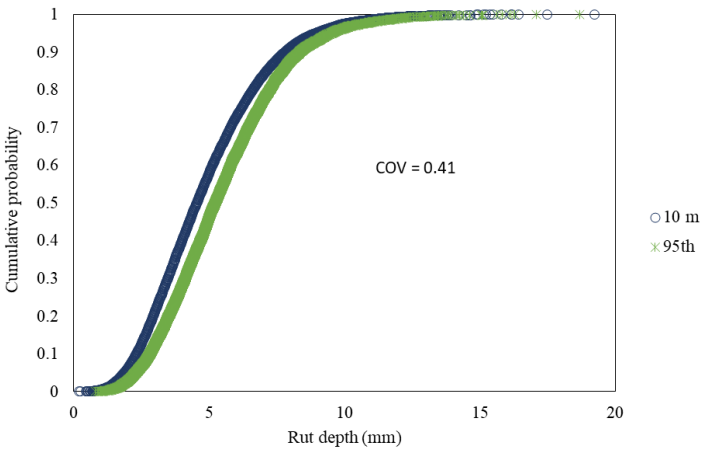


**Figure H-4: Sample 1 cumulative distribution for 95th percentile 20 m section lengths**

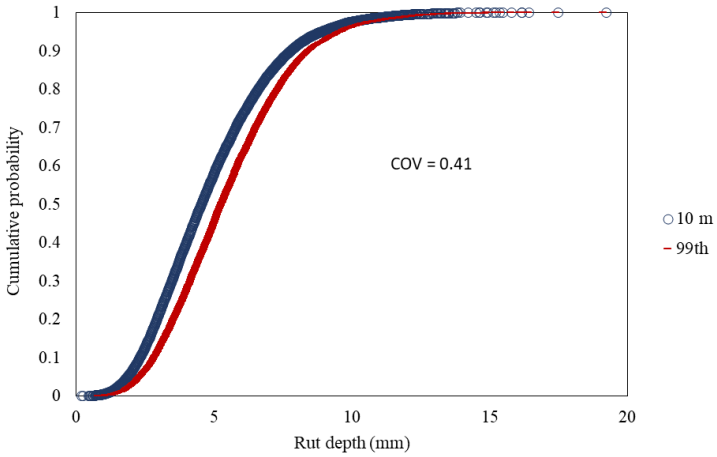


**Figure H-5: Sample 1 cumulative distribution for 99th percentile 20 m section lengths**

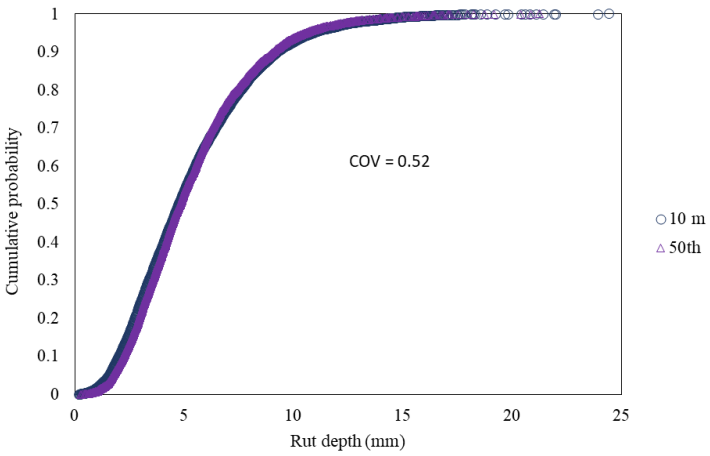


**Figure H-6: Sample 2 cumulative distribution for 50th percentile 20 m section lengths**

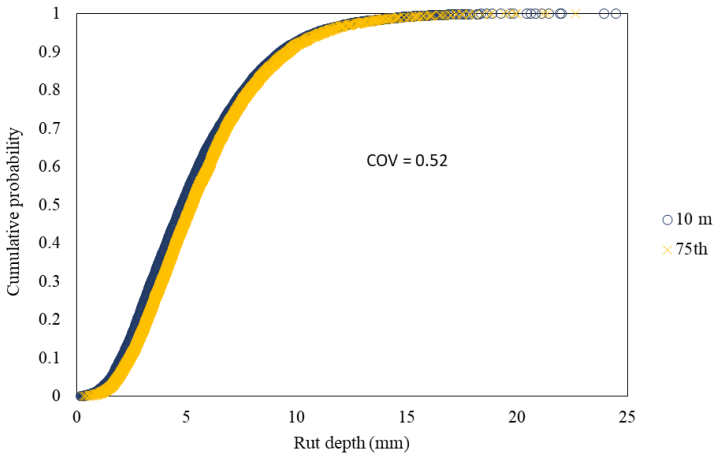


**Figure H-7: Sample 2 cumulative distribution for 75th percentile 20 m section lengths**

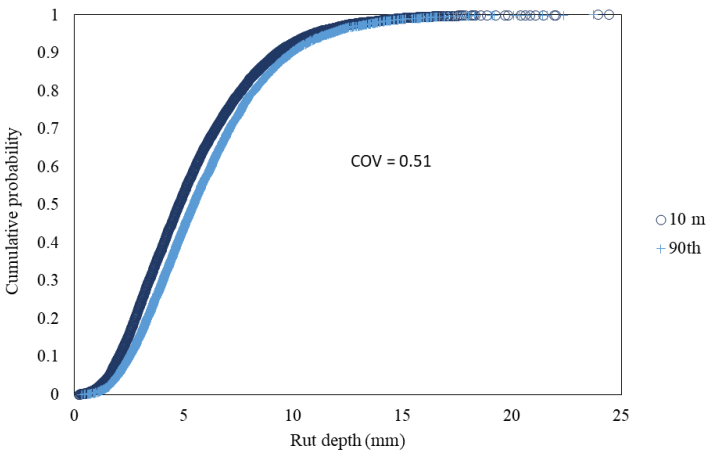


**Figure H-8: Sample 2 cumulative distribution for 90th percentile 20 m section lengths**

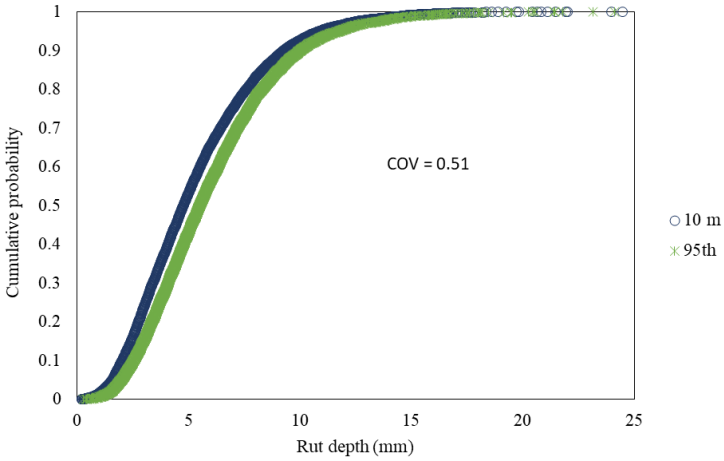


**Figure H-9: Sample 2 cumulative distribution for 95th percentile 20 m section lengths**

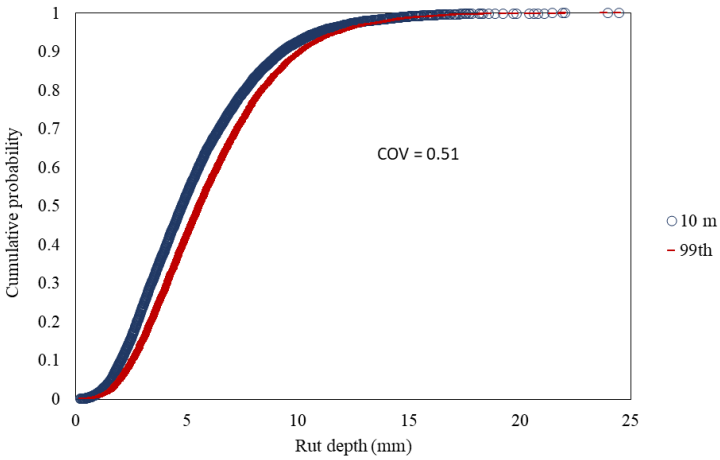


**Figure H-10: Sample 2 cumulative distribution for 99th percentile 20 m section lengths**

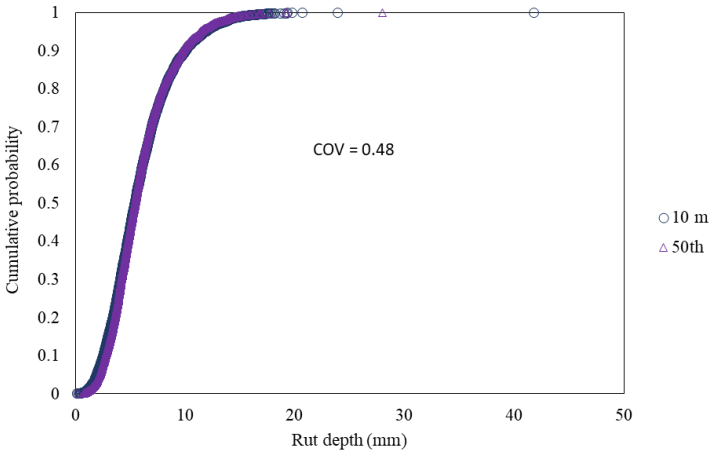


**Figure H-11: Sample 3 cumulative distribution for 50th percentile 20 m section lengths**

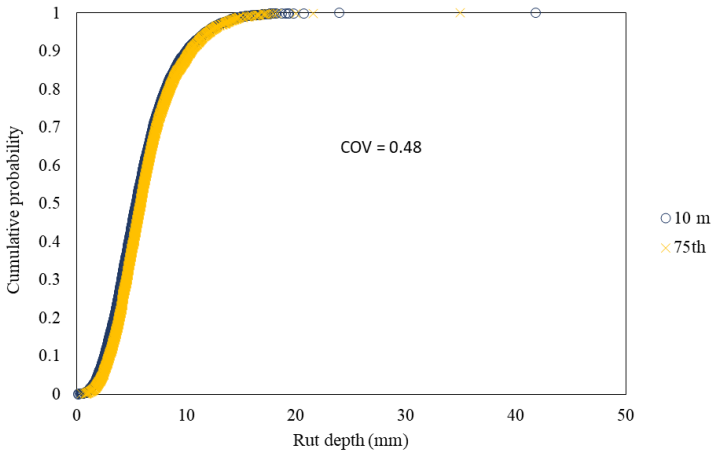


**Figure H-12: Sample 3 cumulative distribution for 75th percentile 20 m section lengths**

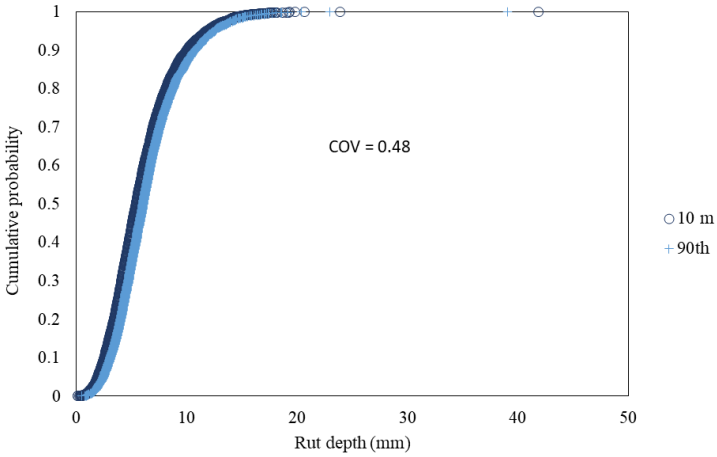


**Figure H-13: Sample 3 cumulative distribution for 90th percentile 20 m section lengths**

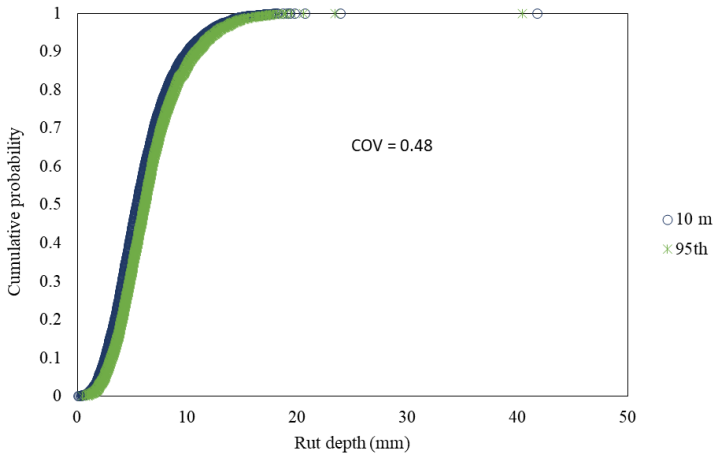


**Figure H-14: Sample 3 cumulative distribution for 95th percentile 20 m section lengths**

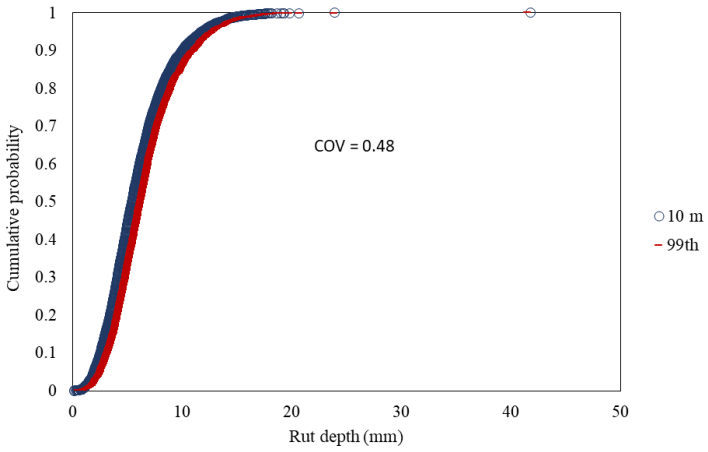


**Figure H-15: Sample 3 cumulative distribution for 99th percentile 20 m section lengths**

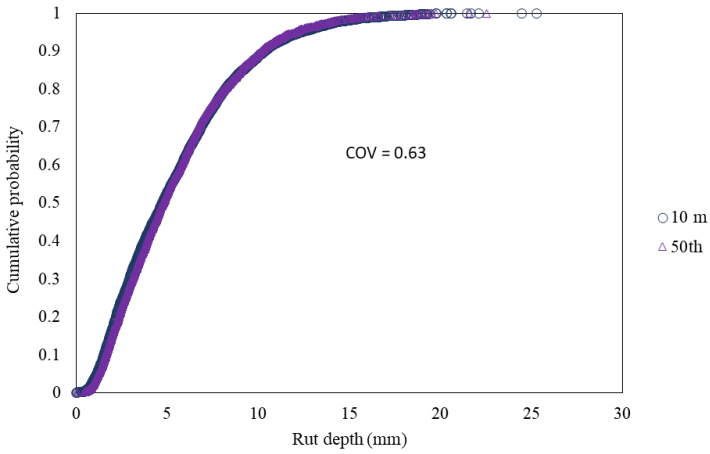


**Figure H-16: Sample 4 cumulative distribution for 50th percentile 20 m section lengths**

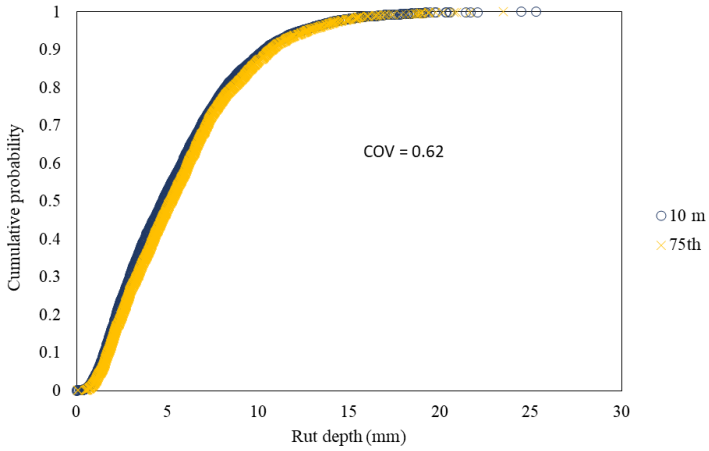


**Figure H-17: Sample 4 cumulative distribution for 75th percentile 20 m section lengths**

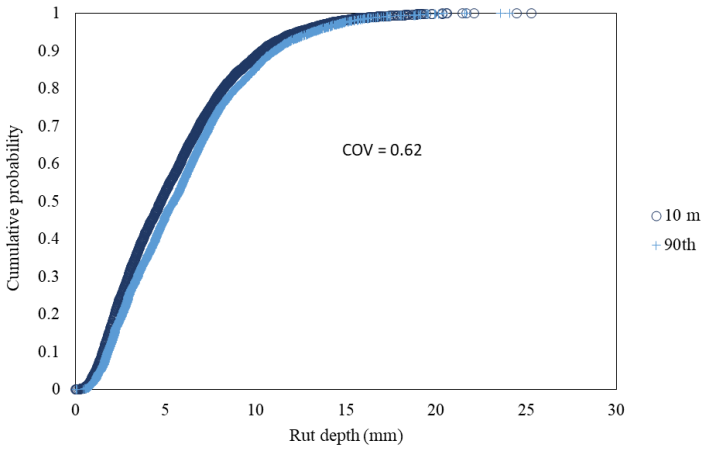


**Figure H-18: Sample 4 cumulative distribution for 90th percentile 20 m section lengths**

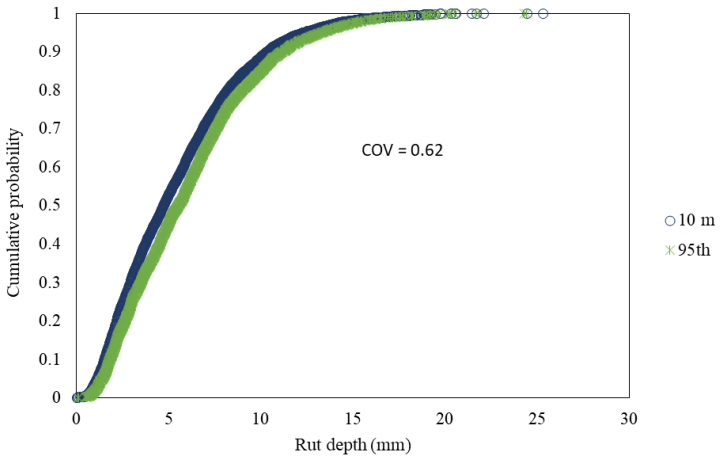


**Figure H-19: Sample 4 cumulative distribution for 95th percentile 20 m section lengths**

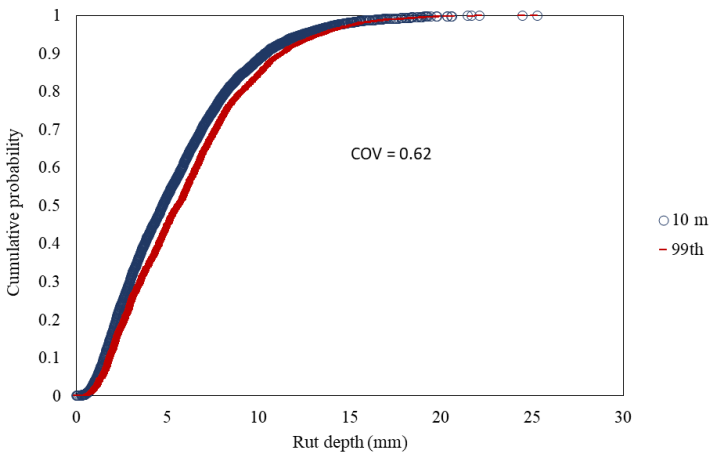


**Figure H-20: Sample 4 cumulative distribution for 99th percentile 20 m section lengths**

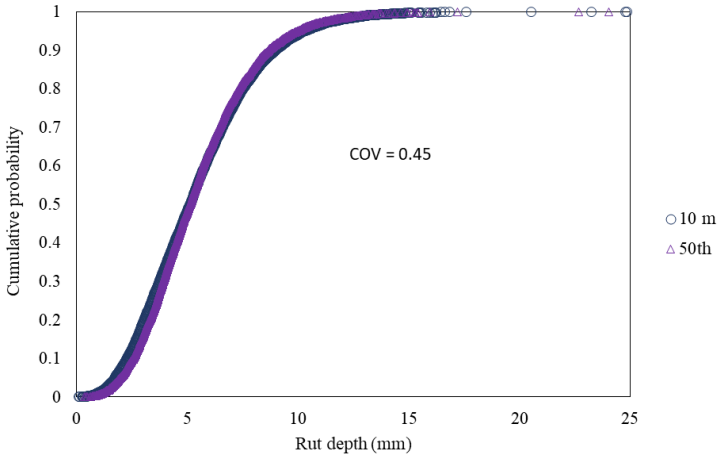


**Figure H-21: Sample 5 cumulative distribution for 50th percentile 20 m section lengths**

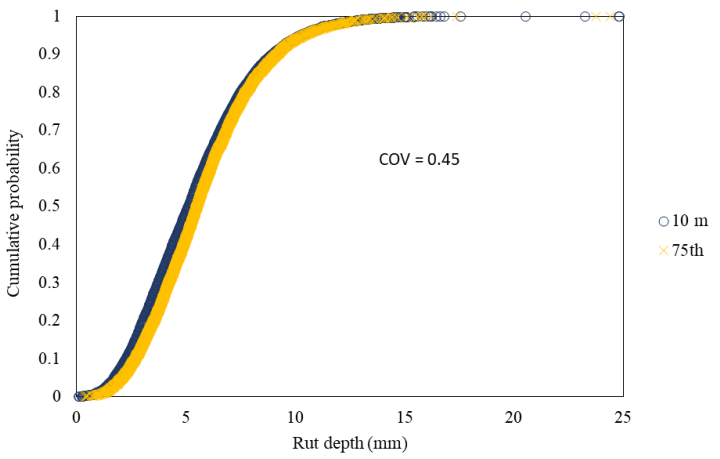


**Figure H-22: Sample 5 cumulative distribution for 75th percentile 20 m section lengths**

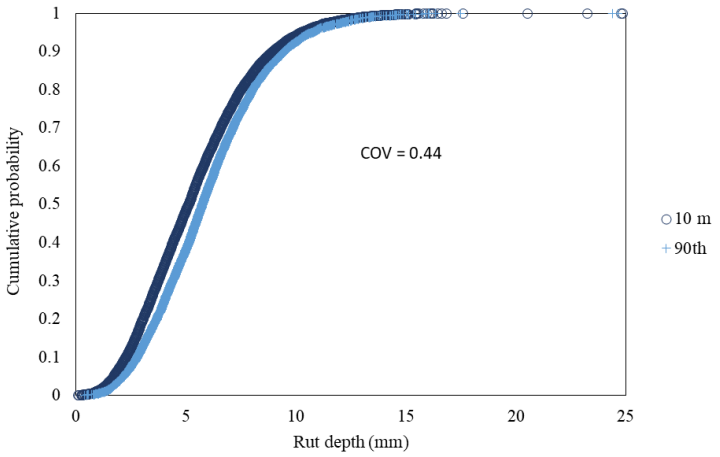


**Figure H-23: Sample 5 cumulative distribution for 90th percentile 20 m section lengths**

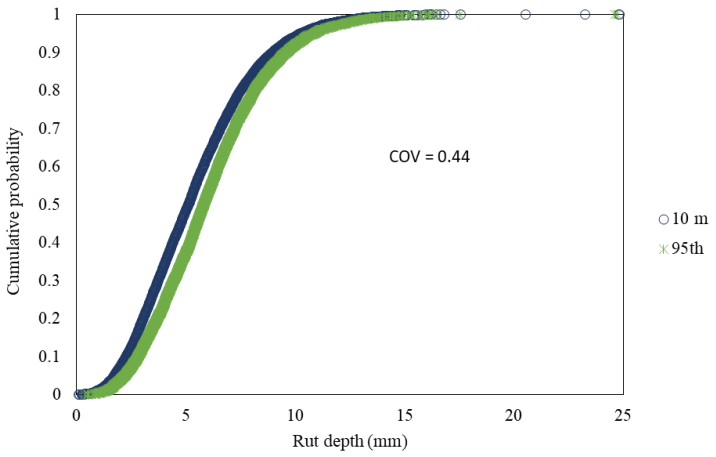


**Figure H-24: Sample 5 cumulative distribution for 95th percentile 20 m section lengths**

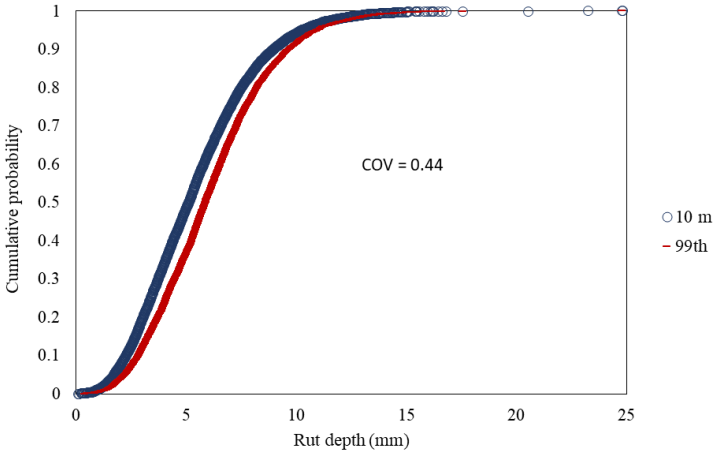


**Figure H-25: Sample 5 cumulative distribution for 99th percentile 20 m section lengths**

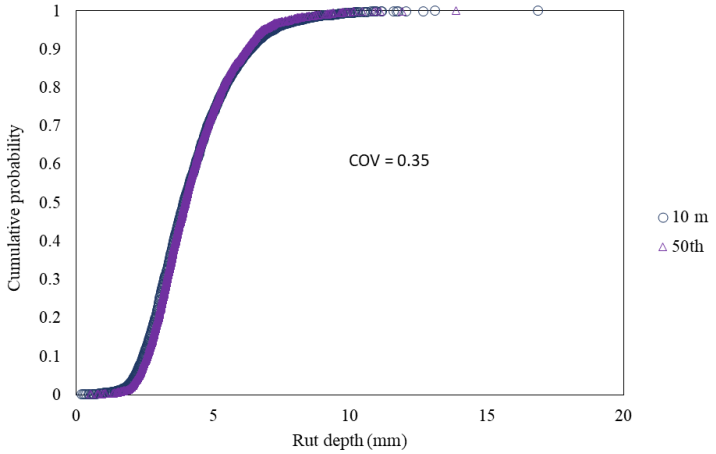


**Figure H-26: Sample 6 cumulative distribution for 50th percentile 20 m section lengths**

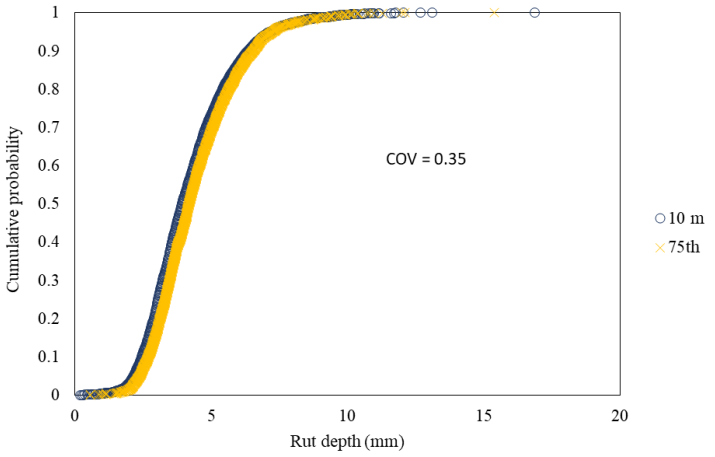


**Figure H-27: Sample 6 cumulative distribution for 75th percentile 20 m section lengths**

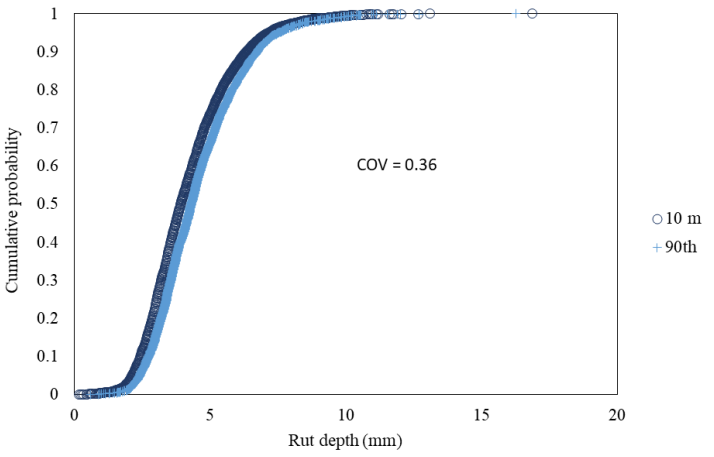


**Figure H-28: Sample 6 cumulative distribution for 90th percentile 20 m section lengths**

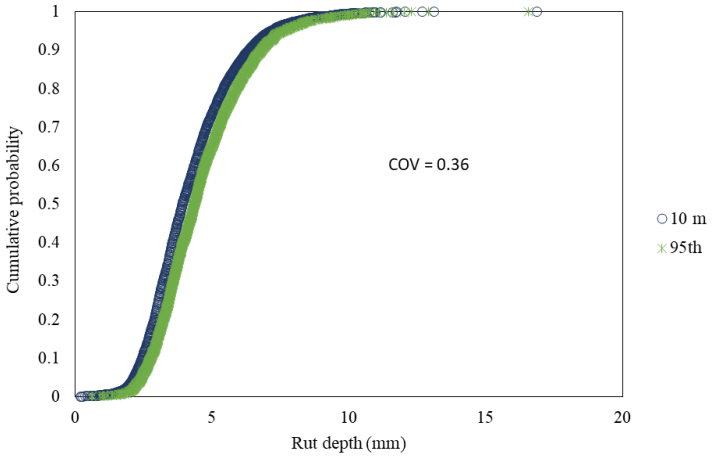


**Figure H-29: Sample 6 cumulative distribution for 95th percentile 20 m section lengths**

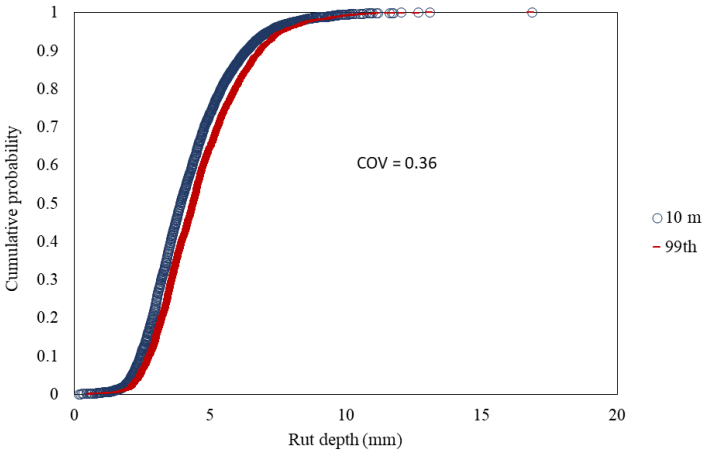


**Figure H-30: Sample 6 cumulative distribution for 99th percentile 20 m section lengths**

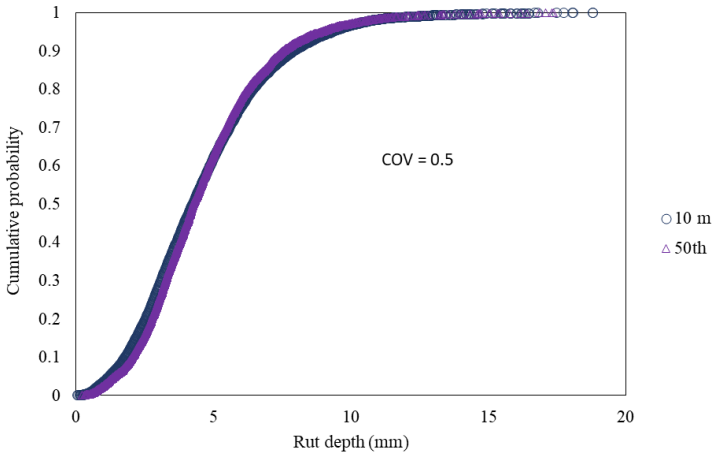


**Figure H-31: Sample 7 cumulative distribution for 50th percentile 20 m section lengths**

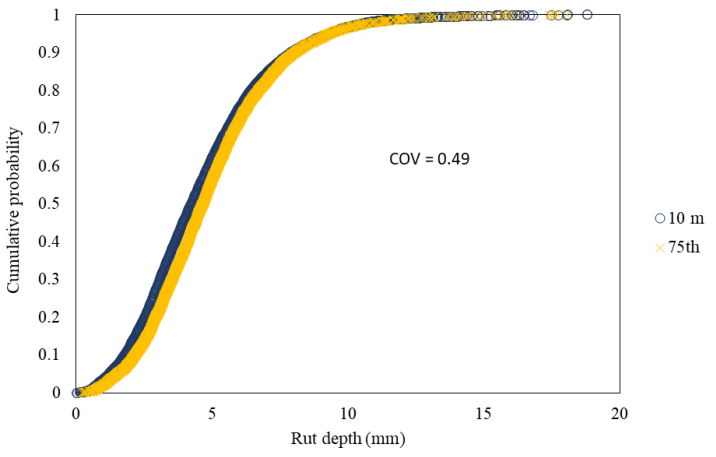


**Figure H-32: Sample 7 cumulative distribution for 75th percentile 20 m section lengths**

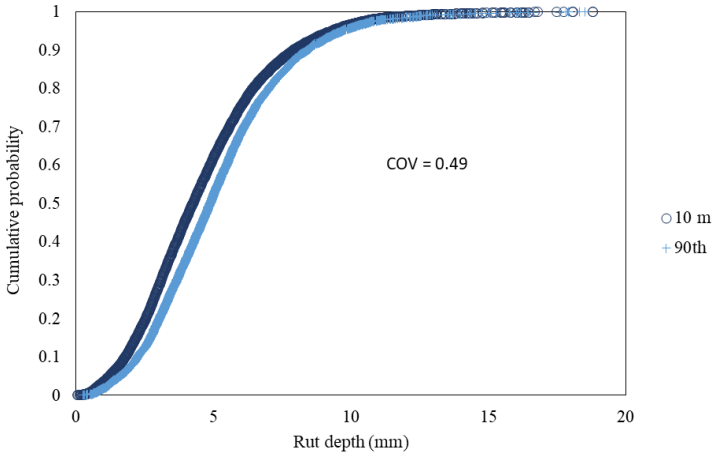


**Figure H-33: Sample 7 cumulative distribution for 90th percentile 20 m section lengths**

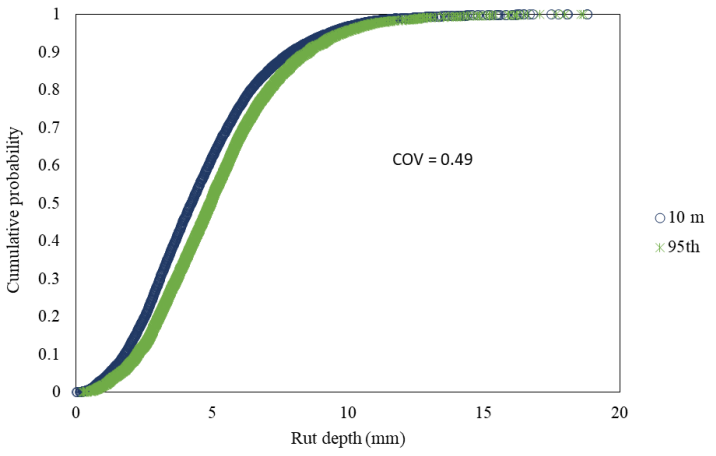


**Figure H-34: Sample 7 cumulative distribution for 95th percentile 20 m section lengths**

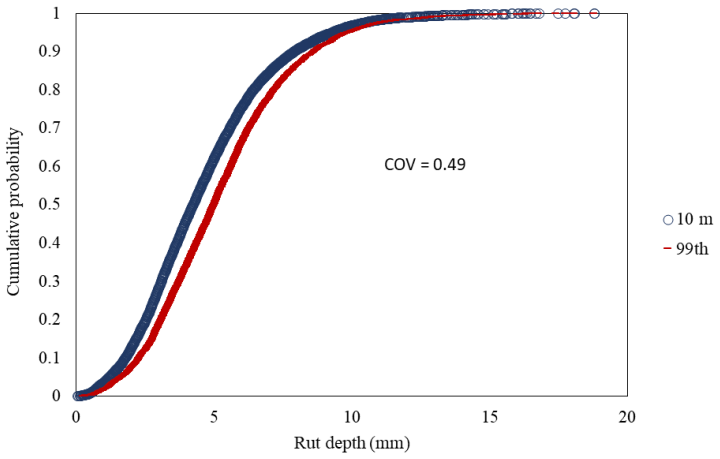


**Figure H-35: Sample 7 cumulative distribution for 99th percentile 20 m section lengths**

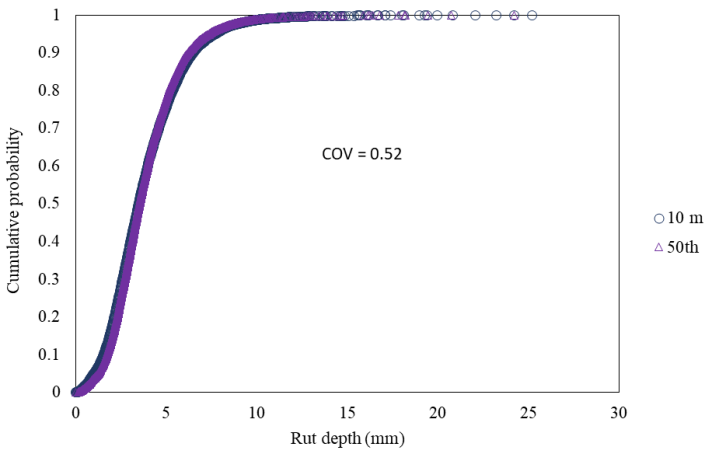


**Figure H-36: Sample 8 cumulative distribution for 50th percentile 20 m section lengths**

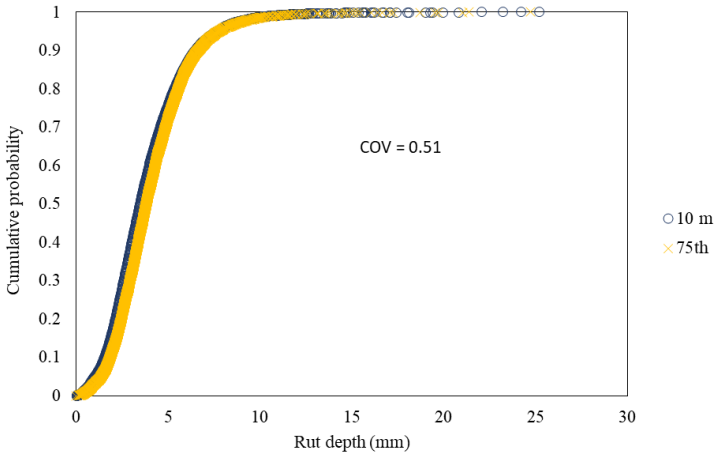


**Figure H-37: Sample 8 cumulative distribution for 75th percentile 20 m section lengths**

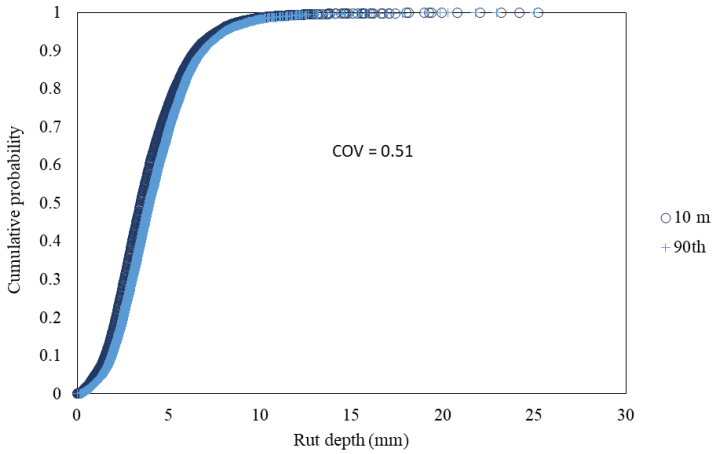


**Figure H-38: Sample 8 cumulative distribution for 90th percentile 20 m section lengths**

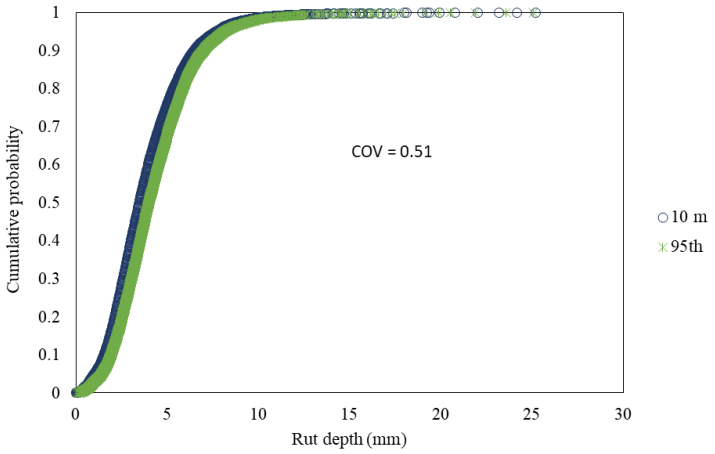


**Figure H-39: Sample 8 cumulative distribution for 95th percentile 20 m section lengths**

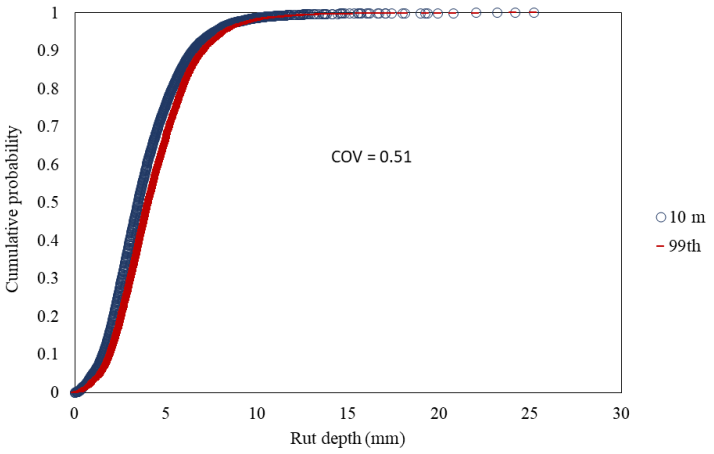


**Figure H-40: Sample 8 cumulative distribution for 99th percentile 20 m section lengths**

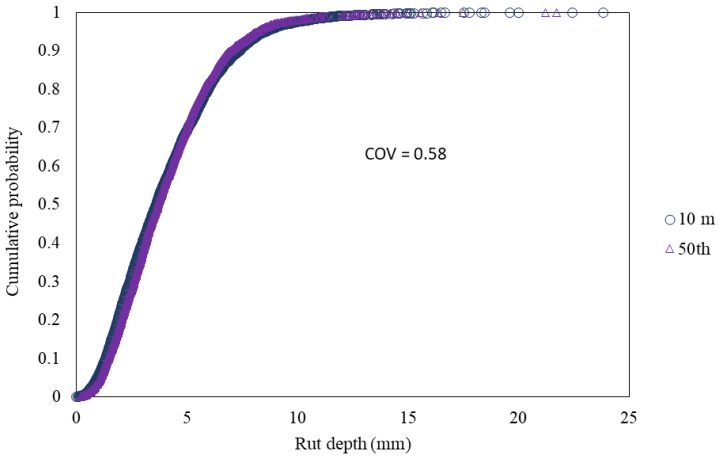


**Figure H-41: Sample 9 cumulative distribution for 50th percentile 20 m section lengths**

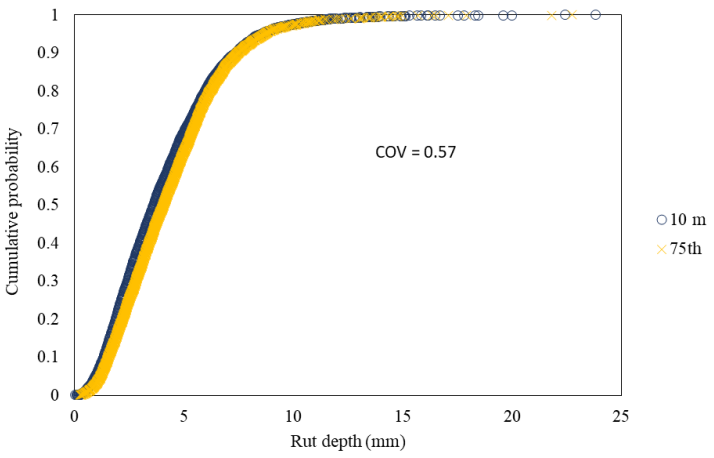


**Figure H-42: Sample 9 cumulative distribution for 75th percentile 20 m section lengths**

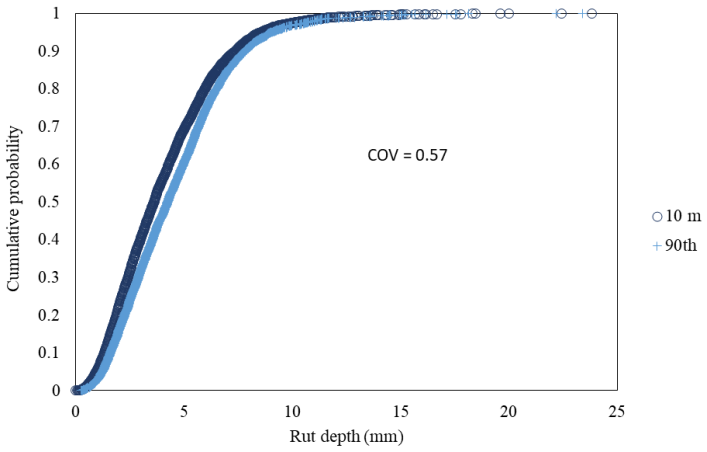


**Figure H-43: Sample 9 cumulative distribution for 90th percentile 20 m section lengths**

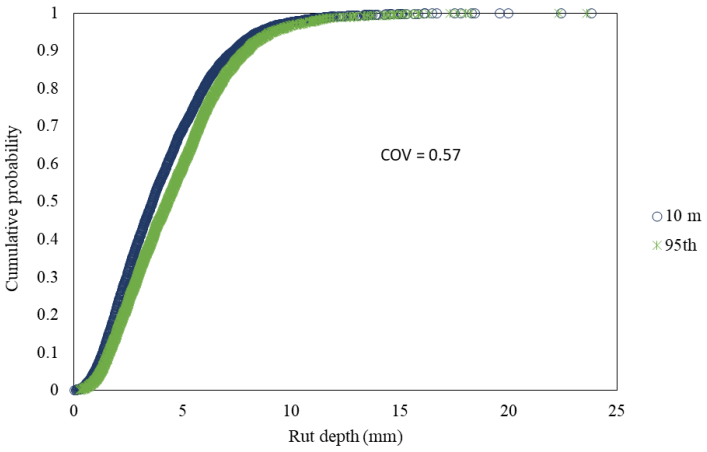


**Figure H-44: Sample 9 cumulative distribution for 95th percentile 20 m section lengths**

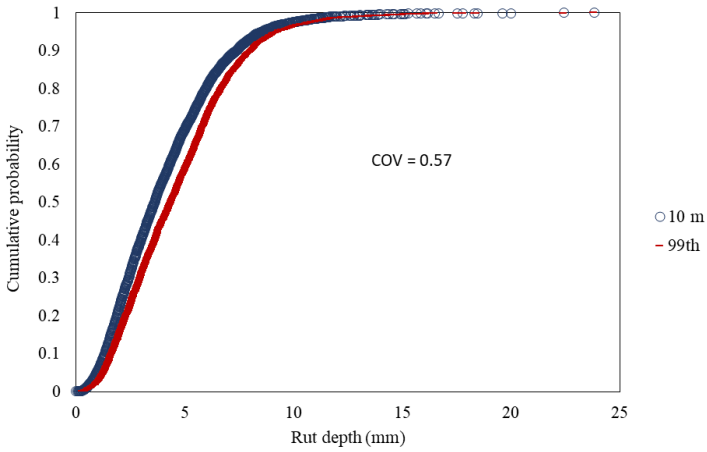


**Figure H-45: Sample 9 cumulative distribution for 99th percentile 20 m section lengths**

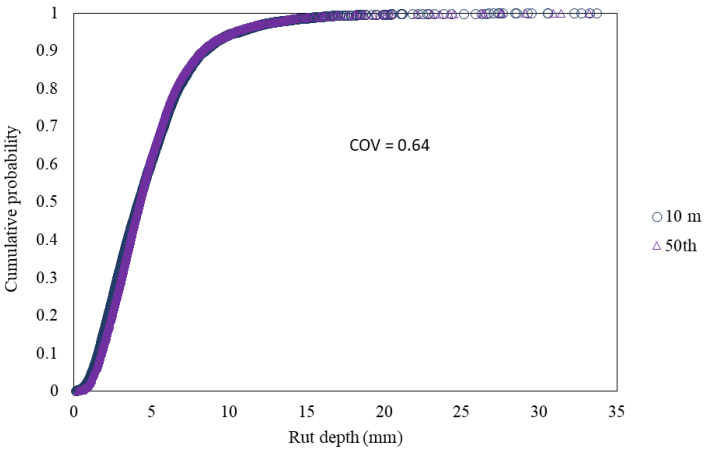


**Figure H-46: Sample 10 cumulative distribution for 50th percentile 20 m section lengths**

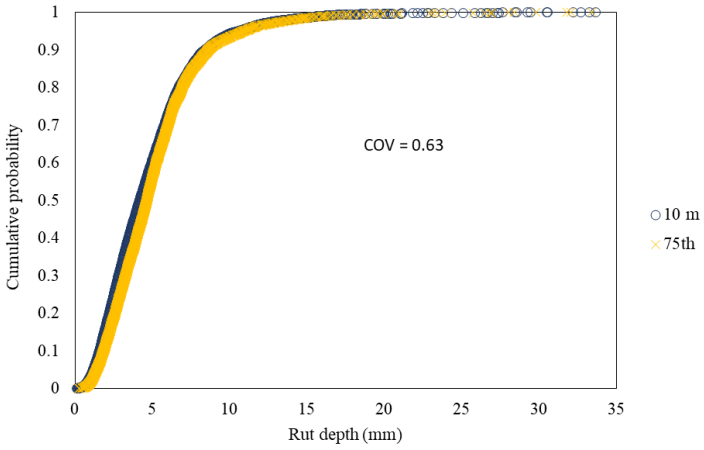


**Figure H-47: Sample 10 cumulative distribution for 75th percentile 20 m section lengths**

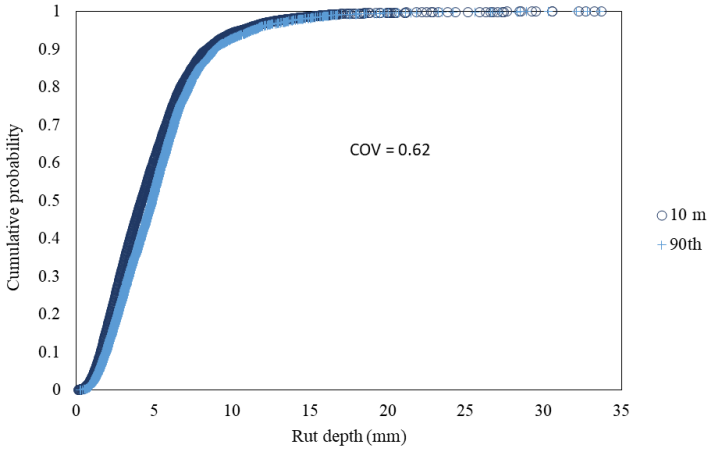


**Figure H-48: Sample 10 cumulative distribution for 90th percentile 20 m section lengths**

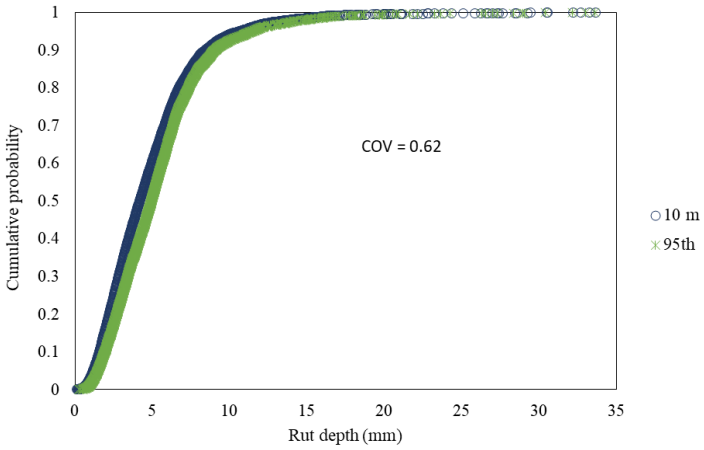


**Figure H-49: Sample 10 cumulative distribution for 95th percentile 20 m section lengths**

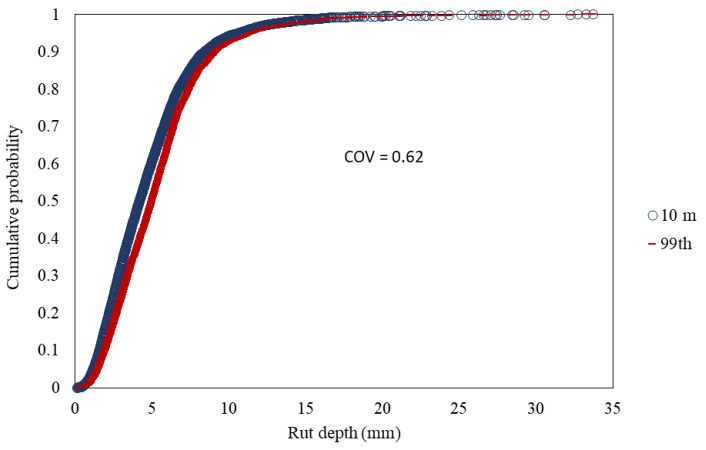


**Figure H-50: Sample 10 cumulative distribution for 99th percentile 20 m section lengths**

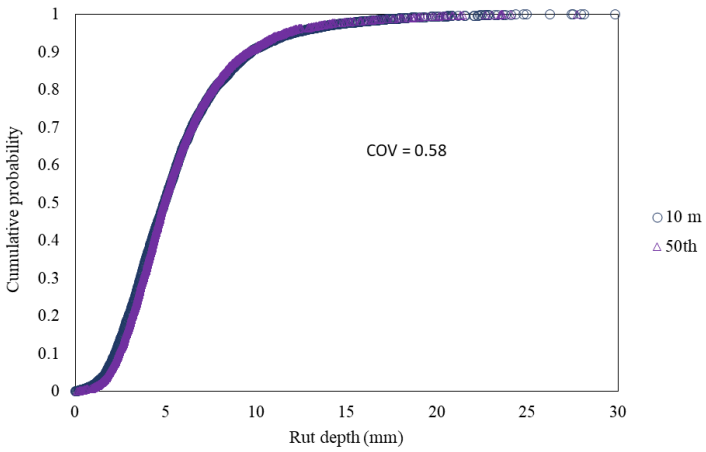


**Figure H-51: Sample 11 cumulative distribution for 50th percentile 20 m section lengths**

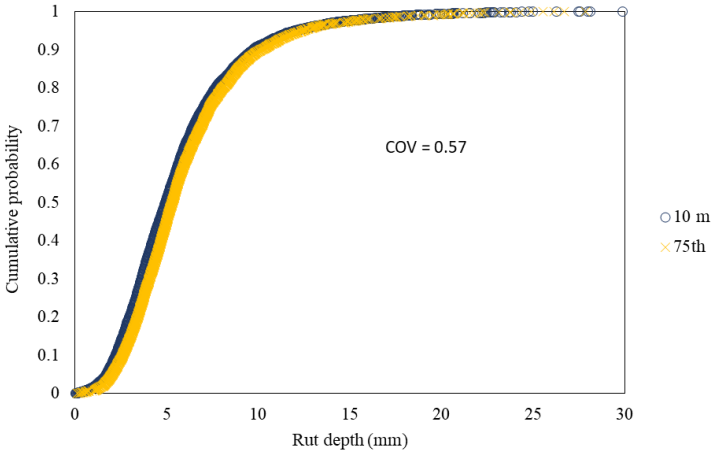


**Figure H-52: Sample 11 cumulative distribution for 75th percentile 20 m section lengths**

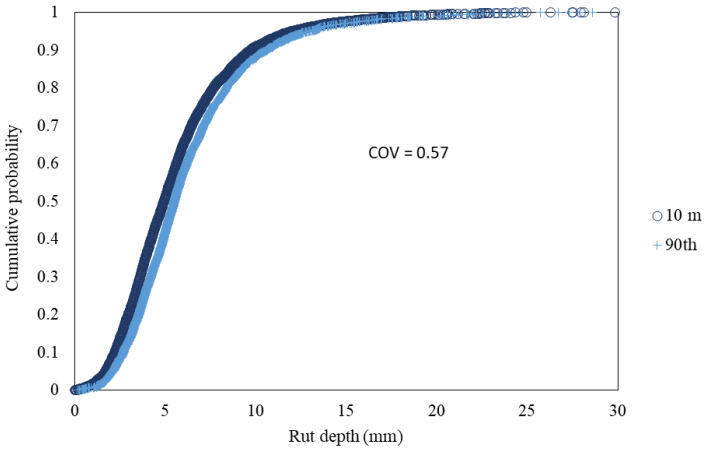


**Figure H-53: Sample 11 cumulative distribution for 90th percentile 20 m section lengths**

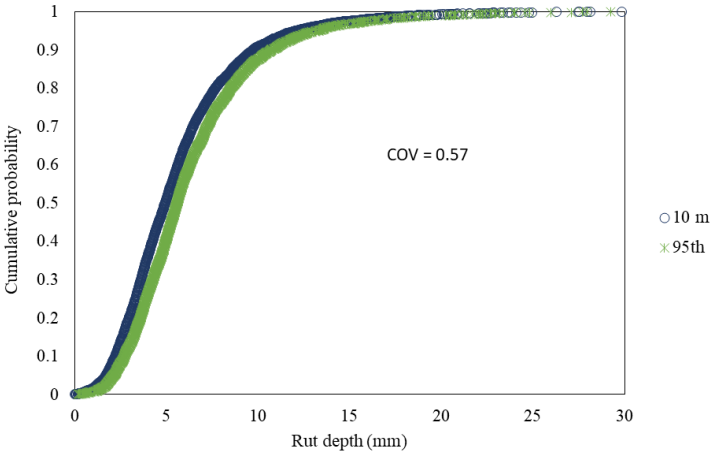


**Figure H-54: Sample 11 cumulative distribution for 95th percentile 20 m section lengths**

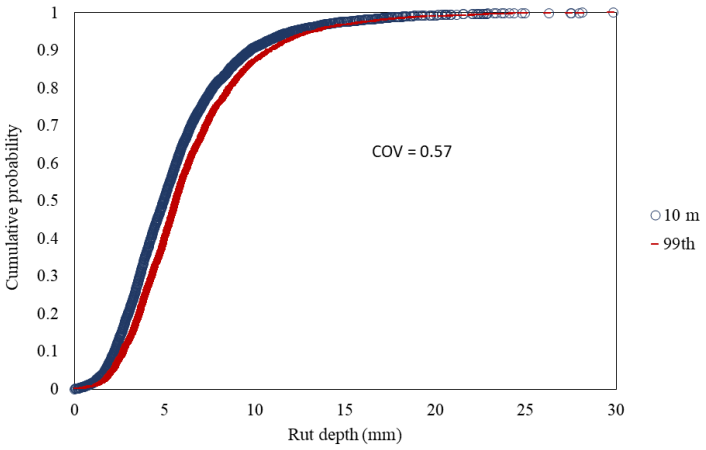


**Figure H-55: Sample 11 cumulative distribution for 99th percentile 20 m section lengths**

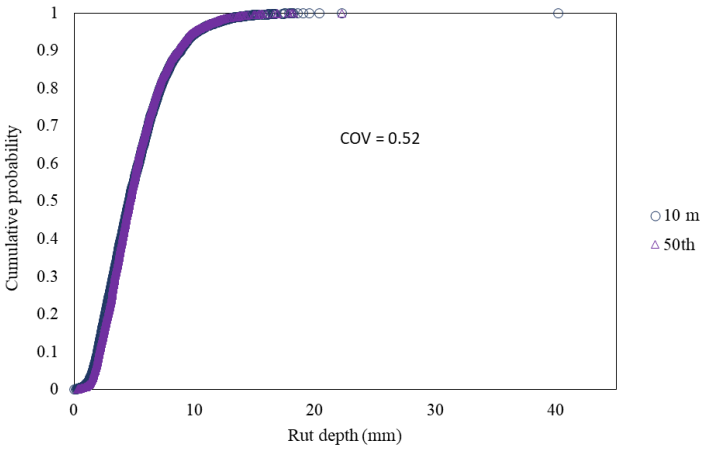


**Figure H-56: Sample 12 cumulative distribution for 50th percentile 20 m section lengths**

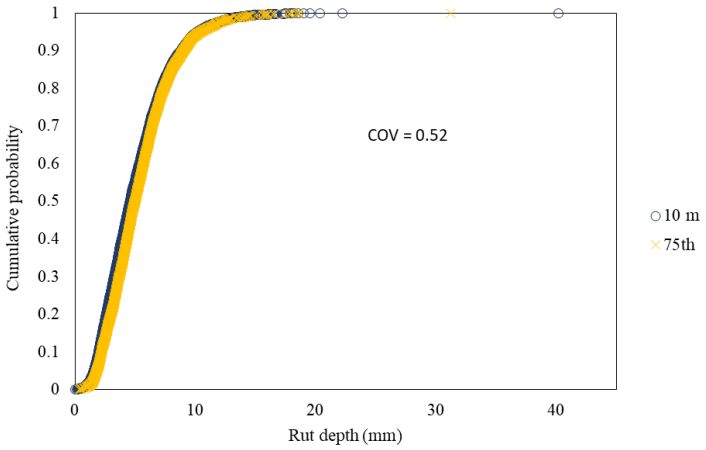


**Figure H-57: Sample 12 cumulative distribution for 75th percentile 20 m section lengths**

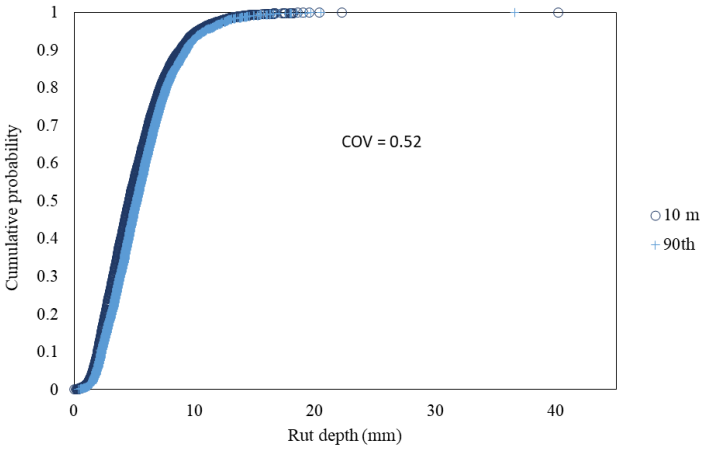


**Figure H-58: Sample 12 cumulative distribution for 90th percentile 20 m section lengths**

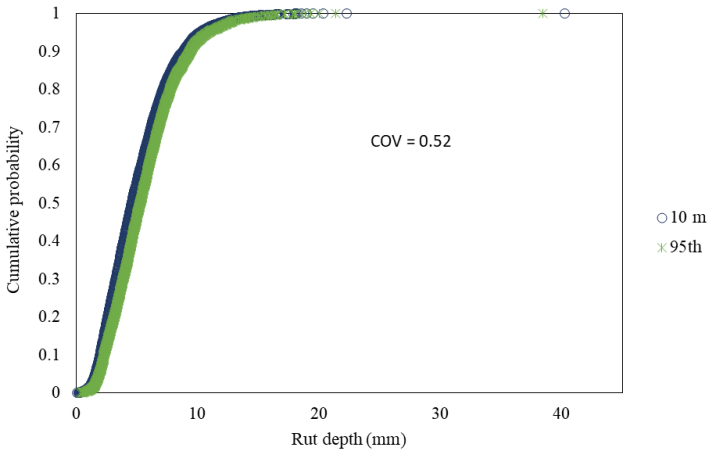


**Figure H-59: Sample 12 cumulative distribution for 95th percentile 20 m section lengths**

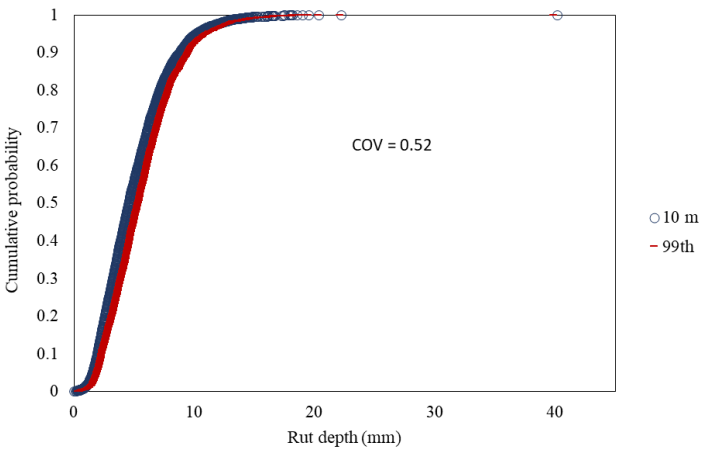


**Figure H-60: Sample 12 cumulative distribution for 99th percentile 20 m section lengths**

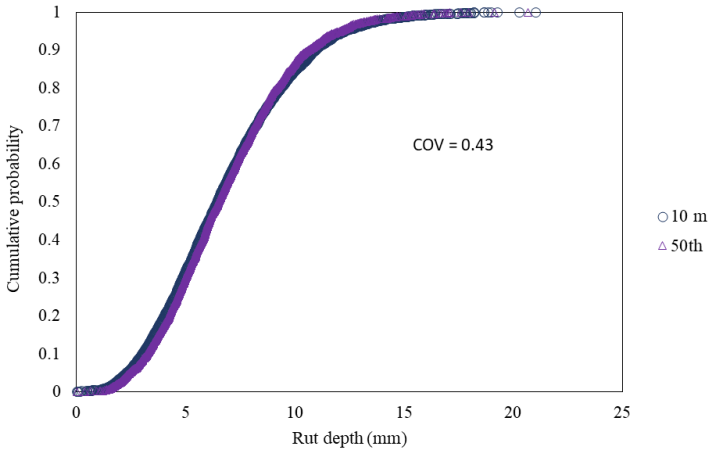


**Figure H-61: Sample 13 cumulative distribution for 50th percentile 20 m section lengths**

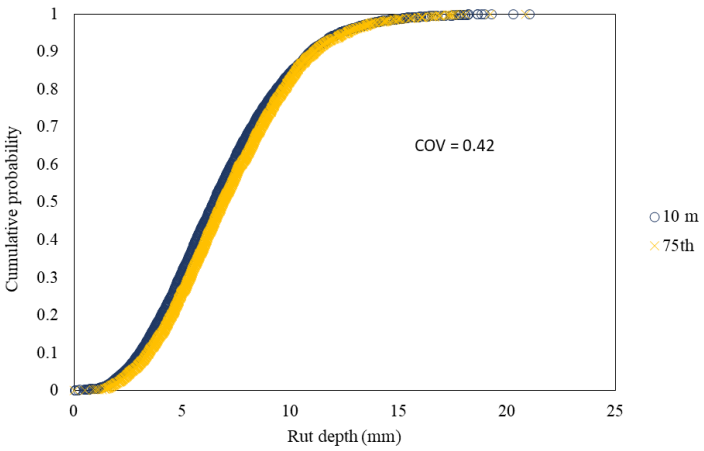


**Figure H-62: Sample 13 cumulative distribution for 75th percentile 20 m section lengths**

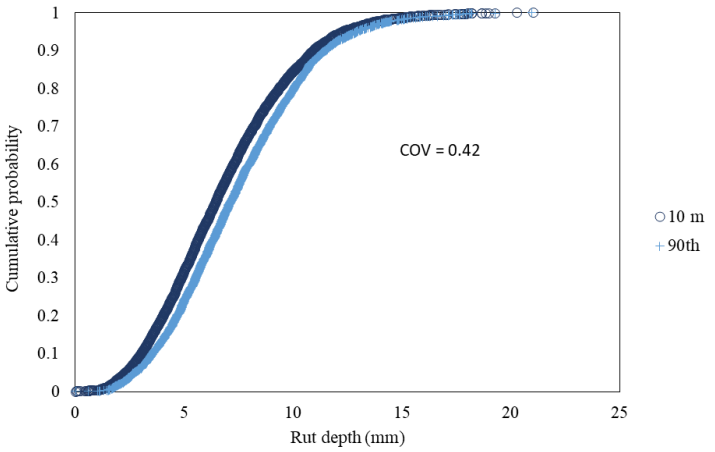


**Figure H-63: Sample 13 cumulative distribution for 90th percentile 20 m section lengths**

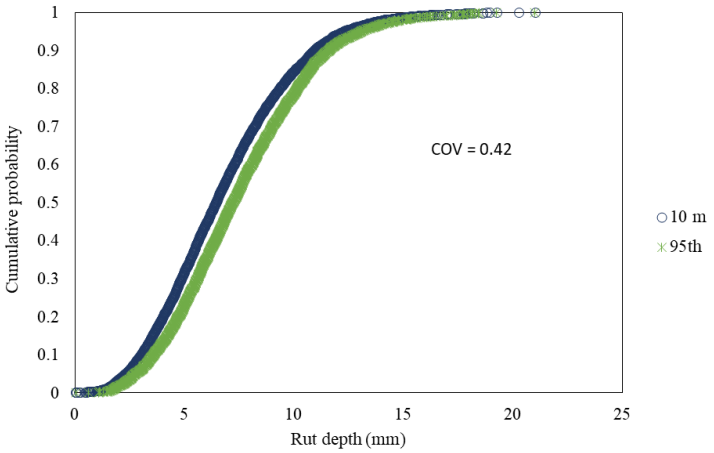


**Figure H-64: Sample 13 cumulative distribution for 95th percentile 20 m section lengths**

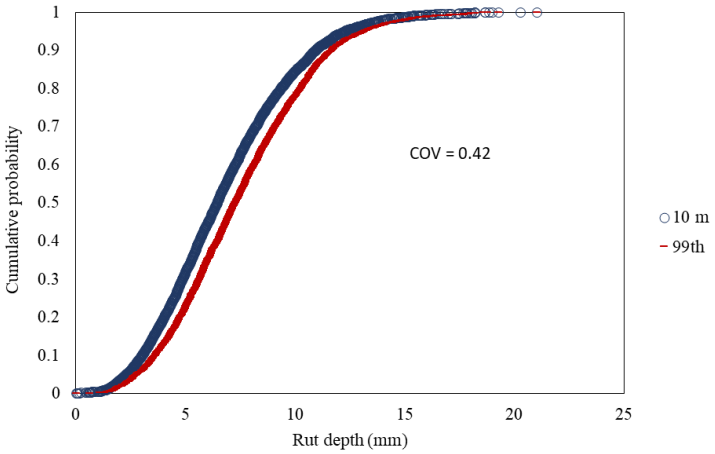


**Figure H-65: Sample 13 cumulative distribution for 99th percentile 20 m section lengths**

# APPENDIX I

# APPLICATION WITHIN THE SOUTH AFRICAN NRA (1999) SPECIFICATION

# APPENDIX I APPLICATION WITHIN THE SOUTH AFRICAN NRA (1999) SPECIFICATION

## I.1 INTRODUCTION

The cumulative distribution graphs of the 5 samples analysed to study the influence of average and percentile statistical aggregation methods on the NRA (1999) acceptance criteria are presented in the sections that follow.

## I.2 CUMULATIVE DISTRIBUTION OF RUT DEPTH

Figure I-1 to Figure I-5 present the cumulative distribution graphs of discrete 10 m, 100 m average, and 100 m 50th, 75th, 90th, 95th, and 99th percentile rut depth measurements for all 5 samples.

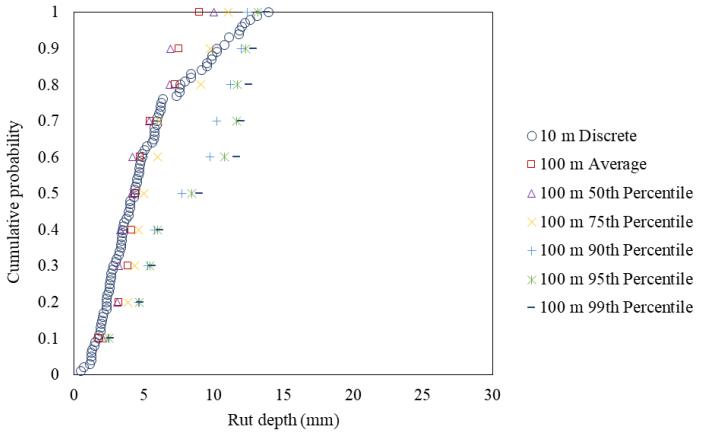


**Figure I-1: Sample 1 cumulative distribution**

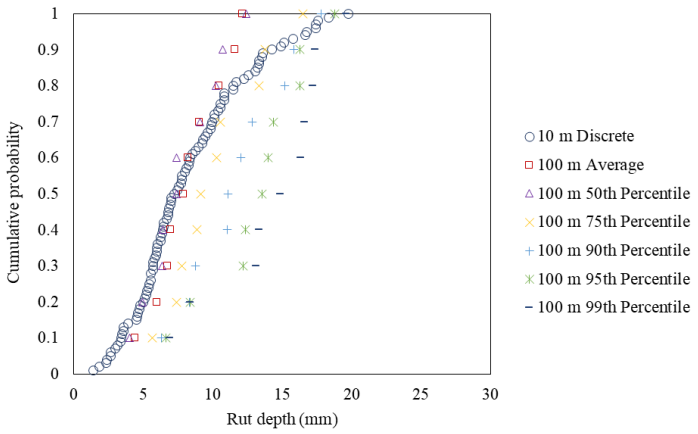


**Figure I-2: Sample 2 cumulative distribution**

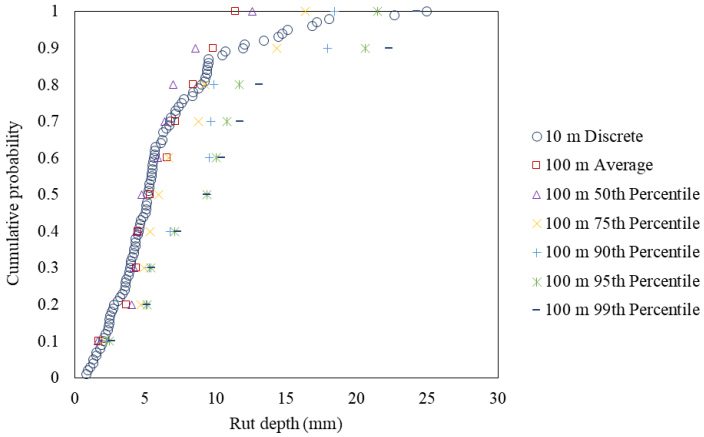


**Figure I-3: Sample 3 cumulative distribution**

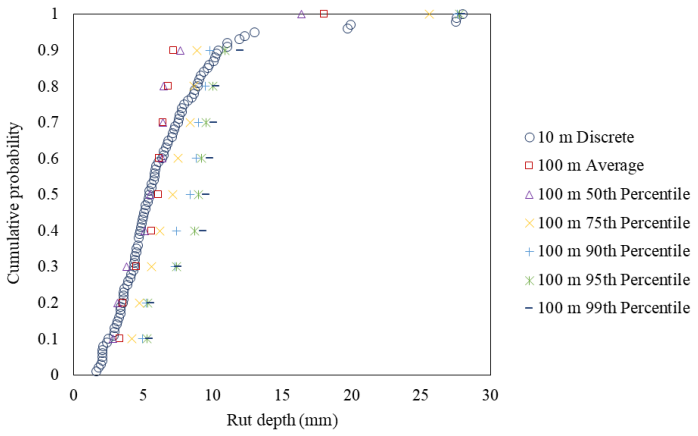


**Figure I-4: Sample 4 cumulative distribution**

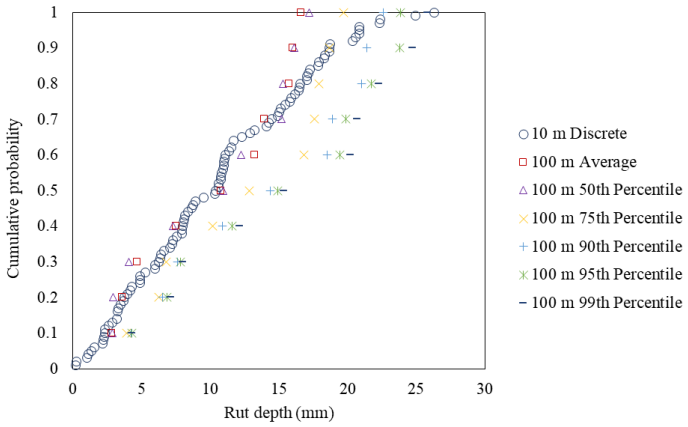


**Figure I-5: Sample 5 cumulative distribution**